

U.S. DEPARTMENT OF COMMERCE
National Oceanic and Atmospheric Administration
National Ocean Service
Center for Operational Oceanographic Products and Services

Tidal Analysis and Prediction

NOAA Special Publication NOS CO-OPS 3

Tidal Analysis and Prediction



Bruce B. Parker, Ph.D.

Silver Spring, Maryland

July 2007

Library of Congress Control Number: 2007925298

U.S. DEPARTMENT OF COMMERCE
Carlos M. Gutierrez , Secretary

National Oceanic and Atmospheric Administration
Conrad C. Lautenbacher, Jr.
Undersecretary of Commerce for Oceans and Atmosphere and NOAA Administrator

National Ocean Service
John H. Dunnigan, Assistant Administrator

Center for Operational Oceanographic Products and Services
Michael Szabados, Director

NOTICE

Mention of a commercial company or product does not constitute an endorsement by NOAA. Use for publicity or advertising purposes of information from this publication concerning proprietary products or the tests of such products is not authorized.

Request for copies should be addressed to
Center for Operational Oceanographic Products and Services
1305 East West Highway
SSMC IV, Rm 6616
Silver Spring, Maryland 20910-3281
Phone (301) 713-2981 ext. 125

<http://tidesandcurrents.noaa.gov>

Table of Contents

	page
1. Introduction	1
1.1 Purpose of This Book	1
1.2 Relationship to Previous Tidal Analysis and Prediction Books and Manuals	3
1.3 The Uses For Tidal Analysis and Prediction	6
1.4 Brief Historical Background	7
1.5 The Importance of Hydrodynamics	10
1.6 Organization of This Book	11
2. Theory Behind Tidal Analysis and Prediction	15
2.1 Short Introductory Overview – the Big Picture	15
2.1.1 Some Definitions	15
2.1.2 The Generation of Tides	24
2.2 Astronomical Considerations	27
2.2.2 The Orbits of the Moon Around the Earth and the Earth Around the Sun	27
2.2.2 The Origins of the Largest Tidal Harmonic Constituents	31
2.2.3 Derivation of Tidal Frequencies from the Basic Astronomical Frequencies – Insights from Tidal Spectra	35
2.2.4 The Origin of Node Factors and Equilibrium Arguments	39
2.2.5 Definitions Revisited, With Relationship to Harmonic Constants	42
2.3 Hydrodynamic Considerations	48
2.3.1 Hydrodynamic Effects On Tide Ranges, Phase Lags and Tidal Current Speeds	49
2.3.2 Nonlinear Effects of Shallow Water – Overtides and Compound Tides	55
2.3.3 Nonlinear Tidal Interaction With River Flow and Storm Surge	62
2.3.4 Nonlinear Hydrodynamic Effects On Node Factors	67
2.3.5 Zero-frequency Effects From Nonlinear Tidal Interactions	69
2.3.6 Special Aspects of Tidal Currents	69
3. Methods of Tidal Analysis and Prediction	81
3.1 Introduction	81
3.2 Simple Demonstration of Extracting Tidal Constituents From a Data Time Series	82

3.3	<i>The Synodic Period – Length of Time Series Needed To Separate Two Constituents</i>	84
3.4	<i>Harmonic Analysis</i>	90
3.4.1	Introduction	90
3.4.2	The Harmonic Tide Prediction Equation	90
3.4.3	The Harmonic Tidal Current Prediction Equations	95
3.4.4	Fourier-based Harmonic Analysis	97
3.4.5	Least-squares-based Harmonic Analysis	99
3.5	<i>Other Frequency Domain Methods</i>	102
3.5.1	The Response Method	102
3.5.2	The Harmonic Shallow-Water Corrections Method	103
3.5.3	The Species Concordance Method	104
3.5.4	The Method for Superfine Resolution of Harmonic Constituents	105
3.5.5	Continuous Wavelet Transform Method	105
3.5.6	Harmonic Constants From a Long Series of High and Low Waters	106
3.6	<i>Nonharmonic Comparison Methods</i>	109
3.6.1	Overview and Short Historical Background	109
3.6.2	Types of Nonharmonic Analyses	111
3.6.3	Variations In Nonharmonically Determined Time and Height Differences	112
3.7	<i>Analyses for determining Sa and Ssa</i>	119
3.7.1	The Meteorological Origins of Sa and Ssa	119
3.7.2	Considerations In Whether To Use Sa and Ssa In a Prediction	120
3.7.3	Methods for Calculating Sa and Ssa	122
3.8	<i>Tidal Filtering and Detiding</i>	123
3.8.1	Introduction	123
3.8.2	Specially Designed Tidal Filters	127
3.9	<i>Calculating Consistently Defined Maxima and Minima</i>	129
3.9.1	Consistently Defined High and Low Waters	129
3.9.2	Consistently Defined Maximum Floods and Ebbs and Slacks (or Minimums)	131
3.10	<i>Spectral Analysis and EOF Analysis</i>	132
3.10.1	Spectral Analysis of Water Level Data Time Series	133
3.10.2	Tidal Cusps In Spectra	134
3.10.3	Spectral Analysis of Current Data Time Series – Rotary Spectra	135
3.10.4	Cross-spectral Analysis	136
3.10.5	Empirical Orthogonal Function (Principal Component) Analysis	137
4.	<i>Harmonic Analysis of Water Level Data</i>	139
4.1	<i>Considerations In Carrying Out the Analysis</i>	139
4.1.1	Which Tidal Constituents Should Be Solved For	139
4.1.2	Keeping or Rejecting Small Constituents	142
4.1.3	Instrument Errors and Their Effects On Analysis Results	142
4.1.4	Assessing the Potential Effects of Nontidal Influences	146
4.1.5	Use of Node Factors and Equilibrium Arguments (or of Satellite Constituents)	148
4.2	<i>Methods for Analyzing Short Time Series</i>	150

Table of Contents

4.2.1	Schureman's Inference and Elimination Technique	152
4.2.2	Use of a Reference Station To Improve the Results of a Short Analysis	153
4.2.3	Inference In the Frequency Domain	155
4.2.4	Other methods	156
4.3	<i>Assessing the Quality of the Predicted Tide Series</i>	158
4.3.1	Introduction	158
4.3.2	Comparison of High and Low Waters In the Predicted Time Series Versus In the Observed Time Series	160
4.3.3	Spectral Analysis of the Residual Time Series	161
4.3.4	Examination of the Residual Time Series For Periods With Transient Tidal Oscillations	162
4.3.5	The Use and Misuse of "Build-up Factors"	162
4.3.6	Looking For Changes in Bathymetry or Shoreline	163
4.4	<i>Producing a Reference Station for Table 1 of a Tide Table</i>	164
4.5	<i>Summary Overview: Steps In Harmonically Analyzing Water Level Data</i>	165
5.	Harmonic Analysis of Current Data	169
5.1	<i>Special Problems With Current Data</i>	169
5.2	<i>Tidal Current Harmonic Constituent Ellipses</i>	174
5.3	<i>Considerations In Carrying Out the Analysis</i>	181
5.3.1	Which Tidal Current Constituents Should Be Solved For	181
5.3.2	Selection of Orthogonal Axes	181
5.3.3	Instrument Errors and Their Effects On Analysis Results	182
5.3.4	Assessing the Potential Effects of Nontidal Influences	186
5.3.5	Whether To Include the Calculated Mean In a Tidal Current Prediction	188
5.3.6	Use of Node Factors and Equilibrium Arguments (or of Satellite Constituents)	189
5.4	<i>Methods for Analyzing Short Time Series</i>	189
5.5	<i>Assessing the Quality of the Predicted Tidal Current Series</i>	190
5.5.1	Introduction	190
5.5.2	Comparison of Maximum Floods and Ebbs and Slacks In the Predicted Time Series Versus In the Observed Time Series	190
5.5.3	Spectral Analysis of the Residual Time Series	191
5.5.4	Examination of the Residual Time Series For Periods With Transient Tidal Current Oscillations	192
5.5.5	Looking For Changes in Bathymetry or Shoreline	192
5.6	<i>Producing a Reference Station for Table 1 of a Tidal Current Table</i>	193
5.7	<i>Summary Overview: Steps In Harmonically Analyzing Current Data</i>	194
6.	Nonharmonic Analysis of Water Level and Current Data	195
6.1	<i>The Need For Nonharmonic Tidal Analyses</i>	196
6.2	<i>Hydrodynamic Considerations</i>	196
6.3	<i>Monthly Mean Tide Analysis</i>	197
6.3.1	Details of the Analysis	197
6.3.2	The Limitations of the Monthly Mean Tide Analysis	202

6.4 Tide-by-Tide Analysis	202
6.4.1 Details of the Analysis	202
6.4.2 The Benefits and Limitations of the Tide-by-Tide Analysis	202
6.5 Reversing Reduction Analysis for Tidal Currents	205
6.5.1 Details of the Analysis	205
6.5.2 Advantages and Limitations of the Reversing Reduction Analysis	210
6.6 Rotary Reduction Analysis for Tidal Currents	210
6.6.1 The Benefits of Using the Rotary Analysis	210
6.6.2 The Limitations of the Rotary Analysis	212
6.6.3 Details of the Analysis	212
6.6.4 Special Consideration and Choices To Be Made For the Rotary Analysis	215
6.7 Selecting a Reference Station	217
6.8 Putting a Subordinate Station In a Tidal Current Table and On a Tidal Current Chart	218
6.9. Minimizing the Errors Due to the Variations Throughout the Month of Nonharmonically Determined Time and Height Differences	219
6.10 <u>Summary Overview:</u> Steps In Analyzing Water Level or Current Data With a Nonharmonic Comparison Method	220

7. Interpretation of Tidal Analysis Results Based On Hydrodynamics

7.1 Products for showing Tidal Analysis Results	223
7.1.1 Cotidal, Corange, and Co-amplitude Charts	223
7.1.2 Cospeed and Cophase Charts	226
7.1.3 Tidal Current Ellipses	226
7.1.4 Various Types of Graphs	229
7.2 Spatial Variation in Tidal and Tidal Current Parameters In a Waterway Due to Hydrodynamic Processes	229
7.3 The Equations of Motion as the Basis for Tidal Hydrodynamic Models	232
7.3.1 The Equation of Continuity	232
7.3.2 The Momentum Equations	233
7.3.3 Simplifying the Equations of Motion For Idealized Cases	236
7.4 Tidal Variations Along a Very Narrow Waterway	238
7.4.1 Tidal Variations In a Narrow Rectangular Waterway	238
7.4.2 Tidal Variations In a Narrowing Waterway	247
7.5. Tidal Variations Along Wider Waterways – the Effect of Coriolis	251
7.6. Nonlinear Shallow-water Effects on Tides	254
7.6.1 The Nonlinear Terms In the Equations of Motion	254
7.6.2 The Generation of Compound Tides and Overtides	256
7.6.3 The Nonlinear Interaction of the Tide With River Flow	260
7.6.4 The Nonlinear Interaction of the Tide With Low-Frequency Storm Surge	262
7.6.5 A Physical Explanation of the Nonlinear Mechanisms	263
7.6.6 A Real-World Example of Nonlinear Shallow-water Effects Using a Numerical Model	267
7.6.7 The Effect of the Nonlinear Lateral Inertial Terms	273

7.7. Variation of Tidal Currents With Depth	274
7.8. Tidal Dynamics of the Oceans of the World	277
8. The Use of Numerical Hydrodynamic Models For Predicting Tides and Tidal Currents	281
8.1 Introduction	281
8.2 The Workings of a Very Simple Numerical Hydrodynamic Model	281
8.3 Advantages of Using a Numerical Hydrodynamic Model	284
8.4 Disadvantages of Using a Numerical Hydrodynamic Model	287
8.5 Proper Tidal Forcing of a Numerical Hydrodynamic Model	288
8.6 Tidal Validation of a Numerical Hydrodynamic Model	290
8.7 The Operational Use of Numerical Hydrodynamic Models	293
8.7.1 Creation of Tidal Current Charts, Forecast Atlases and Digital Tidal Prediction Products	293
8.7.2 Tide-Based Corrections In Hydrographic Surveys	295
8.7.3 Real-time Based Nowcast/Forecast Model Prediction Systems	296
9. Products for Presenting Tide and Tidal Current Predictions	299
9.1 Introduction	299
9.2 Tide Tables	299
9.2.1 Table 1 – Daily Predictions for References Stations	300
9.2.2 Table 2 – Time and Height Differences for Subordinate Stations	302
9.2.3 Table 8 – Tide Prediction Accuracy	304
9.2.4 Other Tables and Information in the Tide Tables	306
9.2.5 Limitations of Tide Tables	307
9.2.6 The Construction of Tide Tables	308
9.3 Tidal Current Tables	309
9.3.1 Table 1 – Daily Predictions for References Stations	310
9.3.2 Table 2 – Differences and Ratios for Subordinate Stations	310
9.3.3 Table 5 – Rotary Tidal Currents	313
9.3.4 Other Tables and Information In the Tidal Current Tables	313
9.3.5 Current Diagrams	314
9.3.6 Limitations of Tidal Current Tables	316
9.3.7 The Construction of Tidal Current Tables	317
9.4 Tidal Current Charts	318
9.4.1 Description of Tidal Current Charts	318
9.4.2 The Advantages and Limitations of Tidal Current Charts	321
9.4.3 The Construction of the Tidal Current Charts	322
9.5 Tidal Circulation and Water Level Forecast Atlases	323
9.6 Tide and Light Diagrams – a bit of history	326
9.7 Digital Tidal Prediction Products	330
Appendices	333
References	345

List of Figures	359
List of Tables	366
Acknowledgments	367
Index	369

1. Introduction

1.1 Purpose of This Book

The purpose of this book is to provide the reader with the knowledge required to carry out the most accurate tidal analysis and tidal prediction possible using any set of water level or current data that he or she may have available. The book is also intended to provide the reader with tools to interpret the analysis results with respect to the hydrodynamics (the physics of the water movement) of the bay or ocean from which the data were obtained, so that these results can best be used for particular oceanographic applications. Tidal analysis and prediction involves more than simply running a harmonic analysis program to obtain tidal harmonic constants and then putting them in a tidal prediction program. It requires understanding both the astronomical and the hydrodynamic aspects of the tide. Lack of such an understanding can lead to problems when performing a tidal analysis. A few examples of such problems are very briefly mentioned below (they are explained in more detail later in this book, and the technical terms used below are defined in Chapter 2).

It is the astronomy, namely the relative periodic motions of the earth, moon, and sun, that determines the frequencies at which tidal energy is found. The contribution to the tide by the energy at each tidal frequency is usually represented by a *tidal harmonic constituent*, for which there will be an amplitude and a phase lag. The pairs of amplitudes and phase lags are referred to as *harmonic constants*. Which of these tidal constituents can be included in a harmonic analysis depends on the length of the data times series one has available. The longer the time series the more tidal constituents that can be included in the analysis and the more accurate the tidal predictions will be. Attempting to include in the analysis more tidal constituents than can be resolved with the available length of the time series can lead to erroneous results, or even to no results at all because in such cases numerical instability can cause the harmonic analysis program to fail (“blow up”). Even when the appropriate tidal constituents are included in a harmonic analysis, one must remember that the energy of the tidal constituents that could not be included in the harmonic analysis (because they were too close in frequency to other larger tidal constituents) will still affect the constituents that were included in the analysis. As a result one may see errors, namely, differences between the tide predictions and the actual water level data, that slowly oscillate in time due to the missing tidal constituents. Such errors may be significant if one has analyzed only 15 days of data or even 29 days.

It is the hydrodynamics of the ocean and bay that determines how large the tide or tidal current will be at a particular location, as well as the timing of high and low waters, maximum floods and ebbs, and slack waters. In shallow water the hydrodynamics becomes nonlinear, distorting the tide and adding new higher harmonic tidal constituents (*overtides*) and new tidal constituents within the semidiurnal tidal band (*compound tides*), some with the same frequencies as some of the original astronomically caused tidal constituents. Knowing whether an analyzed constituent is a compound

tidal constituent or an astronomical tidal constituent (with the same frequency) can make a difference in the accuracy of the subsequent tide predictions, especially when making predictions for years other than the year whose data was used for the analysis.

Shallow-water hydrodynamics also causes nonlinear interactions between the tide and nontidal phenomena such as river flow and wind-produced changes in water level (storm surges) and currents. For example, high river flow reduces the tide range and distorts the tide curve (modifying the astronomical tidal constituents and adding additional higher harmonic constituents, the *overtides*). And so, if water level data obtained during a time period with high river flow are analyzed and then tide predictions are made using the harmonic constants derived from those data, the predicted high waters will be too small throughout the rest of the year. Likewise data obtained during strong wind events may have tides that are modified by low-frequency storm surge and thus are not representative of the rest of the year.

In most cases water level or current data are only available at a few distinct locations in a bay or along a coast. Often some of these locations have data times series that are not long enough to allow a useful harmonic analysis, so oceanographers developed other ways to extract tidal information from locations with short data time series. For decades this has been done nonharmonically, by simply comparing the high and low waters in water level data from the short stations (usually called *subordinate stations*, or *secondary ports*) with the high and low waters in predictions harmonically derived from longer stations (usually called *reference stations*, or *standard ports*). However, there can be severe limitations on how well this can work, due to the hydrodynamics of the location where the data were obtained.

Although this book provides some “rules of thumb” for carrying out tidal analysis and prediction, the intent is to go well beyond this. This book explains not just the “how” but also the “why”, namely it provides explanations of the astronomical causes of the tide and the hydrodynamic modifications of the tide, so the reader can determine how to maximize the accuracy of the analysis results and predictions. This understanding is also important for interpreting the analysis results.

This book explains and illustrates all state-of-the-art tidal analysis and prediction methods presently in use, as well as the astronomical, hydrodynamic, and statistical theories behind them. This is not intended to be a complete textbook on tides. The emphasis here is on subjects the reader must understand in order to carry out accurate tidal analyses and to make skillful tidal predictions. However, in meeting this objective, the result is a reasonably complete study of the tides (with references for subjects not covered in detail). The book provides practical operational procedures, including considerations related to maximum analysis accuracy and maximum prediction skill.

The book is written at an introductory level, so that the reader should need little background in tidal or oceanographic theory. With an eye toward the teaching aspects of this book, it begins with a general overview of the subject of tides, so that the reader can first see the big picture. Then as the material becomes more detailed, the reader will be able to understand that material within a larger context. Since the astronomical and hydrodynamic aspects of the subject affect each other, it was felt that such an overview should be given first, rather than simply jumping right into detailed astronomical theory followed by detailed hydrodynamic theory. Because of this approach, there may occasionally be some redundancy, as well as frequent references to other sections in the book. Although this book is written at a level accessible to the nonexpert, it is also hoped that tidal experts will still find of interest some of the topics that they may not have dealt with themselves.

1.2 Relationship to Previous Tidal Analysis and Prediction Books and Manuals

The Center for Operational Oceanographic Products and Services (CO-OPS) in NOAA's National Ocean Service (NOS) continues to print and provide tidal analysis and prediction manuals and reports produced in the past (under previous organizational names such as the Coast Survey, the Coast and Geodetic Survey, and the National Ocean Survey). In particular the *Manual of Harmonic Analysis and Prediction of Tides* by Paul Schureman (first published in 1924, revised in 1940, and reprinted with corrections in 1958) and the review/update of that manual, *Computer Applications to Tides in the National Ocean Survey*, by Bernard Zetler (1982) are still useful. The technical report *A User's Guide to a Computer Program for Harmonic Analysis of Data at Tidal Frequencies* by Robert Dennis and Elmo Long (1971) describes the first computer implementation of Schureman's harmonic analysis method, for data time series of length 15 days or 29 days. When Schureman's manual was first printed in 1924 (and for four decades thereafter) harmonic analyses were done by hand using special paper "keys". These keys were a series of paper templates with holes in them, each of which was placed over sheets of paper that had long columns of hourly tidal heights. The numbers showing through the holes were added with mechanical adding machines as part of a very time consuming process. Once the harmonic constants were calculated, tide predictions were then produced using large brass analog tide predicting machines with dozens of pulleys and gears representing the tidal harmonic constituents that came out of the hand analysis (see Figure 1.1).

These past manuals, besides being out of date in numerous respects, are also generally narrow in their scope, concentrating only on the one rendition of the harmonic analysis method developed by Schureman. Schureman's original work (often simply referred to as S.P. 98) is still quite valuable from the standpoint of the elaborate astronomical equations that he worked out, and the (sometimes limited) explanations behind them. The 1982 Zetler review/update of the Schureman manual made a few corrections to Schureman's text (very few actually, considering the extensive astronomical/mathematical work done by Schureman). He also put Schureman's work in the context of important British work done by Arthur Doodson (a contemporary of Schureman's) and by David Cartwright (a contemporary of Zetler, but who was still to contribute a great deal more after 1982). Zetler also updated Schureman's node factor and equilibrium argument tables to the year 2025. None of these manuals provided much insight on the best way to use the harmonic method for producing the most accurate results. Also, there was only some mention of the importance of hydrodynamic effects on tidal analysis and prediction.

Prior to Schureman's manual there were also books or sections of major Coast Survey reports that dealt with tidal analysis and prediction and which in many cases provided the bases for Schureman's work. These included William E. Ferrel's *Tidal Researches* (1874) and Rollin A. Harris's five part *Manual of Tides* (1897-1907). These reports included much original research and analysis, and were not really instructional manuals. Harry A. Marmer's *The Tide* (1926) was not a manual but rather an introduction to the subject, which included an explanation of harmonic analysis and prediction.

For some decades now, the Schureman harmonic method (based on Fourier analysis) has only been used at CO-OPS with data series of 15 and 29 days duration. That computer program (Dennis and Long, 1972) makes use of Schureman's particular method of inference and elimination to infer some additional tidal constants that cannot be calculated from only 15 or 29 days of data. It also corrects the constituents that could be calculated for the effects of those constituents that could not be calculated (see Section 4.2.1). Schureman's method of inference and elimination is based on

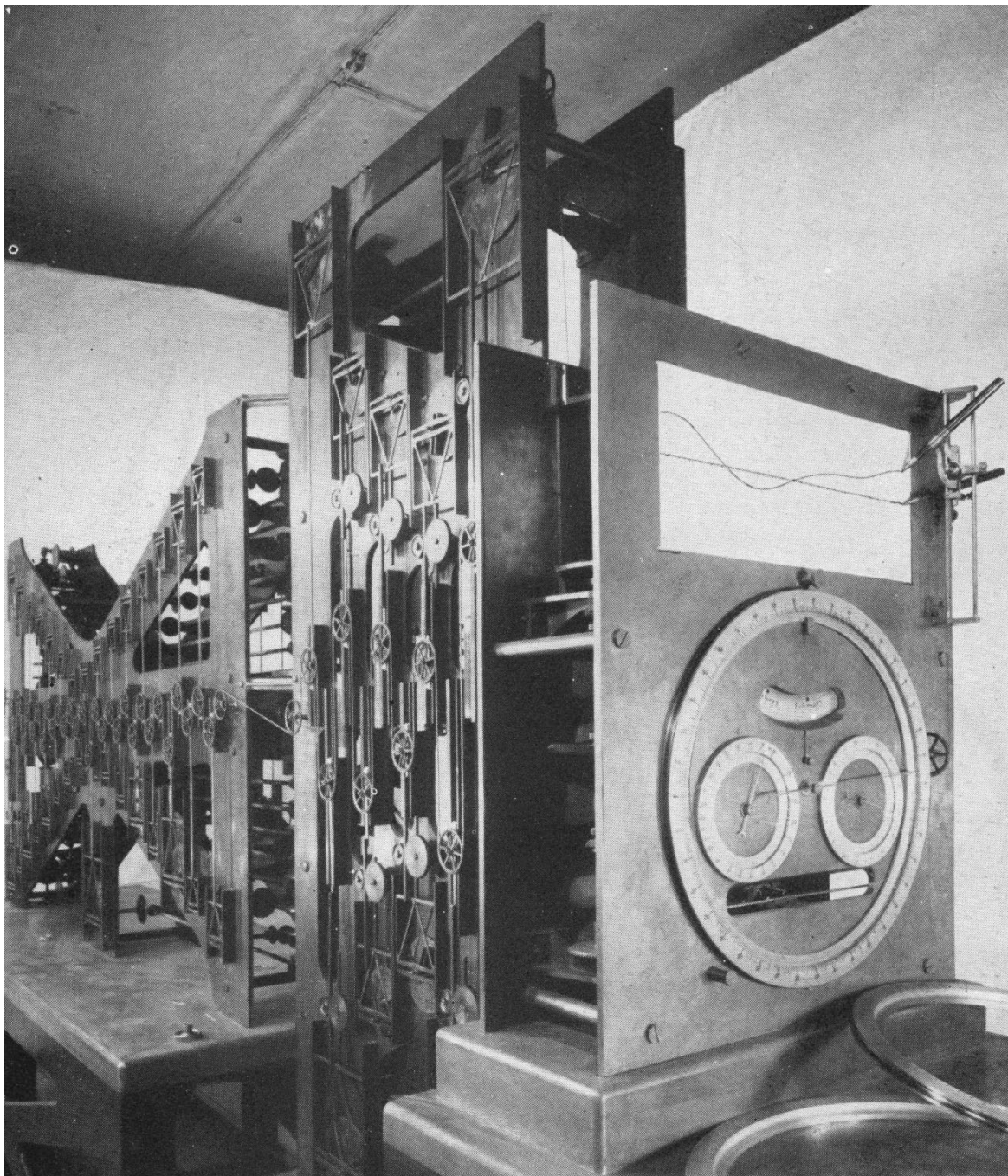


Figure 1.1. The Harris-Fischer tide predicting machine.

astronomical considerations (in the form of the so-called equilibrium theory, see Section 2.1.2), and so does not always work well in the real world, where hydrodynamics has a major influence.

Another program has been the primary method used for tidal analysis at CO-OPS. It was originally written in the 1960's by D. Lee Harris using a least squares harmonic analysis technique (Harris, *et al.*, 1963). Unfortunately there has never been more than an informal in-house manual for that program, although the program listing is provided in the Zetler publication mentioned above. Over the years the Schureman/Dennis&Long program and the Harris program have both been

1. Introduction

modified by the author of this book and by others in CO-OPS (and its predecessor organizations) for use with tidal currents and for additional refinements. Here again the only manuals have been in-house manuals, although they have sometimes been documented in journals and other scientific literature (which are included in References at the end of this book). A recent CO-OPS technical report (Zervas, 1999) serves as an updated operational manual with instructions on how to run specific CO-OPS tidal analysis and prediction computer programs with current data.

Of course, outside of CO-OPS and its predecessor organizations other versions of harmonic analysis have been developed, as well as other types of tidal analysis techniques, of which the *response method* of Munk and Cartwright (1966) is best known. These other methods are also described in this book. Some of the manuals, books, and papers describing these methods are reasonably broad in scope. Probably the classic tidal analysis and prediction manual of all time is the *Admiralty Manual of Tides* by Doodson and Warburg (1941), which includes much of Arthur T. Doodson's important original work in tidal analysis and prediction. A broader coverage of the subject of tides that included much more hydrodynamics was J.J. Dronkers' *Tidal Computations In Rivers and Coastal Waters* (1964), as well as Albert Defant's *Physical Oceanography* (1961; 272 pages of volume II are devoted to tides). The first of Gabriel Godin's two books on tides *The Analysis of Tides* (1972), as the title indicates, concentrated on tidal analysis and prediction and was the basis for the analysis and predictions programs used in Canada written by Mike Foreman (Foreman, 2004). Godin's second book, simply called *Tides* (1988) and published in Mexico, goes well beyond analysis and prediction and includes a great deal of hydrodynamics, including nonlinear effects. A year earlier David T. Pugh published *Tides, Surges, and Mean Sea-Level* (1987), which includes a chapter on analysis and prediction as part of a broader coverage of the tidal and nontidal effects on water level and currents. Pugh's more recent book *Changing Sea Levels* (Pugh, 2004) has four chapters on tides including one on analysis and prediction.

The book *Tidal Hydrodynamics* (Parker, 1991), edited by the author of this book, includes many chapters on analysis and prediction by the world's leading tidal experts at that time, as well as chapters on the hydrodynamic influences on tides. In 1999, David E. Cartwright published *Tides – A Scientific History*, which although a history, provides a great deal of information and insights on tidal analysis and prediction. Just recently published is *Understanding the Tide* by Steacy Hicks (2006), a basic introduction to tides including analysis and prediction. These are all valuable and useful books.

In addition there have been various manuals for specific analysis and prediction computer programs, which primarily provide instructions on how to run those programs, but sometimes also provide additional useful information related to the particular statistical technique and/or tidal theory behind it. A good example are the manuals written by Mike Foreman (Foreman, 2004a, 2004b).

The present book is positioned somewhere between the manuals mentioned above (both inside CO-OPS and outside) and the more theoretical texts, books, and papers also mentioned above. It is like a manual in its "how to" slant, while still providing a good deal of theoretical background, both astronomical and hydrodynamic. That theoretical background, however, is provided in the context of helping the reader carry out better tidal analyses and produce more accurate tidal predictions. Although the emphasis is on harmonic and nonharmonic analyses, this book also includes other methods of tidal analysis and prediction. It includes descriptions of the statistical, astronomical, and hydrodynamic theories on which the analysis and prediction techniques are based, and which must be understood for appropriate interpretation of the results. It includes practical operational step-by-step instructions on how to carry out an analysis and prediction, as well as

specific things to look for in the data and in the hydrodynamic situation that could affect or even compromise the results.

This book does not provide instructions on how to run specific computer analysis and prediction programs, because such programs generally involve data formats and particular parameters that require certain values, and there are technical reports or in-house manuals for that purpose. Knowing how to run a computer program is different than understanding what the program is doing, how to choose the data properly, and how to use the results. This book also does not repeat the elaborate mathematical derivations of the equations dealing with the tide producing forces or the astronomical aspects of the various analysis techniques (found in Schureman, and in papers or reports by Ferrel, Harris, Doodson, Cartwright, and many others), but references are given. This book also may not cover some theoretical aspects of the tides included in some textbooks. The emphasis here is on the knowledge required to carry out the most accurate tidal analysis and tidal prediction possible for a particular set of water level or current data, and to interpret the results.

1.3 The Uses for Tidal Analysis and Prediction

There are various causes of changes in water level and currents, but for most coastal and marine inland waterways the astronomical tide is usually the dominant cause. The tide and tidal current are by far much more predictable than changes in water level and currents caused by changes in the wind (usually the second most dominant cause, except during storms when it dominates the tide), changes in atmospheric pressure, changes in river flow (which can be dominant during spring runoff periods), or changes in density (caused by changes in temperature and salinity). Throughout the centuries, because of the tide's usual dominance and its predictability, changes in water level have often been simply referred to as "the tide" even when other effects were included. Extreme changes in water level that cause flooding during a storm are still often referred to as the *storm tide*, even though the wind component (the *storm surge*) is often larger than the astronomical tide component. For any situation where there has been a need to know the water level, the mariner has typically used a tide prediction, even in place of an actual water level observation. Recently, however, mariners have begun using real-time water level information [from systems such as CO-OPS' Physical Oceanographic Real-Time System (PORTS)] when making on-the-water decisions, although they still rely on tide predictions for planning purposes.

There are a whole host of needs for water level information. The most frequent use was (and probably still is) for navigation. For a deep-draft vessel especially, having sufficient water depth under its keel is critical so that it does not run aground. Many large vessels, such as tankers, cargo ships, and container ships, plan their departure from or arrival at a port to coincide with the time of high water, and thus critically depend on tide predictions. Even in waterways where real-time systems like PORTS are used to provide more accurate information about actual water level values (which includes wind and other effects), it is still the tide prediction that is used for advanced planning. When hurricanes or storms are projected to hit a coast and cause flooding, the height of the tide during its landfall is critical to how much flooding there will be (and to whether the National Weather Service will issue coastal flood warnings). For areas with large tide ranges, there will be less damage if a storm makes landfall near the time of low water. Tide predictions are thus used for emergency management planning. The tide often determines the type of habitats that can exist in specific locations or the degree to which waves can erode beaches or harm a wetland. Since the depth soundings and the shorelines depicted on all nautical charts are referenced to a *tidal datum* (a vertical reference level based on the average high or low tides), tide predictions are also critical

1. Introduction

during the hydrographic and photogrammetric surveys that obtain the data for those charts. Even today as hydrographic/bathymetric and shoreline surveys make use of real-time water level observations and the global positioning system (GPS), tide predictions are still important for planning the surveys.

Often it is information on currents that is needed, and here again for most coastal and marine inland waterways it is the tidal current that is the dominant component, and the component that is far more predictable than the wind-driven component or the gravitational component (caused by salinity differences up an estuary). There are many reasons for wanting to know the currents. Navigation again is one use, since strong currents can greatly affect the maneuvering of a ship (especially when docking), so much so that the prediction of slack water is an important requirement. In some narrow channels where large vessels must pass each other in opposite directions, the right of way is given to the ship moving with the *fair tide* (i.e., to the ship moving with the tidal current) because it has less maneuverability. Tidal current predictions are often used to determine this. Currents are critical for transporting oil spills, flushing pollutants from a harbor or estuary, transporting particular species of marine life, and stirring up and transporting sediments (and attached pollutants). Tidal current predictions are therefore used by responders to oil spills, environmental managers, fishermen, and ecologists, to name just a few.

Today numerical hydrodynamic computer models are used for a whole range of activities from water quality modeling to coastal engineering to harmful algal bloom landfall forecasts. Tide predictions are needed as a primary forcing to run such models, which are used to provide forecasts and to produce scenarios for planning.

Ironically the most accurate tidal predictions are sometimes needed for studies where the tidal signal must be removed from data records, for example, for global sea level studies dealing with seasonal-to-interannual phenomena such as the El Niño Southern Oscillation (ENSO), or for studies of basin-scale circulation using satellite altimetry. It is especially important for removing the tidal aliasing from satellite altimetry data, which not only have large time intervals between data points at a specific geographic location (from 3 to 20 days, depending on the satellite) but can have orbit errors that fall in the tidal frequency bands. In these applications centimeter accuracy is required. For tsunami warning systems, water level station observations during tsunami events are detided using predicted tides so that the signature of a tsunami wave can be more clearly seen in the data record.

1.4 Brief Historical Background

Only a very brief historical background on tidal analysis and prediction is included here. For a much more complete treatment see Cartwright (1999), as well as a much earlier but also interesting work by Harris (1897). Hicks (1967) presents a history dealing specifically with the Coast Survey, which was renamed the Coast and Geodetic Survey (C&GS), of which CO-OPS' predecessor organizational units were a part. Zetler (1987, 1991) extends that history another 20 years, by which time C&GS had become the National Ocean Service (NOS) and was part of NOAA. [Prior to this, NOS was briefly known as the National Ocean Survey, when it was part of the Environmental Science Services Administration (ESSA).]

Tidal prediction is the oldest form of ocean prediction, and is still the most accurate. The two earliest tide tables that have so far been discovered were for the tidal bore in the Tsientang River in China in 1056 and for London Bridge on the Thames River in England in the early 1200's. The long history of tide prediction is a result of the long-recognized correlation between the tide and the

changing position and phases of the moon. That correlation was obvious even to ancient civilizations. Centuries ago mariners invented rule-of-thumb techniques for tide prediction, which were often treated as treasured family secrets and passed on to the next generation. Beginning in the late 1700's fairly sophisticated *nonharmonic* techniques using various lunar characteristics were used to predict the tide. For example, for a particular place, high tide might occur a certain number of hours after the moon was directly overhead, and the highest (spring) tide might occur a certain number of days after full moon or after new moon. In 1752 Daniel Bernoulli produced the first practically reliable tide table in France using luni-tidal intervals (see Section 2.2.5) that took into account the moon's elliptical orbit (see Section 2.2.1). In 1832 John Lubbock produced tide tables in England using a nonharmonic method that also included the effect of lunar declination (see Section 2.2.1).

It was not until 1867 that the much more accurate *harmonic method* was developed by Sir William Thomson (later called Lord Kelvin) (1869, 1881). This was 180 years after Sir Isaac Newton first explained how tides are generated by the gravitational effects of the moon and sun, and 91 years after Pierre Simon Marquis de Laplace first suggested representing the tide as a series of harmonic oscillations. The harmonic method was modified and improved by George Darwin (1883) and Arthur Doodson (1921, 1928) in England. In the U.S., William Ferrel (1874) in the Coast and Geodetic Survey developed harmonic analysis and prediction totally separate from the work of Thomson and Darwin, Ferrel basing his work on the papers of Laplace as had Thomson. This work was further improved and added to by Rollin Harris (1897-1907). About twenty years later, at the same time that Doodson was carrying out his tidal work in Britain, Paul Schureman was also working out the needed astronomical equations and Fourier techniques for harmonic analysis and prediction (Schureman, 1924).

Understanding that all the energy in the tide is found at particular frequencies (mostly in the semidiurnal and diurnal bands) these researchers used a harmonic method to analyze a time series of water level measurements and to determine how much energy is at each of these tidal frequencies, for the specific location of the water level measurements. [Back then such water level measurements were made by hand by noting where the surface of the water was with respect to a long graduated staff permanently mounted on the side of a pier or some other solid structure.] They represented the contribution to the tide of the energy at each tidal frequency using a *tidal harmonic constituent*, for which there was an amplitude and a phase lag (called an *epoch*), which were referred to as *harmonic constants*. The amplitude is the maximum height that a tidal constituent contributes to the tide, and the epoch is the time when this maximum constituent contribution occurs (relative to a reference time, such as the moon's transit over a local time meridian). By combining the amplitudes and epochs of all the tidal constituents, one can predict the tide at any time on any day of any year.

In that pre-computer era Thomson came up with an ingenious way to automate tide predictions using harmonic tidal constituents. He invented a mechanical analog tide predicting machine, a machine made up of dozens of gears and pulleys, with a wire running over all the pulleys and then connected to a pen touching a moving roll of paper. Each tidal constituent was represented by one gear with a pin and yoke arrangement that turned the rotating motion of the gear into an up and down motion, moving a pulley up and down and thus providing that constituent's contribution to the tide curve being drawn by the pen on the moving roll of paper (see Figure 1.2). The machines built to predict the tides were made out of brass and were finely crafted. Thomson's first tide predicting machine was built in London in 1872 by the Légé Engineering Company and summed the contributions of the ten most important tidal constituents. In the U.S., Ferrel was not far behind, designing a 19-constituent machine for the U.S. Coast and Geodetic Survey that was built in

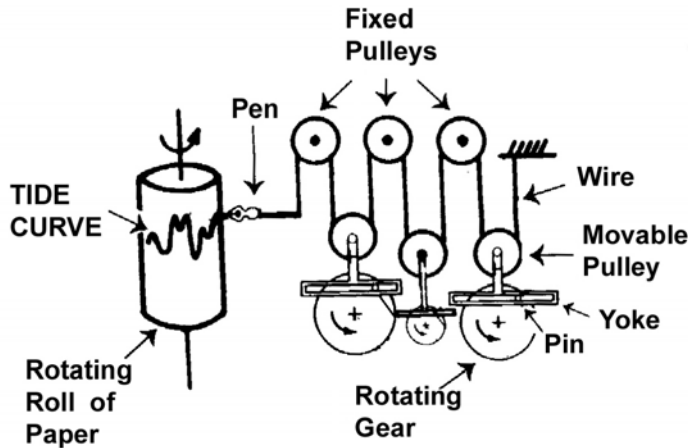


Figure 1.2. Gear and pulley system of an early analog tide predicting machine. Each gear and pulley combination represents one tidal harmonic constituent. The wire running over all the pulleys sums the motions and moves a pen on a moving roll of paper to draw the tide curve.

Washington in 1882 by Fauth & Company. Ferrel's machine directly predicted high and low waters instead of tide elevations. In 1894 in the U.S., Rollin Harris designed a second tide predicting machine, which was completed in 1912 in the workshops of the U.S. Coast and Geodetic Survey. It used 37 tidal constituents and predicted tide elevations or tidal currents (see Figure 1.1).

By the time that World War II broke out in 1939 many maritime nations had one of these huge brass tide predicting machines, and accurate tide predictions for the major ports of the world were commonplace. However, it still required a major manual effort to harmonically analyze water level data in order to calculate the tidal harmonic constants that would be represented by the numerous wheels on one of these machines. The records from the tide gauges used at that time were long analog strip-chart graphs from which hourly heights were scaled off and written onto specially designed forms, along with the times and heights of high and low waters. To perform a harmonic analysis, a series of "keys" or stencils were overlaid. These stencils were sheets of paper with holes revealing only particular observations for use in subsequent summation of a particular constituent onto another form. This manual iterative process could take a week or more to harmonically analyzed a year's worth of data. It takes seconds on a computer today.

The brass tide predicting machines were used by numerous countries until the mid 1960s when computers took over. Today both tidal analyses and tidal predictions are done on high-speed computers, but the statistical techniques used do not differ that much from those earlier methods, although there have been refinements based on modern numerical techniques.

Likewise there have been improvements in obtaining water level data. The tide staff attached to a pier was eventually replaced by a stilling well (to damp out wave action) with a float inside, which was attached to a wire that moved a pen on a moving roll of paper. More recently, acoustic methods have been commonly used, where the height of the water surface relative to some reference point above the surface can be determined by the time it takes sound to reach the water surface and reflect back. Other techniques have also been used such as satellite altimetry, GPS receivers on buoys, laser systems, and radar systems. (More information on water level measurement is found

in Section 4.1.3. Current data measurement methods are briefly discussed in Section 5.3.3.) Modern communication techniques and the Internet have made real-time systems such as PORTS a reality. Most important for data analysis, data from these modern systems are obtained in real time, so that quality control procedures can spot malfunctions that might have led to weeks of bad or missing data in self-recording instruments.

In the U.S. the first published tide predictions appeared in *The American Almanac* in 1830. They were produced by the U.S. Coast Survey, the nation's first scientific agency, established in 1807 by Thomas Jefferson. These predictions consisted merely of high water predictions for Boston, New York, and Charleston, along with time differences for 96 other locations, along with the spring range predictions for 84 locations. (see Hicks, 1967). Low water predictions were not included until 1887. In 1844 tide notes began to appear on nautical charts. Finally in 1867 the first official U.S. Tide Tables were published, produced by the Tide Division of the Coast Survey, the first national government agency to take responsibility for publishing tide predictions (in Great Britain tide tables were produced by private companies; Cartwright, 1999, p.91).

In 1885 tide predictions in the U.S. were produced for the first time using the brass analog tide prediction machine designed by Ferrel. This was the first time the harmonic prediction method was used in the U.S., in this case accounting for 19 tidal constituents. (Prior to 1885, daily predictions had used a nonharmonic method making use of lunital intervals.) In 1887 low waters began to be predicted, and three years after that, tidal currents began to be predicted. In 1912 the Ferrel machine was replaced by the Harris-Fischer tide predicting machine, which used 37 tidal constituents. In 1923 tidal current predictions were published in two volumes separate from the four volumes of tide predictions. In 1966 electronic computers finally replaced the Harris-Fischer analog tide predicting machine in producing the nation's Tide and Tidal Current Tables, using a program written by Harris, Pore, and Cummings (1965). Since that time numerous improvements and additions have been made to tide and tidal current analysis and prediction in the Coast and Geodetic Survey and its later reincarnations (as government agencies were reorganized) leading to the present Center for Operational Oceanographic Products and Services (CO-OPS) in the National Ocean Service (NOS) in the National Oceanic and Atmospheric Administration (NOAA) in the U.S. Department of Commerce (DOC). These improvements and additions are mentioned at appropriate places in the following chapters of this book.

1.5 The Importance of Hydrodynamics

The traditional harmonic tidal prediction methods mentioned in the last section ignore hydrodynamics (that is, the physics of the water movement). They rely only on a knowledge of the astronomically produced tidal frequencies. The forced hydrodynamic system guarantees that tidal energy in a water level data time series (or a current data time series) will appear only at those particular astronomical frequencies. All that is required then to make an accurate tide or tidal current prediction at a particular location is a water level data series (or current data time series) that is long enough so that, when it is harmonically analyzed, the most important of these lunar and solar tidal frequencies can be resolved, and an amplitude and epoch (phase lag) can be determined for each tidal constituent.

As a tide wave propagates in the ocean, onto the continental shelf, and up into bays and estuaries, the hydrodynamics of these bodies of water (e.g., full and partial reflections, continuity effects, inertial effects, and frictional damping, all of which are discussed in this book) affects the tide range and phase lag of the tide, and the amplitude and epoch of each of the tidal constituents.

In shallow waterways the hydrodynamics, through various nonlinear processes, also transfers tidal energy to new tidal frequencies. However, these new frequencies can be determined, and additional *shallow-water tidal constituents* can then simply be included in the harmonic analysis. The details of how these *overtides* (higher harmonics of the astronomical constituents) and *compound tides* (new tidal constituents resulting from the interaction of two or more astronomical constituents) are actually generated have often been ignored. In some cases the mechanisms that produced them were not even fully understood, and the shallow-water constituent frequencies were merely determined by adding or subtracting astronomical frequencies. Not understanding the nonlinear hydrodynamics that generate these constituents can cause problems in tidal prediction accuracy for years other than the one whose data were analyzed. Improvements in tidal prediction have come about as a result of taking hydrodynamics into account.

In recent years numerical hydrodynamic models, which include all the necessary ocean physics, have been used to produce tide and tidal current predictions. These models have the advantage of being able to provide predictions at hundreds and even thousands of locations. This is especially beneficial for tidal currents, which can vary dramatically over short distances. For example, tidal currents near the sea bottom can be very different in speed and direction than those near the water surface. Tidal currents can also be quite different in a channel and in the shallows just a few feet away. Numerical hydrodynamic models can also inherently handle the nonlinear interaction between the tide and nontidal phenomena such as storm surge and river flow. However, such models still depend on having very accurate tide predictions to force the models at their seaward open boundary. While these hydrodynamic models can provide predictions at an almost limitless number of locations they are still rarely as accurate as tide predictions derived from a well-done harmonic analysis at a location with a sufficiently long data time series. However, there will be situations where a model should be able to provide better tidal current predictions than can be obtained from harmonically analyzing current data. The degree of accuracy required, of course, varies considerably with the application for which the predictions are to be used, and for many applications the accuracies from numerical models are more than sufficient.

1.6 *Organization of This Book*

Chapter 2 begins with a general overview of the subject of tides that summarizes in introductory terms both its astronomical and hydrodynamic aspects. This is intended to give the reader the big picture first, so that when the material becomes more detailed, the reader will be able to understand that material within a larger context. Since the astronomical and hydrodynamic aspects of the tide are interrelated, it will be helpful to understand this connection before jumping right into detailed astronomical theory followed by detailed hydrodynamic theory. However, because of this approach, there may occasionally be some redundancy, as well as frequent references to other sections in the book.

This overview (including many basic definitions) is followed by a section providing an introduction to the astronomical aspects of the tide. It describes which frequencies have tidal energy and the specific aspects of the moon's orbit around the Earth and of the Earth's orbit around the sun which are responsible for this energy. This is followed by a section dealing with the hydrodynamic aspects of the tide. It is the hydrodynamics (determined by the dimensions of the ocean, continental shelves, bays, and rivers) that determines how large the tide range will be, how fast the tidal currents will flow, the time of high and low waters (and maximum floods and ebbs and slack waters), and the type of tide (that is, whether it is semidiurnal, diurnal, or somewhere in between). This section

also explains how shallow water (through nonlinear processes) causes the transfer of tidal energy to other frequencies, including higher harmonics of the original astronomical tidal frequencies and the corresponding distortion of the tide and tidal current curve. These same nonlinear processes in shallow water lead to interactions between the tide and various nontidal phenomena such as river flow and storm surge. Finally, Chapter 2 ends with a section devoted to the special aspects of tidal currents not found in the tide.

Chapter 3, before giving an overview of the various methods for tidal analysis and prediction, explains the important effect that the length of the data time series has on the ability to resolve nearby tidal frequencies. The longer the data time series is the more tidal energy that can be accurately represented and the more accurate the tidal predictions will be. This chapter discusses harmonic analysis (using either a Fourier technique or a least squares technique), the response method, and several other frequency domain methods. It also discusses several nonharmonic comparison analysis techniques, which are still important today because of their use in calculating time and height differences for thousands of so-called subordinate stations (or secondary ports) listed in tide tables, those differences being relative to a nearby (harmonically produced) reference station. In addition, Chapter 3 covers tidal filtering (and detiding), spectral analysis, empirical orthogonal function analysis, the importance of calculating consistently defined maxima and minima, and the dominant meteorological energy found in the annual and semiannual tidal constituents S_a and S_{sa} .

Chapter 4 describes in more detail the harmonic analysis of water level data including specific things to look for in the data and in the hydrodynamic situation that could affect or even compromise the results, including the potential effects of nontidal influences. It includes a discussion of methods for analyzing short data time series, for which one could normally not obtain information about all the required tidal frequencies. There is a discussion on assessing the quality of predicted tide series produced with the harmonic constants that come out of the harmonic analysis. The chapter ends with a detailed list of all the steps that should be taken to harmonically analyze water level data.

Chapter 5 is similar to Chapter 4, except that it deals in detail with the harmonic analysis of current data. This chapter covers the same basic topics as the previous chapter, but prefacing this discussion with an explanation of the special problems that one has to deal with in the analysis of currents. It explains the use of tidal currents ellipses, and again ends with a detailed list of all the steps that should be taken to harmonically analyze current data.

Chapter 6 deals in detail with four basic types of nonharmonic comparison analyses, including how to deal with the variations of the time and height differences (or current speed ratios) that occur throughout the month, and which can be quite significant if the subordinate station and reference station are not similar enough in their harmonic makeup. Such variations translate into prediction errors when these time and height differences (or current speed ratios) are used to make predictions at a subordinate station. This chapter also ends with a detailed list of all the steps that should be taken to nonharmonically analyze water level or current data.

Chapter 7 goes back to look again at tidal hydrodynamics, but in more detail than how it was first presented in Chapter 2. The information in Chapter 2 was meant to provide enough hydrodynamic background to allow one to make the best choices when statistically analyzing the tides and tidal currents. Chapter 7 looks at the hydrodynamics more thoroughly in order to help in the interpretation of the results that come out of this statistical tidal analysis, especially the spatial variation of tidal parameters over a waterway. Such insights are gained through the use of simple analytical hydrodynamic models, whose derivation from the equations of motion (which explain the physics of the water movement) is also explained. These simple models allow one to understand

1. Introduction

why the tide range, times of high and low water, tidal current speeds, type of tide, and other features of the tide change spatially in ways that ultimately depend on the length, depth, and width of the waterway. This chapter also explains in more detail the nonlinear effects of shallow water on the tides and tidal currents, and the nonlinear interaction between the tide and nontidal phenomena (such as river flow and storm surge), making use of a nonlinear numerical model and a Fourier decomposition of the equations of motion.

Chapters 3 through 6 describe statistical methods for predicting the tide and tidal current, but Chapter 8 looks at the use of numerical hydrodynamic models for this purpose, and the situations where such models may do a better job than the statistical methods. The chapter discusses both the advantages and disadvantage of using such models. The chapter also explains the importance of and the methods for proper forcing of a numerical model, as well as the importance of and methods for tidal validation of such a model. Chapter 8 ends with a description of three important applications where numerical hydrodynamic models are being used today.

Finally, Chapter 9 discusses in some detail the various products that have been created to present tide and tidal current predictions. This includes, of course, tide tables and tidal current tables. It also includes tidal current charts and the related tidal circulation and water level forecast atlases, as well as the tide and light diagrams used for a special purpose in the past. The chapter ends with a discussion of the advantages of harmonically produced digital tidal prediction products.

Tidal Analysis and Prediction

2. Theory Behind Tidal Analysis and Prediction

2.1 Short Introductory Overview – the Big Picture

Before looking in depth at tidal analysis and prediction, a short overview of the entire subject will be presented. This look at the big picture will allow the reader to put the specific discussions to follow within a larger context – to see where it fits and how it is affected by other aspects of the tide. This overview will begin with some basic tidal terminology to make sure that the reader is clear on the specific meanings of some key terms.

2.1.1 Some Definitions

Tides are the periodic motion of the waters of the sea caused by the changing gravitational effects of the moon and the sun as they change position relative to the rotating Earth (which will be explained in more detail in Section 2.1.2). The tides in the oceans are actually very long waves hundreds or thousands of miles long. Although produced by *astronomical* forces, their behavior in the oceans and connected bays (and the size of the resulting water level oscillations) is determined by *hydrodynamics*, that is, by the physics of the water movement. To fully understand and predict the tides one must understand both its astronomical forcing and the hydrodynamics of the oceans, bays, and rivers.

The vertical rise and fall of the water surface is usually referred to as the *tide*, while the accompanying horizontal movement is referred to as the *tidal current* (or as the *tidal stream* in some countries). In its simplest form (such as at the coast of an island in the open ocean) the plot of changing tidal height looks like a sine wave, with the maximum height reached by the water surface called *high water*, while the minimum height is called *low water* (see Figure 2.1.). In this figure the sine curve oscillates above and below *mean sea level* (MSL). The difference in height between high water and low water is the *tide range*. The *period* of this tidal oscillation is the time from one high water to the next high water (or likewise, from one low water to the next low water) and is typically 12.42 hours for most waterways of the world, but can be 24.84 for some areas. The *tidal frequency* is the inverse of the tidal period, and so is one complete tidal cycle in 12.42 hours, or 1.932 cycles per day (cpd) [this referring to a *solar day*], or 2.0 cycles per lunar day [a lunar day being 24.84 hours long, as will be seen in Section 2.2.1]. Classically, in tidal science, frequency has been called the *angular speed*. The angular speed is expressed in degrees per hour ($^{\circ}/\text{hour}$), where 360° is equal to one complete tidal constituent cycle. One can obtain the frequency in cycles per hour (cph) by dividing its angular speed by 360° (to make it cpd, multiply by 24). The primary tidal frequency of 1.932 cpd is equivalent to an angular speed of $28.9841^{\circ}/\text{hour}$. However, tidal energy occurs at many

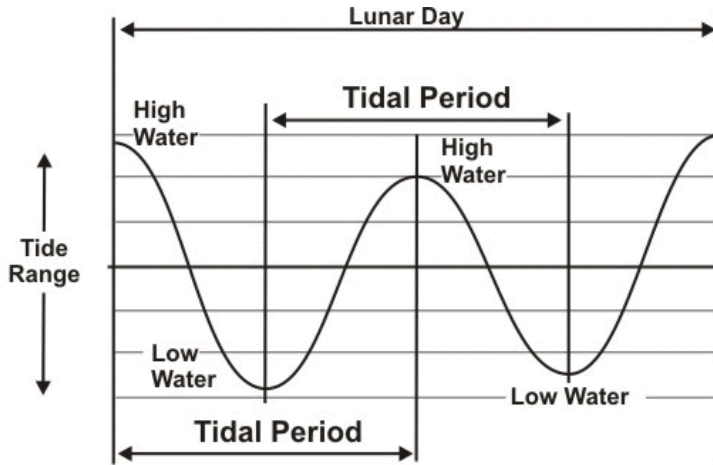


Figure 2.1. A simple tide curve with some definitions of terms. (A lunar day is approximately 24.84 hours, or two tidal periods.)

frequencies, with each frequency being related to some aspect of the relative movements of the Earth, moon and sun, due to the moon-Earth orbit, the orbit of the Earth around the sun, and the rotation of the Earth on its axis.

The tide range varies from day to day throughout the month (see Figure 2.2). The most obvious change correlates with the phases of the moon. Near the times of new moon or full moon the tides have a larger range and are called *spring tides*. Near times of first quarter and third quarter the tides have smaller ranges and are called *neap tides*. Springs tides occur when the Earth, moon, and sun are all lined up, so that the tidal bulges caused by the moon and by the sun add to each other (see Section 2.1.2). Neap tides occur when the moon and the sun work against each other.

There are other variations in tide range throughout the month which will be described in Section 2.2.1, such as due to the changing distance between the moon and Earth, or due to the changing angle of the plane of the moon-Earth orbit relative to the Earth's equatorial plane. From month to month throughout the year there is also some variation in tide range on a smaller scale, due to the changing angle of the plane of the Earth's orbit around the sun relative to the Earth's equatorial plane, or due to certain of the monthly variations coming into and going out of sync. There are also variations from year to year throughout the 18.6-year lunar nodal cycle which are smaller, on the order of 5 to 10% of the average tidal range. The reasons for this variation will be discussed in Section 2.2.1 and 2.2.4. Times of high water or low water are usually given relative to the moon's transit over a particular location or over a time meridian (time zone), which can be local or the zero time meridian at Greenwich, UK (referred to as Greenwich meridian Time, GMT, or Universal time, UT).

The tidal current flow into a bay is called the *flood current* and the tidal flow out of a bay is called the *ebb current*. If the bay or channel is very narrow, a plot of changing tidal current looks like a tide curve except the sine curve is above and below a zero speed line, which serves the same reference function as a datum does for the tide (see Figure 2.3). This *reversing tidal current*, like the tide, is a one-dimensional scalar quantity. In one tidal cycle, the current goes from its maximum positive value, *maximum flood*, through the zero current speed (called *slack water*) to the maximum negative value, *maximum ebb*, and back again through slack water to maximum flood. The slacks are usually referred to as slack before flood (SBF) and slack before ebb (SBE). [Alternative names for the above, include *flood strength*, *ebb strength*, *slack flood begins* (SFB), and *slack ebb begins* (SEB).]

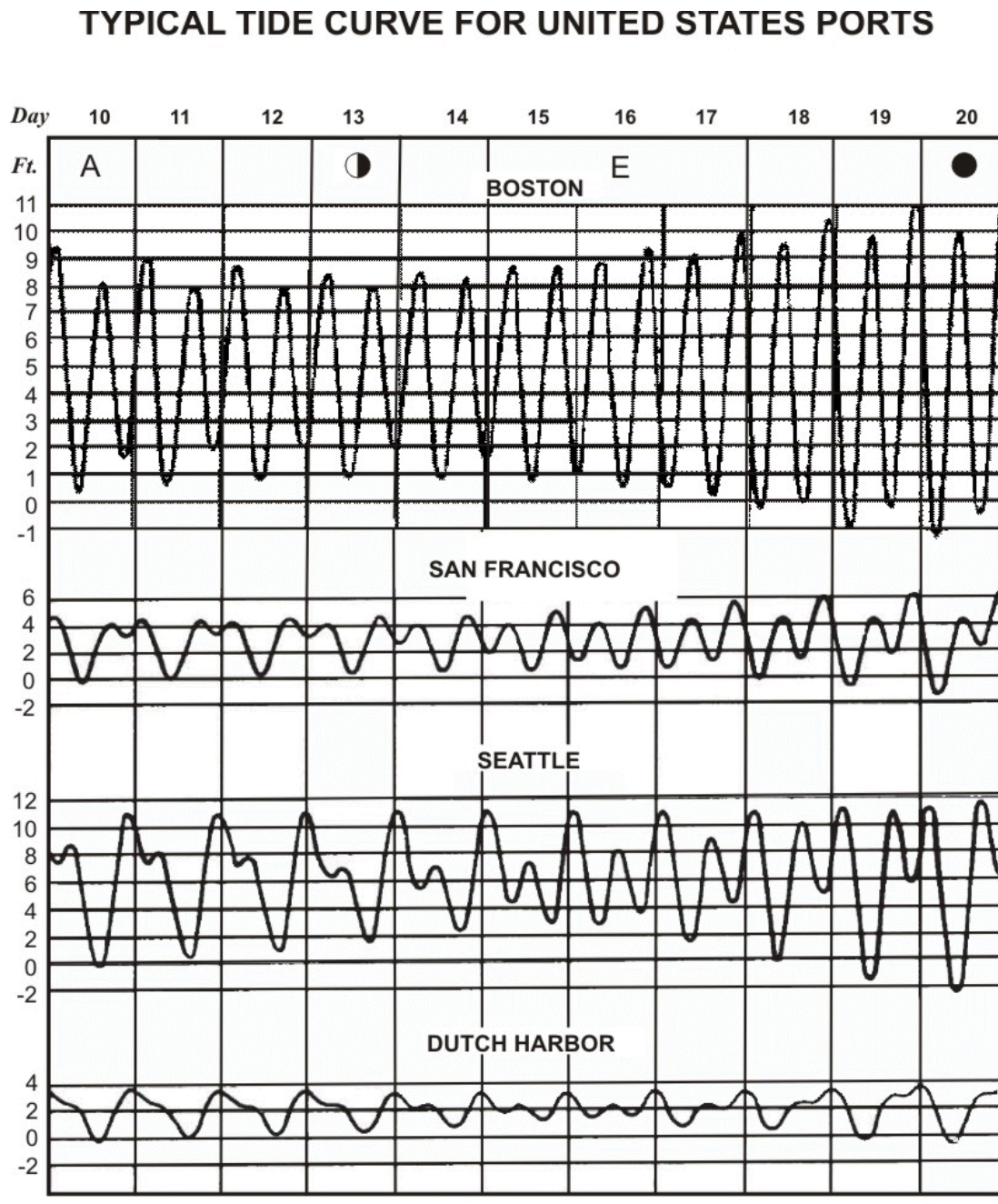


Figure 2.2. Four tide curves showing how the tide range varies through the month. These curves also illustrate different *types of tides*: a semidiurnal tide at Boston; a mixed tide at both San Francisco and Seattle; and a diurnal tide at Dutch Harbor.

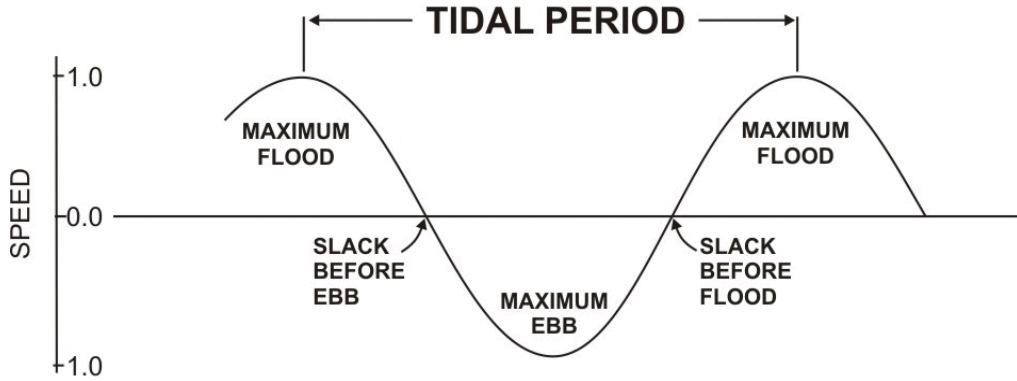


Figure 2.3. A simple tidal current curve with definitions for a reversing tidal current.

However, for wider waterways, and especially in the open ocean, the tidal current is a two-dimensional vector property. For this *rotary tidal current* the direction of flow rotates around the compass, the tip of the current vector tracing out an ellipse (or a circle in the open ocean). (See Figure 2.4) This rotation is due to both the Earth's rotation and certain geographic conditions.

In most waterways of the Earth, the rise and fall (and the flood and ebb) of the tide occur twice a day, in which case the tide is referred to as a *semidiurnal* tide. In most locations, for at least half

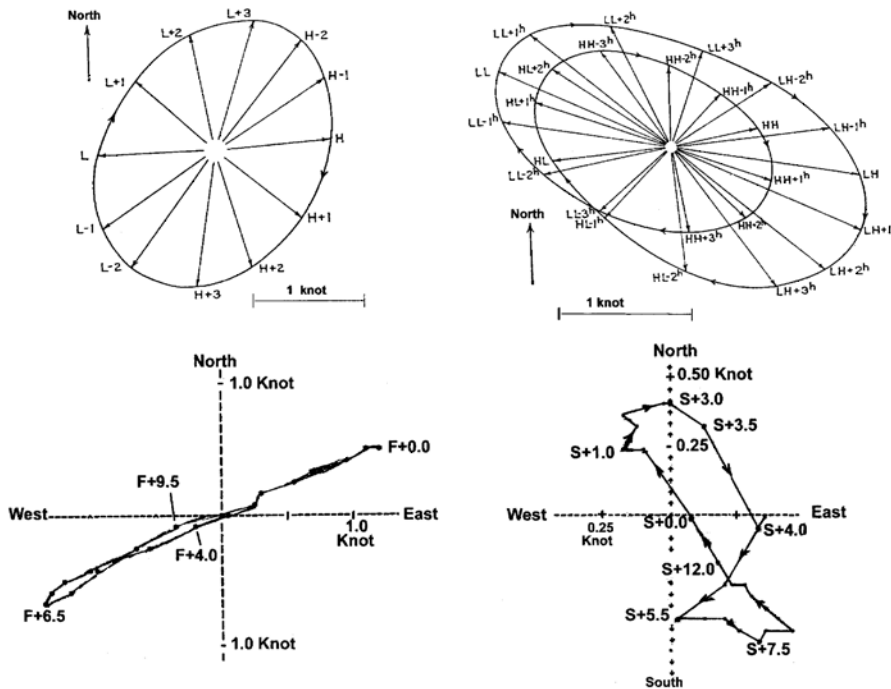


Figure 2.4. Examples of three rotary tidal currents and one reversing tidal current. The first two are off an ocean coast and are idealized. The last two are within a bay and are from actual data. In each example, each vector shows the speed and direction of flow for that hour of the tidal cycle, but for the last two examples only the tips of the vectors are shown (and connected).

2. Theory Behind Tidal Analysis and Prediction

of every month, the two high waters on a given day are not exactly the same in height, nor are the two low waters. The higher of each pair of high waters is referred to as *higher high water* (HHW) and the lower as *lower high water* (LHW), and likewise for each pair of low waters, i.e., *higher low water* (HLW) and *lower low water* (LLW). The height difference between two successive high waters (that is between HHW and LHW) is called the *high water diurnal inequality* and the height difference between two successive low waters (HLW and LLW) is called the *low water diurnal inequality*.

When the diurnal inequality of two high waters (or of two low waters) is significant, then the tide is usually referred to as a *mixed* tide. But even for a mixed tide the diurnal inequality can disappear twice a month when the moon is over the equator (equatorial declination). In some waterways the height difference between the two successive high waters or the two successive low waters becomes so extreme that in reality there is only one high water per day and one low water per day, in which case the tide is referred to as a *diurnal* tide.

When one refers to the *type of tide*, that means the tide is either semidiurnal, mixed, or diurnal. (See Figure 2.2). However, one needs to be careful and very specific how one uses *type of tide*, for it can be confusing. One should specify whether one is talking about the tide on a particular day at a station, or whether one is classifying the station itself. For example, a station might be classified as being *mixed*, but on a few days of the year the tide on a particular day at that station might be *diurnal*. This will be discussed more in Section 2.2.5 and will include the use of harmonic tidal constituents in trying to develop criteria for classifying stations with regard to the type of tide. The *type of tidal current* may also be semidiurnal, mixed, or diurnal, but in many locations the type of tidal current will be quite different than the type of tide because of the hydrodynamics (as will be seen in Section 2.3.1).

The tide is not the only phenomenon in the ocean that produces variations in water level and currents. Such variations can also be caused by changes in wind speed and direction, changes in atmospheric pressure, changes in river discharge, and changes in water density (due to changes in salinity and temperature). But these nontidal changes are not periodic like the astronomical tide and are not nearly as predictable, since they are associated with changing weather (or, on slower time scales, with changing climate). There are cases where there can be short-lived periodic currents due to meteorological effects such as land breeze-sea breeze and inertial currents, both discussed in Section 2.3.6. One will also see annual variations in water level and currents due to seasonal effects on temperature and winds, which vary from year to year, as discussed in Section 3.7. Nontidal water level changes caused by changes in the wind and barometric pressure are usually referred to as *storm surges* (even when the wind speeds are below what might be considered storm level). The term *sea level* is generally used for longer-period slower changes in water level. *Mean sea level* is the average of water level measurements over some time period (such as a day, a month, or a year), which averages out shorter-term oscillations like the tide.

The tide dominates our thinking about changes in water level, not only because it usually causes the largest water level changes (except during storms), but also because it is very predictable (especially in comparison to how well the weather can be predicted). After analyzing only a month's worth of water level measurements from a water level gauge the tide can be predicted quite accurately (for that location) for years into the future. This high predictability is due to the tide's periodic nature and our very precise knowledge of its astronomical forcing. The Earth-moon orbit, the revolution of the Earth around the sun, and the rotation of the Earth on its axis involve periodic motions with fixed and precisely known time periods. Tidal energy is found at the frequencies determined by these astronomical motions.

While it is the astronomical forcing of the tide that is the basis for the tide's predictability, it is the hydrodynamics of the tide that is responsible for the size of the tide range, the timing of high and low waters, and the type of tide, as well as the speed and timing of the tidal current. It is the length, width, and depth of the bay or river (and of any adjoining waterways) that control the hydrodynamics. Because of the hydrodynamics, tide ranges, times/phase lags of high and low tides, the tide regime, and the relationship between the tide and tidal current vary with horizontal (geographic) distance throughout a waterway, especially in shallower water. The variation in tide range over a waterway is usually depicted on *corange charts* and the variation in the phase lag of high water is likewise depicted on *cotidal charts*. [See Figures 2.5 and 2.6.] As will be seen later in this chapter and later in the book, such charts are useful in understanding the hydrodynamics of the tide in a particular waterway.

In addition, it is because of hydrodynamics that tidal currents often vary significantly with depth and with horizontal distance. In shallow waterways the hydrodynamics also transfers tidal energy to new frequencies, and distorts the shape of the tide curve away from a perfect sine curve. These

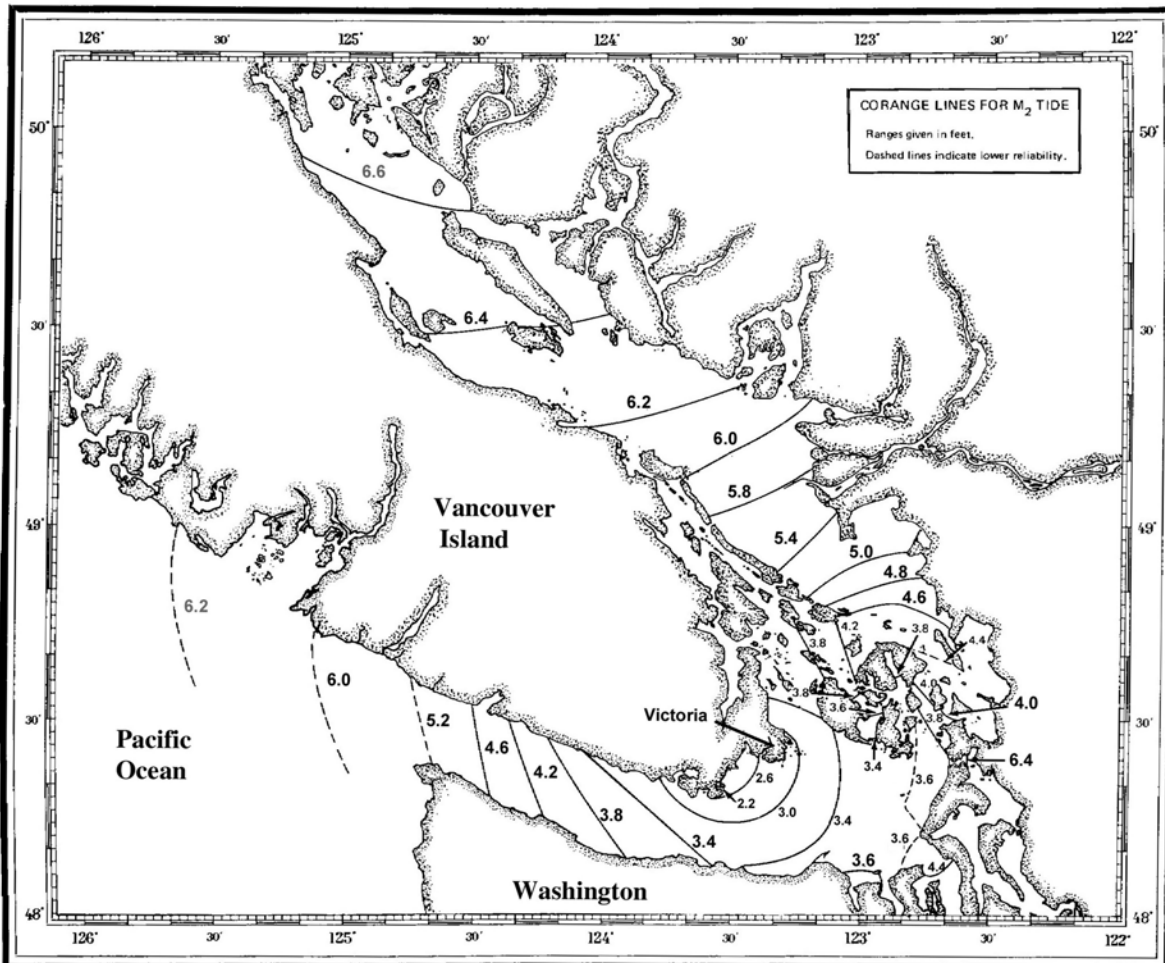


Figure 2.5. A corange chart showing the geographic variation of the tide range of the largest tidal constituent M_2 (defined in Section 2.2.2) for the Strait of Juan de Fuca - Strait of Georgia, located between the U.S. and Canada (from Parker, 1977).

2. Theory Behind Tidal Analysis and Prediction

same shallow-water processes also lead to interactions between the tide and nontidal phenomena such as storm surge and river discharge that can temporarily modify the tide for some period of time.

The largest tide ranges occur in shallow coastal waters, in particular, at the ends of certain bays or along coasts with very wide continental shelves. (Why shallow water increases the tidal range will be described in Section 2.3.1.) The increase in tide range and tidal current speeds that one sees in the shallow waters of bays, rivers and straits can go to dramatic extremes if the circumstances are right. Tide ranges greater than 50 feet (15 meters) can occur in Minas Basin in the Bay of Fundy and at the southern end of Ungava Bay, both in Canada. Tidal ranges greater than 40 feet (12 m) occur at locations such as the northern end of Cook Inlet near Anchorage, Alaska, in the Magellan Strait in Chile, in the Gulf of Cambay in India, along the Gulf of St. Malo portion of the French coast bordering the English Channel, in the Severn River in England, and along the open coast of southern Argentina. Tidal current speeds greater than 15 knots (7.7 m/sec) occur in the Saltstraumen Strait (on the western coast of Norway) and in Seymour Narrows (between Vancouver Island and

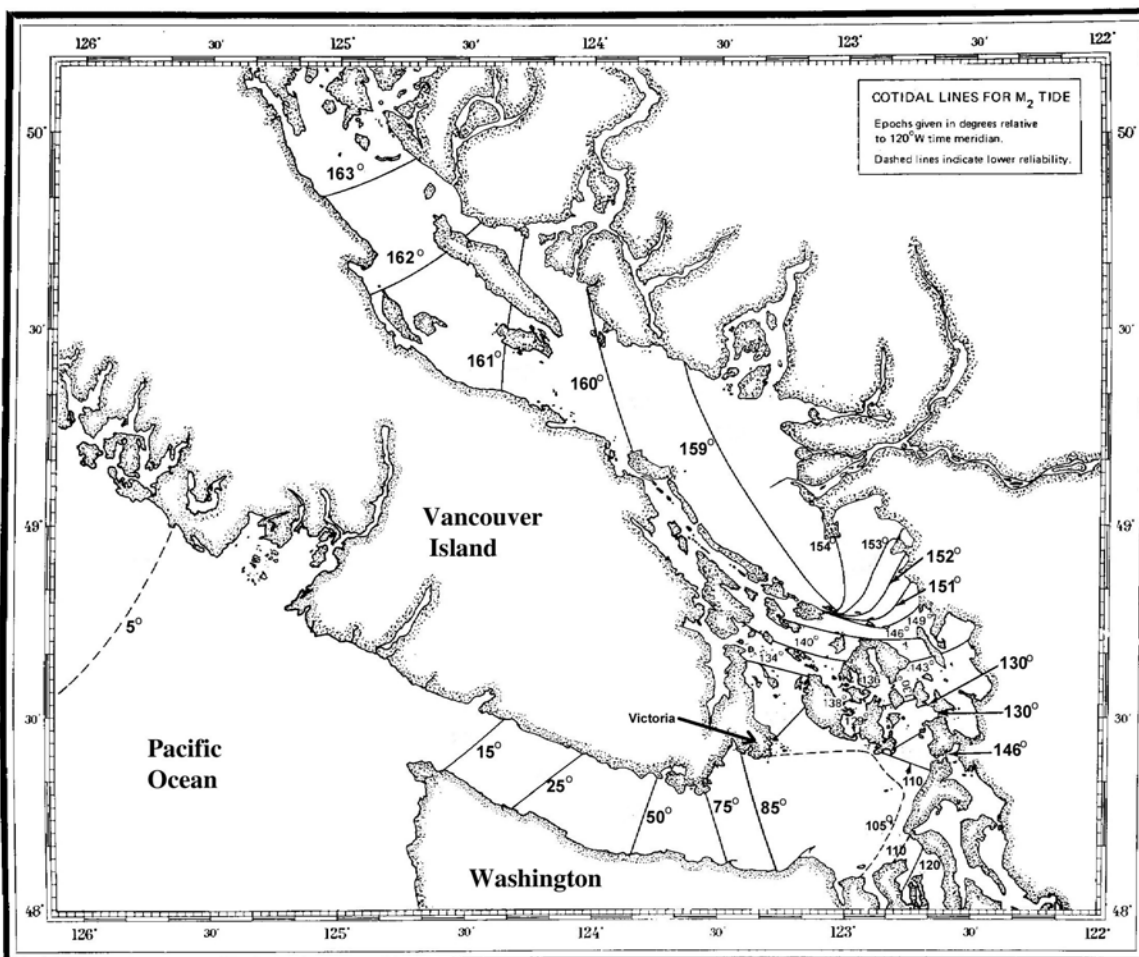


Figure 2.6. A cotidal chart showing the geographic variation of the time (phase) of high water for the largest tidal constituent M_2 for the Strait of Juan de Fuca - Strait of Georgia. The time (phase) of high water is expressed in degrees of an M_2 cycle; dividing by 360° and multiplying by 12.42 hours converts this to hours. It takes 5.2 hours (150°) for high water to progress from the entrance to the head of the waterway. (from Parker, 1977).

the mainland of British Columbia, Canada). Tidal currents of 10 knots (5.1 m/sec) are found in South Inian Pass in Southeast Alaska and in Kanmon Strait, Japan.

When measuring the water level with a *water level gauge* (still referred to by many as a *tide gauge*, because of the usual dominance of the tide) there must be a reference level for the measurement of height of the water surface. This reference level is called a *vertical datum*. Vertical datums have traditionally come in two categories: those based on tidally derived surfaces of high or low water, called *tidal datums*, and those based on the gravity field of the Earth, called *orthometric datums*. More recently a third category has become very important, the so-called 3D or *ellipsoid* datums realized through space-based systems such as the Global Positioning System (GPS).

A *tidal datum* at a particular location is generally defined as an average height of a particular stage of the tide. To minimize all significant tidal variations (daily, monthly and yearly), a tidal datum such as mean high water (MHW) is defined as the average of all the high water elevations over a 19-year National Tidal Datum Epoch period (for example, 1983-2001). Nineteen years is selected because it averages out the variations in the tide due to the 18.6-year lunar nodal cycle (explained in Section 2.2.4). Such a long time period also averages out most meteorological effects on water level, which could bias a tidal datum computed from a shorter length data time series. Even after averaging over a 19-year period there are some climatic variations that may not be eliminated, and with the slow rise in mean sea level (due to land subsidence and/or global warming) the National Tidal Datum Epoch is often updated after a number of years. Slow vertical land movement also shows up as a slow change in mean sea level. The sea level change seen in a water level record is actually a *relative sea level change* (i.e., relative to land). It can be made an *absolute sea level change* only by subtracting out any land movement (such as glacial rebound, subsidence due to sediment compaction, or tectonic movement). Upward land movement from glacial rebound, for example, produces a lowering in mean sea level, while sinking of the land due to sediment compaction produces a rise in mean sea level (which is sometimes confused with the rise due to global warming).

Just as the tide regime varies with horizontal (geographic) distance, so do tidal datum elevations, especially in shallower waters. They usually vary more rapidly in the horizontal direction than do orthometric or 3D/ellipsoid vertical datums.

Tidal datums provide the vertical reference for bathymetry and shoreline on NOAA's nautical charts. There are many tidal datums (e.g., mean lower low water, mean low water, mean sea level, mean tide level, mean high water, mean higher high water, etc.), but in the U.S. two of these are most important – mean lower low water and mean high water. *Chart datum* on a nautical chart in the United States is defined as the mean lower low water (MLLW) at each location, which is the average of all the lower low waters over some time period, usually 19 years. Depth soundings on a nautical chart are the depths below the chart datum, and the predicted tidal heights found in Tide Tables are the heights above the chart datum. Adding the two together gives the total water depth at that moment in time. The legal shoreline in the U.S. is the shoreline depicted on NOAA's nautical charts, which is the mean high water (MHW) shoreline. More specifically, *each point on a MHW shoreline represents the horizontal position of the land-water interface at the time when the water level at that point is at a height equal to the MHW elevation value at that point* (Parker, 2003). Bridge clearances are also referenced to MHW.

These tidal datums also provide the legal definition of *marine boundaries* (see Figure 2.7). MLLW, for example, is the dividing line between Federal territorial seas and State submerged lands, and MHW is the dividing line between many State tidelands and private uplands. All tidal datums

2. Theory Behind Tidal Analysis and Prediction

at a water level gauge are referenced to the land through geodetic leveling to a number of *benchmarks*, which are brass markers driven into solid rock or other permanent structures. Tidal datums can change over decades if the land subsides (or rises due to glacial rebound) or if relative sea level rises due to effects such as global warming.

In some other countries the *lowest astronomical tide* (LAT) is used as chart datum. LAT is defined as the lowest level which can be predicted to occur under average meteorological conditions and under any astronomical condition (Pugh, 1987). There seems to be no generally accepted method to determine LAT, although one commonly used technique is to select the lowest tide from many years of astronomical tide predictions (often 19 years). Another method is to make predictions for known astronomical extremes. LAT appears to have come into favor mainly because it eliminates negative predicted low water values that occur occasionally in tide tables when MLLW (or MLW) is used as the chart datum. LAT has been agreed to by members of the International Hydrographic Organization for use on international charts and as a target chart datum for all countries. Although the U.S. chart datum is MLLW, CO-OPS also calculates LAT and HAT (highest astronomical tide) for reference stations in the U.S. Tide Tables based on 19 years of tide predictions (usually for the National Tidal Datum Epoch, which is presently 1983-2001).

In addition to tidal datums, there are two important geodetic vertical reference systems – *orthometric* datums and *3D/ellipsoid* datums. It is important to know the relationship among all three types of datums for modern application to surveying and mapping. Orthometric heights are determined by geodetic leveling (surveying) relative to the *geoid*. The geoid is defined by a specific gravitational equipotential surface which best fits (in the least squares sense) theoretical global mean

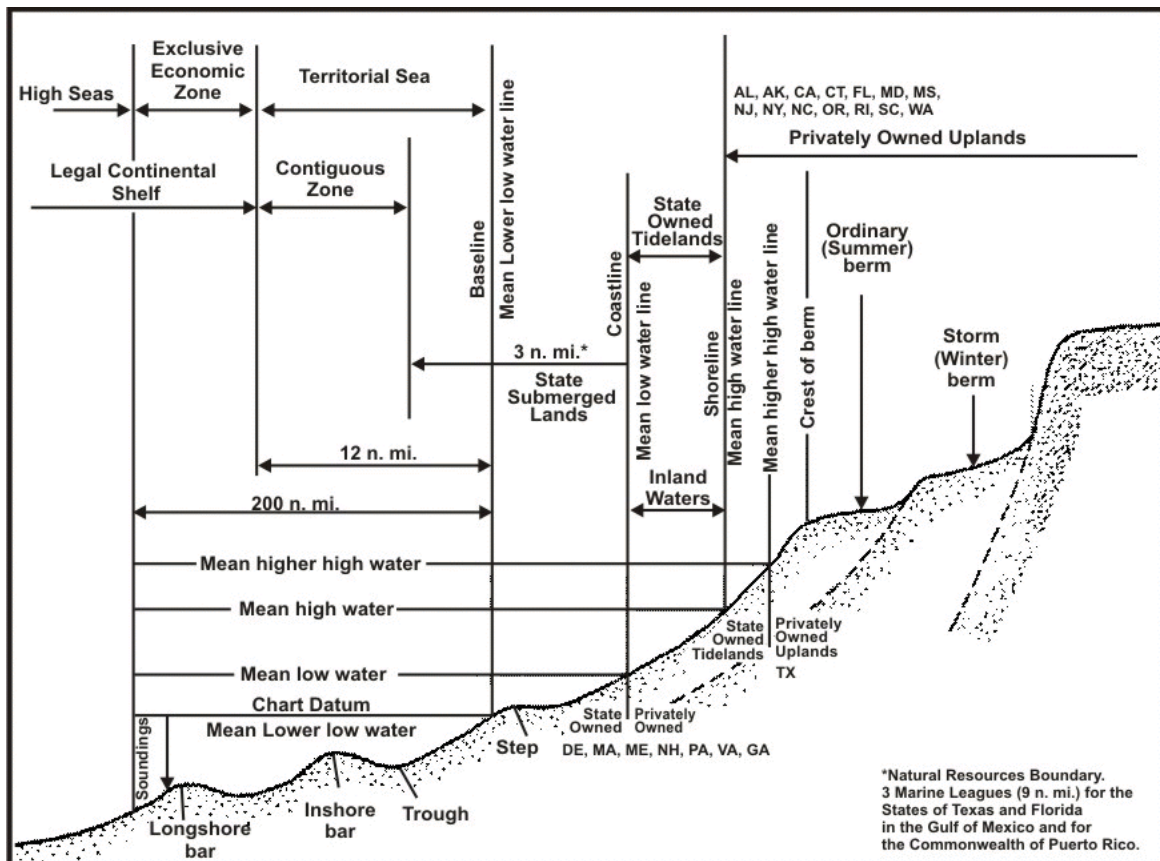


Figure 2.7. Various tidal datums and their relationship to U.S. marine boundaries.

sea level. The current orthometric vertical control system is the North American Vertical Datum (NAVD88), which was established by NOS's National Geodetic Survey (NGS) in 1991. NAVD88 is based on North American-wide adjustment of leveling observations holding fixed the elevation of mean sea level at one water level station on the east coast of Canada. This replaced the older National Geodetic Vertical Datum of 1929 (NGVD29), whose leveling adjustments were originally adjusted to the local mean sea level elevations determined in 1929 at several water level stations on the east and west coasts. Due to sea level change, crustal motion, subsidence and uplift, the loss of bench mark networks and unwieldy adjustments, NGVD29 became severely outdated and cumbersome to use. NGVD29 has often been used incorrectly as equivalent to present day local mean sea level, mainly because it was the vertical reference datum used on topographic maps (e.g., from the U.S. Geological Survey). NAVD88 should also not be used as equivalent to local mean sea level. All GPS positioning data are referenced to one of many 3D/ellipsoid datums, which are based on a geometric model, i.e., the ellipsoid. The ellipsoid is a two-parameter mathematically modeled smooth theoretical surface that approximates the Earth's surface without the topography, i.e., it does not take into account irregularities such as mountains and ocean trenches that the geoid attempts to model. Two frequently used ellipsoid datums, the North American Datum of 1983 (NAD 83) and the World Geodetic System of 1984 (WGS 84) differ by as much as two meters. GEOID03, a geoid model developed by the National Geodetic Survey (NGS) in NOS in NOAA, specifically relates NAD 83 ellipsoid heights to NAVD 88 orthometric heights. *VDatum*, a vertical datum transformation tool developed in NOS (Parker *et al*, 2003), allows the transformation of elevation data between any two vertical datums among a choice of 30 vertical datums, including tidal datums, orthometric datums, and 3D ellipsoid datums. Use of tide prediction models in producing *VDatum* will be described in Section 8.7.2.

In this section only some of the most basic terms have been covered. Others will be introduced throughout the book. In Section 2.2.5 some of the definitions given above will revisited from the perspective of their relationship to harmonic tidal constituents.

2.1.2 The Generation of Tides

The tides are caused by both the moon and the sun. Although the sun is about 27 million times more massive than the moon, its effect is smaller than that of the moon since the sun is 93 million miles away. This is because the influence of a celestial body (the moon or the sun) on the tides of the Earth is directly proportional to the mass of that celestial body but inversely proportional to the cube of its distance from the Earth (for derivation of the formula with this relation, see Dean, 1966; Defant, 1961, Pugh, 1987, Godin, 1988, or Forrester, 1988).

Although the moon appears to orbit around the Earth, the Earth and moon both actually revolve around a common point, which, because the Earth is 82 times more massive than the moon, is inside the Earth, but not at the Earth's center (see Figure 2.8). At the center of the Earth there is a balance between gravitational attraction (trying to pull the Earth and moon together) and centrifugal force (trying to push the Earth and moon apart as they revolve around that common point). At a location on the Earth's surface closest to the moon, the gravitational attraction of the moon is greater than the centrifugal force of the Earth (moving around the center of the revolving Earth-moon system). On the opposite side of the Earth, facing away from the moon, the centrifugal force is greater than the moon's gravitational attraction. In a hypothetical ocean covering the whole Earth with no continents (see Figure 2.8) there will be *two* tidal bulges resulting from these imbalances of gravitational and centrifugal forces, one facing the moon (where the gravitational force is greater

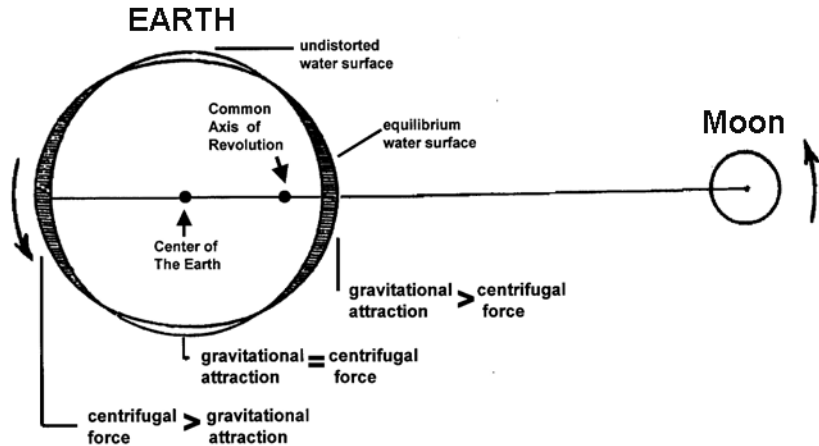


Figure 2.8. The Earth-Moon system (viewed from very high above the North Pole) revolving around a common point. A hypothetical ocean is shown covering the entire Earth (with no continents) with two tidal bulges resulting from the imbalances of gravitational and centrifugal forces.

than the centrifugal force) and one facing away from the moon (where the centrifugal force is greater than the gravitational force).

However, the *tide-producing forces* that result from the difference between the moon's gravitational attraction and the centrifugal force of the Earth's revolution around the center of the Earth-moon system are actually quite small – much smaller than the Earth's own gravitational force. Thus, at the equator on the side of the Earth facing the moon, the tide producing force (which at the equator is vertically upward from the Earth toward the moon) is so small compared to the Earth's gravitational force that it could not cause the tidal bulge. Further north or south of the equator,

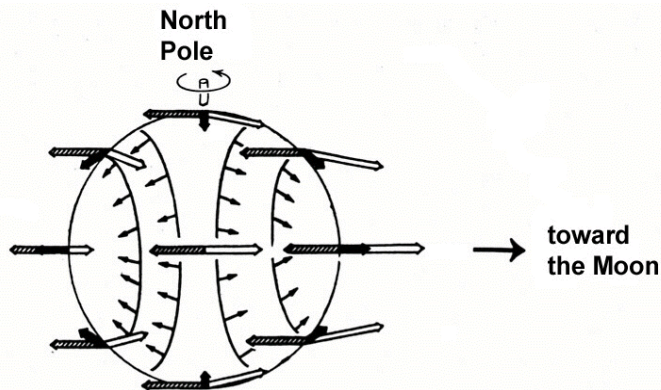


Figure 2.9. The tide generating forces (the thick black arrows) on the Earth resulting from the difference between gravitation attraction (the open arrows) and centrifugal force (the hatched arrows). The small thin arrows are the horizontal components of the tide generating forces, which tend to move the water into the two bulges.

however, at another point on the Earth that is not directly under the moon, the small tide producing force is still pointing toward the moon, but is no longer perfectly vertical relative to the Earth (see Figure 2.9). At this point, the force toward the moon can be separated in a vertical component and a horizontal component, the latter one being tangential to the Earth's surface. This horizontal component of the tide-producing force, though small, has nothing opposing it, and so it can move the water in the ocean. One can see from Figure 2.9 that all the horizontal components tend to move the water toward the equator, causing a bulge centered around the point that is directly under the moon. Similarly, on the other side of the Earth another bulge results.

One can envision the Earth rotating under these two bulges in this hypothetical ocean that covers the entire Earth. In one complete rotation in one day there will be two high tides (when under a bulge) and two low tides (when halfway between bulges), and thus one tidal cycle would be completed in approximately half a day (actually 12.42 hours, for reasons to be explained below). However, this is an extreme simplification (called the *equilibrium tide*) used merely to show how the tide generating forces change as the Earth rotates. Not only are the continents left out (which affect the tides via hydrodynamics), but the equilibrium tide assumes that the oceans respond instantly to the tide-generating forces, which they do not. However, as will be seen later (e.g., in Section 4.2.1), the idea of a simplified equilibrium tide has sometimes been made use of in tidal analysis and prediction.

Now continents are added and only one of the oceans is looked at with a bay connected to it (see Figure 2.10). The tide-generating forces are too small to cause a tide directly in a small body of water like a bay. Only in a large ocean are the cumulative effects of the tide-generating forces throughout the ocean large enough to produce a tide. What is actually generated is a very long wave with a small amplitude (i.e., a small tide range, the range equaling twice the amplitude), on the order of a foot or less. However, when this long wave reaches the reduced depths of the continental shelf, there is a partial reflection of the wave, and the part of the wave that continues toward the coast is

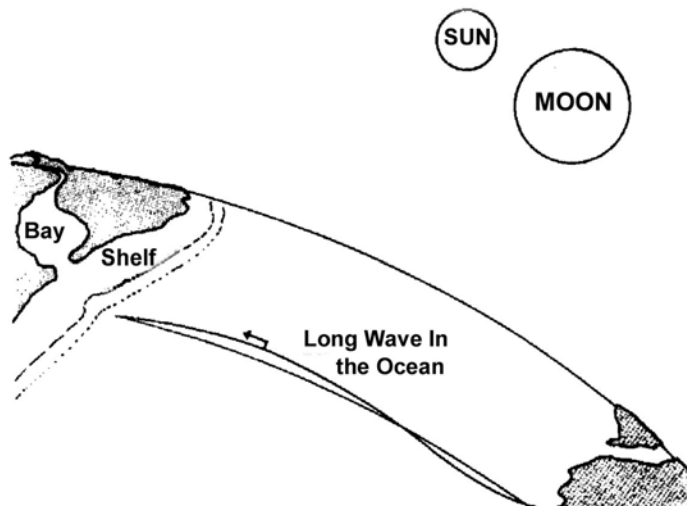


Figure 2.10. The tide generating forces caused by the moon and the sun produce a very long wave of relatively small amplitude in the ocean. When this long wave reaches the continental shelf, then the coast, and finally propagates up a bay, it is amplified by an amount that depends on the depth and length of the basins.

2. Theory Behind Tidal Analysis and Prediction

increased in amplitude. At the coast another reflection further increases the amplitude of this long wave, now reaching three feet or more along most coasts. When the wave moves up into a bay there can be even more amplification depending on the depth, length, and width of the bay, with tidal ranges reaching 15, 30, or even 50 feet for bays with the right dimensions. The propagation of this tide wave is also influenced by the Coriolis force (due to the Earth's rotation), which affects the tide ranges. This will be discussed in Sections 2.3.1 and 7.5.

How large the tide range is depends on how close the natural period of free oscillation of the basin is to the period of the tide-generating force. Much like a pendulum, which swings back and forth with a specific period determined by its length, the water in a basin sloshes back and forth with a specific period determined by its depth and length, which is called its *natural period of oscillation*. If the natural period of the basin is the same as the period of the tide-generating force, then the energy from the tidal forcing will be input in the same direction as the water is already moving and the resulting tide range will be larger. This is called *resonance*.

The natural period of oscillation of a basin, depends on its length and its depth. The longer the basin, the larger the period of oscillation, but the deeper the basin the smaller the period of oscillation. The length has the greater effect. More precisely, the natural period of the basin, T_n , (for the special case of no friction) is given by the formula

$$T_n = \frac{2L}{(gD)^{\frac{1}{2}}}$$

where L is the length of the basin, D is the depth, and g is the acceleration due to gravity. (This result ignores friction, which can have a very significant effect in shallow water, as will be seen in Section 7.4.) The Atlantic Ocean is too wide for there to be resonance (its 19-hour natural period being much longer than the 12.42-hour tidal period). The largest tide ranges in the world are in shallower basins with just the right length and depth combination to have natural periods close to the tidal period. Narrowing widths in rivers and bays also amplify the tide range due to a continuity effect. These hydrodynamic effects will be discussed in more detail in Chapter 7.

While the hydrodynamics, as determined by the dimensions of the ocean, bays, and rivers, determines the tide ranges and times of high and low waters, it is the astronomy that determines the particular frequencies at which tidal energy will be found. Because the system is a forced hydrodynamic system, the energy remains in those astronomically determined frequencies, and it is because of this that tides are so predictable using the methods to be explained in this book. In the next section these particular frequencies will be identified and their origins explained.

2.2 Astronomical Considerations

2.2.1 The Orbits of the Moon Around the Earth and the Earth Around the Sun

As mentioned above, because the ocean and connected bays are a forced oscillating system, the tide will oscillate with the same frequencies as the astronomical tide-producing forces, which are determined by the relative motions of the Earth, moon, and sun. There are many different tidal frequencies because of the complex nature of the orbit of the moon around the Earth and of the orbit of the Earth around the sun. Astronomers have very precisely determined all of the required astronomical frequencies. The fact that tidal energy will always be at known frequencies allows one

to predict the tide at a specific location for any time in the future, as long as there are data to analyze to determine the amplitude and epoch (phase lag) for each important tidal constituent (the amplitude and epoch not being known ahead of time because they are determined by the hydrodynamics).

If the moon-Earth orbit and the Earth-sun orbit were both circular and were both in the plane of the Earth's equator, there would only be two tidal frequencies. One could then predict the tide using only two semidiurnal tidal harmonic constituents (M_2 and S_2 , which are defined in Section 2.2.2). However, the orbital motions are much more complicated. Both orbits are elliptical, so the distance between the moon and Earth changes throughout the month, and the distance between the Earth and sun changes throughout the year. Both orbital planes are also at angles relative to the Earth's equatorial plane. Because of the angle between the moon's orbit and the plane of the Earth's equator, the moon appears to an observer on Earth to move north of the equator and then south of the equator and back north of the equator over roughly a month (actually 27.3 days). Similarly, the sun appears north of the equator half of the year (summer in the Northern Hemisphere) and south of the equator the other half of the year (winter in the Northern Hemisphere). To further complicate matters, the angles between the orbital planes and the equator also slowly change periodically over the years. All these motions modulate (that is, periodically vary the strength of) the tidal forces, so that tidal energy is spread out among many more frequencies (in addition to M_2 and S_2).

The fact that the moon's monthly orbit around the Earth is angled to the Earth's equatorial plane means that the moon will be over the equator only twice a month (*equatorial declination*). The rest of the month the moon will appear either north or south of the equator and the two tidal bulges (on the opposite sides of the Earth) will be asymmetric with respect to the axis of rotation (see Figure 2.11; here as in Figure 2.8, the idealized equilibrium tide is being considered, i.e., an ocean covering the whole earth with no continents). As a result there will be a once per day inequality in the elevation of the two high waters (and in the elevation of the two low waters) formed by the tidal bulge at any given latitude. This asymmetric declination effect puts energy into diurnal tidal frequencies. The strength of the resulting diurnal tide will vary in strength from zero when the moon

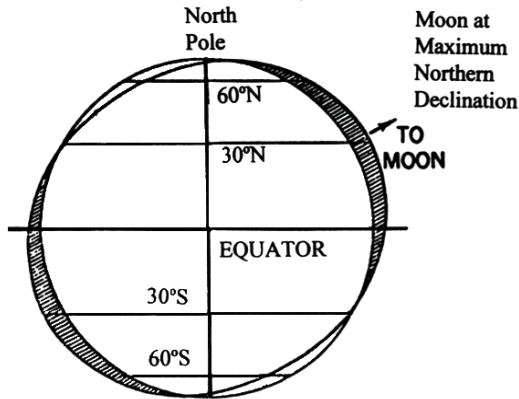


Figure 2.11. When the moon is at maximum declination north or south of the equator, the tidal bulges also shift north or south, and a location on the Earth will rotate under two different height bulges. The result will be a diurnal tidal component. In the real world with continents, hydrodynamics will actually determine which waterways have stronger diurnal signals.

2. Theory Behind Tidal Analysis and Prediction

is over the equator, to a maximum value when the moon appears (to an observer on the Earth) farthest north of the equator (*northern declination*) or farthest south of it (*southern declination*).

The fact that the Earth's yearly orbit around the sun is at an angle to the plane of the Earth's equator means that the sun will be over the equator only twice a year, March 21st (*vernal equinox*) and September 21st (*autumnal equinox*). The rest of the year the sun appears north of the equator half of the year (summer in the Northern Hemisphere) and south of the equator the other half of the year (winter in the Northern Hemisphere). The sun is farthest north of the equator on June 21st (*summer solstice*) and farthest south of the equator December 21st (*winter solstice*). This also produces diurnal tidal frequencies because the two tidal bulges caused by the sun (on the opposite sides of the Earth) will be again asymmetric with respect to the axis of rotation (Figure 2.11 also applies, with the moon replaced by the sun).

The fundamental astronomical periods of the motions of the Earth, moon, and sun are shown in Table 2.1. This includes three types of *day* – the *solar day* (24.000 hours), the *lunar day* (24.8412 hours), and the *sidereal day* (23.9344 hours). These differ from each other with respect to the reference for measuring one complete rotation of the Earth. The solar day is one complete rotation with respect to the sun. The lunar day is one complete rotation with respect to the moon, and is longer than the solar day because the moon revolves around the Earth in the same direction as the Earth rotates, so the Earth must rotate a little farther (and longer) to catch up with the revolving moon. The sidereal day is one complete rotation of the Earth with respect to the *vernal equinox*, which in this context means the location of the intersection of the plane of the Earth's equator and the plane of the Earth's orbit around the sun (called the *ecliptic*). The angle between these two planes is 23½°. The sidereal day differs only slightly from a day referenced to a fixed star in space, and the vernal equinox is usually used as the primary reference point for astronomical discussions.

Table 2.1 also includes the *tropical month* (27.3216 days), which is the period of the lunar declination. It is the time it takes the moon to revolve around the Earth with respect to the vernal

Description	Frequency notation (1/period)	Period (mean solar units)
Sidereal day (one rotation wrt vernal equinox)	Ω	23.9344 hours
Mean solar day (one rotation wrt to the sun)	ω_s	24.0000 hours
Mean lunar day (one rotation wrt to the moon)	ω_L	24.8412 hours
Period of lunar declination (tropical month)	ω_1	27.3216 days
Period of solar declination (tropical year)	ω_2	365.2422 days
Period of lunar perigee	ω_3	8.847 years
Period of lunar node	ω_4	18.613 years
Period of perihelion	ω_5	20,940 years

Table 2.1. The fundamental astronomical periods of the motions of the earth, moon, and sun (reworked from Platzman, 1971). The frequency notation is referred to in Table 2.2 and in the text. (“wrt” = “with respect to”)

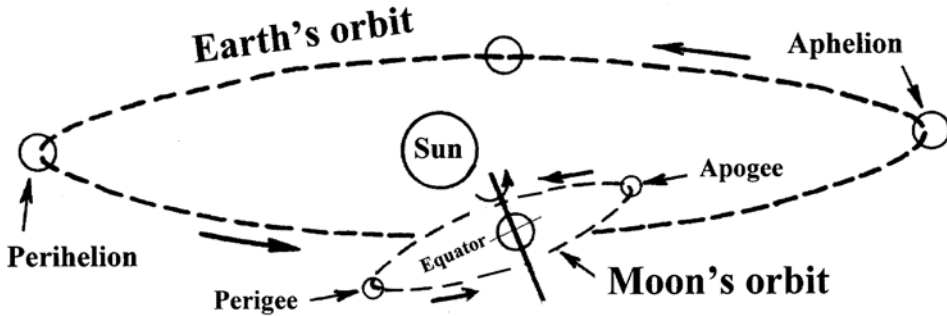


Figure 2.12. The orbits of the moon around the Earth and of the Earth around the sun, as viewed from a distant star. See text for discussion. (Modified from Dean, 1966)

equinox. In other words, it is the time it takes the moon to go from maximum northern declination to the next maximum northern declination. There are also other types of months, the only difference being the reference point against which the revolution of the moon is measured. If it is measured with respect to the sun it is called the *synodic month* (29.5301 days, on average), which is the month commonly observed when one notices the changing phases of the moon. This is longer than the tropical month, because, due to the Earth's orbit around the sun, it takes a little more time for the moon to get back to the same position with respect to the sun.

The Earth-moon orbit is elliptical (Figure 2.12), so that the distance between them varies from *perigee* (the moon closest to the Earth) to *apogee* (the moon farthest from the Earth). The period from perigee to apogee to the next perigee is on average 27.5546 days. The elliptical shape of the moon's orbit also slowly changes, causing the position of perigee to slowly move over an 8.847-year period. The angle between the plane through the moon's orbit and the plane through the equator varies over a 18.613-year period. This is referred to as *lunar nodal regression* because the intersection of the moon's orbital plane with the ecliptic, called the *ascending lunar node*, regresses backwards along the ecliptic over this 18.6-year period (see Figure 2.13).

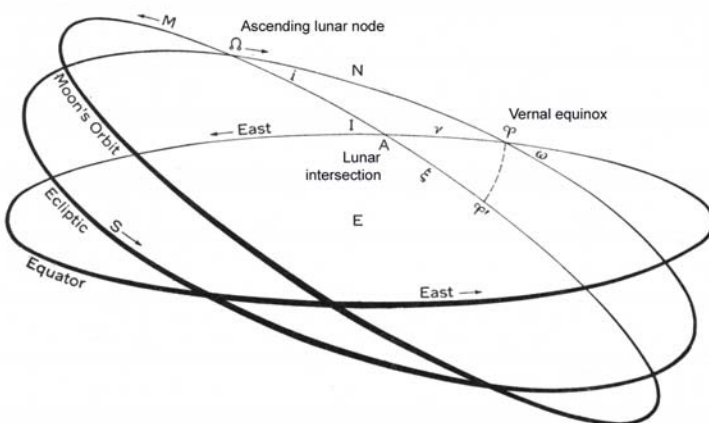


Figure 2.13. The moon's orbit and the sun's orbit (the ecliptic) with respect to the Earth's equatorial plane. See text for explanation of terms. (From Schureman, 1958)

2. Theory Behind Tidal Analysis and Prediction

The *tropical year* (365.2422 days) is the length of time for the Earth to revolve around the sun with respect to the vernal equinox. The orbit of the Earth around the sun is also elliptical, so that the distance between the Earth and the sun varies from *perihelion* (the Earth closest to the sun; also called the *solar perigee*) to *aphelion* (the Earth farthest from the sun; also called the *solar apogee*). However, this orbit also very slowly changes, so that the position of perihelion very slowly moves over a period of 20,940 years (too long to worry about in tide predictions, but important in long-term climate studies).

A simplified schematic of the relative motions of the Earth, moon, and sun, from the view point of a distant star is shown in Figure 2.12. In this figure one sees the plane of the moon's orbit around the Earth inclined at an angle of $5^{\circ}9'$ relative to a plane through the Earth's equator. The plane of the Earth's orbit around the sun (the *ecliptic*) is inclined to the plane of the Earth's equator at an angle of $23^{\circ}27'$. These same two orbital planes and the Earth's equatorial plane are also shown in Figure 2.13, but from the point of view of the Earth. Since one is used to seeing the moon and sun overhead moving across the sky and around the Earth, using Figure 2.13 it is usually easier to visualize the effects of the orbits on the tidal bulges. In Figure 2.13, ω is the angle between the plane of the Earth's orbit (the ecliptic) and the plane of the Earth's equator and equals $23^{\circ}27'$; it is called the *obliquity of the ecliptic*. In the same figure, i is the angle between plane of the Earth's orbit and the plane of the moon's orbit, and it is $5^{\circ}9'$. I is the angle between the plane of the moon's orbit and the plane of the Earth's equator, and it changes with the movement of the ascending lunar node, which moves through one cycle in 18.6 years. Thus this angle goes from approximately $28\frac{1}{2}^{\circ}$ to $18\frac{1}{2}^{\circ}$ and back in 18.6 years and has an important effect on the tide range.

The periods for the (three types of) day, month, year, lunar perigee, lunar node, and perihelion are listed in Table 2.1. ω_L , and ω_1 through ω_5 in Table 2.1 are the notation for the equivalent frequencies for these periods. As will be seen in Section 2.2.3, combinations of these frequencies will produce the frequencies of all the tidal constituents (Table 2.2). Before examining Table 2.2 it will be instructive to see how the frequencies of some of the most important tidal constituents are derived.

2.2.2 The Origins of the Largest Tidal Harmonic Constituents

As was mentioned in Chapter 1, the contribution to the tide by the energy at a particular frequency is usually represented by a *tidal harmonic constituent*, for which there is an amplitude and a phase lag (called an *epoch*). Harmonic tidal prediction involves the summing of a set of cosine curves representing the various tidal harmonic constituents (see Section 3.4.2). The nomenclature for most tidal harmonic constituents is to name each constituent with a capital letter followed by a subscript indicating the approximate number of cycles per day for that constituent, for example M_2 , S_2 , N_2 , K_1 , and O_1 (all of these constituents are discussed in this section). There are also a few tidal constituents named with Greek letters (e.g., μ_2 , v_2 , λ_2 , and ρ_1), as well as compound tides, whose names have more than one capital letter (e.g., $2MN_2$, $2MS_2$, MK_3 , MN_4 , etc.) indicating the primary constituents from which the compound constituent was nonlinearly generated by shallow water. There are also long-period tides which tend to have names with a capital letter and one or more lower case letter (e.g., Mn , Mf , Sa , Ssa , etc.). At the end of Section 2.2.3 there is some discussion of where this naming convention came from.

This section will explain the origin of some of the most important tidal harmonic constituents, namely, why there is tidal energy at a particular frequency and the particular aspect of the Moon's orbit or the Earth's orbit that is responsible.

The moon orbits around the Earth in the same approximate direction as the rotation of the Earth, so that one lunar day (i.e. one complete rotation of the Earth *with respect to the moon*) is longer than the 24-hour solar day, because, by the time the Earth has rotated the moon has revolved a small distance. So a lunar day is 24.8412 hours long ($1/\omega_L$). There are two tidal high water bulges on the Earth, so the period of the largest semidiurnal lunar harmonic constituent, M_2 , is half a lunar day, or 12.4206 hours. Its frequency (1/tidal period) is $2\omega_L$, which is $(1/12.4206 \text{ hours}) = 1.9323$ cycles per (solar) day.

The Earth turns under the sun exactly once every solar day, which leads to the main solar semidiurnal tidal constituent, S_2 , with a period of 12.0000 hours. Its frequency is $2\omega_s$, which is 2.0000 cycles per day. Although the sun is approximately 27 million times more massive than the moon, it is approximately 339 times farther from Earth than the moon, and since the tidal force is inversely proportional to the cube of the distance, S_2 is usually much smaller in size than M_2 . When the moon and sun are in alignment at new and full moons their tidal forces work together to produce larger tide ranges (called *spring tides*). When the moon and sun are at first and third quarters they work against each other to produce smaller ranges (called *neap tides*). In Figure 2.14 in the upper plot, two sine curves, one representing the M_2 tide and one representing the S_2 tide, are plotted together. In that plot they begin in sync, with their tide-producing forces adding to each other, thus causing the larger spring tides seen in the lower plot (where the M_2 and S_2 contributions are summed). After roughly 7 days the two sine curves in the upper plot are now out of sync and their tide-producing forces are now subtracting from each other, thus causing the smaller neap tides seen in the lower plot. After another 7 days they are back in sync and producing spring tides once again. This sequence could represent going from full moon to third quarter to new moon, or likewise, going from new moon to first quarter to full moon. The cartoon representation of the relative positions of the Earth, moon, and sun for these two alignments of the moon and sun are shown in the upper most part of Figure 2.14.

The Earth-moon orbit is elliptical, so that the distance between them varies over a 27.5546-day period ($1/[\omega_1 - \omega_3]$), from *perigee* (the moon closest to the Earth, and so a stronger tidal force) to *apogee* (the moon farthest from the Earth, and so a weaker tidal force) and back to perigee. This periodic change in the distance from the moon to the Earth *modulates* the lunar tidal force, that is, it slowly increases and then decreases the tidal force over the 27.5546-day period. Such a modulation of M_2 can be represented by combining it with another semidiurnal lunar tidal constituent with a period of 12.6583 hours, which is called N_2 . [The effect of the 27-day variation in the moon's distance to the Earth is often referred to as the parallax effect. In this context *parallax* is the angle between two lines from the center of the moon, one to the center of the Earth and one to the surface of the Earth (tangent to the Earth's surface). Because this angle is very small it is approximately equal to the sine of the angle, which is equal to the ratio of the Earth's radius to the distance from the moon to the Earth. Since the parallax is a function of the distance to the moon, the term is applied to tidal inequalities arising from this changing distance.]

The plots in Figure 2.14 can be used to illustrate the perigee-apogee effect, if, in that figure, S_2 is replaced with N_2 , spring tide is replaced with perigean tide, and neap tide is replaced with apogean tide. However, in using this figure it must be remembered that these are two very different situations. The difference is that with the M_2 plus S_2 case, there really are two distinct effects being added, the lunar tide and the solar tide. However, in the case of the changing distance between the moon and Earth, that changing distance directly affects the amplitude of the lunar tide, and this modulating amplitude of the lunar tide is being represented by adding an N_2 tidal constituent to the M_2 tidal constituent. The stronger *perigean* tidal force is represented when M_2 and N_2 come into

2. Theory Behind Tidal Analysis and Prediction

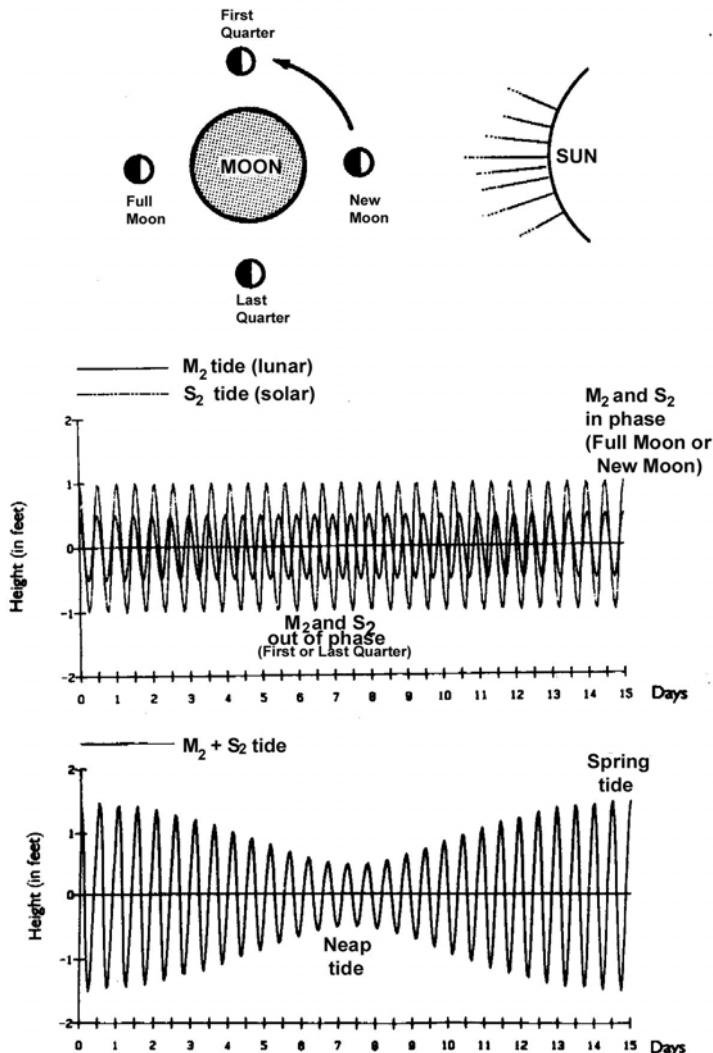


Figure 2.14. The combined effect of the moon and sun varies throughout the month. When the moon and sun are working with each other (at Full Moon and New Moon) there are larger tide ranges (spring tides). At First Quarter and at Last Quarter the moon and the sun work against each other resulting in smaller tide ranges (neap tides).

phase (leading to larger tidal ranges), while the weaker *apo*gean tidal force occurs when M₂ and N₂ are exactly out of phase (leading to smaller tidal ranges). However, that being said, if one carries out a spectral analysis of a water level data series (that is, if one calculates how energy is spread out over the entire frequency domain), one will find that to the left of the M₂ spectral line (1.9323 cpd), there is another spectral line at 1.8960 cpd, which is the frequency of another tidal constituent, N₂ (see next section). Thus, this is really more than just finding a convenient tidal constituent with a frequency, that when added to the M₂ constituent, will produce the correct modulation. The perigee-apogee modulation of M₂ actually transfers energy from M₂ to another frequency, N₂.

There are several times a year when lunar perigee is reasonably close in time to new or full moon, the result being much larger tidal ranges called *perigean spring tides*. Similarly, much smaller tidal ranges (called *apo*gean neap tides) result when lunar apogee occurs near first or third

quarter phases of the moon. With respect to the tide-producing forces S_2 should be larger than N_2 and for many waterways it is, but for other waterways N_2 is larger than S_2 , this being due to the effect of the hydrodynamics in such waterways that amplifies N_2 more than S_2 . They are both, or course, much smaller than M_2 . (But even here there is an exception, at Tahiti, where the hydrodynamics of the Pacific Ocean causes there to be a minimum in M_2 near Tahiti, allowing S_2 to be of comparable size, and therefore leading to the very unusual situation of high water occurring at approximately the same time every day. See Marmer, 1926.)

As mentioned in the last section, the plane of the moon's orbit around the Earth is at an angle to the plane through the Earth's equator. As the Earth rotates under the moon, there will be times of the month when the moon is north of the equator (*Northern Declination*), over the equator (*Equatorial Declination*), and south of the equator (*Southern Declination*). When the moon is north or south of the equator, one of the tidal bulges is more north of the equator and one is more south, so that at a particular location on the Earth there will either be only one high water per day (a diurnal tide), or, if there are two, they will be of different heights, the difference being the *diurnal inequality* (for example, see the San Francisco tide curve in Figure 2.12). The diurnal lunar tidal forces resulting from lunar declination are represented by two diurnal tidal constituents, O_1 and K_1 , with periods of 25.8193 and 23.9345 hours (and frequencies of 0.9295 cpd and 1.0027 cpd). The minimum combined effect of these two constituents occurs every 13.66 days ($1/(2\omega_1)$), at the times when the moon is over the equator. Their maximum combined effect occurs at maximum declination. The sum of the O_1 and K_1 frequencies is equal to the M_2 frequency, so that the time of the diurnal high water does not change with respect to the times of the two semidiurnal high waters. (The maximum angle between the plane of the moon's orbit and the Earth's equator varies from 18.3° to 28.5° over a 18.6-year period, the lunar nodal cycle; see Section 2.2.4 for further discussion.)

As mentioned in the last section, the plane of the Earth's orbit around the sun (the *ecliptic*) is also at an angle to the plane through the Earth's equator. Around December 21st the sun is furthest south of the equator (December solstice) and around June 21st it is furthest north of the equator (June solstice), the angle between the ecliptic and the equator reaching 23.5° in each case. December solstice marks the beginning of winter in the Northern Hemisphere and the beginning of summer in the Southern Hemisphere, and vice versa for June solstice. Around March 21st the sun is over the equator (*vernal equinox*) and again around September 21st (*autumnal equinox*). This movement of the sun north and south of the equator also leads to diurnal tidal constituents, which represent this very slow modulation, in this case P_1 with a period of 24.0658 hours [$1/(\omega_S - \omega_2)$], and another K_1 . Thus, the K_1 used for tidal prediction has both lunar and solar parts. P_1 and the solar part of K_1 have a minimum combined effect every 182 days, at vernal and autumnal equinoxes, and have their maximum combined effects at winter and summer solstices.

Although with respect to the tide producing forces, K_1 and O_1 should always be smaller than M_2 , there are in fact many waterways where hydrodynamics amplifies the diurnal constituents and/or reduces the semidiurnal constituents, so that $K_1 + O_1$ is comparable to or larger than M_2 . In this case the result is a *diurnal tide*, that is, one high water and one low water per day (see Sections 2.3.1 and 7.4.1).

2.2.3. Derivation of Tidal Frequencies from the Basic Astronomical Frequencies – Insights from Tidal Spectra

In the last section, with the exception of M_2 and S_2 , each of the other tidal constituent frequencies looked at represented a modulation of the lunar or solar tide due to some orbital effect. That modulating effect could be represented by using additional tidal constituents in combination with M_2 or S_2 . For example, it was seen that the variation in tidal forces due to the elliptical shape of the moon's orbit (i.e., going from apogee to perigee) could be represented by adding N_2 to M_2 . It was also seen that the diurnal variation in tidal forces due to the changing declination of the moon (i.e., the moon being north of and then south of the equator) could be represented by two tidal constituents, K_1 and O_1 , in combination with M_2 .

It was also seen that the use of tidal constituents like N_2 , K_1 , and O_1 is more than just a convenience. If one carries out a spectral analysis of water level data or current data (which calculates the energy at all frequencies), one will find spectral lines clearly above the nontidal *continuum* (see Section 3.1) at the exact frequencies of N_2 , K_1 , and O_1 . The modulation of the M_2 tidal oscillation by the variation in the moon-Earth distance (from apogee to perigee and back) has indeed transferred energy from the M_2 frequency to N_2 frequency. Likewise, the modulation of the M_2 tide by the changing declination of the moon has also transferred energy to the K_1 and O_1 frequencies. In a water level spectrum one will also find many more spectral lines, which are additional smaller tidal constituents also produced by some variation in the moon-Earth orbit or the Earth's orbit around the sun. Now it will be explained where those constituents come from (and Tables 2.1 and 2.2 will be more closely looked at).

First consider a typical spectral analysis of a water level times series (for example that shown in Figure 2.16). The longer the data time series the smaller the interval one can have as one moves along the frequency domain from zero frequency (i.e., the mean energy over the time series length) to the highest frequency for which energy can be calculated. The resolution frequency is simply the reciprocal of the length of the time series. The highest frequency for which energy can be calculated is determined by the sampling rate, Δt , and is known as the *Nyquist frequency*, defined as $f_N = 1/(2\Delta t)$. For example, for a time series with an hourly sampling rate ($\Delta t = 1$ hour) the highest frequency in the calculated spectrum will be one cycle in two hours, i.e., $f_N = 12$ cycles per day (cpd). So for looking at the tidal spectral lines at most stations, even those in very shallow water, an hour sampling rate is usually more than adequate. However, there are a few shallow-water areas with large tidal ranges where higher harmonics beyond 12 cpd can actually be detected. In such cases a higher sampling rate is required. Water level gauges presently operated by CO-OPS usually have a sampling rate of 6 minutes (which would allow one to do spectral analysis out to 5 cph or 120 cpd).

The Nyquist frequency is also called the *folding frequency*, because the energy at frequencies above the Nyquist frequency affect the calculated energy at frequencies below the Nyquist frequency – they fold back in. This is known as *aliasing* or *folding*. For example, Figure 2.15 shows a sinusoid with a frequency (f) higher than the Nyquist frequency (f_N). In such a case the sampled data points take energy from different phases of the high-frequency sinusoid, and the result looks like a much lower-frequency sinusoid (i.e., with a sinusoid with a frequency, $f_N - f$, which is lower than the Nyquist frequency). So if the sampling interval is too large, not only will the higher tidal frequencies not be included in the spectrum, but that higher-frequency energy will actually be folded back in (through the aliasing) and affect the values of the spectrum that can be calculated. (However, one can sometimes use known aliasing to help reduce computations. See Section 3.5.2.)

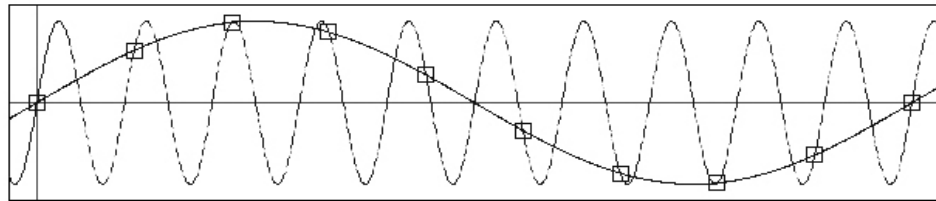


Figure 2.15. A demonstration of aliasing. The higher-frequency sine wave has a frequency greater than the Nyquist frequency (namely, the sampling interval is too large), so the data points (the small boxes) appear to describe a much lower-frequency sine wave (see text).

A spectral analysis of an hourly time series that is a year long, will show us how much energy is at frequencies from 0 cpd to 12 cpd, at frequency intervals of approximately 0.00274 cpd. Two tidal constituents whose frequencies are closer to each other than 0.0027 cpd will, for this case, not be separated and will be seen in one spectral line. (Actually, in Section 3.3 it will be seen that this rule, the so-called *Rayleigh criterion*, may actually be affected by the signal-to-noise ratio of the data time series, and for cases with high signal-to-noise may be too restrictive.)

Figure 2.16 shows the tidal bands from a typical spectral analysis of water level data, in this case from Anchorage, Alaska. The tidal spectral lines are grouped in *bands*, one band for each tidal *species* – semidiurnal and diurnal, as well as the higher harmonics (the overtones). The long-period tides tend to be overwhelmed and hidden by low-frequency nontidal energy. The surface of the ocean moves up and down due to other nontidal phenomena which do not have most of their energy concentrated in a few frequencies. Thus, in the plot of a water level spectrum, the energy from winds, atmospheric pressure, and temperature and salinity changes shows up primarily as a smooth

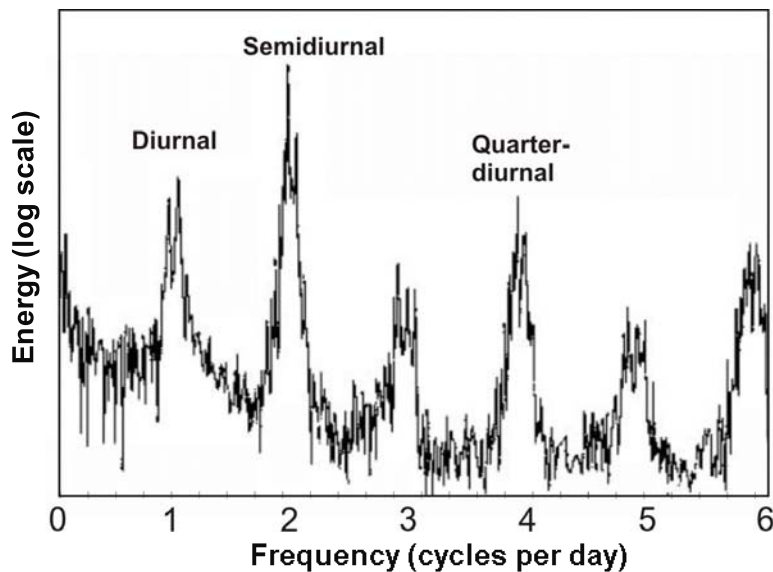


Figure 2.16. A water level spectrum from near Anchorage, Alaska, at the northern end of Cook Inlet, where the water is shallow and the tide range large.

2. Theory Behind Tidal Analysis and Prediction

continuous curve covering a broad range of frequencies, called the *continuum*, ranging from wind waves at the higher frequencies to low-frequency storm surges at the lowest frequencies. The tidal bands (or on a fine scale the tidal lines) rise above this continuum. The continuum curve at a water level station near the coast or in a bay is often highest near zero cpd (which represents the mean of the data time series), with the very low frequencies near zero cpd representing very slow changes in the height of the water surface due to the effects of wind, atmospheric pressure, density changes, and/or river discharge.

As Munk and Cartwright (1966) pointed out, in the language of *spectroscopy* (i.e., the study of spectra) each tidal species shows three orders of “splitting”: monthly splitting, a finer yearly splitting, and hyperfine splitting from long-period effects such as the variation in lunar perigee and nodal regression. This “splitting” is another way of saying that modulation of the lunar and solar tide producing forces by monthly, yearly, and longer-period variations adds additional spectral lines to the tidal spectra, each line of which can be represented by a tidal harmonic constituent. In the previous section, in describing how some of the more important tidal constituents are produced, it was not mentioned that each modulation actually produces two additional tidal constituents (the second usually much smaller) – and thus the term “splitting”. Thus, around each tidal spectral line, a monthly variation will produce two additional spectral lines, one on each side, often referred to as a pair of side-band lines. The longer the period of the modulating effect the closer the lines are to the central line.

Thus, for example, the monthly modulation of M_2 due to the changing distance between the moon and the Earth (the perigee-apogee effect of the Moon’s elliptical orbit), produces two additional spectral lines around the M_2 spectral line, the N_2 and L_2 spectral lines. M_2 has a frequency of $1/(12.4206 \text{ hr}) = 1.9323 \text{ cpd}$, and 0.0363 cpd to the left and right of this spectral line one will find N_2 [$1/(12.658 \text{ hr}) = 1.8960 \text{ cpd}$] and L_2 [$1/12.192 \text{ hr} = 1.9686 \text{ cpd}$], respectively.

Similarly, the yearly modulation of S_2 due to the effects of the elliptical orbit of the Earth around the sun (the perihelion-aphelion effect) produces two additional tidal constituents around S_2 , both 0.0027 cpd from S_2 ; the frequencies of T_2 , S_2 , and R_2 are respectively, 1.9973 , 2.0000 , and 2.0027 cpd (see Figure 2.17).

Likewise, the 18.6-year modulation of the lunar tidal forces due to the lunar nodal regression can be represented by many additional tidal constituents, usually referred to as *satellite constituents*. If one has 19 years of data, one can include these additional satellite constituents and not need to use node factors (which will be discussed more in Section 2.2.4).

The modulating forces that produce additional semidiurnal and diurnal tidal constituents also directly produce other smaller tidal constituents that have the same frequencies as the modulation. For example, there is a tidal constituent **Mm**, the *lunar monthly constituent*, which has a period of 27.55 days (a frequency of 0.036 cpd) and is directly produced by variation in tidal force due to the moon’s elliptical orbit. There is a tidal constituent **Mf**, the *lunar fortnightly constituent*, which has a period of 13.66 days (a frequency of 0.073 cpd) and is directly produced by the variation in tidal force due to the moon’s declination. There is a tidal constituent **MSf**, the *lunar synodic fortnightly constituent*, which has a period of 13.77 days (a frequency of 0.068 cpd) and is also directly produced by the variation in tidal force due to the moon’s declination. All of these long-term tidal constituents are very small, and are often dominated by meteorological effects on water level and currents that can put energy into these same frequencies. More important, however, nonlinear shallow-water effects produce compound tides with the same frequencies as these fortnightly and monthly constituents, but with larger amplitudes. (See Section 2.3.2 and Table 2.4.) For

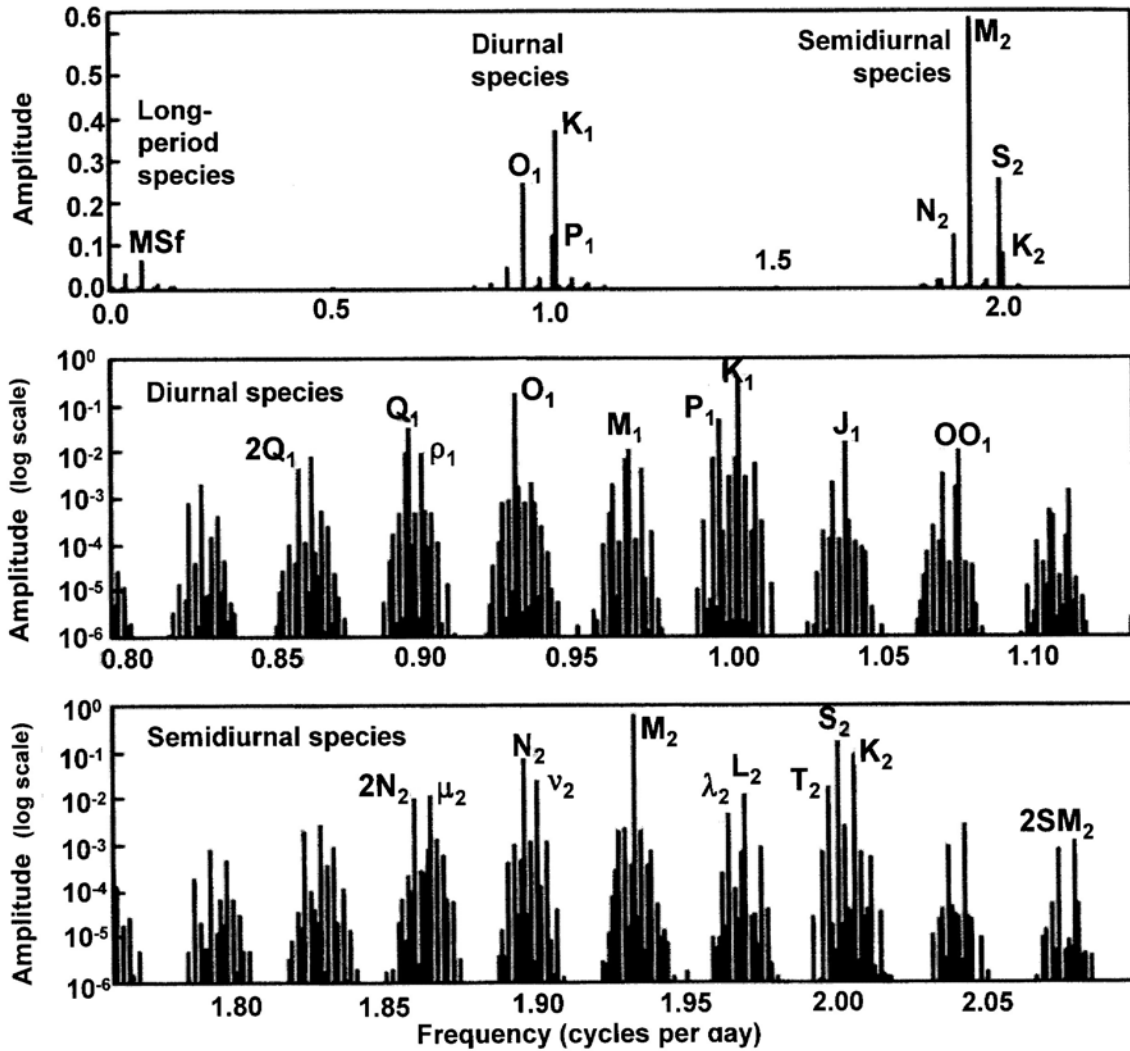


Figure 2.17. Tidal spectral lines for the semidiurnal, diurnal, and long-period constituents (top panel) and with greater resolution for the diurnal constituents (middle panel) and for the semidiurnal constituents (lower panel).

example, the nonlinear interaction of M_2 and S_2 produces the shallow-water constituent MS with the same frequency as **MSf**.

Also dominated by meteorological forces are the even longer-period and even smaller tidal constituents directly produced by yearly variations in the orbits. Sa and Ssa are very small tidal constituents directly generated by the nonuniform changes in the Sun's declination and distance (the perihelion-aphelion effect). The solar annual constituent, Sa, has a period of 365 days (a frequency of 0.0027 cpd) and the solar semiannual constituent, Ssa, has a period of 183 days (a frequency of 0.0055 cpd). These constituents and their dominance in data time series by meteorological effects will be discussed more in Section 3.7.

Although these and other additional tidal constituents represent the tidal energy at new frequencies due to the modulating effects of the moon's and Earth's orbits, early tide researchers found it convenient to think of each as being produced by a separate and distinct heavenly body, like the moon and sun. This idea was first proposed by Laplace, who called it *astres fictifs*, or *fictional*

2. Theory Behind Tidal Analysis and Prediction

celestial bodies, and the idea was then used by Thomson (Lord Kelvin). These celestial bodies could be thought of as each moving in the Earth's equatorial plane with a constant angular speed (which may be one reason why the term "angular speed" was used in tides to mean "frequency"). The more modern name for these fictitious heavenly bodies is *satellites*, and as was just mentioned, this term has come into use again when carrying out 19-year or long harmonic analyses and using satellite constituents instead of node factors.

The naming of the actual tidal constituents themselves (at least the larger ones studied by the earliest researchers) appear to primarily have come from Thomson and Darwin and used the letters K, L, M, N, O, P, Q, R, S, and T. The logic for M for moon and S for sun is obvious. The letters L and N for the two semidiurnal constituents with periods less than and greater than M, probably were used so that alphabetical order matched the order of increasing tidal constituent period, and similarly for R and T around S, but the reason for choosing the letters K, O, and Q seems less obvious. In the U.S., Ferrel developed his own harmonic development of the tide completely independent of Thomson and Darwin (but following on the work of Laplace) and had a totally different naming scheme which involved only numerical suffixes. However, the British naming system found favor and by the time Schureman first published his work on harmonic analysis and prediction in 1924 he was also using the British naming system.

When harmonically analyzing the forces involved in the moon's and Earth's orbits, Doodson (1921) came up with over 400 tidal constituents (admittedly most were very small). This remained the standard reference work for tidal analysis and prediction for fifty years, until it was finally recalculated and updated by Cartwright and Tayler (1971) and Cartwright and Edden (1973), who used an ephemeris of high precision for the moon and sun and the latest I.A.U. astronomical constants.

In Doodson's and others' work, the harmonic development was actually done on the *tide-generating potential*. The tide potential is related to the tidal force by the formula $\mathbf{F} = -\nabla V$, where ∇ stands for the gradient operator, which turns the scalar V into a vector \mathbf{F} . It is mainly a mathematical convenience, and one can think of the tide-generating potential as merely representing the tide-producing force (see Godin, 1972).

Figure 2.17 shows some of the tidal spectral lines. For each tidal frequency there is a tidal constituent for which the amplitudes and epochs (phase lags) are calculated during a harmonic analysis of a data time series. Those amplitudes and epochs are then used to make tidal predictions. Table 2.2 shows how key tidal constituents are derived from these fundamental astronomical frequencies.

The classic *Doodson number* used in many tidal papers is a shorthand notation that indicates which of the six frequencies, ω_L , and ω_1 through ω_5 from Table 2.1, are used to produce a particular tidal constituent (e.g., the examples shown in Table 2.2). Doodson added 5 to each number (except the first) to keep them from being negative. *Cartwright numbers* are the same as the Doodson numbers but without the added 5's. The six digits of a Cartwright number are the multiplying coefficients in front of the six frequencies ω_L , and ω_1 through ω_5 from Table 2.1. Cartwright numbers for each astronomical tidal constituent are given in Tables 3.2, A.1, and A.2.

2.2.4. The Origin of Node Factors and Equilibrium Arguments

As mentioned earlier, there are some very slow variations in the tide-producing forces with periods on the order of many years. Most important of these is the 18.6-year variation in the angle between the plane through the moon's orbit and the plane through the Earth's equator (ω_4 in Table 2.1).

Symbol	Period	Speed (°/hr)	Description	Derived from	Coeff. C
<i>Semidiurnal tides</i>					
K_2^L	11.967 hours	30.0821373	declinational to M_2	$2\omega_L + 2\omega_1 (=2\Omega)$	0.0768
K_2^S	11.967 hours	30.0821373	declinational to S_2	$2\omega_S + 2\omega_2 (=2\Omega)$	0.0365
S_2	12.000 hours	30.0000000	principal solar	$2\omega_S$	0.4299
M_2	12.421 hours	28.9841042	principal lunar	$2\omega_L$	0.9081
N_2	12.658 hours	28.4397295	elliptical to M_2	$2\omega_L - (\omega_1 - \omega_3)$	0.1739
L_2	12.192 hours	29.5284789	elliptical to M_2	$2\omega_L + (\omega_1 - \omega_3)$	0.0257
<i>Diurnal tides</i>					
K_1^L	23.934 hours	15.0410686	declinational to O_1	$(\omega_L - \omega_1) + 2\omega_1 (= \Omega)$	0.3623
K_1^S	23.934 hours	15.0410686	declinational to P_1	$(\omega_S - \omega_2) + 2\omega_2 (= \Omega)$	0.1682
P_1	24.066 hours	14.9589314	principal solar	$(\omega_S - \omega_2)$	0.1755
O_1	25.819 hours	13.9430356	principal lunar	$(\omega_L - \omega_1)$	0.3769
Q_1	26.868 hours	13.3986609	elliptical to O_1	$(\omega_L - \omega_1) - (\omega_1 - \omega_3)$	0.0722
<i>Long-period tides</i>					
Mf	13.661 days	1.0980331	declinational to M_o	$2\omega_1$	0.1564
Mm	27.555 days	0.5443747	elliptical to M_o	$(\omega_1 - \omega_3)$	0.0825
Ssa	182.621 days	0.0821373	declinational to S_o	$2\omega_2$	0.0729

Table 2.2. Tidal constituents and their origin from astronomical frequencies. The “speed” is the angular speed, a classical form of frequency (see text). M_o and S_o represent constant lunar and solar forces. The coefficient C gives a global measure of each constituent’s relative portion of the tide potential (reworked from Platzman, 1971).

This is referred to as the *lunar nodal regression* because the intersection of the moon’s orbital plane with the ecliptic (the Earth’s orbital plane around the sun), called the ascending lunar node, regresses backwards along the ecliptic over this 18.6-year period. Also significant is the 8.85-year variation in lunar distance due to the rotation of the longitude of the lunar perigee (ω_3 in Table 2.1). These longer-term variations in the tide (and especially the 18.6-year variation) are clearly evident in water level records. The 100-year record of monthly and annual mean tide ranges at Seattle, Washington, in Figure 2.18, provides one example. In this figure one can see five complete 18.6-year cycles in the plot of the annual mean tide range. These cycles are also observable in the plot of the monthly mean tide ranges, although that graph shows much greater variability, probably due to the nonlinear interaction effects of various nontidal influences on water level.

2. Theory Behind Tidal Analysis and Prediction

These longer-term modulating effects can also be represented as tidal harmonic constituents, but to do so one must use one or more additional satellite constituents for every lunar tidal constituent already considered. The frequencies of these additional constituents will be extremely close in frequency to those original constituents. (As was seen in Section 2.2.1, the spectral splitting due to these very *long-period* effects puts small spectral lines very close to each tidal spectral line.) Because these additional constituents are so close in frequency to the original constituents, one must analyze a very long data time series, namely 18.6 years of data. When this is done, these additional constituents are usually referred to as *satellite* constituents (see Zetler, et al, 1985; Amin, 1976; and Foreman and Neufeld, 1991).

In the pre-computer era, analyzing 19 years of data was much too labor intensive, especially since these additional constituents accounted for too little variation to be worth the large computing effort. But oceanographers did not want to ignore their effects. The 18.6-year variation due to the lunar nodal regression cycle can affect M_2 by as much as ± 4 percent, and K_1 by as much as ± 11 percent. So a method was devised that included the effect of the lunar nodal regression by including it in a form that directly represents the modulation of each lunar tidal constituent. This method involved using a multiplicative factor (usually called f), one for each tidal constituent, as well as a phase difference (u) that also varied over the 18.6 years. In Section 3.4.2 it will be seen that f and u are explicitly included in the harmonic prediction equation.

The multiplicative factor f is called the *node factor*, even though this method is also used to include the effect of the 8.85-year variation in lunar distance due to the rotation of the longitude of the lunar perigee. Each node factor, for a specific tidal constituent, is a factor that multiplies the tidal amplitude and fluctuates around 1.0. For M_2 , for example, it fluctuates from 0.963 to 1.038 and back to 0.963 over the 18.6-year period. f has usually been obtained from a table created with the appropriate astronomical formulas, such as Table 14 in Schureman, 1958 (a portion of which originally appeared in Harris, 1897). Zetler (1982) extended this table through the year 2025.

In the U.S. a single value of f has typically been used for each year, for each tidal constituent, that value being for the middle of the year, it being assumed that the variation in f was slow enough that the midyear value could be used for the whole year. However, some oceanographers prefer to use f values for every one- or two-month period. The largest variation in f over a 18.6-year period (for the most important tidal constituents) is found in O_1 , which varies $\pm 18\%$, and in K_1 , which varies $\pm 11\%$. (There is a 40% variation in Mf , but that constituent is usually relatively small and usually overwhelmed by meteorological energy.) The variation of f for M_2 is $\pm 4\%$, but since in many locations M_2 is often much larger than O_1 and K_1 , it may only be the 4% variation with which one is most concerned. Since this is a lunar effect, there is no direct nodal effect on solar constituents such as S_2 or P_1 (but, as will be seen later, there may be nonlinear hydrodynamic effects that can lead to variations in S_2 and P_1 over the 18.6-year cycle).

The phase difference associated with the 18.6-year or 8.85-year modulations is also treated in the U.S. as a constant for each year and is included as part of the so-called *equilibrium argument*, which is described in Section 3.4.2. Schureman's Table 15 provides the equilibrium argument value for various tidal constituents for the beginnings of the years 1850 through 2000, the first hundred years being taken from Harris, and Zetler extending it through 2025 (the u part of the equilibrium is actually for the center of each year). His Tables 16, 17, and 18 allow one to adapt the equilibrium arguments ($V_o + u$) in Table 15 to any month, day, and hour, but in these tables the u portion is still considered constant for an entire year. These tables apply to the Greenwich time meridian, but can be modified to apply to other time meridians and other longitudes (see Section 3.4.2).

**VARIATIONS IN MEAN RANGE OF TIDE AT SEATTLE, WA
1900 - 1996**

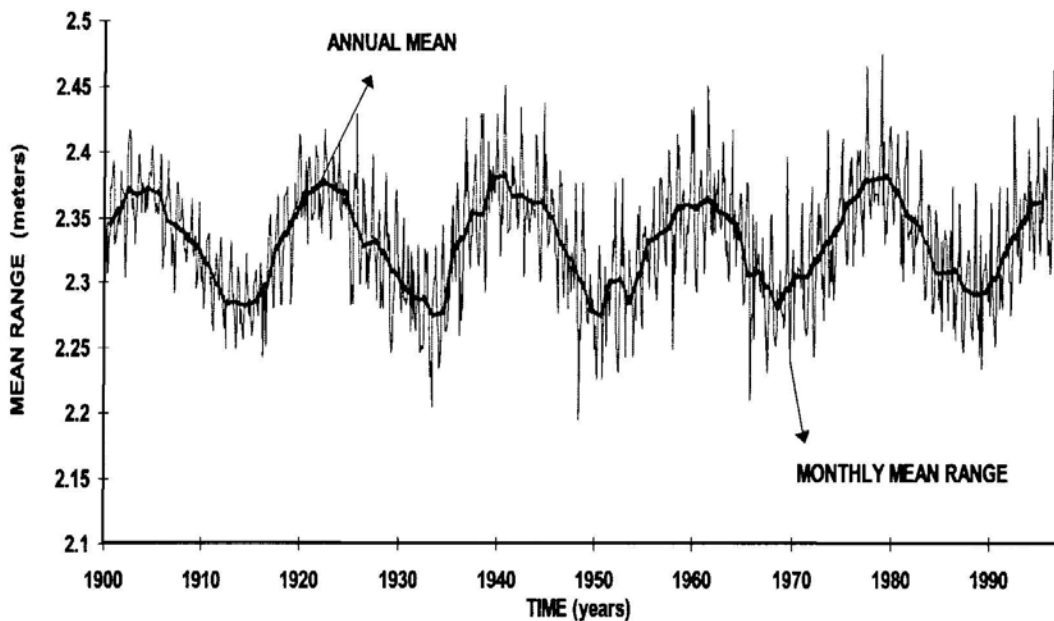


Figure 2.18. A 100-year record of monthly (light line) and annual mean (dark line) tide ranges at Seattle, illustrating the 18.6-year lunar nodal cycle (from Gill and Schultz, 2001).

In a traditional tidal prediction the amplitude of each tidal harmonic constituent is multiplied by the node factor for the year that the tidal prediction is being made for. When a traditional harmonic analysis is carried out, the resulting tidal constituent amplitudes are divided by the node factor for the year that the data were obtained. (Or similarly, multiplied by the inverse of the node factor, which Schureman calls the *reduction factor* and labels as F .) Although tables like those in Schureman are often used, both the node factor and the equilibrium argument can be directly included in harmonic analysis and prediction programs through use of the appropriate astronomical equations. Of course, if a full set of satellite constituents is used, no node factors will be used, but this is still typically not done for routine operational tidal predictions, and is primarily used only in research activities.

Schureman (1958) and others used equilibrium theory when calculating the node factors and the u portion of the equilibrium argument, but f and u can be affected by the hydrodynamics of the oceans and adjoining waterways (see Section 2.3.4). However, except for the most precise analyses and predictions, the use of f and u should be quite adequate. The use of satellite constituents, if one has a 19-year data time series, will get around this problem, although it may take plots such as those shown in Section 2.3.4 to understand and visualize the variation of each tidal constituent over the 19- (or longer) year period and the possible reasons for that variation.

2.2.5 Definitions Revisited, With Relationship to Harmonic Constants

In this section some of the basic definitions of various tidal quantities presented in Section 2.1.1 will again be looked at along with some new ones. In addition, the relationship of these tidal quantities to particular combinations of tidal harmonic constants will be looked at. Although most

2. Theory Behind Tidal Analysis and Prediction

of these tidal quantities are typically derived directly from data, namely, from tabulations of observed high waters and low waters, in some cases they can also be calculated from the amplitudes and phase lags resulting from a harmonic analysis (although not always with a simple formula). For shorter data series, the harmonic constituent method has sometimes been preferred, the assumption being that it eliminates meteorological effects, which for a short data time series could contaminate the results. On the other hand, if the data series is too short, the harmonic constants being used may not be accurate enough (see Section 3.3). The harmonic method does have the advantage of providing some insight as to where such quantities come from and how they may vary with time, but generally these quantities are still usually obtained directly from long data time series. Much of what is presented in this section is covered in more detail in Special Publication 260 (S.P.260) (U.S. C&GS,1952), which includes some additional terms not covered here.

Type of tide was defined in Section 2.1.1 as being either *semidiurnal*, *mixed*, or *diurnal*, and examples of stations that are semidiurnal, mixed, or diurnal were shown in Figure 2.1. However, there was a caution given about the difference between applying this phrase (as well as the terms semidiurnal, mixed, and diurnal) to the tide on a particular day at a station versus applying this phrase to the station itself, in the sense of classifying that station as being semidiurnal, mixed, or diurnal. A station might be classified as being *mixed*, but there will be days at that station where there will be only one HW and one LW and thus the tide on such days would be called *diurnal*.

There have been a variety of definitions proposed for classifying a station according to type-of-tide categories and these definitions make use of the tidal harmonic constants at the station. Such definitions are usually based on the $(K_1+O_1)/M_2$ amplitude ratio [or the $(K_1+O_1)/(M_2+S_2)$ ratio], and sometimes take into consideration the difference in their epochs (phase lags), usually defined as $\frac{1}{2}(M_2^\circ-K_1^\circ-O_1^\circ)$. When using one of these type-of-tide classification schemes, one must remember that the chosen classification is an overall one and does not apply to every day of the month. Stations will look mixed (that is, have two unequal high waters a day) at one time of the month but can look diurnal (have only one high water per day) at other times of the month. The combined effect of the K_1 and O_1 contributions varies throughout the month. The maximum K_1+O_1 combined effect occurs once every 13.66 days, near maximum northern declination of the moon or maximum southern declination (referred to as *tropic tides*). This occurs when the K_1 and O_1 constituent curves are in phase and the maximum contribution is the sum of the amplitudes of $K_1 + O_1$. Likewise the phase difference between the M_2 , K_1 , and O_1 contributions also varies throughout the month. Figure 2.19 (which is reworked from S.P. 260, 1952) shows examples of tide curves for particular combinations of changing $(K_1+O_1)/M_2$ contribution ratios and changing $\frac{1}{2}(M_2^\circ-K_1^\circ-O_1^\circ)$ contribution phase differences, which show examples of semidiurnal, mixed, and diurnal tides.

In S.P.260 it is stated that if the $(K_1+O_1)/M_2$ ratio is less than 2.0, then the tide will be semidiurnal all the time, no matter what the phase relation among M_2 , K_1 , and O_1 . If the contribution ratio is greater than 4.0, then the tide will be diurnal all the time, no matter what the phase relation. However, these statements are being technically very picky, since they consider even a slight indication of a second low water or of a second high water as making the tide mixed. But as one can see in Figure 2.19, the curves for a ratio of 3.0 also look diurnal. And even the curves for a ratio of 2.0 look diurnal (but with what might be called double high waters or double low waters).

With regard to classifying *a station* as being semidiurnal, mixed, or diurnal, there has been a difference of opinion with regards to a standard set of tidal constituent amplitude ratio values that could be used for defining the type of tide at a station. The CO-OPS' *Tides and Currents Glossary* (CO-OPS, 2000) has for some time referenced the values used by Dietrich (1967), who gives four classifications: (1) a *semidiurnal* tide, which has a $(K_1+O_1)/M_2$ tidal constituent amplitude ratio of

less than 0.25; (2) a *mixed, mainly semidiurnal* tide, which has a ratio from 0.25 to 1.5; (3) a *mixed, mainly diurnal* tide, which has a ratio from 1.5 to 3.0; and (4) a *diurnal* tide, which has a ratio greater than 3.0. Using this classification scheme, the tide curve examples shown in Figure 2.1 include semidiurnal, mixed, and diurnal tide curves. Boston has an $(K_1+O_1)/M_2$ amplitude ratio of 0.19 and is semidiurnal. San Francisco (Golden Gate) has an $(K_1+O_1)/M_2$ amplitude ratio of 1.03 and is mixed, mainly semidiurnal. Seattle has an $(K_1+O_1)/M_2$ amplitude ratio of 1.21 and is also mixed, mainly semidiurnal (but with a stronger diurnal signal). Dutch Harbor, Alaska, has an $(K_1+O_1)/M_2$ amplitude ratio of 2.07 and is mixed, mainly diurnal.

Dronkers (1964) references earlier ratio values given by the Coast and Geodetic Survey, which are also given by Marmer (1926), which includes 0.5 as the upper limit for semidiurnal tides and 2.0 as the lower limit for diurnal tides, with mixed tides in between. Dronkers also states that the French (in 1964) instead use the $(K_1+O_1)/(M_2+S_2)$ tidal constituent ratio, and define semidiurnal as below 0.25, diurnal as above 1.25, and mixed as in between 0.25 and 1.25. Defant (1961) also uses $(K_1+O_1)/(M_2+S_2)$ ratios, but his categories are: semidiurnal for a ratio less than 0.25; mixed, mainly semidiurnal for ratios between 0.25 and 1.5; mixed, mainly diurnal for ratios between 1.5 and 3.0; and diurnal for ratios above 3.0. Parker (1977) uses Defant's classification for classifying the type of tide in his study of the tidal hydrodynamics of the Strait of Juan de Fuca - Strait of Georgia. The

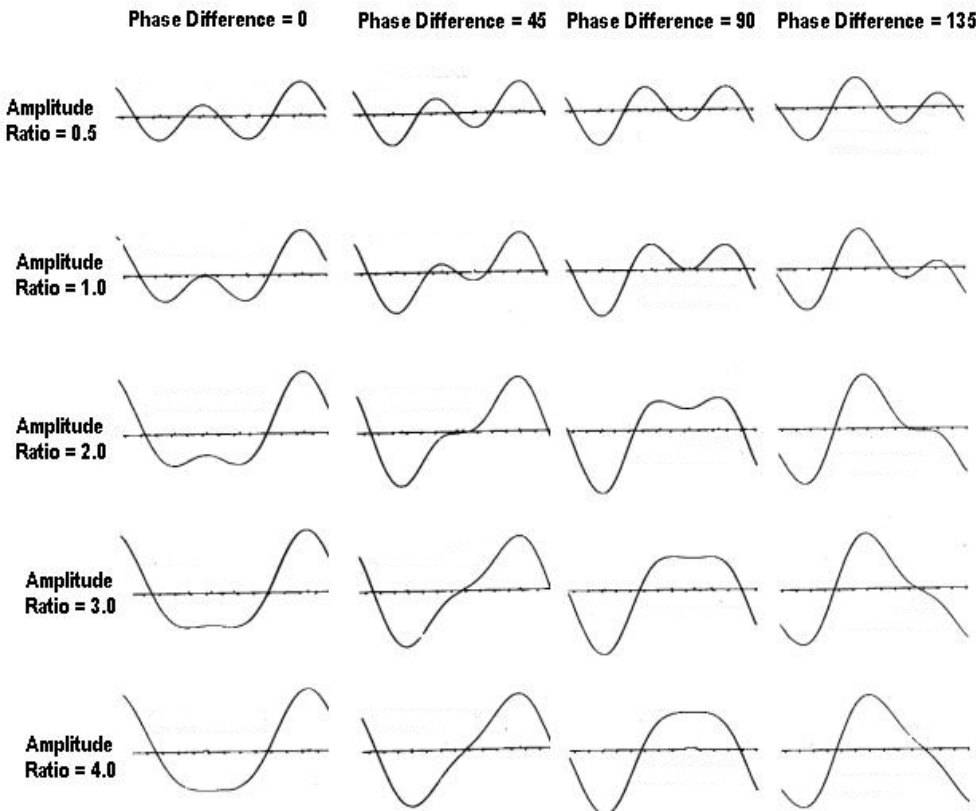


Figure 2.19. Tide curves for particular combinations of $(K_1+O_1)/M_2$ amplitude ratios and phase differences (in degrees) defined as $\frac{1}{2}(M_2^\circ-K_1^\circ-O_1^\circ)$. See text for discussion. Each tick along the horizontal axis is two hours. (Reworked from S.P. 260, 1952. The second row is also found in Zetler (1959), but with the phase difference defined without the “ $\frac{1}{2}$ ”.)

2. Theory Behind Tidal Analysis and Prediction

results are shown in Figure 2.20. The type of tide in this long deep waterway begins at the entrance to the Strait of Juan de Fuca as *mixed, mainly semidiurnal*, then slowly changes to *mixed, mainly diurnal*, and then slowly changes back to *mixed, mainly semidiurnal* up the entire Strait of Georgia. The highest $(K_1 + O_1)/(M_2 + S_2)$ tidal constituent amplitude ratio is 2.3 at Pedder Bay, a little southwest of Victoria, British Columbia, Canada. The tide station at Victoria is classified as *mixed, mainly diurnal*, but if one looks in the Tide Tables, the tide at Victoria with one HW and one LW on a given day (thus being diurnal for that day) occurs 44% of the time. This percentage is an average for a whole year, since it will vary from month to month. However, this again might be considered as a technical fine point, since when one looks at the Tide Tables there are many days that show two HWS and two LWS, but the LHW and HHW are close in value and the HLW between them is also close in value, so that the tide looks diurnal with a double high water. Calling the tide diurnal on days when this happens, the tides are actually diurnal 77% of the time at Victoria.

When the tide is mixed the order in which HHW, LHW, HLW, and LLW occur is called the *sequence of tide*. Table 2.3 (reworked from S.P. 260) shows the sequence of tide for different phase relationships among the contributions of M_2 , K_1 , and O_1 , this phase difference being the $\frac{1}{2}(M_2^{\circ} - K_1^{\circ} - O_1^{\circ})$. Thus, for example, the sequence of tide might be HHW, LLW, LHW, HLW or it might be

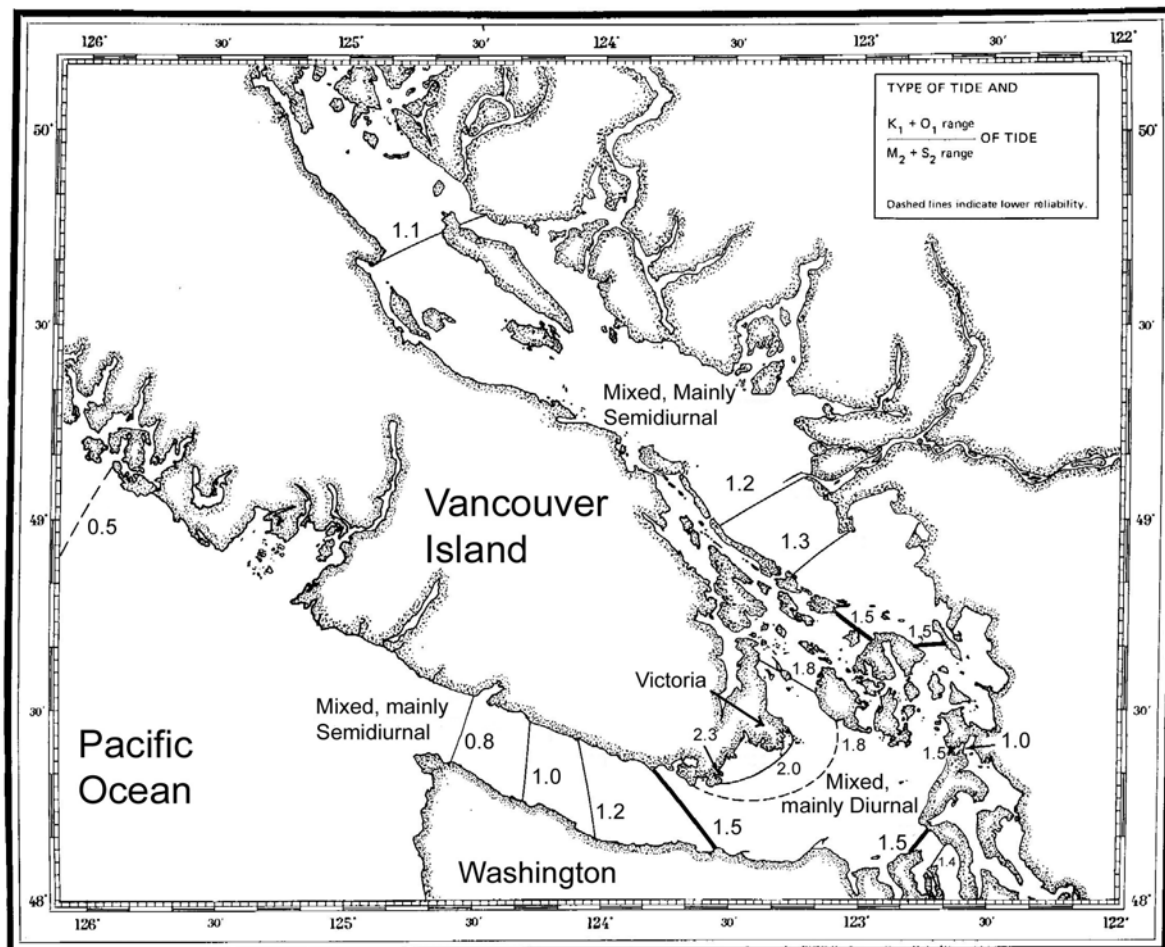


Figure 2.20. Chart illustrating the geographic variation in the $(K_1 + O_1)/(M_2 + S_2)$ tidal constituent amplitude ratio, as well as the *type of tide* classification for each region in the Strait of Juan de Fuca – Strait of Georgia. (From Parker, 1977)

LLW, HHW, HLW, LHW, or situations where the two low waters are almost equal or the two high waters are almost equal.

When there is a mixed tide, the diurnal effect can *accelerate* the time of high water, that is, make high water occur earlier than if there was no diurnal effect, or *retard* the time of high water, that is, make high water occur later. The acceleration or retardation of the high and low waters are also indicated in Table 2.3 for different phase relations.

One can also see in Figure 2.19 examples of the sequence of tide and acceleration/retardation of HW or LW indicated in Table 2.3. For example, in this figure when the phase difference of the M_2 , K_1 , and O_1 contributions has become 45° and the contribution ratio is 0.5, one can see that the sequence of tide is HHW, LLW, LHW, HLW, and that the HHW is accelerated while the LLW is retarded (thus the tide rises more quickly to high water and falls more slowly to low water).

With all the various effects on the heights of high and low waters (and thus on the tide range) and their timing, one ends up with a whole host of tidal definitions. *Mean high water* (MHW) is the average of all the high waters over some time period, and similarly for *mean low water* (MLW). In practice this time period is typically 19 years (the 18.6-year lunar nodal cycle rounded to the nearest year) and is called the National Tidal Datum Epoch. The *mean range* of tide (M_n) is the difference between mean MHW and MLW, in other words, the average of all the tidal ranges over some time period. The average height of the high waters at spring tide is called *mean high water springs* (MHWS) or *spring high water*, and similarly for *mean low water springs* (MLWS). The (mean) *spring range* (S_g) is MHWS minus MLWS and is the average range occurring at the time of spring tides. It is larger than the mean range, but is used only if the type of tide does not have a strong diurnal signal. In the latter case the diurnal range is used (see below). Analogously, the (mean) *perigean range* (P_n) is the average range occurring at the time of perigean tides.

When there is a significant diurnal inequality, a different set of high and low water and tidal range definitions is more useful. *Mean higher high water* is the average of all the higher high waters for some time period (again usually 18.6 years), and similarly for *mean lower low water* (MLLW), *mean lower high water* (MLHW), and *mean higher low water* (MHLW). The *great diurnal range*,

Table 2.3. Table showing the effect of the phase difference $P = \frac{1}{2}(M_2^\circ - K_1^\circ - O_1^\circ)$ on the sequence of tide and the acceleration (acc) or retardation (ret) of the high or low water.

$P = \frac{1}{2}(M_2^\circ - K_1^\circ - O_1^\circ)$	1 st HW of day	1 st LW of day	2 nd HW of day	2 nd LW of day
0°	HHW same	LW* ret	LHW same	LW* acc
$0^\circ < P < 90^\circ$	HHW acc	LLW ret	LHW ret	HLW acc
90°	HW* acc	LLW same	HW* ret	HLW same
$90^\circ < P < 180^\circ$	LHW acc	LLW acc	HHW ret	HLW ret
180°	LHW same	LW* acc	HHW same	LW* ret
$180^\circ < P < 270^\circ$	LHW ret	HLW acc	HHW acc	LLW ret
270°	HW* ret	HLW same	HW* acc	LLW same
$270^\circ < P < 360^\circ$	HHW ret	HLW ret	LHW acc	LLW acc

2. Theory Behind Tidal Analysis and Prediction

or just referred to as the *diurnal range*, is the difference in height between MHHW and MLLW. The (mean) *tropic higher high water* is the average of the higher high waters occurring at times of maximum lunar declination, and likewise for the (mean) *tropic lower low water*. The *great tropic range* (G_c), or just *tropic range*, is the difference in height between tropic higher high water and tropic lower low water.

The timing of high waters has always been referenced to the moon's transit, either over the location of the tide gauge or over a time meridian. A *lunitidal interval* is the interval between the moon's transit (upper or lower) over the local time meridian or the Greenwich meridian and the following high or low water. (The transit is designated as *upper transit* when it crosses the time meridian near the tide gauge, and as *lower transit* when it crosses the meridian that is 180 degrees from the tide gauge location.) The *mean high water lunitidal interval*, or simply the *high water interval* (HWI), is the average of all intervals between the moon's transit and the following high waters, for all phases of the moon, and similarly for *mean low water lunitidal interval*, or simply the *low water interval* (LWI). When there is a diurnal inequality in the tide, separate intervals are calculated for the higher high waters, lower high waters, higher low waters, and lower low waters. These are designated respectively as *higher high water interval* (HHWI), *lower high water interval* (LHWI), *higher low water interval* (HLWI), and *lower low water interval* (LLWI). In such cases, and also when the tide is diurnal, it is necessary to distinguish between the upper and lower transit of the Moon with reference to its declination. Intervals referenced to the moon's upper transit at the time of its north declination or the lower transit at the time of south declination are usually marked **a**. Intervals referenced to the moon's lower transit at the time of its north declination or to the upper transit at the time of south declination are usually marked **b**. There is also a historical term that is sometimes still seen, the *establishment of the port* (also called the *vulgar establishment*), which is the average high water interval on days of the New Moon and Full Moon. The term *high water full and change* (HWF&C) is more often used today. HWF&C is typically ten or fifteen minutes earlier than HWI.

There is usually a delay between the exact occurrence of new moon or full moon and the occurrence of spring tides. That delay is called the *age of the tide* (or sometimes the *age of phase inequality* or simply the *phase age*) and is often on the order of a day or two, but it can be negative (that is, spring tide in some locations, due to hydrodynamics, can come before new moon or full moon).

There are also a variety of other *ages*. The *age of parallax inequality* is the interval between the exact time when the moon reaches perigee and when the maximum effect (of the smaller distance between the moon and Earth) is seen on the tide range. The *age of diurnal inequality* is the interval between the exact time when the moon reaches maximum northern declination or maximum southern declination and the maximum effect of this upon the range of tide (the tropic tide).

All of these *ages* can be calculated from the relevant tidal harmonic constituent epochs. The age of tide is the time required for the M_2 and S_2 tidal constituents to arrive at a phase agreement. It can therefore be obtained by dividing the difference in their epochs by the difference in their frequencies (i.e., their angular speeds). The resulting formula for the age of the tide is thus

$$\text{Age of the tide (in hours)} = 0.984 (S_2^\circ - M_2^\circ)$$

in which the epochs can be local or Greenwich. Similarly, the age of parallax inequality is the time required for the M_2 and N_2 tidal constituents to arrive at a phase agreement. Again, dividing the

difference in their epochs by the difference in their angular speeds, the formula for the age of parallax inequality is thus

$$\text{Age of parallax inequality (in hours)} = 1.837 (M_2^\circ - N_2^\circ).$$

And similarly, the age of diurnal inequality is the time required for K_1 and O_1 to arrive at phase agreement, and the appropriate formula is

$$\text{Age of diurnal inequality (in hours)} = 0.911 (K_1^\circ - O_1^\circ)$$

Each of the types of tide range can also be defined according to the amplitudes of particular tidal harmonic constants, but the formulas are not as simple as one might expect unless one is interested in an approximate result. In S.P.260 one finds fairly elaborate formulas that require the use of a form (Form 180) and tables in order to calculate values. Doodson and Warburg (1941, page 95) on the other hand, provide much simpler formulas for what they term “approximate” values of the tidal quantities. They give approximate values of the mean range of tide, the spring range, and the neap range as:

$$\begin{aligned}\text{Mean range} &= 2M_2 \\ \text{Spring range} &= 2(M_2 + S_2) \\ \text{Neap range} &= 2(M_2 - S_2)\end{aligned}$$

These formulas assume there are not significant shallow-water overtones, M_4 and M_6 .

S.P.260, however, states that the mean range is actually a little larger than twice the M_2 amplitude because of the effects of some other semidiurnal constituents (even ignoring the effects of M_4 and M_6). It uses a table (Table 4, page 50) showing the effect of S_2 on the range of tide, and another (Table 5, page 51) showing the effect of K_1 and O_1 on the range of tide. Zetler (1959) provides approximate average values based on S.P.260 that are still quite simple and a small refinement of the Doodson and Warburg values, i.e.,

$$\begin{aligned}\text{Mean range (long period average)} &= 2.2 M_2 \\ \text{Spring range (at new and full moon)} &= 2.1 (M_2 + S_2) \\ \text{Neap range (at quadrature)} &= 2.1 (M_2 - S_2) \\ \text{Perigean range (moon closest to Earth)} &= 2.2 (M_2 + N_2) \\ \text{Apogean range (moon farthest from Earth)} &= 2.2 M_2 - 1.7 N_2 \\ \text{Tropic range (diurnal range at extreme declination)} \\ \text{for the special case of } M_2 \ll (K_1 + O_1) &= 2 (K_1 + O_1)\end{aligned}$$

2.3 Hydrodynamic Considerations

Only the oceans are large enough for the tide-generating forces to directly produce a tide of significant size. As the tide wave generated in the ocean propagates onto the continental shelf and into bays and estuaries (Figure 2.10), it is hydrodynamics (determined by the dimensions of the ocean, bays, and rivers) that becomes the critical issue. It is the hydrodynamics that determines how large the tide range will be and when the high and low waters will occur. It is the hydrodynamics that determines how fast the tidal currents will flow and when slack waters will occur; and it is the

2. Theory Behind Tidal Analysis and Prediction

hydrodynamics that determines how significant the diurnal signal will be compared with the semidiurnal signal.

In terms of harmonic analysis and prediction, the tidal frequencies may be determined by the astronomy, but the values of the amplitudes and epochs result from the hydrodynamics. Full and partial reflections of the very long tidal waves, the nearness of basin lengths or shelf widths to resonance for particular tidal frequencies, continuity effects, frictional damping, and advective/inertial effects all affect the tide and tidal currents. Even very long-term variations such as that due to the 18.6-year regression of the lunar node can be affected by nonlinear hydrodynamics, so that 18.6-year variations in a tidal constituent may not exactly match the variation expected from astronomical considerations.

In shallow waterways the hydrodynamics also transfers tidal energy, through various nonlinear processes, to new frequencies, creating overtides and compound tides (especially within the semidiurnal band). These so-called *shallow-water tidal constituents* can be larger than many of the astronomically generated tidal constituents. These same nonlinear processes also lead to interactions between the tide and other nontidal phenomena such as storm surge and river discharge, which must be considered when analyzing water level or current data for the tidal signal. To fully understand the tide and to be able to interpret the results of a tidal analysis, one must have a basic understanding of tidal hydrodynamics, an overview of which is provided in the following sections. More details will be provided in Chapter 7 as determined from mathematical models.

2.3.1 Hydrodynamic Effects On Tide Ranges and Phase Lags and Tidal Current Speeds

When the very long tide wave generated in the ocean reaches the shallow water of the continental shelf and the even shallower water of the bays and rivers, it is slowed up, amplified, modulated, and distorted by a number of hydrodynamic mechanisms.

To understand what happens to a tide wave in a bay or river, it is helpful to first look at two opposite extremes in idealized waves. Neither of these tide waves actually exist in a real waterway, because they ignore friction, but they are useful in visualizing a real tide wave, which is always some where between these two extremes.

If there is no friction and a long tide wave enters an endless river (that is, this tide wave is not reflected back at some point), that wave will propagate up the river as a *progressive wave* (see Figure 2.21). For a progressive tide wave, the crest of the wave (namely, high water) moves progressively up the river, as does the trough of the wave (namely, low water). In such a progressive tide wave the maximum flood current (namely, when the current is flowing the fastest up the river) occurs at the same time as high water, and the maximum ebb current (namely, when the current is flowing the fastest down the river) occurs at the same time as low water. Slack water, when the current speed is zero, occurs exactly half way between high water and low water. (In a real river with the energy dissipating effects of bottom friction, such a progressive wave would be damped, and thus would slowly decrease in amplitude, and high water and maximum flood current would not coincide. For now, however, this discussion will assume that there is no friction.)

If the river is of constant width, the amplitude (tide range) of this frictionless progressive tide wave will not change as it moves up the river. However, if the width decreases as one moves up the river, then the amplitude (tide range) will increase, because the same amount of water is being forced through a smaller opening. If the depth of the river decreases there is a similar though less dramatic amplifying effect (which in the real world is generally out weighed by the increased frictional energy loss due to the shallower depths).

If this frictionless river is closed off at some point (e.g. by a dam) or there is a frictionless bay, then the tide wave progressing up the river or bay will be reflected at the closed end, and will travel back down the river or bay. This reflected wave is not observable by someone on the shore because it is superimposed on the next incoming tide wave propagating up the bay, and it is the combination of the two waves that is observed. The resulting combined wave is called a *standing wave*, because the high and low waters do not progress up the bay (see Figure 2.22). The water surface simply moves up and down everywhere at the same time, with the greatest tide range at the head of the bay.

With a standing tide wave, the tide range decreases as one moves from the head of the bay toward the ocean entrance, and if the bay is long enough, reaches a point where the tide range is zero (for this idealized frictionless example), that point being called a *node*, and then starts increasing again (see Figure 2.22). This node occurs at $\frac{1}{4}$ of a tidal wavelength from the head of the bay. (In a progressive wave, high water comes $\frac{1}{2}$ a wavelength before low water, so if the high water of a progressive wave travels a distance equal to $\frac{1}{4}$ of a tidal wavelength up the bay to the head, where it is reflected, and then travels $\frac{1}{4}$ of a wavelength back down the bay, it will have gone $\frac{1}{2}$ a wavelength and so coincide with low water of the next incoming progressive wave, and the two will cancel each other out at that location, producing a zero tide range, the node.) For a standing wave, high waters occur at the same time everywhere on one side of the node, which is the same time that low waters occur on the other side of the node. The strongest tidal currents occur when water level is near mean tide level, halfway between the times of low water and high water. At the times of high water and low water there is no current flow (slack water). The water flows into the bay, stopping the inward flow at high water, reverses direction, flows out of the bay until low water, at which time it reverses again and starts flowing into the bay again.

One finds the largest tide ranges in bays that are exactly $\frac{1}{4}$ of a tidal wavelength long, due to what is called *resonance*. When the water in the bay is forced to move up and down by the tide at

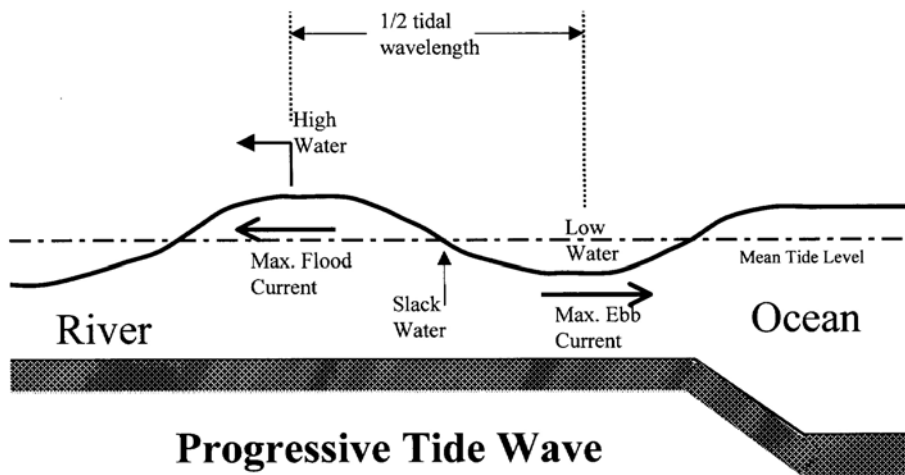


Figure 2.21. An idealized frictionless tide wave propagating up a river as a progressive wave. High water occurs later as one moves upstream, and maximum flood occurs at the same time as high water. The tidal wavelength is typically on the order of hundreds of miles. (From Parker, 2004.)

2. Theory Behind Tidal Analysis and Prediction

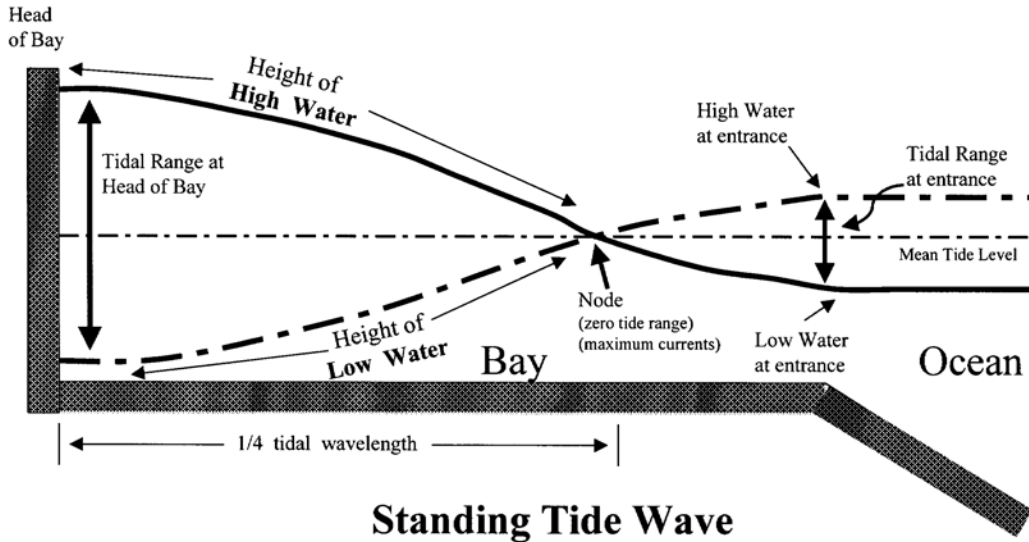


Figure 2.22. An idealized frictionless tide in a bay as a standing wave (the water level is shown for two opposite extremes, high water and low). High water occurs at the same time everywhere on one side of the node (the point of zero range) and maximum flood current occurs half way between low water and high water. With friction there is no point of zero tide range, only a point with a minimum tide range, and the times of high water progress slightly up the bay. (From Parker, 2004.)

the entrance, it will freely oscillate (slosh up and down and back and forth) with a natural period that depends directly on the bay's length and inversely on the square root of its depth. If the basin has the right combination of length and depth so that the natural period is exactly the same as the tidal period, then the oscillation inside the bay will be synchronized with the oscillation at the entrance due to the ocean tide. In other words, the next ocean tide will be raising the water level in the bay at the same time that it would already be rising due to its natural oscillation (stimulated by the previous ocean tide wave), so that both are working together, thus making the tide range inside higher. (In the real world friction keeps these resonating oscillations from being infinitely large, by taking away some of the energy.) The tidal wavelength is determined by the depth of the bay, and when the length of the bay equals $\frac{1}{4}$ of a tidal wavelength, then the bay's natural period of oscillation will be the same as the tidal period.

In the above discussions bottom friction was left out of the discussion, but bottom friction greatly affects all hydrodynamics and is especially important in shallow waters. Because of bottom friction the tide wave in real bays actually falls in between the extremes of pure progressive wave and pure standing wave described above. This is because friction reduces the amplitude of the tide wave as it travels. Thus, the reflected wave will always be smaller than the incoming wave, especially near the bay entrance (since the reflected wave has traveled the longest to get all the way back to the entrance), and the combination of the two *frictionally damped progressive waves* will not be a pure standing wave. There will be no point of zero tidal range (no real node), but only an area of minimum tidal range (a *quasinode*). There will be some progression of high waters and low waters up the bay, but not as quickly as a pure progressive wave. This progression will be faster near the entrance and slowest near the head of the bay. Maximum flood or ebb currents will not occur exactly half way between high water and low water. A basin $\frac{1}{4}$ of a wavelength long will still

produce the largest possible tidal range at the head of the bay, but friction keeps that tide range much smaller than it would be without friction.

In some bays the very high tide range at the head of the bay is due to a combination of both a narrowing width and a near resonant situation (due to the right length and depth). The highest tide ranges may involve several amplifications, the bay being perhaps connected to a gulf which is perhaps connected to a wide continental shelf, with amplifications of the tide wave occurring in each basin. This is the case with the Bay of Fundy tides, the tide wave being already amplified by the continental shelf and the Gulf of Maine prior to entering the Bay of Fundy (see Section 7.4.2).

(Formulas representing the effects described above are derived mathematically in Section 7.4.1, except for the width effects, which are derived in Section 7.4.2.)

If a bay is wide enough one also sees larger tide ranges on the right side of the bay (looking up the bay) due to the Coriolis effect. The Coriolis force, a fictitious force due to observing motion from the rotating reference frame of the Earth (see Parker, 1998), acts perpendicular to the flow of the water, thus pushing water currents to the right in the Northern Hemisphere (and to the left in the Southern Hemisphere) as they flow. For a pure progressive tide wave (no friction), at high water the tidal current flows up the bay, so the tidal height will be greater on the right-hand shore than on the left-hand shore. At low water the tidal current flows down the bay, so the tidal height will be lower on the right-hand shore than on the left hand shore. The result is that the tide range (high water minus low water) will be greatest on the right-hand shore (looking up the bay).

For a pure standing wave (no friction) the pattern of high water caused by the Coriolis force is more complicated, and is shown in the upper half of Figure 2.23. This figure shows lines of constant tidal range (*corange lines*), as well as lines of locations with the same time of high water (*cotidal lines*), in an idealized rectangular basin for the case where the effect of bottom friction is ignored. A single point of zero tidal range (a *node*) occurs in the center of the bay $\frac{1}{4}$ of a tidal wavelength from the head of the bay. This figure comes close to representing the corange and cotidal lines in a bay that is very deep. A more typical case, including the damping effect of bottom friction, is shown in the bottom half of Figure 2.23. In this case the node has moved to the left (when looking up the bay) and becomes a *virtual node* since it is on land. (See Section 7.5 for derived mathematical formulas describing this effect.) One can see some similarity between the pattern of corange lines in the lower half of Figure 2.23 and the corange lines in Figure 2.5 for the Strait of Juan de Fuca - Strait of Georgia, (although the latter has many geographic variations not included in the simple regular basin of Figure 2.23), and likewise for the cotidal lines in Figure 2.23 and Figure 2.6. In Figure 2.5 the pattern of a quasinode is also seen to the southwest of Victoria. A similar pattern, including a quasinode on the western shore near Smith Point, is also apparent in the M_2 coamplitude (half the tide range) chart for Chesapeake Bay shown in Figure 2.24.

The largest tide ranges are found in bays that are close to $\frac{1}{4}$ of an M_2 tidal wavelength long, such as the Bay of Fundy-Gulf of Maine (Canada), Ungava Bay (Canada), Bristol Bay (United Kingdom), Gulf of St. Malo (France), Cook Inlet (Alaska, US), the Gulf of Cambay (India), and the eastern end of the Magellan Strait (Chile). Huge tide ranges are not restricted to bays. If the continental shelf is the right combination of depth and width, a near resonant situation can also result. This is the reason for the 40-foot tidal ranges along the coast of southern Argentina. The continental shelf there is over 600 miles wide, and includes the Falkland Islands near the edge of the shelf (where the tide range only reaches 6.5 feet). The distance from the Argentinean coast to the edge of the shelf is fairly close to $\frac{1}{4}$ of a tidal wavelength for that depth of water. Essentially, that wide shelf has a natural period of oscillation that is fairly close to the tidal period.

2. Theory Behind Tidal Analysis and Prediction

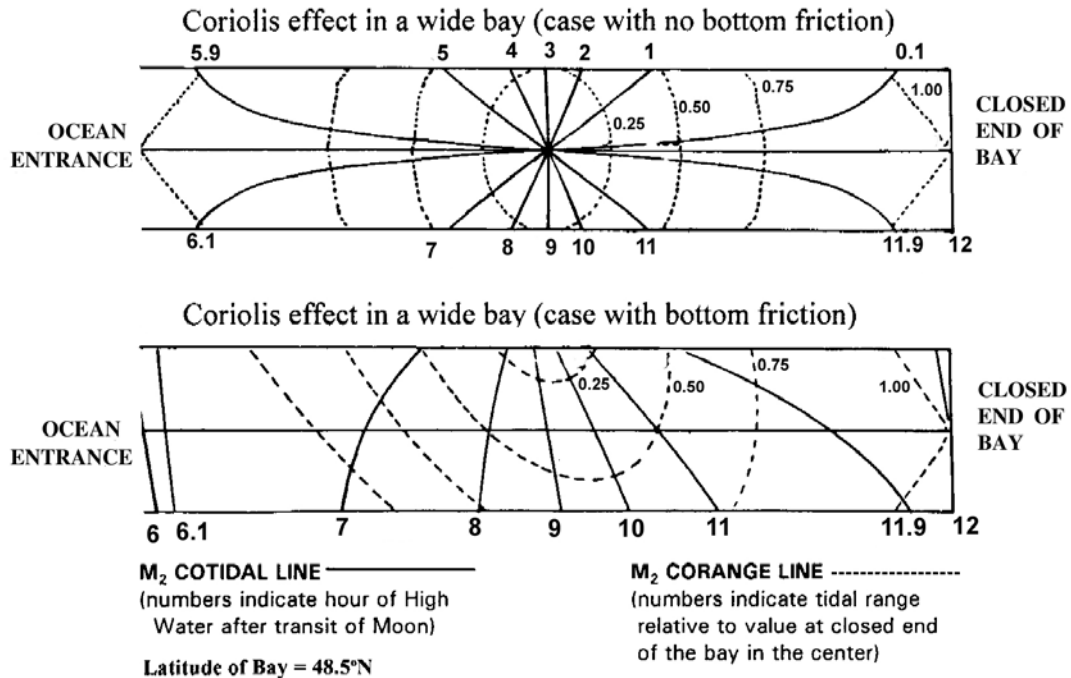


Figure 2.23. The effect of Coriolis force on the M₂ tide range (corange lines) and the time of high water (cotidal lines) for an idealized rectangular bay. The top panel shows the case with no bottom friction and has a single point of zero tide range (the node) in the middle of the bay. The bottom panel includes the effect of bottom friction, and there is no point of zero tide range.

The largest tidal currents in bays tend to be near the entrances. Maximum tidal current speeds are zero at the head of the bay (since there is no place for the water to flow). As one moves down the bay toward the ocean the maximum flood and maximum ebb tidal current speeds increase, with the greatest speeds occurring at the entrance, or, if the bay is long enough, at the area of smallest tide range (the nodal area). However, if the width of the bay decreases at any point, the current speeds will be increased in that narrow region (since the same volume of water is being forced to flow through a smaller cross-section, it must flow faster). This can be especially dramatic if there is a sudden decrease in width and depth. The largest tidal currents are found in narrow straits in which the tides at either end have different ranges or times of high water (see Section 2.3.6g). Where a strait suddenly becomes very narrow or where it bends, eddies and whirlpools can be formed as the result of the sheltering effect of the land and the inertia of the coastal flow.

The dimensions of a basin can also determine the size of the diurnal tidal signal compared with the usually dominant semidiurnal tidal signal (also see Section 7.4.1). A particular bay could have a natural period of oscillation that is closer to the diurnal tidal period (approximately 24.84 hours) than to the semidiurnal period, thus amplifying the diurnal forcing at the entrance to the bay more than the semidiurnal signal. Depending on the size of the diurnal signal at the entrance the result could be a mixed tide or a diurnal tide. At such locations (such as parts of the Gulf of Mexico) the tide will be diurnal near times of maximum lunar declination, but will be mixed near times when the moon is over the equator.

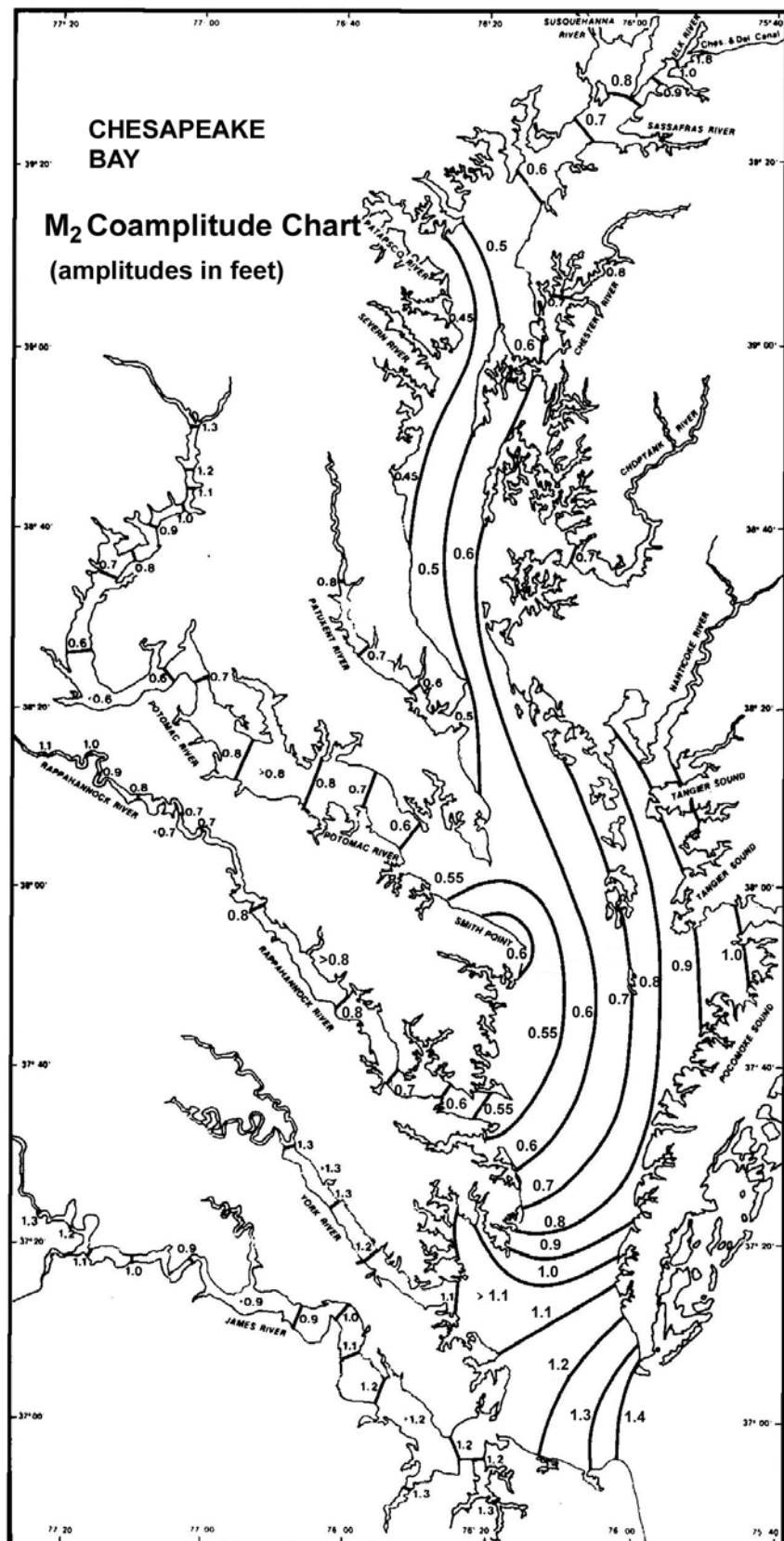


Figure 2.24. M₂ coamplitude chart for Chesapeake Bay (in feet). (From Fisher, 1986.)

2. Theory Behind Tidal Analysis and Prediction

The wavelength, λ , of a tide wave in a bay depends on the depth of the water, D , and on the tidal period, T , according to $\lambda = T(gD)^{1/2}$ (if frictional effects are ignored). The shallower the bay the shorter the wavelength. The longer the tidal period the longer the wavelength. A diurnal tidal component has a wavelength twice as long as a semidiurnal tidal component since its period is twice as long. When a waterway is shallow enough and long enough so that more than $1/4$ of a semidiurnal wavelength fits in the waterway, there will be a nodal area with a very small semidiurnal tidal range. This will be an area where the diurnal tide could dominate, since the diurnal tide would still be large at the semidiurnal nodal area (the diurnal node being twice as far from the head of the bay). Thus near the head of the waterway the tide could be semidiurnal, but near the semidiurnal nodal area the tide could be mixed or even diurnal. This is the case near Victoria, British Columbia, at the southeastern end of Vancouver Island (see Figure 2.20). At that location along the Strait of Georgia–Strait of Juan de Fuca waterway, the semidiurnal tidal component decreases to a minimum, but the diurnal component does not, and so the tide becomes diurnal, while at the northern end of the Strait of Georgia the tide is mixed, mainly semidiurnal.

Whether due to a basin size conducive to amplifying the diurnal signal or due to the existence of a semidiurnal nodal area (leaving the diurnal signal as the dominant one), there are numerous areas around the world with strong diurnal tides – places like Norton Sound in Alaska near the Bering Strait, and various (but not all) locations in the Philippines, New Guinea, and the islands of Indonesia. In southern China, at Beihai, and at Do Son, Vietnam, the diurnal signal is very dominant, with tidal ranges that reach 15 feet and 10 feet respectively (near times of maximum southern declination of the moon). In these locations the tide remains diurnal even when the moon is over the equator.

2.3.2 Nonlinear Effects of Shallow Water – Overtides and Compound Tides

The shallower the water depth is the more the tidal wavelength will shorten and the faster the tidal characteristics of a waterway will change with horizontal (geographic) distance. When the tidal wavelength is shortened to near the length of a bay or river basin, this can bring the dynamic situation closer to resonance and increase the tide ranges. [Or, one can also look at it from the point of view of the shallower depths increasing the natural periods of a bay or river basin to be closer to the tidal period.]

Shallow water, however, can have other effects on the tide. It can, for example, distort the shape of the tide wave, that is, make it very asymmetric, so that its rise and fall (and its flood and ebb) are no longer equal (see the second curve in Figure 2.25). The tide can then no longer be described by a simple sine wave (the first curve in Figure 2.25). In some cases such distortion leads to double high waters or double low waters (see the third curve in Figure 2.25). The extreme case of distortion is a tidal bore (the fourth curve in Figure 2.25), when the tide wave becomes so steep that it is essentially breaking and it moves up a river as a turbulent wall of water.

Shallow water distorts the tide through several mechanisms that are *nonlinear* – that is, in the equations of motion (which will be discussed in Sections 7.3 and 7.6) each mechanism can be tied to a specific term in which key parameters (such as elevation, η , or velocity, \mathbf{u}) multiply each other, which leads to energy transfer. (Linear terms contain only one key parameter and their separate effects simply add, with no interaction.)

The speed, **C**, at which a long tide wave travels depends on the depth of the water, **D**, approximately as the formula $C=(gD)^{1/2}$. When the depth of the water is much greater than the tidal range, the speed of the crest of a tide wave and the speed of the trough are virtually the same, since the tide wave itself has only a very small effect on the total water depth. However, in the shallow water where the depth is not much greater than the tide range, the total water depth under the crest is significantly larger than the total water depth under the trough. In this case, the crest of the wave (high water) travels faster than the trough of the wave (low water). If the tide wave travels far

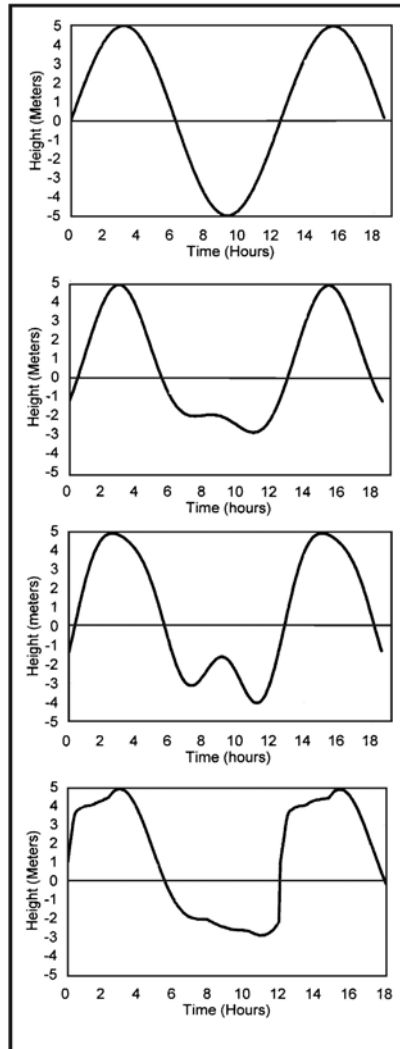


Figure 2.25. Typical tide curves (over 1½ tidal cycles) for an area with no shallow-water effect (top panel) and for three areas with increasing degrees of distortion caused by the shallow water. The third panel shows a double low water. The fourth panel shows the almost instantaneous rise in water level due to the passage of a tidal bore. (From Parker, 1999)

2. Theory Behind Tidal Analysis and Prediction

enough, the crest begins to catch up with the trough ahead of it (which is falling behind the crest ahead of it). Thus, high water arrives sooner than it would in deeper water, and there is a faster rise to high water and a slower fall to low water. This can be seen in the water level curves in Figure 2.26 as one moves further up the Gironde River (in France).

In other waterways the tide wave will not be progressive since it will reflect back from a closed end (or from a sudden width decrease) and produce a more standing wave. Most waterways are somewhere in between progressive and standing (see Section 7.4.1). The shape of the tide curve could perhaps look more like that shown in the second curve in Figure 2.25 (or one of the curves in Figure 2.26). In terms of harmonic constituents, this distortion transfers energy from M_2 into the second harmonic, a constituent called M_4 , with half the period of M_2 . Combining an M_2 tide curve and an M_4 tide curve, one can produce the distorted tide curves shown in Figure 2.25, with the M_4/M_2 ratio increasing as one goes from top curve to bottom curve in that figure. The third curve shows a double low water, but with a different phase relationship between M_2 and M_4 one could obtain a double high water.

Another shallow-water distorting mechanism is caused by bottom friction, which can have both asymmetric and symmetric effects. The asymmetric effect (similar to that just discussed and represented in Figure 2.25) results because friction has a greater effect in shallow water than in deep water (there being less water to have to slow down), and so it slows down the trough more than the crest, contributing to the distortion of the tide wave and the generation of M_4 . The symmetric effect results because energy loss due to friction is proportional to the square of the current speed. This means that there will be much more energy loss during times of maximum flood and maximum ebb

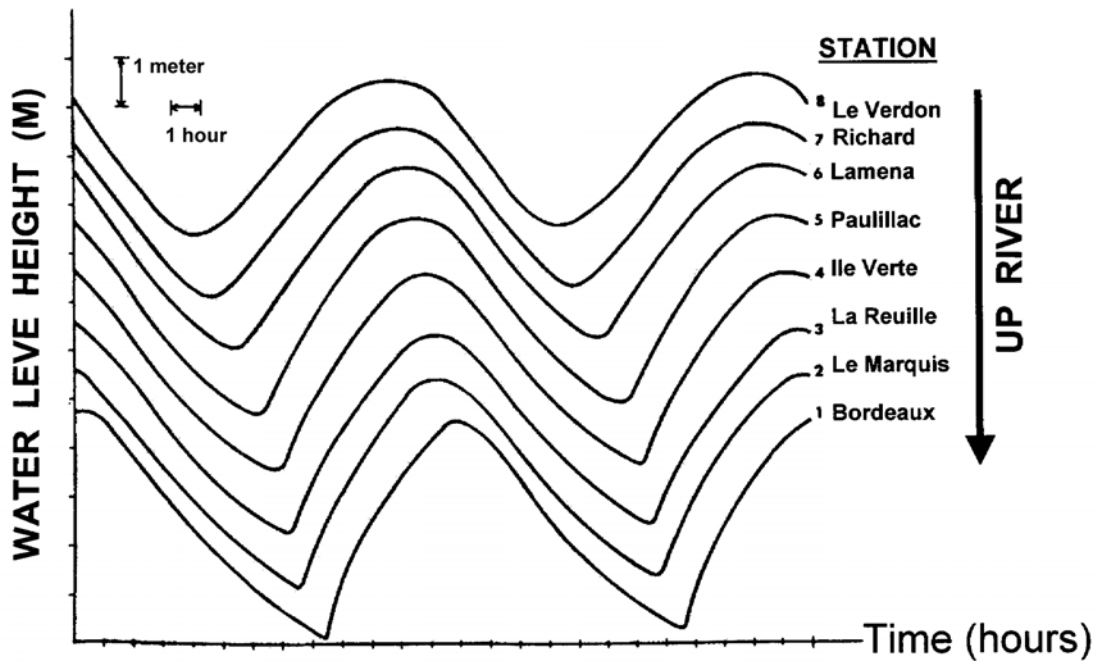


Figure 2.26. Water level curves from the Gironde River in France showing the effect of nonlinear shallow-water distortion. At LeVerdon (just inside the river entrance) the rise to high water takes about an hour longer than the fall to low water, while at Bordeaux the fall takes 4 hours longer than the rise. (Reworked from George and Simon, 1984.)

than near times of slack water (or minimum flow). This results in the generation of another higher harmonic, M_6 , with a period of one third that of M_2 . This effect, combined with the asymmetric effect, can lead to double high or low waters (see third curve in Figure 2.25).

Higher harmonic tidal constituents like M_4 and M_6 are referred to as *overtides* (a term analogous to the term *overtones* in acoustics). M_4 is the first overtide, and the second harmonic of M_2 . M_6 is the second overtide and the third harmonic of M_2 . M_8 is the third overtide and the fourth harmonic of M_2 . Whereas M_4 and M_6 are generated by first-order nonlinear processes, M_8 is generated by second-order nonlinear processes (that is, it is generated by nonlinear effects on M_6).

Friction dissipates energy from the entire tide wave and slowly wears the entire wave down. However, if, as the tide wave propagates up the river, the river's width is decreasing significantly, this can keep the amplitude of the wave high in spite of the friction. Thus, the tide wave can continue to travel up a narrowing river, getting more and more distorted in shape. A further distortion can be caused by the river flow interacting with the tide (see below). In the extreme case the distortion from all these effects can lead to the creation of a tidal bore (see fourth curve in Figure 2.25).

The above symmetric quadratic friction effect also causes the interaction of two tidal constituents, such as M_2 and N_2 . M_2 and N_2 go in and out of phase over a 27.6-day cycle (perigee to apogee to perigee). In this case the greatest energy loss occurs when M_2 and N_2 are in phase and producing the strongest tidal currents, and the lowest energy loss occurs 13.8 days later with M_2 and N_2 are out of phase and producing the weakest tidal currents. Because energy loss is proportional to the square of the current speed, the increased energy loss when M_2 and N_2 are in phase is greater than the decreased energy loss when they are out of phase, and the result is that each constituent will be smaller than if it existed without the other present. The reduction in N_2 (due to M_2) will be greater than the reduction in M_2 (due to N_2), because M_2 is much greater than N_2 . However, M_2 will be reduced by the combined interactions of all the other tidal constituents.

There is a 27.6-day modulation of this energy loss from M_2 and N_2 and this produces two new *compound* tidal constituents called $2MN_2$ and $2NM_2$. (Similarly, the above asymmetric mechanisms also cause interactions between constituents, producing higher frequency constituents such as MN_4 from M_2 and N_2 .) Table 2.4 lists many overtides and compound tides and shows which nonlinear mechanisms can produce them. These shallow-water effects that distort and modulate the tide (and, as will be seen, cause interactions with storm surge and river discharge) are called *nonlinear* effects because the mechanisms that produce these effects are represented by several *nonlinear* terms in the equations of motion used to model the tidal hydrodynamics. These various nonlinear mechanisms that lead to the generation of overtides and compound tides are described in more detail in Section 7.6, with mathematical derivations and physical explanations. Table 2.4 is based on a Fourier decomposition of the one-dimensional nonlinear hydrodynamic equations (described in Section 7.6), from which four basic nonlinear mechanisms are identified for this simple one-dimensional case.

The two classical nonlinear shallow-water terms, $\partial(\eta\mathbf{u})/\partial\mathbf{x}$ in the one-dimensional continuity equation, and $\mathbf{u}\partial\mathbf{u}/\partial\mathbf{x}$ in the one-dimensional momentum equation (where η is the water level elevation, \mathbf{u} is the current, and \mathbf{x} is distance), produce asymmetric effects, that is they affect one half of the tidal cycle differently than the other half of the cycle, and this leads to even harmonic overtides and low-frequency compound tides. The same asymmetric results are also produced by the effect of elevation on the frictional momentum loss per unit volume of fluid, as first pointed out by Parker (1984).

2. Theory Behind Tidal Analysis and Prediction

M_2 interacting with constituent $C \Downarrow$	Tidal Constituents Generated With Frequency:				
	$ \sigma_{M2} - \sigma_C $	$(2\sigma_{M2} - \sigma_C)$	$(\sigma_{M2} + \sigma_C)$	$(2\sigma_{M2} + \sigma_C)$	$(4\sigma_{M2} - \sigma_C)$
M_2	mean *	-----	M_4	M_6	M_6
N_2	MN (Mm)	$2MN_2$ (L_2)	MN_4	$2MN_6$	$4MN_6$
S_2	MS (MSf)	$2MS_2$ (μ_2)	MS_4	$2MS_6$	$4MS_6$
K_1	MK_1 (O_1)	$2MK_3$ [MO_3]	MK_3 [$2MO_3$]	$2MK_5$ [$3MO_5$]	$4MK_7$ [$3MO_7$]
O_1	MO_1 (K_1)	$2MO_3$ [MK_3]	MO_3 [$2MK_3$]	$2MO_5$ [$3MK_5$]	$4MO_7$ [$3MK_7$]
Nonlinear terms responsible →	$\partial(\eta u)/\partial x$ $\eta u u $ $u \partial u / \partial x$ $u u $ with a mean flow	$u u $	$\partial(\eta u)/\partial x$ $\eta u u $ $u \partial u / \partial x$ $u u $ with a mean flow	$u u $	$u u $
symmetric or asymmetric NL mechanism	asymmetric	symmetric	asymmetric	symmetric	symmetric
in terms of σ_r **	σ_r	$\sigma_{M2} + \sigma_r$	$\sigma_{M2} - \sigma_r$	$3\sigma_{M2} - \sigma_r$	$3\sigma_{M2} + \sigma_r$

* the mean can be in the form of a residual mean circulation or a shift in mean sea level
** $\sigma_r = |\sigma_{M2} - \sigma_C|$

Table 2.4. Compound and overtide constituents generated by four nonlinear terms in the one-dimensional equations of motion. The nonlinear terms are explained in the text. C is any tidal constituent listed in the first column. A constituent in () is an astronomical constituent with the same frequency as the compound tidal constituent. A constituent in [] is another compound constituent with the same frequency. See text, as well as Sections 7.3 and 7.6 for the mathematical treatment behind this table. (reworked from Parker, 1991a)

This is represented by the term $\eta u |u|$, which is actually the second term of the binomial expansion of the one-dimensional friction term, $u |u|/(1+\epsilon\eta)$, where the elevation is in the denominator and ϵ is a scaling factor (ϵ = tidal amplitude/depth). (See Section 7.6.) Quadratic friction, $u |u|$, can also produce an asymmetric effect and these same constituents if there is a mean flow present, such as river flow. However, without a mean flow present, quadratic friction primarily produces symmetric effects that lead to odd harmonic over tides as well as to compound tides in the semidiurnal band. A few of these compound tides have the same frequencies as particular astronomical constituents, for example, $2MN_2$ has the same frequency as L_2 , and $2MS_2$ has the same frequency as μ_2 . And two compound tidal constituents produced by different nonlinear mechanisms can also have the same frequency, such as $2MK_3$ and MO_3 . Not shown in this table, the lateral inertial terms in the 2-dimensional or 3-dimensional momentum equations can also produce asymmetric effects in tidal currents similar to those produced by the four terms mentioned above (see Section 7.6.7 and Parker, 1991a).

Until the 1970's tidal analysts had simply treated these shallow-water tidal constituents as being the sums or differences of the astronomical constituents, and paid little attention to the specific

nonlinear hydrodynamic mechanism that produced them. In particular the quadratic frictional nonlinear mechanism for generating compound tides and over tides was ignored for decades after Proudman (1923) had first proposed it. For example, it was assumed that M_6 was produced from M_4 via the classic shallow-water nonlinear continuity term (actually a second-order effect) rather than directly from M_2 via quadratic friction (a first-order effect).

Quadratic friction produces many compound tidal constituents that have the same frequency as particular astronomical constituents. The compound tidal constituent $2MN_2$, for example, has the same frequency as the astronomical constituent L_2 , but a very different node factor. In coastal regions and especially up into bays and estuaries, $2MN_2$ is much larger than L_2 , yet L_2 was often still used for predictions. Use of the L_2 node factor for (in reality) the $2MN_2$ constituent can lead to the effect of this constituent being doubled or halved in predictions for other years (than the year that was analyzed). The compound tidal constituent $2MS_2$ has the same frequency as the astronomical constituent μ_2 , but in this case both constituents should theoretically have the same node factor.

The node factor for M_6 was often calculated by cubing the node factor for M_2 (for example, this was erroneously done in Schureman, 1958), as though M_6 was a third-order harmonic resulting from the same asymmetric nonlinear phenomenon that produces M_4 , i.e. generating M_6 from M_4 in the same way that M_4 is generated from M_2 . However, a Fourier decomposition of the hydrodynamic equations (see Section 7.6) shows that M_6 is primarily due to the symmetric nonlinear effect of quadratic friction and is a first-order effect, so that the node factor should equal the square of the node factor for M_2 . The effect of not understanding the origin of shallow-water constituents, and thus of perhaps choosing the wrong node factor, can really add up for a location like Anchorage,

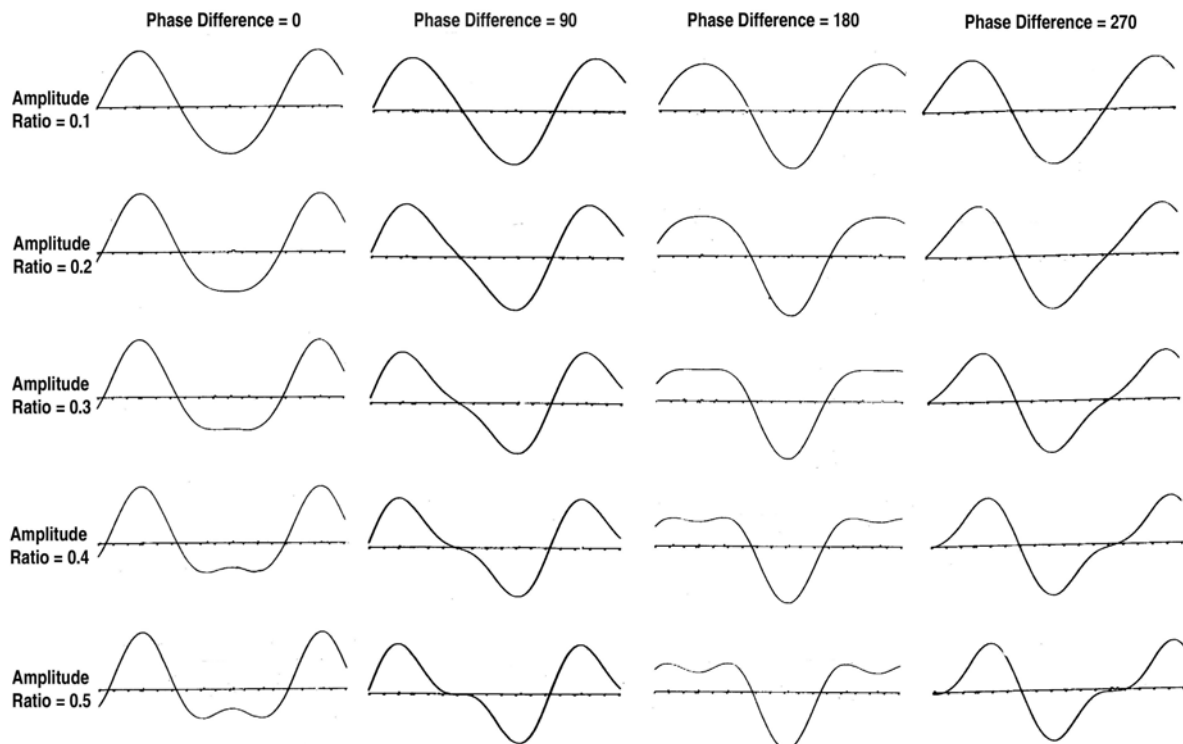


Figure 2.27. Tide curves for particular combinations of M_4/M_2 amplitude ratios and $2M_2^{\circ}-M_4^{\circ}$ phase differences (in degrees). See text. Each tick on the horizontal axis is one hour. (Reworked from S.P.260, U.S.C.&G.S., 1952.)

2. Theory Behind Tidal Analysis and Prediction

Alaska, at the northern end of Cook Inlet, where most of the 114 constituents used by CO-OPS to predict the 30-foot range tides are shallow-water constituents.

The way in which a tide or tidal current curve is distorted by the nonlinear effects of shallow water depends on the hydrodynamics of the particular waterway. There is a correlation between the particular shape of the curve and the amplitudes and epochs of the overtide constituents relative to the semidiurnal constituents. Figure 2.27 shows examples of tide curves for particular combinations of M_4/M_2 amplitude ratios and phase differences between M_4 and M_2 (defined as $2M_2^{\circ} - M_4^{\circ}$). The effect of M_4 on M_2 is asymmetric, that is, it affects one half of the tidal cycle differently than the other half. For an amplitude ratio of 0.3 and a phase difference of 0° , one sees in this figure a steepening of high water and a flattening of the low water, the latter often referred to as a *stand of tide* (at low water). If the amplitude ratio approaches 0.5, one sees double low waters. The same applies to high waters if the phase difference is 180° , in which case for an amplitude ratio of 0.3 there will be a stand of tide at high water and a steeping of low water, and for a ratio of 0.5 there will be double high waters. For a phase difference of 90° one sees a flattened area of the curve near the mean tide level point of the falling tide; here the tide has a slow fall from high water to low water and a rapid rise from low water to high water. For a phase difference of 270° there is again a flattened area around mean tide level, but this time during the rising tide, which is now slower than the rapid fall.

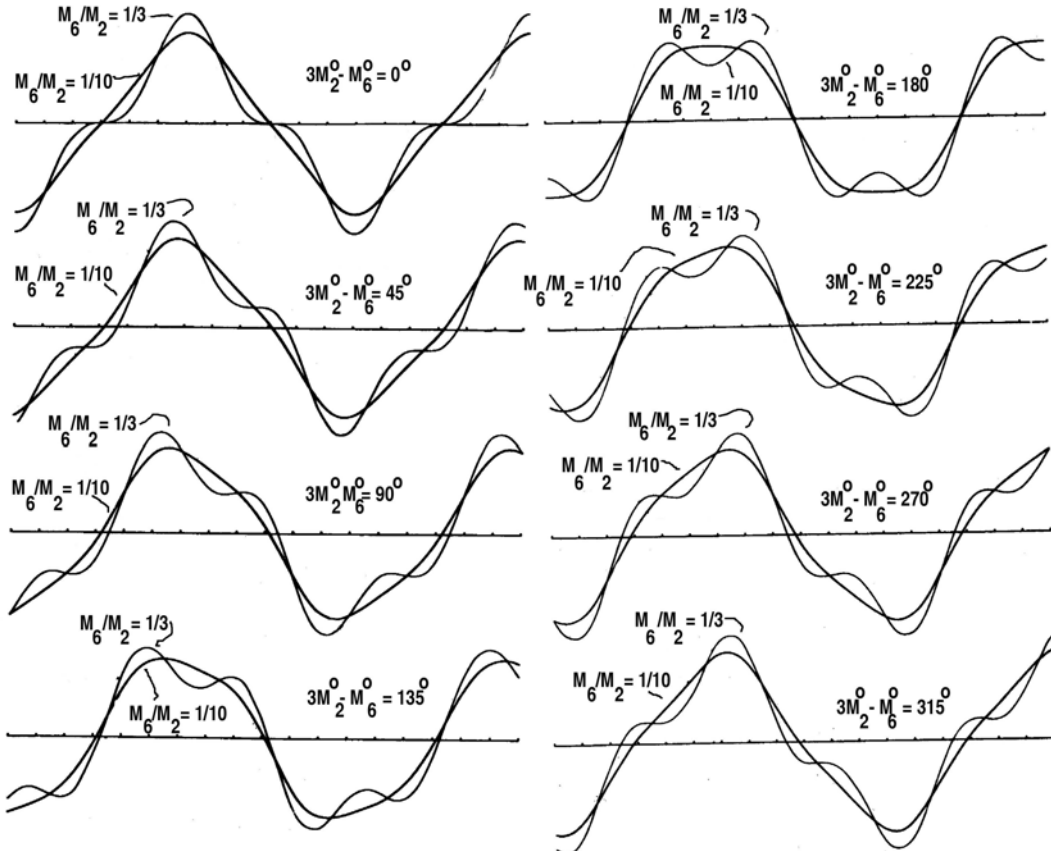


Figure 2.28. Tide curves for particular combinations of M_6/M_2 amplitude ratios and $3M_2^{\circ} - M_6^{\circ}$ phase differences. Each tick mark along the horizontal axis is one hour. (Reworked from S.P. 260, U.S.C.&G.S., 1952.)

Figure 2.28 shows examples of tide curves for particular combinations of M_6/M_2 amplitude ratios and phase differences between M_6 and M_2 (defined as $3M_2^{\circ}-M_6^{\circ}$). The effect of M_6 on M_2 is symmetric, that is, it affects both high waters and low waters in the same way. Depending on the phase difference this can mean flattening both high and low waters or making them both steeper. However, if M_6 is present there will always be an M_4 , so M_6 would never act solely on M_2 . A double high water, for example, is more likely caused by a combination the effects of both M_4 and M_6 , with, for example, M_4 flattening out high water and M_6 causing the minimum between two high water peaks. M_6 can affect the overall tide range. The asymmetric effect of M_4 will probably not significantly affect the overall tide range, but it will significantly shift the times of high water (often earlier) and low water (often later).

M_8 is often larger than many of the compound constituents shown in Table 2.4. This table only goes up to seventh diurnal tidal constituents (e.g., $4MK_7$), because it includes only constituents generated by a first-order nonlinear interaction between two astronomical constituents. M_8 is generated by the interaction of M_6 with M_2 via the asymmetric nonlinear terms. It often reaches a significant size only because M_2 is usually so much larger than the other tidal constituents.

2.3.3 Nonlinear Tidal Interaction With River Flow and Storm Surge

In a tidal river, water flow is due to both the tidal current and the river current itself (i.e., the fresh water flowing downhill). The result of the combined tidal current and river current is a faster and longer lasting ebb current phase and a slower shorter flood current phase. Far enough up a river, where the river flow is faster than the strongest tidal current, the flow of water will always be downstream. In this case, the speed of flow will oscillate, flowing the fastest downstream at the time when maximum ebb occurs further down the river and flowing the slowest downstream at the time when maximum flood occurs further down the river. This is a simple linear addition of the river current to the tidal current.

However, because of the shallow water, the river flow also nonlinearly interacts with the tide and distorts it, mainly due to the effect of bottom friction. As already mentioned, energy loss due to friction is proportional to the square of the total current speed. During ebb, the tidal current is in the same direction as the river current and the result is a larger combined ebb current, with increased energy loss. During flood, the tidal current is in the opposite direction as the river current and the result is a smaller combined current, with reduced energy loss. This not only has an asymmetric effect that distorts the tide (causing a faster rise to high water, delaying the time of low water, and increasing the size of M_4), but it also further wears down the entire wave because the increased energy loss during ebb is larger than the decreased energy loss during flood. In Figure 2.29 one can see the tide range shrink when the river discharge increases. (See also Sections 7.6.3 and 7.6.6c for the mathematical treatment of this effect.)

Another type of shallow-water effect causes interactions between the tide and low-frequency storm surges (generated by the wind) that have periods longer than tidal periods. In this case, when the water level is raised by an onshore wind, the water depth increases and changes the tidal dynamics, usually increasing the tide range. When an offshore wind lowers the water level, decreasing the water depth, the result is usually a decreased tidal range. As will be seen in Sections 7.6.4, 7.6.5, and 7.6.6d, it is the two asymmetric nonlinear terms that involve elevation (η) that have the most significant effect (e.g., see Table 7.1 in Section 7.6.6d).

Knowing that river discharge and storm surge can modify the tide, it is important when harmonically analyzing water level data to make sure that these data were not taken only during such

2. Theory Behind Tidal Analysis and Prediction

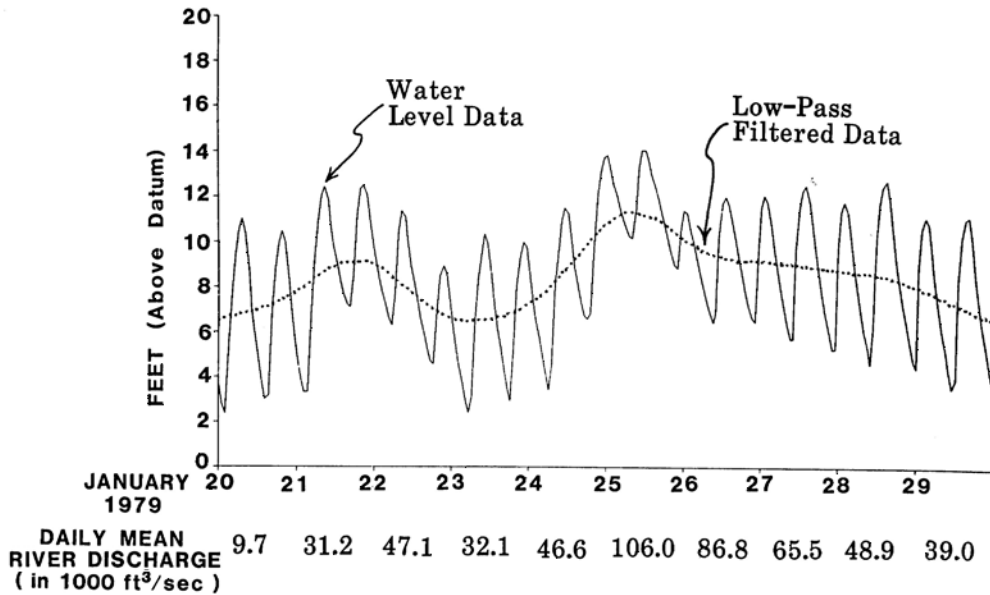


Figure 2.29. Water level data from the tide gauge at Trenton, NJ, during a high river discharge period (January 20-29, 1979). The tide range is reduced when the river discharge is high. (From Parker, 1984.)

meteorological events. For example, Figure 2.30 shows the results of a harmonic analysis of 15 days of data taken from six NOS water level stations during a high runoff period in the Delaware River in March 1978, compared with the results of a 15-day analysis of a low runoff period (chosen to have similar astronomical conditions). The three upriver stations show the effects of the higher river current speeds on the harmonic constants – the M_2 amplitude is reduced and the M_4/M_2 ratio is increased when the river flow is greatest. Down river, where it is wider and deeper and the river current speeds are much slower, these effects are not seen.

If a water level data time series includes a period with higher than average river runoff, and the harmonic constants calculated from this data record are used to make a tide prediction, then the tide will be under predicted for the rest of the year. This may be seen by looking at the two curves in Figure 2.31, which shows another high runoff period at the Trenton tide gauge in the Delaware River. The solid curve shows the tidal (high-pass filtered) portion of the water level record from that high runoff period. The dashed curve is the predicted tide for that time period if there had been no river runoff (based on 31 harmonic constants from a 7-month period when there wasn't high runoff). If one didn't have those harmonic constants from the 7-month data record, but only had constants from the high runoff period, then one would produce tide predictions (for the entire year) that would look more like the solid curve (including the distortion due to the increased M_4/M_2 ratio) than the dashed curve. This river example is a fairly extreme one, heavy runoff during a freshet period after a snow melt. Such extremes, with differences on the order of 3 to 5 feet in tidal range, are usually limited to only a short part of each year (at least for this river).

Storm surges, however, occur throughout the year (although they are generally more frequent and larger during the winter months). Subtidal storm surges (with periods longer than the tidal period) are the largest wind induced changes in water level, and, like river flow, they can also interact

15-Day Harmonic Analysis Results

LOW RUNOFF PERIOD:

August 11 - 25, 1979

Discharge: $4,593 \text{ ft}^3/\text{sec.}$

HIGH RUNOFF PERIOD

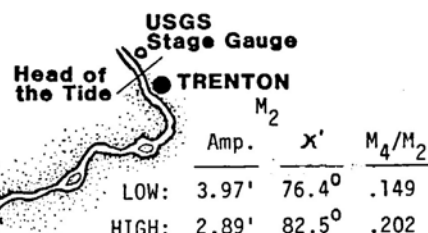
January 18 - February 1, 1979

Discharge: $40,826 \text{ ft}^3/\text{sec.}$

CHESAPEAKE AND
DELAWARE CANAL

PHILADELPHIA

	Amp.	M_2	κ'	M_4/M_2
LOW:	2.90'	44.3°	.093	
HIGH:	2.51'	45.1°	.120	



	Amp.	M_2	κ'	M_4/M_2
LOW:	2.90'	44.3°	.093	
HIGH:	2.51'	45.1°	.120	

ARTIFICIAL ISLAND

	Amp.	M_2	κ'	M_4/M_2
LOW:	2.87'	307.3°	.067	
HIGH:	2.53'	319.2°	.075	

Delaware Bay

	Amp.	M_2	κ'	M_4/M_2
LOW:	2.42'	248.2°	.019	
HIGH:	2.34'	246.4°	.010	

NAUTICAL MILES
0 5 10

LEWES
CAPE HENlopen

ATLANTIC
OCEAN

Figure 2.30. Comparison of 15-day harmonic analyses of water level from Delaware River and Bay during a high runoff period and during a low runoff period, both periods with similar astronomical conditions. κ' is the local epoch, i.e., the phase lag relative to the local time meridian (75°W). (From Parker, 1991a)

2. Theory Behind Tidal Analysis and Prediction

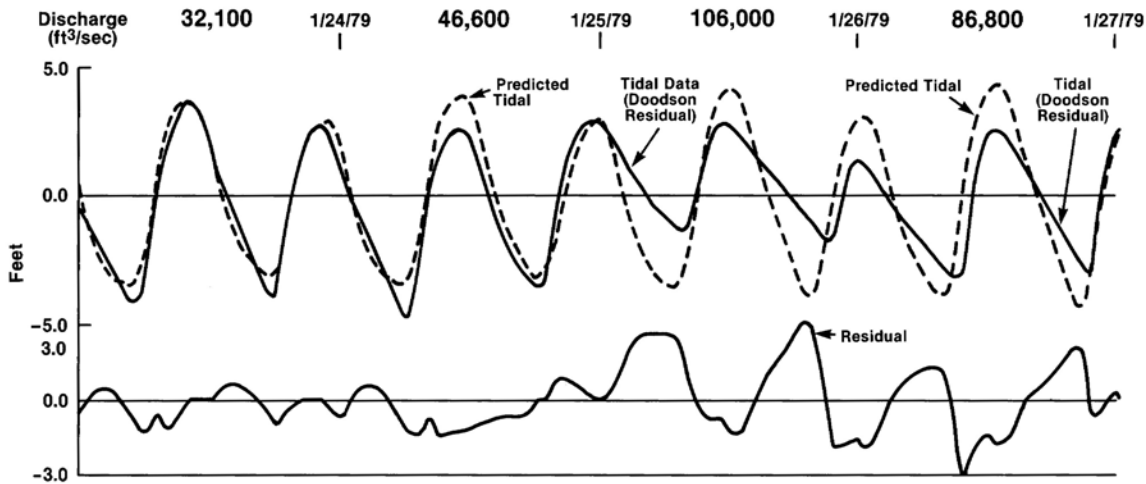


Figure 2.31. The tidal portion of a water level record from Trenton, NJ, on the Delaware River, during a high river discharge period (solid line) plotted with the tide predictions for the same time period as if there were no river discharge (dashed line). The difference in the two curves is shown in the lower plot. The tidal portion of the water level record was produced by filtering the water level with a Doodson tidal filter (see Section 3.8.2) and subtracting it from the water level time series. (From Parker, 1991a)

with and modify the tide. Figure 2.32 shows an example, also from Delaware Bay. This figure shows the tidal portion of water level records from NOS four water level stations in Delaware Bay and from the NOS water level station at Atlantic City (outside the Bay on the Atlantic Coast) along with the predicted tide curves based on harmonic constants from seven months of data. The bottom curve in the figure shows the subtidal water level signal at Atlantic City. The trough of a subtidal storm surge occurs on January 18th. Within the Bay there is not only a water level drop (not shown in these high passed water level curves), but a tide range reduction which increases as one moves up the Bay to Trenton. Late on the January 19th and into the 20th one sees crest conditions for the subtidal signal, and a corresponding tide range increase up the Bay (before the increased river discharge on the January 21st starts to have an effect).

Again, harmonic constants calculated from a time period with significant storm surge could have errors, especially if the record is short. If the record is not short and includes several subtidal crests and troughs, there may not be a dramatic affect on the harmonic constituents. What does happen, as seen in the frequency domain, is that the some of the energy in a tidal spectral line is smeared to both sides, forming a "cusp" around the line (see Section 3.10.2). This implies that some energy is lost from the tidal lines, and that the harmonic constant amplitudes are reduced to some degree.

During periods with large river discharge or large storm surge, the tide or tidal current cannot be predicted accurately using statistical/harmonic analysis methods. No matter how accurate the tidal harmonic constants are (in predicting the tide during most of the year), they cannot provide accurate predictions during strong nontidal events, because the tide has been changed by those strong nontidal events. If the nontidal phenomena themselves cannot be accurately predicted (which is often the case), then one cannot predict how the harmonic constants will be modified by those nontidal phenomena. Recently a statistical method called the *continuous wavelet transform* method

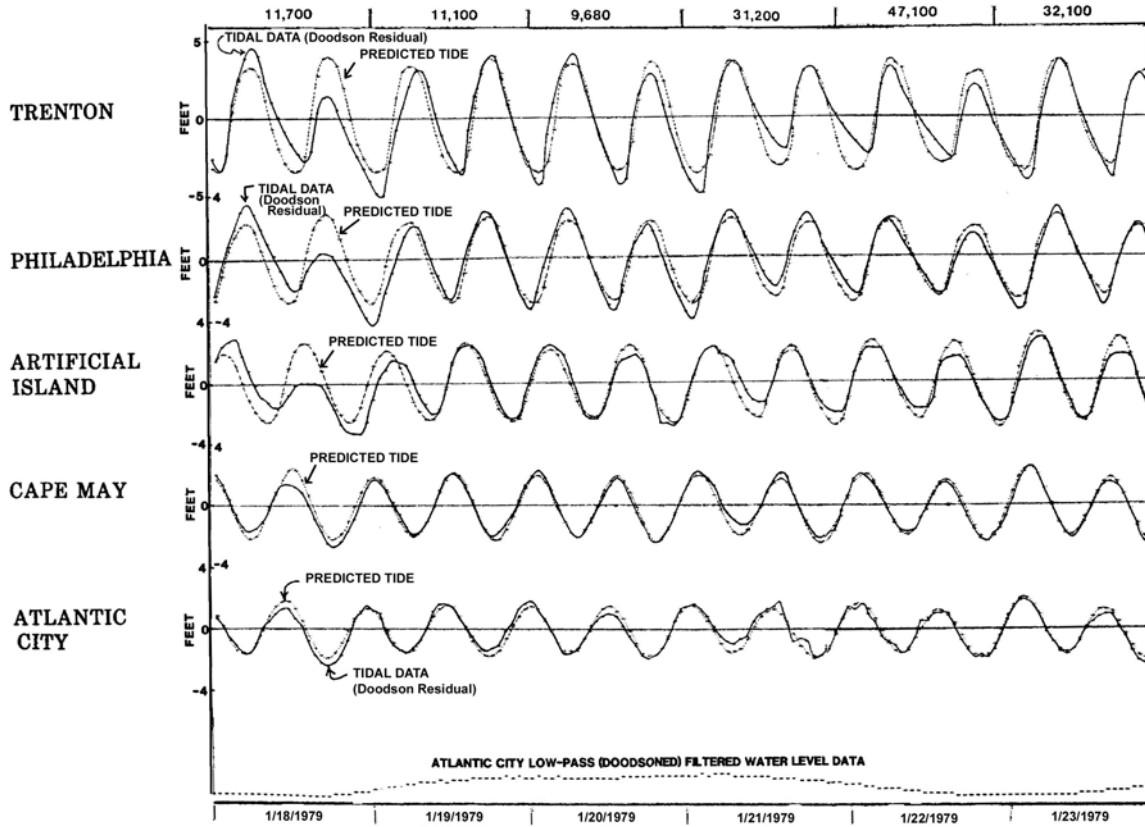


Figure 2.32. The tidal portion of the water level record plotted with tide predictions for three locations along the Delaware River and Bay and a station on the Atlantic Coast outside the Bay. The bottom curve is the low-pass filtered water level record from Atlantic City showing a subtidal storm surge. The upper curves show the effect of the storm surge on the tide (see text). (From Parker, 1991a)

was developed to try to deal statistically with the effect of strong nontidal events on the tide and tidal current. This method will be discussed in Section 3.5.5. Fully nonlinear hydrodynamic numerical models can easily handle the nonlinear interaction between the tide and river flow or storm surge, and they can do a fine job hindcasting or nowcasting strong nontidal events. They can also be used to forecast the water level (and currents) during such events if reasonably accurate forecast surface winds and other forecast meteorological parameters can be input into them.

Over the last two decades there has been much progress in providing real-time water level and current information to the maritime community. Such real-time data is needed because tide and tidal current predictions alone cannot give the mariner information about the often dramatic effects of wind on water levels and currents (Parker, 1986, 1995), and so the actual water level and current data are needed. For predictions into the future (beyond the time of the last real-time data points) numerical hydrodynamic models are also now being used operationally by NOS (driven by tide predictions, forecast winds, forecast atmospheric pressure, and forecast fresh water inflows) to find ways to forecast the nontidally-induced water level changes and current and their interactions with the tide and tidal current (see Section 8.6.3). Since such models are nonlinear, they automatically reduce (or increase) and distort the tide as necessary.

2.3.4 Nonlinear Hydrodynamic Effects On Node Factors

As discussed in Section 2.2.4, the 18.6-year variation in the lunar tidal force has typically been handled in a form that directly represents the modulation of each lunar tidal constituent using a *lunar node factor*, f . The f for each lunar tidal constituent is usually regarded as constant for the period of analysis (or prediction) and is typically obtained from astronomically-determined tables, such as Table 14 in Schureman (1958). However, there are hydrodynamic effects on these node factors, specifically through nonlinear interactions due to shallow water. To illustrate this one can look at how closely the long-term variation of uncorrected tidal constituents actually matches the variation predicted by astronomical considerations (using equilibrium tide theory).

Figure 2.33 shows the node factors calculated from harmonically analyzed water level data, specifically 19 uncorrected one-year least squares harmonic analyses of water level data from Philadelphia, Pennsylvania, on the Delaware River. For each tidal constituent, the 19 calculated (and uncorrected) amplitudes were averaged, and then each individual one-year constituent amplitude was divided by this 19-year average to obtain the calculated node factor. Also plotted in the figure are the astronomically determined mid-year node factors taken from Table 14 of Schureman (1958). Philadelphia is in a very dynamic location, located half way up a shallow estuary and affected by river discharge as well as storm surges that propagate into Delaware Bay from the wide Atlantic continental shelf.

It is apparent from the plots in Figure 2.33 that for most of the tidal constituents, the calculated node factor curve does not match the astronomical node factor curve very well. Before looking at these curves too closely, it should be remembered that other factors can affect tidal amplitudes over long periods beside the 18.6-year nodal cycle. For example, if a basin depth changed over the years due either to shoaling or dredging or land subsidence, the tide range could also change over the years. This could affect different tidal constituents differently depending on whether the change brings a constituent closer to or farther from resonance. Also, due to nonlinear frictional interactions, a change that made M_2 tidal currents stronger might decrease the other constituents. River discharge could also vary over the years, which would also make the tidal range vary. Changing frequency or size of storm surges over the years might also have a long-term effect. Thus, there are many potential causes of the year-to-year variation of tidal constituents, along with the 18.6 year-variation. Here, however, one merely is trying to see if there is any apparent 18.6-year variation, and if so, whether it is similar to the astronomically determined variation.

The two M_2 node factor curves in Figure 2.33 are difficult to compare because of the trend in the calculated curve (which shows an increasing M_2 tidal range over the 19 years). Removing that trend would give a minimum node factor at 1930, about 1.5 years earlier than the astronomical minimum node factor. The N_2 calculated node factor curve looks very little like the astronomical curve, and S_2 , being a solar constituent, should not show any lunar nodal variation at all (hence the straight dashed curve), but there are obviously variations from year to year. The two M_4 curves have minima at the same year, but do not look very similar otherwise. Only the two diurnal constituents show strong similarities between calculated and astronomical curves, with the two O_1 node factor curves showing a very good match, and the two K_1 node factor curves looking very similar but with the calculated curve lagging the astronomical curve by about a year.

There may be two reasons for the good match with the diurnal constituents. Quadratic-friction-caused interactions among the tidal constituents have more of an effect in the semidiurnal band, but perhaps more important may be the shape of the Delaware River and Bay estuary. The width of the upper Delaware estuary decreases exponentially at such a rate that, if the hydrodynamic system were

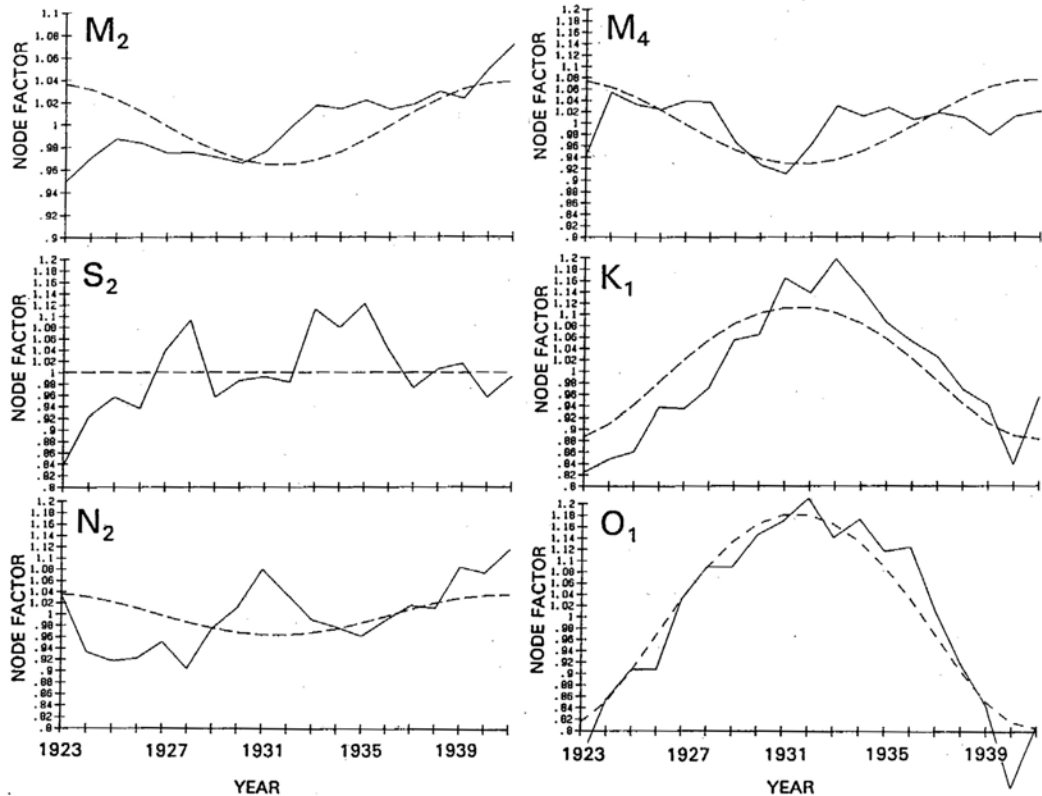


Figure 2.33. Calculated node factors (solid line) from 19 one-year uncorrected least squares harmonic analyses of Philadelphia water level data, plotted with the node factors determined from astronomical (equilibrium tide) consideration (dashed line), the latter taken from Schureman (1958). (From Parker, *et al*, 1999.)

frictionless, the dimensionless cutoff frequency, above which the solution is oscillatory and below which the solution is monotonic, would fall between the diurnal and semidiurnal bands (see Section 7.4.2). With friction included the monotonic solution becomes oscillatory, but the exponential width decrease still increases the K_1 wavelength much more than the M_2 wavelength, and the O_1 wavelength even more. It would seem that the exponential width decrease inhibits the hydrodynamics and thus inhibits the nonlinear interactions that would have modified the calculated diurnal node factor curves. (See Parker, 1984)

The fact that observed node variations for the semidiurnal constituents were found to be different than those values typically used in tide prediction (which were determined from astronomical/equilibrium tide considerations) has been pointed out by Amin (1976) and Godin (1986) for other waterways.

Thus, if for a particular application, one needs to obtain the highest possible accuracy in tidal harmonic constants and/or tidal predictions, one might consider (if they have very long water level time series) carrying out an analysis similar to the one done above for Delaware Bay above, and using the node factor variation obtained in that way rather than from astronomically based tables like in Schureman (1958). If one has a short station one could use the variation in node factor at a nearby long station. However, this is only useful for self-prediction or predictions into past time periods

2. Theory Behind Tidal Analysis and Prediction

with data. For future predictions, one would have to try to extrapolate the node factor curves into the future.

If one does have at least 19 years of data, one can also use satellite constituents (see Sections 2.2.4 and 4.1.5) in the harmonic analysis and do away with the use of node factors and the u portion of the equilibrium arguments altogether. This will work for the future as well as the past. This will include hydrodynamic effects on the 18.6-year variations, as well as any other long-term periodic variation for which satellite constituents were included. The only drawback of using satellite constituents is that it might be somewhat difficult to interpret the results. The plots such as those shown above are easier to understand and it is easier to visualize the variation of each tidal constituent over the 19- (or longer) year period and the possible reasons for that variation.

2.3.5 Zero-frequency Effects From Nonlinear Tidal Interaction

Tidal heights are referenced to some type of datum (see Section 2.1.1), typically the mean level of a particular key point on the tide curve. Datums such as mean lower low water (MLW) or mean high water (MHW) or mean tide level (MTL) are usually calculated by averaging over 19 years of data to eliminate the lunar nodal variations. Such datums may slowly change over the years due to a change in sea level, or due to slow vertical land movement (e.g., due to glacial rebound or sediment compaction), the latter looking like a sea level change to the water level gauge, which is held fast to the moving land. All the datums slowly move up and down with the long-term changes in relative sea level.

However, in shallow-water areas there can also be a *tidally induced change in "mean sea level"* due to nonlinear tidal effects. Here the "mean" results from averaging an asymmetry within a tidal cycle caused by the nonlinear effects, rather than from a uniform shifting up or down of the water level on which the tide propagates, but this is an effect that is included in the datum calculation. It is therefore an effect that should be considered when assessing long-term changes in sea level in a shallow-water area, since something as simple as dredging or shoaling can change the tidal hydrodynamics of a waterway and then also affect the value of mean sea level (and thus all the tidal datums). As one example, Parker (1984) used a nonlinear numerical model of the Delaware River and Bay to show that shallow-water nonlinear effects increased the mean sea level value near Philadelphia by an amount equivalent to 8% of the M_2 amplitude.

Tidal currents do not require datums, the zero current speed serving that purpose (if there is no mean current from a nontidal source). If there is a mean permanent current, such as due to a mean river flow or a mean wind drift, then the tidal current oscillates about that mean flow. Or, as was seen in Figure 2.4 (the fourth example), the entire tidal current ellipse can be shifted in the direction of the mean flow. But here again, the mean current can also be affected by the nonlinear tidal hydrodynamics causing an asymmetry within the tidal cycle. This can be due to not only shallow-water effects, but even more importantly by nonlinear lateral inertia effects (that do not need shallow water). Such *tidally induced residual currents* effects are discussed in Section 2.3.6e, as one of the many phenomena that appear in tidal currents but not in the tide.

2.3.6 Special Aspects of Tidal Currents

As will be seen in Chapter 5, the same methods of tidal analysis and prediction can be used for tidal currents, except that, since currents are vectors, the analysis is done twice, once for each of two orthogonal components (e.g., for the major and minor axes). However, there are many more

difficulties with tidal current analysis and prediction than with tide analysis and prediction. Godin (1988, 1991) describes various analysis approaches for tidal currents, and generally takes a very pessimistic view about how accurately they can be predicted. In this book we take a much less pessimistic view, for as long as the special aspects of tidal currents are kept in mind and accounted for in some fashion, there is no reason why accurate tidal current predictions cannot be made for most situations.

2.3.6a *Short current data times series*

In the past most current data records have been much shorter than water level data records, and shorter time series led to fewer tidal constituents that could be resolved and thus less accurate tidal current predictions and to the need for special methods to try to improve the accuracy of such predictions (see Section 5.4). These shorter time series were because current measurements have been more difficult and more expensive to acquire than water level measurements. Water level measurements are usually made on a pier or other coastal structure, where the gauge can be easily maintained, provided with power, connected to a real-time data acquisition system, and repaired if there is a malfunction. Until recently, current measurements could not be made from a pier or from land. Now with sideward-looking acoustic Doppler current profilers (ADCPs) and high frequency (HF) radar systems, that is no longer true, although there are still some limitations in these two new systems that make *in situ* current meters or bottom-mounted upward looking ADCPs still necessary. Such systems can now be more easily maintained for long periods of times, but they are still more expensive (in terms of operational maintenance cost) than water level gauges.

Current meters also tended to have fouling problem due to biological growth, or debris clogging the sensor (especially when propellers or rotors were used), so that only portions of a data time series could be used. Today's current sensors are less susceptible to fouling problems. Even ADCP's partially covered by sand waves have been shown to work well (up to a point). (See Section 5.3.3.)

2.3.6b *Noisy current data*

Current data also tends to be noisier than water level data, usually due to the effects of surface waves (water level data are also affected by waves, but usually not to the same extent). Wave motion can not only show up in the current data (and have to be averaged out in some fashion), but it can also cause various motions in the current meters themselves. This additional noise, however, varies considerably depending on the type of instrument used to measure the currents. In past decades current meters were hung from surface buoys that were very susceptible to the pitching and rolling caused by waves (although some buoys were specially designed to minimize such motions). Some of the early current meters were more susceptible to wave action, in terms of adding noise to the data record. For example, many current meters used savonius rotors to measure the current speed and a separate small vane to measure the current direction. The S-shaped savonius rotor would turn no matter which way the water was flowing (unlike a propeller), so fairly high (apparent) current speeds could be seen by a savonius rotor even during times of slack water, because the wave action would be turning the rotor. The small size of the vane allowed it to move so easily that the result was very noisy direction data. The savonius-rotor-small-vane combination led to serious noise problems when there was any kind of wave action at the water surface. Vector-averaging current meters, usually of the electromagnetic variety (but one variety had two propellers at right

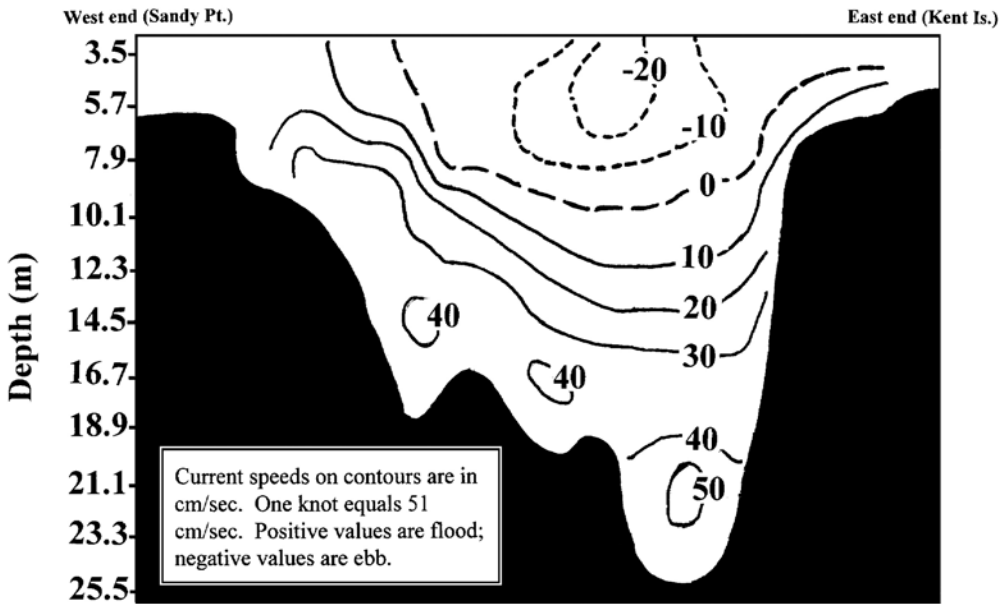


Figure 2.34. Current flow at one moment in time through a cross section near the Chesapeake Bay Bridge. (From Parker, 1997.)

angles to each other), did a much better job of not letting wave action influence the data. ADCPs also break up the current vector into orthogonal components (in this case covering portions of the water column), and also average over some time interval. Such time averaging (and spatial averaging in the case of the ADCP) reduces higher frequency noise (including the orbital motions of the waves). (See Section 5.3.3.)

2.3.6c Dramatic Spatial Variation in Tidal Currents – Vertically

Perhaps most important, the spatial variation of tidal currents, both vertically in the water column and horizontally (i.e., geographically), is much more complex than for tides. The tide, being the movement of the water surface, does not have a depth variation. Tidal currents, however, vary considerably from the surface to the bottom. Bottom friction is a major cause of this variation. The tidal current is slowest near the bottom and faster nearer to (but usually not at) the water surface. Usually the tidal current will turn (from flooding to ebbing, or vice versa) earlier near the bottom than near the water surface, so there will be times when the tidal current is going in the opposite direction at one depth than at another depth. One example of the variation in tidal current speed across a cross section of Chesapeake Bay is shown in Figure 2.34. In this figure one sees the current flooding (i.e., flowing up the Bay) in the deeper depths and ebbing (i.e., flowing down the Bay) near the water's surface (except on the west side, where it is still flooding).

There are also other effects that can also make the tidal current vary vertically. Tidal currents can be modified by *baroclinic* effects, that is, by density differences vertically along the water column, due to salinity difference (in estuaries that are not well mixed) or temperature differences (offshore in the coastal ocean), which allow the propagation of *internal tide waves*. Such baroclinic effects on tidal currents are often seen in the middle of the water column but not near the bottom or near the water surface, where frictionally caused mixing takes place. [No direct baroclinic effect is

usually noticeable in the tide, although in estuaries there may be indirect effects due to differences in energy dissipation caused by stratification. In the deep ocean, surface manifestations of internal tides have been detected (see Ray and Mitchum, 1997.)] Other types of currents, such as wind-induced currents and river flow, also vary from the water surface to the bottom, and these currents can nonlinearly interact with the tidal currents.

2.3.6d Dramatic Spatial Variation in Tidal Currents – Horizontally

Horizontally (i.e., geographically), the tide varies quite smoothly due to the hydrodynamic effects of such things as changing depths and widths, resonance, and Coriolis. Such variations can often be reproduced or predicted with even simple analytical models. Although tidal currents are also affected by the same hydrodynamics and can change in similar ways, there are other hydrodynamic effects which can make tidal currents change dramatically in the horizontal direction over surprisingly short distances. One example is the tidal current in a navigation channel compared with the tidal current in the nearby shallows. The tidal current is much faster in the deeper channel than in the shallows, and the times of slacks and of maximum floods and ebbs can be quite different than those in the nearby shallows. One does not require a dramatic change in depth to see

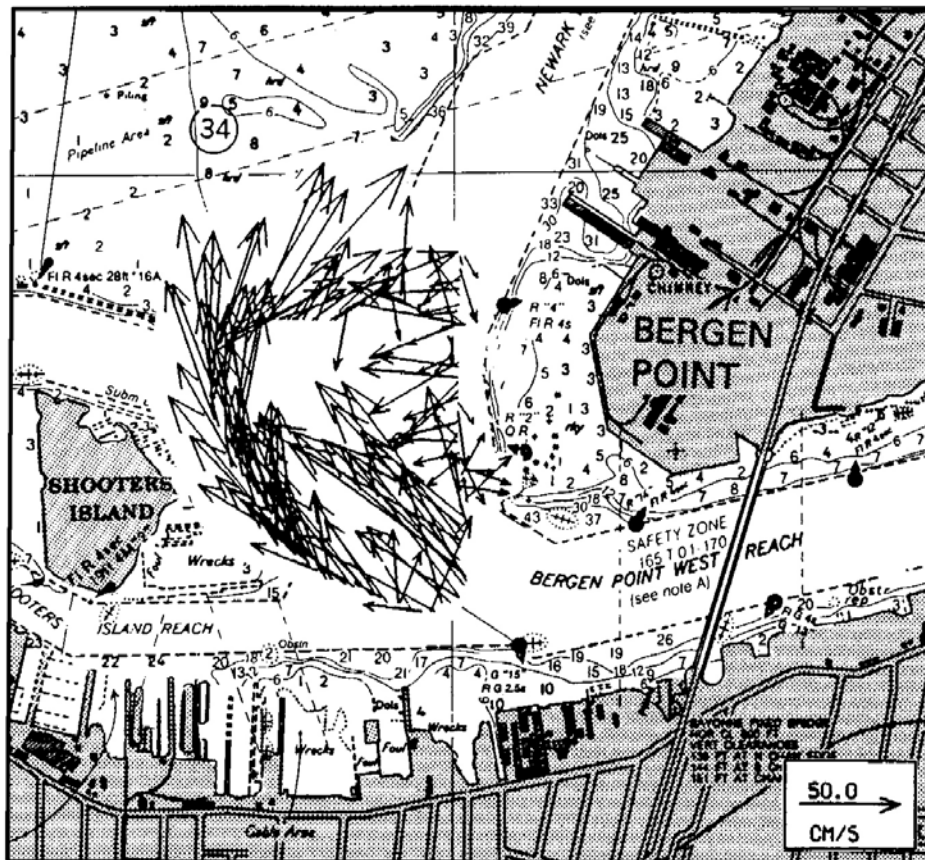


Figure 2.35. The spatial variation in tidal current near the surface to the west of Bergen Point in the Port of New York and New Jersey acquired from a towed acoustic doppler current profiler. (From Parker, 1977.)

2. Theory Behind Tidal Analysis and Prediction

differences in the tidal currents. Even in a wide bay, changes in bathymetry will affect the tidal currents. Not only will current speeds vary with horizontal distance (as mentioned above) but the bathymetry will steer the current. Also, currents within a channel or constricted portion of bathymetry will tend to be more reversing than currents in a more open and flat part of the bay, where a more rotary tidal current will be possible.

In Figure 2.34, where vertical variation in the tidal currents were seen, there were also horizontal variation along the width of the bay. Another example with more rapid horizontal variation in the tidal currents is shown in Figure 2.35, which presents a synoptic view (from above) of tidal current vectors in different locations in a small region of the Port of New York and New Jersey.

In decades past when current meters were primarily hung from surface buoys, those buoys would swing around with the changing current direction carrying the current meter to a location where the tidal current could be different. Such a difference could be quite significant, if, for example, there was a long mooring line and the buoy swung from over a deep channel to over shallow water next to the channel. Bottom mounted acoustic Doppler current profilers (ADCPs) are much more stable, but even they can be moved by storms or strong currents, and here again the tidal currents in the new location can be slightly (or not so slightly) different. (So with current data, one must always pay careful attention to the exact latitude and longitude of the measurements, and note when that changes due to movement of the current meter.)

Bottom friction is often the main reason for the horizontal variation in tidal current, due to the changing waters depth as one moves horizontally. However, there are many other causes of horizontal variation in tidal currents, such as that discussed in the next section.

2.3.6e Nonlinear Lateral Inertial Effects On Tidal Currents

One effect which can be even more dramatic than the frictional effect (due to changing depths) is found where there is a bending waterway, a channel bend, a point of land sticking out into the waterway, or some other similar geographic variation in the shoreline. Such a feature can cause the formation of an eddy during one or both phases of the tidal current. A point sticking out into a waterway, produces an eddy on the side of the point sheltered from the tidal current. Thus, during the flood phase there will be an eddy on the backside of the point, and during the ebb phase there will be an eddy on the front side of the point. This is a *lateral inertial* effect (see Section 7.6.7). After the ebb phase is done, for example, the water on the backside of the point keeps moving roughly in the same flood direction, because that location is sheltered from the opposing flood currents by the point of land and inertia keeps the sheltered water moving.

If one harmonically analyzes current data from a location within this eddy, one will obtain a consistent mean current, which is usually referred to as a *tidally-induced residual flow* (and the process that causes it is often called *tidal rectification*). However, one will also see that the size of the tidal harmonic constants is very different than those for the waters not sheltered by the point of land, because the inherent asymmetry leads to energy being transferred to the second harmonics of the tidal constituents. Thus, the ratio of semidiurnal-to-diurnal constituents in the tidal current will be larger in sheltered locations than in unsheltered locations (and thus, the usually shown diurnal-to-semidiurnal constituent ratio will be smaller). Similarly the ratio of quarter diurnal tidal current constituents to semidiurnal tidal current constituents will also be larger, leading to distorted tidal current curves. None of this affects the tide, and one will not see such dramatic variations in tide constituents across the waterway.

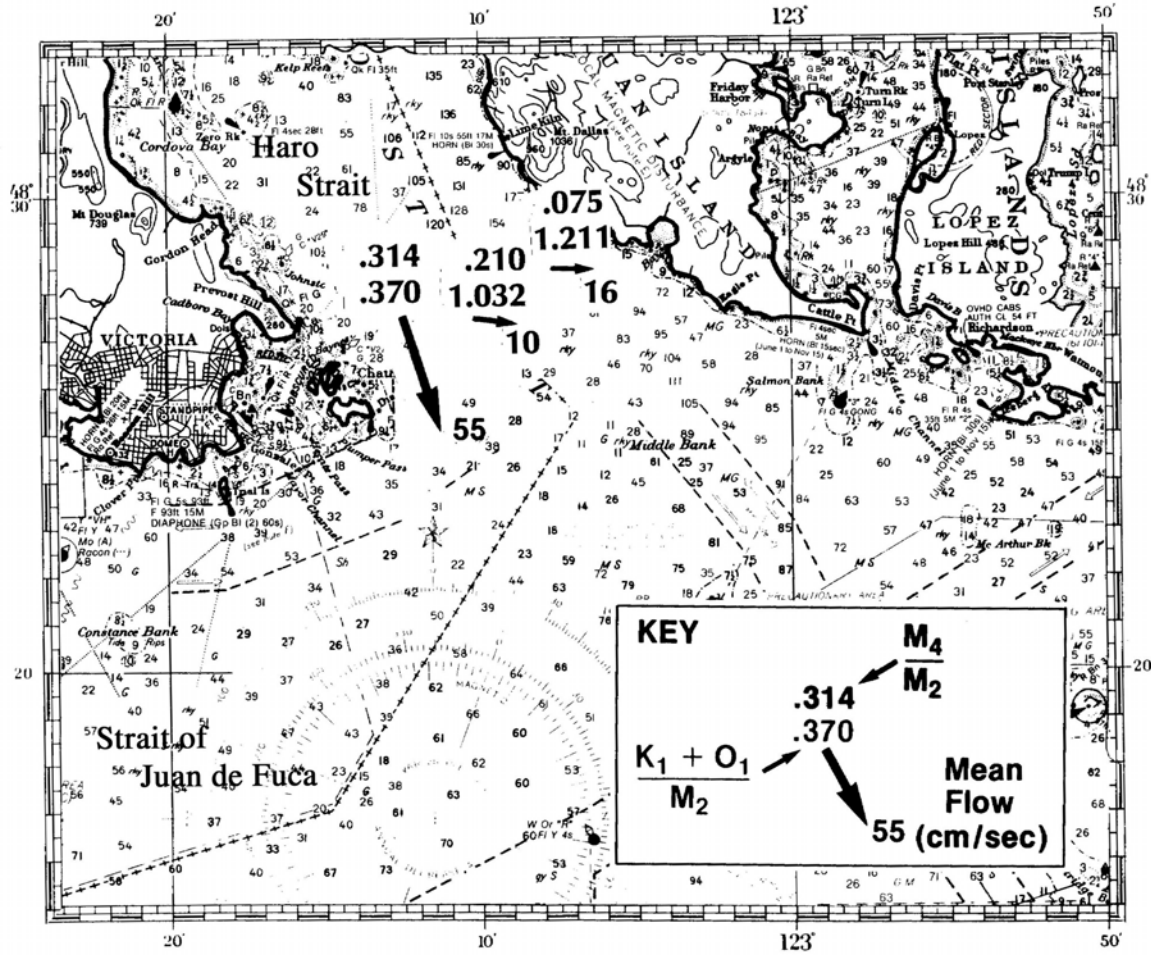


Figure 2.36. Variation in $(K_1 + O_1)/M_2$ and M_4/M_2 tidal current amplitude ratios, and in tidally induced residual currents, at three stations across the entrance to Haro Strait at a depth of 70 feet (21m) below MLLW. (From Parker, 1991a.)

This inertial effect is one of many nonlinear effects which can modify tidal currents, however, this effect does not depend on the water depth being shallow, as most nonlinear effects do (see next section). When looking at the 2-dimensional or 3-dimensional momentum equations (see Sections 7.3.2), it is the lateral advective/inertial terms that produce the tidally-induced residual current and the transfer of energy to higher frequency tidal constituents. This rectification of tidal currents can be demonstrated by a Fourier decomposition of the inertial terms (see Section 7.6.7) and as mentioned above is a result of the inherent asymmetry in the problem.

Figure 2.36 shows a good example of these inertial effects on tidal currents, for the region where the Strait of Juan de Fuca meets Haro Strait (between Canada and the U.S.). Both are deep waterways, but they meet at an angle, namely the waterway bends significantly to the north near Victoria, BC. Thus, the flood current in the Strait of Juan de Fuca flowing past Victoria cannot make a sharp left turn because inertia keeps it moving eastward, allowing the southerly ebb current at the western-most current station in Haro Strait to keep moving longer than at the current station on the eastern side of the waterway. Figure 2.36 shows analysis results from three NOS current stations across the entrance to Haro Strait (entering from the Strait of Juan de Fuca). The

2. Theory Behind Tidal Analysis and Prediction

$(K_1+O_1)/M_2$ amplitude ratio in the tidal current varies dramatically, decreasing from 1.21 on the eastern side of the waterway to 0.37 on the sheltered western side (while for the tide the $(K_1+O_1)/M_2$ ratio does not change much, only from 2.25 to 2.50). The M_4/M_2 ratio for the tidal current also varies significantly across the waterway, from 0.075 on the eastern side to 0.314 on the western side.

2.3.6f Nonlinear Shallow-water Effects On Tidal Currents

The shallow-water nonlinear processes that affect the tide (see Section 2.3.2) also affect the tidal currents, and in many situations those shallow-water effects are seen to be more dramatic in the tidal current than in the tide. When one considers distorted tidal currents one usually speaks of *flood dominance* or *ebb dominance*. The asymmetric tidal current can have: (1) a shorter flood phase with higher speeds and a longer ebb phase with slower speeds (called flood dominance because of the higher flood current speeds); (2) a shorter ebb phase with higher speeds and a longer flood phase with slower speeds (ebb dominance); or (3) the case midway between (where one of the slacks can last for a couple of hours). Asymmetry in the tidal current is important in the transport of sediment and pollutants. The transport of coarse sediment depends on the maximum speeds achieved, and so might be transported up an estuary with a flood dominant situation. Fine sediment stays suspended except near slacks, so the case with longer slacks before ebb might lead to deposition at that time. (See Speer, *et al*, 1991, for more discussion on flood and ebb dominance.)

The distortion in tidal currents can be greatly enhanced by a strictly linear superposition effect, that in fact, will not similarly enhance the distortion in the tide. Parker (1991a) shows an extreme example in Ramshorn Creek, a small shallow channel connecting the shallow Cooper and New Rivers, both part of the intracoastal waterway in South Carolina and both connected to the Atlantic Ocean (Figure 2.37). Two tide waves, each distorted by shallow water, enter Ramshorn Creek at

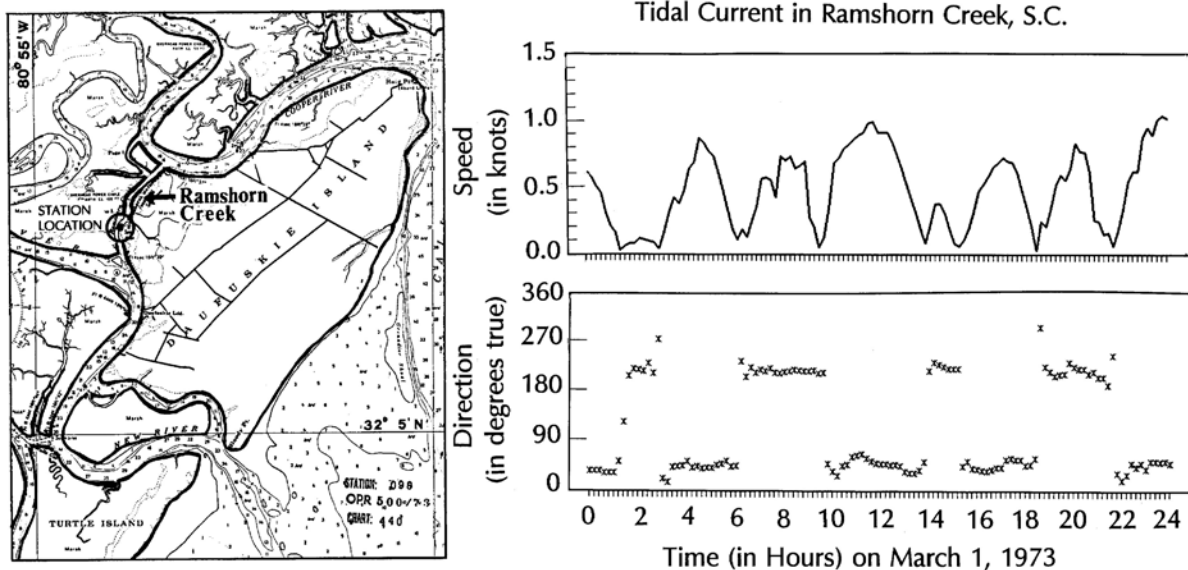


Figure 2.37. Current speed (top panel on right) and direction (lower panel) plots of the unusual occurrence of dominant quarter-diurnal tidal currents at an NOS current station in Ramshorn Creek, SC. There are four cycles per day in the tidal currents (see text). (From Parker, 1991a.)

opposite ends and cross, superimposing their effects. The M_2 flood currents for the two waves are in opposite directions, and so the superposition of the two waves leads to a reduction in the M_2 tidal current. Each tide wave is distorted to a different degree because the two waterways leading to Ramshorn Creek do not have exactly the same width or depth. Thus, there is a different $2M_2^o - M_4^o$ phase relationship, so that when the M_4 tidal constituent waves are superimposed the two waves add together (rather than cancel each other out like the M_2 constituent waves) thus increasing the M_4 tidal current. For this particular situation the result is the very unusual situation of dominant quarter-diurnal tidal currents (Figure 2.37), that is, the tidal current actually changes directions eight times a day instead of four (i.e., there are four tidal current cycles per day instead of two). There are other waterways in the salt marsh estuaries of South Carolina and Georgia that also exhibit the effects of two tide waves entering from opposite ends and crossing. Most are not as extreme as in Ramshorn Creek, but the result is very distorted tidal current curves. (This superposition effect does not lead to a dominant M_4 in the tide because the two M_2 waves add positively at the crossover point, not negatively as with the tidal current.)

2.3.6g Hydraulic Tidal Currents

There is another type of tidal current which involves the crossing of two tide waves from the opposite ends of a waterway. In this case the waterway is a short and narrow strait, and there is often a significant difference in tide range at each end of the strait and/or a difference in timing in the high waters at the two ends. For example, the very fast currents in Seymour Narrows (noted in Section 2.1.1) are due to tidal height differences between the Strait of Georgia end and the Queen Charlotte Strait end, the tide being approximately 180° out of phase at opposite ends. Tidal currents in such straits, which can have very high speeds, were given the name *hydraulic currents*. Since in the past it was difficult to maintain a current meter where there were very fast currents (now one can put an upward-looking ADCP successfully on the sea bottom or a sideward-looking ADCP on a pier), another method to predict the tidal currents in a strait was devised which used the predicted water level differences at the opposite ends of the strait.

Two often cited examples in the U.S. of hydraulic currents driven by tidal height differences at opposite ends of a strait are Deception Pass, Washington (between Rosario Strait and Reservation Bay), where the tidal currents reach speeds over 8 knots, and the East River (connecting New York Harbor and Long Island Sound), where the tidal current speed reaches over 5 knots at Hell Gate, about half way between the entrances. These two stations, and four others with hydraulic currents (Cape Cod Canal, Chesapeake and Delaware Canal, Sergius Narrows, and Isanotski Strait) still appear as reference stations in the U.S. Tidal Current Tables.

The daily predictions for each of these six hydraulic current stations are based on harmonic constants that were derived from the harmonic constants at the tide stations at the opposite ends of each of the straits (and in some cases were modified based on a small amount of actual current data). Differences in the water level at opposite ends of the strait are partly due to any difference in the tidal range at the two ends and partly due to any difference in the time of the high waters at the two ends. In the method described in *The Manual of Current Observations* (U.S. C&GS, 1950, S.P.215, pp78-83), the current speed is assumed to vary as the square root of the water level difference. By the reasoning of this method, the current speed will be a maximum when the difference in water level is greatest, and will be zero (slack current) when the water levels are the same at opposite ends. However, this ignores friction and inertia (and other details of the actual hydrodynamics that would occur in the strait), so there will usually be a lag in the response of the currents due to the difference

2. Theory Behind Tidal Analysis and Prediction

in the water levels at opposite ends. This lag was usually determined by obtaining a short record of current data by whatever technique could work for a few tidal cycles in the fast currents.

This method was developed in the pre-computer era and before the numerous modern methods which can be used today to measure fast currents in a strait, such as an upward-looking ADCP on the sea bottom, a sideward-looking ADCP on a pier, or HF or microwave radar. It is no longer necessary, and was only a reasonable approximation. If one is interested in it, one can look at S.P.215.

2.3.6h Limitations On Tidal Current Predictions

Because of these various effects on tidal currents (that do not similarly affect the tide), there are several limitations that should be remembered about tidal current predictions, which will be discussed below.

Tidal current predictions are only accurate for the exact depth and location where the current data were obtained. Such predictions may be usable at nearby locations (preferably at the same depth), but only if the bathymetry does not change dramatically.

It is also very important to remember that bathymetry and shoreline can slowly change over the years, which means that the tidal currents can also slowly change over the years (while in most cases the tide will not similarly change over the years). Thus, for shallow-water areas (i.e., for many bays and estuaries), new current measurements may have to be made and new tidal current harmonic constants calculated, because the bathymetry has changed (while the harmonic constants for the tide are still perfectly acceptable). Dramatic changes in bathymetry, such as due to dredging or rapid shoaling or due to the dramatic movement of sediments after a large storm, can make the predictions in the Tidal Current Tables invalid (or at least much less accurate) for any locations within the area of the dredging or shoaling or storm movement. Even for this extreme situation the tide predictions may not be affected at all, unless the bay or estuary is very small and the changes due to the dredging or shoaling represent a significant portion of the total volume of the waterway. (For example, dredging in a small bay can increase the tide range.)

As will be discussed in Section 3.6.1, since many current stations have short data time series tidal current predictions at these stations are often produced using time differences and amplitude ratios (found in Table 2 of the Tidal Current Tables), calculated through a nonharmonic comparison analysis. For a nonharmonic comparison tidal analysis (and the resulting predictions) to be reasonably accurate, it is crucial that the reference and subordinate stations have very similar frequency domain characteristics, that is, the ratios of diurnal-to-semidiurnal constituents should be very similar, as well as the ratios of quarterdiurnal-to-semidiurnal constituents. From what has been seen in this section, there can be significant variation of tidal currents over a geographic region, making it more difficult for all these short (subordinate) stations to have the same frequency characteristics as the reference station(s) being used. For example, in the waterway shown in Figure 2.36 and other waterways nearby, there is such a dramatic variation over geographic distance in the diurnal-to-semidiurnal ratios in the tidal currents, that it is difficult to have enough reference stations to handle all the subordinate stations accurately.

Another bad situation arose sometimes in the past, when the lack of a long-term current data time series led to the use of a tide station as the reference station for tidal current stations. However, when one wishes to compare the tidal current to the tide one must remember that basic linear hydrodynamics determines that the tidal characteristics can be very different for tidal currents and tides at the same location. For example, the quasinode for a constituent of the tide will occur 1/4

of a wavelength from the head of bay (where the reflection of the tide wave takes place), where as for a constituent of the tidal current the quasinode will occur $\frac{1}{2}$ of a wavelength from the head of bay (see Section 7.4.1). Thus, near the M_2 quasinode of the tide, where the diurnal effect is therefore stronger and the tide may be mixed or diurnal, the tidal currents will still be semidiurnal. This occurs in the eastern end of the Strait of Juan de Fuca near Victoria, British Columbia (see Parker, 1977).

All these various geographic and bathymetric effects can also cause the directions of the maximum flood current and the maximum ebb current at a particular location to not be directly opposite of each other, that is, to not be 180° apart. The direction difference between maximum flood and maximum ebb tidal currents will depend on exactly where the current meter is positioned. If placed in a straight section of channel, then flood and ebb directions will be 180° apart. However, if the current meter is placed at a bend in the channel, the difference between flood and ebb directions can be very different than 180° . When this latter situation occurs, and one harmonically analyzes the tidal current data, there will be an apparent mean current and an artificially large overtide, i.e., M_4 , that comes out of the analysis of the two orthogonal components (see Section 5.1).

Because of all these mechanisms that can cause significant variation in tidal currents over depth and horizontal/geographic distance, this is an area of tidal prediction where (high-resolution) numerical hydrodynamic models are most useful, and may actually do a better job than obtaining many current records and obtaining harmonic constants for each. (See Section 8.3). Given that slightly moving a current meter can change the harmonic constants significantly, and not knowing the location where the current meter would be most representative of the local area, it may be better to rely on the predicted tidal currents over the small area of a grid cell in a carefully calibrated numerical model (that is forced at the entrance with very accurate tide predictions). That being said, one must remember that there can be problems with how well a model might represent the currents, especially if it does not have high enough spatial resolution. Thus, for locations with uniform geography and bathymetry for which one has a long data time series of high quality current data, it will usually be better to rely on harmonic analysis of the current data and the subsequent prediction of the tidal current from the calculated harmonic constants.

There is another aspect of current data that does not apply to water level data. In current data one is more likely to find energy at frequencies close to tidal frequencies that is not caused by the tide. In the summer in many coastal locations one will see a *land breeze-sea breeze*, where the name comes from that fact that generally the wind blows toward the land during the day (the landward wind replacing rising heated air over the warmer land surface) and toward the sea at night (the opposite situation), although the change in direction of flow can in many locations actually rotate around the compass over the 24-hour period. (This is mainly due to the Coriolis effect, so rotations of the land breeze-sea breeze are clockwise in the Northern Hemisphere, although the orientation and shape of the coastline can often significantly affect this.) This changing wind speed and direction has a 24-hour period and thus would show up in a harmonic analysis as S_1 . To notice this effect, however, one would need a year-long time series to separate this meteorological S_1 from K_1 . Since in many locations the land breeze-sea breeze usually only occurs in the summer, the S_1 value would be very different in the summer than in the winter. One should remember this effect when one is analyzing current data obtained during the summer, because it may have a noticeable effect on the K_1 value that comes out of a harmonic analysis.

Along these same lines (that is, of energy from a nontidal source occurring at a frequency near to one of the tidal frequencies), at some latitudes one must also consider the possibility of *inertial currents*. Inertial currents are caused by Coriolis effects on the wind. They are oscillatory currents

2. Theory Behind Tidal Analysis and Prediction

that rotate in a clockwise direction in the Northern Hemisphere (and counterclockwise in the Southern Hemisphere), and they have energy at a frequency that depends on latitude. The formula for the period of an inertial current is $T_i = 11.97 / \sin \varphi$, where the numerator is half a sidereal day in hours and φ is the latitude in degrees. While generally transient and usually lasting only a few days, they may last long enough to affect a tidal current analysis, at least in locations where the inertial frequency is at or close to the frequency of a particular tidal constituent. Thus, in the Arctic Ocean (or in the Ross Sea and Weddell Sea next to Antarctica) inertial currents may affect the calculated M_2 harmonic constants, because the inertial period at 75°N is the same as the M_2 period. At latitude 30°N inertial currents will have their energy at exactly the K_1 tidal frequency, and at 27.6°N the inertial energy will be at exactly the frequency of O_1 , and thus they might affect the calculations for these diurnal constituents in large parts of the Atlantic or Pacific Oceans.

Thus, as has been seen, there are many aspects of tidal currents that make them more difficult to analyze and predict accurately than the tide, but keeping these problems in mind, one should be able to produce useful results. The next chapter will look at the various methods of time series analysis that can be used for this purpose.

Tidal Analysis and Prediction

3. Methods of Tidal Analysis and Prediction

3.1 Introduction

The prediction of tides and tidal currents is unique in the world of geophysical prediction on Earth. There is no other geophysical phenomenon where all its energy is known *a priori* to be found only at very specific frequencies – which as explained in the last chapter, are determined by the relative astronomical movements of the Earth, moon, and sun in their various orbits, rotations, and axis tiltings. For other geophysical systems, notably weather (and on a longer time scale, climate) only a small portion of the energy is found at known frequencies – primarily the daily cycle (heating during the day and cooling at night) and the annual cycle (more heating in the summer and less in the winter). Like the tides, these cycles are astronomical in origin, but unlike the tides, the complex physics of weather and climate systems is so chaotic that the daily and annual cycles are only a part of the whole story. Although tidal systems can also be very nonlinear in shallow waterways, they are not chaotic. The nonlinearity of the tides simply transfers energy from some (astronomical) tidal frequencies to other new tidal frequencies, which in the time domain show up as distorted tide and tidal current curves and asymmetries between the flood phase and the ebb phase. The tides are a periodic *deterministic* process, whereas the processes affecting weather are *stochastic* processes that involve random and aperiodic fluctuations.

[In shallow waterways nonlinear processes also cause an interaction between the (deterministic periodic) tide and the (stochastic random/aperiodic) weather-induced effects (such as river discharge or storm surges). The tide can be temporarily changed by these nontidal effects (through this nonlinear interaction; see Sections 2.3.3, 7.6.3, and 7.6.4), thus bringing a stochastic element into the analysis and prediction of tides. When dealing with random processes one usually is concerned with whether the process (data) is *stationary*, meaning that the average properties computed over short intervals do not vary significantly from interval to interval. When the tide is nonlinearly modified by random meteorological effects in shallow water, the tide is no longer stationary. But a random (usually small) modification to strongly periodic deterministic process like the tide, does not make the tide a stochastic process in the same sense as other geophysical phenomena, and the methods for dealing with these nonlinear modifications require a different approach than might be used with other nonstationary processes.]

Tidal data analysis and tidal prediction are a special subcategory of *time series analysis* (and a further subcategory of statistics). As with any other time series of data, water level data and current data can be looked at in the *time domain* and in the *frequency domain*. In the time domain one looks at actual real-world measured data as well as tide and tidal current predictions – the water level heights or current speeds and directions plotted against time. In the frequency domain one looks at plots showing how the energy found in the data time series is spread over different frequencies. As was seen in Section 2.2.3, when one looks at a frequency domain plot resulting from the spectral

analysis of the time series, one again sees the uniqueness of the tides, because the tidal energy is represented by a series of spikes at only a number of specific frequencies. If the time series analyzed is fairly short one will see spikes at semidiurnal and diurnal frequencies (and at higher harmonics of these frequencies if the data came from a shallow waterway), each spike trailing off from a peak in the middle of the band. However, for a longer time series (which allows finer resolution along the frequency axis of the spectral plot), one can see the actual *tidal spectral lines* for the various tidal constituents. Between these tidal spikes is the rest of the spectrum, resulting from the assortment of nontidal phenomena that can make the ocean move up and down (or horizontally), but these effects do not have most of their energy concentrated in a few frequencies. In a plot of a water level spectrum, the energy from winds, atmospheric pressure, and temperature and salinity changes shows up primarily as a smooth continuous curve covering a broad range of frequencies, called the *continuum*, ranging from wind waves at the higher frequencies to low-frequency storm surges at the lowest frequencies (see Figure 2.16). The tidal spikes or lines rise above this continuum. The continuum curve at a water level station near the coast or in a bay is often highest near zero cycles per day (where zero cpd represents the mean), with the very low frequencies near zero cpd representing very slow changes in the height of the water surface due to the effects of wind, atmospheric pressure, density changes, and/or river discharge.

As was mentioned in Section 2.2.3, one can use spectral analysis for tidal analysis, but the results merely give us an idea of how strong the tidal signal is, the relative importance of the diurnal and semidiurnal bands (and thus information on the type of tide), and whether there are strong higher harmonics due to shallow water. The spectral results are of no use for tidal prediction, for they provide no phase information, that is, there is no information about the timing of these effects. Since one already knows at exactly which frequencies the tidal energy will be found (because of its astronomical origin), there are much better ways to analyze a water level record or a current record in order to both characterize the tidal signal, and more importantly, to be able to predict the tide or tidal current using the results of the analysis.

3.2 *Simple Demonstration of Extracting Tidal Constituents From a Data Time Series*

The general methodology for extracting tidal constituents from a data time series, taking advantage of our *a priori* knowledge of the frequencies where the tidal energy will be found, can be seen with a simple demonstration. If one would like to see the contribution to the tide of, for example, the M_2 tidal constituent, which has a period of approximately 12.4206 hours, one simply takes a water level time series and breaks it up into consecutive pieces, each 12.4206 hours long. One then superimposes these 12.4206-hour-long pieces (i.e., adds them up) and averages them. For each of these pieces the M_2 contribution will be in sync, that is, the maximum M_2 contribution will be at the same time within each piece of the chopped up data time series, but the other tidal constituent frequencies will not stay in sync. For S_2 , which has a period of 12.0000 hours, the time of the maximum S_2 contribution to the tide (within each 12.4206-hour piece) will slowly shift earlier as one moves from piece to piece. This is illustrated in Figure 3.1. The top plot in this figure shows the contributions of M_2 and S_2 for the first 12.4206-hour piece. The M_2 maximum and the S_2 maximum start out in sync, but by the end of the second segment the S_2 maximum is slightly to the left of the M_2 maximum. In the next plot below it, showing the next consecutive 12.4206-hour piece from a couple of days later, the S_2 maximum has shifted even more to the left. By the fourth plot down (about 7.38 days after the first data point), the S_2 maximum occurs at the same time as the M_2

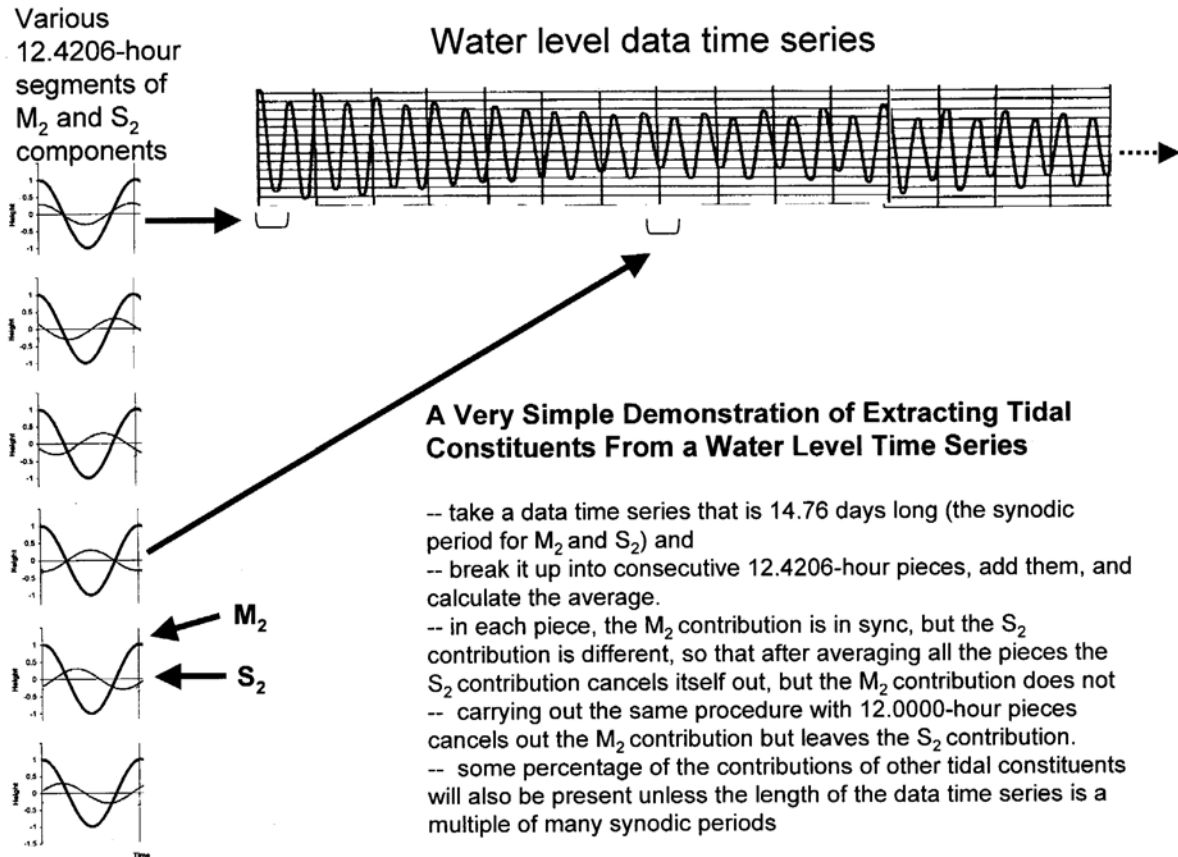


Figure 3.1. A very simple demonstration of extracting tidal constituents from a water level data time series (see text).

minimum. After enough pieces (about 14.76 days after the first data point), the S_2 maximum will come back to the same time (within the piece), and again be in sync with the M_2 maximum.

When one adds up all the 12.4206-hour pieces of the data time series, the S_2 portion of the tide will cancel itself out. The same thing will happen with the other tidal constituents – all that will be left will be the M_2 contribution. For the moment it has been assumed that one has a very long time series so the contributions of all the other tidal constituents will cancel out. The result of averaging all these M_2 -period-long pieces is an average M_2 cycle, from which one can obtain the M_2 amplitude (half the M_2 range, i.e., half the height difference between the M_2 high water and the M_2 low water). One can also obtain the M_2 phase lag, which is the time of the maximum M_2 high water from the beginning of the mean curve (which itself will have a time relationship to some other time reference point, such as the time of the moon's transit over a particular time meridian).

So far it has been assumed that one has a very long data times series, so that all the other constituents would cancel themselves out over that long period of time. However, when one does not have such a long data record, one may not want to use the entire length of the record when extracting (in this case) the M_2 signal. For example, in the above procedure, one needs a 14.76-day long time series of data in order to cancel out the S_2 tidal constituent. This 14.76-day length of series is determined by the difference in the periods of M_2 and S_2 . The difference between the M_2

period (12.4206 hours) and the S_2 period (12.0000 hours) is 0.4206 hours, and thus the maximum S_2 contribution shifts to the left in each successive piece of the time series by 0.4206 hours. It therefore takes $(12.0000/0.4206)=28.53$ M_2 cycles (or 14.765 days) for the S_2 maximum to sequence through completely (as was seen in Figure 3.1). If one had a time series that was 20 days long, one would still only want to use 14.76 days of that time series, because using the entire 20 day would leave in some of the S_2 contribution. One could, however, use 29.53 days, or any multiple of 14.76 days.

The closer in tidal period a tidal constituent is to M_2 , the longer the data times series must for its effects to be completely canceled out. The period of N_2 is 12.6583 hours. The difference between the periods of M_2 and N_2 is 0.2377 hour. This is smaller than the difference between the period of M_2 and S_2 , so it will require a longer time series to cancel out the N_2 contribution. In this case it requires 27.560 days long ($12.6583/0.2377=53.25$ M_2 cycles), or some multiple of that. The period of K_1 (23.9345 hours) is not close to that of M_2 , and thus only 1.1 days of data (or some multiple of that) are needed to cancel out the effect of K_1 . The period of K_1 is closer to the period of O_1 (25.8193 hours) and so 13.66 days are needed to cancel out the O_1 effect when calculating K_1 and vice versa.

One can obtain the contribution of another tidal constituent by going through the same procedure, but choosing a different time period for chopping the time series up into pieces. For S_2 , one would chop the time series up into consecutive pieces, each with a length of exactly 12.00 hours long. For N_2 , one would chop the times series up into pieces, each with a length of 12.658 hours long. And so on. When doing this procedure for K_1 (23.094 hours), the two closest important tidal constituents are O_1 (25.819 hours) and P_1 (24.066 hours). For O_1 therefore, 13.66 days of data (or some multiple) are required to cancel out the O_1 contribution when trying to extract K_1 . For P_1 , since it is much closer to K_1 , 182.6 days of data (or some multiple) are required.

3.3 *The Synodic Period – Length of Time Series Needed To Separate Two Constituents*

The time (typically) required to separate the effects of two nearby tidal constituents is called the *synodic period*, and it is defined as the interval between two consecutive conjunctions of phase of the two constituents (Schureman, 1940, p 51). This time period includes N oscillations of the lower frequency constituent wave and $N+1$ oscillations of the higher frequency constituent wave. This criterion for the minimum length of series required to resolve two constituents is also called the *Rayleigh criterion* (Godin, 1972), because it was first proposed by Lord Rayleigh in optics, dealing with the criterion for resolving two adjacent frequency components when light is shone on a diffraction grating. Although the demonstration in Section 3.2 was carried out in the time domain, the most straight forward way to calculate the synodic period, T_{syn} , is simply to find the inverse of the difference in the frequency between two tidal constituents. Thus, the difference in the M_2 and N_2 frequencies is 0.0015 cycles per hour, so the synodic period for M_2 and N_2 is $T_{\text{syn}} = (1/0.0015)\text{cph} = 661$ hours = 27.560 days. Or likewise, in the classical notation of angular speeds, the synodic period is 360° divided by the difference in the angular speeds of the two tidal constituents. Another way of stating Rayleigh's criterion is: to resolve two frequencies their difference must be greater than the inverse of the length of the data time series analyzed, i.e.,

$$|\sigma_2 - \sigma_1| > T^{-1}$$

3. Methods of Tidal Analysis and Prediction

Table 39.—*Synodic periods of constituents*

DIURNAL CONSTITUENTS										
	J ₁	K ₁	M ₁	O ₁	OO ₁	P ₁	Q ₁	2Q ₁	S ₁	p ₁
K ₁	Days. 27.555	Days. 27.555	Days. 27.555	Days. 27.555	Days. 6.830	Days. 14.765	Days. 12.710	Days. —	Days. —	Days. —
M ₁	13.777	—	—	—	—	—	—	—	—	—
O ₁	9.133	13.661	27.555	—	—	—	—	—	—	—
OO ₁	27.093	13.661	9.133	6.830	—	—	—	—	—	—
P ₁	23.942	182.621	32.451	14.765	—	—	—	—	—	—
Q ₁	6.859	9.133	13.661	27.555	5.474	9.614	—	—	—	—
2Q ₁	5.492	6.859	9.133	13.777	4.566	7.127	27.555	—	—	—
S ₁	25.622	365.243	29.803	14.192	13.168	365.243	9.367	6.991	—	—
p ₁	7.096	9.557	14.632	31.812	5.623	10.085	205.892	24.302	9.814	—

SEMIDIURNAL CONSTITUENTS											
	K ₂	L ₂	M ₂	N ₂	2N	R ₂	S ₂	T ₂	λ ₂	μ ₂	ν ₂
L ₂	Days. 27.093	Days. 27.555	Days. 27.555	Days. 27.555	Days. 27.555	Days. 6.991	Days. 7.127	Days. 365.259	Days. —	Days. —	Days. —
M ₂	13.661	—	—	—	—	—	—	—	—	—	—
N ₂	9.133	13.777	27.555	—	—	—	—	—	—	—	—
2N	6.859	9.185	13.777	27.555	—	—	—	—	—	—	—
R ₂	365.225	29.263	14.192	9.367	6.991	—	—	—	—	—	—
S ₂	182.621	31.812	14.765	9.614	7.127	365.259	—	—	—	—	—
T ₂	121.748	34.847	15.387	9.874	7.269	182.630	365.259	—	—	—	—
λ ₂	23.942	205.892	31.812	14.765	9.614	25.622	27.555	29.803	—	—	—
μ ₂	7.096	9.614	14.765	31.812	205.892	7.236	7.383	7.535	10.085	—	—
ν ₂	9.557	14.765	31.812	205.892	24.302	9.814	10.085	10.371	15.906	27.555	—
2SM	16.064	10.085	7.383	5.823	4.807	15.387	14.765	14.192	9.614	4.922	5.992

Table 3.1. Schureman's Table 39 showing the synodic periods for a number of pairs of semidiurnal and diurnal tidal constituents. (From Schureman, 1958.)

or, in other words, the length of the time series must be greater than (or, in reality, approximately equal to) the synodic period, i.e., $T > T_{\text{syn}}$.

Schureman's Table 39 (reproduced here as Table 3.1) shows the synodic periods for a number of pairs of semidiurnal tidal constituents (bottom table) and for a number of pairs of diurnal tidal constituents (top table). (There is no need to consider the synodic period between a semidiurnal constituent and a diurnal constituent, since it will be on the order of a day.) For a particular constituent, the most important synodic period will be the longest synodic period with another tidal constituent that is expected to have a larger amplitude than it. For example, in Table 3.1, one sees that to separate P₁ from J₁, K₁, M₁, O₁, and OO₁ (the fifth row of the diurnal table) one needs data times series of lengths 23.942, 182.621, 32.451, 14.765, and 12.710 days, respectively, and to separate P₁ from Q₁, 2Q₁, S₁, and p₁ (the sixth column of the diurnal table), one needs data times series of lengths 9.614, 7.127, 365.243, and 10.085 days, respectively. But because K₁ is the diurnal constituent with the largest amplitude, it is the 182.632-day synodic period that is important. If one has less than 183 days of data, according to the Rayleigh criterion (but see caveat below) one could analyze either for K₁ or for P₁, but not both. One would naturally choose K₁ because it will always have a larger amplitude than P₁. But the K₁ harmonic constants (amplitude and phase lag) that come out of such an analysis will include an error caused by the effect of the P₁ energy that could not be separated out. Table 3.2 shows the synodic period (fourth column in that Table) for each tidal constituents with respect to a larger tidal constituent from which it must be separated.

In both Tables 3.1 and 3.2 one notices that once there is at least a month of data there are no significant astronomical tidal constituents that adversely affect M_2 or O_1 . However, for the rest of the primary tidal constituents there are interfering tidal constituents with half-yearly and yearly synodic periods. Thus, unless one has (approximately) a half year of data, K_1 will be affected by P_1 , and S_2 will be affected by K_2 , and N_2 will be affected by v_2 . Unless one has (approximately) a year of data K_1 will be affected by S_1 , and S_2 will be affected by both R_2 and T_2 .

If one was interested in separating only two tidal constituents the minimum length of the time series would be straightforward, i.e., it must have a length equal to the synodic period for those two constituents. But since one needs to correctly separate many pairs of constituents, all with different synodic periods, the key question is – what should the length of a time series be in order to separate the most tidal constituents? For a particular data time series one could use a length that is the best compromise for the most important tidal constituents. This involves not just the longest synodic period found in Table 3.1 for key tidal constituents, but also multiples of other key synodic periods. For example, in Table 3.2 one sees some natural groupings near 15 days, 29 days, a half year, and a year. Schureman suggests that 369 days should be considered as a standard length for harmonic analysis because it is supposed to “conform very closely to multiples of the synodic periods of practically all of the short-period constituents.” In practice, however, and especially if one is using a least squares harmonic analysis technique (see Section 3.4.5) 365 days of data should work fine (Schureman used a Fourier series technique).

However, a number of authors have felt that the Rayleigh criterion is overly restrictive. Munk and Hasselman (1964) suggested that the length of the time series determined by the Rayleigh criterion could be shortened if there was not much noise in the data time series (either from meteorological effects or from the instrument itself). In fact, they specifically suggested that the required data series length can be reduced by the ratio of the signal-to-noise standard deviation, and they referred to this as “super resolution”. Thus, Munk and Hasselman replaced the Rayleigh criterion with another relation. They said that meaningful information can be gained about the frequencies, σ_1 and σ_2 , provided that

$$|\sigma_2 - \sigma_1| > \frac{T^{-1}}{(\text{signal/noise level})^{1/2}}$$

This seems to imply that for a signal-to-noise ratio of 1 that the classic Rayleigh criterion is a good rule. It also seems to imply that if one has (e.g.) a water level record with a very strong tidal signal then one may be able to extract more tidal constituents than would be expected for the length of time series available. The extreme example would be a time series produced by a model forced at the entrance by only tidal predictions, which does not contain any noise. In this case it may be possible to use much shorter records than specified in Table 3.1 (see Foreman and Henry, 1989). Similarly, if one has a weak tide signal, one may not be able obtain good harmonic constants even if one has a record length that is longer than the synodic period. It also implies that for a data record with some noise a large tidal constituent might be obtained very accurately, but a small constituents down in the nontidal noise might be determined less accurately (or not at all). This would be a separate effect from this small constituent being overwhelmed by meteorological fluctuations that happened to fall at its particular frequency, yet it might not be distinguishable from that effect, since one would expect the noise closest in frequency to the tidal line to have the most effect. Either way, the only good way to check the quality of harmonic constants (if one has enough data available) is

3. Methods of Tidal Analysis and Prediction

to analyze several different data sets (with the same data length) and see how consistent the amplitudes and epochs are from data set to data set.

However, there still seems to be a lot of room for interpretation. Pugh (1987) suggests that in practice, “the Rayleigh criterion is a good guide for tidal analyses of continental shelf data from middle and high latitudes, but finer resolution is feasible in ideal conditions such as tropical oceanic sites.” There is also experience to show that the nature of the least squares technique used in most modern harmonic analysis programs sometimes allows one to use time series lengths shorter than that determined by the Rayleigh criterion. In some cases, for example, P_1 has been reasonably accurately determined from length of series a month or two shorter than the six months suggested by the Rayleigh criterion, but this has not happened for all such cases, and it may possibly be affected by the relative positions of the K_1 and P_1 maximums in the particular time series used. (See also Godin, 1972, Foreman, 1977, and Jay and Flinchem, 1999).

A reasonable approach is to initially use the synodic period (Rayleigh criterion) as a guideline when carrying out a harmonic analysis. Then, especially if one’s time series is a little shorter than one of the key lengths of series (see Table 3.2), rerun the harmonic analysis with one or more additional constituents included that one should be able to obtain with the next highest length of series.

The procedure described in the simple demonstration in Section 3.2 is not a very efficient one, especially when many tidal constituents have to be resolved from each other, and as will be seen there are more sophisticated ways to accomplish this. Each of the tidal analysis methods described in the following sections has a different technique for extracting the amplitude and phase lag (epoch) of each tidal constituent. But the above demonstration provides the basic idea behind most tidal analyses whose results are presented in the frequency domain, and the Rayleigh criterion (at least as a useful guide) is true for all tidal analyses in the frequency domain – the longer the data time series the more tidal constituents that can be accurately resolved, that is, whose effects can be separated from each other. Another way of saying this, the closer in frequency two important tidal constituents are, the longer the time series that is needed to resolve them.

Although the most accurate tidal analysis methods will deal with the frequency domain (that is, they will produce results for particular tidal frequencies), there are also tidal analysis methods that deal only with the time domain. Such *nonharmonic* methods simply compare the data time series at one location (station) with the data time series at another. This is usually done only for key recognizable points in the time series, such as high waters and low waters on a water level curve, or maximum floods, maximum ebbs, and slacks waters (or minimum flows) on a tidal current curve. Thus, the time of high water at a subordinate station will be calculated as occurring a certain amount of time after the corresponding high water at a reference station, and being a certain number of feet higher or lower than the high water at the reference station. The results of such nonharmonic methods are used for stations listed in Table 2 of the Tide and Tidal Current Tables. Such time domain methods were historically the first kinds of tidal analysis used. The earliest methods used the time of each of the moon’s transit overhead as the time reference points, a certain number of hours after which high water would be calculated to occur. [A nonharmonic comparison method is also the basis for how tidal datums are computed at a short-term station and referenced to a 19-year period (see CO-OPS, 2003).]

In the following sections various methods will be described that are used for tidal analysis and prediction. The most commonly used methods are based on the theory of harmonic analysis, not much different from that developed by Thomson, Ferrel, and Darwin in the late 1800s, except that the Fourier analysis solution technique (Schureman, 1958) has generally been replaced by a least

Tidal Harmonic Constituent	Origin of Constituent	Cartwright No	Shallow-water equivalent	NL mechanism sym or asym	Angular Speed (/hour)	Freq. (cpd)	Period (hours)	Synodic Period (days)	wrt const.	Cartwright Potential Coeff.	Amplitude at Trenton
M ₂	lunar	2 0 0 0 0 0	KO ₂	asym	28.9841042	1.9323	12.4206	---	—	0.90809	3.547
M ₄	shallow	4 0 0 0 0 0	M ₄	asym	57.9682084	3.8645	6.2103	0.5	M ₂		0.517
M ₆	shallow	6 0 0 0 0 0	M ₆	sym	86.9523127	5.7968	4.1402	0.5	M ₄		0.266
M ₈	shallow	8 0 0 0 0 0	M ₈	both	115.9364169	7.7291	3.1052	0.5	M ₆		0.120
K ₁	luni-solar	1 1 0 0 0 0	MO ₁	asym	15.0410686	1.0027	23.9345	1.1	M ₂	0.53011	0.349
S ₆ **	shallow	6 -6 0 0 0 0	S ₆	sym	90.0000000	6.0000	4.0000	4.9	M ₆		0.005
O ₁	lunar	1 -1 0 0 0 0	MK ₁	asym	13.9430356	0.9295	25.8193	13.7	K ₁	0.37694	0.288
OO ₁	lunar	1 3 0 0 0 0			16.1391017	1.0759	22.3061	13.7	K ₁	0.01624	0.030
2MK ₃ (MO ₃)	shallow	3 -1 0 0 0 0	2MK ₃ (MO ₃)	sym (asym)	42.9271398	2.8618	8.3863	13.7	MK ₃		0.120
MK ₃ (2MO ₃)	shallow	3 1 0 0 0 0	MK ₃ (2MO ₃)	asym (sym)	44.0251729	2.9350	8.1771	13.7	2MK ₃		0.116
2Q ₁	lunar	1 -3 0 2 0 0			12.8542862	0.8570	28.0062	13.8	O ₁	0.0955	0.028
S ₂	solar	2 2 -2 0 0 0	KP ₂	asym	30.0000000	2.0000	12.0000	14.8	M ₂	0.42248	0.461
2SM ₂	shallow	2 4 -4 0 0 0	2SM ₂	sym	31.0158958	2.0677	11.6070	14.8	S ₂		0.025
MS ₄	shallow	4 2 -2 0 0 0	MS ₄	asym	58.9841042	3.9323	6.1033	14.8	M ₄		0.148
S ₄	shallow	4 4 -4 0 0 0	S ₄	asym	60.0000000	4.0000	6.0000	14.8	MS ₄		0.005
M ₁	lunar	1 0 0 1 0 0	NO ₁	asym	14.4920521	0.9661	24.8412	27.3	K ₁	0.02964	0.027
M ₃	lunar	3 0 0 0 0 0			43.4761563	2.8984	8.2804	27.3	MK ₃	0.01188	0.034
N ₂	lunar	2 -1 0 1 0 0			28.4397295	1.8960	12.6583	27.6	M ₂	0.17386	0.553
Q ₁	lunar	1 -2 0 1 0 0			13.3986609	0.8932	26.8684	27.6	O ₁	0.07217	0.022
J ₁	lunar	1 2 0 -1 0 0			15.5854433	1.0390	23.0985	27.6	K ₁	0.02964	0.016
MN ₄	shallow	4 -1 0 1 0 0	MN ₄	asym	57.4238337	3.8283	6.2692	27.6	M ₄		0.176
L ₂	lunar	2 1 0 -1 0 0	2MN ₂	sym	29.5284789	1.9686	12.1916	31.8	S ₂	0.02567	0.409
U ₂	lunar	2 -2 2 0 0 0	2MS ₂	sym	27.9682084	1.8645	12.8718	31.8	N ₂	0.02776	0.219
Mm	lunar (*met)	0 1 0 -1 0 0	MN	asym	0.5443747	0.0363	661.3092	31.8	MSF	0.08254	0.124
P ₁	lunar	1 1 -2 0 0 0	SK ₁	asym	14.9589314	0.9973	24.0659	182.6	K ₁	0.17543	0.110
K ₂	luni-solar	2 2 0 0 0 0			30.0821373	2.0055	11.9672	182.6	S ₂	0.11498	0.094
MSf	lunar (*met)	0 2 -2 0 0 0	MS	asym	1.0158958	0.0677	354.3671	182.6	Mf	0.01369	0.186
Mf	lunar (*met)	0 2 0 0 0 0	KO	asym	1.0980331	0.0732	327.8590	182.6	MSf	0.15647	0.132
v ₂	lunar	2 -1 2 -1 0 0			28.5125831	1.9008	12.6260	205.9	N ₂	0.03302	0.210
λ ₂	lunar	2 1 -2 1 0 0			29.4556253	1.9637	12.2218	205.9	L ₂	0.00670	0.102
2N ₂	lunar	2 -2 0 2 0 0	2NM ₂	sym	27.8953548	1.8597	12.9054	205.9	2MS ₂	0.02301	0.042

3. Methods of Tidal Analysis and Prediction

$2N_2$	lunar	2 -2 0 2 0 0	$2N\bar{M}_2$	sym	27.8953548	1.8597	12.9054	205.9	$2MS_2$	0.02301	0.042
P_1	lunar	1 -2 2 -1 0 0			13.4715145	0.8981	26.7231	205.9	Q_1	0.01371	0.013
S_a	solar (*met)	0 0 1 0 0 0			0.0410686	0.0027	8765.8211	365.2	Ssa	0.01156	0.430
S_{sa}	solar (*met)	0 0 2 0 0 0			0.0821373	0.0055	4382.9052	365.2	Sa	0.07281	0.169
$S1$	solar (*met)	1 1 -1 0 0 0			15.0000000	1.0000	24.0000	365.2	K_1	0.00416	0.062
R_2	solar	2 2 -1 0 0 -1	SK_2		30.0410667	2.0027	11.9836	365.3	S_2	0.00355	0.028
T_2	solar	2 2 -3 0 0 1			29.9589333	1.9973	12.0164	365.3	S_2	0.02476	0.056

Table 3.2. The 37 tidal harmonic constituents that typically had been included in a harmonic analysis at CO-OPS and its predecessor organizations (unless it was an extreme shallow-water situation).

In the 2nd column (“origin of constituent”), the term “shallow” indicates that the constituent was produced by nonlinear mechanisms in shallow water. A “(*met)” indicates that the calculated harmonic constants for this constituent usually include mostly quasi-periodic meteorological effects. (S_6 is marked with a **, because this is one constituent that was a poor choice to be included in the standard 37, since it is usually much smaller than two other sixth diurnal constituents which could have been chosen instead, MS_6 and MN_6 .)

The 4th column (“shallow-water equivalent”) gives the shallow-water constituent with the same frequency as the astronomical constituent listed in the 1st column. The 5th column (“NL mechanism, sym or asym”) indicates whether this shallow-water constituent is produced by the symmetric nonlinear mechanism ($\mathbf{u}|\mathbf{u}|$) or by the asymmetric nonlinear mechanisms ($\partial(\mathbf{q}\mathbf{u})/\partial\mathbf{x}$, $\mathbf{u}\partial\mathbf{u}/\partial\mathbf{x}$, and $\mathbf{q}|\mathbf{u}|$) as indicated in Table 2.4. Constituents listed as asymmetric can also be produced by the lateral initial terms as discussed in Section 7.6.7.

The 3rd column (“Cartwright number”) gives the six digits that indicate which combination of astronomical frequencies (from Table 2.1) produces that astronomical tidal constituent (examples are shown in Table 2.2). These six digits are the multiplying coefficients in front of the six frequencies ω_1 , ω_2 , and ω_3 through ω_5 from Table 2.1. The classic *Doodson numbers* are the same as the Cartwright numbers but with a 5 added to each digit (except the first), which Doodson did to keep these digits from being negative.

The 6th column gives the “angular speed” of the constituent in degrees per hour. Dividing the angular speed by 360° (= one cycle) and multiplying by 24 gives the frequency of the constituent in cycles per day (cpd), shown in the 7th column. Dividing 360° by the angular speed gives the period of the constituent in hours, shown in the 8th column.

The 9th column gives the synodic period for the constituent with respect to (wt) the constituent which is closest in frequency among the constituents with a larger amplitude (shown in the 10th column). Table 3.1 showed several synodic periods for each constituent, each paired with another constituent, but only the longest synodic period for the larger constituents is shown in the 9th column.

The 11th column shows the relative coefficient of the strength of the tide potential (the tide producing force) for each astronomical constituent as determined by Cartwright and Edden (1973), in order to give one a first guess at the expected relative sizes of the tidal constituents (at least the astronomical ones).

However, hydrodynamics will change these relative strengths, and the 12th column gives, as just one example, the constituent amplitudes for a water level station at Trenton, NJ, on the Delaware River. In this latter case, one will notice that N_2 is larger than S_2 , unlike in the tide producing force. Also, for that station one is really calculating $2MN_2$ and not L_2 , and likewise $2MS_2$ not μ_2 .

The tables in Appendix A include many additional tidal constituents.

squares solution technique (Harris, 1965; Foreman, 1977; Foreman and Henry, 1989; Dronkers, 1964). The daily predictions for reference stations in all nationally published Tide and Tidal Current Tables are produced from the harmonic constants that come out of tidal harmonic analysis. Nonharmonic analysis, which is simply one of several methods of comparing the tide or tidal current at two locations, is used to calculate the time differences, height differences, velocity ratios, etc. for the thousands of subordinate stations in these tables that are referred to the reference stations. Several refinements to the harmonic methods were developed in recent decades, as well as the cross-spectral approach of the response method developed by Munk and Cartwright (1966). All of these methods will be described below. Whatever the method used, some principles will always apply. As mentioned above, the analysis of longer data times series will lead to better predictions no matter which type of analysis is used, because more tidal frequencies can be resolved with a longer time series.

3.4 *Harmonic Analysis*

3.4.1 Introduction

Tidal harmonic analysis was first developed by William Thomson (later Lord Kelvin) in England in 1867, but was developed independently in 1874 in the U.S. by William Ferrel. In England, Thomson's work was modified and improved by George Darwin (1883) and Arthur Doodson (1921, 1928) and others, and in the U.S. Ferrel's work was modified and improved by Rollin Harris (1897-1907), Paul Schureman (1924) and others in the U.S. Coast and Geodetic Survey. Harmonic analysis takes advantage of the fact that one knows *a priori* all the frequencies at which tidal energy will be found in a data times series. As already mentioned, most of these frequencies are astronomically caused but many are due to the nonlinear hydrodynamic effects of shallow water. The demonstration in Section 3.1 provides the basic idea of how to find the amplitude and epoch (phase lag) of each tidal constituent's contribution to the tide or tidal current. But when one looks more specifically at the exact mathematical technique for finding the amplitudes and epoch of tidal harmonic constituents, there are differences in the various forms of harmonic analysis techniques. The biggest difference (between older and more recent techniques) is that the Fourier analysis solution technique (e.g., Schureman, 1958) has generally been replaced by a least-squares solution technique (e.g., Harris *et al*, 1963; Foreman, 2004), the latter based on minimizing the squared differences between tidal data and computed tidal predictions.

Before looking at the actual methods for extracting the tidal harmonic constants from a time series of data, one must first look at the harmonic tidal prediction equation. This is the equation into which the tidal harmonic constants (amplitudes and phase lags) are put in order to make a tidal prediction.

3.4.2 The Harmonic Tide Prediction Equation

A tide prediction can be made by summing up the oscillating contributions of some number of tidal constituents. The tide, being a single scalar quantity, requires only a single tide prediction equation. However, Section 3.4.3 will deal with prediction of the tidal current, a vector quantity, which must be broken up into two orthogonal components, so that two prediction equations are needed. (Another option for the tidal current case, however, is to treat the two components together using complex algebra, in which case one can use one prediction equation instead of two.)

3. Methods of Tidal Analysis and Prediction

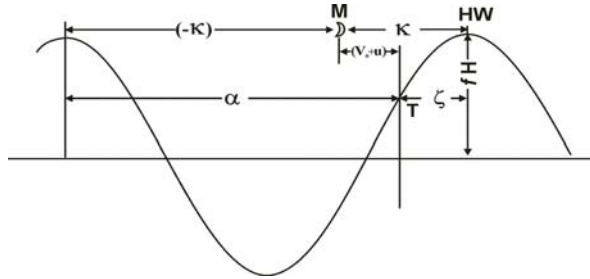


Figure 3.2. A graphical representation of the amplitude and epoch (phase lag) of a single tidal constituent and its time relationship to the moon's transit (over the tide station). (From Schureman, 1958.)

The formula for the height of one tidal constituent, h_1 , at time equal zero, can be written as

$$h_1 = f H \cos(V_o + u - \kappa)$$

which is represented graphically in Figure 3.2. The contribution of a tidal constituent for a specific tidal frequency (each frequency being classically symbolized by the *angular speed*, a ; see Section 2.1.1) is represented by a cosine curve with an amplitude and phase. The amplitude is often called H , but as will be seen, that H is often multiplied by a node factor, f , so that the modulation effect of the 18.6-year lunar nodal cycle can be included (see Sections 2.2.4 and 4.1.5). The phase is usually made up of three parts, the first changing with time and determined by the frequency (angular speed), the second a phase relationship for the idealized equilibrium tide based on astronomical variations (discussed below), and the third, a phase lag relative to the equilibrium tide. This third part, a phase lag for that particular constituent (relative to the moon's transit over the tide station), is usually called the *epoch*, κ .

It is the amplitude H and the epoch κ that are needed for each tidal constituent to make a prediction (and it is H and κ for each constituent that are calculated from a data time series using harmonic analysis). In Figure 3.2, T is a particular time of interest, and M is the time when the constituent argument equals zero, so that the interval from M (the moon's transit over the tide station) to the following high water (HW) is the epoch κ . The time interval from the previous high water to M is measured by the *explement* of κ (i.e., $360^\circ - \kappa$), which can be expressed as $-\kappa$. The phase of the constituent argument at time T is reckoned from M and is equal to $V_o + u$. The phase of the constituent at this time is reckoned from the previous high water and is equal to $V_o + u - \kappa$.

The epoch of the tidal constituent determines when the maximum effect of the tidal constituent occurs, relative to the maximum effect of this same constituent in the theoretical (and idealized) equilibrium tide (which, as was seen in Section 2.1.2, is the tide that would occur on an Earth covered with water and without continents and with the tide responding instantly to the tide producing forces). More specifically, the epoch κ is the angular retardation of the maximum of a tidal constituent of the observed tide behind the corresponding maximum of the same constituent of the theoretical equilibrium tide. Thus it may also be defined as the phase difference between a tidal constituent and its *equilibrium argument*. The *equilibrium argument* is the theoretical phase of a constituent of the equilibrium tide. It is usually represented by the expression $(V + u)$, in which V is a uniformly changing angular quantity involving multiples of the hour angle of the mean Sun, the mean longitudes of the Moon and Sun, and the mean longitude of lunar or solar perigee. As was

mentioned in Section 2.2.4, u is a slowly changing angle depending upon the longitude of the Moon's node and varies over the 18.6-year lunar nodal cycle. When pertaining to an initial instant of time, such as the beginning of a series of observations, the equilibrium argument is expressed by ($V_o + u$).

To account for the effect of the 18.6-year lunar nodal cycle (also see Section 2.2.4) on the amplitude of the tidal constituent, H is usually multiplied by a node factor, f . However, f is not used (nor is u) if the so-called *satellite* tidal constituents are included in the prediction (see Section 4.1.5).

The height of the tide, h , at any time, t , is typically represented by a formula summing up the contributions of the individual tidal constituents, such as the formula below from Schureman (1958):

$$h(t) = H_o + \sum_{i=1 \text{ to } n} f_i H_i \cos(a_i t + \{V_o + u\}_i - \kappa_i) \quad (3.1)$$

where

$h(t)$	=	height (above some reference datum) of the tide at any time t
n	=	the number tidal constituents being used to make the prediction
H_o	=	mean height of water level above the datum
H_i	=	amplitude of tidal constituent i
a_i	=	angular speed of tidal constituent i (i.e., its frequency) [in degrees/hour]
t	=	time, reckoned from some initial epoch (e.g., $t=0$ at the beginning of the year) [in hours]
κ_i	=	epoch (phase lag) of tidal constituent i [in degrees] relative to the moon's transit over the tide station
f_i	=	node factor for tidal constituent i
$\{V_o + u\}_i$	=	equilibrium argument for tidal constituent i at $t=0$. [in degrees]
$(a_i t + \{V_o + u\}_i - \kappa_i)$	=	the phase at any time t (sometimes called the <i>argument</i>) relative to the moon's transit over the tide station

Usually an entire predicted time series of tidal heights is produced using this equation, and then some standardized technique is used to pick off the times and heights of the high waters and the times and heights of low waters (see Section 3.9). Figure 3.3 shows four days of the predicted tide at San Diego, CA (second to bottom plot), compared with the observed water level curve (bottom plot), along with the plotted contributions of four semidiurnal constituents (M_2 , S_2 , N_2 , K_2) and three diurnal constituents (K_1 , O_1 , and P_1).

In the U.S. the reference datum is typically the mean lower low water (MLLW) datum, which is referred to as *chart datum*, because all the depths on U.S. nautical charts are depths *below* chart datum. Tidal predictions are heights *above* chart datum, so the total water depth at any moment in time at a specific location on a nautical chart is the tidal height added to the charted depth.

3. Methods of Tidal Analysis and Prediction

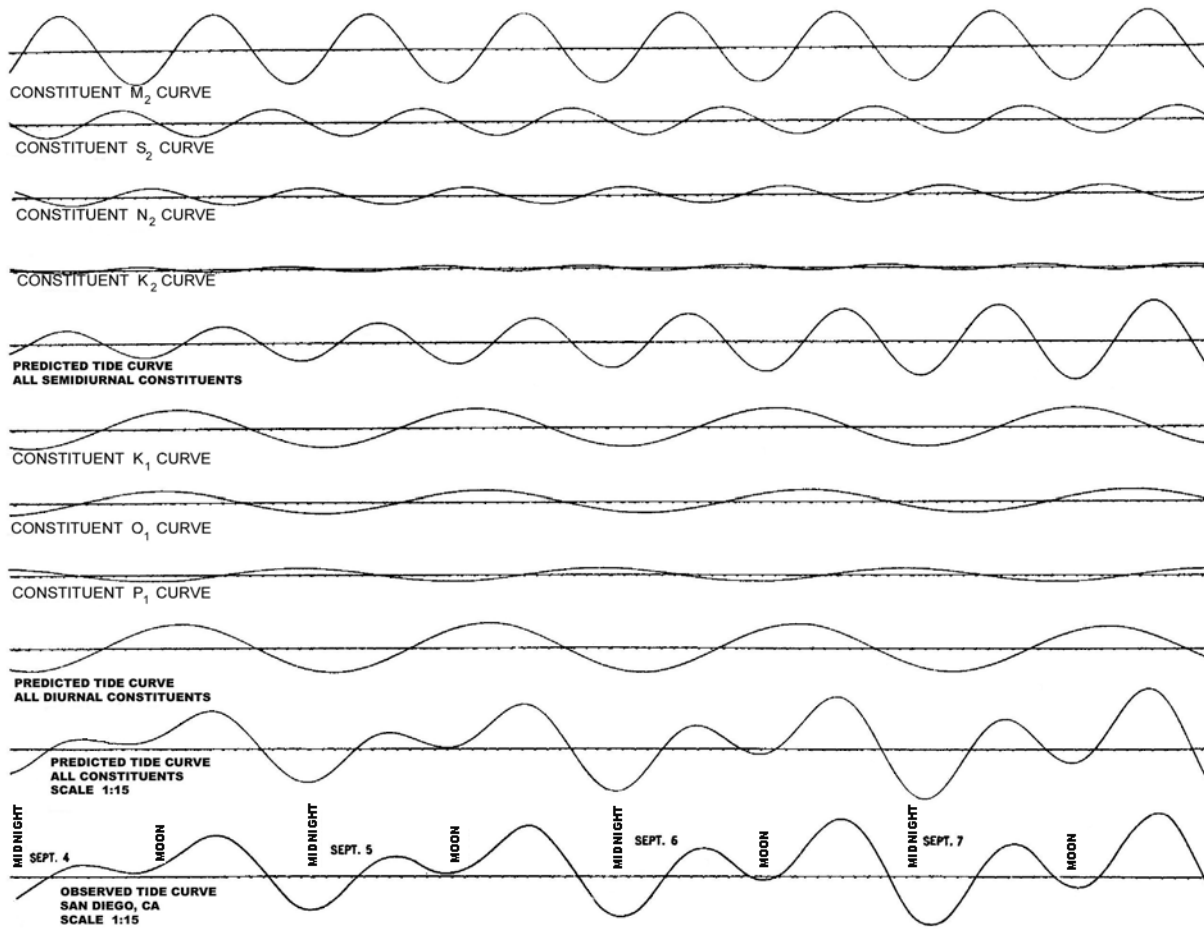


Figure 3.3. Example of a tide curve (second from the bottom) produced with the harmonic tide prediction equation, along with curves for seven of the tidal constituents used to make the prediction. The bottom curve is from water level observations for the same time period as the tide predictions.

As mentioned in Section 2.1.1, the *angular speed* of a constituent is merely a traditionally used form of *frequency* and is given in terms of degrees per solar hour, where 360° is one complete constituent cycle. M_2 , for example, has a speed of $28.984104^\circ/\text{hour}$. One can obtain the frequency of a tidal constituent in cycles per hour by dividing its speed by 360° . Thus, dividing $28.984104^\circ/\text{hour}$ by 360° gives the M_2 frequency of 0.081 cycles per hour, or 1.932 cycles per day. One can obtain the period of a tidal constituent by dividing 360° by its speed. Thus, dividing 360° by $28.984104^\circ/\text{hour}$ gives the M_2 period of 12.4206 hours.

The tidal harmonic constants that come out of a harmonic analysis are the n pairs of amplitudes and epochs, H and κ . The tidal amplitude H is modified by the node factor, f , which allows one to include the modulating effect of the 18.6-year lunar nodal cycle without having to use numerous additional tidal harmonic constant (the *satellite* tidal constituents). Schureman (1958) provides in his Table 14 the values of f for 37 tidal constituents for the years 1850 through 2000. Zetler (1982) extended this table to the year 2025. In this table f is considered to be constant for each entire year (using the midyear value of f). However, if more accuracy is desired, one can use the original

astronomical formulas to calculate f for any time and any time series length. These formulas are provided by Schureman in his Table 2. These node factor formulas have been built into some harmonic analysis and tidal prediction programs, while other programs require the user to read in the node factors as data obtained from Tables like those in Schureman.

The tidal epoch (phase lag) κ' is referenced to the time when the moon passes directly over the exact location of the tide station, the data from which the tidal harmonic constants were calculated. However, using κ' is very inconvenient, since time is always referenced to a local time meridian (or sometimes to the Greenwich time meridian). Also, comparison of phase lags at different locations is not possible without the phase lags having the same time reference system. When the epoch is given in terms of the local time meridian, it is usually called κ' (or g). When the epoch is referred to the Greenwich time meridian (0°) it is called G . The relationship among these three defined epoch terms is described by the following formula:

$$\kappa' (= g) = \kappa + pL - \frac{aS}{15} \quad (3.2)$$

where

- L = west longitude of the tide station (in degrees); it will be negative if the station has east longitude
- a = angular speed of the tidal constituent (in degrees/hour)
- S = west longitude (in degrees) of the local time meridian
- p = the species of the tidal constituent (i.e., = 0 for long-period, = 1 for diurnal, = 2 for semidiurnal, = 4 for quarter-diurnal, etc.)

$\kappa + pL = G$ = the epoch relative to the Greenwich meridian

Time meridians around the world are every 15° of longitude, that is, one hour of time change for every 15° of longitude. In the above formula, the 15 is actually 15 degrees/hour. Thus, for example, the time meridian of 75°W , for the East Coast Standard Time in the U.S., is $(75/15 =)$ 5 hours earlier than at the Greenwich time meridian (0°). Typical tidal analysis and tidal prediction programs allow the use of any of these three versions of the epoch, but one should know the relationship among the three versions. They become especially relevant when considering the *equilibrium argument*, $\{V_o+u\}$.

$\{V_o+u\}$ is not only different for each tidal constituent, it is different for every longitude on Earth. Schureman (1958) provides in his Table 15 the values of $\{V_o+u\}$ for 37 tidal constituents at the Greenwich meridian for the years 1850 through 2000. Zetler (1982) extended this table to the year 2025. As mentioned earlier, V_o is a uniformly varying part of the equilibrium argument, and is referenced by Schureman to the beginning each year. u is a very slowing varying part of the equilibrium argument due to changes in the moon's node, and is (like the node factor, f) referenced by Schureman to the middle of the year and assumed to be constant throughout the year. $\{V_o+u\}$ must, therefore, be corrected for the longitude of the tide station being predicted and for the time meridian used for time referencing. This is accomplished using a formula that looks similar to the one above, namely, the equilibrium argument at a location that is L° west of Greenwich, using the local time meridian, which is S° west of Greenwich, is

$$\{V_o+u\} = \{V_o+u\}_{\text{Greenwich}} + \frac{aS}{15} - pL$$

The tidal prediction equation can thus now be written:

3. Methods of Tidal Analysis and Prediction

$$h(t) = H_o + \sum_{i=1 \text{ to } n} f_i H_i \cos(a_i t + [V_o + u]_{\text{Greenwich}} + \frac{aS}{15} - pL)_i - \kappa_i)$$

which simplifies to

$$h(t) = H_o + \sum_{i=1 \text{ to } n} f_i H_i \cos(a_i t + \{V_o + u\}_{i \text{ Greenwich}} - \kappa'_i) \quad (3.3)$$

so one can now use Schureman's Greenwich equilibrium arguments as well as epochs referenced to the local time meridian (shown here as κ' , but also called g).

However, as mentioned above, the value for the u portion of the equilibrium argument due to changes in the moon's node is assumed to be the midyear value and constant for the entire year (as is f). If one would like a little more accuracy one can use the actual (fairly messy) astronomical formulas for V , u , and f provided by Schureman. These have been computerized and used in some tidal analysis and tidal prediction programs.

3.4.3 The Harmonic Tidal Current Prediction Equations

The tidal current is a vector quantity usually given in terms of a speed and a direction. To harmonically analyze current data one must first transform each speed and direction pair into two orthogonal components, such as north and east components (see Figure 3.4). If s_i is the current speed and θ_i is the current direction clockwise from north (i indicating a particular data point pair), then the north and east components are simply

$$N_i = s_i \cos \theta_i \quad \text{and} \quad E_i = s_i \sin \theta_i$$

Any pair of orthogonal components can be used, and it is common to use major and minor components, where the direction of the major axis is usually the direction of maximum flood, and the direction of the minor axis is 90° clockwise from the major axis (see Figure 3.4), namely

$$Mj_i = s_i \cos(\theta_i - \theta_{\text{major}}) \quad \text{and} \quad Mn_i = s_i \sin(\theta_i - \theta_{\text{major}})$$

Each current vector data time series will be turned into two current component data time series, such as N_i and E_i (or Mj_i and Mn_i), and thus for each tidal current constituent there will be two harmonic constant pairs, namely, an amplitude and epoch for (e.g.) the north component, and an amplitude and epoch for the east component (or likewise for the major and minor components).

And thus for tidal currents, the harmonic prediction equation (3.1) will be used twice, once for each orthogonal component (with the h replaced by an N or E , or by a Mj or Mn). Two predicted component data times series will be produced, and then will be combined to produce predicted speed and direction time series using

$$s_i = (\dot{N}_i^2 + \dot{E}_i^2)^{\frac{1}{2}} \quad \text{and} \quad \theta_i = \tan^{-1}(E_i/N_i)$$

or

$$s_i = (\dot{Mj}_i^2 + \dot{Mn}_i^2)^{\frac{1}{2}} \quad \text{and} \quad \theta_i = \tan^{-1}(Mn_i/Mj_i) + \theta_{\text{major}}$$

Times and amplitudes of maximum floods and maximum ebbs can then be picked off the speed time series, s_i (see Section 3.9.2). The minimums (or slacks, if the current speed goes down to zero and

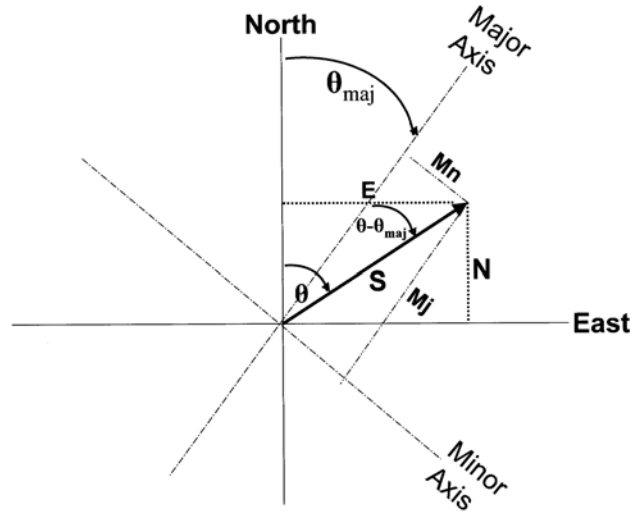


Figure 3.4. A current vector with speed \mathbf{S} and direction θ , broken up into north and east components (\mathbf{N} and \mathbf{E}) and into major and minor components (\mathbf{M}_j and \mathbf{M}_n).

the tidal current becomes truly reversing) are usually found by looking at the speed values when the current flow is directly perpendicular to the major axis as flow (see Section 3.9.2).

The orthogonal pair of harmonic constants for each tidal current harmonic constituent can also be combined (in a way analogous to combining the predicted component time series). This will allow us to see how the speed and direction of flow due to a particular tidal constituent changes each hour, and to watch it rotate around the compass over a tidal constituent cycle. The result will be an elliptical representation of the flow due to that tidal constituent. The technique for producing these harmonic *constituent ellipses* will be described in Section 5.2.

If the two orthogonal components chosen were major-minor components, and the major axis was chosen to be the direction of maximum flood, then by looking at these harmonic constants one can get some understanding of the harmonic makeup of the tidal current in the up-channel direction (i.e., the primary flood and ebb flow), as well as the harmonic makeup of the cross-channel/cross-bay component of the tidal current. [If one originally chose north-east components (as has often been done by default) and these do not line up with the predominant major-minor axes of flow, then interpretation of the results is limited until the harmonic constant pairs are transformed into a major-minor system (see Section 5.2).] The tidal constituent ellipse produced from the pair of orthogonal harmonic constants, provides more information, showing how the flow from that tidal current constituent changes over the whole constituent cycle, which way it rotates, and the direction of its major axis (which may be somewhat different than the mean flood direction and also may be different than that for other constituents, even though one would think that the bathymetry would affect all the constituents the same). One can also decompose each constituent ellipse into different pairs of harmonic constants for two polarized counter-rotating circular motions, one for clockwise motion and one for counter-clockwise motion. This is often done with spectra obtained from currents, and are called *rotary spectra* (see Section 3.10.3).

One can also treat the two orthogonal components together using complex algebra (Pawlucz, et al, 2002). In this case there is one prediction equation instead of two, since the current vector is

3. Methods of Tidal Analysis and Prediction

represented by the complex number $u + iv$ (where u and v are the orthogonal components of the tidal current, but the complex algebra allows them to be treated together). This complex prediction equation looks like

$$v(t) = v_0 + \sum_{i=1 \text{ to } n} a_i e^{i\sigma_i t} + a_{-i} e^{-i\sigma_i t}$$

where $v(t)$ is used to indicate velocity, but this equation could also be used for the scalar tidal heights. a_i and a_{-i} are complex conjugates of the amplitude if $v(t)$ is a real series. For more information see Pawlowicz, et al, (2002).

3.4.4 Fourier-based Harmonic Analysis

The tidal prediction equation itself appears fairly simple – and it is, because various scientists have already worked out the great mathematical complexity behind it, i.e., that dealing with the derivation of the tidal frequencies from astronomical equations, and with the variation of the tide producing forces with time, again based on astronomical equations. The present chapter has unfortunately provided only a little insight into the complexity of this astronomically based work. For a proper appreciation of it one should read Doodson (1921 and 1928) and Schureman (1958, originally published in 1924), Godin (1972), and the more recently Cartwright and Tayler (1971), and Cartwright and Edden (1973). With that work accomplished, one is left with simply having to put some tidal harmonic constants into the tidal prediction equation, and then predicting the tide for any time in the future or the past. These tidal harmonic constants have to be determined from water level data (or current data) because their amplitudes and epochs are determined by the hydrodynamics of the waterways from where the data were obtained, and not by the astronomy.

The more demanding part of the job of tidal analysis and prediction is the analysis part, that is, the calculation of the most accurate tidal harmonic constants possible from whatever data time series may be available. Tidal analysis, of course, also relies on these same astronomical equations, looking for energy at those same astronomical frequencies, and using the equations that determine the variation in tidal forcing with time. And again, that part has been worked out. But extracting accurate tidal harmonic constants from a data time series is trickier than making tide predictions using those harmonic constants.

There have been two primary techniques within the idea of harmonic analysis for extracting harmonic constants from a data time series – using a *Fourier series technique* or using a *least squares technique*. In Fourier-based harmonic analysis, each tidal constituent is solved for separately, and this type of analysis resembles to some extent our demonstration in Section 3.2. In the least-squares-based harmonic analysis (which is described in detail in the next Section), all the tidal constituents are solved for simultaneously, the approach being to minimize the squared differences between measurements and computed tidal predictions. As will be seen, the least squares method has many advantages and is the method generally used today. But the Fourier-based method, which was the first method to be developed, is still worth looking at, at the very least as a lead in to the least squares technique treated in the next section.

Although in CO-OPS a harmonic analysis program based on the least squares technique is the primary method for extracting tidal harmonic constants from data, there is still in use a program based on the Fourier analysis technique developed by Schuremen (1958) for time periods of 15 or 29 days. This latter program, written by Dennis and Long (documented in 1971) has probably remained in use because it is easy to use. Its inference and elimination routines infer some

constituents that cannot be solved for with only 15 or 29 days of data and correct the solved-for constituents for the adverse effects of the unsolved-for constituents (see Section 4.2.1).

Sir Isaac Newton, who in 1687 first explained that the tide was a consequence of the gravitation attraction between the moon and the Earth, was certainly aware of the numerous astronomically caused periodicities in the tide. However, it was the French scientist Pierre-Simon Marquis de Laplace, who in 1775, following up on Newton's work, first suggested the idea of harmonic analysis. He had derived the hydrodynamic equations of motion for tides on a rotating earth, and solved them for the special case of an Earth entirely covered by one ocean. Using that solution he became the first to separate the tide into three species – semidiurnal tides, diurnal tides, and long-period tides, and he went on to say that the tides could be represented by the sum of cosines representing the many periodic forces involved. However, it was not until 1867 that Sir William Thomson (later Lord Kelvin) actually developed and used a practical harmonic analysis method. In the U.S. only seven years later, William Ferrel, a scientist in the U.S. Coast and Geodetic Survey, unaware of Thompson's work, independently developed the harmonic analysis technique in 1874, also basing his method on Laplace's work. In each country, those original harmonic analysis methods were further modified and improved, in England by George Darwin (1883) and later Arthur Doodson (1921), and in the U.S. by Rollin Harris (1897-1907) and Paul Schureman (1924) of the U.S. Coast and Geodetic Survey.

Much of the work of these scientists was astronomical and oceanographic. To actually extract the tidal harmonic constants from the tide data, they all used some form of Fourier series technique. As an example the form of the Fourier-base technique in the U.S. Coast and Geodetic Survey developed by Schureman (in 1924, but revised in 1940) and computerized by Dennis & Long (1971) will be briefly looked at.

Traditionally, before a Fourier-series-based harmonic analysis is carried out, the tidal prediction equation is changed to an equivalent form involving the sums of sines and cosines. Doing this, the tidal prediction equation (3.1) becomes (for a prediction taking into consideration n tidal frequencies a_i)

$$h(t) = H_o + \sum_{i=1 \text{ to } n} c_i \cos a_i t + \sum_{i=1 \text{ to } n} s_i \sin a_i t \quad (3.4)$$

where

$$f_i H_i = (c_i^2 + s_i^2)^{1/2} \quad (3.5)$$

and

$$(V_o + u) - \kappa' i = -\tan^{-1} \frac{s_i}{c_i}$$

Then c_i and s_i can be found from the following two summations:

$$c_i = \frac{2}{N} \sum_{k=0 \text{ to } N-1} h_k \cos a_i k \delta \quad \text{and} \quad s_i = \frac{2}{N} \sum_{k=0 \text{ to } N-1} h_k \sin a_i k \delta \quad (3.6)$$

where time t is now represented by $(k \delta)$, δ being the sampling interval of the data time series and k being the number of the data point (from 0 to $N-1$). Although these summations can be carried out in seconds in the Dennis&Long program (see their subroutine FORAN), in the pre-computer era they had to be done by hand. Years before Schureman's work, special paper stencils or "keys" (i.e., sheets with holes in it that were laid over sheets of tabulated hourly heights) were invented by Leland P. Shidy in 1885, and Schureman incorporated them into his analysis scheme. As Schureman

3. Methods of Tidal Analysis and Prediction

put it, they “resulted in a very great saving of labor,” but it could still take a week or more to do a harmonic analysis by hand compared with seconds on a computer.

As mentioned earlier, the length of the data time series, N , is chosen to be one of the key synodic period lengths (although in the Dennis & Long program that can only be 15 or 29 days). The pairs of c_i and s_i would then be converted to pairs of amplitudes and epochs using formulas (3.6). The epochs are then adjusted for proper time reference using the equilibrium argument $\{V_o + u\}$, which includes the nodal effect of u . The amplitudes are likewise adjusted by dividing them by the node factor f for the time period at the particular data time series that was analyzed. In the Dennis & Long program (1971), the f and u are determined directly from the appropriate astronomical equations (from Harris, 1897, and Schureman, 1941). The program then goes on to implement Schureman’s inference and elimination routines (see Section 4.2.1).

The next section will describe the numerical technique most commonly used today for extracting tidal constituent amplitudes and epochs from a data time series – the least squares technique.

3.4.5 Least-squares-based Harmonic Analysis

As mentioned above, most harmonic analysis programs today use the least squares technique instead of the Fourier series technique described in the last section. Because of its computational demands the least squares technique could not really be used until the computers became available in the 1960s. The least squares technique simultaneously solves for all harmonic constituents (that can be separated with the length of the available data time series). The harmonic constants determined are those that minimize the sum of the square of the residuals, that is, minimize the sum of the squared differences between the original data time series and the predicted time series (i.e., the fit to that series using the calculated harmonic constants). This method has several advantages over the Fourier series method, including: (1) one is not restricted to continuous equally spaced data with no gaps; in fact, the data can be completely random in time and can have large gaps; (2) there is more flexibility on the length of the time series; one does not have to stick strictly to lengths that match a particular synodic period, or a multiple of synodic periods; and (3) one can determine how the variance between the data time series and the predicted time series from the calculated harmonic constants is reduced by each additional constituent included in the analysis.

The least squares harmonic analysis used in CO-OPS is the program originally written by D. Lee Harris in the 1960s. Most other harmonic analysis programs commonly used today also use some type of least squares technique (e.g., Foreman, 2004a). First, the typical least squares technique will be discussed, and then the Harris version will be briefly looked at. In that technique the harmonic constants are derived using a multiple correlation screening process which can be terminated when the regression equation contains a specified number of terms or when the next constituent will not explain some preselected fraction of the variance.

To reiterate the problem, one has a time series of (in this case) water level data, $h(t)$ with N observations, from which one wants to extract the amplitudes (H_i) and phase lags (κ'_i) of the greatest possible number (n) of tidal harmonic constituents, whose frequencies are known. Fitting n harmonic curves to the time series with N observations (where $n \ll N$) is an *over-determined* problem, so there is no solution which could exactly match all the data points, and one looks instead for an approximate solution that best matches the data points. To do this one uses some type of *optimization technique*. Most common of these techniques is the *least squares* technique, in which one will estimate the amplitudes and phase lags by minimizing the squared difference (i.e., “the least

squares'') between the original data time series and the predicted time series created using these calculated amplitudes and phase lags.

Again one starts with the tide prediction equation (3.1) but here one has $\mathbf{h}(t)$ as the actual observed data time series, and so an additional term is included to represent the residual time series, $\mathbf{h}_r(t)$:

$$\mathbf{h}(t) = \mathbf{H}_o + \sum_{i=1 \text{ to } n} f_i \mathbf{H}_i \cos(\alpha_i t + \{\mathbf{V}_o + \mathbf{u}\}_i - \kappa_i) + \mathbf{h}_r(t)$$

with the definitions of the other parameters given in Section 3.4.2. The residual time series is equal to the observed data series $\mathbf{h}(t)$ minus the predicted time series created using the n harmonic constants (\mathbf{H}_i and κ_i). The residual series contains nontidal water level variations due to meteorological effects (such as wind, atmospheric pressure, and river discharge) as well as tidal oscillations caused by any harmonic constants not among the n resolvable constituents used to make the prediction. The residual time series may or may not include \mathbf{H}_o , but one typically demeans the data time series before the harmonic analysis is carried out (in order to minimize roundoff errors), in which case \mathbf{H}_o is taken out of the problem. (This is especially important to do for water level data, which may be referenced to a datum which can be quite a large value.)

And again (as was done in Section 3.4.4) the above water level equation can be transformed into an equivalent form involving the sums of sines and cosines (but with the residual series added)

$$\mathbf{h}(t) = \mathbf{H}_o + \sum_{i=1 \text{ to } n} c_i \cos \alpha_i t + \sum_{i=1 \text{ to } n} s_i \sin \alpha_i t + \mathbf{h}_r(t) \quad (3.7)$$

where

$$f_i \mathbf{H}_i = (c_i^2 + s_i^2)^{1/2} \quad (3.8)$$

and

$$(\mathbf{V}_o + \mathbf{u}) - \kappa_i = -\tan^{-1} \frac{s_i}{c_i}$$

Since one is dealing with digital data, with individual data points, it is clearer to put (3.7) into a digital form. The equation for each individual data point, the k^{th} data point, is

$$\mathbf{h}_k = \mathbf{H}_o + \sum_{i=1 \text{ to } n} c_i \cos \alpha_i t_k + \sum_{i=1 \text{ to } n} s_i \sin \alpha_i t_k + \mathbf{h}_{r_k} \quad (3.9)$$

where k goes from 1 to N . Our objective is to minimize the variance of the residual series, e^2 , i.e., minimize

$$e^2 = \sum_{k=1 \text{ to } N} \mathbf{h}_{r_k}^2 = \sum_{k=1 \text{ to } N} \left\{ \mathbf{h}_k - \sum_{i=1 \text{ to } n} [c_i \cos \alpha_i t_k + s_i \sin \alpha_i t_k] \right\}^2 \quad (3.10)$$

To find the minimum of e^2 one takes partial derivatives of the residual equation (3.10) with respect to the unknown coefficients c_i and s_i , and set the results equal to zero. This produces $2n+1$ simultaneous equations for $n+1$ tidal constituents. These equations are solved using matrix algebra [solution of a $(n+1)$ by $(n+1)$ matrix equation], but the specific solution technique can vary, and various ways of simplifying the matrix can be used to improve the ease and numerical efficiency of the solution. For example, although most least-square-based harmonic analysis programs can handle random data and data with large gaps, one usually has to turn on that option, since there are more

3. Methods of Tidal Analysis and Prediction

efficient matrix solutions that can be used when the data is continuous and equally spaced. (See pages 18-23 of Foreman, 2004; as well as Emery and Thomson, 2001.)

As has been mentioned, with a Fourier-series-based harmonic analysis, one should stick fairly closely to the guidance of synodic periods, but when using a least squares harmonic analysis, there seems to be some leeway, and often less data (than based on synodic periods) will still do a good job. Some oceanographers have managed to obtain good harmonic constants with almost half as much data as would seem to be required by the Rayleigh criterion, and not necessarily with noiseless data (see the end Section 3.3). But this has not always been the case, and there is some thinking that it may depend on the relative phases of the two constituents trying to be resolved with too little data.

Now one particular type of least squares harmonic analysis will be briefly looked at, namely, one using a numerical approach developed by D. Lee Harris (1965). A program using Harris' method is used in CO-OPS. Harris' original Fortran code can be found in Zetler (1982). This method uses a step-wise linear regression algorithm and a multiple-correlation screening process. In the first step of the analysis, the tidal constituent which is most highly correlated with the observed tide is selected and the program derives the harmonic constants for this constituent which provide the best prediction (in a least squares sense, i.e., the residual is minimized). In the second step, the next constituent that will make the greatest improvement to the first prediction is selected, and then the program computes the harmonic constants for both these constituents which will provide the best prediction (again in the least squares sense). The next step is the same, except the third most important constituents is included, and so on. At each step the reduction in variance brought about by the last constituent is calculated. This process continues until either all the user-specified constituents have been considered, or until the reduction in variance brought about by the last tidal constituent considered is below some user-specified value. In other words, if none of the remaining tidal constituents make an appreciable difference, the calculation will end and these remaining constituents will be left out.

[In the program implementing Harris' method, subroutine SCREEN (see Zetler, 1987) solves a large multiple regression equation, but treats the variables one at a time or in pairs, in order to avoid stability problems. Two algebraically equivalent solution procedures are used, one based on a correlation matrix and the other on a covariance or product matrix, because they have different convergence properties, making each preferable for certain calculations. The matrix (of covariance or of correlation) is inverted to solve for the amplitudes and phases of the harmonic constituents. The contribution of the constituent with the highest correlation is then subtracted from the observed data time series and the matrix is recalculated with the residual time series (in place of the observed time series). In each iteration all unused variables are examined to determine which will make the greatest contribution to the solution. The matrix is rearranged if necessary to facilitate the solution for selected variables. A check for potential instability is made along with this procedure and if a potential or real instability can be recognized with any predictor, that predictor is set aside for consideration after all the apparently stable predictors have been considered. Calculations are ended when none of the remaining predictors will make a significant contribution.]

A user's guide for running the most recent version in CO-OPS of Harris's least square harmonic analysis program (called LSQHA) can be found in Zervas (1999). It is presently set up to handle 175 tidal constituents. The program can handle water level or current data. In addition to the harmonic constants (amplitudes and epochs) the program also outputs the variance accounted for by each constituent, the cumulative variance, the observed mean, the observed variance, the observed standard deviation, the residual variance, the residual standard deviation, and the regression constant.

3.5 Other Frequency Domain Methods

3.5.1 The Response Method

Of all the alternatives to harmonic analysis for tidal analysis and prediction the *response method* is the technique most often used, and the one often felt to be an improvement over the harmonic technique, although such improvements are actually minor in terms of producing accurate predictions. The response method is simpler in some ways (requiring fewer arbitrary constants), but the results are usually not as easy to interpret as those from a harmonic analysis, whose amplitudes and phase lags for each tidal frequency, whether astronomical or of nonlinear shallow-water origin, are quite straight forward to interpret with regard to the effects of the hydrodynamics of the ocean and connecting waterways. Expert use of the response technique requires some background in spectral analysis and other areas of time series analysis. Here only a short summary of this technique is provided, along with references to numerous papers.

The response method was first proposed by Walter Munk and David Cartwright in their well-known paper “Tidal Spectroscopy and Prediction” (Munk and Cartwright, 1966). They note that in the harmonic method the Kepler-Newtonian mechanics (representing the many aspects of the Earth-moon orbit, the Earth’s orbit around the sun, and the Earth’s rotation and wobble) is only used to identify the principal tidal frequencies (Table 2.1). In their response method, however, they directly take into account the actual Kepler-Newtonian mechanics. From the basic astronomical equations they generate a time series of the tidal potential itself (i.e., the tide-producing forces) for the same time period as a water level data time series. They then treat the problem essentially like a “black box” system, where the tide potential is the input to the system, the water level time series is the output of the system, and the response of the system is determined by comparing the output with the input in some manner. The response of the system once determined (for the particular location of the water level station) can then be applied to a tide potential time series generated for another time period to produce tide predictions for that time period.

The “black box” system essentially represents all the hydrodynamic effects of the ocean and any connecting waterways on the tide (at that specific location), yet it is determined strictly statistically, by cross correlating the time variation of the potential with the observed time variation in the water level. This involves the use of a weighted sum of past and present values of the potential. If $\eta(t)$ is the water level time series and $V(t)$ is the astronomically generated tidal potential time series, then a predicted water level time series $\tilde{\eta}(t)$ can be produced according to

$$\tilde{\eta}(t) = \sum_s w(s) V(t-\tau_s),$$

where the weights w are determined so that the prediction error $\eta(t) - \tilde{\eta}(t)$ is a minimum in the least-square sense. [This is referred to as taking the *convolution* of w and V , where V has been reversed and shifted in time.] These weights represent the “sea level response” at the location of the water level gauge to a unit impulse $V(t)=\delta(t)$, which is where Munk and Cartwright got the name *response method*. The actual input potential $V(t)$ was regarded as a sequence of such impulses. Munk and Cartwright expanded $V(t)$ in spherical harmonics, which converged rapidly so only a few terms were needed. This input potential, in the form of time-variable spherical harmonics confined to the tidal bands (0, 1, and 2 cycles per day), is cross-correlated with the output, and the response is expressed in terms of frequency-dependent *admittances* (amplitudes and phase lags). (The admittance is the cross spectrum of the input and output functions divided by the power spectrum of the input

3. Methods of Tidal Analysis and Prediction

function, the cross spectrum being a measure of the part of the output spectrum that is coherent with the input spectrum. Each admittance has an amplitude and a phase.)

A key assumption of this method, called the *credo of smoothness*, is that these admittances should vary smoothly over each narrow tidal band. This appears to work fine for deep water stations, but in shallow-water areas, where the admittances are no longer as smooth, one has to include some additional nonlinear input functions to handle the shallow-water tides (which is done as a second step in the analysis).

One can also include other inputs, for example, a *radiational* input included by Munk and Cartwright to represent some solar/meteorological effects (some of which show up in the S_a , S_{sa} , and S_i harmonic constants in a harmonic analysis). (See also Zetler, 1971.)

The variability of the admittances for a tidal band varies with the number of complex weights in the response analysis. The number of complex weights that can be resolved depends on the length of the series being analyzed (Zetler and Munk, 1975), just as do the number of constituents that can be resolved with the harmonic method. In fact, Zetler, *et al* (1969) provides a method for deriving harmonic constants from response admittances. The response method has proved to be very useful for tidal research, but only slightly improves tidal prediction accuracy (Zetler, *et al*, 1979; Amin, 1977, and Smith, *et al*, 1997). See also discussions in Pugh, 1987 and Godin, 1988.

From the standpoint of doing a self-prediction, the response method with a radiational input may do a better job than a harmonic analysis because it does a better job at handling the low-frequency (annual, semiannual, and other periods) variations due to nontidal/meteorological effects (wind, pressure, temperature, river runoff). However, these low-frequency nontidal variations vary considerably from year to year (as will be seen in Section 3.7.1), and so for predictions into the future, when one does not know what the response to the radiational input will be (the chaotic atmosphere being the key intermediary, since it produces the winds, atmospheric pressure, etc), one would not expect as much prediction skill. Also with regards to prediction skill, there is always an effect of the length of series (also affected by noise) no matter what the method of analysis (response method or harmonic analysis). The response method has been used with short data time series by using the water level time series (or predicted tide series) from a nearby longer reference station as its input instead of the tidal potential. As was mentioned already (and will be discussed in more detail in Section 4.2) there are also various ways to use a reference station with harmonic analysis.

3.5.2 The Harmonic Shallow-Water Corrections Method

In shallow water the nonlinear hydrodynamics transfers energy to many additional frequencies, which must be included in a harmonic analysis if accurate predictions are to be made. For shallow waterways with large tide ranges many dozens of additional harmonic constants are required, the majority in higher frequency bands. Today with modern computing capabilities one can easily handle a hundred or more tidal constituents, but in the pre-computer era this presented a serious problem. Tide predicting machines could not handle that many tidal constituents and the effort to determine the additional harmonic constants manually was excessive. This was a significant problem in the United Kingdom, which has many bays and estuaries that are shallow and have large tide ranges.

To deal with this problem Arthur Doodson developed a special technique, which came to be called the *harmonic shallow water corrections (HSWC) method* (Doodson, 1957). This method was intended to improve the predicted heights and times of high and low waters for locations in

waterways with strongly nonlinear tides. The HSWC method used a two-step process. First a tide prediction was made using the best available harmonic constants, from which high and low waters were calculated. Then in the second step, corrections to these high and low waters were made that took into account the distortions of the tide caused by the shallow water. To make these corrections Doodson actually took advantage of the aliasing caused by the energy at frequencies greater than the Nyquist frequency (see Section 2.2.3). In this case, because (in the second step) his data points were only high and low waters, he was dealing with a sampling interval of a lunar day. He was able to derive formulas where the differences in the heights and times of the high and low waters depended only on the folded frequencies obtained by this mean-lunar-day sampling. (See also Godin, 1972, pp 154-61) Doodson also was able to do the initial harmonic prediction at a reference station (e.g., at the entrance to a bay where the shallow-water effects were not strong) instead of at the actual station where the strong shallow-water effects were, and then could correct those predictions for the shallow-water effects at this second station. This made for a more efficient process if there were many shallow-water stations to be predicted, since they could all use the same reference station for the harmonically predicted first step of the process (especially since all calculations were done by hand and all harmonic predictions were done on a tide predicting machine).

In the modern computer age the HSWC is still a useful method for extreme situations where one does not want to deal with hundreds of harmonic constituents. Amin (1977) did a comparison between the HSWC method, the response method, and an extended harmonic method (i.e., one using more than a 100 harmonic constituents) and found that all three were comparable to each other with respect to the accuracy of the predicted high and low waters. However, he also points out that the HSWC method does not work well in waterways with strong diurnal signals, i.e., where K_1 approaches the magnitude of M_2 .

3.5.3 Species Concordance Method

Extreme shallow-water situations can be handled by the harmonic method of analysis and prediction, but the number of additional shallow-water tidal constituents needed (to capture all of the energy that the nonlinear hydrodynamic mechanisms have transferred to new frequencies) can become quite large for a shallow waterway with a large tide range. For example, Zetler and Cummings (1967) used 114 constituents for the tide at Anchorage, Alaska, as did Rossiter and Lennon (1967) for the tide in the Thames estuary in the United Kingdom (although only 74 constituents of each 114 were the same for both groups).

In the Gironde estuary in France, George and Simon carried out spectral analyses of water level data that showed tidal lines out to 38 cycles per day (cpd) at Bordeaux, about 100km (39 miles) up the estuary. They were already using 100 constituents to predict the distorted tide at Bordeaux, but they increased that to several hundred. With so many constituents needed it gets very messy trying to determine the particular constituents that should be included in the analysis, since there can be many different combinations of the astronomical frequencies that can produce the same high-frequency compound tidal constituents. And it takes more than a year of data to separate many of them. In 1978 the Bordeaux Harbor Authority asked the French Hydrographic Service to improve the accuracy of the tide table predictions for the Gironde estuary including Bordeaux Harbor. The result was the *species concordance method*, which was first used in 1980 to produce those improved tables (George and Simon, 1984; Simon, 1991).

3. Methods of Tidal Analysis and Prediction

The *species concordance method* relies on the nonlinear relation between species of the tide at the station to be analyzed (and predicted) and at a reference station where the tide is well known and easily predicted (often at the mouth of an estuary). The efficiency of the method results from its application to the predictable part of the water level variation, which is confined to narrow bands of the spectrum. Each species may be analyzed individually. This method is similar to the response method in that it involves a convolution (see Section 3.5.1), but without using the tidal force (or potential) as the input as the latter method does.

Like Doodson's harmonic shallow water corrections method (Section 3.5.2) this is a two-step method, and it also uses a reference station (e.g.) near the entrance of an estuary where the shallow-water effects have not built up. The harmonic method is used to predict the relatively undistorted tide at the mouth of the estuary, and a secondary technique is then used to predict the tide at the stations up the estuary where the shallow-water effects are significant. The relationship between the tide at the reference station and the tide at a station up the estuary is expressed in terms of so-called *reduced vectors*, which are the complex amplitudes of the tide in particular species, and which vary slowly. Reduced heights are computed from these using the Fast Fourier Transform, and then real heights by quadratic interpolation. (See George and Simon, 1984; Simon, 1991).

The species concordance method has been used successfully not only to account for the many higher frequency tidal species (e.g., up 36 cycles per day for Rouen on the upper Seine River), but also to account for the effects of river discharge. Average seasonal variations in river discharge can be input, but river discharges can vary considerably throughout the year, so in the species concordance method the fresh water level may be explicitly introduced by the user so that events like freshets can be handled.

3.5.4 Method for Superfine Resolution of Harmonic Constituents

Amin (1976, 1991) developed a refinement to the harmonic method, the method for *superfine resolution of tidal harmonic constituents*, in which a corrective step is added to the harmonic method. The tidal species are divided into subgroups of common origin, such as those due to gravitational (astronomical) or advective or frictional forces. Then, in conjunction with functional representation of the response of the sea and of nonlinear interaction coefficients within a subgroup, harmonic analysis is used to improve the resolved tide and to compute estimates for some additional terms (constituents). The interaction coefficients of the resolved nonlinear tides are computed using the analytical solution of the hydrodynamic equations (see Chapter 7). Then the unresolved nonlinear terms are estimated by interpolating these coefficients. Using this method, estimates of nodal terms can be obtained from analysis of a few years of tide gauge records and the variance of the principle tides can be reduced. See Amin (1976, 1991) for more details.

3.5.5 Continuous Wavelet Transform Method

As was shown in Section 2.3.3, there are times when in shallow water the nonlinear interaction between the tide and a nontidal phenomenon (such as river flow or storm surge) can lead to a temporary change in the tide range, as well as a distortion in the tide indicated by a change in the shape of the tide curve and an increase in the overtide constituents (M_4 , M_6 , and M_8). This, of course, can also be seen in the tidal current, which in addition can also be affected by changes in density (due to changes in salinity or temperature) through the temporary generation of internal tide waves or other baroclinic effects.

Any harmonic constants calculated from data obtained when nontidal effects are very significant cannot be used at other times to predict the tides. They might only be usable for a self prediction during the time period from which they were derived, and possibly for a future period when the same nontidal effect was predicted to occur. For example, as was seen Section 2.3.3 a high fresh water flow in the early spring in some rivers will lead to a dramatic shrinkage in the tide range and a distortion of the tide curve (a higher M_4/M_2 ratio). The harmonic constants derived from (e.g.) a 15-day harmonic analysis for a period covering this freshet, if used to make predictions for the rest of the year would greatly underpredict the tide ranges. But even using these harmonic constants to try to predict the water level during the freshet event may not work well either, since the event most likely was much shorter than 15 days, the 15-day analysis came up with average harmonic constants for the whole 15-days (hence spreading the two- or three-day effect over the entire 15 days). The effect of the shorter period freshet was not captured, since one could not do a quality harmonic analysis with only a few days of data.

For this type of situation, i.e., a relatively short nontidal event which is known to affect the tide through some type of nonlinear interaction mechanism (usually due to shallow water, or for currents perhaps a lateral inertial effect as seen in Section 2.36e) a special type of tidal analysis was developed by David Jay called the *continuous wavelet transform* (CWT) method (Jay and Flinchem, 1999; Jay and Kukulka, 2003). This method is used for those special applications where one wants to better understand the dynamics of a short nontidal event that significantly affects the tide or tidal current, or one wants to be able to do a self prediction for that time period. Also, if one has an independent way of accurately predicting the nontidal event, then the CWT method could possibly be used to make a more accurate future prediction of the total effect of such an event, involving both the tide and the nontidal influence. [This, of course, can also be done using a nonlinear numerical hydrodynamic model, if one has such a calibrated and verified model for the particular waterway of interest.]

Like the species concordance method, the CWT method does not use tidal constituents, but instead uses just tidal species, usually the semidiurnal band, the diurnal band, and the higher harmonic (overtide) bands. For short nontidal events, one cannot separate out the effects of (e.g.) the various semidiurnal constituents, but the effect of not knowing N_2 and S_2 in addition to M_2 is much smaller than the nonlinear effect of the nontidal phenomenon on the tide. Thus, for this special situation a species approach is fine.

3.5.6 Harmonic Constants From a Long Series of High and Low Waters

Before modern automated water level gauges were invented, water level measurements were made using a tide staff attached to a pier or some other permanent structure. Because the measurements had to be made by sight and recorded by hand, it could be quite labor intensive to record hourly water level heights. At some locations therefore only the height and time of high waters and low waters were recorded, but sometimes such data series lasted for years. Such historical data time series may only have one or two data points a day, but they can still be used to extract harmonic constants. Although, as will be seen elsewhere in this book, the high and low waters (and especially their timing) are very sensitive to the effects of nonlinear shallow-water dynamics as well as to the accuracy and/or bias of particular observers, useful harmonic constants should still be obtainable, if the time series is long enough (see more below).

When such data are found today (through some data archeological effort) it can easily be harmonically analyzed with a least squares technique written for handling random data. However,

3. Methods of Tidal Analysis and Prediction

in the pre-computer era when these high and low water data series were created, other methods had to be devised, but these were still quite elaborate and labor intensive to carry out.

The first in the U.S. to derive harmonic constituents from a series of high and low waters was probably William Ferrel (1874, pp 160-83), who applied his method to a 19-year data series from Brest, France, that had originally been analyzed by Laplace. [One result of Ferrel's work was his calculation that the moon's mass was 1/78.0 of the Earth's mass (p.189), a value that is closer to today's accepted value of 1/81.3 than the value that Laplace had calculated, 1/75. He went on to obtain an even closer value, 1/81.7, from a 19-year data series from Boston Harbor. (see Cartwright, 1999, p 104).] In 1890 George Darwin published his method of harmonic analysis of tidal observations, which he said was needed because "Extensive use of the tide gauge has only been in recent years, and by far the largest number of tidal records consist only of observations of high and low water." (Darwin, 1890) He also states "My objective has been to make the whole process a purely mechanical one, and, although nothing can render the reduction of tidal observations a light piece of work, I believe that it is here presented in a form which is nearly as short as possible." However, 61 years later Arthur Doodson would say that due to the complexity of the method designed by Sir George Darwin he would "rule it out as a practical method" (Doodson, 1951). Doodson came up with a clever method that treated the high and low water times and heights as low-frequency harmonic series, but it still took him 65 pages to explain and demonstrate his method. Twenty years earlier Doodson published a method of analyzing and predicting tidal currents based on analysis of only the slack waters (Doodson, 1928b), which also could be applied to the tide.

In 1924 Paul Schureman also referred to Darwin's method as "an elaborate mode of analysis" and provided his own simpler method of harmonically analyzing high and low waters (Schureman, 1924, rev. in 1940), which was partially based on a method developed by Rollin Harris at the turn of the century. Only a few highlights of that method will be mentioned here (see pages 100-104 in Schureman for more details) to give the reader an idea of the process, which involved the use of the old Coast & Geodetic (C&GS) forms and stencils. The first step was simply to make the "usual high and low water reductions, including the computation of the lunitidal intervals." This involved tabulating the times and heights of all the high and low waters, along with the times of the moon's transits, and the calculation of the interval between each transit and the following high or low water (he used C&GS Form 138 for this). Then separate means were found of all the low water intervals and of all the high water intervals. For semidiurnal tides the approximate amplitude and epoch for M_2 could be obtained directly from these results. The amplitude of M_2 was found by multiplying the mean tide range by 0.47 (or by the ratio of M_2 amplitude to mean tide range at a nearby water level station), and then corrected for the longitude of the moon's node using factor F from Schureman's Table 12.. The epoch of M_2 was obtained from the high and low water lunitidal intervals, HWI and LWI, using the formula

$$M_2^o = \frac{1}{2} (HWI + LWI) \times 28.944 + 90^\circ$$

where HWI must be larger than LWI, and so 12.42 hours could be added to HWI if necessary. M_4 is the main cause of the difference between the average duration of the rise and fall of the tide, and this was used to calculate an approximate M_4 . Schureman ended up with the following formula for the amplitude of M_4

$$M_4 = \mp \frac{1}{2} \frac{\cos \frac{1}{2} a DR}{\cos a DR} M_2$$

where a = the angular speed (frequency) of M_2 and DR = the average duration of the rise of the tide. Schureman then found approximate values for S_2 , N_2 , K_1 , and O_1 using the following procedure. First he added the mean tide range value to each low water height, and copied the high and modified low water heights onto the form usually used for hourly height (C&GS Form 362). Then he summed for the desired constituents using the same stencils normally used for analyzing the regular harmonic analysis of hourly heights. He then went through a second procedure to improve these results, making use of a tide predicting machine. With this machine he made tide predictions with the harmonic constants calculated so far (plus some smaller inferred constituents) and tabulated the differences between the heights of the predicted high and low waters and the heights of the observed high and low waters. These differences were then summed and analyzed in the same manner as the original observed heights of high and low water. The result from this analysis of the residuals was then combined with the previously calculated constants. For the combination of the previously calculated harmonic constant with the amplitude and epoch corrections, Schureman used the following two formulas:

$$A = [(A' \cos \kappa' + A'' \cos \kappa'')^2 + (A' \sin \kappa' + A'' \sin \kappa'')^2]^{1/2}$$

and

$$\kappa = \tan^{-1} \frac{A' \sin \kappa' + A'' \sin \kappa''}{A' \cos \kappa' + A'' \cos \kappa''}$$

where A and κ are the final corrected constituent amplitude and epoch, A' and κ' are the original uncorrected amplitude and epoch, and A'' and κ'' are the corrections.

Another specialized example of deriving harmonic constants from nonharmonic tidal quantities was published in 1952 by Bernard Zetler, in this case a relatively simple procedure to infer M_2 and (K_1+O_1) amplitudes from the mean diurnal high water inequality (DHQ) and the mean diurnal low water inequality (DLQ). DHQ is the difference between the mean higher high water (MHHW) and the mean high water (MHW), and DLQ is the difference between the mean lower low water (MLLW) and the mean low water (MLW).

The ratio of (K_1+O_1) to M_2 is often used for the classification of the type of tide (see Section 2.2.5), but in this case there was a different motivation for this technique, which was developed during World War II. About 250 secondary stations in the Philippines had to be assigned to several new reference stations (which were required because of the great variability in the diurnal-to-semidiurnal ratio throughout the islands). Because of this great variability, the values for M_2 and (K_1+O_1) were needed in order to assign a secondary station to the most appropriate reference station. However, no water level data were available for these stations, only the DHQ and DLQ values in the tide tables. And so Zetler developed the following method, publishing it six years after the war ended.

Zetler ended up with two seemingly very simple formulas for the (K_1+O_1) amplitudes

$$\text{if } DHQ > DLQ, \text{ then } (K_1+O_1) = DHQ/F_1$$

and

$$\text{if } DHQ < DLQ, \text{ then } (K_1+O_1) = DLQ/F_1$$

where F_1 is provided by Table 1 found in Zetler (1952) and ranged from 0.46 to 0.64, chosen according to a DHQ/DLQ (or DLQ/DHQ) ratio ranging from 1.0 to 3.6. He also presented a seemingly simple formula for the M_2 amplitude from the mean range (Mn)

3. Methods of Tidal Analysis and Prediction

$$M_2 = M_n / (2.19 + F_2)$$

where F_2 is provided by Table 2 in the same publication and ranged from 0.00 to 0.65. Of course, the complexity came in developing the Tables for F_1 and for F_2 , which is explained in Zetler (1952) and makes use of Tables in S.P. 260 (C&GS, 1952).

As mentioned at the beginning of this section, with today's modern computer capabilities, the use of the least squares harmonic analysis technique is the best way to derive harmonic constants from a time series of high and low waters. Zetler, *et al* (1965) were one of the first to assess the usefulness of this approach. They created one month predicted tide records with 100 or less random data points selected over that period but restricted to 11 hours of daylight (which comes down to 3 or less data points per day). Although these random data points were not necessarily high or low waters, they were equally as sparse. (They actually represented the time density of observations of currents measured photogrammetrically from airplanes which flew only during the daytime.) They were able to obtain accurate harmonic constants for a variety of cases. Most cases were noise free (since the data points selected were actually tide predictions), but in four cases they added noise by reducing the number of significant figures in the data points.

Foreman and Henry (2004) also carried out numerical tests, this time specifically analyzing one month of observed high and low waters with a least squares technique. Good harmonic constants were obtained for all the test cases, which included: adding gaps, adding timing errors, using inference and not using inference, and using daytime only values. They also added an option to the least squares error-minimization equation in which they included a zero derivative representing the fact that they were looking only at high and low waters. Including this option gave better results, but the results without this option were still quite good. Foreman and Henry also provide a program and manual for carrying out the harmonic analyses of high and low waters. Because there are much fewer data points when analyzing high and low waters (versus analyzing hourly data) their high-low water analysis program uses a different least squares solution technique than the program they use to analyze hourly data (Foreman, 2004a).

Theoretically, with such least squares methods, one may not be able to accurately calculate overtides or other higher frequency compound tides, since the (approximate) sampling rate determines the highest frequency that can be calculated and when using only high and low waters (an approximate sampling interval of 6 hours) the upper limit is somewhere between the semidiurnal and quarterdiurnal bands. However, was seen with Schureman's method, one should at least be able to approximate the M_4 constituent by looking at the duration of the rise of tide from low water to high water.

3.6 Nonharmonic Comparison Methods

3.6.1 Overview and short historical background

In the past, tidal analysis and prediction manuals or books have usually paid most attention to harmonic or other frequency-domain methods. That is understandable from the standpoint that such methods provide the greatest prediction accuracy and also the greatest understanding of the tidal dynamics. However, throughout history the methods that have been used most often for tidal prediction have been *nonharmonic methods*. Such methods relate the tide, both its height and its timing, to either the passage of the moon overhead (and the day of the lunar month) or to the tide

at another location (where it is presumably well known and accurately predicted, being based on harmonic analysis). The earliest methods of tide prediction by ancient man correlated the times of high water with the moon's passage overhead, and also, of course, correlated the size of the tide range with the phases of the moon. (The latter was probably what convinced ancient man that there was some type of connection between the moon and the tide.)

The world's oldest known tide table, produced by the Chinese (more than 200 years before the English tide tables for London Bridge) to predict the occurrence of the tidal bore in the Qiantang River near Hangzhou, was based on a nonharmonic analysis. The tide table was first carved in stone on the Zhejiang Ting pavilion on the bank of the Qiantang at Yanguan, and later a printed version was produced in 1056 A.D. The tide table gave the time for two occurrences of the bore for each day (to the nearest 2 hours) for each lunar month in each of four seasons of the year. The two-hour time intervals of each day were called the "twelve earthly branches", which began at 11:00pm, each branch being named for an animal – rat, ox, tiger, hare, dragon, snake, horse, sheep, monkey, cock, dog, and pig. The heights of the bore, from lowest to highest, were seven characters translated as lowest, very low, low, fairly high, high, very high, and highest (see Zuosheng, *et al.*, 1989). The English tide table for London Bridge was also based on a nonharmonic method and simply related the tide to the *age of the moon* (the number of days since the last new moon). As was mentioned in Section 1.4, John Lubbock greatly perfected the nonharmonic method for tide tables he produced in England in 1832. Eighty years earlier Daniel Bernoulli also produced very useful tide tables in France using a nonharmonic method.

Those earlier nonharmonic methods compared the elevation and times of high waters (and sometimes low waters) to various astronomical occurrences such as the moon's transit, times of new moon and full moon, times of apogee and perigee, etc. More recently, and for many decades now, the main use for nonharmonic tidal analysis has been to compare one or more aspects of the tide (or tidal current) at two tide (or tidal current) stations. A typical nonharmonic comparison analysis might, for example, calculate the time difference between the occurrence of high water at two tide stations, as well as the height difference, and similarly for low waters at the two stations. Although this type of analysis is not very sophisticated, it has been used to analyze data at thousands of locations, i.e. at the so-called *subordinate stations* (or *secondary ports*) in national tide and tidal current tables. In the U.S. Tide Tables, daily predictions of high and low waters for particular *reference stations* (called *standard ports* in other nations), produced using harmonic constants, are found in Table 1. The nonharmonic comparison analysis is used to compare a subordinate station to a reference station, and the resulting time differences and height differences are listed in Table 2. The same is true for current data, but here there are four sets of differences in Table 2, for maximum flood, maximum ebb, slack before flood, and slack before ebb. In some cases, where the current is not strictly reversing the slacks are replaced with minimums. In some cases current speed comparisons between the subordinate and reference station are handled with ratios instead of differences, and in some rare cases both differences and ratios are used.

The use of nonharmonic comparison methods has been necessary for two reasons. First, there is limited space in the annually published paper Tide Tables. If daily predictions (i.e., the times and heights of high and low waters) were included for the thousands of tide stations in these tables, they would have many thousand of pages (typically there have been four pages per harmonically predicted reference station in Table 1 of the Tide Tables). However, the time and height differences for a subordinate station (relating it to a reference station) takes only one line in Table 2 (with typically 60 stations to a page). Thus, the only way to manageably include the thousands of stations is to calculate time and height differences using a nonharmonic comparison method. Second, in the

3. Methods of Tidal Analysis and Prediction

past at least, many stations had too few days of data to carry out a reliable harmonic analysis. This was especially true of stations with current data. Those data records were typically short because current meters were much more difficult to deploy and maintain compared with land-based coastal water level gauges.

An average time or height difference that comes out of a nonharmonic comparison analysis is implicitly assumed to be constant and to apply at all times so that it can be used to adjust the harmonically-predicted (e.g) high waters at the reference station in order to predict the high waters at the subordinate station. However, it is important to remember (and it will be demonstrated in Section 3.6.3) that such differences and ratios actually vary throughout the month as astronomical forces change. The closer the reference and subordinate stations are in their tidal characteristics the smaller this variation will be. But often these two stations are not as similar as one would like, and this variation throughout the month can be the greatest source of error in producing a tide or tidal current prediction for a subordinate station. This is especially true in waterways with a significant diurnal inequality. Such errors are minimized by using a reference station that is close enough to the subordinate station to have very similar tidal characteristics, but as mentioned above this has not always been possible in the past. It can be especially difficult for current stations, since the frequency characteristics of the current can change significantly over fairly small distances by such things as channel bends and points of land through inertial effects (as seen in Section 2.3.6).

3.6.2 Types of Nonharmonic Analyses

There are three basic types of nonharmonic analysis: (1) the monthly mean analysis; (2) the *mean cycle analysis* (or *rotary analysis* when analyzing current data); and (3) the *cycle-by-cycle analysis* (or *reversing reduction analysis* when analyzing current data). The first two analyses derive differences between two stations from average values calculated at each station over some time period (a month for the first analysis). The third method, however, calculates differences and/or ratios for every individual tidal cycle in a data series. The first and third analyses look at only key points in the tidal cycle (high and waters or maximum floods and ebb and slacks), while the second analysis produces an entire mean tide or mean tidal current curve.

The *monthly mean analysis* is typically done on water level data (U.S. C&GS, 1965). Times and heights of high water and low water are tabulated at a station and mean values are calculated for one or more months. These mean results are then directly compared with the mean results from a reference station to give time and height differences (and/or height ratios). A month-by-month comparison ignores the greatest tidal variations, those that take place within each month from cycle to cycle. It also provides no information between the high and low waters, and thus cannot represent distortions in the tide curve caused by nonlinear shallow-water effects.

The *rotary reduction analysis* has been used primarily with current data (U.S. C&GS, 1950) and is so named because it was originally used with data taken from offshore current stations where the current flow was rotary. At such stations the direction of flow rotated around the compass in one tidal cycle and no distinct direction of maximum flood or maximum ebb could be determined. In a rotary analysis the velocity time series is divided into tidal cycles, which are superimposed and vectorially averaged to produce mean tidal current curves (speed and direction plots, and a polar plot with the equivalent of a current rose only the tips of each vector are usually connected). The division of the data series into tidal-cycle pieces is determined by the times of a single key point in the tidal cycle (e.g. times of maximum flood) at the reference station. The rotary analysis is useful for all current stations where one is interested in the values in between the times of maximum flood

or ebb or the times of slack (minimum). It is especially useful in shallow-water areas where the tidal current curve can be distorted (away from a perfect cosine curve) due to over tides, and it can even show double floods or ebbs. The rotary analysis is also very useful in producing tidal current charts that depict the tidal flow in a waterway for each hour of the tidal cycle; the actual rotation of the current at each location can then be depicted. The equivalent *mean cycle analysis* is not often done with tide data, although a mean tide curve would also be useful in shallow-water areas where the curve is significantly distorted.

In the *cycle-by-cycle analysis* (also called the *tide-by-tide analysis* or, for currents, the *reversing reduction*) key points are picked off two time series of data or predictions (U.S. C&GS, 1950). For tide data or tide predictions, the key points are usually high water and low water. For current data the key points are usually slack (or minimum) before flood, maximum flood, slack (or minimum) before ebb, and maximum ebb. The time differences between corresponding key points at the two stations for each tidal cycle are tabulated and then an average value is calculated. Heights at corresponding high or low waters, or speeds at corresponding maximum floods or ebbs, are similarly compared; the latter generally is in the form of ratios, while the former has been typically been in the form of height differences, height ratios, or a combination of both. These methods depend on having an accurate and consistent method for selecting maximums and minimums and slacks from water level and current data times series. This especially becomes an issue when shallow water has distorted the tide or tidal current curve. As will be seen in the next section, the cycle-by-cycle analysis is very useful because it allows us to see how the differences between the two stations vary throughout the month, thus giving us some idea of the quality of a tide prediction made using these differences in Table 2 of the Tide Tables or Tidal Current Tables.

3.6.3 Variations In Nonharmonically Determined Time and Height Differences Throughout a Month

There is one key fact that must always be remembered when carrying out a nonharmonic comparison analysis (and especially when putting the results in Table 2 of a Tide or Tidal Current Table):

the time and height differences between corresponding high waters (or low waters) at two tide stations vary from tidal cycle to tidal cycle throughout the month (and similarly for tidal current stations).

The greater the difference between the tidal harmonic characteristics of the two stations, the larger the variation in time and height difference (or current speed ratios) will be throughout the month. This variation can be seen when using cycle-by-cycle analysis; it cannot be seen when using a monthly mean analysis or a rotary reduction analysis.

If a cycle-by-cycle analysis is done on observed data, then the time and height differences can include the effects of nontidal influences such as wind or river discharge, in addition to the effects of changing astronomical conditions. However, if a cycle-by-cycle analysis is done to compare tide predictions from two stations, then the variation in these differences are solely the effect of changing astronomical conditions at the two stations (which do not have identical tidal characteristics). In this latter case, the variation in differences over the month, around a mean difference, corresponds to the error that would result when making a prediction at a subordinate station using the mean differences

3. Methods of Tidal Analysis and Prediction

that come out of a nonharmonic comparison analysis (i.e., the value that is put in Table 2 of the Tide Table or Tidal Current Table). Thus, the cycle-by-cycle analysis can serve an important role in the quality assurance analysis of subordinate stations. If there is too much variation in the time or height differences over a month, then one needs to use a different reference station, one with more similar tidal characteristics (usually geographically closer).

The average time difference between, for example, high waters at the two stations will approximately equal the time difference between the two respective M_2 high waters. But other constituents, each with different phase (time) differences, will also affect high water, so that the time difference between high water at the two stations will vary throughout the month, i.e. from springs to neaps, and from apogee to perigee, and from maximum lunar declination to equatorial declination to southern declination and back.

Generally, the greater the geographical distance between two stations the greater the difference in harmonic makeup and the greater the variation in time differences. The key consideration is how quickly the tidal characteristics change with distance in the vicinity of the two stations. When producing a tide or tidal current table, the intention, of course, is to have enough reference stations so that no subordinate station is forced to be associated with a reference station whose tidal characteristics are dissimilar enough that significant variations in time differences and other differences or ratios will occur. In mixed tidal regimes the reference stations need to be closer because the diurnal-to-semidiurnal ratios change more quickly with distance than do the ratios between two semidiurnal constituents. The phase differences between K_1 and between O_1 , at two stations, have a significant effect on the average (essentially M_2) time differences.

This will be illustrated with examples from San Francisco Bay, where the tide and tidal current regimes are mixed and there is a significant diurnal inequality, so that the diurnal-to-semidiurnal ratios change relatively quickly with geographic distance. Figure 3.5 shows the tidal harmonic characteristics for two water level stations and two current stations in San Francisco Bay. The two tide stations, at Golden Gate and Port Chicago, are only about 18 nautical miles apart. One-year least-squares harmonic analyses were carried out for both stations for the year 1980. The $(K_1+O_1)/M_2$ ratio is 1.048 at Golden Gate and 0.900 at Port Chicago; the phase differences, $(M_2^{\circ}-K_1^{\circ}-O_1^{\circ})/2$, are 247° and 241° , respectively. One-year predictions were made at both these stations, and the times and heights of high water and low water were determined for each set. Cycle-by-cycle comparisons of the two stations were made. Figure 3.6a shows a plot of the differences between predicted low water times at Port Chicago and predicted low water times at Golden Gate, for the first 120 tidal cycles of 1980. The solid line connects the first of each pair of cycles, and the dashed line connects the second of each pair.

The average time difference between low water at the two stations is 2.99 hours; namely, low water at Port Chicago is 2.99 hours later than low water at Golden Gate, on the average. It can be seen from the plot, however, that this average value is only good at certain times of the month. Over the first 120 cycles the time difference can be as large as 3.43 hours and as small as 2.47 hours. The maximum time difference occurs in the first of each pair of cycles, just after maximum southern lunar declination (S).

If Golden Gate is used as a reference station and Port Chicago is used as a subordinate station, then 2.99 would be the value that would appear in Table 2 of the Tide Table for Port Chicago. A prediction of low water at the subordinate station Port Chicago, calculated by using this 2.99-hour time difference to adjust the predicted low waters at the reference station (Golden Gate), would give tide predictions for Port Chicago that would have an error ranging from -0.44 hour to +0.52 hour.

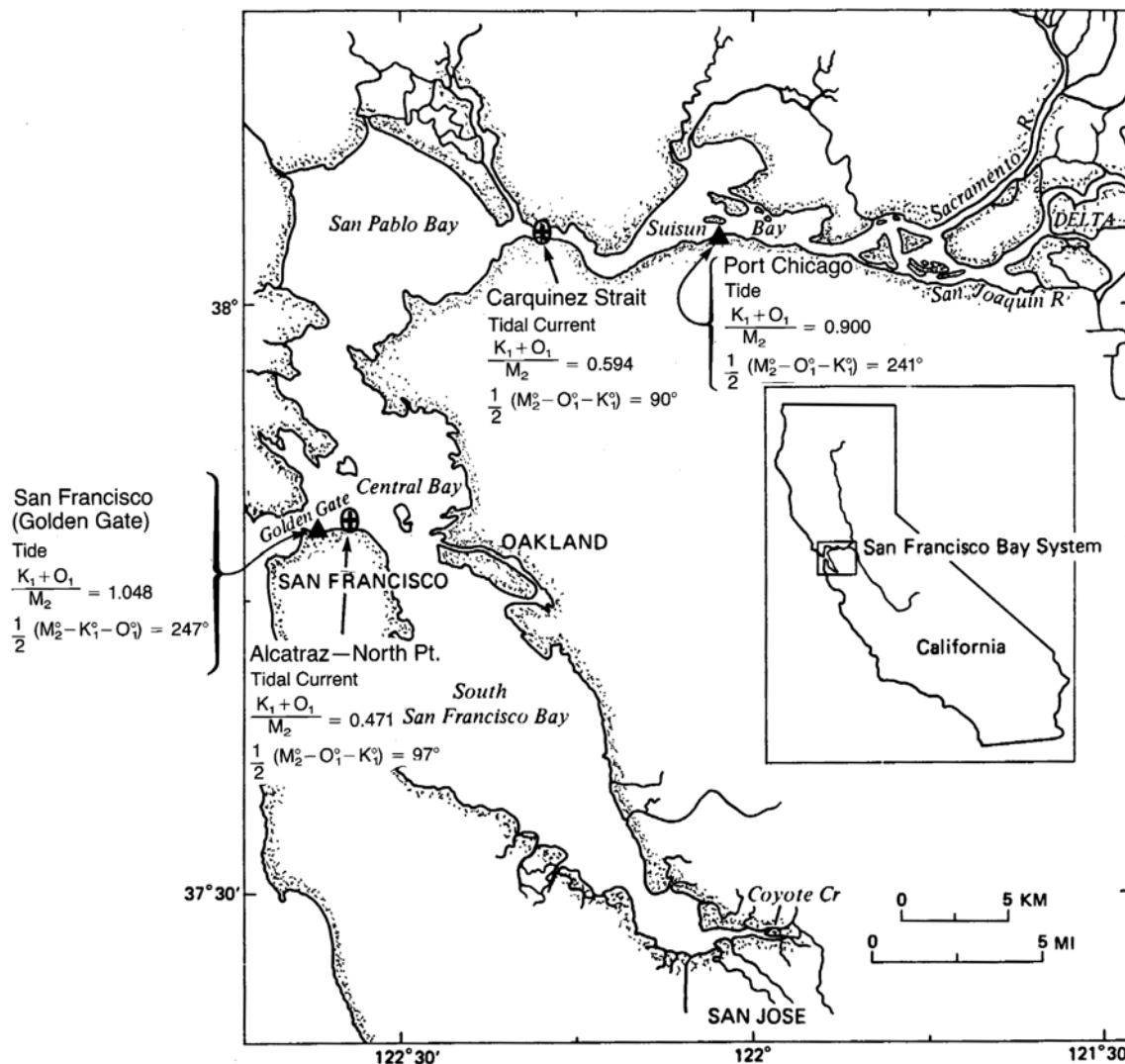


Figure 3.5. The harmonic characteristics for two water level stations and two current stations in San Francisco Bay, where the tide regime is mixed. (From Parker, 1991b)

Such errors would be even larger at locations further up the estuary. Similar variations in time differences are also seen for high waters.

Figure 3.6b shows a similar plot of the differences between the heights of predicted low waters at Port Chicago and the heights of predicted low waters at Golden Gate. The average height difference for low waters at the two stations is -0.41 foot ; namely, low water at Port Chicago will be 0.41 foot (0.12 m) lower than low water at Golden Gate, on the average. However, it can be seen from the plot, that the height difference can as great as as -1.10 feet (with Port Chicago much lower than Golden Gate) or as great as +0.70 foot (with Port Chicago actually higher than Golden Gate). The greater height differences occur just after maximum southern lunar declination (S) for the first of each pair of cycles. Again, -0.41 is the value that would appear in the tide table for Port Chicago. A prediction of low water at Port Chicago calculated by adjusting the predicted height at Golden Gate would have an error ranging from -1.11 feet to+0.69 foot. These San Francisco Bay results

3. Methods of Tidal Analysis and Prediction

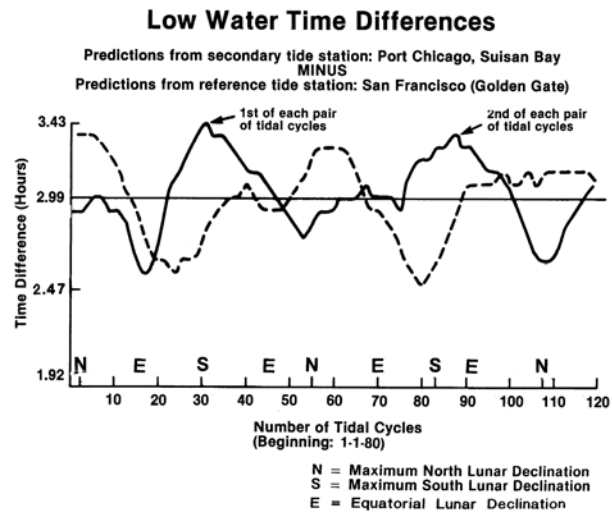


Figure 3.6a. Plot of the differences between harmonically predicted low water times at Port Chicago and at Golden Gate, for the first 120 tidal cycles of 1980. The solid line connects the first of each pair of tidal cycles, and the dashed line the second. N and S are the times of maximum north and south lunar declination. (From Parker, 1991b)

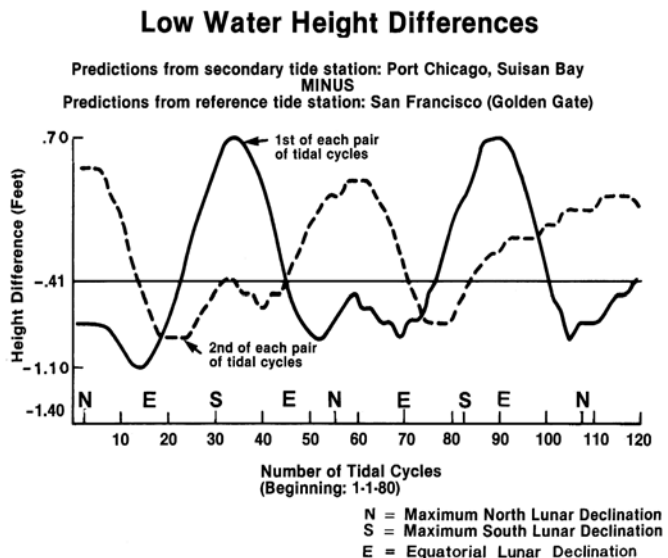


Figure 3.6b. Plot of the height differences between the harmonically predicted low waters at Port Chicago and at Golden Gate. (From Parker, 1991b.)

suggest that the use of a second reference station in the northern part of the estuary would improve the tide predictions for stations in that area. (This in fact did happen and Port Chicago was added as a reference station in the U.S. Tide Tables because of the results displayed in Figures 36a and 36b.) But in some areas a second reference station may not always be possible until a new long-term station is installed.

Shallow-water-generated distortions in the tide or tidal current may also lead to variations in time differences between two stations. An example is provided by the results of a reversing reduction analysis of two current stations in Delaware River and Bay that show sudden large maximum ebb time differences at certain times of the month, for the first of each pair of cycles (see Figure 3.7). These sudden jumps in the plots are caused by the effect of higher-frequency shallow-water constituents (the overtides) on the times of maximum at Philadelphia, where the overtides are larger than at the Bay entrance. Although these constituents are not large enough to greatly change the speed value of maximum ebb, they do distort the shape of the tidal current curve enough to shift the times of maximum ebb later or earlier by a considerable amount. Examples of the shifting of high and low waters in the tide were seen in Section 2.2.5. Figure 3.8 shows an example of this with the tidal currents near Philadelphia (see also Figure 9.3).

When the overtides were removed from the Philadelphia prediction the time differences between Philadelphia and the bay entrance became quite small (Figure 3.9). Here the method of selecting maximum flood (see Section 3.9.2) makes a difference. In cases like this where the time of (in this case) maximum flood is shifted by the shallow-water distortion of the tidal current (but the maximum speed is not changed much), it would make more sense not to use the time of the actual maximum flood value, but to use a time more in the center of the flattened out area, e.g. the center

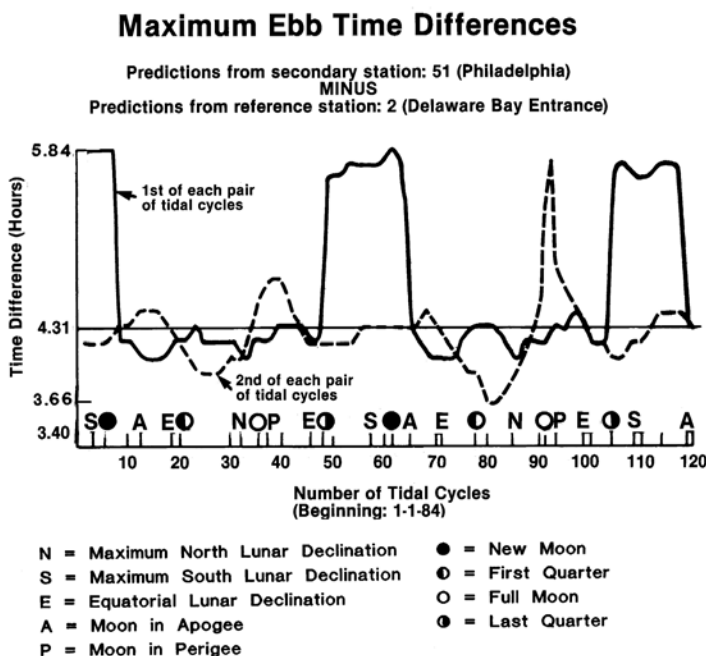


Figure 3.7. Plot of the time differences between harmonically predicted maximum ebbs at two station in Delaware River and Bay. The solid line connects the first of each pair of tidal cycles, and the dashed line the second. (From Parker, 1991b.)

3. Methods of Tidal Analysis and Prediction

time of all values greater than 90 percent of the actual maximum. This would provide more consistency from cycle to cycle in such flattened out cases, while still accurately picking maximums for strongly distorted, steeper cases.

Tidal currents have an additional problem. It was noted at the end of Section 2.3.6 that the lateral advective/inertial terms in the 2-dimensional momentum equation (see also Section 7.3.2) shift energy into the next harmonic (especially off points and around channel bends), changing, for example, the $(K_1 + O_1)/M_2$ ratio or the M_4/M_2 ratio in the tidal current (see Figure 2.35). The area around the San Juan Islands (between British Columbia and the state of Washington), including the Strait of Juan de Fuca, Haro Strait, and many other connecting waterways, provides an extreme example. Here a combination of the large diurnal inequalities and the inertial effects due to the complex geometry lead to tidal current characteristics that can change dramatically over a short distance. While the $(K_1 + O_1)/M_2$ ratio for the tide changes gradually and smoothly in this area, the $(K_1 + O_1)/M_2$ ratio for the tidal current varies considerably (Parker, 1977). The six reference stations in the NOS Tidal Current Tables for this area are not really sufficient and there are times during the month when some subordinate stations will become diurnal a day earlier or later than the reference station, making it almost impossible to make a prediction using a nonharmonically-derived correction. Even at times of the month when both reference station and subordinate station have not become diurnal, there is large variation in time differences and speed ratios. One really needs several values for each tidal parameter (e.g. one set for maximum southern declination, one set for equatorial lunar declination, and one set for maximum northern lunar declination), and that may still not work well enough.

Although the Tide and Tidal Current Tables must use nonharmonically-produced correction factors for thousands of stations in order to avoid adding thousands of extra pages to the Tables, as will be seen in Section 9.7, there is no reason to continue using this method in digital tidal prediction products, which with today's computer power can be based totally on harmonic methods. Most subordinate (i.e., Table 2) water level stations usually have at least 29 days of data, and thus harmonic constants are available. However, most subordinate stations in Tidal Current Tables have less than 15 days of data, and so new current data would have to be obtained. The improvement in the tidal prediction accuracy would be significant, especially in waterways with a strong diurnal signal. CO-OPS is, in fact, moving toward delivering harmonically based predictions for more locations than just reference stations.

Chapter 6 will look at how to carry out the various kinds of nonharmonic tidal analysis of water level and current data times series, the best methods for including the analysis results in Table 2 of the Tide and Tidal Current Tables, and ways to minimize the errors that can easily result from making predictions using the corrections factors put in Table 2.

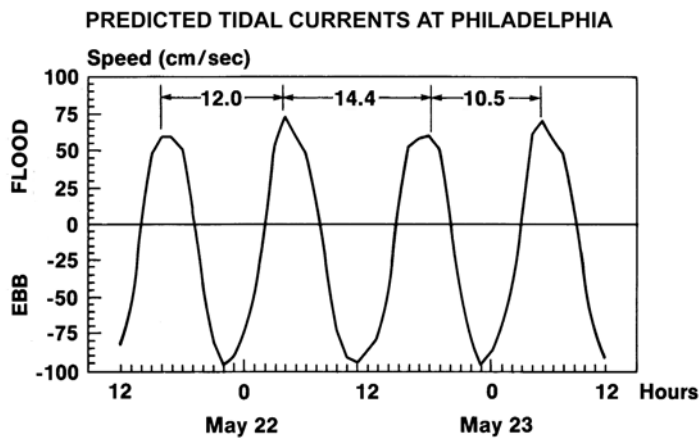


Figure 3.8. Predicted tidal current at Philadelphia on the Delaware River illustrating the dramatically varying time interval between successive maximum flood and between successive maximum ebbs due to shallow-water effects. (From Parker, 1991b.)

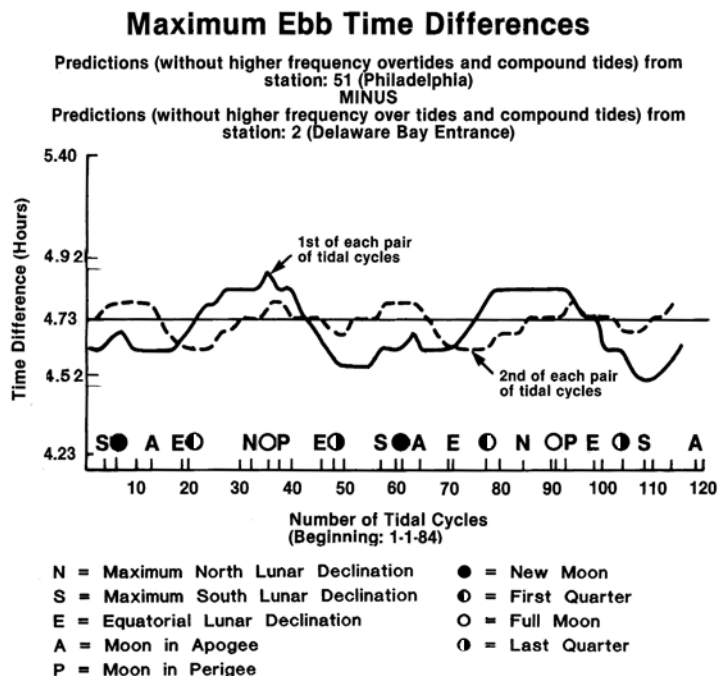


Figure 3.9. Plot of the time differences between harmonically predicted (but leaving out the overtones and compound tides) maximum ebbs at two current stations in Delaware River and Bay.

3.7 Analyses For Determining Sa and Ssa₇

3.7.1 The Meteorological Origins of Sa and Ssa

Sa and Ssa are long-term tidal constituents directly generated by the nonuniform changes in the Sun's declination and distance (the perihelion-aphelion effect). The solar annual constituent, Sa, has a period of 365 days (a frequency of 0.0027 cpd) and the solar semiannual constituent, Ssa, has a period of 183 days (a frequency of 0.0055 cpd). Sa and Ssa are very small compared to other tidal constituents, and insignificant for most applications. However, if one includes Sa and Ssa in a year-long harmonic analysis of water level data one may initially be surprised that their calculated values come out much larger than would be expected from astronomical forcing. This is because the energy at the one cycle per year (Sa) and one cycle per half year (Ssa) found by the analysis is actually meteorological in origin, namely, caused by the seasonal changes in wind, temperature, and atmospheric pressure that affect water level.

For example, summer heating of the upper layer of ocean causes the water to expand, raising the coastal water level. This is usually referred to as a *steric* sea level change. The expansion in the summer and contraction in the winter puts energy into the Sa constituent. Since this annual raising and falling water level due to annual warming and cooling is not perfectly sinusoidal (that is, there is some asymmetry in this variation), some of the energy will also show up in the next higher harmonic, i.e., at two cycles per year, which is the Ssa constituent. For example, if most of the heating and expansion took place in just a few summer months and the rest of the year there was slow cooling and contraction, that asymmetric effect would put some of the energy into Ssa.

Sa and Ssa can be produced by the seasonal cycle of any meteorological effect on water level. There are, for example, annual patterns of changing coastal winds, that during part of the year can push the water toward the shore, raising the water level, and during other parts of the year push the water away from the shore, lowering the water level (putting energy into Sa). And again whatever asymmetry is involved will also put energy into Ssa. Similarly, seasonal changes in atmospheric pressure will push the water down or lift it up (the inverted barometer effects), and changes in river discharge will also raise the water level in a river (during spring freshets), the latter effect being very asymmetric, since the largest water level increase usually occurs during only one month of the year. Similar seasonal effects can also be seen in long-term current records, where other effects, such as seasonal changes in salinity, may also come into play.

One can get an idea of how large and varied (from location to location) meteorologically caused Sa and Ssa can be by looking at Figure 3.10. This figure shows the mean annual sea level cycle at 13 water stations along the East Coast of the U.S. and part of the Gulf Coast, as well as at the island of Bermuda east of the U.S. East Coast. (Since the tide is being averaged out as well as other higher frequency water level variations, this is referred to as *sea level*.) This mean seasonal sea level cycle was produced by taking monthly averages of 37 years of water level data at each station (1948-1984; which includes two 18.6-year periods). One can see a clear annual cycle at each station, but many of the stations have strong asymmetries. The northern most station, at Halifax, Canada, has an almost sinusoidal shape, but the stations get more and more asymmetric as one moves south. For most of these stations the maximum sea level value occurs in September or October. The asymmetry gets so strong at Charleston and Fernandina Beach that their annual cycle curves show double maximums, the larger one peaking in October, but a second smaller one peaking at the beginning of June. The range of the annual cycle for each station, which is given in the figure to the right

of each station name, is largest at Charleston and Fernandina Beach, and generally larger in the south than in the north.

Bermuda, which is far to the east of the U.S. East Coast, has a sinusoidal annual sea level cycle, which is due to steric effects, namely, due to a similar variation in annual water temperature. With most of the coastal stations, the annual cycle of varying wind speed and direction is the dominant cause of the annual water level cycle. Seasonal changes in the Gulf Stream transport may also have an effect on the seasonal water level curves at stations along the southern part of the U.S. East Coast (see Noble and Gelfenbaum, 1992), with maximum transport causing lower sea levels at the coast, and vice versa. The largest Gulf Stream transport usually occurs in July-August, which matches a minimum sea level at Charleston, Fernandina Beach, and Miami, while the lowest Gulf Stream transport usually occurs in October which matches the maximum sea level at these three stations. Extensions of the Gulf Stream, in the form of the Florida Current and the Loop Current (in the Gulf of Mexico) might also account for the slight dip in sea level in July at other stations heading into the Gulf of Mexico.

The variation in annual cycle and semiannual cycle seen in Figure 3.10 (from Parker, 1994) is not an isolated example. Similar variation in these cycles is seen in the results of Tsimplis and Woodworth (1994), who used data from 1043 water level stations around the world to determine the amplitude and phases of the annual and semiannual cycles at each location.

Seeing these examples of numerous meteorologically caused seasonal changes in sea level, one could rightly decide not to use any S_a or S_{sa} values that come out of a harmonic analysis when making a tidal prediction. Some oceanographers have, however, proposed that to make the best “water level” prediction possible, one could include these meteorologically caused S_a and S_{sa} harmonic constants. That would make sense if the calculated S_a and S_{sa} values were expected to be consistent from year to year. In fact, they can vary fairly dramatically from year to year, as can be seen in Figure 3.11, which shows the variation from year to year of the seasonal sea level range from 1935 to 1992 at four stations along the U.S. Atlantic coast. In this figure one can see that (e.g.) the three southern stations had large seasonal sea level ranges in 1958 and small ranges in 1980. At Fernandina Beach the mean sea level range was 0.99 feet (from Figure 3.10), but its seasonal range in 1958 was 1.92 ft and in 1980 its range was 0.54 ft. From this one can see that S_a and S_{sa} (obtained from one-year harmonic analyses) would vary considerably from year to year.

3.7.2 Considerations In Whether To Use S_a and S_{sa} In a Prediction

From the results presented in the last section, one would still not know what value of S_a and S_{sa} should be used for a future year. Choosing an S_a and S_{sa} for next year, the mean values obtained from Figure 3.10 could be a poor choice, because (from the variation seen in Figure 3.11) they might do a poor job of representing that year. One might try projecting into the future based on a figure like Figure 3.11 (but more specifically for values of S_a and S_{sa} for each year), but, from the sudden changes one sees in Figure 3.11, that may not do a very good job. Including S_a and S_{sa} in a self prediction (i.e., predicting the same year as the data used to produce the harmonic constants) can be justified, if one is looking to make a water level prediction (i.e., the tide plus any other known periodic water level variation) as close as possible to an actual water level record, and to reduce the energy in the residual time series. But for a prediction in another year, this is not likely to be the case, because of the significant variation from year to year in the meteorologically caused variations at the annual and semi-annual frequencies that are not predictable.

3. Methods of Tidal Analysis and Prediction

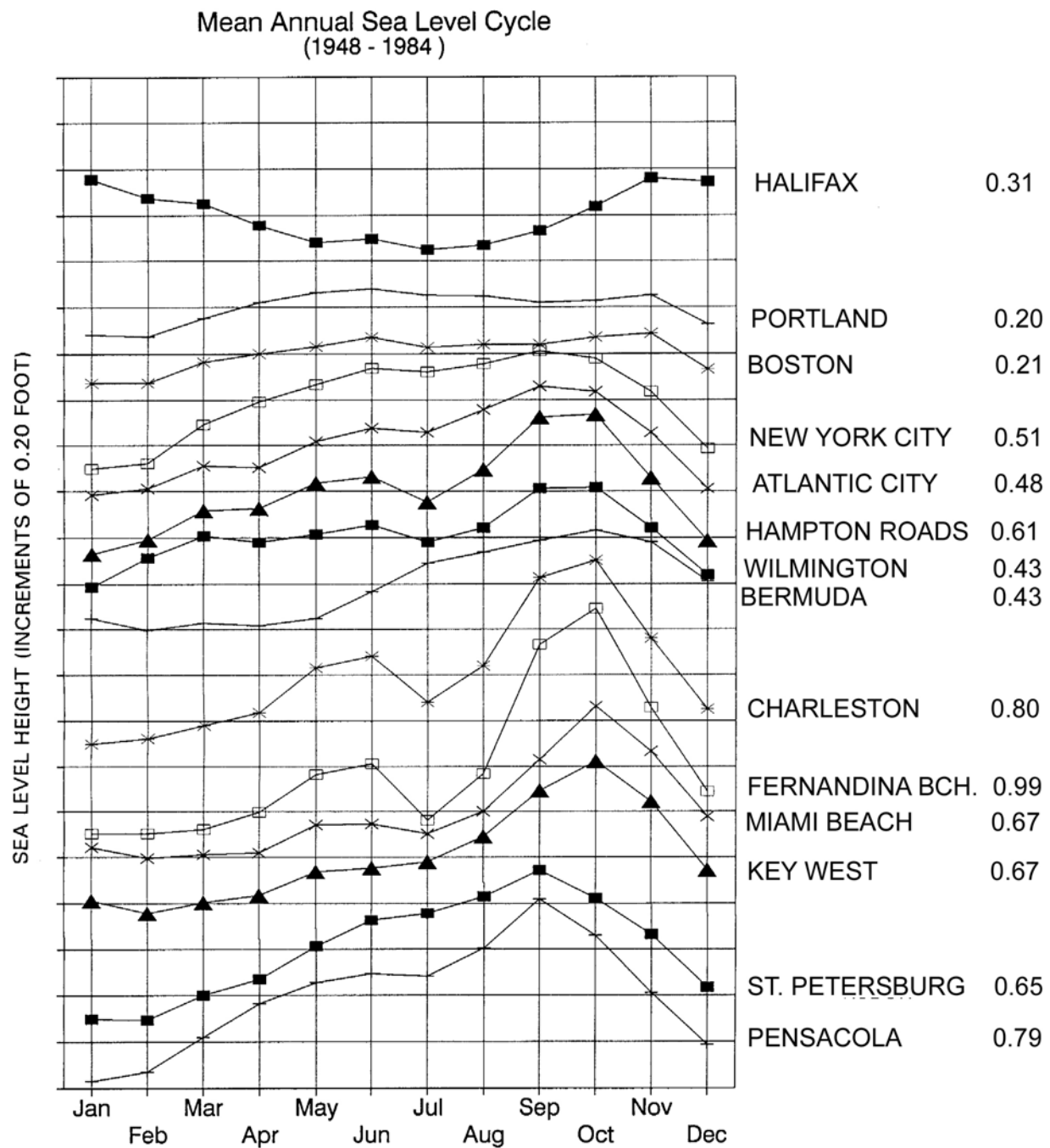


Figure 3.10. The mean annual sea level cycle at fourteen NOS stations along the East Coast and Gulf Coast of the U.S. for the period 1948-1984. The number to the right of each station name gives the mean range of that stations seasonal cycle. All values are in feet; increments along the vertical axis are 0.2 foot. (From Parker, 1994.)

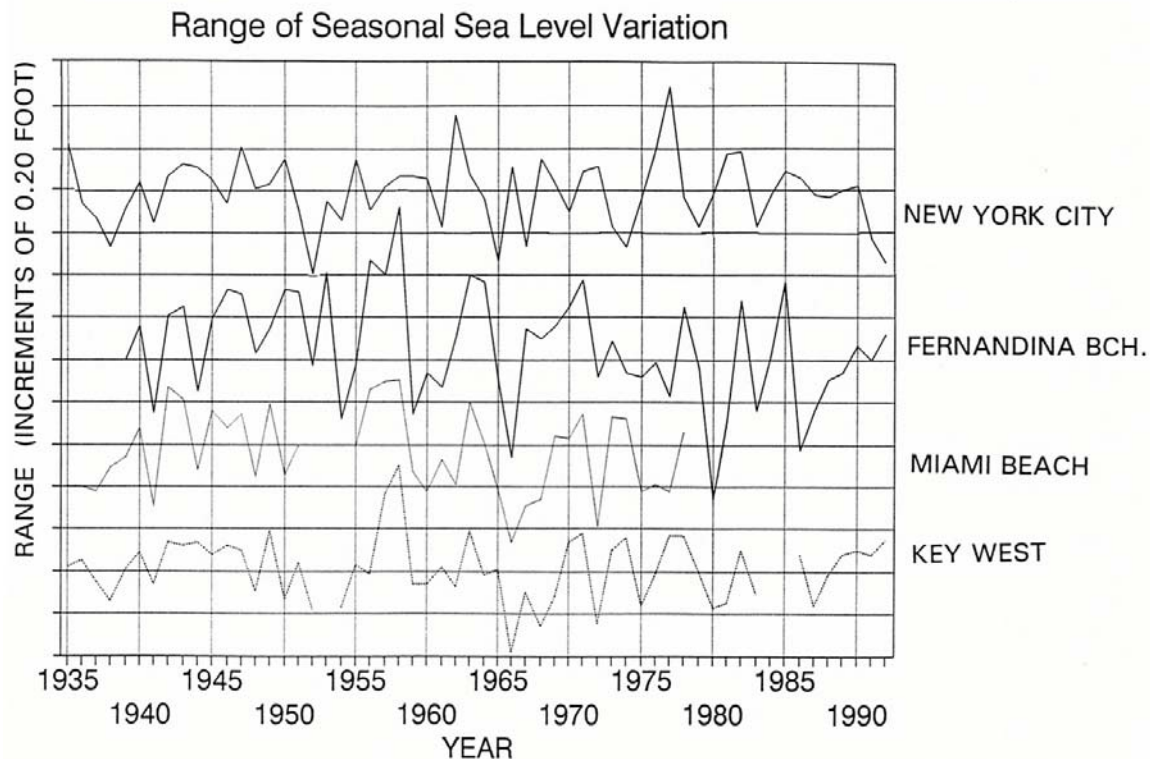


Figure 3.11. The variation from year to year of the seasonal sea level range from 1935 to 1992 at four NOS stations along the U.S. East Coast. Increments along the vertical axis are 0.2 foot. (From Parker, 1994.)

Instead of using the S_a and S_{sa} values that come out of a least squares harmonic analysis of a year's worth of data, sometimes a special analysis is carried out with many years of data, which produces much smaller values of S_a and S_{sa} , more representative of an average annual and semi-annual cycle. Although much smaller than the values from an individual year analysis, these S_a and S_{sa} values still contain meteorological energy and still are greater than if they truly represented only the astronomical tidal energy at those frequencies. They are usually too small to make much difference in a water level prediction.

So whether the calculated values of S_a and S_{sa} are used or not, becomes almost a philosophical question, based on one's application, the amount of data one has, and the dynamics at the particular location from which the data came. Often tide predictions are subtracted from actual water level data in order to look at only the nontidal signal (and perhaps correlate it with changes in the wind and barometric pressure or steric changes). In such a case, one would not want to use the essentially meteorological S_a and S_{sa} harmonic constants in the prediction. Even for producing the "most accurate" water level predictions for other purposes, for many locations the use of the S_a and S_{sa} may not change the prediction that much, and may not represent the annual cycle for a particular year very well anyway.

3.7.3 Methods for Calculating S_a and S_{sa}

Today the simplest (and perhaps best way) to calculate S_a and S_{sa} is simply to include them in a one-year least squares harmonic analysis, and to carry out as many one-year analyses as possible

3. Methods of Tidal Analysis and Prediction

with the available data. Then one can see how S_a and S_{sa} varies from year to year. One can also do longer analyses (e.g., two-year or five year analyses, or even a 19-year analysis) to see how much the amplitudes are reduced and how the phase lags are changed in the longer analysis. Greatly reduced amplitudes in the longer analysis compared with the shorter analyses indicates that the inclusion of S_a and S_{sa} in an accepted set of harmonic constants for a particular station will not be very useful for a tide prediction.

There are also methods to extract S_a and S_{sa} from tabulations of monthly means of mean sea level. This again can be done with a least squares harmonic analysis. In the pre-computer era, other methods were devised. Schureman (1958, page 114) provides a method for determining S_a and S_{sa} from monthly means of sea level using C&GS Form 194. This form was originally designed for a regular harmonic analysis using hourly means. Such analyses were done by hand so the various steps in the arithmetic on the form were designed with labor savings in mind (and so the method behind may not be very clear), and it also involves the use of logarithms (unnecessary now in the computer age).

If one decides that they want to include S_a and S_{sa} in a set of harmonic constants, it is probably wisest to analyze a 19-year set of monthly means, or to include S_a and S_{sa} in a least squares harmonic analysis of a 19-year water level time series.

3.8 *Tidal Filtering and Detiding*

3.8.1 Introduction

There are often applications where one wishes to remove the tidal energy from a data time series. A good way to accomplish that is to do a harmonic analysis of the available observed data time series and then make a tidal prediction for the same time period. Subtracting the predicted times series from the observed series produces a *residual time series*, which should contain only (or predominantly) nontidal energy. This is usually referred to as *detiding*. Here, of course, one has the same limitations as discussed throughout this book, namely, the shorter the time series the fewer harmonic constants that can be used to make the prediction. However, this limitation may not be quite as serious a problem for this application, since here one is making a self-prediction (i.e., predicting for the same time period as the analyzed data series). Energy from the unsolved-for constituents is included in the solved-for constituents, and although the harmonic constants that come out of a short harmonic analysis may not do a good job of predicting for other time periods (since the phase relationship between the unsolved-for constituents and the solved-for constituents will be different and unknown), they are able to do a fairly good job predicting for the period of the analysis. Still, if the data time series is very short, for example less than 15 days, this harmonic method of producing a residual series may not do a good enough job of removing the tidal energy.

The alternative (and much more direct and economical) method for removing tidal energy is to use *filtering*. Filtering in its simplest form is merely taking running averages (running means) as one moves through a data time series. For example, suppose one wants to remove M_2 energy from a data time series that has a sampling rate of one hour. M_2 (frequency = 1.93 cpd) has a period of 12.42 hours, so if one averages 13 hourly data points, most of the M_2 energy should cancel out, since the M_2 contribution would have gone through an entire M_2 cycle. Since, for this example, a 13-hour running mean filter (a 13-hour *box filter*) is being used, and the M_2 period is 12.42 hours, there will actually be a small amount of M_2 energy left, an important concern as will be seen. To filter out (a lot of) the M_2 energy from a time series, one can average the first 13 data points (call them data point

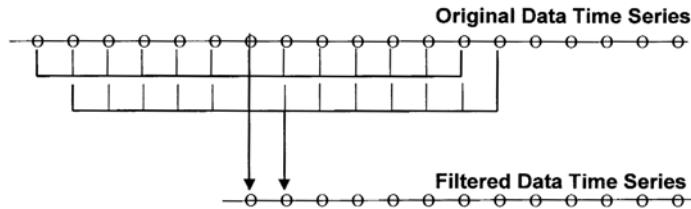


Figure 3.12a. Filtering a data time series. In this simple example each group of 13 points is averaged to produce one data point in the filtered series (see text).

1 through 13) and save the averaged result (it will have the same time as original data point number 7), then average data points 2 through 14 and save the result (at the time of original data point 8), then average data points 3 through 15, etc, etc (see Figure 3.12a). When this is finished there will result a new (filtered) time series with most of the M_2 energy eliminated (see Figure 3.12b, but this actually shows better results than a simple box filter for M_2 could accomplish.). Because of the filtering process, this new filtered time series will be 12 points shorter than the original time series, beginning 6 hours later and ending 6 hours sooner. As a result of this process, one has also taken out some of the S_2 tidal energy, but not as much as the M_2 energy, since the S_2 period is 12.00 hours and thus averaging over 13 hours would leave more of the S_2 energy. To eliminate the energy at all the tidal frequencies one would have to go through this process many times, using running means of different lengths. This would be very time consuming, and with each pass through with another running mean our filtered time series would become shorter and shorter. One could instead use a 25-hour running mean filter, which loses only 24 data points and filters out energy from both semidiurnal and diurnal tidal constituents. However, this filter still leaves too much tidal energy for most applications.

To avoid this problem, special filters have been designed to eliminate most tidal energy on one pass through the time series. In this case the process is to take *weighted* running averages as one moves through the time series. The way this is usually represented is the following:

$$y(t) = \sum_{i=-n}^n w_i x(t-i)$$

where

$y(t)$	=	a single data point in the output filtered time series (at time t)
$x(t-i)$	=	a single data point in the input data time series; $2n+1$ data points of these input data points (centered at time t) are averaged to produce a single output data point, $y(t)$
w_i	=	one of the $2n+1$ <i>weights</i> that multiply times the $2n+1$ input data points
$2n+1$	=	the <i>length of the filter</i> (i.e., from $i=-n$ to $i=n$), i.e., the number of weights in the filter, and the number of input data points averaged to create each new filtered output data point

An odd number of weights are usually chosen, with values symmetric about t , so that the filtered time series will occur at the same times as the original data series (minus the $2n$ data points lost, of

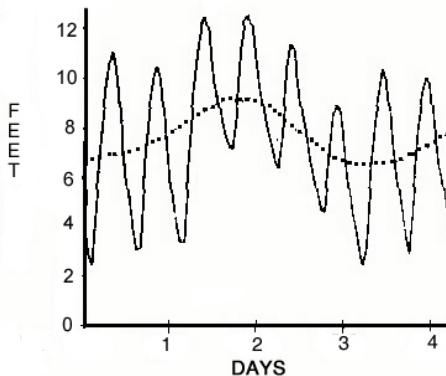


Figure 3.12b. A water level time series (solid line) filtered to remove the tidal oscillations and leave a predominantly nontidal time series (dotted line).

course). Each weight has a value less than 1, and the sum of the $2n+1$ weights must equal 1, so that no energy is artificially taken away or added. These two requirements are written:

$$\mathbf{W}_i = \mathbf{W}_{-i} \quad \text{and} \quad \sum_{i=-n}^n \mathbf{W}_i = 1$$

For the simple running mean the \mathbf{W}_i 's are all equal to $1/(2n+1)$. Thus in the simple M_2 example above, the \mathbf{W}_i 's are all equal to $1/13 (= 0.077)$. For a 25-hour running mean the \mathbf{W}_i 's are all equal to $1/25 (= 0.04)$.

The next section will look at several filters specially designed to filter out most tidal energy. Each filter will have different capabilities and different drawbacks.

When using tidal filters it is very important to remember that *a tidal filter will also eliminate energy at other nontidal frequencies*. Such filters reduce nontidal energy not only at frequencies near tidal frequencies, but also at frequencies not close to tidal frequencies. For example, although tidal filters are generally *low pass filters* (i.e., they eliminate most high frequency energy and allow low frequency energy to “pass” through), a typical tidal filter can still reduce some subtidal energy by as much as 60%.

When deciding to use tidal filtering (instead of detiding the data series by creating a residual series using tidal harmonic prediction) one must look at the intended application. If one wishes primarily to eliminate higher frequency energy (including tidal energy) from a data record, then tidal filtering is a reasonable choice. However, if one does not want to lose 60% of the subtidal energy as a result of this filtering, then it would be wiser to detide the data series using tidal harmonic analysis. This detided series will still have higher frequency nontidal energy, but that can then be eliminated with a shorter filter.

There are other possible situations where tidal filtering would be better to use than creating a residual series using tidal harmonic prediction. As was seen in Section 2.3.3, in shallow waterways nontidal phenomena such as river flow and low-frequency storm surge can affect the amplitudes and phases of tidal harmonic constants obtained from a harmonic analysis. Thus, one should not create a residual series using accepted harmonic constants (probably calculated from a one-year analysis), because those constants will not predict the tide accurately for a time period with strong nontidal influences (because the tide was changed by that strong nontidal influence). Because those

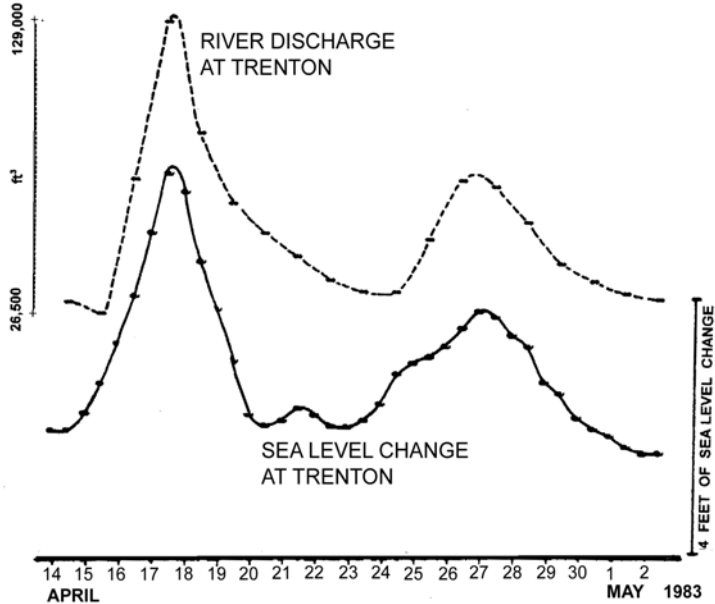


Figure 3.13. Water level data from Trenton, NJ, filtered with a tidal filter, and compared with river discharge data also filtered with the same tidal filter. (From Parker, 1984.)

harmonic constants are wrong for the period of the nontidal event there will still be tidal energy in the residual time series, whereas tidal filtering will eliminate it. Even trying to calculate new harmonic constants just for the time period of the (e.g.) strong river flow will not work well, because such events are usually shorter than the length of series needed for a reasonable harmonic analysis (although one could try the continuous wavelet transform method; see Section 3.5.5).

If one decides to use tidal filtering, and one is going to compare the filtered tidal series to some other data time series, it is usually wise to also filter that other data time series with the same tidal filter (even if one does not expect there to be tidal energy in that other data time series), so that the nontidal energy in both times series will be treated the same way. This is because, as mentioned above, the tidal filter will also remove some nontidal energy, and if one is looking to compare the results of a filtered water level time series to (e.g.) a wind or pressure data series, they should also be filtered in order to take out the same percentage of nontidal energy. Figures 3.13 and 3.14 provide two examples of this.

Figure 3.13 shows a tidally filtered water level record from Trenton, NJ, during a heavy river runoff period on the Delaware River and a river discharge record for the same time period (also from Trenton, but above the rapids) which was also tidally filtered even though there was no tidal signal in the river discharge data. The purpose of this application was to look for similarities in the two resulting curves that might indicate how much the river discharge affects the water level at Trenton.

Figure 3.14 illustrates an application of tidal filtering in Massachusetts Bay, where tidally filtered water level records are compared with tidally filtered wind records. In this case, two water levels records (Boston and Sandwich) at opposite ends of the Bay (see map in Figure 3.14) were tidally filtered and subtracted from each other to look at the changing sea level difference between the two ends of the Bay. The wind record for Boston (Logan Airport) was also tidally filtered (and squared, since wind stress was being looked at). The component of this wind stress along the axis of the Bay is plotted in the figure along with the sea level difference curve (between Boston and

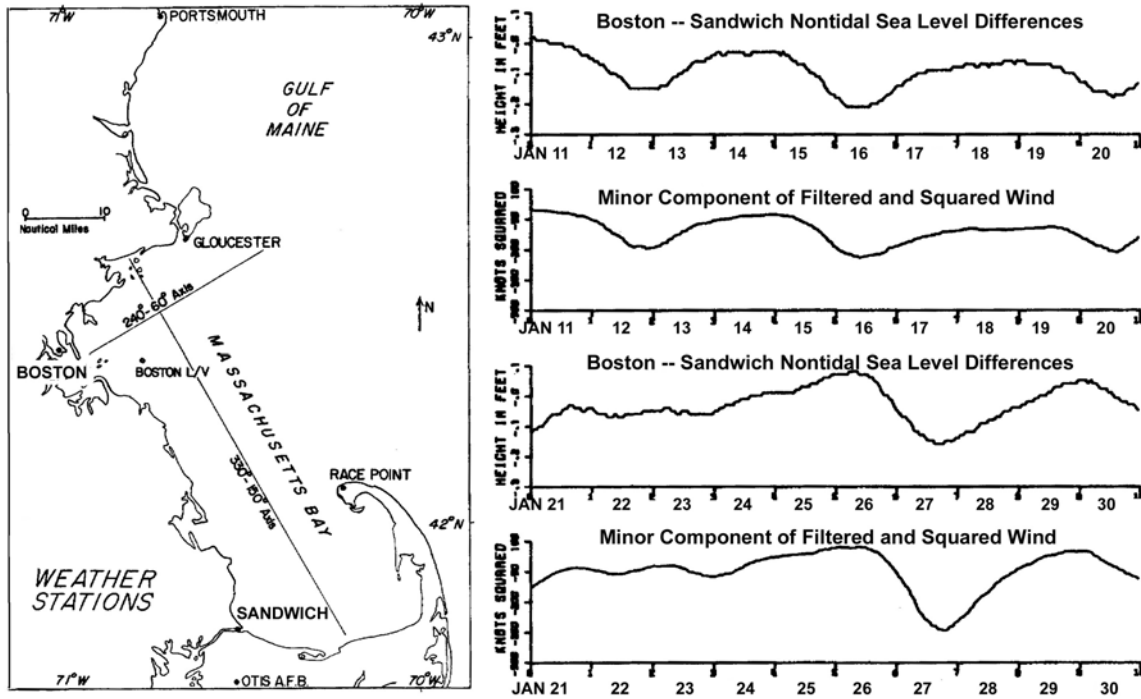


Figure 3.14. Plots (right panel) of the difference between two tidally filtered water level records at opposite ends of Massachusetts Bay (left panel) compared with plots of wind stress along the axis of the Bay, which were similarly filtered. (From Parker and Pearce, 1975.)

Sandwich) to see how much the wind stress along the longitudinal axis of the Bay affected the longitudinal tilt of the sea surface.

3.8.2 Specially Designed Tidal Filters

Numerous filters have been developed to eliminate energy at the tidal frequencies (see Groves, 1955, and Godin, 1972), each having specific weights (W_i 's) and specific lengths ($2n+1$). Such filters are usually designed to try to accomplish three objectives: (1) to eliminate the maximum amount of tidal energy; (2) minimize the amount of nontidal energy eliminated; and (3) to have minimum adverse effects on other frequencies through side-band effects. The box filter, which is the running mean (see Figure 3.15), is especially bad in terms of side-band effects, that is, it adds energy to higher harmonics of the frequency being filtered for. Other filters can have similar effects. In the right-hand plot in Figure 3.15, which shows the effect of the running mean in the frequency domain, one sees that it passes through all the energy at zero frequency and almost none at the frequency being filtered for, but it also filters out some of the low-frequency energy. One also sees the side bands, which are a result of the abruptness of the box filter (running mean), i.e., it has a value of 1.0 and then suddenly a value of 0.0. Filters which have a gradual decrease from the center (e.g., Gaussian and cosine filters) show a frequency response that gradually decreases from the frequency, without side bands effect, but unfortunately filtering out more low-frequency energy.

Filters generally are classified as: *low-pass filters*, i.e., they allow energy to be passed through below a designated frequency; *high-pass filters*, i.e. they allow energy to be passed through above a designated frequency; *band-pass filters*, i.e., they allow energy to be passed through between two

designated frequencies; or *band-stop filters* (or band-rejection filters), i.e., they pass through the energy at most frequencies except those between two designated frequencies. A high-pass filter is the opposite of a low-pass filter, and a high-pass filtered time series can be obtained by subtracting a low-pass filtered time series from the original data time series, and vice versa. Similarly, a band-stop filter is the opposite of a band-pass filter, and one can get one filtered time series by subtracting the other filtered time series from the original data time series. Since tidal filters are designed to eliminate the energy in the tidal bands (diurnal, semidiurnal, and higher harmonic bands) they are band-stop filters, but if most of the surrounding frequencies and higher frequencies are also reduced, then they are essentially low-pass filters.

One of the earliest and most widely used tidal filter is the Doodson filter (Doodson and Warburg, 1941; they referred to it as “multipliers of sea level”). The Doodson filter has a length of 39 hours (i.e., $2n+1 = 39$), and the following 39 weights:

$$W_i = \begin{cases} 0 & \text{for } i = 0, 5, 8, 10, 13, 15, 16, 18 \\ 1/30 & \text{for } i = 2, 3, 6, 7, 11, 12, 14, 17, 19 \\ 2/30 & \text{for } i = 1, 4, 9 \end{cases}$$

According to Groves (1955), the Doodson filter eliminates 99.94 percent of tidal energy at the semidiurnal frequencies, 99.79 percent of the tidal energy at the diurnal frequencies, and 99.38 percent of the tidal energy at the overtide frequencies. However, it also reduces nontidal energy at subtidal frequencies, e.g. by 60% at 0.5 cpd and by smaller amounts below that frequency. It has generally smaller side bands (than the 24-hour running mean) at the first few harmonics, but surprisingly high sidebands at the 9th harmonic, and so for some cases additional high-frequency smoothing may be recommended if the original data series has energy in this area of the frequency domain. (The Doodson filter was the filter used to produce the plots in Figures 3.13 and 3.14.)

The Doodson filter was originally developed by combining other simple filters, each of which discriminated against one or more tidal constituents. Groves (1955) used a similar method of combining simple filters to produce many other tidal filters. There are numerous papers on the subject of tidal filtering and many opinions on which filters work the best. Emery and Thomson

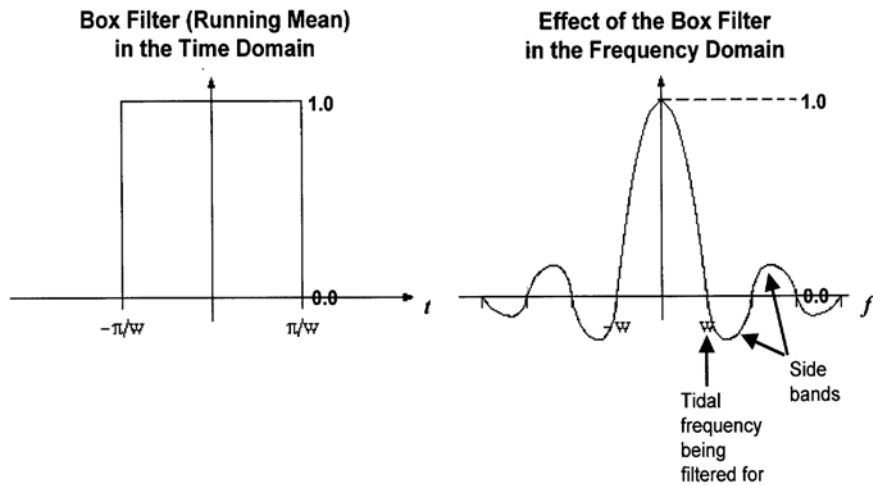


Figure 3.15. The simple box filter (running mean) and its effect in the frequency domain.

(2001) have a good discussion on filtering and seem to like Butterworth filters. In the end it comes down to the particular application and probably personal taste.

3.9 Calculating Consistently Defined Maxima and Minima

3.9.1 Consistently Defined High and Low Waters

The tidal prediction equation is generally used to predict a series of tidal heights from which the times and heights of high and low waters are calculated for each tidal cycle. It is these high and low waters that are listed in Table 1 of the U.S. Tide Tables, and presented in numerous media outlets such as in newspapers and on TV news shows during the weather report. Similarly, high and low waters are also calculated for each tidal cycle of the actual observed water level data time series that was analyzed. A typical quality control test for the tide prediction is the comparison of the high and low waters from the predicted tide series with the high and low waters from the actual water level data time series.

It would seem to be a relatively simple operation to pick off the maximums and minimums from a tide curve, and that is usually true if the curve is relatively smooth (with little or no noise) and undistorted by shallow water effects. Actual water level data curves (and especially tidal current data curves) can be noisy due to wave effects, which can make the determination of high or low water (or maximum flood or ebb) a little less obvious. There will be no noise in a predicted tide curve, but it can have distortions due to the nonlinear effects of shallow-water (see Section 2.3.2), as can the actual data curve. For example, the high water portion of the tide curve might be severely flattened so that it is not obvious what the time of the actual high water should be.

There have been various methods of selecting high and low waters (and maximum flood and ebbs and slack waters) to handle noise and distortions. Which ever method is used, the important thing is *consistency*, namely, to use the same method for all the data and predictions. If one is comparing the high and low waters at two stations (for a nonharmonic comparison analysis) or comparing the predicted and actual high and low waters at the same station (for quality controlling the prediction), is important that the same method of calculating these high and low waters is used for both time series. As will be seen below, failure to do this can lead to some very misleading results.

In most cases today the water level data time series will generally be fairly smooth because modern acoustic water level gauges average out most of the higher frequency waves. With older water level gauges, a float (connected by a wire to a recording device) moved up and down inside a stilling well, which protected it from waves, damping out much of the wave effects on the water level data. Instrument errors, if not removed with some type of quality control methodology can also add noise and possibly make selection of maximums and minimums difficult. (As will be seen in the next section, current data is much noisier than water level data, and it can often be more difficult to pick off the maxima.)

In very shallow waterways the tide curve is distorted by the nonlinear mechanisms (see Sections 2.3.2 and 7.6.2). In such cases the tide curve will no longer be a simple sine curve. Sometimes one part of the curve will be flattened while the other half of the cycle will have a sharper peak. Examples were given in Figure 2.26. The extreme case is when one sees double high waters, that is, when the water level rises to a maximum, starts to fall, but then rises again to a second maximum, before finally falling all the way down to a low water. Or there can be double low waters, or instead the curve might flatten out near mean tide level.

Prior to the use of electronic computers and automated data processing, high and low waters were selected by hand from a paper tide roll or some other paper graph. This method continued for many years even after computers were used for other functions. In order to make this manual operation as consistent as possible from person to person, the following instructions were given in the *Manual of Tide Observations* (C&GS, 1965, page 48):

“In selecting the time of high or low water from the tide curve attention should be given to the general trend of the curve rather than the individual peaks arising for various causes. The aim should be to take the middle of a smooth arc covering an hour or more during the high or low water period.” “In determining the times of the high and low waters to the nearest tenth of an hour it may be found convenient to construct a small scale 1 inch long and divided into 10 equal parts for use between hour marks on the curve. An experience tabulator, however, will usually be able to estimate the tenth accurately without use of such a scale.”

For smooth predicted curves high and low water selection was generally not a problem. However, for noisy data or for portions of tides curves flattened by nonlinear shallow-water effects, there might be a difference of opinion on where the actual maximum or actual minimum is located on the curve. One of the benefits of an accepted computerized routine for selecting high and low waters, besides the much greater operational efficiency, is the consistency – all high and low waters are selected using the same method. But it is still important to make sure that the same method is used on both predictions and data. Even after computer routines began to be used, the results were often checked manually, by looking at the selected high and low waters plotted on top of the tide curve, and sometimes manual corrections were made.

One basic aspect of all methods for selecting high and low waters from a predicted or observed time series is keeping tracking of each tidal cycle, since usually there is only one true high water and one true low water per cycle. But there are two key exceptions that must be accounted for in any maximum/minimum selection routine.

The first exception is when the nonlinear effects of shallow water distort the shape of a tide curve and lead to double high waters or double low waters (see Section 2.3.2). The high water/low water selection method must be able to recognize when the tide curve is rising and when it is falling and thus be able to keep track of all maximums and minimums throughout each cycle. And, if there is more than one maximum (or minimum) it must decide whether the second maximum is significant enough to be considered as a double high water.

The second exception occurs where there is a strong *mixed* tide regime (see Section 2.1.1), so that the tide actually is diurnal part of the month. The high water/low water selection method must be able to handle the transition from the tide having two high waters (and two low waters) per day to the tide having one high water (and one low water) per day.

A less extreme and more common shallow-water effect leads to a situation that can be very misleading. Shallow water can, for example, greatly flatten the high water part of the tide curve. The actual high water is usually not much higher than the rest of the high water part of the tide curve, but the time of high water can be shifted to the right end or the left end of the high water part of the tide curve. Often the maximum will be near one end of this *plateau*, rather than in the middle (see Figure 3.8), and if this is listed as the high water it can be very misleading (e.g.) to a mariner using a Tide or Tidal Current Table, since high waters are usually thought of as being in the middle

3. Methods of Tidal Analysis and Prediction

of the high water part of the tide curve. In such cases one would be better off selecting the midpoint of the high water part of the curve as the time of high water.

Another bad consequence of this type of situation is that the time of high water will often shift around in time from cycle to cycle, as the relative phases of the (especially overtide) constituents change. As was seen in Sections 3.6.3 this shifting of the time of the high water can lead to problems with nonharmonic analyses. It could also lead to great variability in an error analysis comparing predicted and observed high and low waters.

Many computerized high and low water selection routines use some type of curve fit to select the maximum or minimum. Often these take into consideration the amount of noise in the data. The higher the noise level the more data points that are used in the curve fit. Some also look for the type of nonlinear asymmetric situation described above, where high water may cover a long period as flat plateau, in which case high water is selected as being midway between the slacks.

Standard computerized algorithms are used by NOS to tabulate and quality control high and low waters from 6-minute interval water level data. Six-minute data, even with the mechanical and numerical filtering used in water level measurement systems, can be noisy due to waves, so a polynomial curve fit is used to determine the times and heights of the high and low waters. The tabulation routines contain error diagnostics for flat tides, curve fit failures, etc, for the analyst to review. The algorithms also use some cut-off criteria to eliminate unwanted computer selections during periods of high frequency noise (e.g., not tabulating preliminary computer selections if they are not greater than 0.03m apart in elevation or greater than 2.0 hours in duration).

3.9.2 Consistently Defined Maximum Floods and Ebbs and Slacks (or Minimums)

All that has been said in the last section about consistently selecting high and low waters also applies to finding maximum floods and ebbs and slacks (or minimums) before floods and ebbs (and one should read that section before reading the present section). However, maximums and minimums in tidal current predictions and especially current data are usually more difficult to calculate for a variety of reasons.

First, current data is usually noisier than water level data, especially for offshore current stations. Of course, this will depend a great deal on the type of current measurement device used, as was discussed in Section 2.3.6.

Second, tidal currents are much more susceptible to distortion by shallow water and the distortion can be much more extreme than that seen in the tide. Flattened ebb cycles are very common, with the choice of the time of maximum ebb not always easy to determine (using the midpoint of the ebb phase being the safest choice). In Section 2.3.6 a case was shown where the tidal currents were distorted by shallow-water so much that they are actually quarter-diurnal (with four tidal current cycles per day) – few standardized max/min selection programs could handle that special case.

Third, tidal currents are most often rotary (see Section 2.3.6 and Section 3.4.3), that is, the direction of flow of the current rotates around the compass over one tidal cycle. In the extreme case, in the open ocean far off the coast, the tip of the current vector as it changes direction traces out a circle, and there is no obvious time of maximum flood or maximum ebb. When such stations are put in the Tidal Current Tables, no maximums are picked and instead hourly values for a mean tidal current cycle are put in Table 5 (see Section 9.3.3). In most other cases, ellipses are traced out by the tip of the current vector as it changes direction, and a clear maximum flood and maximum ebb are observable. In narrow channels the ellipse is usually so narrow, that the tidal current is

essentially reversing, with a complete stoppage of flow (*slack water*) halfway between the maximum flood and the maximum ebb. In this case the tidal current speed curve looks like a tide curve (with the zero speed line serving the role of a datum).

Most rotary tidal currents fall between these two extremes (i.e., between circular rotary flow and reversing flow), with their flow vectors tracing out ellipses of varying widths, with slacks replaced by flow minimum, when for a short time the flow is perpendicular to the main flood-ebb axis of flow. However, geography (i.e., bathymetry and shoreline shapes) can make these rotary flows complicated, adding asymmetry in a variety of ways, so that the curves traced out by the changing flow vectors do not look like ellipses at all, and often are strange shapes (see for example the fifth plot in Figure 2.4). Selecting maximums may not always be as straightforward as one would hope. For example, if one has current data (or harmonically produced vector tidal current predictions that show the rotating current) at a location where three channels meet, one may see three maximum flows, one each for when the tidal current is flowing into each channel. For such a case, it may be difficult to decide whether one of those maximums is a maximum flood or a maximum ebb.

Typically the methods for selecting maximum floods and ebbs from a predicted tidal current time series and from an observed current data time series are similar to those used for the tide. Again, one aspect of all methods is the keeping track of each tidal cycle. All of the complications just discussed (as well as the two exceptions discussed for tides) must be somehow accounted for in any maximum selection routine (or in a few of the extreme cases, they must be discovered manually, after looking at the maxima and minima that the computerized routine selected).

There are different methods for selecting slack waters (if the tidal current is reversing) or minimums (if the tidal current is rotary). For selecting slack waters (one before flood and one before ebb) in a predicted tidal current curve, it is simply a matter of finding the smallest positive (flood) speed value and the smallest negative (ebb) speed value (right next to it) and interpolating between them to find the time of the zero speed. Or in some cases one may actually have a predicted value that is zero. For selecting slack waters in a current data curve, the noise may lead to several calculated times of slack, in which case some type of averaging/smoothing scheme over some number of data points can be used to come up with only one slack water. For selecting the times, speeds and directions of the minimum before flood and the minimum before ebb, one usually vectorially averages a group of points with the smallest speeds. One should obtain directions for the minimums that are approximately perpendicular to the flood-ebb axis.

3.10 Spectral Analysis and EOF Analyses

Spectral analysis was mentioned in Section 2.2.3 as a way of determining (and easily visualizing) the amount of energy present in the tidal frequency bands as well as in the nontidal continuum between those bands. In general the results of spectral analysis are not very useful for accurately predicting tides or tidal currents. The exception to this statement, as was seen with the response method, is when a cross-spectral analysis is done (e.g.) between a water level time series and a time series of the tide potential (or the time series of a reference tide station), in which case there will result amplitudes and phase lags that can be used to predict the tide (relative to the input tide potential or reference tide station). So more precisely, it should be said that the results of an autospectrum are not very useful for accurately predicting tides and tidal currents.

Such results are, however, very useful for assessing which tidal constituent signals in a data time series are large enough so that they should be included in a harmonic analysis. Spectral analysis, for example, comes in very handy in determining how important the higher order bands (i.e., the

3. Methods of Tidal Analysis and Prediction

quarter-diurnal and higher bands) will be at a station from a shallow-water area. One can then make some decisions as to which additional tidal constituents will be needed to be included in the harmonic analysis in order to accurately capture most of the tidal energy and ultimately to make the most accurate tidal prediction possible.

3.10.1 Spectral Analysis of Water Level Data Time Series

Only a very brief description of spectral analysis techniques themselves will be given here. For a much more thorough treatment of the material presented below see Emery and Thomson, 2001, as well as Press, et al, 1992 (or one of the latter's many later editions for different computer languages). Although in many ways very different than harmonic analysis, some of the insights gained by understanding those differences can be useful for appreciating what the very act of sampling a data time series and analyzing it can do to that data's inherent frequency make up. This section will concentrate on analyzing water level data, a scalar data times series, but in Section 3.11.3 one will see how this is extended to vector time series, i.e. current data time series.

Technically the spectrum has usually been called a energy spectrum or power spectrum, and it involves at some point squaring the data values in the time series or squaring the individual results in the frequency domain. A theorem called *Parseval's theorem* says that the total energy will be the same whether computed in the time domain or in the frequency domain. A spectrum from only one time series is referred to as an *autospectrum*. When one has two time series for the same time period and one wants to see the frequency make up of what might be characterized as shared power between them, one calculates a *cross-spectrum* (see Section 3.10.4). Prior to carrying out a spectral analysis one first removes (subtracts) the mean from the data time series, as well as its trend, because leaving them in can have an adverse effect on the estimated low-frequency components of the spectrum. Sometimes a low-frequency component itself will be removed if it can be reliably determined.

The frequency resolution of spectral analysis, like all time series analyses (including harmonic analysis) depends on the length of the time series – the longer the time series analyzed the finer the resolution in the frequency domain (see Sections 2.2.3 and 3.3). However, with spectral analysis one typically gives up some of the maximum possible resolution in order to improve the reliability of the analysis result. This is because the data being analyzed with the spectral analysis has many nontidal random and aperiodic fluctuations (which are *stochastic*, and thus unpredictable, except in a probabilistic sense), along with the periodic tidal oscillations (which are *deterministic* and predictable). To make the raw spectrum of a stochastic process more reliable some type of averaging is done, either in the time domain or in the frequency domain. In the time domain this is done by chopping the time series into some number of equal length segments, doing spectral analysis on each segment, and averaging the results. In the frequency domain the same thing is accomplished by averaging several adjacent raw spectral estimates into wider frequency bands. Both processes reduce the frequency resolution in the final (but more reliable) result. (One does not usually choose to do this with harmonic analysis because of the periodic deterministic character of the tides.)

The original type of spectral analysis was the autocorrelation method (Blackman and Tukey, 1958), where the power spectrum is calculated by taking the Fourier transform of the autocorrelation function using some number of lag intervals. (As the name implies, the autocorrelation function is a way of showing how well the time series correlates with itself shifted in time.) When computers began to be used, a numerical technique called the Fast Fourier Transform (FFT) allowed the use

of a better method usually called the *periodogram method* or the *direct method using the FFT* (Cooley and Tukey, 1965). Here the data itself is directly transformed into its Fourier components with the FFT. Both of these methods are sometimes referred to being *nonparametric methods* (Emery and Thomson, 2001) because such methods are not data specific like the so-called *parametric methods*, which use some kind of predetermined statistical model to modify the time series.

The first of the parametric methods was the so-called *maximum entropy method* (MEM) (Burg, 1972), where the name comes from the fact that a maximum entropy condition is used, that is, it is required that the spectral estimate be the most random of any power spectrum which is consistent with the data. *Autoregressive methods* (AR) are very similar to MEM. MEM/AR methods provide finer frequency resolution (although they lose some accuracy), and they allow one to better deal with short time series. These methods can therefore better find the location of peaks, but may not do as good a job calculating an accurate spectral energy at those peaks. Other types of parametric spectral analysis have also been developed such as the *maximum likelihood method*.

The mathematical details of these (and other types of) spectral analysis methods are left to the references mentioned above. [Emery and Thomson (2001, pp 461-2) provide a step-by-step standard spectral analysis approach.] What the reader of this manual mainly needs to know are (1) the advantages and disadvantages of a spectral analysis method that he or she may want to use; and (2) how to interpret and use the resulting spectra that come from that method.

As was mentioned in Section 2.2.3 the spectrum for a typical water level time series (such as that shown in Figure 2.16) shows a continuous curve with spikes above it at the tidal frequencies. The portion of the spectra plot between these tidal spikes is the nontidal continuum and usually is higher at the lower frequencies. This is referred to as a “red” spectrum (in analogy to optics where red light has lower frequencies and longer wavelengths than the rest of visible light). For a long enough time series the frequency resolution can be made small enough to allow the energy in each tidal constituent to show up in its own vertical spectral line (see Figure 2.17).

3.10.2 Tidal Cusps In Spectra

If one looks at a water level spectrum with even greater resolution (e.g., from a time series length of a year or greater) one sees that between the tidal spectral lines the nontidal continuum curve rises up to meet each tidal spectral line on both sides, forming a cusp-like shape (this being usually most noticeable around semidiurnal tidal lines). Such *tidal cusps* were first described in papers by Munk, *et al* (1965) and Munk and Cartwright (1966). They felt that the simplest explanation for these cusps were that they were “presumably due to non-linear interaction between the lines with the low-frequency continuum,” namely that they “represented the sidebands due to the modulation of a carrier (the tides) by a low-frequency noise (the continuum at very low frequencies).” This seems to make sense, but they could not identify any dynamic mechanism that seemed to be able to produce the cusps seen in the water spectra from the locations analyzed by these authors and others. As Cartwright (1999) would write 33 years later, “Their precise cause was hard to identify, but the most promising suggestion was that they were due to the surface manifestation of internal tides.” Such surface manifestations of internal tides would slowly vary as the stratification of the ocean varied (or even disappear if the water became well mixed). This was, in fact, demonstrated by Ray and Mitchum (1997) at Hawaiian water level gauges.

Parker (1991) suggested that, at least for shallow water areas, the same nonlinear mechanisms that lead to the interaction of the tide with storm surge, should produce tidal cusps in a water level

3. Methods of Tidal Analysis and Prediction

spectrum. If a low-frequency storm surge was periodic, the Fourier decomposition analysis of the hydrodynamic equations of motion (see Section 7.6) that showed how the various nonlinear terms could produce overtides and compound tide, could also be used to determine the effect of such a “periodic” storm surge on the tide. If periodic, such subtidal storm surges would produce side bands around each astronomical constituent spectral line via primarily the $\partial(\eta u)/\partial x$ and $\eta u|u|$ terms (the effect of $u \partial u/\partial x$ would probably be negligible because of the small current speeds associated with low-frequency surges). The low-frequency water level spectrum has the highest amplitudes nearer the zero frequency and then slowly decreases with increasing frequency. A “periodic” storm surge with a frequency close to zero would lead to side bands very close to the tidal spectral line, and these would be larger than the side bands caused by a slightly higher-frequency “periodic” storm surge (which would be further from zero frequency and thus have a smaller amplitude). A visualization of this effect in the frequency domain does, in fact, correspond to the idealized picture in a figure presented by Munk, *et al* (1965), and recreated in Figure 3.16. But storm surges are, of course, transient and vary in frequency. The result is a smearing of each spectral line to create a cusp-like shape in the nonlinear continuum around the tidal spectral line.

Whatever their cause the presence of cusps is one more source of noise that might adversely affect the calculation of the smaller harmonic constants. (See discussion in Section 3.3.) And it also implies that some energy is lost from the tidal lines, and that harmonic constant amplitudes would be somewhat larger if there was no nontidal noise and thus no tidal cusps.

3.10.3 Spectral Analysis of Current Data Time Series – Rotary Spectra

Since tidal currents are vectors and since the speed and direction time series are typically transformed into two orthogonal component time series (such as major-minor or north-east component series), there are several choices on what type of spectrum can one can produce from a current data time series. For very reversing tidal currents, or even for tidal currents where the flow in flood or ebb directions is much larger than the perpendicular flow near times of minimums (i.e., for narrow elliptical rotation), one may wish to simply do one spectral analysis, on either the speed time series (with ebb flows given negative values) or on the major-component time series only. For other cases, however, one will want to carry out two spectra analyses, one on the major-axis time series and one on the minor-axis time series. In some cases the spectra of the minor-axis time series will look different than the major-axis time series, e.g., sometimes having more energy in the quarter-diurnal tidal band.

Another option is to carry out a what is usually referred to as a *rotary spectral analysis*, first developed by Gonella (1972) and Mooers (1973). The energy in a current vector time series (i.e., speed and direction time series) does not have to be partitioned into two orthogonal components; it can instead be decomposed into two polarized counter-rotating components, that separately represent the clockwise energy and the counterclockwise energy in the time series. At each frequency, the two counter-rotating circular components can be combined to produce an ellipse for that frequency (the same one that would be produced by combining the two orthogonal results at that frequency). An ellipse from a rotary spectrum at a particular frequency is analogous to the ellipse from a harmonic analysis, created by combining the harmonic constants for two orthogonal components (see Sections 3.4.3 and 5.2). Rotary spectra can be calculated from their Cartesian counterparts (i.e., the spectra for the north-east or major-minor components). (See Emery and Thomson, 2001.)

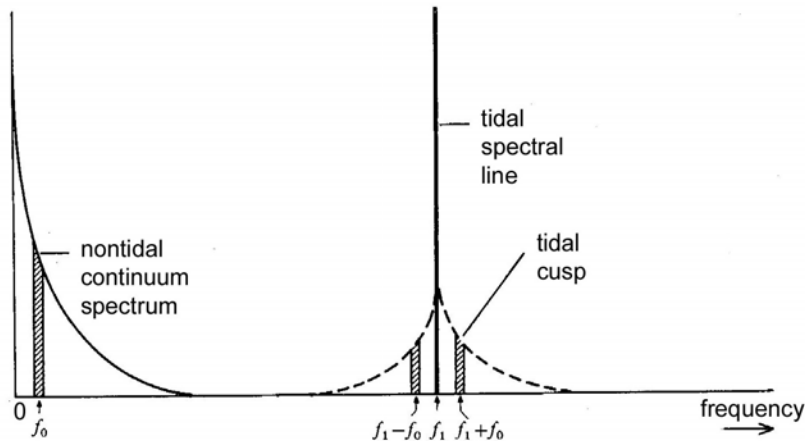


Figure 3.16. An idealized low-frequency nontidal continuum decreasing from its highest value near zero frequency, but then rising up around a tidal spectral line in the shape of a so-called tidal cusp (see text). (From Munk, *et al*, 1965.)

Rotary spectra are useful because there are situations where energy may be predominant in either the clockwise or the counter-clockwise component. Inertial currents (which can be close to tidal frequencies at particular latitudes) rotate clockwise in the northern hemisphere and counter-clockwise in the southern hemisphere due to Coriolis effects. Sometimes one will see the dominance of one type of rotation offshore, and the opposite rotation or perhaps rectilinear motion (i.e., equal amounts of energy in both clockwise and counter-clockwise) close to shore. Each of these types of spectra will provide not only information on how much energy is left at the various tidal frequencies, but also might also provide insights (some more than others depending on the situation and location) into possible hydrodynamic reasons why the energy is there.

3.10.4 Cross-spectral Analysis

The calculation of an autospectrum deals only with the frequency characteristics of a single data time series. The calculation of a cross-spectrum deals with the frequency characteristics common to two data time series from the same time period. At each frequency in the cross spectrum one will see the highest values at frequencies where there is energy in both the time series. At each frequency there will be an amplitude and a relative phase, showing the relationship between the two time series at that frequency. The two times series are often the same parameter but at two different locations, such as two water level records from two locations along a waterway (from which, for example, the cross spectrum might tell us something about the response of the tide at the second station relative to the tide at the first station). However, the two data time series can be for two different parameters, such as the water level and wind, or current and water temperature, again to learn something about the connection between the two parameters over the frequency domain. One often sees higher values only over certain frequency bands, implying a possible causal connection between those parameters for those frequencies.

We have already seen one example of the use of cross-spectral analysis with tides, i.e., the response method (see Section 3.5.1). Here a cross-spectral analysis is done (e.g.) between a water level time series and a time series of the tide potential (or the time series of a reference tide station),

3. Methods of Tidal Analysis and Prediction

in which case there will result amplitudes and phase lags that can then be used to predict the tide (relative to the input tide potential or reference tide station).

One can also carry out a cross-spectral analysis of more than two data time series, and in fact, this approach is recommended if one believes that more than one input (e.g., tidal forcing, wind, changing water temperature) to a physical system is important in producing the output (e.g., changing water level). Such a *multi-input cross spectral analysis* takes into account the mutual correlation among all the inputs, and calculates the relative contribution of each input to the output. Wunsch (1972) used this method to look at the sea level at Bermuda in relation to the tides, weather, and fluctuations in water temperature. Cartwright (1968) also used it to carry out a unified analysis of tides and surges along the coasts of Britain. Similarly, Groves and Hannan (1968) used it to look at the effects of weather on sea level.

One can also calculate *rotary cross spectra* for two vector times series (Mooers, 1973). Here one is essentially trying to ascertain the similarity between the two vector time series in terms of their circularly polarized rotary components. This includes the common energy in the two co-rotating components as well as in the two counter-rotating components. One might, for example, want to look at the rotary cross spectra in currents and wind, as part of an investigation of the effect of a sea breeze-land breeze on the currents (O'Brien and Pillsbury, 1974), and perhaps also see how this might affect nearby tidal frequencies.

(See Emery and Thomson, 2001, and Godin, 1972, for a much more thorough discussion of cross-spectra and rotary cross-spectra.)

3.10.5 Empirical Orthogonal Function (Principal Component) Analysis

All the discussions in this chapter have only dealt with analysis techniques in the time domain (and thus also in the frequency domain). Variations in the space domain (and analogously in the wave number domain) were only mentioned in terms of displaying the time series analysis results on a graph or on a chart, where the results at different locations are plotted. For example, for tides one produces cotidal and corange charts, or graphs the increase in various tidal constituents amplitudes as one moves up a waterway. This serves an important visualization function, and it also is necessary for comparison with the output of hydrodynamic models used to explain the physics behind the variations in the relevant physical oceanographic parameters, including the tides and tidal current.

However, there is a whole field of spatial analysis of time varying *data fields*, that is, when there are literally hundreds or thousands of time series being produced by an instrument or a model at hundreds or thousands of (usually evenly spaced) locations. Such techniques become very useful when one wishes to analyze such time varying data fields, for example, time varying surface current fields from an HF radar system, or time varying elevation fields from satellite altimetry (from which fields of tidal variation can be extracted), or various time varying fields from a hydrodynamic numerical model of a waterway. Here one wishes to understand not only how the frequency makeup varies in space, but one also wants to extract some type of wave number information (in the spatial domain the wave number is the inverse of the wavelength, just as in the time domain the frequency is the inverse of the wave period).

The most common technique used in the analysis of time-varying data fields is *empirical orthogonal function (EOF) analysis*, also called *principal component analysis (PCA)*. EOF analysis essentially allows one to characterize the spatial variation in the time-varying fields using orthogonal functions or *modes*. It does this in a more economical manner than one might expect, because often

most of the variance of a spatially distributed time series is captured by the first few orthogonal functions (in many cases the first orthogonal mode can account for more than half of the variation). For an EOF analysis of sea level data over a region, for example, the first mode might represent the portion of the energy for the water level going up and down together at all the stations, while the second mode might represent a standing wave oscillation where the water level at some of the stations moves up together while at other stations it moves down. The higher modes may have oscillations with decreasing wave length (increasing wave number).

One then usually tries to somehow interpret or correlate the patterns seen in these modes with respect to the spatial variation in particular hydrodynamics mechanisms. This may not always be easy, since these modes are a statistical entity and should not be confused with a particular oscillation that comes out of the hydrodynamic equations. In that respect EOF modes are not the spatial analog of the harmonic constants produced by a harmonic analysis. Where the analogy does hold is that the few modes that come out of an EOF analysis can be used to economically reproduce the spatial variation over a waterway that, for example, may previously been represented by data from dozens of water level stations (just like a few harmonic constants can represent most of the temporal variation in a water level time series). As another example, using an EOF analysis of vertical or cross-sectional current velocity profiles it might be possible to separate the current flow into a few modes of variance, from which one might be able to ascertain the relative importance of the baroclinic contribution (due to perhaps internal waves) compared with the basic barotropic contribution (of the dominant tide wave, wind, or other effects).

For more information on the math behind this technique and its practical application see Preisendorfer (1988) and Emery and Thomson (2001).

4. Harmonic Analysis of Water Level Data

4.1 Considerations In Carrying Out the Analysis

Using the astronomical and hydrodynamic considerations discussed in Chapter 2 and the least squares harmonic analysis method described in Chapter 3, this chapter will look specifically at the things to be considered when harmonically analyzing water level data. (Harmonically analyzing current data will be treated in Chapter 5, and nonharmonically analyzing water level and current data will be treated in Chapter 6.) At the end of this chapter, in summary, all the steps to be considered in a harmonic analysis of water level data will be listed.

4.1.1 Which Tidal Constituents Should Be Solved For

4.1.1a Based on Length of the Data Time Series (the Synodic Period)

As was seen in Section 3.3, the most important consideration affecting the accuracy of calculated harmonic constants (and skill of the tide predictions made with those harmonic constants) is the length of the data time series that is to be analyzed. *The key to an accurate tidal prediction is determining the amplitudes and epochs for the most tidal constituents that can be calculated with a given length data time series.* The longer the time series, the closer in frequency two tidal constituents can be and still both be solved for. Or stated another way, if the synodic period (i.e., the time required to separate the effects of two nearby constituents) is shorter than the data record length, then both those constituents can be included in the harmonic analysis.

If a time series is not long enough to separate two nearby tidal constituents, then only one of these two constituents can be solved for in the harmonic analysis. This will have two effects. First, some tidal energy of the unsolved-for constituent will not be captured. Second, some of the energy of the unsolved-for constituent will be wrongly incorporated in the harmonic amplitude and phase lag of the constituent that is solved for. Since the two close constituents will go in and out of phase over their synodic period (see Section 3.3), the astronomical conditions during the data record will determine how much of an adverse effect this will have on the harmonic constants. As will be seen in Section 4.2, for cases where the time series is too short, methods have been developed to infer the unsolved-for tidal constituents, and also to adjust the solved-for constituents for the degrading effects of the unsolved-for constituents.

Table 3.2 lists the 37 tidal constituents that have typically been solved for in a standard one-year harmonic analysis at CO-OPS (and its predecessor organizations). The list starts with M_2 , generally the largest of all the constituents (except for some locations with an extreme diurnal situation) and then follows with other constituents listed in the order of their most important synodic period, that is, the length of the series required to separate them from a nearby (usually) larger constituent. Once

one gets past K_1 (and overtones) there are four natural groupings with respect to the synodic period: half month, month, half year, and year.

This table provides guidance for which constituents to include in a harmonic analysis, but (as was discussed in Sections 3.3 and 3.4.5) when using a least square harmonic analysis there may be some leeway, especially when there is a very strong tidal signal. Thus, if one has less data than Table 3.2 says is required to be able to include a particular constituent in our harmonic analysis (so that it can be separated from another key constituent), one may still be able to analyze for both constituents because of the least squares technique. The best procedure is probably do several analyses, following the recommendations of Table 3.2 with the first analysis, and then adding a key constituent with the second analysis, and if necessary adding additional constituents in additional analyses. For each analysis redone with an added constituent, examine carefully the other tidal constituents to see how much they have changed compared with the results of the previous analysis. Large changes probably indicate that the program has been pushed too far (and in fact, the program will crash if one really pushes it too far).

As but one example, suppose one has 5 months of water level data from a waterway with a strong enough diurnal signal that one wants to be able to solve for P_1 , because it is the third largest diurnal tidal constituent. However, Table 3.2 says that to be able to include P_1 in a harmonic analysis one should have 182.6 days of data (the synodic period for resolving P_1 from K_1). The time series length is a month short, but since a least squares harmonic analysis technique is being used, and since one expects P_1 to be a strong signal (well above the noise level of the water level record), one can decide to try a 150-day analysis. This analysis will most likely turn out fine, but one can check this (as just mentioned) by comparing the K_1 value from this analysis with the K_1 value from an analysis without P_1 included. If they are reasonably similar, then there was little adverse affect of P_1 on K_1 . Also, if one has analysis results from a nearby longer period station, one can see if the P_1/K_1 ratio at that station is similar to the P_1/K_1 ratio at this newly analyzed shorter station (and likewise that the difference in the K_1 and P_1 epochs are similar). If the results do not look reasonable, the analysis results without solving for P_1 will have to be used, and then the amplitude and phase of P_1 can be inferred using one of the methods talked about in Section 4.2.

As another example, suppose one has only 15 days of data. Then a harmonic analysis will provide values for the major constituents M_2 , S_2 , K_1 , and O_1 , plus a few higher harmonics and a couple of less important constituents. However, these calculated values will also include energy from the constituents that could not be separated out in only 15 days. Most important, M_2 will include energy from N_2 (which could have been resolved from M_2 if there had been 29 days of data). This N_2 contribution could make the M_2 value calculated from 15 days of data larger than it should be, or smaller than it should be, depending on when the data were measured. Likewise (as in the above example but more extreme here), since P_1 cannot be separated from K_1 , K_1 will include the effects of P_1 . If one had more data and harmonically analyzed successive 15-day periods, one would see the amplitude of K_1 slowly vary over a 6-month period because of the influence of P_1 . One would also see the amplitude of M_2 vary from 15-day to 15-day period, but to clearly show the 29-day modulation one would need to start each 15-day analysis only a few days after the previous one. For a record as short as 15 days, use of a method to infer important missing tidal constituents such as N_2 and P_1 is definitely required.

Table 3.2 is quite adequate for many situations, but for shallow-water areas with large tide ranges, or if one wants to include every possible constituent that can be calculated using a data time series that is longer than a year, then one needs to look at Table A.2 in Appendix A, which includes

4. Harmonic Analysis of Water Level Data

149 tidal constituents (including 103 shallow-water constituents) and extends beyond a year for the synodic periods of some very small constituents.

4.1.1b Compound Constituents Versus Astronomical Constituents (with the same frequency)

There is another consideration when deciding which constituents to include in a harmonic analysis. In shallow-water areas, compound tides will be produced (by the nonlinear processes discussed in Sections 2.3.2 and 7.6) and some of these compound tides will have frequencies that are the same as particular astronomical constituents. Although they have the same frequencies, they may have different node factors (and equilibrium arguments), so that if the wrong choice is made between using the astronomical constituent versus using the shallow-water compound constituent, then there will be errors in future predictions (but not in the self-prediction for the year of the analyzed data).

A usually important example of this is that the shallow-water constituent $2MN_2$ has the same frequency as L_2 , but has a different node factor. There is no way to separate two such constituents unless one has 18.6 years of data, in which case the satellite constituents corresponding to these two constituents would handle the different long-term variation (that is represented by the different node factors when not using satellite constituents). To decide which constituent to use, one can initially use L_2 but then look at the analysis results for locations throughout the waterway. If one sees that L_2 increases in amplitude (as one moves up a waterway) at a rate that is greater than the rate of increase in M_2 or S_2 (for example see Figure 7.5) then L_2 is probably really $2MN_2$. [L_2 would increase at a rate similar to the rate of increase of M_2 , because both would be affected by how close the waterway is to a resonance condition (see Sections 2.3.1 and 7.4.1), but $2MN_2$ would increase at a faster rate because nonlinear processes would be extracting energy from M_2 and N_2 and putting it into $2MN_2$ all the way up the waterway.] If the constituent is $2MN_2$, the analysis does not have to be redone, but the final amplitude and epoch should be adjusted for the correct node factor and equilibrium argument.

In some cases, where the amplitude of the constituent does not grow at a rate greater than the rate of increase of M_2 , it may not be possible to tell how much of it is L_2 and how much of it is $2MN_2$. (If one had an numerical hydrodynamic model, one could tell by running the model with and without the appropriate nonlinear terms turned on, but this is much too much effort.) However, in this case the amplitude of the constituent is probably small enough that simply sticking with L_2 is fine. If the water level station is on an oceanic island or along an ocean coast (especially one with a deep and/or narrow continental shelf) one is very safe in using L_2 . For most other shallower waterways, since L_2 is usually small, it has been simplest just to use only $2MN_2$.

Another example is that the shallow-water compound constituent $2MS_2$ and μ_2 have the same frequency. In shallow estuaries one sees $2MS_2$ increase at a rate faster than the rate of increase of M_2 or S_2 (also see Figure 7.5). Here, however, it does not matter whether the analyzed constituent is $2MS_2$ or μ_2 , because they have the same node factor.

For very shallow-water areas with large tide ranges one adds many additional shallow-water compound constituents, and some of these may end up with the same frequency. In such cases one has to look at the nonlinear generating mechanism and try to decide which of the candidate constituents to use. One should also first determine whether their node factors will even be different. If they are not, it doesn't matter what name one gives that constituent.

4.1.2 Keeping or Rejecting Small Constituents

Many of the constituents included in the harmonic analysis will come out with very small amplitudes. If these constituents are so small that they fall within the nontidal continuum, they may not be real (that is, one has not been able to calculate the actual tidal constituent, only the amplitude and phase lag of some transient nontidal periodic signal). Sometimes there has been an arbitrary lower limit set, below which the harmonic constants are rejected (see Section 4.3.5). However, there can be cases where harmonic constants are real even if their amplitudes fall below that lower cutoff level. The best way to determine this, if one has enough data, is to run more than one harmonic analysis and to look at the phase lag (epoch) and see if it is consistent from analysis to analysis. If it is, then the harmonic constants probably do represent the tidal constituent solved for (and not just some transient periodic nontidal energy).

The reason it is important not to reject small tidal constituents unnecessarily, is that the lost tidal energy can add up if several small constituents are rejected. Then the predicted high waters (on average) will be too small (and low waters on average will be too high) compared with the high and low waters in the data (also on average, so that meteorological effects are averaged out). Such a situation has sometimes been “solved” by simply increasing all the constituent amplitudes by some percentage (see Section 4.3.5) in order to make the mean predicted high and low waters better match the mean high and low waters from the data. This so-called “build-up” factor adds energy in the wrong places and does not really make the tidal predictions more accurate (only the average of all the high waters and the average of all the low waters are more accurate).

4.1.3 Instrument Errors and Their Effects On Analysis Results

When data is referred to as being “bad” or “unreal”, one is essentially talking about instrument error, i.e., values that do not represent the actual water level at the time of measurement because of some error related to the measurement process itself. There will also be natural noise in the data record due to various nontidal phenomena, but being natural such noise is considered real and not errors (although one may wish to filter them out at some point, if one feels they might adversely affect our tidal analysis). Techniques for evaluating the quality of a data time series and techniques for editing out (or possibly repairing) data points that are determined to be “bad” or “unreal” can vary significantly, and there is no need to discuss any particular method here. Commonly one tries to find and then remove (or “correct”) data points that are obvious outliers, which is fairly simple when there is a clear tidal signal in the data. One also tries to discover if possible other types of variations in the data that may not be of natural origin (and thus must have come from the instrument) which might affect the analysis results.

What is important is to acquire some feeling for the potential sources of errors and how different types of errors might affect the results of a harmonic analysis. Errors in a water level data time series may be electronic, mechanical, the effect of temperature changes on the instrument (as opposed to its effect on the water level), etc, or have to do with movement of the water level gauge itself.

The types of potential errors are different for each different type of water level gauge. However, with an eye toward their effect on harmonic analysis results, these types of error can be classified as either:

(Type 1) *random errors* [which will tend to average out during a harmonic analysis];

4. Harmonic Analysis of Water Level Data

- (Type 2) *sudden shifts*, when from some point in time forward, the entire time series of measured heights are all larger or smaller by some amount than they were before that point in time [which would incorrectly change mean sea level, but probably not affect the amplitudes of harmonic constants, except perhaps the longer-period constituents (such as Sa and Ssa) depending on the length of the erroneous offset];
- (Type 3) *slowly changing errors*, where an error might slowly grow over months or longer [which might change the harmonic constants];
- (Type 4) *slowly changing time measurement*, such as when a clock may be running slow [which would essentially spread out time and reduce the frequencies of the tidal constituents, so that when a harmonic analysis looks for energy at the correct tidal frequencies the result will be smaller amplitudes and changed phase lags]; or
- (Type 5) *periodic errors*, which might, for example, be due to meteorological effects on the instrument (as opposed to meteorological effects on the water level itself) [which might change particular tidal constituents].

From 1807 until the mid 1850's, in the U.S. Coast Survey the simple *tide staff* was the primary method used for measuring water level. A tide staff had graduated markings on it in feet and tenths of a foot, and was fastened firmly to a pier or piling or some other structure that was (hopefully) unlikely to move vertically. In remote areas, supporting structures had to be constructed so that a stable tide staff could be read during the time period of a hydrographic survey. In many instances, the tide staff was not read continuously, often being read only around the times of high water or low water. In such cases, either the harmonic methods discussed in Section 3.5.6 or nonharmonic methods (Chapter 6) had to be used for analysis and prediction purposes.

To make a water level observation an observer simply tried to determine where the water level fell on the staff, and wrote down the time and height of the water level elevation. That was often made difficult by the fact that the water level was usually oscillating up and down due to the action of (higher frequency) wind waves. The *Manual of Tide Observations* (U.S. C&GS, 1963, page 33) provided the following guidance for the tide observer using a tide staff:

“In taking the tide staff reading, both the highest and lowest points reached by the waves are to be recorded, the two readings being separated by a dash or in some other distinctive manner.”

For this type of water level measurement, errors were mostly likely human error during the visual process of estimating each water level elevation (and any errors were hopefully of Type 1). If the observers changed, there might also be a change in bias of how each person tended to make the observation (which would be error Type 2). Another error could result if the tide staff suddenly shifted position on the pier (again error Type 2), but it also could also have slowly slipped lower over a period of time (error Type 3). [The pier itself could also be shifting, which is a potential problem for all types of water level gauges (see below).]

One type of tide staff occasionally used had a *glass tube* attached to its full length. This glass tube was partially closed at the lower end (which was always in the water), the purpose being to dampen the action of waves so that the water in the tube would not oscillate as much as the water outside the tube. This was intended to make it easier for the observer to make an accurate visual measurement of the water level. Such a tube might get clogged which could lead to errors of Type 2, or might be prone in some areas to slow biological growth, which might cause errors of Type 3.

It was also subject to random errors by the observer (error Type 1), as well as to a change in bias (on the way a particular observer made a visual measurement) when observers changed (error Type 2).

From the mid 1850's until the last couple of decades, the most common method for water level measurement was the use of a *float* inside a *stilling well* (sometimes also called a *float well*). The float was at the end of a wire which was attached (usually by pulleys) to some type of measuring/recording device. Before it became an automated system and measurements were still made visually by an observer, the wire was a tape which was either graduated itself (in feet and tenths of a foot) or had a pointer which would move up and down along a graduated scale. This pre-automated version was also subject to random errors by the observer (error Type 1), as well as to a change in observer bias when observers changed (error Type 2). The stilling well was intended to dampen (or “still”) wave effects on the vertical movement of the float. It had a small opening at the bottom, typically a 1½ inch opening in a well of from 4 to 12 inches in diameter, but the opening could be as small as 3/4 inch in areas exposed to heavy seas. The stilling well could become clogged with floating debris, which could lead to errors of Type 2, or it could be slowly clogged by biological growth, which might cause errors of Type 3.

When the float tide gauge system became an *automated system* (not requiring an observer to make a visual reading), the wire moving up and down operated a worm screw on the gauge, which in turn moved a pencil back and forth across a moving strip of paper. The paper moved forward at a known uniform rate by a clock motor, the result being a continuous graph of the rise and fall of the water level. There was still a human aspect to making the measurement (and a chance for human error of Types 1 or 2), but it was now in how the time and height were taken off the graph of the tide on the paper roll, which involved not only determining the times and heights of high and low waters, but also the heights at hourly intervals. Tide observers were still important in the field, however, since once a day they made independent measurements using a tide staff, unclogged the stilling well, and made clock adjustments to keep the tide gauge clock on the correct time. In the mid 1960's, the analog strip charts were replaced by analog-to-digital (ADR) punched paper tape. The punched paper tape allowed the use of an automated data processing system. This reduced some of the processing and tabulation errors, tide gauges still had clock drift, and tide staffs were still required to be read by tide observers. Slowly degrading bearings in the ADR gauge system due to the salt-water environment could also lead to slowly changing errors (Type 3).

The stilling well was also a potential source of another type of error when there were fast tidal currents (Shih and Baer, 1991). Such currents could cause a pull-down effect as the water flowed past the smaller opening (the orifice) at the bottom of the well. Such an effect would be periodic (error Type 5) with the frequency of the primary tidal constituent, and thus could affect that tidal constituent and other constituents in the same frequency band. However, the maximum effect would be at both maximum flood current and at maximum ebb current, so the result might also affect the overtide constituents. As a solution to this problem, in locations with strong tidal currents, large parallel plates were mounted below the orifice to reduce the pull down effect.

At locations where a tide station could not be installed on a solid structure along the shore, a *gas-purging pressure tide gauge* (or *bubbler gauge*) was used, being placed on the sea bottom (usually 2000 feet or less from the shore, the maximum length of tube between the bubbler and the data recorder onshore). As explained in The *Manual of Tide Observations*, when gas is bubbled freely into a liquid from the fixed end of a tube, the pressure in the entire length of the tube is approximately equal to the pressure head of the liquid over the bubble orifice. Any change in the hydrostatic pressure (such as caused by the rise and fall of the tide) is transmitted by gas pressure through the tubing to the transducer bellows of the recorder where pressure variations are recorded

4. Harmonic Analysis of Water Level Data

as changes in depth of water. The changes in the pressure pushing down on the bubbler gauge (sitting on the sea bottom) can also be caused by changes in water density due to changes in salinity or water temperature. Since in estuaries tidal currents can periodically change the salinity and water temperature (e.g., perhaps being saltier during the flood current phase and fresher during the ebb current phase), this is a potential source of error (Type 5) that can affect the tidal harmonic constants calculated from the water level data obtained with this instrument. Seasonal changes in water temperature and salinity can also have an effect (also a Type 5 error, but with a longer period and so more likely affecting the constituents Sa and Ssa; see Section 3.7). For bubbler gauges deployed for short time periods, this seasonal effect would not be obvious in the data. However, in the early 1970's, bubbler tide gauges were installed at most long-term stations to serve as an independent backup system to the float and stilling well system. More recently, the density effect problem has been reduced by using dual bubbler orifice systems with the pressure fed into two highly precise Paroscientific pressure transducers. The pressure difference between the two bubbler orifices is used to estimate water density, which is then used to correct the elevations calculated from the pressure data.

When automated systems began to be used, which involved time keeping with clocks, there was the added possible problem of clock errors, both sudden changes and very slow changes in time that occur over days, months, or years. Slow changes in time can have a significant effects on harmonic analysis results (error Type 4). A slow clock would lead to data samples being taken at time intervals slightly longer than the intended sampling interval. If this was not recognized and corrected (and the time was erroneously assigned to the data points as though the clock were correct), then the tidal energy in this data time series (with erroneously assigned times) would appear at slightly higher frequencies than the tidal frequencies. (For a fast clock, the opposite would happen.) Analyzing such data for the frequencies where one expects to find tidal energy could then lead to erroneous harmonic constants (depending on how slow or fast the clock was). A sudden shift in time also decreases the amplitudes of the constituents and changes the phase lags (like Type 4). With today's real-time systems, timing errors are no longer a problem, as timing is controlled by a small antenna that receives precise timing from the GPS system.

The present water level measurement system used by CO-OPS is an acoustic one, where again there is a well, although more open than a stilling well to reduce the aliasing effect of the stilling well when there are waves (Shih and Baer, 1991). Water level elevation is now measured by the time it takes a sound pulse to leave a transducer, travel to the surface of the water, reflect off it and return, the sound pulse actually traveling through a 13 mm diameter PVC tube. The speed of sound in the tube is determined using a second reflection from a discontinuity in the tube at a known distance from the transducer (this section of the tube being referred to as the calibration tube). There is a new potential source of error, caused by changes in air temperature, which changes the density of the air, which in turn changes the speed of sound, but the use of the calibration tube is designed to take care of that. However, care must be taken to assure that the temperature in the calibration tube is the same as in the rest of the tube, and this is accomplished by various means (including ventilation, keeping the calibration tube in the same environmental conditions as the rest of the tube, and painting the protective well a light reflective color). But for water level stations where there is a large tide range, the PVC tube is very long and so there is more of a chance for temperature effects. To deal with this problem, there are also two thermistors, one in the calibration tube and one in the rest of the tube. If the temperature at these two locations is different enough, they can be used to make corrections to the speed of sound (and thus of the water level measurement). If temperature errors do occur, since the air temperature changes over a daily cycle, such errors would

be Type 5, and there could be seasonal variations as well. (See Gill, *et al.*, 1993, and Porter and Shih, 1996.)

The switch from the float gauge to an acoustic gauge at a particular stations can also potentially cause an error Type 2. However, to minimize such an effect (which would not affect harmonic constants, but could affect sea level determinations, and in fact look like a small change in sea level), both gauges were run simultaneously side by side for a year, in order to make the necessary adjustments, and assure continuation of the datums.

A potential problem for all types of water level gauges is that the pier itself could shift vertically, either suddenly (perhaps due to a storm, which is easy to recognize; error Type 2) or slowly over the years (error Type 3). The land itself, of course, can also move vertically, both suddenly (due to an earthquake) or very slowly (due to things such as glacial rebound, sediment compaction, extraction of fluids from the ground nearby). Operational standard operating procedures require annual leveling to check for pier and/or local vertical movement in bench marks on land. Special levels are run after earthquakes or known hits by storms or ships to check for vertical movement. To track slow regional vertical land movement, tide stations are now being tied into nearby continuously operating GPS systems that track land movement. These errors when they occur are usually very small and mainly are of concern in the determination of long-term sea level change and the updating of tidal datums. However, one should be aware of the possibility of some of these errors affecting the results of a harmonic analysis of the data.

There are a variety of other very recent techniques for measuring water level, which are not yet used on a regular basis, such as GPS receivers on buoys, laser systems, and land-based radar systems. These will also have some type of potential instrument-caused errors, but they are still new enough so that such potential errors have not yet been fully assessed. For a recent discussion and assessment of water level measurement techniques see the Intergovernmental Oceanographic Commissions's *Manual of Sea Level Measurement and Interpretation*, volume IV (IOC, 2006).

4.1.4 Assessing the Potential Effects of Nontidal Influences

As was seen in Section 2.3.3, in shallow-water areas the tide can be modified by the nonlinear interaction of nontidal phenomena such as river discharge and storm surge. It was shown, for example, that strong river discharge during a spring runoff period can shrink the tide range and shift energy into the first overtide, increasing the M_4/M_2 ratio and distorting the shape of the tide curve (perhaps leading to a more rapid rise to high water and a slower drop to low water). Storm surge with frequencies below the tidal frequency bands (so that the water level change due to the storm surge takes place slowly over a couple of days) also affects the tide through shallow-water nonlinear mechanisms. The tide range might, for example, increase when the nontidal water level is higher due to the storm surge, and decrease when the nontidal water level is lower due to the storm surge. Changing water density (due to changing salinity in estuaries, or to changing water temperature offshore) can cause various baroclinic effects (including internal tide waves), which though they primarily affect tidal currents, could indirectly affect the tide through effects on energy dissipation (see Section 2.3.6). There can also be seasonal effects on water level, such as higher water levels during the summer due to the thermal expansion of the warmer upper layer of the ocean (see Section 3.7.1), during which time the tide range (and most tidal constituents) might be higher.

When one is harmonically analyzing a water level data time series one must therefore be aware of the potential effects of nontidal phenomena on the harmonic constants that come out of the analysis. If one needs harmonic constants from which accurate predictions can be made for most

4. Harmonic Analysis of Water Level Data

of the year, then one might consider leaving out sections of the time series that include strong nontidal events and using the gap option of the least squares harmonic analysis program. If one has a short time series of water level data that includes a major nontidal event, one will probably not be able to use the harmonic constants that come out of the analysis to make tide predictions for “normal” time periods, i.e., for time periods without those strong nontidal phenomena. In fact, one can probably not even use those harmonic constants to make a tide prediction for the time period that included the nontidal event, because the effect of the nontidal event (which probably only lasted a couple of days) was spread out over the length of the analysis. So even the results of a 15-day harmonic analysis will not be useful. In such cases, one can try using the continuous wavelet transform method (see Section 3.5.5).

To discover those periods in an observed water level data time series when a nontidal phenomenon may have a strong influence, one can first tidally filter (see Section 3.8) the water level time series. Although the filtering process may reduce the amplitude of such an effect, one should still see periods when the nontidal water level is raised and then lowered (or vice versa). These may be sections of the time series that one will ultimately decide to leave out of the harmonic analysis, but initially at least one should analyze the entire time series, produce a predicted time series for the entire period of the observations, and subtract the predicted series from the observed series to produce a residual series. Then one should carefully examine the residual series. At those same periods in time where one saw changes in nontidal water level in the filtered time series, one is likely now to see oscillations at a tidal period appear and then disappear. One might even see transient tidal oscillation at time periods without an obvious change in nontidal water level in the filtered time series (which would imply the effects from nontidal currents or changing water density).

When these transient tidal oscillations occur, it will usually be due to the effect of the nonlinear interaction between the tide and a transient nontidal phenomenon, such as a large river discharge (see Figure 4.1) or storm surge. During these periods of interaction, the nontidal phenomenon has temporarily changed the hydrodynamics of the situation and thus changed the amplitudes and/or

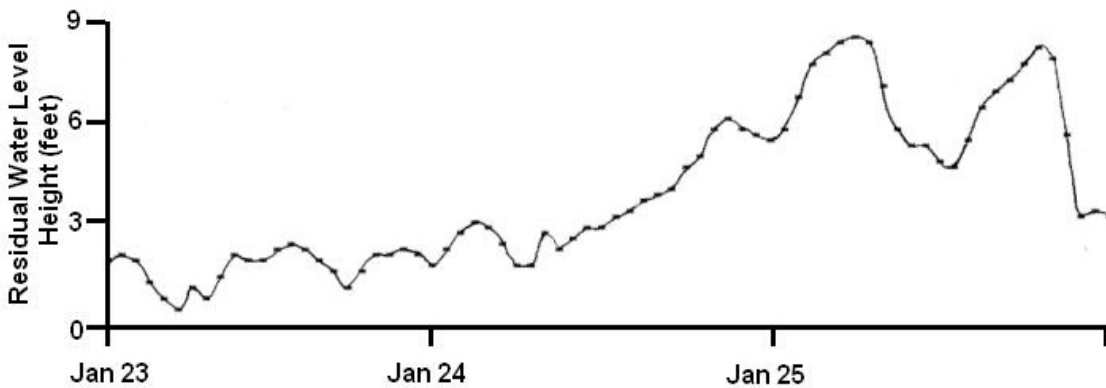


Figure 4.1. The residual water level at Trenton, NJ, on the Delaware River, during a period of increasing river discharge. The residual series was produced by subtracting the predicted tide series (based on harmonic constants from a one-year analysis) from the water level data time series. In addition to raising the nontidal water level, the high river discharge shrinks the tide range and distorts the tide curve, so that tidal energy temporarily shows up in the residual time series (see text, and also Figures 2.29 and 2.31).

phase lags of the tidal constituents. Thus, by subtracting the predictions based on the average tidal constituents (obtained from the analysis of the entire time series) one leaves some tidal energy for that particular time period. The transient tidal oscillation seen at time periods without an obvious change in nontidal water level (in the filtered time series) would be time periods when there are nonlinear effects of nontidal currents or perhaps even the indirect effect of a change in water density that allowed a baroclinic effect to occur (although this effect is much more important for affecting tidal currents).

When one sees nontidal events in the filtered time series and/or transient tidal oscillations in the residual time series, one should look at wind or river or other data records for the potential nontidal influences that may have caused the temporarily different tidal constituents. If such incidents occur frequently, one may wish to add a footnote in a Tide Table about when such incidents occur. (However, in cases where it is large nontidal water level changes that are nonlinearly modifying the tide, those nontidal changes may overshadow any changes seen in the tide.) If such incidents occur frequently, then water level prediction with a real-time driven water level forecast numerical model may be the best route to take, because it can include not only the nontidal phenomena but also the effects of their nonlinear interaction with the tide.

If there is a strong seasonal effect on nontidal water levels and, for example, one sees larger tide ranges on average in the summer, one might need additional tidal harmonic constants in order to include the essentially semiannual modulation of the tide range. The actual higher nontidal water level in the summer might also be included in the Sa constituent, even though it is not tidal. (See Section 3.7.)

4.1.5 Use of Node Factors and Equilibrium Arguments (or of Satellite Constituents)

As was seen in Section 2.2.4 there are some very slow modulations of the tide-producing forces with periods of many years. The two most important are the 18.6-year lunar nodal regression, i.e., the variation in the angle between the plane of the moon's orbits and the plane of the Earth's equator, and the 8.85-year variation in the lunar distance from the Earth due to the rotation of the longitude of the lunar perigee. To include these effects in a complete harmonic analysis one must add dozens of additional satellite tidal constituents, at least one for each of the lunar tidal constituents, with frequencies very close to the frequencies of those usual tidal constituents (e.g., a separation of .0022°/hour or .0015 cpd), and one must analyze 19 years of data. Classically such a method was not used because of the enormous required work effort (which could not even be attempted prior to electronic computers) and because of the lack of 19-year long time series for many stations.

The alternative approach, as explained in Section 2.2.4 is the use the node factor, f , a factor that multiplies the amplitude of each tidal constituent (directly representing the modulation of the tidal forces), as well as a phase difference, u , included in the equilibrium argument, that also varies over the 18.6 years. Each node factor fluctuates around 1.0, with a variation of $\pm 4\%$ for M_2 , $\pm 11\%$ for K_1 , $\pm 18\%$ for O_1 , etc. The solar constituents such as S_2 or P_1 do not have node factors.

Because of the slowness of the variation in f and u , they would not change much in value over the length of a typical harmonic analysis or tidal prediction, which is usually for a year or less. Thus, for convenience, it became regular practice in the U.S. C&GS to use only a single value of f and a single value of u for the entire analysis or prediction, and to use values for the center of the time duration of the analysis or prediction. In some countries the values of f and u used in prediction programs are changed every month (e.g., in the UK and in Canada). Typically the f and u values

4. Harmonic Analysis of Water Level Data

(for the center of a particular year) were obtained from tables (such as Table 14 and 15 in Schureman, 1958, or Zetler, 1982), but the astronomical equations with which they are calculated can be included in any harmonic analysis or tidal prediction program and often were.

However, as was seen in Section 2.3.4, these astronomically determined node factors are based on equilibrium theory and thus ignore the modifying influences of hydrodynamic effects. Although the frequency of the typical tidal harmonic constituents is determined by astronomy, their amplitudes and phase lags are determined by the hydrodynamics of the ocean and waterways on the Earth. The same is true of the 18.6 and 8.85-year variations, and one should expect some modification of f and u due to hydrodynamics. Because of the very low frequencies involved, however, the modifications may be more due to nonlinear interactions than to typical near-resonance-type effects (see Section 2.3.1).

Figure 2.32 shows the true variation in the amplitude of six harmonic constants over 19 years as determined from uncorrected one-year harmonic analyses (and compared with the variation based on equilibrium theory), and in only one case does the variation in the node factor calculated from actual data closely match the astronomically determined node factor (for O_1 , see Section 2.3.4 for the reason). In these plots, besides the 18.6-year variation one sees other variations due to other effects, some of which may be due to small wind-, river-, or temperature-caused changes in the hydrodynamic system for a particular year.

The use of satellite constituents might capture some of this hydrodynamically caused modification of the astronomical node factor, but only those variations that are periodic. Instead of using the astronomically determined node factors, one could instead use calculated node factors (like those in Figure 2.32), which could be from a nearby reference station if there is not enough data at the station being analyzed or predicted. Using node factors calculated from actual water level data will work for self predictions and predictions into the past, but not for predictions into the future. In such a case, one would try to extrapolate forward the periodic signals seen in the most recent 19-year or 38-year (or longer) analysis. But for many applications the increase in the accuracy obtained may not be worth that effort.

Zetler, Long, and Ku (1985) did a study on the accuracy of tide predictions using satellite constituents versus node factors (as well as comparing the use of an annual f and u , a bimonthly f and u , and a monthly f and u). They did this by first doing a 19-year harmonic analysis of water level data from Seattle, Washington, using 55 tidal constituents of which 30 were satellite constituents. Tide predictions were made with these 55 constituents (the use of f and u was not needed), and these predictions were subtracted from the observed time series to produce a residual series. Similar predictions were then made using the primary 25 tidal constituents (i.e., no satellite constituents), but using f and u , and again producing residual series. This was done three times, the f and u held constant for each year, the f and u held constant for two month intervals, and the f and u held constant for one month intervals. A fifth prediction was also made using satellite constituents that were inferred (using the ratio of the satellite constituent to the main constituent as found in the tide-generating potential in Cartwright and Edden, 1973). The residual variances were best for the predictions using the satellite constituents obtained from the 19-year analysis, but only by a few percentage points. Among the predictions using f and u , the results using f and u held constant for one month or two month intervals were just barely better than the results when f and u were held constant for a year, as were the results gotten from using the inferred satellite constituents.

Another thorough analysis of 19 years (and 38 years) of water level data using satellite constituents was carried out by Foreman and Neufeld (1991). They used over 500 constituents. They found that predictions based on a 19-year harmonic analysis with satellite constituents were

only slightly better than those based on averages from 19 one-year analyses using Godin's (1972) satellite correction algorithm and satellite inference (based on tide potential theory relationships).

To give the reader some feel for a 19-year analysis done using satellite constituents, Table 4.1 is reproduced from Zetler, Long, and Ku (1985) showing the 25 main tidal constituents plus the 30 satellite constituents that were calculated from 19 years of Seattle water level data. In this table one can see the main harmonic constants (amplitudes and epochs) obtained from standard 19-year analyses with and without satellite constituents, along with the inferred satellite constituents. The very slight difference in angular speed (i.e., frequency) between corresponding main and satellite constituents is apparent in the third column of the table, and the cause of this difference, either the lunar node variation or the variation in lunar distance, is indicated by the change in 4th and/or 5th Cartwright number (in the second column of the table) (see the end of Section 2.2.3). Some main constituents only have lunar nodal satellite constituents (e.g., M₂, N₂, K₁, O₁, etc.), one or two satellite constituents per main constituent. M₁ and L₂ have both lunar node and lunar distance satellites, in which case there are four satellite constituents per main constituent. Solar constituents have no satellite constituents.

In spite of the possible error in using a node factor (mentioned above and in Section 2.3.4), the tendency has been to stay with that approach (versus using satellite constituents) for several reasons:

- (1) there are still many water level stations without 19 years of data, and to be consistent the same method has been used for all stations;
- (2) it is a familiar approach that is more intuitively understandable than using dozens of additional small satellite constituents;
- (3) the additional accuracy does not seem to warrant (in most cases) the extra work of analyzing for dozens of additional constituents and needing nearly 19 years of data for the analysis;
- (4) even when there is some hydrodynamic nonlinear interaction that affects the 18.6-year modulation so that it may not look very similar to the astronomically determined variation, that nonlinearly-determined variation is more understandable in terms of its affect on the astronomical nodal variation than trying to understand the changes in the many satellite constituents.

4.2 *Methods for Analyzing Short Time Series*

As was seen earlier in this book (Sections 3.3 and 4.1.1) the number of tidal constituents that one can accurately determine using harmonic analysis depends on the length of the data time series. The length of the time series determines the frequency resolution of the analysis, that is, how close two constituents can be in frequency and still be separated by the harmonic analysis. If one has two tidal constituents that are closer in frequency than can be separated by the analysis (i.e., the time series is too short), then only one of those two constituents (the one expected to be larger) can be solved for. The calculated value for this larger constituent will not be as accurate as one would like, because its value will include an unknown contribution from the second constituent that could not be solved for. This contribution from the nearby unsolved-for constituent will vary from month to month throughout the year.

When this occurs there are methods to try to improve the analysis results – both to obtain values for constituents that could not be included in the original harmonic analysis (called *inference*) and to improve the value of constituents that were in the analysis but were adversely affected by the constituents that were left out of the analysis (called *elimination*). Several of these methods for inferring constituents that could not be solved for with the available time series, and for eliminating

4. Harmonic Analysis of Water Level Data

Seattle Harmonic Constants

Constituent			Amplitude in cm			g (kappa Prime) in °		
Name	Cartwright Number	Speed in °/h	NOS analysis	added inferred	19-yr. analysis	NOS analysis	added inferred	19-yr. analysis
Sa	001000	0.04106864	7.38		6.93	289.1		289.2
Ssa	002000	0.08213728	2.71		2.99	214.0		218.0
2Q ₁ (-1)	1-302-10	12.85207974		0.22	0.18		130.7	158.3
2Q ₁	1-30200	12.85428615	1.19		0.83	130.7	144.7	
Q ₁ (-1)	1-201-10	13.39645444		1.42	1.49		143.5	138.6
Q ₁	1-20100	13.39866086	7.53		7.42	143.5		141.8
p ₁ (-1)	1-22-1-10	13.46930806		0.33	0.32		138.3	136.0
p ₁	1-22-100	13.47151447	1.74		1.49	138.3		140.2
O ₁ (-1)	1-100-10	13.94082915		8.64	8.85		143.9	141.6
O ₁	1-10000	13.94303556	45.81		45.64	143.9		143.6
M ₁ (-2, -1)	100-1-10	14.48520386		0.26	0.48		172.0	131.3
M ₁ (-2, 0)....	100-100	14.48741027		1.40	2.13		172.0	135.0
M ₁ (-1)	1001-10	14.49448752		0.11	0.10		172.0	1.0
M ₁	100100	14.49669393	3.90		3.53	172.0		174.4
M ₁ (+1)	100110	14.49890034		0.78	0.91		172.0	159.4
P ₁ (-1).....	11-20-10	14.95672495		0.28	0.70		154.9	132.7
P ₁	11-2000	14.95893136	25.24		25.36	154.9		155.0
S ₁	11-1000	15.00000000	1.77		1.94	262.1		235.7
K ₁ (-1)	1100-10	15.03886223		1.65	1.41		157.0	172.1
K ₁	110000	15.04106864	83.06		82.74	157.0		156.9
K ₁ (+1)	110010	15.04327505		11.26	11.38		157.0	155.0
J ₁ (-1)	120-1-10	15.58323693		0.11	0.04		163.6	95.2
J ₁	120-100	15.58544334	3.63		4.04	163.6		189.6
J ₁ (+1)	120-110	15.58764976		0.72	0.99		163.6	174.7
OO ₁	130000	16.13910171	1.98		2.98	170.1		202.0
OO ₁ (+1)	130010	16.14130812		1.27	1.86		170.1	196.3
OO ₁ (+2)....	130020	16.14351454		0.27	0.47		170.1	180.8
2N ₂ (-1)	2-202-10	27.89314838		0.11	0.02		85.9	287.2
2N ₂	2-20200	27.89535479	2.83		2.35	85.9		86.4
μ_2 (-1).....	2-220-10	27.96600199		0.12	0.28		7.0	340.6
μ_2	2-22000	27.96820840	3.20		3.24	7.0		12.1
N ₂ (-1)	2-101-10	28.43752308		0.79	0.74		112.7	108.9
N ₂	2-10100	28.43972949	21.24		21.28	112.7		113.1
v ₂ (-1)	2-12-1-10	28.51037670		0.13	0.07		132.2	29.9
v ₂	2-12-100	28.51258311	3.60		4.38	132.2		127.0
M ₂ (-1)	2000-10	28.98189779		3.99	3.96		139.6	141.0
M ₂	200000	28.98410420	106.95		106.86	139.6		139.3
λ_2 (-1)	21-21-10	29.45341888		0.08	0.24		164.6	182.9
λ_2	21-2100	29.45562529	1.71		2.13	164.6		171.5
L ₂ (-1).....	210-1-10	29.52627250		0.18	0.48		185.6	181.2
L ₂	210-100	29.52847891	4.97		4.76	185.6		180.6
L ₂ (+2, 0)....	210100	29.53776257		1.24	0.27		185.6	196.7
L ₂ (+2, +1)	210110	29.53996898		0.55	0.31		185.6	52.0
T ₂	22-3001	29.95893342	1.52		1.57	158.2		136.9
S ₂	22-2000	30.00000000	25.82		25.79	157.9		157.5
K ₂ (-1)	2200-10	30.07993086		0.09	0.11		155.9	94.4
K ₂	220000	30.08213728	7.22		7.50	155.9		156.4
K ₂ (+1)	220010	30.08434369		2.15	2.42		155.9	158.0
K ₂ (+2)	220020	30.08655010		0.23	0.26		155.9	157.2
M ₄ (-1)	4000-10	57.96600199		0.16	0.13		91.2	99.3
M ₄	400000	57.96820840	2.10		2.14	91.2		98.2
MS ₄ (-1)	42-20-10	58.98189779		0.04	0.04		119.0	186.9
MS ₄	42-2000	58.98410420	1.01		1.11	119.0		121.5
M ₆ (-1)	6000-10	86.95010619		0.10	0.14		326.3	332.5
M ₆	600000	86.95231260	0.91		0.90	326.3		333.5

Table 4.1. 55 tidal constituents from a 19-year harmonic analysis of Seattle water level data, including 30 satellite constituents (indicated by a number in parentheses following the name); see text. (From Zetler, Long, and Ku, 1985.)

the adverse effects of these missing constituents from those constituents that were solved for, are presented in the next sections.

4.2.1 Schureman's Inference and Elimination Technique

4.2.1a Inferring Tidal Constituents Not Solved For

To infer tidal constituents that could not be solved for because the data times series was too short, and to eliminate the effects of these missing constituents on those constituents that were solved for, Schureman (1958, pages 78-87) uses a technique that first makes the assumption that “the amplitudes of the constituents of a similar type at any place, although differing greatly from their theoretical values, have a relation that, in general, agrees fairly closely with the relations of their theoretical coefficients.” This technique also assumes that “the difference in the epochs or lags of the constituents have a relation conforming, in general, with the relation of the differences in their speeds” [i.e., frequencies]. Schureman recognized that the hydrodynamics of a waterway will make the harmonic constants at a tide station quite different than they would be if equilibrium theory was true (i.e., if the Earth was totally covered by one ocean and the tide responded instantaneously to the astronomical tide producing forces; see Section 2.1.2), but for the purpose of his technique he assumed that the relationships between pairs of particular harmonic constants will still be similar to relationships between them if equilibrium theory were true. In reality this is only approximately true, as the hydrodynamics of a waterway can significantly affect the relationships between two tidal constituents, especially in shallow waterways. But to a first approximation this is still useful, and for many areas, especially deep-water open-ocean areas, it can work reasonably well. (As will be seen in the next section, there are ways to further improve this, if one has a long-term station nearby.)

Thus, based on his first assumption above, to infer the amplitude, $H(B)$, of a tidal constituent B, based on another tidal constituent A with amplitude $H(A)$, Schureman uses the formula

$$H(B) = \frac{\text{mean coefficient of } B}{\text{mean coefficient of } A} H(A).$$

The “mean coefficients” in this formula are values calculated by Schureman from astronomical considerations (pages 21-24), which are listed in his Table 2 (pages 164-7). The relative magnitudes of tidal constituents based on equilibrium theory are proportional to the mean constituent coefficients.

Based on the second assumption above, to infer the epoch (i.e., the phase lag), $\kappa(C)$, of a tidal constituent C, whose angular speed c is close to the angular speeds a and b of tidal constituents A and B [whose epochs are $\kappa(A)$ and $\kappa(B)$], Schureman uses the formula

$$\kappa(C) = \kappa(A) + \frac{c-a}{b-a} [\kappa(B) - \kappa(A)].$$

By substituting the mean coefficient values (from Schureman’s Table 2) into the first formula, and the angular speeds into the second formula, Schureman produced the special formulas shown in Figure 4.2.

Schureman’s inference technique is built into the CO-OPS computer program version of Schureman’s Fourier harmonic analysis method, the original version written by Dennis and Long,

4. Harmonic Analysis of Water Level Data

Diurnal constituents

$$\begin{aligned}
 H(J_1) &= 0.079 H(O_1); \quad \kappa(J_1) = \kappa(K_1) + 0.496 [\kappa(K_1) - \kappa(O_1)] \\
 H(M_1) &= 0.071 H(O_1); \quad \kappa(M_1) = \kappa(K_1) - 0.500 [\kappa(K_1) - \kappa(O_1)] \\
 H(OO) &= 0.043 H(O_1); \quad \kappa(OO) = \kappa(K_1) + 1.000 [\kappa(K_1) - \kappa(O_1)] \\
 H(P_1) &= 0.331 H(K_1); \quad \kappa(P_1) = \kappa(K_1) - 0.075 [\kappa(K_1) - \kappa(O_1)] \\
 H(Q_1) &= 0.194 H(O_1); \quad \kappa(Q_1) = \kappa(K_1) - 1.496 [\kappa(K_1) - \kappa(O_1)] \\
 H(2Q) &= 0.026 H(O_1); \quad \kappa(2Q) = \kappa(K_1) - 1.992 [\kappa(K_1) - \kappa(O_1)] \\
 H(\rho_1) &= 0.038 H(O_1); \quad \kappa(\rho_1) = \kappa(K_1) - 1.429 [\kappa(K_1) - \kappa(O_1)]
 \end{aligned}$$

Semidiurnal constituents

$$\begin{aligned}
 H(K_2) &= 0.272 H(S_2); \quad \kappa(K_2) = \kappa(S_2) + 0.081 [\kappa(S_2) - \kappa(M_2)] \\
 H(L_2) &= 0.028 H(M_2); \quad \kappa(L_2) = \kappa(S_2) - 0.464 [\kappa(S_2) - \kappa(M_2)] \\
 &\quad = 0.143 H(N_2); \quad \kappa(N_2) = \kappa(M_2) + 1.000 [\kappa(M_2) - \kappa(N_2)] \\
 H(N_2) &= 0.194 H(M_2); \quad \kappa(N_2) = \kappa(S_2) - 1.536 [\kappa(S_2) - \kappa(M_2)] \\
 H(2N) &= 0.026 H(M_2); \quad \kappa(2N) = \kappa(S_2) - 2.072 [\kappa(S_2) - \kappa(M_2)] \\
 &\quad = 0.133 H(N_2); \quad \kappa(N_2) = \kappa(M_2) - 2.000 [\kappa(M_2) - \kappa(N_2)] \\
 H(R_2) &= 0.008 H(S_2); \quad \kappa(R_2) = \kappa(S_2) + 0.040 [\kappa(S_2) - \kappa(M_2)] \\
 H(T_2) &= 0.059 H(S_2); \quad \kappa(T_2) = \kappa(S_2) - 0.040 [\kappa(S_2) - \kappa(M_2)] \\
 H(\lambda_2) &= 0.007 H(M_2); \quad \kappa(\lambda_2) = \kappa(S_2) - 0.536 [\kappa(S_2) - \kappa(M_2)] \\
 H(\mu_2) &= 0.024 H(M_2); \quad \kappa(\mu_2) = \kappa(S_2) - 2.000 [\kappa(S_2) - \kappa(M_2)] \\
 H(\nu_2) &= 0.038 H(M_2); \quad \kappa(\nu_2) = \kappa(S_2) - 1.464 [\kappa(S_2) - \kappa(M_2)] \\
 &\quad = 0.194 H(N_2); \quad \kappa(N_2) = \kappa(M_2) - 0.866 [\kappa(M_2) - \kappa(N_2)]
 \end{aligned}$$

Figure 4.2. Schureman's formulas for inferring tidal constituents from constituents already calculated. (From Schureman, 1958, page 79, or Dennis and Long, 1971, page 6.)

1971 (the FORTRAN code for the inference technique is shown on pages 18 and 19 of that publication). C&GS Form 452, page 115 in Schureman, 1958, was used in the hand analysis.

Schureman did a test of the reliability of his inference technique using 60 tide stations “representing various types of tide in different parts of the world.” (He does not mention the exact locations of the stations, nor how many stations were on the ocean coast versus inside shallow bays.) He compared actual calculated values of M_1 , P_1 , Q_1 , K_2 , L_2 , and ν_2 (presumably from a one-year harmonic analysis) with the inferred values obtained by using the appropriate formulas from Figure 4.2. He characterized his reliability test results (shown on page 80 of Schureman, 1958) as “fairly good”, but admits that “the inferred constants, especially the epochs, cannot be depended upon for a high degree of refinement.” For P_1 , the most important constituent inferred in a 29-day analysis, he found an average difference of 0.03 feet between the inferred amplitude and the actual amplitude, and an average difference of 8° between the inferred epoch and the actual epoch. The largest difference between inferred and actual amplitudes and epochs for P_1 was 0.27 feet and 49° (one would guess from a station in a shallow bay perhaps, but Schureman does not say). The results for the rest of the test constituents were worse. Without knowing the locations of the 60 stations tested one cannot make total use of these results. Hydrodynamics will change the relationships among tidal constituents, even those close in frequency (speed), the magnitude of that change depending on the particular hydrodynamic situation. As a general rule one would expect the most change in long shallow-water bays, estuaries, or rivers (where the tidal wavelength has been shortened by the shallow water).

4.2.1b *Eliminating the Effects of Missing Constituents on Constituents That Were Solved For*

Schureman's technique for eliminating the effects of *tidal constituents that could not be solved for* on those *tidal constituents that were solved for* is complex enough that the numerous equations will not be repeated here (see pages 80-87 of Schureman, 1958, as well as his Tables 21-26). The FORTRAN code for this technique as implemented by Dennis and Long (1971) can be found within their program on their pages 17, 18, 22, and 28 (which has Schureman's Tables 21-26). [C&GS Form 245 on page 117 in Schureman was used in the hand analysis.] The most important constituents considered are the disturbing effects on K_1 by P_1 and the disturbing effects on S_2 by K_2 and T_2 . This is corrected (as best it can be by this equilibrium/astronomical-based method) by accounting for the phase displacement and amplitude modification of the major constituents K_1 and S_2 by the minor constituents P_1 , K_2 , and T_2 , for which the inferred values obtained by Schureman's technique are used. Since the method must begin with inferred values, a series of successive approximations is used (each time using the newly eliminated values for the disturbing constituents in Schureman's formulas). Thus any degree of refinement could theoretically be achieved, but the first approximation has generally been used, realizing that there are other effects that would probably limit the benefit of continuing.

4.2.2 Use of a Reference Station To Improve the Results of a Short Analysis

Schureman's inference and elimination technique (at least for 15-day analyses) is better than nothing, but its results are not as accurate as one would like for many applications. Schureman's method assumes that equilibrium (i.e., astronomical) relationships among the tidal constituents hold, that is, that the relative strengths and timing of these constituents is the same as in the tide producing forces. Thus, the hydrodynamics of the oceans and connected bays and rivers is ignored.

One can improve on this by making use of the tidal harmonic constants from a nearby long-term water level station, as long as the two stations are close enough to have similar tidal characteristics. In most cases it is more likely that, for example, the N_2/M_2 ratio at the station with the short time series will be closer to the N_2/M_2 ratio at a nearby reference tide station than to the N_2/M_2 ratio in the astronomical tide producing forces.

The use of a nearby reference station is very straight forward. One merely needs a water level data time series at the reference station for the same time period as the station with the short time series. (If the reference tide station was not in operation during that period, one can use a harmonically predicted time series for that period.) Then one harmonically analyzes that short series from the reference station in exactly the same way the short data time series at the subordinate station was analyzed. The results from this short analysis at the reference station are then compared with the equivalent results from the one-year harmonic analysis at the reference station. For example, the one-year M_2 amplitude is divided by the short-analysis M_2 amplitude (both from the reference station), and the resulting ratio is then used to correct the M_2 amplitude from the short analysis at the subordinate station (by multiplying it with the ratio). Likewise, the short-analysis M_2 epoch (phase lag) is subtracted from the one-year M_2 epoch (both from the reference station), and the resulting difference is used to correct the epoch at the subordinate station (by adding the phase difference to it).

Another way to look at this, is that the results of, for example, a 29-day analysis at the subordinate station will be different than the results that could have been obtained from a one-year analysis (if one had had the data). This difference is due to the particular astronomical conditions

4. Harmonic Analysis of Water Level Data

during those particular 29 days. One expects to see a similar difference at a nearby reference stations during those same 29 days, but for this reference stations one does have one-year harmonic analysis results, so one knows what that difference is. Thus one can correct the short subordinate station using this knowledge from the reference station.

This method was used by Parker (1977) to correct the 29-day harmonic analysis results for numerous tides stations along the Strait of Juan de Fuca – Strait of Georgia, in order to construct corange and cophase (cotidal) charts for the most important tidal constituents. Before using this method it was found that the harmonic constants did not change smoothly along this waterway, and it was suspected that the variation in the harmonic analysis results was due to the short records being analyzed at most of the tide stations. Such variation was obvious because the waterway was deep and thus the tide regime changed slowly, with tide stations separated along the coast by one or two degrees of phase (which translates into only 2 to 4 minutes difference in M_2 high waters, and 4 to 8 minutes difference in K_1 high waters). The errors in a 29-day analysis, even one corrected using Schureman's method based on astronomical/equilibrium theory can easily be larger than one or two degrees of phase. And similarly for the amplitudes.

For this waterway there were ten longer-period tide stations for which one-year least squares harmonic analyses were able to be carried out, and 58 stations for which 29-day harmonic analyses had to be used (using Schureman's Fourier method and his inference and elimination technique). Table 4.2 shows the correction factors that were calculated for one particular 29-day period at the ten longer-period stations for the six largest tidal constituents. One sees that the correction factors are different at each station, because of the changing tide regime with location. The largest changes (i.e., ratios most different from 1.000) are found in the diurnal constituents, since for this waterway P_1 (which was inferred in the 29-day Schureman harmonic analysis) is the fourth largest tidal constituent and requires a half year of data to separate it from K_1 .

Each of the 58 tide stations that had been analyzed using Schureman's 29-day analysis was corrected using a pair of correction factors (for amplitude and epoch) from one of the ten long-period stations (listed in Table 4.2), usually the closest geographically to the 29-day station. The method appeared to work quite well. Prior to correction, harmonic constants from nearby 29-day stations that had been operated during different time periods often were quite different. However, once corrected they were closer in value and seemed to fit in much better with the geographic change in values moving up the waterway. Phase corrections as large as 10° were made, with the results fitting in better with surrounding stations. Three of the resulting charts from this process are shown in Figures 2.5, 2.6, and 2.9.

Another way in which to accomplish the same type of correction of the harmonic constants of a short station (secondary station) based on the harmonic constants at a nearby long-term station (reference station), and a method that would make the process a little more automated, would be to incorporate it into Schureman's inference and elimination technique, but to use the relationships among the tidal constituents based on the nearby reference station instead of based on equilibrium/astronomical relationships. This is, in fact, done in the least squares harmonic analysis program by Foreman (2004) based on the method of Godin (1972) (see Section 4.2.4), as well as in a recent version of the harmonic analysis program based on Schureman.

4.2.3 Inference In the Frequency Domain

By plotting the amplitudes of tidal constituents (of the same species) in the frequency domain (and similarly for the epochs of the tidal constituents), one will gain some insights that one might

Sta. No.	Station	M ₂		S ₂		N ₂		K ₁		O ₁		P ₁	
		H _{YR} H ₂₉	(g _{yr} -g ₂₉)	H _{YR} H ₂₉	(g _{yr} -g ₂₉)	H _{YR} H ₂₉	(g _{yr} -g ₂₉)	H _{YR} H ₂₉	(g _{yr} -g ₂₉)	H _{YR} H ₂₉	(g _{yr} -g ₂₉)	H _{YR} H ₂₉	(g _{yr} -g ₂₉)
1	Neah Bay	1.019	0.8	1.005	1.2	.985	-0.5	.833	0.4	1.059	-1.2	.840	-3.5
11	Port Townsend	1.011	-3.9	.967	-4.6	.940	0.0	.917	0.1	1.040	0.5	.866	-2.3
20	Reservation Bay	1.018	-2.0	1.036	-3.0	.964	1.7	.912	1.5	1.037	1.0	.866	-3.8
22	Yokeko Point	1.005	-1.3	.992	-0.9	.998	1.9	.908	1.8	1.028	1.6	.843	-2.2
47	Hanbury Point	.998	-1.9	1.007	-4.6	.928	1.4	.910	0.9	1.023	1.4	.855	-2.8
26	Anacortes	.987	-1.2	.957	-0.1	.965	3.4	.903	2.5	1.031	2.0	.842	-0.3
34	Bellingham	.975	-0.8	1.008	-0.8	1.008	4.8	.894	4.1	1.044	1.0	.833	0.9
39	Cherry Point	.981	1.1	.998	-0.3	1.004	4.7	.907	3.0	1.035	3.1	.866	-0.3
44	North Beach	.979	-5.4	.943	-5.2	.921	-1.9	.905	0.3	1.023	0.2	.852	-3.0
49	Friday Harbor	.974	-4.0	1.098	-1.4	.899	9.0	.922	6.3	1.027	8.6	.867	2.4

$\frac{H_{YR}}{H_{29}}$ = amplitude from year analysis divided by amplitude from 29-day analysis.

$(g_{yr}-g_{29})$ = epoch from year analysis minus epoch from 29-day analysis (in degrees).

Table 4.2. Correction factors for ten different reference stations in the Strait of Juan de Fuca – Strait of Georgia for the 29-day period beginning March 1, 1974, for use in correcting the harmonic constants from other stations with only 29 days of data. (From Parker, 1977.)

initially hope would allow one to infer the amplitude and epoch of missing tidal constituents, i.e., those that could not be analyzed with the available length of data time series. In doing so, one must remember (again) that the variations in tidal constants throughout a waterway are due to hydrodynamics, and barring the use of a hydrodynamic model, one is only looking for statistical ways to essentially guess what those missing constituents will look like.

One would expect that the closer that two tidal constituents are in frequency the less the relationship between those tidal constituents will change as one moves to another geographic location, but it must be remembered that this is only true of the original astronomical tidal constituents. In shallow waterways the nonlinearly produced shallow-water constituents (see Sections 2.3.2 and 7.6.2) will typically grow much faster (and change phase faster) than nearby astronomical constituents, so one must separate astronomical constituents from shallow-water constituents when developing any inference and elimination scheme. The amplification and phase change of all the astronomical constituents in a species (e.g., the semidiurnal band) will depend on the nearness of the waterway to resonance conditions based on the length, depth, and (sometimes) width of the waterway (see Sections 2.3.1 and 7.4.1). The amplification and phase change of all the shallow-water constituents in a species (e.g., the semidiurnal band) will depend on the energy transfer into them from the relevant astronomical constituents via one or more nonlinear mechanisms. (The astronomical constituents will be reduced by this energy transfer, but not as dramatically as the shallow-water constituents will be increased; see, for example, Figure 7.5.)

So the first question is, can one look at the tidal constituents (of similar nature, either astronomical or shallow-water) surrounding a missing constituent and be able to infer a reasonable amplitude and phase lag for that missing constituent. The answer is no. Without a nearby reference

4. Harmonic Analysis of Water Level Data

station to look at, one will have no idea what the relative sizes of those astronomical constituents should be. For example, in many waterways S_2 is larger than N_2 , but in many others (including the East Coast of the U.S.) N_2 is larger than S_2 . This is because even for constituents fairly close in frequency the hydrodynamics of a large waterway (like an ocean) can cause them to be fairly different in certain locations (when tide waves travel long distances, there is plenty of time for two constituents close in frequency to become quite different in amplitude and phase). Likewise shallow-water constituents may grow at roughly the same rate in an estuary, but their energy comes from astronomical constituents with different sizes, so here again one will have no idea what their relative sizes should be (without looking at a nearby reference station).

Godin (1972, in his Figure 2.16, pp 180-1) shows how the relationship between close pairs of constituents varies at 21 Canadian water level stations (from all its coasts). As would be expected, there is a lot of scatter in his diagrams. Some have less scatter than others (e.g., the diagram for P_1K_1 and the one K_2S_2), but these amplitude ratios and phase lags differences still depend on the hydrodynamics of the particular locations chosen for the analysis, and there is no reason to assume particular values for them (except initially the values from equilibrium theory, for lack of anything else) unless one has values from a nearby (reference) station.

Thus, to infer missing constituents one is stuck with needing a nearby reference station (with presumably similar harmonic characteristics). Schureman's "reference station" was actually the tide producing forces themselves via equilibrium theory.

4.2.4 Other methods

Inference and elimination/correction is included in the least squares harmonic analysis program of Foreman (2004) based on the method of Godin (1972). In that program one inputs, for a nearby reference station, the amplitude ratio of the constituent to be inferred to the constituent that is included in the actual harmonic analysis (which is close in frequency), and likewise the differences in phase lags for the two constituents. The program calculates the amplitude and phase lag for the missing constituent, as well as the corrected amplitude and phase lag for the close constituent that was solved for in the analysis (and which had been influenced by the energy from the missing constituent).

The mathematics behind this inference and correction process is given on pages 27-28 of Foreman (2004), but it is useful to summarize it here (although using different notation). It involves two assumptions (one not explicitly stated). First, it assumes that all the energy from the unsolved-for constituent (the one to be inferred) was incorporated in the amplitude and phase lag for the nearby solved-for constituent that came out of the least squares harmonic analysis. Thus, the contribution to the tidal elevation of the uncorrected solved-for constituent (h_1^o) is assumed equal to the contributions of the two constituents after inference and correction have been carried out ($h_1 + h_2$), namely,

$$h_1^o = h_1 + h_2$$

or

$$H_1^o \cos(a_1 t - \kappa_1^o) = H_1 \cos(a_1 t - \kappa_1) + H_2 \cos(a_2 t - \kappa_2) \quad (4.1)$$

where a_1 and a_2 are the angular speeds (frequencies) of the two constituents (the first constituent being the one solved for in the least squares harmonic analysis), H_1^o , H_1 , and H_2 are the amplitudes of the uncorrected solved-for constituent, the corrected solved-for constituent, and the unsolved-for constituent (the one being inferred), and likewise for the phase lags (epochs) κ_1^o , κ_1 , and κ_2 . Here

the node factors and equilibrium arguments have been left out for simplicity. Now let r_{12} be the ratio of the inferred constituent amplitude to the corrected solved-for constituent, i.e.

$$r_{12} = \frac{H_2}{H_1}$$

and let ζ be the difference in the phase lags of these two constituents, i.e.

$$\zeta = \kappa_1 - \kappa_2$$

Then equation (4.1) becomes

$$\begin{aligned} H_1^o \cos(a_1 t - \kappa_1^o) &= H_1 \cos(a_1 t - \kappa_1) + r_{12} H_1 \cos\{(a_1 t - \kappa_1) + (a_2 - a_1)t + \zeta\} \\ &= H_1 \cos(a_1 t - \kappa_1) + r_{12} H_1 \cos(a_1 t - \kappa_1) \cos[(a_2 - a_1)t + \zeta] \\ &\quad - r_{12} H_1 \sin(a_1 t - \kappa_1) \sin[(a_2 - a_1)t + \zeta] \\ H_1^o \cos(a_1 t - \kappa_1^o) &= H_1 \cos(a_1 t - \kappa_1) \{1 + r_{12} \cos[(a_2 - a_1)t + \zeta]\} \\ &\quad - H_1 \sin(a_1 t - \kappa_1) \{r_{12} \sin[(a_2 - a_1)t + \zeta]\} \end{aligned} \quad (4.2)$$

Since the length of the time series was not long enough to separate these two constituents, one knows that the Rayleigh criteria was not met (see Section 3.3) and so the difference in the frequencies was not greater than the frequency resolution of the analysis (i.e., $1/T$, where T is the length of the series). However, a second assumption is now made, that the difference in frequencies is much smaller than $1/T$. This is done to allow one to approximate the values in the {} in equation (4.2), with their average value over the length of the series. After some further substitutions and manipulations (see Foreman, 2004, page 28), one ends up with the amplitude and phase lag for the corrected solved-for constituent as

$$H_1 = \frac{H_1^o}{(C^2 + S^2)^{1/2}} \quad \text{and} \quad \kappa_1 = \kappa_1^o + \frac{\tan^{-1}(S/C)}{2\pi}$$

and the amplitude and phase lag for the inferred constituent as

$$H_2 = r_{12} H_1 \quad \text{and} \quad \kappa_2 = \kappa_1 - \zeta$$

where S and C are the terms that include the average value over the length of the series of the cosine and sine terms in equation (4.2), which are

$$S = \frac{r_{12} \sin[(a_2 - a_1)t]}{(a_2 - a_1)t} \sin \zeta \quad \text{and} \quad C = 1 + \frac{r_{12} \sin[(a_2 - a_1)t]}{(a_2 - a_1)t} \cos \zeta$$

(The equations in Foreman, 2004 used frequency instead of angular speed. The angular speed is in %/hour, where as the frequency in Foreman is in cycles per hour. One can go from angular speed to frequency by dividing by 360° . For example, the angular speed for M_2 is 28.984104, and its frequency is 0.081 cycles per hour, or 1.932 cycles per day.)

Other discussions of methods for inferring tidal constituents from short data time series can be found in Zetler, et al (1965), Dronkers (1964), and Zetler, et al (1985) in the latter case inferring satellite constituents based on the tide potential. The continuous wavelet transform method (see

Section 3.5.5) is also useful for analyzing short data time series, although it does not use tidal constituents (Jay and Flinchem, 1999; Jay and Kukulka, 2003).

4.3 Assessing the Quality of the Predicted Tide Series

4.3.1 Introduction

The typical way to evaluate the quality of the final *set* of harmonic constants (amplitudes and epochs) that result from a harmonic analysis process (including any inference and elimination and node factor application done after the actual least squares analysis) is to produce a *tide prediction* time series with that *set of those harmonic constants* and then evaluate the quality of those tide predictions. The need for a set of harmonic constants has been specifically referred to, because no matter how accurate the constants may be for individual tidal constituents, it is the entire set that is important. It does little good to have very accurate constants for M_2 and K_1 , but not have other constituents, since an accurate tide prediction can only be made if the harmonic constants for all the important constituents are available (so that as much as possible of the tidal energy has been accounted for). (Of course, for particular hydrodynamic research involving perhaps the hydrodynamics of only M_2 , such a limited analysis might be acceptable, but even here most hydrodynamics studies should really include all the important constituents.)

In addition to making tide predictions, one also subtracts these predictions from a simultaneous *observed* water level data time series to create a so-called *residual* time series. This observed water level time series might be the data that were analyzed to produce the set of harmonic constants, or it might be from another time period. If it is the data that were analyzed, then the prediction for that time period is referred as a *self-prediction*. As will be discussed, there are some limitations on using a self-prediction to assess the quality of the set of harmonic constants, versus using predictions for other time periods, but often one has no other data other than that which were analyzed. The residual series will show all the variations in the time domain that are left over once the tide predictions have been removed.

Obviously there will be water level variations in the observed series caused by nontidal phenomena, such as wind, atmospheric pressure, river discharge, and changing salinity and water temperature (steric effects), and which will not be in the predicted tide time series. The residual series will have predominantly those nontidal water level variations (unless one has poor harmonic constants, in which a great deal of tidal variations will show up in the residual series). Because of these nontidal variations (which of course can be very large when there is storm or a heavy river flow event) the tide prediction can be very different than the actual water level data on some days and be very close to the water level data on other days. That is beyond one's control (and if one wishes to do a good job of predicting the actual water level, one needs to use real-time based hydrodynamic forecast models). The most one can do is hope to produce tide predictions which on average match the water level time series as well as possible. However, as will be seen, it will still be valuable to investigate the tide predictions on individual days as well as on the whole. For shallow-water areas there will be times when such nontidal influences will change the tide through nonlinear interaction (although in cases such as with storm surges, these changes will be still be smaller than the nontidal variations that caused them).

No matter what type of evaluation method one uses, the issue of self-prediction versus prediction for time periods other than that used to calculate the harmonic constants will be important. If other data are available besides that which was used for the analysis, it is important to use them in a

thorough quality assessment. This is because one can often produce a high quality self-prediction, even if one has not managed to calculate the optimum set of harmonic constants, because these constants have been best fit to produce the best possible prediction for the analyzed data. Energy from missing constituents (that should have been included in the harmonic analysis) will often still be included in the constituents that were solved for. Those same constituents, however, may not do as good a job predicting for other time periods.

If one does not have any data other than the data that were analyzed, one could in some situations face making a choice between: (1) using all the data for the analysis and getting the maximum number of constituents possible (but having no independent data to check the predictions against); or (2) analyzing some portion of the data and using the other portion to check the predictions (but perhaps having to solve for a smaller number of harmonic constituents). Generally, where possible, one usually will opt for using as much of the data as possible to obtain as many tidal harmonic constituents possible. If, for example, one had close to six months of data, one would certainly want to use all the data and be able to calculate P_1 . But sometimes the length of the available data time series will fall between two of the preferred lengths (e.g., between 6 months and a year), in which case one can choose to use less than all the data (in this case, 6 months) and use the remainder for testing the results. However, even here, when one is using the least squares technique, one might still be able to successfully solve for additional tidal constituents with synodic periods of one year, in which case all the data will again be used.

Even before getting to the point of making predictions with the best set of harmonic constants that came out of the analysis, there is an advantage to having more than one time period with data. In this case, however, one wants to do additional analyses to see if the epochs of the smallest constituents are consistent from analysis to analysis. This consistency would be a sign that these constants really represent those tidal constituents and are not just the amplitudes and phase lags for some transient periodic nontidal phenomena.

Before doing the analysis, one might want to test the harmonic analysis program, to see how well it does on a predicted tide time series generated from known harmonic constants. One would like to see if the harmonic analysis program can reproduce exactly the harmonic constants that were used to make the predicted tide time series, and if not, where energy is lost (or possibly gained). However, a predicted tide time series has no noise, and as was discussed in Section 3.3 with reference to Munk and Hasselman (1964), a low tidal signal-to-noise ratio can adversely effect the calculation of the smaller tidal constituents, especially ones close in frequency to other constituents. So if the harmonic analysis program passed the test with a pure predicted time series, one might repeat the tests with additional noise added each time.

There are a number of ways to evaluate the quality of the tide predictions produced with a set of harmonic constants. Three approaches will be primarily looked at:

- (1) directly compare the high and low waters of the predicted time series with the high and low waters of a simultaneous water level data time series;
- (2) carry out and examine a spectral analysis of the residual time series; and
- (3) examine the residual time series itself for periods with transient tidal oscillations.

4.3.2 Comparison of High and Low Waters In the Predicted Time Series Versus In the Observed Time Series

A frequently used method for assessing the quality of a tide prediction time series is to compare the heights and times of corresponding high waters (and low waters) in the predicted series and the observed water level series. Here it is important to use the same method for calculating high and low waters for both time series (see Section 3.9.1). Usually one looks at the height differences and time differences between each pair of corresponding high waters (and low waters), the mean differences, the standard deviations, and other statistical parameters.

This method is typically used to check the quality of the daily predictions for reference stations in Table 1 of a Tide Table. The water level stations from which the harmonic constants for the predictions were extracted are typically permanent stations, so that data are available every year to evaluate the predictions. Each year some one checks how close the predicted high waters and low waters are to the observed high and low waters. If each year they are getting further apart, then one assumes that something is changing the hydrodynamic situation in the waterway. (And investigations of possible changes to the bathymetry and/or shoreline of the waterway are carried out.) One might keep the same harmonic constants until the differences between the predicted tide series and the observed water level series are larger than some predetermined criteria based on typical applications that use the predicted tide (such as safe navigation of deep-draft ships), but often new harmonic constants will be produced before that point is reached.

It is important to remember that the observed series high waters and low waters includes nontidal contributions, so there will be differences between the predicted high and low waters and the observed high and low waters due to these nontidal contributions. These should mostly average out when one is calculating a mean difference over a long enough time period. However, when averaging over only a year, there can still be asymmetries in seasonal effects on the nontidal water level that will not average out and will show up in the mean time and height differences. This can be seen in Table 8 from the Tide Tables for the *East Coast of North and South America* (shown in Figure 8.4). [Table 8 shows some statistical figures on “tide prediction accuracy” at 32 reference stations in the Tide Table. However, technically, since one is comparing predicted and observed values, one is not really looking at the accuracy of the tide prediction, but how well the tide prediction can represent the actual water level (on average over a year). However, the statistical information in Table 8 is useful for mariners who use tide prediction as the best estimate of actual high and low waters that they will experience with their ships. See Section 9.2.3.]

Thus, in Figure 8.4, one sees larger mean differences between predicted and observed high waters at Philadelphia, which is on the upper Delaware River. This station is influenced by the changes in water level caused by the river flow, which will produce much higher water levels during the strong freshets in the spring. Since the mean differences in Table 8, being based on only one year of data, may primarily represent the nontidal contributions, the astronomical tide itself could, in fact, be totally captured by the harmonically produced tide predictions, and thus could really be 99.99% accurate. If the comparison between predicted and observed high waters for Table 8 had been done over many years, the mean difference values would be smaller, and probably more representative of any missing tidal energy in the tide prediction (and thus a truer indication of the accuracy of the astronomical tide prediction). In Section 3.7.1 and specifically in Figure 3.11 one saw how much the seasonal sea level range can vary from year to year. The year chosen for the statistics in Table 8 could have been a typical year or an unusual year. However, Table 8 is simply an example provided in the Tide Tables. More than one year of high and low waters are typically

used to assess the quality of a tide prediction (and the set harmonic constants on which that prediction is based).

Standard deviations (also presented in Table 8 of the Tide Tables) will always be affected by the nontidal water level variations, no matter how long the time series of differences that is analyzed. The four stations from the northern Gulf of Mexico (Pensacola, Mobile, Grand Isle, and Galveston) shown in Table 8 in Figure 9.4 all have large standard deviations for the time differences between predicted and observed times of high water and low water. At these locations the tide range is small and is often dominated by water level variations caused by wind and pressure effects (i.e., storm surge), which are usually stronger during the fall months.

Even with these nontidally caused differences it is still useful to look at how the individual time and height difference values change throughout each month and from month to month. For example, one might see a periodicity in the height (or time) differences that points to a problem with a specific harmonic constant. Other longer periodicities or patterns in the height (or time) differences might be due to nontidal seasonal effects. For example, both predicted high and low waters might appear consistently too low in the summer because thermal expansion of the upper water layer has raised sea level and thus raised both the high waters and the low waters. Such an effect, though not tidal, might be captured to some degree in the S_a constituent, although its variance from year to year can be considerable, and is another the reason why one cannot really include harmonic constants that represent even quasi-periodic meteorological effects.

4.3.3 Spectral Analysis of the Residual Time Series

A typical way to check the quality of the calculated harmonic constants (i.e., some type of *error estimation*) is to make a tide prediction for the time period of the data analyzed, subtract the predicted time series from the original observed times to produce a *residual time series*, and then to see how much energy is left in the residual time series at the tidal frequencies using a spectral analysis. If there is a significant amount of tidal energy still present (relative to some predetermined criterion), then possibly not enough tidal constituents were included in the harmonic analysis (or possibly constituents with small amplitudes were erroneously rejected). If the number of constituents was limited by the length of the available data time series, then additional constituents probably need to be inferred. However, it is also possible that the tidal energy in the residual series is due to erroneously inferred tidal constituents. Perhaps they were based only on the equilibrium theory relationships, and one needs to use the relationships at a nearby longer-period station.

Although a spectral analysis is quite straight forward, when assessing the spectrum of the residual series one should always remember (as mentioned above) that a self prediction can often look good, even when an important constituent has been left out of the analysis (perhaps due to a short data time series) and the harmonic constants that come out of the analysis are not as accurate as they could be. This is because the constituents solved for are best fit to the data. The energy of constituents not included in the analysis will be incorporated into one or more of the constituents that are solved for, so that a self prediction for the same time period can look reasonable. The key question, however, is whether one can predict accurately for other time periods. When predicting for time periods other than the one analyzed, the way that the energy from the unsolved-for constituents was incorporated into the solved-for constituents will not work for those other time periods, because there will different phase relationships between the unsolved-for constituents and the solved-for constituents for those other time periods.

4.3.4 Examination of the Residual Time Series For Periods With Transient Tidal Oscillations

In addition to doing the spectral analysis, one should also examine the residual time series itself and look for time periods where oscillations with a tidal period appear and then disappear (see Section 4.1.4). When these occur, it will usually be due to the effect of the nonlinear interaction between the tide and some transient nontidal phenomenon, such as a large river discharge or storm surge (or perhaps even the indirect effect of a change in water density that allowed a baroclinic effect to occur, although this effect is much more important for tidal currents). During these periods of interaction, the nontidal phenomenon has temporarily changed the hydrodynamics of the situation and thus temporarily changed the amplitude and/or phase lag of one or more tidal constituents, and so by subtracting the predictions based on the average tidal constituents (from the analysis of the entire time series) one leaves some tidal energy for that particular time period. These various events with temporary tidal energy will not show up in the spectral analysis because they will have different phase relationships and cancel each other out in the overall average values determined by the analysis.

When such incidents occur, one should look at the nontidal influences (such as wind, river discharge, etc.) to try to determine the cause of the temporarily different tidal constituents. If such incidents occur frequently, one may wish to add a footnote in a Tide Table about when such incidents occur. However, some nontidal effects itself (such a storm surge or a river freshet) will usually be larger than its nonlinear influence on the tide, and so the changes to the tide may be of less importance. (If such incidents occur frequently, then water level prediction with a real-time driven water level forecast numerical model may be the best route to take, because it can include not only the nontidal phenomena but also the effects of their nonlinear interaction with the tide. See Chapter 8.)

4.3.5 The Use and Misuse of “Build-up Factors”

In some cases, when one compares the high and low waters from a predicted tide time series with those from an observed water level series, one will find that the high waters from the observed series are on average higher than those from the predicted series and that the low waters from the observed series are on average lower than those from the predicted series. In other words, the predicted tide range (on average) is smaller than the actual measured mean tide range.

When this happens, one solution in the past has been to increase the amplitude of all the harmonic constants (from which the prediction was made) by a percentage that will allow the predicted high and low waters to have the same heights (on average) as the high and low waters in the observed series. This has usually been referred to as the *build-up factor*. It was sometimes reasoned that the harmonic analysis program itself probably lost some energy, and the assumption was made that this energy was probably lost similarly over all tidal bands, so that one could compensate by increasing all the tidal constituent amplitudes by the same percentage.

However, the more likely cause of this missing tidal energy is that certain tidal constituents were probably not included in the analysis, and if they had been included that they would have accounted for the missing energy. The missing constituents may have been left out because the analyzed data series was too short (and not enough of them were inferred). Or, the missing constituents may have been smaller constituents from the analysis that were rejected because their amplitude fell below the criteria of 0.03 foot (about a cm), which was standard procedure at the U.S. C&GS since the time of Schureman [who apparently “in an informal office memorandum, rejected all analyzed amplitudes

less than 0.03 foot" (Zetler, *et al.*, 1985)]. If numerous small constituents were rejected that were in fact perfectly good, that would account for much or most of the missing energy that would later be compensated for with the build-up factor. For stations with enough data, a better criteria for rejection of small constituents is a lack of consistency in the phase lag from year to year. If there is consistency, then the constituent results are probably really tidal and should be used. When using a least squares harmonic analysis program that determines the best order to solve for each additional constituent and that calculates the reduction in variance after each additional constituent, one should be able to ignore a constituent that does not add to the cumulative reduction of variance. However, the opposite may not be true. A small constituent that reduces the variance could be representing transient periodic nontidal energy. Again, if possible, one needs constituent results from the analysis of at least one other time period.

Trying to compensate for missing tidal constituents by increasing the amplitudes of the other tidal constituents will in fact lead to errors. Although the mean of the predicted high waters will now match the mean of the observed high waters, some of the predicted high waters will end up being too large and some will end up being too small (and likewise for low waters), because the phases relationships involving the missing tidal constituents are different than the phase relationships of the included (and built-up) tidal constituents.

The solution for a reference station or other permanent water level station (since one has plenty of data) is to carry out a harmonic analysis on a longer time series and to include more tidal harmonic constants. For a water level station with a limited time series length, the solution is more difficult, and for many applications the predictions made using "built-up" harmonic constants may be okay. If more accuracy is wanted, one can try inferring additional tidal constituents (see Section 4.2), and then re-evaluating the predicted and observed high and low waters.

4.3.6 Looking For Changes in Bathymetry or Shoreline

Although more important for tidal current predictions, changes in the depth of a waterway can affect the tide, especially if the waterway is small and the change in volume of water in the waterway during a tidal cycle is a significant portion of the total volume of water in the waterway. Such changes in depth over time at a location may be rapid due to a hurricane or extratropical storm, relatively fast due to a dredging project in a navigation channel, or fairly slow due to year-to-year erosion and movement of sediment in the waterway.

When a dredging project to deepen a navigation channel in a small waterway has been completed, one will know from the project report (and any follow-up hydrographic surveys) how much the depths have changed. Tide stations will have been installed during and after the project, so one will also be able to determine whether there has been a significant change in tide range has occurred. If significant changes have occurred, new harmonic constants should be calculated from a new (preferably at least year-long) data record taken after the dredging is complete. Similarly, when the shoreline is changed significantly by filling in water areas to create land, or to create artificial island, that may also change the tide in a small waterway.

When a hurricane or large storm has hit a small waterway, one should harmonically analyze post-storm water level data and compare it to analyses of pre-storm water level data, to look for possible changes in the tide which might warrant calculating new harmonic constants and new tide predictions. The effect of slower changes (due to year-to-year erosion and sediment transport in a small waterway) might not be seen unless one compares water level records and harmonic constants separated by several years. In all these cases, the smaller the waterway the more likely that changes

4. Harmonic Analysis of Water Level Data

in depth will have an effect on the tide (whereas for tidal currents, even local changes in depth in a large waterway will affect the tidal currents).

4.4. Producing a Reference Station for Table 1 of a Tide Table

Very accurate tidal harmonic constants are required for a reference station that appears in Table 1 of the Tide Tables, since accurate tide predictions using those harmonic constants will be made for many years in the future, and many subordinate stations in Table 2 will be referenced to that station. The water level data time series for such a station must be long (at least a year) in order to be able to use as many tidal constituents as possible in the harmonic analysis. Since most tide reference stations in Table 1 coincide with one of the permanently installed water level stations operated by CO-OPS, there will usually be many decades of data available. However, the most recent should be used especially in small waterways in case there have been bathymetric changes which may have affected the tide regime. A long data time series not only allows one to calculate as many tidal harmonic constituents as are needed to produce an accurate prediction (with the limit on tidal constituents determined mainly by whether the smaller tidal spectral lines are sufficiently above the nontidal continuum), but it also allows one to accurately determine the effects of the 18.6-year lunar nodal cycle. In fact, if one wanted to, one could abandon the use of node factors and simply add dozens of additional satellite constituents when carrying out the harmonic analysis and subsequent tide predictions. However, the tendency has been to stay with the node factor approach for reasons given in Section 4.1.5.

Typically the standard 37 constituents (listed in Table 3.2) have been used in CO-OPS (and its predecessor organizations) unless the station is located in a shallow waterway with a large tide range, in which case additional shallow-water tidal constituents are used (see Tables A.2). For example, 114 tidal constituents were used for the reference station at Anchorage, Alaska. The 77 additional constituents were shallow-water constituents that were needed because of the 30-ft tide range and the very shallow-water conditions at the upper end of Cook Inlet (there is even a tidal bore that occurs at Turnagain Arm near Anchorage). However, when creating a new reference station, or updating an old reference station, one should not feel it necessary to stick with the standard 37 constituents (even for waterways that are not as extreme as upper Cook Inlet). One should use the methods mentioned in Section 4.3 for assessing the quality of the predicted tide series to decide whether more constituents are needed (and whether a longer time series needs to be analyzed). One should use as many tidal constituents as can be obtained from the available time series (plus inferred constituents, if necessary) in order to accurately capture as much of the tidal energy as possible, and to avoid the temptation to use a build-up factor (see Section 4.3.5). Constituents that come out of a harmonic analysis with amplitudes less than some standard cutoff criterion for acceptance (e.g., 0.03 feet) should not be rejected if they contributed to the cumulative reduction in variance (usually calculated after each step by the least squares program). One should do analyses on different time periods to see if the amplitude and epoch (phase lag) for these small constituents are similar from year to year. Such consistency is a better acceptance criterion than using an arbitrary cutoff criterion, or even looking for a reduction in variance during the analysis.

4.5 Summary Overview: Steps In Harmonically Analyzing Water Level Data

In this section we will summarize the steps in harmonically analyzing a water level data time series. Here we will assume we are using a least squares harmonic analysis program. In many cases more than one harmonic analysis will need to be carried out on the data, with adjustments being made after each analysis if needed (such as adding additional constituents after assessing how much tidal energy is left in a residual series). Some steps may not be necessary for every analysis. Sections where more information can be found are in brackets [] at the end of each step.

These steps, in bullet form are:

- (1) *when first using a harmonic analysis program* it may be a good idea to *test the program on a predicted tide time series* based on known harmonic constants, to see if the program can reproduce exactly the harmonic constants that were used to make the predicted tide time series, and if not, to try to determine where energy is lost (or possibly gained). [Section 4.3.1]
- (2) *determine how much accuracy one needs* in the harmonic constants (and in predictions to be made with those constants) for your particular application; that will affect how many of the steps below one will choose to use;
- (3) *assess the data available at the water level station*; if more than one time series is available, use the longest most recent data; (especially for small shallow waterways) *check the records for dramatic changes in bathymetry* (e.g., due to storms or to dredging); if such changes have occurred, select data (if possible) from after those changes occurred. [Section 4.3.6]
- (4) *determine if there are gaps in the water level data time series*; still use all the data but make sure to select the option in the least squares program that handles gaps (or random time data) since some least square programs distinguish these two cases from a continuous data record (because for the latter, a different numerical scheme is typically used to analyze the data more quickly). [Section 3.4.5]
- (5) *determine which astronomical tidal constituents will be included* in the program, initially based on the length of the water level time series; use Table 3.2 or Tables A.2 or to make this determination, selecting all the constituents with synodic periods less than or almost equal to the length of the data time series; in subsequent runs of the program more constituents may be added, especially if the length of the data time series is fairly close to the next highest synodic period. [Section 4.1.1]
- (6) *determine whether additional shallow-water tidal constituents should be included* in the analysis; this will be obvious for a very shallow waterway with a large tide range, but one may first have to use the standard 37 constituents and see how much energy is left in the higher harmonic tidal bands of a spectrum; for an extreme case, the highest order overtide that can be solved for will depend on the sampling rate of the water level time series, but hourly data is sufficient for almost all locations. [Section 4.1.1]
- (7) *determine how much of the data time series to use* in the harmonic analysis; in Step (5) the longest synodic period within the length of the available data time series was selected, but one may have more data than that (but less than the next highest synodic period); run the first analysis using a segment of the time series whose length is the selected synodic period; if there is enough extra data, it will be useful to run one analysis from the beginning of the time series, and one that includes the end of the time series (and look for consistency in the harmonic constants for each, especially in the smallest constituents); if the length of the available data series is more than half way to the next synodic period, the follow-up

4. Harmonic Analysis of Water Level Data

analyses can use all the available data and include additional harmonic constituents that theoretically require the next highest synodic period; if one has many years of data, one will initially do several one-year analyses, and then decide based on how much tidal energy is left in the residual series (and whether the smaller constituents are consistent from year to year), whether to analyze a two-year or longer time series. [Section 4.1.1]

- (8) *decide whether to use a particular shallow-water compound tidal constituent or the astronomical constituent with the same frequency* (e.g., $2MN_2$ or L_2); for deep-water stations the astronomical constituent is fine, but for shallow-water stations (especially inside bays and rivers) one will probably need to use the shallow-water constituent; if one is unsure, one will have to look at the harmonic analysis results of several stations in the bay and see if the rate of growth moving up the bay is greater than the rate of growth of an astronomical constituent in the same tidal band (e.g., see if $2MN_2$ grows at a faster rate than M_2); for constituent pairs whose node factors are the same (e.g., $2MS_2$ and μ_2) it does not matter which is selected; for pairs with different node factors, if one initially chose the astronomical constituent, but later decides it should have been the shallow-water constituent, one does not have to re-analyze, for one can merely correct for the different node factor and equilibrium argument. [Section 4.1.1]
- (9) check the data file for notes about instrument errors, datum shifts, or other potential problems with the data; if such problems are noted, keep in mind the possible effects of the five types of errors on the harmonic constants; [Section 4.1.3]
- (10) *tidally filter the water level time series to look for strong nontidal events* (like spring river runoff, or storm surge) that may nonlinearly affect the tidal analysis results; if one needs harmonic constants from which predictions can be made for most of the year, one should consider leaving out strong nontidal event periods and using the gap option of the least squares program; if one has a short time series of water level data that includes a major nontidal event, one will probably not be able to use the harmonic constants that come out of the analysis for tide prediction; [Section 4.1.4]
- (11) carry out the least squares harmonic analysis; use all the constituents that contributed to the cumulative reduction in variance, even if their amplitudes are very small (e.g., lower than some standard lower cutoff criterion such as 0.03 feet); if additional data are available, run additional harmonic analyses to see if these smaller constituents are consistent from year to year; inconsistent epochs are grounds for rejecting a constituent; [Section 4.3.5]
- (12) with the harmonic constants from the first harmonic analysis, *make a tide prediction for the same period as the data*, and subtract this predicted time series from the original observed time series to *produce a residual time series*; if one has data for another time period besides the one analyzed, make tide predictions and produce a residual time series for that other time period; this other residual time series will provide more meaningful results in steps (13) and (14) because it does not represent a self-prediction. [Section 4.3.1]
- (13) carry out a *spectral analysis on the residual time series* to see if there is any remaining tidal energy still in the record; also carry out a *spectral analysis on the original observed time series* for comparison purposes. [Section 4.3.3]
- (14) *examine a plot of the residual time series* looking for places where a transient tidal signal may appear; compare to the results of Step (10); investigate the wind, river, or other potential nontidal influences for those time periods; one may have to consider leaving strong nontidal event time periods out of the analysis and rerunning the least squares harmonic analysis using the gap option; if one has a short time series of water level data that includes

- a major nontidal event, one will probably not be able to use the harmonic constants that come out of the analysis for tide prediction. [Section 4.3.4]
- (15) if there still is tidal energy in the residual time series try to *determine what additional tidal constituents might be added to the next harmonic analysis*; most easy to spot will be energy in higher species bands due to shallow-water effects; decide which additional shallow-water constituents are most likely to be important [Table 3.2 or Table A.2]; *for energy left in the semidiurnal or diurnal bands* there may be compound tidal constituents (due to shallow-water effects) that should be added to the next analysis; [Table 3.2 or Table A.2]
- (16) *obtain values for additional constituents*; if one does not have enough data to move to the next synodic period, one can then either:
- use an inference (and elimination) technique* to calculate the amplitudes and epochs for the missing constituents, using a nearby reference station if possible; [Section 4.2]
 - try rerunning the harmonic analysis with these constituents included* using the full length of the available time series, to see if the least squares technique can successfully determine them;
- if one originally carried out a one-year analysis, and has more available data, *consider running a longer analysis* so as to include additional tidal constituents.
- (17) when one has decided that they have the optimum set of harmonic constants for a particular water level station, run a final prediction for a year of data (or for the full length of data, if less than a year) and calculate all the high and low waters; compare the predicted high and low waters with the high and low waters calculated from the data time series, determining all the usual statistics; (if possible, use the same max/min routine for both predicted and data series); if the mean high waters from the data are higher than the mean predicted high waters (and likewise if the mean low waters from the data are lower than the predicted low waters), consider going back to Step (15);
- (18) *for producing predictions for reference stations in the Tide Tables*, use a *build-up factor* on the final harmonic constants only as a last resort, and only if the average predicted high and low waters differ so significantly from the observed mean high and low waters that they would make a noticeable difference to the mariner. [Section 4.3.5]

5 Harmonic Analysis of Current Data

5.1 Special Problems With Current Data

The special aspects of tidal currents were described and explained in Section 2.3.6 (that section should be read before reading this section). Those special aspects are now looked at again with an eye toward the difficulties they might present when harmonically analyzing current data. Many of these problems have led some oceanographers to be very pessimistic about how well one can represent the tidal current using harmonic analysis or other techniques. Here we believe that most of these problems can be overcome if treated carefully, assuming we have good quality data of sufficient length. In some cases, as will be discussed below and in Chapter 8, the use of numerical hydrodynamic models can do a better job than harmonic prediction methods (although, if not properly used, e.g., if too coarse a resolution is used, models will provide less accurate results).

As mentioned in Sections 2.3.6 and 3.4.3, the primary difference between a time series of current data and a time series of water level data is that water level is a simple one-dimensional scalar quantity and the current is a two-dimensional vector quantity (that also varies along a third dimension, i.e. depth). One can directly analyze the time series of water level heights, but to analyze the time series of current speeds and directions one must first convert each speed and direction pair into two orthogonal components, such as north and east components. Often major and minor components are chosen, the major axis usually being the direction of maximum flood with the minor axis 90° clockwise from the major axis. Thus, to harmonically analyze current data one must harmonically analyze two data times series instead of one. This in itself is not a problem; it simply adds little extra work, and it requires some additional knowledge with regards to interpreting the analysis results. The pairs of harmonic constants that come out of a harmonic analysis of current data can be combined into *tidal current constituent ellipses* (which are derived and explained in Section 5.2), which show how the flow from each tidal constituent rotates around the compass during a constituent cycle.

With regard to actual problems with current data, they will be discussed in roughly the same order as they were presented in Section 2.3.6. This discussion will include the possible effect of these problems on the accuracy of the analysis and prediction of the tidal current, and how to avoid or mitigate such problems.

Current data time series have typically been much shorter than water level times series because of the difficulty and expense of maintaining current meters in the open water, as compared with maintaining a water level gauge on a pier or other land-based platform. Current meters also have tended to have a worse fouling problem due to biological growth or debris clogging the sensor (especially when propellers or rotors were used). However, with newer technology this is much less of a problem today, and even if the time series are short, there are ways to get useful information out of the data. So this is now not usually a critical problem.

Current data have also tended to be noisier (in some cases much noisier) than water level data, and that noise could adversely affect the harmonic analysis results especially in locations where the tidal signal is not that strong. The degree of this problem has depended on the type of current meter used, and how much averaging was done to acquire each measurement. Mechanical current meters that used an S-shaped savonius rotor to measure the speed and a separate (generally quite small) vane to measure the direction usually had the worst noise problems, especially when hung from a surface buoy when there were significant surface waves. There was less of an instrument-caused noise problem when using a propeller and a larger vane, and still less when using two propellers at right angles (to measure two orthogonal components directly, instead of speed and direction). There was even less of a noise problem with electromagnetic *in situ* sensors, which also measured two orthogonal components. Likewise, acoustic doppler and high frequency remote sensors have much less noise problems, since there is vectorial averaging over time intervals and over volumes of water. Thus, instrument-caused noise is less of a problem today. There is still natural noise due to meteorological effects, and this is generally more significant for currents than for water levels, but most effects of this noise are eliminated by tidal analysis because of its emphasis on energy at particular frequencies and the inherent averaging. Those effects that can be significant will be talked more about below.

More serious is the spatial variation in tidal currents, which is much more rapid than for the tide. Tidal currents can vary rapidly both vertically and horizontally. Tidal currents vary with depth due to the effects of (especially) bottom friction, surface friction (from the wind), and baroclinic (density) effects, the latter often due to internal tide waves. The most dramatic changes in tidal currents in the horizontal direction are typically in going from deep channels (with faster currents) to shallow water next to the channels (with slower currents). (See examples in Section 2.3.6).

In some cases this spatial variation in the tidal current can be so rapid that the particular placement of a current sensor can make a significant difference in the analysis results. If there is an unintended change in the position of the current sensor during the period of measurement (e.g., it was moved by a storm or by a strong current) and one analyzes the entire record, then one is really combining the results for essentially two different locations. In such cases, one should break the current time series up into two pieces and analyze them separately. If the current sensor slowly changes position through the measurement period (due to strong currents), that is a serious problem, and all one can do is analyze different portions of the record and try to assess whether there is enough similarity (or an obvious trend) so that the results are usable. Another serious problem is when a current sensor is hung from a surface buoy with a long anchor line, and the buoy and sensor swings around to different locations during flood and during ebb. This can be especially bad if the buoy was anchored near the edge of a navigation channel and the buoy and sensor move into shallow water during either the flood or ebb phase.

The solution to many of these problems is proper planning and good field work. One should try to install a current station where one expects less horizontal variation in the tidal current field, such as in the center of a channel, (rather than at the edge) or in the middle of a straight channel (rather than in a channel bend). Although information is still certainly needed at the edge of a channel and in a channel bend, it may be better to use a high-resolution hydrodynamic numerical model to produce those tidal current predictions, and to use a towed ADCP and/or HF radar to obtain observations of such horizontal variation. Most important, one needs to make sure that the current station is not moved during the observation period. If such movement does occur, perhaps due to a storm or due to being dragged by strong currents, then one may need to break up the current time series into one or more pieces to be analyzed separately.

5. Harmonic Analysis of Current Data

Dealing with the change in tidal currents with depth requires a different approach. The effects on tidal currents of internal tide waves or other baroclinic effects are not easy to handle because such effects are generally intermittent. In areas where there is believed to be some stratification, or even a lateral variation in salinity or water temperature, one should take vertical CTD (salinity and temperature) profiles during the current measurement period to be able to assess the changing density fields. In rivers and estuaries one can choose not to harmonically analyze current measurements made during heavy river runoff periods. Offshore, internal tide waves move along density fields due to vertical temperature gradients (of which the thermocline is the most dramatic), but these are more likely to happen during warmer months and when the upper layer is warmer and there is little wind to mix the water column. Data obtained during periods with less baroclinic effects will provide reasonable tidal current predictions for most of the year. For dealing with those periods with baroclinic effects one might consider trying the continuous wavelet transform analysis method (Section 3.5.5), but any results can probably only be included in a Tidal Current Table as a footnote for the particular current station.

Even without baroclinic/density effects, the tidal current speed and times of maximum flow will change with depth due to bottom friction effects, as well as effects near the surface due to wind. And so, one would hope that an *in situ* current sensor could be kept at the same depth throughout the measurement period (or similarly, the bins of an ADCP should be kept consistent). However, this may be more difficult than one would think, if there is a reasonable tide range. In shallow water there can be a difference in the currents measured by a bottom-mounted sensor compared with the currents measured by a sensor attached to a surface float, because the rise and fall of the tide changes the distance from the surface-float-hung sensor to the bottom. The bottom-mounted sensor will be measuring currents at different depths relative to the surface, whereas the sensor hanging from a surface float will be measuring currents at different distances relative to the bottom. Throughout a tidal cycle an HF radar system always measures currents at the surface. In most cases, however, one would expect the differences due to such depth changes to be relatively unimportant for most applications. However, with a bottom-mounted ADCP, one can see how the entire velocity profile changes over a tidal cycle and thus get some idea of the depth dependencies.

Tidal currents are generally much more susceptible to the distortion by nonlinear shallow-water effects. They are also affected by nonlinear lateral inertial effects (see Section 2.3.6e) that do not affect the tide at all. For example, Figure 2.35 provided an example of dramatically changing $(K_1 + O_1)/M_2$ and M_4/M_2 ratios in the tidal currents across a waterway, but there was no such variation in the tide. This is not really a problem, as long as one is aware of this, and makes sure to look for the results of this distortion when analyzing current data. Thus one would expect to see stronger over tides (i.e., higher M_4/M_2 , M_6/M_2 , M_8/M_2 ratios, etc) and stronger compound tides. As already mentioned, a particular compound constituent can have the same frequency as an astronomical constituent but be much larger (e.g., $2MN_2$ is often larger than L_2). These two constituents may have different node factors and equilibrium arguments, and so give different predictions for years other than the one from which the analysis came. ($2MN_2$ and L_2 have different node factors, while $2MS_2$ and μ_2 have the same node factor.) There may also be those very rare occurrences such as seen in Ramshorn Creek (see Figure 2.36) where the shallow-water effect is so strong (in this case enhanced by the superposition of two tide waves crossing) that the tidal current becomes a true quarter-diurnal tidal current. Without recognizing the hydrodynamic cause of this (admittedly rare) occurrence, and upon seeing the tidal current change directions four times a day instead of two, one might think that there was a clock problem with the current sensor.

There is also the special situation which occurs when a current sensor is placed at a channel bend, or any other location where the direction of maximum flood is not exactly 180° from the direction of maximum ebb. When current data from a sensor in such a location are harmonically analyzed, one will see an apparent mean current and artificially higher M_4 values that are not caused by the shallow water (nor even by an inertial effect if the channel is narrow), but are simply due to the geometry of the situation. Figure 5.1 shows such a situation. When analyzing the current data from this location, one would probably select the major axis along neither the flood direction nor the ebb direction, but at some compromise position (in this case in the north direction, with the minor axis pointing eastward). One can see that as the major-axis component goes through one complete cycle, that the minor-axis component will actually go through two complete cycles (the minor axis component will always flow toward the east, but will go through two oscillations for the one oscillation of the major axis). The harmonic analysis would show an M_4 and other apparent overtones. The analysis would also calculate a mean current toward the east, which, of course, *cannot* be interpreted as a real mean current upon which the tidal current was superimposed (as one could interpret a tidal current superimposed on a river current). Again, this should not present a problem, since predictions based on the orthogonal pairs of harmonic constants should reproduce the tidal current accurately, but one must understand what is behind it.

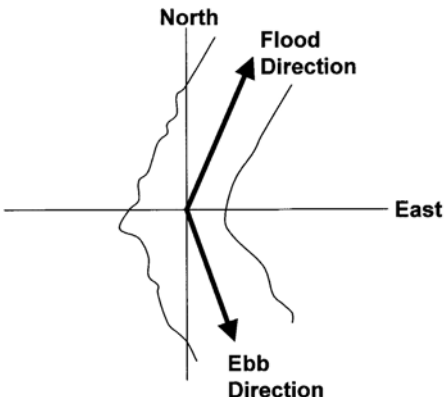


Figure 5.1. A current station deployed at a bend in the waterway, so that the flood direction and the ebb direction are not 180° apart. Because of this geometry a harmonic analysis will show a mean current toward the east and a significant value for M_4 .

5.2 Tidal Current Harmonic Constituent Ellipses

One way to recombine the results of analyzing the two orthogonal component time series is the use of harmonic *constituent ellipses*. The result of the harmonic analysis of a time series of current data is two sets of harmonic constants, one for each of the two orthogonal axes that were chosen when the original speed and direction data time series were turned into two component time series. If the two orthogonal components chosen were major-minor components, and the major axis was chosen to be the direction of maximum flood, then by looking at these harmonic constants one can get some understanding of the harmonic makeup of the tidal current in the up-channel-down-channel direction (i.e., the primary flood and ebb flow), as well as the harmonic makeup in the cross-channel direction. If the two orthogonal components chosen were north-east components (as has often been

5. Harmonic Analysis of Current Data

done by default) and these do not line up with the predominant major-minor axes of flow, then interpretation of the harmonic constants is limited until they are recombined.

To see how the speed and direction of flow due to a particular tidal constituent changes each hour, and to watch it rotate around the compass over a tidal constituent cycle, one needs to combine the two component harmonic constants for that constituent. The result will be an elliptical representation of the flow due to that tidal constituent. The width of the ellipse will vary considerably with location, from very narrow in a narrow waterway to very wide (and thus circular) in the open ocean, with every possible situation in between.

To derive the formula for a tidal constituent ellipse from a pair of harmonic constants for two orthogonal components, the derivation of Doodson and Warburg (1941, pp 180-1) is followed fairly closely, but instead of restricting it to north and east components, the formula is derived for any pair of orthogonal components, since often harmonic analyses are done using major-minor components. However, to keep it as close as possible to Doodson and Warburg, the formula for north-east components is derived first and then modified later for any orthogonal pair. This looks like a messy derivation but it simply involves the use of angle-sum and angle-difference formulas from a standard trigonometry text. The notation of Doodson and Warburg is used as much as possible, but it has been modified slightly for clarity, and here directions are clockwise from north (instead of counterclockwise from east) so that they match up with the standard compass directions.

Figure 3.4 shows a current vector, $W(t)$, and its north and east components, $W_N(t)$ and $W_E(t)$, which are functions of time (that figure also shows a pair of major-minor components, which will correspond to the directions of the axes of the ellipse). The time variation in the north and east components is expressed in the normal fashion, similar to the harmonic prediction equation (3.1) in Section 3.4.2 (but with the h replaced by an N or E , and without the node factor and equilibrium argument, and using Doodson and Warburg's notation for frequency, n), as

$$\begin{aligned} N(t) &= W_N \cos(nt - \kappa_N) & \text{and } E(t) &= W_E \cos(nt - \kappa_E) \\ &= W_N \cos nt \cos \kappa_N + W_N \sin nt \sin \kappa_N & &= W_E \cos nt \cos \kappa_E + W_E \sin nt \sin \kappa_E \\ &= A_2 \cos nt + B_2 \sin nt & &= A_1 \cos nt + B_1 \sin nt \end{aligned}$$

where the second line of each formula has been expanded out from the first (with an angle-difference formula), and the third line has been simplified by using constants A_1 , A_2 , B_1 , and B_2 for the known quantities made up of the component harmonic constants and defined by:

$$A_1 = W_E \cos \kappa_E ; \quad B_1 = W_E \sin \kappa_E ; \quad A_2 = W_N \cos \kappa_N ; \quad B_2 = W_N \sin \kappa_N$$

The square of the current speed at any moment in time can then be given by

$$\begin{aligned} W^2 &= (A_1 \cos nt + B_1 \sin nt)^2 + (A_2 \cos nt + B_2 \sin nt)^2 \\ &= C \cos^2 nt + D \sin^2 nt + 2E \sin nt \cos nt \end{aligned}$$

where

$$C = A_1^2 + A_2^2 \quad D = B_1^2 + B_2^2 \quad E = A_1 B_1 + A_2 B_2 .$$

Letting $F = \frac{1}{2}(C-D)$ and $G = \frac{1}{2}(C+D)$, which equivalently is $C=F+G$ and $D=G-F$, then (using double angle formulas) the equation for W^2 can be written as

$$W^2 = F \cos 2nt + E \sin 2nt + G .$$

This can be further simplified to

$$W^2 = G + H \cos 2(nt - a)$$

where

$$H = \frac{F}{\cos 2a} = \frac{E}{\sin 2a} \quad \text{and} \quad H^2 = E^2 + F^2 \quad \text{and} \quad a = \frac{1}{2} \tan^{-1} \frac{E}{F} .$$

and a is the phase of the maximum constituent current. This occurs when $nt = a$ or when $nt = a + 180^\circ$, in which case

$$W_{\text{major}} = (G + H)^{\frac{1}{2}}$$

This happens twice in a constituent cycle, when the constituent current vector is pointing toward either end of the major axis of the constituent ellipse. The minimum constituent current occurs when $nt = a + 90^\circ$ or $a - 90^\circ$, in which case

$$W_{\text{minor}} = (G - H)^{\frac{1}{2}}$$

This also happens twice in a constituent cycle, when the constituent current vector is pointing toward either end of the minor axis of the constituent ellipse.

This can be described with a drawn constituent ellipse, with the major axis of length twice W_{major} and the minor axis length of twice W_{minor} . The major axis direction (clockwise from north) is

$$\theta_{\text{major}} = \tan^{-1} \left(\frac{A_2 \sin a + B_2 \cos a}{A_1 \sin a + B_1 \cos a} \right) .$$

Likewise the direction of the minor axis (clockwise from north) is

$$\theta_{\text{minor}} = \tan^{-1} \left(\frac{-A_2 \sin a + B_2 \cos a}{-A_1 \sin a + B_1 \cos a} \right) .$$

If $\theta_{\text{minor}} = \theta_{\text{major}} + 90^\circ$, then the rotation of the ellipse is *clockwise*,
 $\theta_{\text{minor}} = \theta_{\text{major}} - 90^\circ$, then the rotation of the ellipse is *councclockwise*.

The phase lag for W_{major} is

$$\kappa_{\text{major}} = \tan^{-1} \frac{E}{F} .$$

The phase lag for W_{minor} is

and $\kappa_{\text{minor}} = \kappa_{\text{major}} + 90^\circ$, when the rotation is clockwise
 $\kappa_{\text{minor}} = \kappa_{\text{major}} - 90^\circ$, when the rotation is counterclockwise.

The *eccentricity* of each ellipse is a measure of how narrow or wide the ellipse is (see Figure 5.2).

It is defined as

$$e = \frac{(W_{\text{major}}^2 - W_{\text{minor}}^2)^{\frac{1}{2}}}{W_{\text{major}}} .$$

Eccentricity will go from 0.0 for a circle (where the major and minor axes are equal, and the current is pure rotary) to 1.0 for a very narrow ellipse (essentially a reversing current)

5. Harmonic Analysis of Current Data

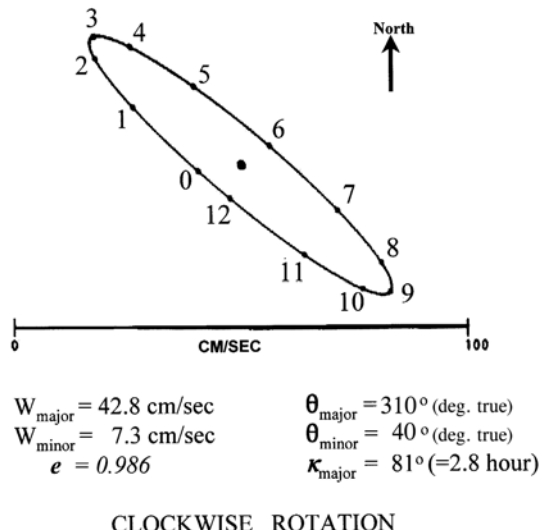


Figure 5.2. A fairly narrow tidal constituent ellipse (i.e., with an eccentricity approaching 1.0). See text for explanation of parameters.

These results based on north-east components, called $N(t)$ and $E(t)$, will now be generalized for any pair of orthogonal components, such as (user-selected) major-minor components, called $MJ(t)$ and $MN(t)$. From Figure 5.3, which shows the geometry and trigonometry for converting between north-east components and major-minor components, the north component in terms of the major and minor components (where θ is the major axis direction clockwise from north) is:

$$\begin{aligned}
 N(t) &= MJ(t) \cos\theta - MN(t) \sin\theta \\
 &= W_{MJ} \cos(nt - \kappa_{MJ}) \cos\theta - W_{MN} \cos(nt - \kappa_{MN}) \sin\theta \\
 &= W_{MJ} \cos nt \cos \kappa_{MJ} \cos\theta + W_{MJ} \sin nt \sin \kappa_{MJ} \cos\theta \\
 &\quad - W_{MN} \cos nt \cos \kappa_{MN} \sin\theta - W_{MN} \sin nt \sin \kappa_{MN} \sin\theta \\
 &= (W_{MJ} \cos \kappa_{MJ} \cos\theta - W_{MN} \cos \kappa_{MN} \sin\theta) \cos nt \\
 &\quad + (W_{MJ} \sin \kappa_{MJ} \cos\theta - W_{MN} \sin \kappa_{MN} \sin\theta) \sin nt \\
 &= A_2 \cos nt + B_2 \sin nt
 \end{aligned}$$

where

$$\begin{aligned}
 A_2 &= W_{MJ} \cos \kappa_{MJ} \cos\theta - W_{MN} \cos \kappa_{MN} \sin\theta \\
 B_2 &= W_{MJ} \sin \kappa_{MJ} \cos\theta - W_{MN} \sin \kappa_{MN} \sin\theta
 \end{aligned}$$

And likewise the east component in terms of the major and minor components is:

$$\begin{aligned}
 E(t) &= MJ(t) \sin\theta + MN(t) \cos\theta \\
 &= W_{MJ} \cos(nt - \kappa_{MJ}) \sin\theta + W_{MN} \cos(nt - \kappa_{MN}) \cos\theta \\
 &= W_{MJ} \cos nt \cos \kappa_{MJ} \sin\theta + W_{MJ} \sin nt \sin \kappa_{MJ} \sin\theta \\
 &\quad + W_{MN} \cos nt \cos \kappa_{MN} \cos\theta + W_{MN} \sin nt \sin \kappa_{MN} \cos\theta \\
 &= (W_{MJ} \cos \kappa_{MJ} \sin\theta + W_{MN} \cos \kappa_{MN} \cos\theta) \cos nt \\
 &\quad + (W_{MJ} \sin \kappa_{MJ} \sin\theta + W_{MN} \sin \kappa_{MN} \cos\theta) \sin nt \\
 &= A_1 \cos nt + B_1 \sin nt
 \end{aligned}$$

where

$$\begin{aligned} A_1 &= W_{MJ} \cos \kappa_{MJ} \sin \theta + W_{MN} \cos \kappa_{MN} \cos \theta \\ B_1 &= W_{MJ} \sin \kappa_{MJ} \sin \theta + W_{MN} \sin \kappa_{MN} \cos \theta. \end{aligned}$$

The same derivation as previously used applies, but now these new values for A_1 , B_1 , A_2 , B_2 are used.

Sometimes it is convenient to be able to convert harmonic constants that were calculated using north-east components directly into harmonic constants for major-minor components, which is a form in which they can be more easily interpreted even without looking at ellipses. There might be cases where the tidal signal in the cross-bay direction (the minor axis) is small enough that one might be worried about extracting accurate harmonic constants for this component. Since there usually is a very strong tidal signal in the flood-ebb direction (the major axis), it might be advantageous to purposely run the analysis with north-east components in order to have a strong tidal signal in both components. Then once the harmonic constants for the north-east components are calculated, they are then converted to major-minor components.

From Figure 5.3 one can start with the formulas

$$MJ(t) = N(t) \cos \theta + E(t) \sin \theta \quad \text{and} \quad MN(t) = E(t) \cos \theta - N(t) \sin \theta ,$$

which will be manipulated (in a manner similar to above) to obtain the formulas for the epoch and amplitude for the major axis component in terms of the epochs and amplitudes of the north and east components, and similarly for the minor axis component. Only a couple of steps are

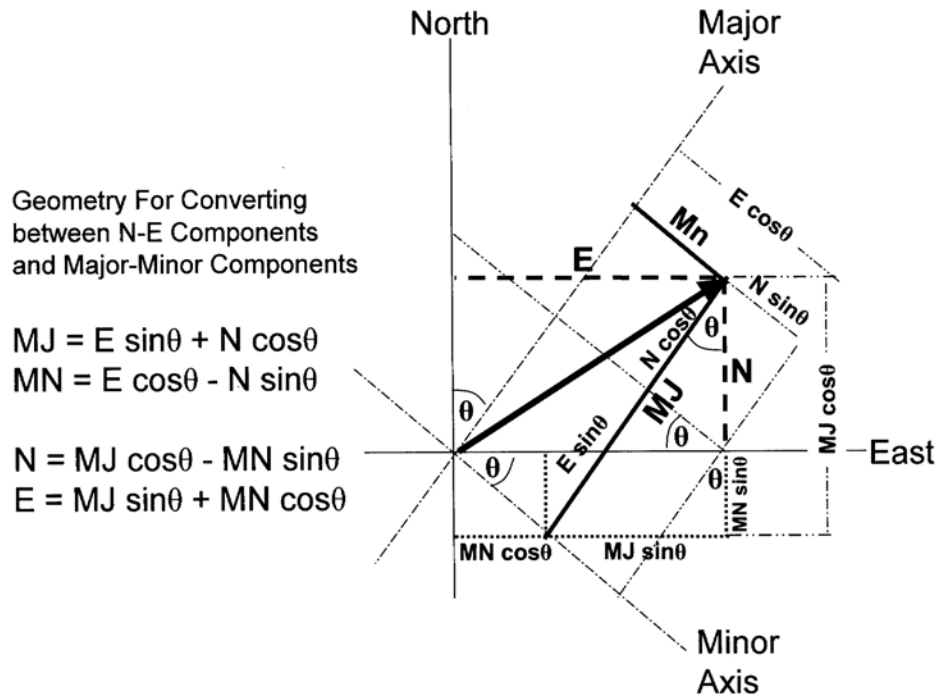


Figure 5.3. The geometry and trigonometry for converting between north-east components and major-minor components.

5. Harmonic Analysis of Current Data

given in finding the major axis epoch and amplitude.

$$\begin{aligned}
 MJ(t) &= N(t) \cos\theta + E(t) \sin\theta \\
 W_{MJ} \cos(nt - \kappa_{MJ}) &= W_N \cos(nt - \kappa_N) \cos\theta + W_E \cos(nt - \kappa_E) \sin\theta \\
 W_{MJ} (\cos nt \cos \kappa_{MJ} + \sin nt \sin \kappa_{MJ}) &= W_N (\cos nt \cos \kappa_N + \sin nt \sin \kappa_N) \cos\theta \\
 &\quad + W_E (\cos nt \cos \kappa_E + \sin nt \sin \kappa_E) \sin\theta \\
 W_{MJ} \cos \kappa_{MJ} \cos nt + W_{MJ} \sin \kappa_{MJ} \sin nt &= (W_N \cos \kappa_N \cos\theta + W_E \cos \kappa_E \sin\theta) \cos nt \\
 &\quad + (W_N \sin \kappa_N \cos\theta + W_E \sin \kappa_E \sin\theta) \sin nt
 \end{aligned}$$

then

$$\begin{aligned}
 W_{MJ} \cos \kappa_{MJ} &= W_N \cos \kappa_N \cos\theta + W_E \cos \kappa_E \sin\theta \\
 W_{MJ} \sin \kappa_{MJ} &= W_N \sin \kappa_N \cos\theta + W_E \sin \kappa_E \sin\theta
 \end{aligned}$$

and dividing the first equation by the second to get $\tan \kappa_{MJ}$ on the left side, the major axis epoch then is

$$\kappa_{MJ} = \tan^{-1} \frac{W_E \sin \kappa_E \sin\theta + W_N \sin \kappa_N \cos\theta}{W_E \cos \kappa_E \sin\theta + W_N \cos \kappa_N \cos\theta}$$

Then the major axis amplitude is

$$W_{MJ} = \frac{W_E \cos \kappa_E \sin\theta + W_N \cos \kappa_N \cos\theta}{\cos \kappa_{MJ}}$$

using the value just obtained for κ_{MJ} .

Similarly for the minor axis component one obtains

$$\kappa_{MN} = \tan^{-1} \frac{W_E \sin \kappa_E \cos\theta - W_N \sin \kappa_N \sin\theta}{W_E \cos \kappa_E \cos\theta - W_N \cos \kappa_N \sin\theta}$$

and

$$W_{MN} = \frac{W_E \cos \kappa_E \cos\theta - W_N \cos \kappa_N \sin\theta}{\cos \kappa_{MN}} .$$

Figure 5.4 shows an example of the constituent ellipses for M_2 , S_2 , N_2 , K_1 , and O_1 for a current station in the Strait of Georgia. One will notice that the eccentricities (and widths) of the constituent ellipses are different. This may be the result of the effect of the nonlinear lateral inertial terms (see Sections 2.3.6 and 7.4.2) being different for the different frequencies. Even more dramatic differences in ellipse width are seen in Figure 7.3 (which shows additional M_2 ellipses at the eastern end of the Strait of Juan de Fuca, Haro and Rosario Straits, and the southern end of the Strait of Georgia). The differences in ellipse widths from location to location are also due to basic continuity effects; for example, the ellipse in a narrow entrance will be faster and narrower than the ellipse in a more open water area.

One will also notice that the major axis directions for these five ellipses are not exactly the same. This is at first somewhat surprising since one would expect that the bathymetry and shorelines would steer all components of the tidal current in the same direction. One might begin looking for some frequency-dependent tidal hydrodynamic effect that could cause the ellipse directions to vary, but it is more likely to be a product of the harmonic analysis itself, where for the smaller constituents the smaller of the two orthogonal components may be more affected by noise, resulting in a value that might shift the direction of its ellipse.

Tidal Analysis and Prediction

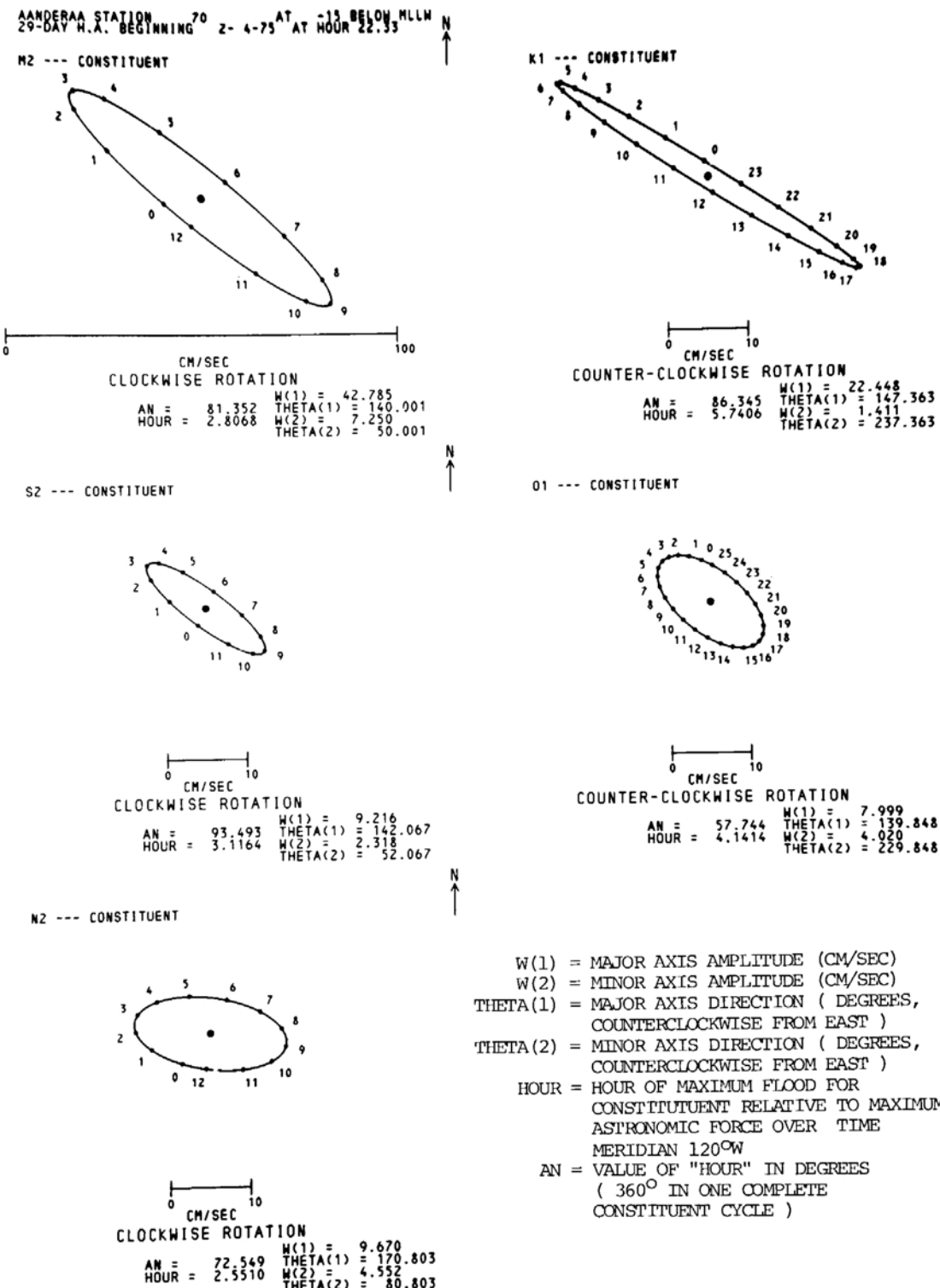


Figure 5.4. Tidal constituent ellipses for M_2 , S_2 , N_2 , K_1 , and O_1 , for current station 70 (at 15 feet below the surface) in the Strait of Georgia, based on a 29-day harmonic analysis of a data time series beginning February 4, 1973. (From Parker, 1977.)

As was mentioned in Section 3.4.3, one can also treat the two orthogonal components together using complex algebra (Pawlowicz, et al, 2002). In this case there is one prediction equation instead of two, since the current vector is represented by the complex number $\mathbf{u} + i\mathbf{v}$ (where \mathbf{u} and \mathbf{v} are the orthogonal components of the tidal current, but the complex algebra allows them to be treated together). The complex prediction equation (for N tidal constituents) looks like

$$\mathbf{x}(t) = \mathbf{x}_0 + \sum_{k=1 \text{ to } N} a_k e^{i\sigma_k t} + a_{-k} e^{-i\sigma_k t}$$

where here $\mathbf{x}(t)$ has been used to indicate velocity, and σ_k to indicate the frequency of each constituent, a_k and a_{-k} to represent the complex amplitudes (a_k and a_{-k} are complex conjugates if the time series is real). The length of the semimajor axis of the ellipse is $|a_k| + |a_{-k}|$ and the length of the semiminor axis is $|a_k| - |a_{-k}|$. (See Pawlowicz, et al, 2002, for more details.)

5.3 Considerations In Carrying Out the Analysis

5.3.1 Which Tidal Current Constituents Should Be Solved For

Almost all the considerations in harmonically analyzing water level data discussed in Section 4.1.1 apply to harmonically analyzing current data. Thus, one should read Section 4.1.1 before proceeding, and should use either Table 3.2 or Table A.2 to determine which tidal constituents to solve for based on the length of the available data time series. Since current data time series are generally shorter than water level time series (there being typically only a few current stations with a year of data or longer), the decisions one will usually be making with regard to current data are whether one can include key constituents like N_2 or P_1 in the analysis, and if not, what will be the best method to infer them.

Since in shallow-water areas, current data are more likely to have larger compound tides and over tides than water level data, extra shallow-water tidal constituents may be needed (some of which can be solved for with the lengths of data time series available, and some of which cannot). However, current data are often noisier than water level data, so these additional tidal constituents will have to be clearly above the nontidal (noise) continuum to be accurately calculated. If one has enough data available to do more than one analysis (perhaps the current station was occupied at two different times, but both records were short) then consistency between the two calculations of the amplitude and epoch for a small constituent will be important in deciding whether the result is accurate. As mentioned before, some of the compound shallow-water constituents will have the same frequency as an astronomically caused tidal constituents. For example, in a shallow waterway there is a very good chance that $2MN_2$ in the tidal current will be a good deal larger than L_2 , and thus $2MN_2$ should be used in the harmonic analysis rather than L_2 .

5.3.2 Selection of Orthogonal Axes

One can choose any pair of orthogonal axes for the analysis, to convert the speed and direction time series into two component time series. Often north-east components have been chosen, really for no particular reason. More often major-minor components are chosen, with the direction of the major axis being the mean direction of maximum flood (which often coincides or is very close to the direction of maximum M_2 flood). Accurate tidal current predictions can be made using any choice of orthogonal components system (north-east works as well as major-minor), but for

interpreting the results one usually feels more comfortable with major-minor. And there may be times when one may only wish to use the major axis component, because either the tidal current is a reversing current, or it is rotary but there is so little energy in the minor component that one may decide to leave out for convenience.

The harmonic analysis itself calculates the mean direction of maximum flood, and the directions of all the tidal constituent flood directions. It also produces ellipses for all the tidal current constituents that came out of the harmonic analysis (by combining the harmonic constants for the two components). Unless one knows ahead of time what the mean direction of maximum flood is, one may end up running the harmonic analysis a second time, using the mean maximum flood direction that came out of the first harmonic analysis as the major axis. However, one does not really need to run the harmonic analysis a second time, if one includes some trigonometric formulas at the end of the harmonic analysis program, which will automatically convert all the harmonic constant pairs (for the orthogonal components used in the analysis) into equivalent pairs for a major-minor orthogonal system using the calculated mean maximum flood direction as the major axis. Formulas for conversion from north-east components to major-minor components were given at the end of Section 5.2.

Sometimes one does wish to include a relatively small minor component when making the prediction, but one may be worried about the quality of the harmonic constants extracted by the harmonic analysis from the minor component time series because the signal-to-noise can be quite low (whereas in the major axis there is very high signal-to-noise). In such cases one could select orthogonal axes so that the strong tidal signal is evenly split between the two components, and then use formulas like those at the end of Section 5.2 to convert them into the preferred major-minor components.

5.3.3 Types of Instrument Errors Possible and Their Effects On Analysis Results

As was mentioned in Section 4.1.3, when data points said to be “bad” or “unreal”, one is essentially talking about instrument error, i.e., values that do not represent the actual current speed and direction at a particular location at the time of measurement because of some error related to the measurement process itself. In Section 5.1 some types of current sensors were mentioned along with the problems they could present (and this will be discussed more below), which included adding instrument noise to the data record. There is also natural noise in a current data record due to various nontidal phenomena (especially wind waves), but being natural they are real and are not considered errors (but one may have to filter out that noise prior to our analysis).

There are many methods for evaluating the quality of a data time series and for editing out data points that are determined to be “bad” or “unreal”, and we will not discuss any particular methods here. Usually one tries to find and then remove (or “correct”) data points that are obvious outliers, which is fairly simple when there is a clear tidal signal in the data, but can be more difficult if the current data is noisy. One also tries to discover other types of variations in the data that may not be of natural origin, and thus must have come from the instrument, which might affect the analysis results.

It is important to acquire some feeling for the potential sources of errors and how different types of errors might affect the results of a harmonic analysis. The errors in a current data time series may be due to electronic, mechanical, or many other causes. It may be helpful to first read Section 4.1.3 for the general discussion on types of errors in water level gauges and the possible effects they can have on the results of a water level harmonic analysis. The five error types

5. Harmonic Analysis of Current Data

discussed in that section are repeated here. The various types of current measurement devices will be looked at, along with the types of errors they can produce. With an eye toward their effect on analysis results, these five types of error are:

- (Type 1) *random errors* [which will tend to average out during a harmonic analysis];
- (Type 2) *sudden shifts*, when from some point in time forward, the entire time series of measured currents are all larger or smaller (or in a different direction) by some constant amount than they were before that point in time, which would change the amplitudes of harmonic constants as well as the measured mean flow (this is a different effect than a sudden shift in tide gauges);
- (Type 3) *slowly changing errors*, where an error might slowly grow over months or longer [which would change the harmonic constants];
- (Type 4) *slowly changing time measurement*, such as when a clock may be running slow [which would essentially spread out time and reduce the frequencies of the tidal constituents, so that when a harmonic analysis looks for energy at the correct tidal frequencies the result will be smaller amplitudes and changed phase lags]; or
- (Type 5) *periodic errors*, which might, for example, be due to meteorological effects on the instrument (as opposed to meteorological effects on the water level itself) [which might change particular tidal constituents].

First, it should be mentioned that many of the methods below for measuring currents involved making those measurements from an anchored boat, or from an anchored buoy, which would swing around when the tidal current changed from flood to ebb or from ebb to flood. Since, as was seen in Section 2.3.6, current speeds and directions can vary significantly over geographic distance (due to changing bathymetry, among other reasons), the measurements made during the flood phase were likely made at a location some distance (depending on the anchor line length) from the location of the measurements during the ebb phase. Thus error Type 5 was quite prevalent. In some cases two or three anchor lines were used to try to minimize the movement of the boat or buoy.

The earliest method for measuring currents used by the Coast and Geodetic Survey on a regular basis was the *current pole* and *log line*. (See *Manual of Current Observations*, U.S. C&GS, 1950, for more details on the current pole and some other early instruments mentioned below.) This was a truly manual method to measure currents, which involved putting a 15-foot-long current pole (weighted at one end to keep it vertical, with the top about a foot above the water's surface) in the water behind an anchored boat with an attached graduated log line that was pulled out as the current moved the pole away from the boat. Using a stop watch to measure how much of the line was pulled out over a specific interval of time, the speed of the current was calculated. A compass or some other device such as a sextant or pelorus was used to measure the direction that the pole moved. [This method of measuring currents is said to go back to the 16th century, when the log line was knotted at regular intervals so that the sailor could easily tell how much line was let out in a set amount of time by counting how many knots passed through his hands, thus leading to the term "knots" as a unit of speed (which came to mean one nautical mile per hour). On the early Coast Survey log lines, the unit graduations were marked by pieces of cotton string in which knots were tied, the number of knots in any string indicating the speed of the current expressed in "knots".]

This method using a current pole and log line did not really measure the current at one specific location in space, since the current pole moved some distance in space during the measurement period. It was really a measurement of the average speed over the distance that the pole traveled, over a depth comparable to the length of the pole, over the time period of the measurement. Since the current speed and direction can vary significantly over space (both with depth and with

geographic distance), the current pole often moved through regions with different current speeds. Using the current pole it was hard enough to accumulate a current data time series long enough for a harmonic analysis, but it was even more difficult to have each data point represent the current for different times over the exact same location. An error analysis of the results of a harmonic analysis of current data measured with a current pole was almost not worth the effort (and all the types of error were possible, most of it human error in a situation that had a low chance of repeatability).

The next improvement in current measurement was to hang over the side of an anchored boat an instrument that could measure the current speed at one location, lowering it to a specific depth. The first of these used regularly by the Coast and Geodetic Survey was the *Price Current Meter*, which had a wheel made of conical shaped cups angled horizontally around the wheel in such a way that the water flow would make the wheel spin. The current speed was calculated by counting the number of rotations of the wheel that occurred during a specific time period. Originally the counting of rotations was done manually by an observer on the deck of the ship with headphones connected electronically to the instrument. A later version was connected to an automatic recording device. Direction was not measured, but was estimated by the observer on the boat. Another current meter used by C&GS that was lowered over the side of a boat and could measure direction as well as speed at one location was the *Ekman current meter*. The Ekman current meter had a screw propeller to measure speed, and a compass-ball receptacle to measure direction, by catching small bronze balls in one or more of 36 ten-degree receptacles around a compass. Although a big improvement over the current pole, this was still a manually intensive way to measure currents, with many chances for human error or human inconsistency.

The next advance in current measurement at C&GS was the Roberts Radio Current Meter, which measured speed and direction, was fully automated, and could be hung from an unmanned buoy. A rotating impeller measured the current speed. A large vane pointed the current meter into the direction of flow, with a magnetic compass device that determined what that direction was relative to magnetic north. The current meter was connected electronically to a radio transmitter on the buoy which sent the data to a nearby receiving station where time was assigned to the data with a chronometer and where a chronograph tape was produced with the times and the data. That tape had to be converted manually into a tabulation of pairs of current speeds and directions.

With later more modern versions of current meters (such as the *Geodyne photographic current meter*, the *TICUS current meter*, the *Plessy Current meter*, and the *Aandera Current meter*), current meter systems became more automated, with various data storage devices (e.g., photographic film and magnetic tape) to save the data internally for a month or longer (depending on the sampling rate). In some cases the method of measurement could cause serious errors in the data, especially when there was significant wave action during the deployment. The Geodyne and TICUS current meters measured current speed with a small S-shaped savonious rotor (which could feel water flow from all directions and so could easily be turned by wave action) and current direction with a small vane (which was easily flipped around, again by wave action). This had a great effect on the harmonic make up of the measured tidal currents, and could often totally mask slack waters in a tidal current. Vector averaging current meters overcame this problem, and deploying these *in situ* current meters from a submerged tautline buoy helped keep the current meters out of the surface wave zone. Current measurement based on remote sensing is now the preferred method, with the two most used systems being the acoustic Doppler profiling current meter (for measuring currents along a depth profile at a specific location, or a horizontal profile at one depth from a pier) and the high frequency radar system (for measuring surface currents over a large area).

5. Harmonic Analysis of Current Data

The following discussion mentions how the five types of errors might be caused by the various current measurement systems. Random errors (Type 1) can be caused by all current sensors. Such errors were probably more frequent and/or larger for the early manual current measurement techniques (such as the current pole and some of the earliest current meters). As long as those errors are random, they tend to be averaged out in a harmonic analysis, but if the human errors become in any way consistent, they could add some type of bias to the measurements, which then would affect the harmonic constants from the analysis.

Sudden shifts or changes in the data (Type 2) were probably most prevalent with mechanical current meters due to the rotor or propeller being clogged by debris in the water. If the clogging totally stopped the rotor or propeller from turning, the current speeds would suddenly go to zero. This was actually preferable to a partial clogging that caused slower speeds to be registered, because the zero-speed data would be recognized and not used, but the slower speeds (especially if it still showed a tidal cycle) might not be noticed, and the data would be used. In the latter case, the amplitudes of all the harmonic constants would be reduced. Such (relatively) sudden changes are still possible with newer instruments, for example, if a great deal of sand suddenly was moved on top of a bottom-mounted acoustic doppler current profiler (ADCP). However, for bottom-mounted ADCPs and for moored *in situ* current sensors, the most common cause of a sudden change in the data is when the instrument is suddenly moved by strong currents during a storm (or perhaps inadvertently by a fishing boat), since the current can change dramatically over horizontal distances.

Slowly changing errors (Type 3) for all current measurement systems (except land-based remote systems) are usually caused by biological fouling, namely, the slow growth of an organism on the sensor in a way that slowly changes the current measurements, usually slowly reducing the measured speeds. For the early current meters fouling would slowly inhibit rotors and propellers or even the movement of the smaller vanes. Such changes would affect all the calculated harmonic constants, mainly reducing their amplitudes. If the change was slow enough (and did not last long enough to bring the current meter to a halt), it might go completely unnoticed, and if noticed might even be assumed to be due to the changing hydrodynamics rather than fouling. Luckily, fouling is less of a problem with modern non-mechanical current sensors.

Slowly changing time measurement (Type 4) was a prevalent problem with the early internal recording current meters. In fact, all such current meters were assumed to have clock drift, and methods were developed to determine how much the clock drifted during a current meter deployment. The usual way was to carefully write down the exact time the current meter was turned on and the exact time the current meter went below the water surface, and likewise the times when the current meter first left the water and when it was turned off. These points in time could be spotted in the current data record (recognizing the water entry and exit was helped considerably if the current meter also had a temperature sensor), and then one could determine how many data points should have been recorded versus how many actually were recorded. One had to assume that the clock drift was constant throughout the data record, but one could then adjust the sampling interval accordingly. Of course, there was always the possibility that individual data points were for some reason not measured or not recorded when they should have been (due to electrical problems). To recognize those occurrences, the instrument makers began adding mechanisms to either mark the hours (since sampling was usually several data points per hour) or to record the time itself for each data point. All this was necessary because effects on the automated time keeping could adversely affect the harmonic constants from an analysis. A slow clock would lead to data samples being taken at time intervals slightly longer than the intended sampling interval. If this was not recognized and corrected (and the time was erroneously assigned to the data points as though

the clock were correct), then the tidal energy in this data time series (with erroneously assigned times) would appear at slightly higher frequencies than the tidal frequencies. (For a fast clock, the opposite would happen.) Analyzing such data for the frequencies where one expects to find tidal energy could then lead to erroneous harmonic constants (depending on how slow or fast the clock was).

There are a number of ways that periodic errors (Type 5) can be caused in various current measurement systems. This includes the previously mentioned current sensors hung from an anchored surface buoy (or boat) that are swung around by the change in current direction from flood to ebb and back to flood. Since current speeds can change dramatically over horizontal distance, especially when the depths are different, being moved horizontally by the currents will put the current sensor in different current regimes. This can be most dramatic when the sensor is in a deep channel (with faster currents) during one phase of the tide, but is over the shallows (with slower current) during the other phase of the tide. This is a periodic effect that will have the most effect on the harmonic constants of the dominant constituent (usually M_2) and other constituents in the semidiurnal band. The inherent asymmetry of this effect could increase the amplitude of M_4 . Since the current regimes over the various depths (that the current meter will pass over as the buoy swings around) may not change smoothly, there are likely to be other effects on the higher harmonic constituents as well. Such changes would be difficult to determine in the data. To avoid this problem methods were often used to try to limit the movement of anchored buoys, such as by using two or three anchor lines.

Another periodic effect influencing sensors hung from both buoys and bottom-mounted tautline moorings, is the effect of the drag on the mooring line (or the line from the surface buoy) due to the currents. The drag of the currents on a tautline mooring will pull the current sensor deeper as the current speeds increase, and thus the measured current speeds will actually be for different depths, which likely will be different than if the sensor had not been pulled deeper, since current speeds often change with depth (due to frictional effects, as well as possibly baroclinic effects; see Section 2.3.6, as well as Figure 7.27). For current sensors hung from surface buoys, the drag on the line due to the currents will pull them shallower. In either case, the effect is periodic, the current sensor moving deeper (for the tautline mooring) or shallower (for the surface buoy) as one approaches maximum flood and again as one approaches maximum ebb. This will again have the greatest effect on the harmonic constants of the dominant constituent (usually M_2) and other constituents in the semidiurnal band. The inherent symmetry of this effect could also affect M_6 . Other higher order constituents might also be affected. Such effects are difficult to determine in a current record, so methods were tried to limit the drag on the line by currents (such as using Kevlar lines to reduce drag).

5.3.4 Assessing the Potential Effects of Nontidal Influences

As was seen in Section 2.3.3, in shallow-water areas both the tide and tidal current can be modified by the nonlinear interaction of nontidal phenomena such as river discharge and storm surge. See Section 4.1.4 for a discussion of the specific effects on the tide; similar effects can occur on the tidal current. In addition, however, as seen in Section 2.3.6 there are effects on the tidal current that one will not see in the tide. There is also periodic nontidal energy in the currents that can occur at or near tidal frequencies, which can affect the results of harmonic analysis. Changing water density due to changing salinity in estuaries or to changing water temperature offshore can allow internal tide waves and other baroclinic effects, which primarily affect tidal currents.

5. Harmonic Analysis of Current Data

When one is harmonically analyzing a current data time series one must therefore be aware of the potential effects of nontidal phenomena on the harmonic constants that come out of the analysis. If one needs harmonic constants from which accurate predictions can be made for most of the year, then one might consider leaving out sections of the time series that include strong nontidal events and using the gap option of the least squares harmonic analysis program. If one has a short time series of current data that includes a major nontidal event, one will probably not be able to use the harmonic constants that come out of the analysis for tide predictions for “normal” time periods, i.e., for time periods without those strong nontidal phenomena. In fact, one can probably not even use those harmonic constants for the time period that included the nontidal event, because the effect of the nontidal event (which probably only lasted a couple of days) was spread out over the length of the analysis. So even the results of a 15-day harmonic analysis will not be useful. In such cases, one can try using the continuous wavelet transform method (see Section 3.5.5).

To discover those periods in an observed current data time series when a nontidal phenomenon may have a strong influence, one can first tidally filter (see Section 3.9) the current data time series. Although the filtering process may reduce the amplitude of such an effect, one should still see periods when the nontidal currents are increased and then decreased. These may be sections of the time series that one will ultimately decide to leave out of the harmonic analysis, but initially one should analyze the entire time series, produce a predicted time series for the entire period of the observations, and then subtract the predicted series from the observed series to produce a residual series. When examining the data, predicted, and residual time series, one will probably have to look at plots of orthogonal components, as well as plots of speed and direction. At those same time periods where one saw changes in nontidal currents in the filtered time series, one is likely to see tidal oscillations appear and then disappear. One might see transient tidal oscillations at time periods without an obvious change in nontidal currents in the filtered time series (which would imply the effects of either changing water density or of changing water level, the latter easily checked in a water level time series from a nearby location).

When these transient tidal current oscillations occur, it will often be due to the effect of the nonlinear interaction between the tide or tidal current with a transient nontidal phenomenon, such as a large river discharge or storm surge. During these periods of interaction, the nontidal phenomenon has temporarily changed the hydrodynamics of the situation and thus changed the amplitude and/or phase lag of one or more tidal current constituents. Thus, by subtracting the predictions based on the average tidal current constituents (obtained from the analysis of the entire time series) one leaves some tidal energy for that particular time period. The transient tidal current oscillation seen at time periods without an obvious change in nontidal currents (in the filtered time series) may be due to the nonlinear effects of a change in water density. Also low-frequency changes in nontidal water level are not accompanied by large changes in nontidal currents, but can have significant effects on both the tide and tidal current. (See Section 4.1.4 and 4.3.4.)

When one sees nontidal events in the filtered time series and/or transient tidal oscillations in the residual times series (or in the residual time series from a nearby water level station), one should look at wind, river, salinity or water temperature data records for the potential nontidal influences that may have caused the temporarily different tidal current constituents. If such incidents occur fairly frequently, one may wish to add a footnote in the Tidal Current Table about when such incidents occur. For such incidents current prediction with a real-time driven forecast numerical circulation model may be the best route to take, because it can include not only the nontidal phenomena but also the effects of their nonlinear interaction with the tide and tidal current.

There can also be nontidal phenomena with (temporary) periodic behavior at frequencies near tidal frequencies. A land breeze-sea breeze (see Section 2.3.6) changes its wind speed and direction over a 24-hour period, and this can produce a wind driven current with the same periodicity. In a tidal current harmonic analysis, this energy will show up in the S_1 constituent, but because the changes are asymmetric there can also be additional energy put into S_2 and maybe even S_4 . To notice this effect on S_1 , one would need a year-long time series to separate this meteorological S_1 from K_1 . Since in many locations the land breeze-sea breeze usually only occurs in the summer, the S_1 value would be very different in the summer than in the winter (and one might see a noticeable change in S_2 as well). One should remember this effect when one is analyzing current data obtained during the summer, because it may have a noticeable effect on the K_1 value that comes out of a harmonic analysis.

For current measurements made at latitudes near 30°N or 30°S , one may have to also consider the possibility of *inertial currents* (see Section 2.3.6) affecting the measurement of diurnal tidal currents. Inertial currents are nontidal but still periodic. At latitude 30°N inertial currents will have their energy at exactly the K_1 tidal frequency, and at 27.6°N the inertial energy will be at exactly the frequency of O_1 . Although generally transient and usually lasting only a few days, inertial currents can last long enough to affect a tidal current analysis. Inertial currents with frequencies in the semidiurnal band will occur near 75°N or 75°S .

There can also be a strong seasonal effect on nontidal currents. For example, stratification during the summer allows internal tide waves to occur which can greatly affect the tidal currents, but such internal waves will not occur during the winter months because of the mixing of the upper water column due to the higher winds from more frequent storms. Also, the sea-breeze-land-breeze effects just mentioned occur most often in the summer, and so one might see some effect on the S_a and S_{sa} constituents.

5.3.5 Whether to Include the Calculated Mean Current In a Tidal Current Prediction

There is one other aspect of nontidal effects in a current series that one must deal with, but from a different perspective. The harmonic analysis will also calculate a mean current for the current time series that was analyzed. That value is the mean current for *only* that particular time period. That particular mean current could have been caused by one or more different possible phenomena, for example, by the winds or river flow. It could be the gravitational current resulting from the salinity gradient going up an estuary. Or it could be a tidally induced residual current produced by the nonlinear lateral inertial terms in the momentum equation, usually due to a bend in the waterway or a point of land sticking out into the waterway, which creates residual eddies due to a sheltering effect (see Sections 2.3.6 and 7.6.7).

All of these mean currents, with the exception of the tidally induced mean current, are transient and the exact value that comes out of the harmonic analysis is probably only good for the particular time period of the analyzed data. Because of this, in most cases the mean current that comes out of the harmonic analysis should not be included in tidal current predictions for future time periods, or for use in Tidal Current Tables. There are two exceptions.

The first exception is if one can determine in some way that the mean current is likely to be permanent because it was tidally induced. A look at the geography around the location of the current station will give one the first clue. If, for example, the current station is in the center of a long narrow waterway, it is highly unlikely that the lateral inertial mechanism could have come into play. On the other hand, one might have a situation like in Figure 2.35, in which case it would make

sense to include the mean current in all tidal current predictions. [Also, if one used orthogonal components to analyze the current data at a location as depicted in Figure 5.1 (with flood and ebb directions that are not 180° apart), one *must* include the apparent mean current, for reasons explained in Section 5.1. (However, for that type of location, an alternative approach is to treat the reversing current as a scalar quantity, with positive flood speeds and negative ebb speeds, so that only one set of harmonic constants is required, in which case there would be no apparent mean current.)]

The second exception is not as strong a case. If one has done a harmonic analysis on a long current data series, and one has reason to believe that they have captured a mean current that exists most of the time (e.g., a typical river flow), then one may decide to include it in the tidal current prediction. Strictly speaking, it is not part of the tidal current, but in some cases it might be included in a prediction for a Tidal Current Table if one is trying to predict as much of the current as possible (for the mariner). However, if it is included, there will be many time periods when the nontidal current will be faster or slower than that mean current.

Actually, there is a third exception, but for a very different circumstance. When one is evaluating the quality of the harmonic constants calculated by comparing the predicted tidal current series with the original observed current data series, one must include the calculated mean current in the prediction (or one must subtract the mean current from the observed series).

5.3.6 Use of Node Factors and Equilibrium Arguments (or of Satellite Constituents)

In Section 2.2.4 it was seen that there are some very slow modulations of the tide-producing forces with periods of many years, the two most important being the 18.6-year variation in the angle between the plane of the moon's orbit and the plane of the Earth's equator, and the 8.85-year variation in the lunar distance from the Earth due to the rotation of the longitude of the lunar perigee. To include these effects in a complete harmonic analysis one can either add dozens of additional satellite tidal constituents, or use the concept of a node factor which represents the modulation of the tidal constituents over these 18.6- and 8.85-year cycles. Consideration of these two approaches for the harmonic analysis of water level data was discussed in Section 4.1.5. That discussion also applies to the harmonic analysis of tidal current data, and so the reader should read that section.

5.4 Methods for Analyzing Short Time Series

In Section 4.2 various methods for analyzing a short time series of water level data were discussed. That discussion applies equally well to currents and in fact is probably more relevant for currents, since typically current data time series have been much shorter than water level times series. As was seen in Section 3.3 the number of tidal constituents that one can accurately determine using harmonic analysis depends on the length of the data time series. One can look at either Table 3.2 or Table A.2 to determine which constituents can be included in a harmonic analysis based on the length of the time series. But there is some leeway in following the guidance in those tables, both due to our use of the least squares harmonic analysis technique, and for high tidal signal-to-low nontidal noise situations, and one should read Section 3.3. When the length of the time series limits the number of tidal constituents one can solve for, there are methods to try to improve the analysis results – both to obtain values for constituents that could not be included in the original harmonic analysis (called *inference*) and to improve the value of constituents that were in the analysis but were adversely affected by the constituents that were left out of the analysis (call *elimination*). Several of these methods for *inferring* constituents that could not be solved for with the available time series,

and for *eliminating* the adverse effects of these missing constituents from those constituents that were solved for, were presented in Sections 4.2.1 through Sections 4.2.5. These methods were applied to water level data, but they can be applied equally well to current data, and one should read those sections.

5.5 Assessing the Quality of the Predicted Tidal Current Series

5.5.1 Introduction

To assess the accuracy of harmonic constants calculated using a harmonic analysis, one usually compares a predicted tidal current time series (made using those harmonic constants) with the observed current data time series from which the harmonic constants were extracted. Even though there will be other nontidal signals in the observed current data time series, there are ways to evaluate the quality of the predicted tidal current time series and thus of the accuracy of the harmonic constants. In Section 4.3 several methods were looked at for assessing the accuracy of the harmonic constants from water level data using the predicted tide time series. That section should be read before reading the sections below.

The same approaches can be used for tidal currents, although there may be some differences due to the vector nature of the tidal current and the need to harmonically analyze two orthogonal component series. The other difference relates to the mean current. The mean current can be large, but since it is usually nontidal and thus unpredictable, one should usually not include it in a tidal current prediction for a Tidal Current Table. (As was discussed in Section 5.3.5, the mean current could be permanent if it is tidally induced by the nonlinear inertial mechanism described in Section 2.3.6.) However, when one does a quality assessment of the harmonic constants by comparing the predicted series to the observed series, the mean current must be included in the predicted series (or subtracted from the observed series).

Also, one usually had a lot less current data than one has water level data, which limits the kind of quality assessment that can be done. Sometimes one will not have a very long current time series, perhaps a month-long record, but one may have two such one-month records. It is important to analyze both records, for comparison, especially of the smallest constituents – ones that might be rejected for being very small unless they show up in both analyses with approximately the same phase lags, which would indicate that they do represent the tidal constituent (and not just some transient periodic nontidal energy).

For tidal currents (as for the tides) the three main approaches for assessing the accuracy of the calculated harmonic using the predicted time series are:

- (1) directly compare the speeds, directions, and times of maximum floods, maximum ebbs, and slack waters (or minimum flows) in the predicted series versus in an observed time series
- (2) carry out and examine a spectral analysis of the residual time series; and
- (3) examine the residual time series itself for periods with transient tidal current oscillations.

5.5.2 Comparison of Maximum Floods and Ebbs and Slacks In the Predicted Time Series Versus In the Observed Time Series

A frequently used method for assessing the quality of a tidal current prediction time series is to compare the speeds, directions, and times of corresponding maximum floods, maximum ebbs, and slack waters (or minimums) in the predicted tidal current series and the observed current series.

5. Harmonic Analysis of Current Data

Here it is important to use the same method for calculating these key points on a tidal current curve for both time series (see Section 3.9.2). Usually one looks at the time differences for each pair of corresponding maximum floods, maximum ebbs, slack waters (or minimums) and the speed ratios for the maximums. If the tidal current predictions were done using only major axis harmonic constituents, there will be no variation in the predicted directions. If the tidal current predictions were done using both major and minor constituents (or north and east constituents) then directions will be predicted, but they usually do not vary enough to enter into a quality assessment.

As with the tide, this method is typically used to check the quality of the daily predictions for reference stations in Table 1 of a Tidal Current Table. However, unlike the tide, there may not be any current data beyond what was analyzed to calculate the harmonic constants, even for a reference station.

As already mentioned, the observed current series includes nontidal effects on the maximum floods and ebb and the slack waters, so there will be differences between the predicted tidal current series and the observed current series due to those nontidal effects. These should average out when one is calculating mean ratios and difference for these parameters. Even with these nontidally caused differences it is useful to look at how the individual time difference and current speed ratio values change throughout each month and from month to month. For example, one might see a periodicity in the current speed ratios or time differences that points to a problem with a specific harmonic constant. Other longer periodicities or patterns in the current speed ratios or time differences might be due to nontidal seasonal effects.

5.5.3 Spectral Analysis of the Residual Time Series

As was seen in Section 4.3.3 one common way to check the quality of the calculated harmonic constants (and to provide some type of *error estimation*) is to make a tidal current prediction for the time period of the data analyzed, subtract the predicted time series from the original observed times to produce a *residual time series*, and then to see how much energy is left in the residual time series at the tidal frequencies using a spectral analysis. The details and comments presented in Section 4.3.3 for tides also apply to tidal currents, and that section should be read.

For tidal currents, since they are vectors and since the speed and direction time series are typically transformed into two orthogonal component time series (such as major-minor or north-east component series), there are several choices on which residual series to look at and what type of spectrum to produce. For reversing tidal currents, or even tidal currents where the flood-ebb axis is much longer than the perpendicular flow axis near minimums (i.e., for narrow elliptical rotation) one may wish to look at the speed residual time series (with ebb flows given negative values) or the major-component residual time series only. But for other cases one will look at both the major and minor residual time series. One can also look at the residual rotary spectra (see Section 3.10.3), i.e., the clockwise component residual time series and the counterclockwise residual time series. Each of these types of residual spectra will provide not only information about how much energy is left at the various tidal frequencies, but might also provide insights (some more than others depending on the situation and location) into possible hydrodynamic reasons why the energy is there.

5.5.4 Examination of the Residual Time Series For Periods With Transient Tidal Current Oscillations

In addition to doing the spectral analysis, one should also examine the residual current time series itself and look for time periods where oscillations at a tidal period appear and then disappear. (See Sections 4.1.4, 4.3.4, and 5.3.4.) When these occur, it will usually be due to the effect of the nonlinear interaction between the tide and some transient nontidal phenomenon, such as a large river discharge or storm surge, or to a change in water density that allowed a baroclinic effect to occur such as an internal tide. This latter effect can be important for tidal currents. During these periods of interaction, the nontidal phenomenon has temporarily changed the hydrodynamics of the situation and thus temporarily changed the amplitude and/or phase lag of one or more tidal constituents, and so by subtracting the predictions based on the average tidal constituents (from the analysis of the entire time series) one leaves some tidal energy for that particular time period. These various events with temporary tidal energy will not show up in the spectral analysis because they will have different phase relationships and cancel each other out in the overall average values determined by analysis.

When such incidents occur, one should look at the nontidal influences (such as changes in wind, river discharge, water density, etc.) to try to determine the cause of the temporarily different tidal constituents. If such incidents occur frequently, one may wish to add a footnote in the Tidal Current Table describing when such incidents occur. However, in some cases the nontidal effect (e.g. river flow) that caused the change in tidal current harmonic constants will be larger than its nonlinear influence on the tidal current, and so such changes to the tidal current may be less important. (If such incidents occur frequently, then tidal current prediction with a real-time driven forecast numerical circulation model may be the best route to take, because it can include not only the nontidal phenomena but also the effects of their nonlinear interaction with the tide and tidal current. See Chapter 8.)

5.5.5 Looking For Changes in Bathymetry or Shoreline

Changes in the depth of a waterway can significantly affect the tidal current. It was seen in Section 2.3.6 how sensitive the currents are to depths, because of friction and other effects. Changes in depth over time at a location may be rapid due to a hurricane or extra-tropical storm, relatively fast due to a dredging project in a navigation channel, or fairly slow due to year-to-year erosion and movement of sediment in the waterway. This effect is most important in shallow waterways where the same amount of depth change will represent a larger percentage of the total depth. Since sediment is almost always on the move, bathymetry is always changing. For very deep bays and estuaries the depth changes will not have much effect on the tidal currents, but for shallow bays and estuaries the same depth changes can significantly affect the tidal currents, so much so that the predictions in the Tidal Current Tables for that bay may no longer be accurate enough, since they are based on harmonic constants calculated from data measured before the depth changed.

When a dredging project to deepen a navigation channel in a small waterway has been completed, it is very likely that the tidal currents will be different (probably faster) in the channel than they were before the dredging project. It would therefore make sense to try to deploy a current sensor in that channel to see how much of a change has occurred. If the change is determined to be significant, then a new current survey is required, and the Tidal Current Tables should be footnoted with a warning until new predictions can be included. Similarly, when the shoreline is changed

significantly by filling in water areas to create land, or to create an artificial island, there also will likely be a change in the tidal currents. Storms and longer-term erosional effects due to the currents themselves (that move sediment around, creating some shoals and eroding others) can significantly change the tidal current regime in a shallow bay or estuary. For some locations, such as the shallow salt-marsh estuaries of South Carolina and Georgia, the changes can be very difficult (and expensive) to try to keep up to date in the Tidal Current Tables.

5.6 Producing a Reference Station for Table 1 of a Tidal Current Table

Very accurate tidal current harmonic constants are required for a reference station that appears in Table 1 of the Tidal Current Tables, since accurate tidal current predictions using these harmonic constants will be made for many years in the future, and many subordinate stations in Table 2 will be referenced to that station. The current data time series for such a station should be as long as possible in order to be able to use as many tidal constituents as possible in the harmonic analysis. Current data time series have typically been much shorter than water level time series, and many of the reference stations in Table 1 of the Tidal Current Tables are less than (some much less than) a year.

Selecting the location for a tidal current reference station is often trickier than for a tide station. One should try to select, if possible, a dynamically simple location, such as in the center of the entrance to the waterway, or in the straight section of a channel, and away from channel bends, junctures of channels, and points sticking out into the waterway. It is preferable, if possible, that this location should also be important for navigational purposes, as many mariners will rely mainly on the reference station and may not want to go through the adjustment process for predicting a subordinate station using Table 2 time differences and speed ratios .

Typically the standard 37 constituents (listed in Table 3.2) have been used in CO-OPS (and its predecessor organizations). However, since nonlinear shallow-water effects are usually larger in tidal currents than in tides, and since nonlinear lateral inertial effects also move energy into the higher harmonics, there is probably room for adding more shallow-water constituents into the harmonic analysis of current data (see Table A.2). One should use the methods mentioned in Section 5.5 for assessing the quality of the predicted tidal current series produced using 37 constituents to decide whether more constituents are needed (and whether a longer time series needs to be acquired from a new deployment).

If the location for the tidal current reference station happens to have a fairly rotary current, that is, its overall current ellipse is wide enough that the minimum flows (perpendicular to the flood-ebb axis) are important enough to be included in the daily predictions, then one must use a set of pairs of harmonic constants from a major-minor harmonic analysis (or a north-east harmonic analysis). If there are analysis results from several current sensors at that location, each for a different depth, one needs to assess each set of harmonic constants to decide which one is best to serve as the reference station. If the current data came from an ADCP then there will be many bin depths from which to choose. The best bin depth will probably be the one with the largest current speeds but far enough below the water surface so that the current data will not be significantly affected by surface wind waves. The other bin depths can be included in Table 2 and treated like subordinate stations.

5.7 Summary Overview: Steps In Harmonically Analyzing Current Data

In this section the steps to take in harmonically analyzing a current data time series will be summarized. Here it is assumed that one is using a least squares harmonic analysis program. In many cases, if the data are available, more than one harmonic analysis will need to be carried out on the data, with adjustments being made after each analysis if needed (such as adding additional constituents after assessing how much tidal energy is left in a residual series). Some steps may not be necessary for every analysis. Sections where more information can be found are in brackets [] at the end of each step.

These steps, in bullet form are:

- (1) *when first using a harmonic analysis program* it may be a good idea to *test it on a predicted tidal current time series* based on known harmonic constants, to see if the program can reproduce exactly the harmonic constants that were used to make the predicted tidal current time series, and if not, try to determine where energy is lost (or possibly gained); this might have to be done on tide data in order to have enough data to do an adequate test; [Section 4.3.1]
- (2) *determine how much accuracy one needs* in the harmonic constants (and in predictions to be made with those constants) for your particular application; that will affect how many of the steps below one will choose to use;
- (3) *assess the data available at the current station*; if more than one time series is available, use the longest most recent data; (especially for small shallow waterways) *check for indications of dramatic changes in bathymetry* (e.g., due to storms or to dredging); if such changes have occurred, select data (if possible) after those changes occurred. [Section 5.5.5]
- (4) *determine if there are gaps in the current data time series*; still use all the data but make sure to select the option in the least squares program that handles gaps (or random time data) since some least squares programs distinguish these two cases from a continuous data record, because the latter can be analyzed more quickly. [Section 3.4.5]
- (5) *determine which astronomical tidal constituents will be included* in the program, initially based on the length of the current data time series; use Table 3.2 or Table A.2 to make this determination, selecting all the constituents with synodic periods less than or almost equal to the length of the data time series; in subsequent runs of the program more constituents may be added, especially if the length of the data time series is fairly close to the next highest synodic period. [Section 5.3.1]
- (6) *determine whether an orthogonal component harmonic analysis should be done* (major-minor or a north-east analysis), or whether the tidal current is reversing enough to treat with only one (major) component;
 - (a) if the waterway is very narrow and the tidal current is essentially reversing, so that a *single component analysis* is to be done, make sure that the flood and ebb directions are 180° apart; if they are not (because there is a bend in the narrow waterway) one should use only the current speed time series, making all ebb speeds negative;
 - (b) if the waterway is wide enough for there to be some rotation in the current directions, then an *orthogonal component harmonic analysis* will be used; one may initially run a major-minor analysis or a north-east analysis, but let the analysis determine the actual mean flood direction (probably the M₂ max flood direction); the analysis can then either be rerun with that new major axis direction, or the constituent can be converted to the new major axis direction; if the signal-to-noise ratio looks small in the minor component, decide whether to

5. Harmonic Analysis of Current Data

choose orthogonal components that put equal amounts of the tidal signal into each component; [Sections 5.2 and 5.3.2]

- (7) *determine whether additional shallow-water tidal current constituents should be included* in the analysis; this will be obvious for a very shallow waterway with strong tidal currents, but one should first use the standard 37 constituents and see how much energy is left in the higher harmonic tidal bands of a spectrum; for an extremely nonlinear case, the highest order overtide that can be solved for will depend on the sampling rate of the current data time series, but the sampling rate of most current sensors (several sample per hour) is more than sufficient. [Section 5.3.1]
- (8) *determine how much of the data time series to use* in the harmonic analysis; in Step (5) the longest synodic period within the length of the available data time series was selected, but one may have more data than that (but less than the next highest synodic period); run the first analysis using a segment of the time series whose length is the selected synodic period; if there is enough extra data, it will be useful to run one analysis from the beginning of the time series and a second analysis that includes the end of the time series (and look for consistency in the harmonic constants for each, especially in the smallest constituents); if the length of the available data series is more than half way to the next synodic period, the follow-up analysis can use all the available data and include additional harmonic constituents that theoretically require the next highest synodic period; if one has a second (also short) data time series, also harmonically analyze that time series and look for consistency in the two sets of constituents; [Section 5.3.1]
- (9) *decide whether to use a particular shallow-water compound tidal current constituent* or the astronomical constituent with the same frequency (e.g., $2M\text{N}_2$ or L_2); for deep-water stations the astronomical constituent is fine, but for shallow-water stations (especially inside bays and rivers) one will probably need to use the shallow-water constituent; if one is unsure, one will have to look at the harmonic analysis results of several current stations in the bay and see if the rate of growth moving up the bay is greater than the rate of growth of an astronomical constituent in the same tidal band (e.g., see if $2M\text{N}_2$ grows at a faster rate than M_2); for constituent pairs whose node factors are the same (e.g., $2M\text{S}_2$ and μ_2) it does not matter which is selected; for pairs with different node factors, if one initially chose the astronomical constituent, but later decides it should have been the shallow-water constituent, one does not have to re-analyze, for one can merely correct for the different node factor and equilibrium argument. [Section 5.3.1]
- (10) check the data file for notes about instrument errors, movement of the current sensor, or other potential problems with the data; if such problems are noted, keep in mind the possible effects of the five types of errors on the harmonic constants; [Section 5.3.3]
- (11) *carry out the least squares harmonic analysis*; if an orthogonal component analysis has been run, *plot the current constituent ellipses*; decide whether to rerun the analysis with a new major axis direction;
- (12) *tidally filter the current data time series to look for strong nontidal events* (like spring river runoff, strong wind currents, or internal tides) that may nonlinearly affect the tidal analysis results; one should probably also look at a tidally filtered water level data series from a nearby station (for storm surges, which do not usually have strong currents associated with them, but which can significantly affect both the tide and the tidal current); if one needs harmonic constants from which predictions can be made for most of the year, one might consider leaving out the nontidal event periods and rerunning the least squares harmonic

- analysis using the gap option; if one has a short time series of current data that includes a major nontidal event, one will probably not be able to use the harmonic constants that come out of the analysis for tidal current prediction. [Section 5.3.4]
- (13) with the harmonic constants from the first harmonic analysis, *make a tidal current prediction for the same period as the data*, and subtract this predicted time series from the original observed time series to *produce a residual time series*; if one has more data than were used to do the harmonic analysis, then also produce predicted and residual time series for that second time period (this other residual time series will provide more meaningful results in steps (15) and (16) than the residual series from the self prediction); [Section 5.5.3]
- (14) carry out a *spectral analysis on the residual time series* to see if there is any remaining tidal energy still in the record; also carry out a *spectral analysis on the original observed time series* for comparison purposes. [Section 5.5.3]
- (15) *examine a plot of the residual time series* looking for places where a transient tidal signal appears; compare to the results of Step (12); investigate the wind, river, water density, or other potential nontidal influences for those time periods; one may have to consider leaving time periods with strong nontidal events out of the analysis and rerunning the least squares harmonic analysis using the gap option; if one has a short time series of current data that includes a major nontidal event, one will probably not be able to use the harmonic constants that come out of the analysis for tide prediction. [Section 5.5.4]
- (16) if there still is tidal energy in the residual time series try to *determine what additional tidal constituents might be added to the harmonic analysis*; most easy to spot will be energy in higher species bands due to shallow-water effects; decide which additional shallow-water constituents are most likely to be important; [Table 3.2 or Table A.2]
for energy left in the semidiurnal or diurnal bands, one should determine which are the next semidiurnal or diurnal constituents that were left out of the analysis because of insufficient length of the time series; there may also be compound tidal constituents (due to shallow-water effects) that should be added to the next analysis; [Table 3.2 or Table A.2]
- (17) *obtain values for additional constituents*; if one does not have enough data to move to the next synodic period, one can then either:
- use an inference (and elimination) technique* to calculate the amplitudes and epochs for the missing constituents (and to correct the amplitudes and epochs of the solved-for constituents; [Section 4.2])
 - try rerunning the harmonic analysis with these constituent included* using the full length of the available time series, to see if the least squares technique can successfully determine them; and
- (18) when it is decided that one has the optimum set of harmonic constants for a particular current station, run a final prediction for the full length of data and calculate all the maximum floods, maximum ebbs, and slack waters (or minimums); compare these predicted maximum floods, maximum ebbs, and slack waters (or minimums) with the equivalent values calculated from the data time series, determining all the usual statistics; (if possible, use the same max/min routine for both predicted and data series); if the mean maximum floods (and the mean maximum ebbs) from the data are larger than the mean predicted maximum floods (and mean predicted maximum ebbs) consider going back to Step (17).

6. Nonharmonic Analysis of Water Level and Current Data

Nonharmonic comparison analysis methods for analyzing the tide and tidal current were introduced and briefly described in Section 3.6. This type of analysis is not very sophisticated, simply comparing one or more aspects of the tide (or tidal current) at two stations. But it has been used to analyze data at thousands of stations which have been put into the Tide or Tidal Current Tables. A nonharmonic comparison analysis is used to compare a subordinate station to a reference station, with the resulting time differences and height differences (for tides) or current speed ratios (for tidal currents) listed in Table 2 of the Tide or Tidal Current Tables. In Section 3.6.3 a key fact was demonstrated (using several detailed examples) about the time and height differences and speed ratios that come out of a nonharmonic comparison analysis:

the time and height differences between corresponding high waters (or low waters) at two tide stations vary from tidal cycle to tidal cycle throughout the month (and similarly for tidal current stations).

If the tidal characteristics at the two stations being compared are very similar, then this variation throughout the month will not be significant (which is the desired result). Often, however, this is not the case. The tidal characteristics of the two stations may not be similar enough because either they are not close enough geographically or because the waterway has a mixed tide with a significant diurnal inequality, which causes the tidal characteristics to change significantly over even fairly short geographic distances. If this is the case then these differences can vary significantly from the mean value when, for example, the moon is at maximum declination.

This fact is important because the main use for the mean time and height differences that come out of a comparison tidal analysis is to produce correction factors for a subordinate station in Table 2 of the Tide Tables. These correction factors are used to produce tide predictions at the subordinate station by applying them to the (harmonically produced) tide predictions at a reference station. A single mean value of the time or height difference is usually used to make these subordinate station predictions, so errors in the prediction will occur at certain times of the month (such as maximum lunar declination, as mentioned above).

This chapter will present more details about using the various types of nonharmonic comparison tidal analysis, including a discussion of the consequences of the variation in nonharmonically determined time and height differences throughout the month. The most important consequence will be errors in making tide predictions using the correction factors found in Table 2 of the Tide and Tidal Current Tables, and ways will be looked at to minimize such errors.

6.1 The Need For Nonharmonic Tidal Analyses

As was mentioned above and in Section 3.6, nonharmonic comparison analysis does not provide as accurate a representation of the tide or tidal current as does harmonic analysis, nor are the predictions made using the time and height differences (or tidal current speed ratios) that come out of a nonharmonic comparison analysis as accurate as predictions made using tidal harmonic constants. Tide predictions made with such time and height differences are made by applying these difference to the harmonically produced tide predictions at a reference station, and the fact that these differences are not accurate for all times of the month degrades the tide prediction to some degree.

In spite of its lesser accuracy, nonharmonic analysis is still required in order to put stations into Table 2 of the Tide and Tidal Current Tables. Table 2 contain thousands of *subordinate* stations which could not feasibly be included as daily predictions in Table 1, even if one wanted to. At four pages per station in Table 1 (versus one line in Table 2), it would take thousands of pages to include these stations in Table 1. For example, in the 2007 edition of *Tide Tables, East Coast of North and South America*, produced by CO-OPS for NOAA, Table 1 consists of daily predictions for 76 harmonically analyzed reference stations, while Table 2 consists of time differences and height differences and/or ratios for 2589 subordinate stations.

Nonharmonic comparison analysis is also required for stations with data times series too short to be accurately analyzed harmonically (usually less than 15 days). Short time series have been especially common for stations with observed current data, which have been much more difficult and expensive to deploy and maintain compared with land-based water level stations. For short stations there is no choice but to analyze such stations nonharmonically and then put them into Table 2.

Tide and Tidal Current tables are still the primary means for providing tidal predictions to users in the marine community, and often hard copy versions are carried by the mariner and recreational boater. However, even if there is an eventual transition to fully digital means of providing tidal predictions, with all predictions produced harmonically (see **Section 9.7**), there are thousand of stations already in Table 2 of the Tide and Tidal Current Tables that are based on short data times series, and these stations would need to be re-occupied (for at least 15 days, and preferably 30) in order to include them in a harmonically-based digital prediction product. Table 2 is therefore likely to remain a part of all Tide and Tidal Current Tables in the near future, and so nonharmonic comparison analyses will continue to be used.

6.2 Hydrodynamic Considerations

A key fact first mentioned in Section 3.6.3 is repeated here again, which should always be remembered when carrying out a nonharmonic comparison analysis (especially when the results are going to be put in Table 2 of the Tide or Tidal Current Tables):

the time and height differences between corresponding high waters (or low waters) at two tide stations vary from tidal cycle to tidal cycle throughout the month (and similarly for tidal current stations).

This variation in time and height differences is a consequence of hydrodynamic effects on the times and heights of high waters and low waters.

Two stations in different parts of a waterway will have a different harmonic makeup because, as was seen in Section 2.3.1, various hydrodynamic effects cause the amplitudes and phase lags of

the harmonic constituents to change with geographic distance, along both the length and width of a waterway, and these changes are frequency dependent. Thus, as one moves along the waterway the ratio of two harmonic constants changes. The larger the difference between the frequencies of the two constituents the faster their ratio changes with distance. The ratio of a diurnal constituent to a semidiurnal constituent, for example, K_1/M_2 , changes much faster than, for example, S_2/M_2 changes. As was seen in Section 3.6.3, in a waterway with a mixed tide and a significant diurnal inequality, two stations do not have to be separated geographically by many miles to lead to large variations throughout the month in the differences between the times and heights of high waters at the two stations. It was also seen in Section 3.6.3 that the distortion of the tide curve or tidal current curves due to nonlinear shallow-water effects can also lead to variations in the time and height differences and speed ratios.

In essence, by using a constant time or height difference or a constant speed ratio throughout the month one is assuming that only M_2 is important, when, in fact, other tidal harmonic constituents are also important. A constant time difference between times of high water at the two locations would also be possible if the two stations in a bay had exactly the same relative harmonic makeup, that is, if the amplitude ratios of and the phase differences between corresponding harmonic constituents were exactly the same. But the hydrodynamics of the bay makes this impossible. Numerous hydrodynamic effects have a frequency dependence that causes them to affect each harmonic tidal constituent differently (see Sections 2.3 and Chapter 7). This includes the effects of partial and full reflections with which the bay affects the amplitude and phase lag of each tidal constituent, as well as frictional effects, continuity effects, and inertial effects, all of which are frequency dependent.

As mentioned above, the average time difference between high waters at the two stations equals approximately the time difference between the two respective M_2 high waters, but other tidal constituents, each with their own phase lag (time) difference, also affect the time and height of high water (and likewise the maximum floods and ebbs in a tidal current). The time difference between high water at the two stations therefore varies throughout the month, varying from springs to neaps or from maximum lunar declination to equatorial declination. Generally, the greater the geographical distance between two stations the greater the change in the tide regime and the greater the difference in harmonic makeup, and thus the greater the variation in time differences. The fundamental consideration is how quickly the tidal characteristics change with distance in the vicinity of the two stations being compared.

Four different types of nonharmonic comparison analyses will now be looked at in some detail, the first two for tides and the second two for tidal currents.

6.3 Monthly Mean Tide Analysis

6.3.1 Details of the Analysis

The monthly mean tidal analysis is described in the *Manual of Tide Observations* (U.S. C&GS, 1965, pages 48, 51-57); see also CO-OPS, 2003. The relevant section in that manual is called “High and Low Water Tabulations” because the bulk of the work was in tabulating the times and heights of high water and low water at a water level station, usually a month at a time. Prior to computer-assisted data processing and analysis, such tabulations were put on a special form, C&GS Form 2211, a copy of which is shown in Figure 6.1 (taken from C&GS, 1965, page 55). One can see in that figure that Form 2211 provided two lines for each calendar day, the morning high water and low water times and heights entered on the first line, and the afternoon values on the second line. A

Tidal Analysis and Prediction

TIDES: HIGH AND LOW WATERS																		
Station: <u>Seattle, Wash.</u>											Lat. <u>47° 36' N</u>							
Time Meridian <u>120° W</u>											Long. <u>123° 20' W</u>							
Year <u>1962</u> Month <u>Jan.</u>											Highest Tide: Date <u>12</u> Height <u>20.3</u> feet							
											Lowest Tide: Date <u>6, 7, 9</u> Height <u>4.6</u> feet							
MOON'S TRANSIT	TIME OF		LUNITIDAL INTERVAL		HEIGHT OF		MOON'S TRANSIT	TIME OF		LUNITIDAL INTERVAL		HEIGHT OF						
DAY	GMT	HW	LW	HW	LW	HW	LW	DAY	GMT	HW	LW	HW	LW					
(1)	Hours	hours	hours	hours	hours	feet	feet		hours	hours	hours	feet	feet					
1	7.6	1.5	6.3	(6.3)	(1.1)	15.4	13.6	18	(10.3)	4.5	9.8	6.7	12.0	18.5	14.6			
	(200)	12.3	19.2	4.7	11.6	18.4	8.8		22.7	14.7	21.8	(4.4)	(11.5)	18.0	5.8			
2	8.4	2.5	7.1	(6.5)	(11.1)	16.7	14.4	19	(11.1)	5.3	10.6	6.6	11.9	18.8	14.5			
	(20.8)	12.9	20.1	4.5	11.7	19.7	8.4		23.5	15.7	22.3	(4.6)	(11.2)	18.2	6.3			
3	9.2	3.5	8.1	(6.7)	(11.3)	18.3	15.7	20	(12.0)	5.8	11.3	6.3	11.8	19.1	14.3			
	(21.6)	13.6	20.8	4.4	11.6	19.4	6.7		—	16.3	22.9	(4.3)	(10.9)	17.9	5.6			
4	10.1	4.3	9.3	(6.7)	(11.7)	18.1	14.8	21	0.4	6.5	11.9	6.1	11.5	18.7	13.7			
	(22.6)	14.5	21.5	4.4	11.4	18.7	5.8		(12.8)	17.1	23.6	(4.3)	(10.8)	17.4	5.9			
5	11.1	5.1	10.1	(6.5)	(11.5)	19.0	15.1	22	1.1	7.1	—	6.0	—	18.6	—			
	(23.6)	15.2	22.3	4.1	11.2	19.3	4.9		(13.5)	17.6	12.5	(4.1)	11.4	17.0	13.3			
6	—	5.8	10.9	(6.2)	(11.3)	19.1	14.4	23	1.9	7.5	0.2	5.6	(10.7)	18.7	6.1			
	12.1	16.1	22.8	4.0	10.7	19.1	4.6		(14.3)	18.3	13.2	(4.0)	11.3	16.8	13.0			
7	(0.6)	6.2	11.7	(5.6)	(11.1)	19.0	14.3	24	2.6	8.1	0.7	5.5	(10.4)	19.0	7.1			
	13.1	16.7	23.6	3.6	10.5	19.1	4.6		(15.0)	19.1	13.8	(4.1)	11.2	16.5	12.9			
8	(1.6)	6.9	—	(5.4)	—	19.9	—	25	3.3	8.4	1.2	5.1	(10.2)	19.5	8.2			
	14.0	17.5	12.4	3.5	(10.8)	18.4	13.8		(15.7)	19.8	14.5	(4.1)	11.2	16.0	12.7			
9	(2.5)	7.6	0.3	(5.1)	10.3	19.0	4.6	26	4.0	8.9	1.8	4.9	(10.1)	19.2	9.2			
	15.0	18.4	13.4	3.4	(10.9)	17.5	12.8		(16.4)	20.7	15.2	(4.3)	11.2	15.6	11.9			
10	(3.5)	8.3	1.1	(4.8)	10.1	19.7	5.2	27	4.7	9.3	2.5	4.6	(10.1)	18.8	10.3			
	15.9	19.4	14.3	3.5	(10.8)	17.1	12.2		(17.1)	21.9	16.2	(4.8)	11.5	14.7	10.8			
11	(4.4)	9.1	1.9	(4.7)	10.0	20.1	6.8	28	5.5	9.9	3.3	4.4	(10.2)	18.4	11.4			
	16.8	20.8	15.3	4.0	(10.9)	16.4	11.7		(17.8)	23.4	16.9	(5.6)	11.4	14.8	9.9			
12	(5.2)	9.8	2.8	(4.6)	10.0	20.3	8.9	29	6.2	10.6	4.3	4.4	(10.5)	18.0	12.7			
	17.6	21.9	16.5	4.3	(11.3)	16.0	10.9		(18.6)	—	17.8	—	11.6	—	9.0			
13	(6.1)	10.4	3.8	(4.3)	10.2	20.0	10.8	30	7.0	0.9	5.6	(6.3)	(11.0)	15.5	13.9			
	18.5	23.7	17.5	5.2	(11.4)	15.7	9.7		(19.4)	11.5	18.6	4.5	11.6	17.9	8.3			
14	(6.9)	11.5	4.9	(4.6)	10.4	20.0	12.4	31	7.8	2.4	6.9	(7.0)	(11.5)	16.5	14.6			
	19.3	—	18.5	—	(11.6)	—	9.2		(20.3)	12.4	19.6	4.6	11.8	18.0	7.6			
15	(7.7)	1.5	6.2	6.2	10.9	16.3	13.8		.	.	.	60	60	60	60			
	20.1	12.3	19.3	(4.6)	(11.6)	18.8	7.4		Sums	.	.	302.3	666.4	1083.1	622.6			
16	(8.6)	2.9	7.7	6.8	11.6	17.2	14.6		Means	.	.	5.04	11.11	18.05	10.38			
	21.0	13.2	20.3	(4.6)	(11.7)	18.7	7.1		Greenwich Interval	.	.	0.62	6.69	.	.			
17	(9.4)	3.6	8.9	6.6	11.9	18.1	14.7		Lunar Interval	.	.	8.44	8.44	7.67	Mn			
	21.8	14.1	21.1	(4.7)	(11.7)	18.2	6.3		Local Interval	.	.	4.60	10.67	14.22	MTL			
REMARKS												Mn	DHQ	DLQ	HHW	LLW		
												Observed	7.67	0.99	3.20	31	29	
												Factor	0.989	0.97	0.97	Sums	590.1	208.3
												Corrected	7.59	0.96	3.10	Means	19.04	7.18
												Tabulated by	Winn			.		
												Reduced by	Winn			11.86	G	
																13.11	(Dr) TL	

-Form 2211 (back), High and low waters.

Figure 6.1. A copy of Form 2211, on which tabulations were done in the pre-computer era when carrying out a monthly mean analysis.

6. Nonharmonic Analysis of Water Level and Current Data

dashed line indicated when there was no high water (or low water) during that 12-hour period, which happens every 14 or 15 days since the time of high water (or low water) gets progressively later every day (usually by roughly 50 minutes). (The dashed line distinguished this situation from missing data, which was simply left blank.)

Also tabulated on this form were the times of *Moon's Transit* over the Greenwich time meridian (these transits also being available in the American Ephemeris and Nautical Almanac). *Lower transits* (i.e., the moon passing over that part of the meridian lying below the polar axis) were enclosed in parentheses to distinguish them from *upper transits* (i.e., the moon passing over that part of the meridian lying above the polar axis). The *lunitidal interval* for each high water (or a low water) was calculated by subtracting the latest moon's transit just prior to the time of high water (or low water). The lunitidal intervals calculated using lower transits were indicated by parentheses. Thus, there were seven values listed for each half calendar day, in order: moon's transit, time of high water, time of low water, lunitidal interval for high water, lunitidal interval for low water, height of high water, and height of low water. At the bottom of the right half of this form the lunitidal intervals were summed, as were the heights of high water and low water; then means were calculated for each. Since the moon's transits were given in Greenwich time but (for convenience) the times of high and low waters were given in Standard Time (for the local time meridian) the means had to be corrected to become Greenwich lunitidal intervals, by adding one hour for every 15° difference between the local time meridian and Greenwich (if the local time meridian is west of Greenwich; if it is east of Greenwich then subtraction is done, and sometimes one had to subtract 12.42 hours if the result is 12.42 hours or greater).

The *local interval* is relative to the moon passing over the longitude of the tide station location (rather than passing over Greenwich). To calculate this one had to know the *lunar interval*, i.e., the time it would take the moon to pass from the Greenwich meridian to the station location. This astronomically-determined value was obtained from a table (Table 7 in U.S. C&GS, 1965, pages 53) but it essentially meant subtracting approximately 0.069 hour for every degree of longitude change (when the station was west of Greenwich), plus subtracting approximately 0.00115 hour for every additional minute of longitude difference.

Form 2211 was also used to calculate the mean high water (MHW) and the mean low water (MLW) for the month of the tabulations. The mean tide range (M_n) was also calculated by subtracting MLW from MHW, and the mean tide level (MTL) was calculated by taking the average of MHW and MLW. For tide stations with a significant diurnal inequality, there were places on the form to sum all the higher high waters and all the lower low waters, so that the mean higher high water (MHHW, but called HHW on Form 2211) and mean lower low water (MLLW, but called LLW on Form 2211) could be calculated. Then the diurnal high water inequality (DHQ) was calculated by subtracting the mean of all the high waters from the mean of all the higher high waters, and likewise for the diurnal low water inequality (DLQ).

The values of M_n , DHQ, and DLQ were the mean range, diurnal high water inequality, and diurnal low water inequality for that particular month of water level data. These values were then corrected for the 18.6-year variation in the procession of the lunar node (see Sections 2.2.4 and 3.4.2), which was accomplished using other tables in U.S. C&GS, 1965 (Tables 8 and 9, pages 56-7), that were based on tables originally found in Harris' *Manual of Tides* (1897-1907). However, these tables also included the effects of the relation of the diurnal tide to the semidiurnal tide at the station, which was represented by the formula $2(DHQ + DLQ)/M_n$, which should be approximately equivalent to $(K_1 + O_1)/M_2$.

Tidal Analysis and Prediction

TIDES: Comparison of Monthly Means												
(A) Subordinate station <u>Angeles (San Luis Obispo Bay), Calif.</u> Lat. <u>35° 10' 2"</u> Long. <u>120° 44' 4"</u> (B) Standard station <u>Los Angeles, Calif.</u> Lat. <u>33° 43' 2"</u> Long. <u>118° 16' 3"</u>												
MONTH	M T L			M S L			H W I			L W I		
	(A) Feet	(B) Feet	(A)-(B) Feet	(A) Feet	(B) Feet	(A)-(B) Feet	(A) Hours	(B) Hours	(A)-(B) Hours	(A) Hours	(B) Hours	(A)-(B) Hours
1948 July	5.86	6.64	-0.78	5.83	6.63	-0.80						
Aug.	5.87	6.64	-0.77	5.83	6.61	-0.78						
Sept.	6.08	6.74	-0.68	6.04	6.73	-0.69						
Oct.	5.84	6.52	-0.68	5.80	6.49	-0.69						
Nov.	5.74	6.54	-0.80	5.68	6.50	-0.82						
Dec.	5.64	6.52	-0.88	5.59	6.46	-0.93						
1949 Jan.	5.82	6.49	-0.66	5.80	6.45	-0.65						
Feb.	5.68	6.46	-0.78	5.65	6.43	-0.78						
Mar.	5.56	6.18	-0.62	5.53	6.14	-0.61						
Apr.	5.53	6.25	-0.72	5.50	6.22	-0.72						
May	5.67	6.34	-0.67	5.60	6.30	-0.70						
June	5.82	6.57	-0.75	5.77	6.53	-0.76						
Sums			-0.79			-0.83						
Means			-0.73			-0.74						
Accepted values for (B)		6.51		XXXXX	XXXXX	6.48	XXXXX	XXXXX		XXXXX	XXXXX	
Corrected values for (A)		5.78		XXXXX	XXXXX	5.74	XXXXX	XXXXX		XXXXX	XXXXX	

Corrected value for MTL, MSL, HWI, and LWI, for subordinate station = accepted value for standard station + mean difference.

MONTH	Mn			D H Q			D L Q					
	(A) Feet	(B) Feet	(A)+(B) Ratio	(A) Feet	(B) Feet	(A)+(B) Ratio	(A) Feet	(B) Feet	(A)+(B) Ratio			
1948 July	3.43	3.57	0.96	0.48	1.02	0.96	1.28	1.18	1.08			
Aug.	3.58	3.72	0.96	0.88	0.85	1.04	1.20	1.11	1.08			
Sept.	3.64	3.90	0.93	0.61	0.66	0.92	1.01	0.92	1.01			
Oct.	3.69	3.94	0.94	0.49	0.55	0.89	1.00	0.89	1.12			
Nov.	3.56	3.75	0.95	0.73	0.78	0.94	1.26	1.15	1.10			
Dec.	3.57	3.67	0.97	0.88	0.97	0.91	1.32	1.23	1.12			
1949 Jan.	3.55	3.67	0.91	0.89	0.93	0.96	1.27	1.18	1.08			
Feb.	3.55	3.73	0.95	0.79	0.77	1.03	1.05	0.97	1.07			
Mar.	3.51	3.80	0.92	0.56	0.58	0.97	0.86	0.80	1.08			
Apr.	3.53	3.74	0.94	0.61	0.66	0.92	1.04	0.94	1.11			
May	3.54	3.65	0.97	0.51	0.89	0.91	1.26	1.14	1.11			
June	3.55	3.64	0.93	0.45	0.49	0.96	1.32	1.21	1.09			
Sums			11.44			11.41			13.15			
Means			0.953			0.951			1.096			
Accepted values for (B)		3.76		XXXXX	XXXXX	0.74	XXXXX	XXXXX	0.95	XXXXX	XXXXX	
Corrected values for (A)		3.57		XXXXX	XXXXX	0.70	XXXXX	XXXXX	1.04	XXXXX	XXXXX	

Corrected value for Mn, DHQ, and DLQ for subordinate station = accepted value for standard station × mean ratio.

Figure 6.2. A copy of Form 657, which was used in the pre-computer era for calculating and recording comparison of monthly means.

In order to find time differences and height differences between a subordinate station (to be put in Table 2 of the Tide Tables) and a reference station, another form, C&GS Form 657, was used. Form 657 is shown in Figure 6.2 (taken from *Tidal Datum Planes* by Marmer, 1951, page 139). This form simply provided three columns for each of seven parameters, the first two columns being values for the subordinate station and for the reference stations (which is referred to as the *standard station* on the form) and the third column being for the difference or ratio of the two values. The seven parameters for which this was done were: mean tide level (MTL), mean sea level (MSL), high water interval (HWI), low water interval (LWI), mean range (Mn), diurnal high water inequality (DHQ), and diurnal low water inequality (DLQ). For the first two parameters the third column is the height difference in feet, for the next two parameters the third column is the time difference in hours, and for the last three parameters the third column is the height ratio. There is one line for each set of monthly means being compared.

6. Nonharmonic Analysis of Water Level and Current Data

FORM 248
(28-59)
USCOMM-DC 27247

U.S. DEPARTMENT OF COMMERCE
COAST AND GEODETIC SURVEY

TIDES : Comparison of Simultaneous Observations

(A) Subordinate station Port Susan Wash. Lat. 48° 8' N Long. 122° 22' W
 (B) Standard station Seattle, Wash. Lat. 47° 36' N Long. 122° 20' W
 Chief of party Time Meridian: (A) 120° W (B) 120° W

DATE. Year.	(A) STATION.		(B) STATION.		(A)-(B)		(A) STATION.		(B) STATION.		(A)-(B)	
	Time of--		Time of--		Time difference.		Height of--		Height of--		Height difference.	
	H.W.	L.W.	H.W.	L.W.	H.W.	L.W.	H.W.	L.W.	H.W.	L.W.	H.W.	L.W.
1962												
Mo. D.	Hours.	Hours.	Hours.	Hours.	Hours.	Hours.	Feet.	Feet.	Feet.	Feet.	Feet.	Feet.
Oct 1	6.5	0.1	6.4	0.1	0.1	0.0	11.0	2.6	18.1	9.4	-7.1	-6.8
	18.2	12.2	18.4	12.3	-0.2	-0.1	11.3	4.5	18.5	11.5	-7.2	-7.0
2	7.2	0.3	7.1	0.5	0.1	-0.2	11.2	2.3	18.4	9.2	-7.2	-6.9
	18.6	12.9	18.6	12.9	0.0	0.0	11.5	5.7	18.7	12.8	-7.2	-7.1
3	7.9	1.0	8.0	1.0	-0.1	0.0	11.0	2.3	18.1	9.1	-7.1	-6.8
	19.2	13.6	19.3	13.6	-0.1	0.0	10.7	6.0	17.8	13.0	-7.1	-7.0
4	9.3	1.4	8.8	1.8	0.5	-0.2	10.7	2.1	17.8	8.7	-7.1	-6.6
	20.0	14.5	19.9	14.3	0.1	0.2	10.1	6.8	17.3	13.8	-7.2	-7.0
5	10.2	2.7	10.2	2.5	0.0	0.2	10.6	2.3	17.6	8.4	-7.0	-6.1
	20.6	15.6	20.5	15.4	0.0	0.2	9.9	7.6	17.0	14.5	-7.1	-6.9
6	11.2	3.2	11.4	3.4	-0.2	-0.2	10.8	1.7	17.9	8.6	-7.1	-6.9
	21.5	17.0	21.6	16.7	-0.1	0.3	9.3	7.8	16.3	14.7	-7.0	-6.9
7	12.8	4.4	12.8	4.5	0.0	-0.1	11.9	1.7	18.9	8.5	-7.0	-6.8
	22.5	18.7	22.8	19.0	-0.3	-0.3	9.4	8.7	16.3	15.5	-6.9	-6.8
Sums.							7 H.W.	7 H.W.	7 H.W.	7 H.W.	7 H.W.	7 H.W.
Means.							7.77.8	47.1	127.5	95.8	-49.7	-48.7
Sums.							11.1	6.73	18.21	13.69	-7.10	-6.96
Means.							7 L.H.W.	7 L.L.W.	7 L.H.W.	7 L.L.W.	7 L.H.W.	7 L.L.W.
							-0.2	-0.2	71.6	15.0	121.2	61.9
							-0.01	-0.01	10.23	2.4	17.31	8.84

(1) = -0.01 | -0.01 = Mean difference in time of high and low water respectively.

(2) = 0.00 | 0.00 = Correction for difference in longitude. (Table on back of form.)

(3) = -0.01 | -0.01 = (1)+(2) = Mean difference in high and low water intervals, respectively.

Ft.

(4) = 11.11 = Mean HHW height at (A).

(5) = 6.73 = Mean HLW height at (A).

(6) = 10.23 = Mean LHW height at (A).

(7) = 2.4 = Mean LLW height at (A).

(8) = 0.88 = (4)-(6) = 2DHQ at (A).

(9) = 4.59 = (5)-(7) = 2DLQ at (A).

(10) = 10.67 = $\frac{1}{2}[(4)+(6)]$ = Mean HW height at (A).

(11) = 4.44 = $\frac{1}{2}[(5)+(7)]$ = Mean LW height at (A).

(12) = 6.23 = (10)-(11) = Mn at (A).

(13) = 7.56 = $\frac{1}{2}[(10)+(11)]$ = MTL at (A).

(14) = -7.10 = Mean HHW difference.

(15) = -6.96 = Mean HLW difference.

(16) = -7.08 = Mean LHW difference.

(17) = -6.70 = Mean LLW difference.

(18) = -0.02 = (14)-(16) = 2DHQ difference.

(19) = -0.26 = (15)-(17) = 2DLQ difference.

(20) = -7.09 = $\frac{1}{2}[(14)+(10)]$ = Mean HW difference.

(21) = -6.83 = $\frac{1}{2}[(15)+(17)]$ = Mean LW difference.

(22) = -0.26 = (20)-(21) = Mn difference.

(23) = -6.96 = $\frac{1}{2}[(20)+(21)]$ = MTL difference.

(24) = 0.960 = (12)+[(12)-(22)] = Mn ratio.

(25) = 0.978 = (8)+[(8)-(18)] = DHQ ratio.

(26) = 0.946 = (9)+[(9)-(19)] = DLQ ratio.

Results from comparison of Stations A and B.		H.W.	L.W.	M.T.L.	Mn.	DHQ.	DL.Q.
Length of Series.		Hours.	Hours.	Feet.	Feet.	Feet.	Feet.
Accepted values for standard station, from	1941-1959	4.52	10.69	14.29	7.6	0.9	2.8
Differences and ratios: (1), (23), (24), (25), (26)		-0.01	-0.01	-6.96	x 0.96	0.978	0.946
Corrected values for subordinate station		4.51	10.68	7.33	7.30	0.88	2.65

Mean LW on staff at subordinate station = MTL - $\frac{1}{2}$ Mn = 3.68 feet.

Mean LLW on staff at subordinate station = MTL - $\frac{1}{2}$ Mn - DLQ = 1.03 feet.

Computed by Winn, 9-6-63 Verified by _____ (Date.)

Form 248, Comparison of simultaneous observations.

Figure 6.3. A copy of Form 248, which was used in the pre-computer era to carry out a comparison of simultaneous observations (a tide-by-tide analysis).

Essentially the same procedures are now done routinely using computers, as part of the standard water level data processing and analysis in CO-OPS.

6.3.2 The Limitations of the Monthly Mean Tide Analysis

The monthly mean tide analysis is routinely carried out for all tide stations for which there is a month of data or more. Most tide stations are occupied for at least a year, and a couple of hundred stations are permanently installed as part of the National Water Level Observation Network (NWLON). Thus many monthly tabulations and monthly means have accumulated at these stations. It is part of standard data processing for water level data.

The major drawback with this method for putting tide stations in Table 2 is that only the monthly means are used to calculate the time and height differences between the subordinate station being put in Table 2 and the reference station. The differences between the two stations are not looked at cycle by cycle, and so there is no way of knowing how much the differences actually vary throughout the month due to changing lunar declination or the change from neaps to springs. One can see variations from month to month, but those variations are much smaller than those that occur within a month.

If the reference station is nearby and has tidal harmonic constant ratios and phase lag differences that are similar to those at the subordinate station, the results from the comparison of the monthly means will be of good quality, but one can not tell how good that is unless one also carries out a tide-by-tide analysis (see next Section).

6.4 Tide-by-Tide Analysis

6.4.1 Details of the Analysis

A tide-by-tide analysis is the cycle-by-cycle analysis applied to water level data (see CO-OPS, 2003). Classically in the Coast and Geodetic Survey it was usually referred to as a “comparison of simultaneous observations” (*Manual of Tide Observations*, C&GS, 1965, page 58), although one could also compare observations from one station to the tide predictions at a nearby reference station, for the same time period. In the pre-computer era a special form was used, C&GS Form 248, which was titled: “TIDES: Comparison of Simultaneous Observations”. This analysis tended to be used only for short series of observations, the monthly mean analysis being typically used when there was a longer data time series. According to the above manual, “for series extended over longer periods, Form 657 for the comparison of monthly means will be found more convenient”. However, as will be seen in the next section, the tide-by-tide analysis has advantages over the monthly mean analysis, and in that pre-computer era it was probably its labor intensiveness that led to it being used only for short time series.

To begin a brief description is given about how the analysis was carried out using Form 248, since that procedure was essentially transferred to computer operation. Form 248 is shown in Figure 6.3. In the form there is one line for each half calendar day, and twelve values on each line. The first four columns are the times of high water and low water for the two stations being compared. The next two columns are the time differences between the high waters and between the low waters at the two stations. The last six columns are the equivalent for the heights of the high and low waters and the height differences.

6. Nonharmonic Analysis of Water Level and Current Data

The sums and means of all the time differences for high water and for low water are calculated and written at the bottom of the sixth and seventh columns. The sums and means for the heights and the height differences for high water and for low water are done separately for: higher high waters, lower high waters, higher low waters, and lower low waters. Further calculations in the spaces provided below the tabulation lead to calculation of mean high water height difference, the mean range ratio, the mean tide level ratio, the DHQ ratio and the DLQ ratio, and the high water interval and low water interval.

The tide-by-tide analysis has been computerized (see CO-COPS, 2003) and a short analysis using that program is shown in Figure 6.4. The analysis is straight forward, the only somewhat tricky parts being: keeping the respective cycles in sync at the two stations; allowing for cases where the tide goes diurnal; and dealing with distorted tide curves in very shallow water. It is also important to use of the same method for selecting the high waters and low waters, if possible.

6.4.2 The Benefits and Limitation of the Tide-by-Tide Analysis

As was seen in Section 3.6.3, the difference between the height of a high water at a subordinate station and the height of a high water at a reference station will vary throughout the month. This variation can be significant if the tidal characteristics of the two stations are not as similar as one would like it to be. Because of the hydrodynamics of the waterway, the further apart two stations are geographically the greater the difference in their tidal characteristics. But such distances need not be very great if the waterway has mixed tides with a strong diurnal signal. It is this mean difference in high water heights between the two stations that ends up in Table 2 of a Tide Table,

Figure 6.4. A short tide-by-tide analysis produced with a recent computer program. (From CO-OPS, 2003)

and which will be used to produce tide predictions at the subordinate station by modifying the tide predictions at the reference station. Since only the mean value of the difference is used, there will be errors at certain times of the month corresponding to those times when the height difference was different than the mean value (usually near maximum lunar declination in mixed tide areas, or during spring tides when there is a significant difference between springs and neaps, that is, when the effect of S_2 is large). This variation in high water height difference (as well as low water height differences, and the time difference for high water and lower) from cycle to cycle cannot be seen in a monthly mean analysis, since only monthly averages are produced and compared. However, the tide-by-tide analysis, as its name would imply, does show the cycle-by-cycle variation.

Stations in waterways with a significant diurnal inequality are usually the ones most poorly represented in Table 2 of the Tide Tables, especially if there are only one or two reference stations for that waterway. An example of this was given in Section 3.6.3 for the comparison of two tide stations in San Francisco Bay, where the tides are mixed and there is a strong diurnal signal (see Figure 3.5). If a tide-by-tide analysis is done on actual observed data, then the differences can result from the effects of nontidal influences such as wind, atmospheric pressure, or river discharge, as well as from changing astronomical conditions. Typically the differences due to nontidal influences will not be cyclical, whereas the cyclical nature of the changing astronomical conditions will stand out. However, to make very clear the effect of the changing astronomical conditions on the differences between two tide stations that do not have similar enough harmonic characteristics, the tide-by-tide analysis can be done on predictions for the two stations. Then the differences are solely the effect of changing astronomical conditions on the tide. This was done in Section 3.6.3.

Figure 3.6a shows a plot of the results of a tide-by-tide analysis, which exhibited significant variation in the time difference throughout the month between low waters at the two tide stations. Figure 3.6b showed a significant variation throughout the month in the height difference between low waters at the two tide stations. In each plot one sees the maximum differences a short while after maximum lunar declination. If the mean time difference and the mean height difference were put into Table 2 for the subordinate station, and then used to make predictions of low water at the subordinate station by modifying the times and heights of low waters at the reference station, then these maximum differences translate into prediction errors ranging from -0.44 hour to + 0.52 hours and from -1.11 feet to +0.69 foot. A new reference station for the subordinate stations in this waterway would thus be called for, and in fact, Port Chicago was added to the U.S. Tide Tables as a reference station because of the results displayed in Figure 3.6.

This analysis is probably the most important of all types of nonharmonic comparison analyses because it shows how the various differences and ratios vary from tidal cycle to tidal cycle. Thus, *this technique can be used for quality assurance analyses of subordinate stations in Table 2.*

However, the tide-by-tide analysis has one limitation. It deals only with high and low waters and does not provide any information about tidal heights in between the high and low waters. For data from deep-water stations this is not a problem, since the tide curve will look like a cosine curve. However, for shallow-water stations the tide curve is distorted away from a pure cosine curve by the nonlinear hydrodynamic effects. It can have a variety of shapes, often with more rapid rises to high water and slow falls to low water. In extreme cases there can be double high waters or double low waters. The only type of nonharmonic comparison analysis that could be provide this information would be a *mean tidal cycle analysis* (analogous to the rotary reduction analysis, Section 6.6). Such an analysis would chop up the water level times series into tidal cycles (based on, for example, the times of high water at a reference station), add them together, and average them. The resulting *mean tide curve* could be used for interpolating between the predicted high and low

waters, instead of using a cosine curve, which would provide erroneous values for a shallow-water station.

6.5 Reversing Reduction Analysis for Tidal Currents

The *reversing reduction analysis* is the cycle-by-cycle analysis applied to current data. Its name comes from the fact that this type of analysis was intended to be used on reversing tidal currents, that is, tidal currents that are bidirectional. In this case the tidal current flows upstream or into a bay (*the flood current*), reaches a maximum flood speed, then slows up until it reaches zero speed (*slack water*), then flows in the opposite direction going downstream or out of a bay (*ebb current*), reaches a maximum ebb speed, then slows up, again reaches another slack water, and reverses flow to the flood direction again. The tidal current speed curve for a reversing tidal current looks like a tide curve, with the zero speed (slack water) line serving the role of a datum, and with flood currents above that zero line (and considered positive) and ebb currents below the line (and considered negative).

However, only in the narrowest waterways are the currents truly reversing. In most cases the tidal current is *rotary* (see Section 6.6), but since the shape traced out by the end of the rotating current vector over a tidal cycle is usually elliptical (except in the open ocean where it is circular), with a clear maximum flood and maximum ebb, the current can still be analyzed as though it was reversing. (In such cases a tidal current speed curve as described above, with flood currents above the zero line and ebb currents below the zero line, will not smoothly pass through this slack-water line, because for such cases there is no real slack water, only minimum currents flowing perpendicular to the flood-ebb axis. Instead two plots are typically produced, one for the absolute current speed, and one for the current direction.) A rotary reduction analysis would be more appropriate, but before the computer era the reversing reduction was used instead because it was much less labor intensive to do by hand. Once computers came on the scene the opposite became true and rotary reduction analyses were predominantly done because that analysis was much easier to program for the computer. Each type of analysis has its benefits and drawbacks, and both really should be done when analyzing a current station.

6.5.1 Details of the Analysis

In a reversing reduction analysis key points are picked off from two time series of current data or tidal current predictions, specifically: maximum flood, maximum ebb, slack water (or minimum current) before flood, and slack water (or minimum current) before ebb. Time differences and speed ratios between corresponding key points (such as maximum flood) at the two current stations are calculated for each tidal cycle. Means for these time differences and speed ratios for each key point are calculated for the entire data record. These means should be close to those that would come out of a rotary reduction analysis, but the real benefit of the reversing reduction analysis is that it also allows one to see how the time differences and speed ratios vary throughout the month.

In the pre-computer era the reversing reduction analysis used was different in a couple of important details. The manual undertaking of this analysis used C&GS Form 451, shown in Figure 6.5 (taken from U.S. C&GS, 1950, page 54). This form had six columns, for the tabulation of the

Tidal Analysis and Prediction

times of slack before flood, strength of flood, slack before ebb, and strength of ebb (where "strength of" means the same as maximum), and for the speed and direction of the strength of flood and strength of ebb (on the form the word "velocity" was used for speed). On this form the reference station used was a tide station and so the times of high water and low water for each cycle were also tabulated in two of the columns. However, as was seen in Section 3.6, referencing a current station to a tide station can cause problems, because generally their tidal harmonic makeup will be different, but back when this form was used there were not many long-term current reference stations. Form 451 was modified in the 1960s to restrict the reference station to being a current station. Thus the two columns for the high and low waters were replaced with six columns for the reference current station, for the same six parameters as in the six columns for the subordinate current station. Both versions of Form 451 showed only time differences for each cycle; speed ratios were not shown for each cycle, and the mean maximum flood speed ratio and mean maximum ebb speed ratio between the two stations were calculated from the calculated mean flood speed and calculated mean ebb

CURRENTS: FLOOD, EBB, AND SLACK														
Station: Savannah (0.5 Mi. N 42° W of City Hall Dome), Savannah Re., Ga.														
Lat. 32° 05.2' N Long. 81° 05.9' W														
Acc. No. T 1863 Party of E. F. Hicks, Jr. Plotted on Chart No. 440 Station No. 19														
Times referred to Pred. Tides at Tybee Light, Ga. Time Meridians: (This Sta.) 75° W														
Velocities corrected for Pred. vels at Tybee Light, Ga. $f = 6.80/6.87 = 0.99$ (Ref. Sta.) 75° W														
DATE Year <i>no. d</i>	HW., LW. <i>h.</i>	TIME OF—				CURRENT INTERVALS				STR. OF FLOOD	STR. OF EBB			
		Slack Before F.	Strength of Flood	Slack Before E.	Strength of Ebb	Slack Before F.	Strength of Flood	Slack Before E.	Strength of Ebb	Direct Add. Tint	Velocity	Direct Mag. True	Velocity	
Pole Average Depth 7 feet	1934													
	May	7	2.3 8.8	11.5		(8.0)	2.7			0.8		(140) (1.8)		
			4.9 21.2	---	15.7	16.5 19.2	---	1.2	1.6	2.0	322	1.4	143 2.0	
			8	3.3 9.7	0.0 2.4	5.0 8.9	2.8	0.9	1.7	0.8	319	1.2	141 2.0	
			9	4.3 10.6	12.3 15.2	17.6 20.4	2.8	0.8	1.6	1.9	320	1.8	142 2.0	
				16.022.3							323	1.4	145 2.0	
			10	5.2 11.4	13.3 15.5	18.8 22.0	2.7	1.4	1.9	1.2	314	1.6	140 2.0	
					2.1 4.3	7.0	---	2.9	0.9	1.8	---	319	1.2	---
							Sums	16.5	6.3	10.5	7.2	1917	8.6	851 11.8
							Divisors	6	6	6	6	6	6	6 6
						Means	+2.75	-1.05	+1.75	-1.20	320	1.43	142 1.97	
						Gr. Intervals, reference station	6.66	0.54	0.34	6.56				
						this station	9.41	11.71	2.09	5.46	1.43		1.95	
						Mean current hour (MCH)			11.82					

<u>computation of mean current hour</u>		
Slack before flood	9.41 + 3.10	= 12.51 hours
Strength of flood		= 11.71 "
Slack before ebb	2.09 - 3.10 + 12.42	= 11.41 "
Strength of ebb	5.46 + 6.21	= 11.67 "
Sum.....		= 47.30 "
Mean current hour.....		= 11.82 "

<u>Velocity reduction</u>		
Best known mean range of tide at reference station.....		6.80 feet
Range for observational period at reference station.....		6.87 "
Reduction factor for tidal current..... $f = 6.80/6.87 =$		0.99
Observed tidal current at this station = $\frac{1}{2}(1.43 + 1.97) =$		1.70 knots
Corrected tidal current..... = $1.70 \times 0.99 =$		1.68 "
Nontidal current..... = $\frac{1}{2}(1.43 - 1.97) =$		-0.27 "
Corrected flood current..... = $1.68 - 0.27 =$		1.41 " "
Corrected ebb current..... = $1.68 + 0.27 =$		1.95 "

Form 451, Flood, ebb, and slack referred to tides.

Figure 6.5. An early version of Form 451, which was used in the pre-computer era to carry out a reversing reduction analysis of current data (from *Manual of Current Observations*, 1950).

6. Nonharmonic Analysis of Water Level and Current Data

speed for each station. Thus, there was no information about how the flood speed ratio or ebb speed ratio changed from tidal cycle to tidal cycle.

When the author of this book computerized the reversing reduction in the 1980s, he added this capability, thus allowing the reversing reduction to be able to serve a quality control function, by determining how much the time differences and speed ratios varied throughout the month, and thus how large errors would be in predictions made using the mean time differences and mean speed ratios that came from the analysis.

The basic reversing reduction analysis is very straightforward, but its accuracy and usefulness depends on having an accurate and consistent method for selecting maximum floods and ebbs, and minimums before flood and ebb, from a current data times series. A combination of sometimes noisy data and sometimes significant distortion by shallow-water effects made this analysis more difficult to program than the rotary reduction analysis (which did not need to pick maximum and minimums until at the end when the data had already been vectorially averaged into one mean tidal current curve).

The computerized version of the reversing reduction analysis was used to produce the plots shown in Figures 3.7 and 3.9 showing the differences in maximum ebb times for tidal currents in the Delaware River near Philadelphia relative to the reference tidal current station at the Delaware Bay Entrance. (The tides option in this program was also used to produced the plots in Figures 3.6a and 3.6b showing the difference in low water times and heights for tides at Port Chicago in San Francisco Bay relative to the reference tide station at Golden Gate Bridge.)

Figure 6.6 shows the tabular output from the computerized reversing reduction analysis, in this case for a current station at Kent Island in Chesapeake Bay relative to the reference tidal current station at the Chesapeake Bay Entrance. Only one page of tabular results is shown, with the first few tidal current cycles and the last few, plus the final mean results. One can see that the time of slack before ebb at Kent Island was on average 8.63 hours later than the time of slack before flood at the Chesapeake Bay Entrance, but that it could be as much as an hour later than that or an hour earlier (see also the plots in Figure 6.7). Thus, if +8.63 hours was used in Table 2 as a correction factor with which to produce tidal current predictions at Kent Island based on the (harmonically produced) tidal current predictions at the Chesapeake Bay Entrance, there would be certain times of the month where the Kent Island prediction could be off by up to an hour, either earlier or later. This is because Kent Island is too far from the Chesapeake Bay Entrance for the two stations to have similar enough tidal harmonic makeup. (And, in fact, in the Tide Tables, Kent Island is referenced to the much closer reference station at Baltimore Harbor Approaches.)

Another example of the results of a reversing reduction, this time for two current stations in San Francisco Bay (Carquinez Strait and Alcatraz-North Point) are given in Figures 6.8 and 6.9. The locations of these two stations are shown in Figure 3.5, along with their diurnal-to-semidiurnal ratios. The $(K_1+O_1)/M_2$ ratio at Carquinez Strait is 0.594, while it is 0.471 at Alcatraz-North Point, and the phase lag differences at the two stations differ by only 7° , yet one sees significant variation in the time differences and speed ratios between the two stations. In Figure 6.8 the difference in maximum ebb times at the two stations varies throughout the month, averaging 3.38 hours, but varying from a half hour smaller than that to a half hour greater. In Figure 6.9 the ratio of maximum ebb speeds at the two stations varies through the month, averaging 1.36, but varying from 0.77 to 1.86.

Tidal Analysis and Prediction

Predictions (2) from Secondary Station #121, Kent Island, Chesapeake Bay
 Predictions (1) from Reference Station #40, Chesapeake Bay Entrance

YEAR 1975	PREDICTIONS (2)								PREDICTIONS (1)								(PRED2-PRED1)				(PRED2/PRED1)		
	---- TIMES ----				Max. Flood	MAX. Ebb	---- TIMES ----				SPEEDS				TIME DIFFERENCES				SPEED RATIOS				
DATE	SBF	NF	SBE	MK	SPD DIR	SPD DIR	SBF	NF	SBE	MK	NF	MK	SBF	NF	SBE	MK	NF	MK	NF	MK			
JAN 1	4.5	7.3	10.0	1.3	.6 ***	-.7 ***	7.5	10.1	1.0	4.4	1.3	-1.6	8.60	9.37	9.17	8.72	.54	.38					
	16.1	19.5	22.7	13.1	.7 ***	-.6 ***	20.2	22.7	13.5	17.0	1.1	-1.6											
JAN 2	5.2	8.1	11.1	2.0	.6 ***	-.7 ***	8.5	11.0	2.0	5.4	1.1	-1.5	8.72	9.43	9.13	8.73	.55	.44					
	17.2	20.4	23.4	14.1	.6 ***	-.5 ***	21.1	23.7	14.3	18.0	1.1	-1.5											
Skipped over 361 days of output for this printout																							
DEC 30	.8	2.8	4.8	8.1	.3 ***	-.4 ***	3.0	5.8	9.5	.1	1.2	-1.4	8.50	9.30	8.48	7.98	.43	.29					
	11.0	14.9	18.7	22.3	.7 ***	-.6 ***	16.1	18.3	21.3	12.0	.8	-1.5	8.00	9.10	9.18	9.30	.58	.40					
DEC 31	1.6	3.6	5.9	9.1	.3 ***	-.4 ***	3.9	6.6	10.3	1.0	1.2	-1.5	8.55	9.35	8.58	8.10	.38	.27					
	12.0	15.8	19.5	23.1	.8 ***	-.6 ***	16.8	19.1	22.2	13.8	.8	-1.6	8.12	9.17	9.20	9.30	.67	.38					
YEAR 1975	PREDICTIONS (2)								PREDICTIONS (1)								(PRED2-PRED1)				(PRED2/PRED1)		
DATE	---- TIMES ----				N.F.	M.E.	---- TIMES ----				SPEEDS				TIME DIFFERENCES				SPEED RATIOS				
	SBF	NF	SBE	MK	SPD DIR	SPD DIR	SBF	NF	SBE	MK	NF	MK	SBF	NF	SBE	MK	NF	MK	NF	MK			
NO. OF OBS.		705	705	706	706		NO. OF OBS.		705	705	704	704	705	705	705	704	705	705	704	705			
MEAN		.50 ***	-.48 ***				MEAN		.83	-.26	8.63	9.18	9.06	8.74		.63	.38						
STAND.DEV.		.16 ***	.12 ***				STAND.DEV.		.29	.26	.52	.25	.21	.34		.12	.08						
MAXIMUM		.90 ***	-.30 ***				MAXIMUM		1.60	-.70	9.62	9.70	9.90	9.53		1.00	.63						
MINIMUM		.20 ***	-.80 ***				MINIMUM		.30	-.190	7.52	8.23	8.43	7.92		.33	.21						
SPRD RATIO FROM MEANS																							
CORRECTED MEAN		.59	-.56				(CORRECTION FACTOR = (1.03/(0.5*(.83 + 1.26)) = .99)																
REFERENCE STATION GREENWICH INTERVALS																							
SECONDARY STATION GREENWICH INTERVALS																							

Figure 6.6. Results of a computerized reversing reduction analysis for Kent Island, MD, relative to a reference station at Chesapeake Bay Entrance. Only 4 days from the 365-day analysis are shown, along with the results.

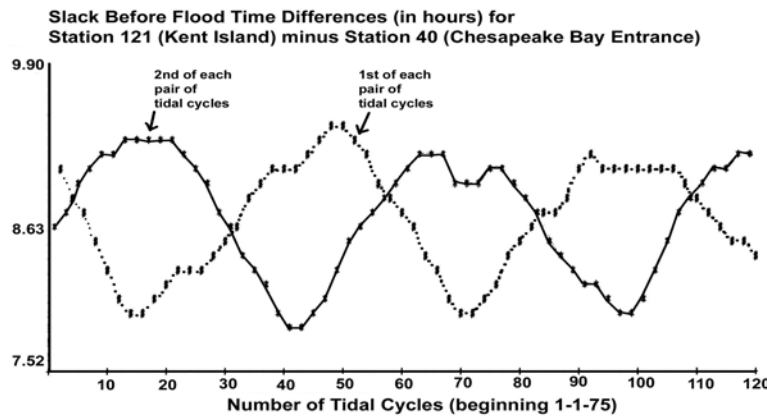


Figure 6.7. Plotted time differences between slack before flood at Kent Island, MD, and a reference station at Chesapeake Bay Entrance.

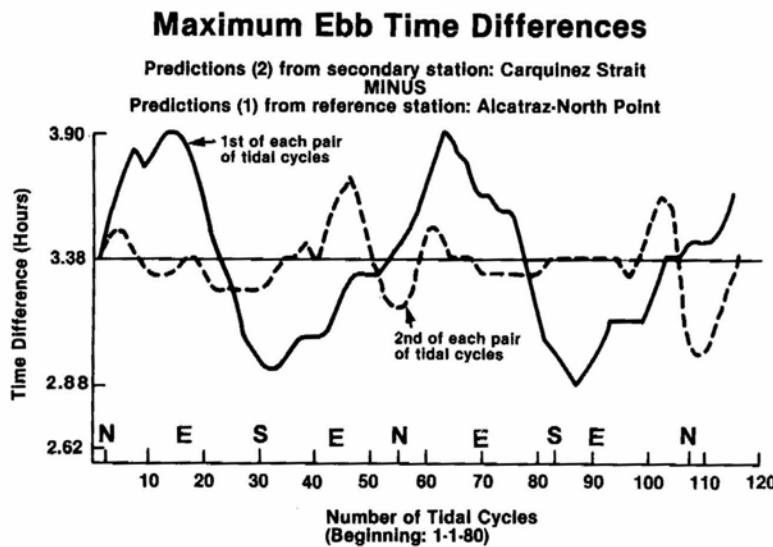


Figure 6.8. Plotted results from a reversing reduction analysis showing the time differences between maximum ebbs at Carquinez Strait and Alcatraz-North Point, both in San Francisco Bay. Along the horizontal axis, **N**=maximum northern lunar declination, **S**=maximum southern lunar declination, and **E**=equatorial lunar declination. (From Parker, 1991b.)

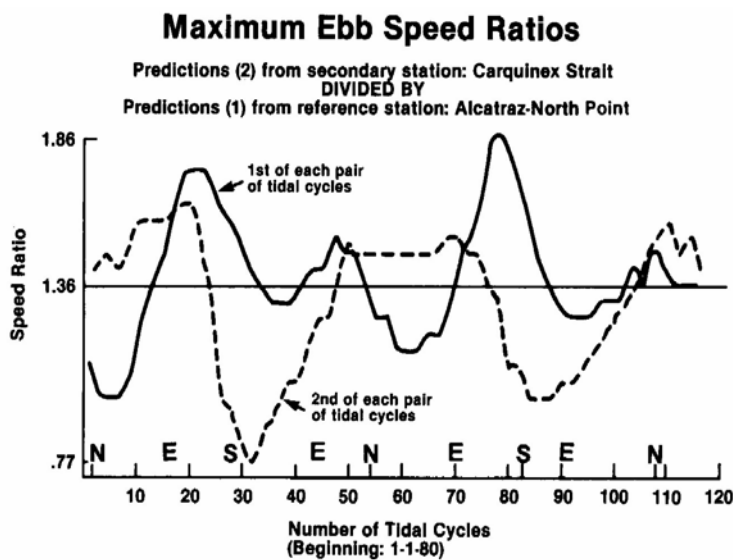


Figure 6.9. Plotted results from a reversing reduction analysis showing the ratio of maximum ebb speeds at Carquinez Strait and Alcatraz-North Point in San Francisco Bay. See Figure 6.8 for the meaning of **N**, **S**, and **E**. (From Parker, 1991b.)

6.5.2 The Advantages and Limitations of the Reversing Reduction Analysis

As mentioned earlier, the main advantage of using the reversing reduction analysis is that one can see cycle by cycle how the time differences and speed ratios vary throughout the month. This knowledge allows one to quality control the resulting mean values that come out of the analysis and that will be put into Table 2 of the Tidal Current Tables. Since these time differences and speed ratios will be used to make predictions for a subordinate station in Table 2 (by applying them to the daily predictions at the nearest reference station in Table 1), the reversing reduction analysis provides a quality analysis of those predictions. (The other nonharmonic comparison analysis used on tidal currents, the rotary reduction analysis, does not provide this capability.)

As discussed before, if the variation in the time difference and speed ratios (which equate to the errors one would see in the predictions using the mean time differences and mean speed ratios), is larger than acceptable (for a particular application, such a maritime safety) then one may need to establish a new (harmonically produced) reference station for this (and other nearby) subordinate current stations. However, if that is not possible, there is another possibility, using the results of the reversing reduction analysis. One can try to use these results to calculate additional types of mean time difference and mean speed ratio, for example, for times of maximum lunar declination. Such values might be added to the Endnotes for Table 2. If there are many subordinate in need of those additional time differences and speed ratios, one could even change the format of the Table 2 page (for those stations) to more efficiently handle it.

The reversing reduction analysis (like the tide-by-tide analysis) does have a limitation, which can be significant for shallow water areas. It deals only with the maximum floods and ebbs and the slacks, and cannot provide information on the currents in-between those points. Except for narrow waterways, the tidal current is rotary, with the tip of its current vector rotating around the compass in one tidal cycle and tracing out an ellipse. None of this information is captured in a reversing reduction. For offshore areas, this tidal current ellipse can even be circular, with no clear maximum flood direction and no clear maximum ebb direction. (Even in the pre-computer era, such ocean stations had to be analyzed using the rotary reduction analysis, done by hand.) Also, the tidal current in shallow waterways is distorted by the nonlinear mechanisms discussed in Sections 2.3.2 and 2.3.6. The tidal current speed curve in such areas does not look at all like a pure cosine curve. It can have short flood durations but with high speeds, and long ebb durations with lower speeds. It can have double maximum floods or double maximum ebbs. None of this information is shown by a reversing reduction analysis. Such information is, however, provided by the rotary reduction analysis described in the next section.

6.6 Rotary Reduction Analysis for Tidal Currents

6.6.1 The Benefits of Using the Rotary Analysis

The rotary reduction analysis (described briefly in Section 3.6.2) is a form of nonharmonic analysis that was originally used only for offshore current stations where the current was rotary, that is, where the direction of the current flow rotated completely around the compass over one tidal cycle. This can be represented by a current rose, but more often the tips of the moving current vectors are connected, and usually trace out an ellipse. For areas away from shore the ellipse is often almost circular, making it difficult to decide what to call the flood direction and what to call the ebb direction (which is the reason the rotary reduction analysis was used instead of the reversing

6. Nonharmonic Analysis of Water Level and Current Data

reduction analysis). Whether circular or elliptical, there are no slack waters. Current always flows in some direction. In locations where there is an ellipse, and for which there is an obvious flood and ebb direction, about half way between maximum flood and maximum ebb the current flows perpendicular to the flood-ebb direction and reaches a minimum speed. The narrower the ellipse the smaller the minimum current speed. (See Figure 2.4.)

In reality, most tidal currents are rotary, with only tidal currents in very narrow channels having true slack waters and being true reversing currents. The rotation of the Earth is the main cause of the rotation offshore, but geography and bathymetry also play a role especially within bays and estuaries.

Before computers, it took much more manual effort to carry out a rotary analysis than a reversing reduction, so rotary analyses were usually carried out only for offshore current stations where there were no obvious flood and ebb directions. Table 5 in each Tidal Current Table (see Section 9.3.3) is a special table for those offshore stations with rotary currents, where the speed and direction of current flow is provided for an entire mean tidal cycle in hourly increments (the time increment can be smaller if needed). Prior to 1972 all current stations put into Table 2 were analyzed using the reversing reduction.

The author of this book first computerized the rotary analysis in 1972. From that point on most current stations that were put into Table 2 were analyzed using the rotary analysis. There were several reasons for this change over.

First, although the rotary analysis took more time to carry out manually, ironically it was much easier to computerize than the reversing analysis (which would not be computerized for another decade, also by the author of this manual). The time savings in using a computerized rotary analysis instead of a manual reversing analysis were enormous.

Second, as mentioned above, all tidal currents are really rotary and the rotary analysis gives a better description of the current, showing the exact speed and direction of flow for every hour of the tidal cycle. The reversing analysis only gives the times and speeds of maximum flood and maximum ebb and the times of the (supposed) slack waters. It gives no information about what is going on in between those times. In the past if such information was wanted it was assumed that a cosine curve could be fitted to those four known points on the tidal current curve – which, in fact, was almost always an erroneous assumption and in shallow waterways dramatically so. After analyzing many current data records with the rotary analysis it became apparent that not only did the current rotate, but often the tips of the current vectors did not always trace out simple ellipses. As a result of the geography of the waterway and especially of the bathymetry, the shapes of the path traced out by the current vector tips could be quite varied, especially at locations where there were channel bends or where several channels met at the locations of the current station. Figure 2.4 shows some examples, including a station where a figure eight was traced out.

Third, for shallow-water areas the tidal current (even more than the tide) is distorted by nonlinear effects. The rotary analysis clearly shows this distortion because the result is an entire mean tidal current curve (not just maximum floods and ebbs and “slacks” as gotten from a reversing reduction). When the current speeds are plotted (like a tide curve) they rarely look like a smooth cosine curve, but are often flattened out in one phase (flood or ebb) and show a sharper peak in the other phase, or other times may stretch out the times of minimum flow significantly. In some cases there may be double floods or double ebbs. These are the same effects represented by the overtide tidal constituents (e.g., M_4 , M_6 , M_8 , and others) in a harmonic analysis. As was seen in Section 2.3.6, superposition of two tide waves can greatly enhance these overtide effects, as can the inertial effects seen at channel bends and in the sheltered areas near points.

Fourth, the rotary analysis is vastly superior for producing Tidal Current Charts. In the past, using a reversing reduction, the 12 charts representing the tidal current flow for each hour increment of a mean tidal cycle were determined by fitting a cosine curve to the maximum flood, slack before ebb, maximum ebb, and slack before flood for each current station. Thus, even in the widest part of a waterway, the tidal current was erroneously shown as being reversing, with the direction of flow represented as being exactly the same throughout the flood phase and then in the opposite direction throughout the ebb phase, and with speeds changing like a cosine curve from slack to maximum to slack. Only after the change over to using the rotary analysis did Tidal Current Charts show rotation of flow, the distortion due to shallow-water effects, and the effects of the bathymetry and geography.

6.6.2 The Limitations of the Rotary Analysis

The rotary analysis calculates the mean tidal current (speeds and directions at a specific time interval) for a mean tidal cycle, the average done for the length of the current data time series available. The main limitation of a rotary analysis is that one cannot see the variation from cycle to cycle throughout the month (and year). That variation is caused by whatever differences there are between the current station being analyzed and the reference station used to break up the current data times series into tidal cycles. If the reference has a very similar tidal harmonic makeup to that of the station being analyzed, this will not be a problem. Such cycle-to-cycle variations can, however, be seen with the reversing reduction analysis, and both types of current analysis should be carried out on every current station.

6.6.3 Details of the Analysis

In a rotary reduction analysis the current velocity time series is divided into tidal cycles, which are superimposed and vectorially averaged to produce a mean tidal current. To do the vectorial average all speeds and direction pairs are first converted to a major-minor component pair, such as north component and east component, or any other orthogonal pair. The resulting mean tidal current is plotted as both speed and direction curves (and can also be plotted as a polar plot with the equivalent of a current rose but with the tips of each vector are usually connected) covering one (mean) tidal cycle..

The division of the data time series into tidal-cycle pieces is usually determined by the times of a single key point in the tidal current cycle at the reference station, for example, the times of all the predicted maximum floods at the reference station that fall within the time period of the data (or the times of the maximum ebbs or of the slacks). However, using two key points, such as using the times of both maximum flood and maximum ebb, is also an option to be considered (which will be discussed in the next section). Each tidal current cycle of data is divided up into increments, which are typically half-hour intervals centered on (e.g.) the time of maximum flood at the reference station, designated here as MF, and each half hour after that, i.e., MF+ $\frac{1}{2}$ hour, MF+1, MF+1 $\frac{1}{2}$, MF+2,, MF+12. (The last interval may not be exactly a half hour, and this may vary from cycle to cycle.) Every data point in the time series will fall into one of these 25 time intervals. After all the data points have been assigned to a half-hour interval, an average current speed and direction is obtained for each of these intervals. The calculation is done vectorially, so first average major and minor components are obtained and then the averages are converted back into speeds and directions.

6. Nonharmonic Analysis of Water Level and Current Data

At this point a vectorial *mean current* for the entire mean tidal cycle is obtained by averaging the 25 half-hour increment values. This mean current, being only for the that particular period of time, requires careful interpretation (discussed in the next section) as to whether it will be incorporated into the final values that are turned into time and height difference for inclusion in Table 2 of the Tidal Current Tables. Next this mean current is subtracted from each of the 25 individual current values covering the tidal cycle, to produce a *tidal-only* current, which again is usually plotted.

The next step is to compensate for the fact that the data times series does not usually cover a time period long enough for all the tidal frequencies to be equally represented. Thus, some type of correction must be made to the analysis results to make them more closely represent the values that would be obtained from a full-year analysis (or actually from a full 19-year analysis, that also eliminates the varying affects of the lunar node). In this step the analysis takes all the speeds of (e.g.) the reference station's maximum floods during the time period of the data from the subordinate station and averages them. Then the true 19-year mean maximum flood speed value for the reference station is divided by this reference station average for the time period of the data to produce a correction ratio. This ratio is then used to multiply all 25 of the tidal-only speed results, to give a *corrected tidal-only* result. Then the mean current is vectorially added back in to give a final *total current*. This total current is usually plotted, both on speed and direction plots, and on a polar plot, the latter being the equivalent of a current rose but with the tips of each vector connected, so one can easily see how the flow rotates. This polar plot makes the most sense for interpretation purposes if it is superimposed on a chartlet showing the current station location and the bathymetry.

At this point the analysis picks off the values from the mean tidal current curves for maximum flood, maximum ebb, minimum before flood, and minimum before ebb, providing a time, speed and direction for each. In the case of a double flood or ebb, it will also pick off the time, speed, and direction for that also.

In NOS the method presently used for the maximums is as follows. For most cases, the maximum flood and ebb are each determined using a parabolic fit to the 3 highest current speed values. If 3 or more speed values are within 5 cm/sec (0.1 knot) of the highest value, then the curve around the maximum value is fairly flat, and in such cases the time of maximum flood (or ebb) is chosen to be the midpoint of this flat interval. The direction of the maximum flood (or ebb) is the average of the directions for the speed values used in the previous calculation. The method presently used for determining the minimums before flood and ebb begins by finding the five current vectors which vectorially are closest to zero. The minimum current vector is the shortest vector perpendicular to one of the four lines connecting the tips of these five current vectors. One should always examine the calculated maximums and minimums and compare them with the linear and polar plots.

The final step is to determine the Greenwich Intervals for the maximum flood, maximum ebb, minimum before flood, and minimum before ebb for the analyzed stations. Those values are known for the reference station and are input into the rotary analysis program. The results of the analysis give the times of these four points of the tidal current with respect to one of these reference times at the reference station, so the Greenwich Interval for that point in the tidal current at the reference station is simply added to the four times from the rotary analysis to produce the Greenwich Intervals at the subordinate station. If the analysis results are to be used in Table 2 of Tidal Current Tables, then the time differences to go into Table 2 are obtained by subtracting the Greenwich Intervals of the reference station from the Greenwich Intervals of the subordinate station.

Tidal Analysis and Prediction

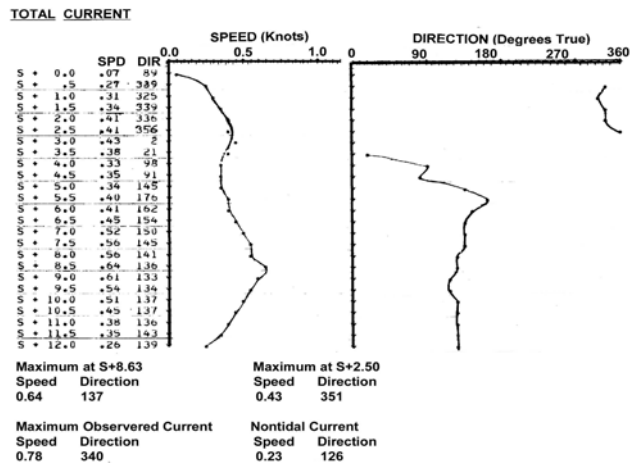


Figure 6.10a. Speed and direction plots of the total current (tidal current plus mean current) resulting from a rotary reduction analysis of current data from Boston Harbor (Station 6 at 10 feet below the surface, May 28 – June 1, 1971). Times are relative to the slack before flood (S) at the reference station (Deer Island Light).

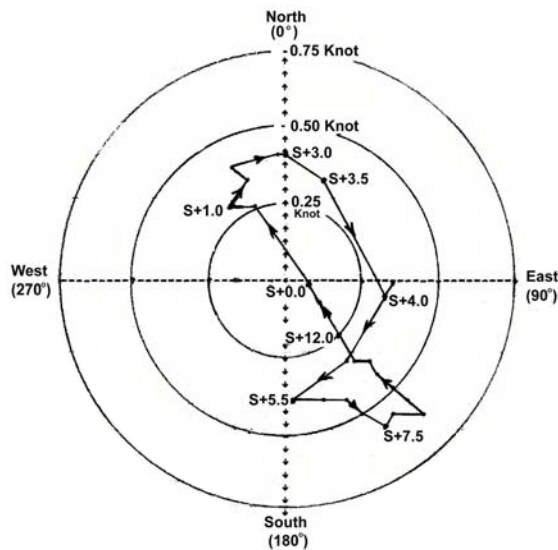


Figure 6.10b. Polar plot showing the rotation of the total current (tidal current plus mean flow) resulting from the same rotary reduction analysis as in Figure 6.10a. Each hourly current vector would be an arrow from the center of the plot to a dot labeled with a time relative to S. Note that the tidal current rotates clockwise from S+11.5 to S+4.5, but counterclockwise for the rest of the tidal cycle.

The plotted results of a typical rotary analysis are shown in Figures 6.10a and 6.10b. Figure 6.10a shows the speed and direction plots for total current (i.e., tidal current plus the mean nontidal flow for the period of the data). In this example the (harmonically) predicted times of slack before flood (S) at the reference station were used to break up the current data time series into tidal cycles. Thus the half hour intervals of the analysis go from S+0.0, S+0.5, S+1.0,, to S+12.0 hours. For each of these 25 half hour intervals a speed and direction are plotted. Below the plots are shown the time (relative to S), speed and direction of the maximum flood and maximum ebb, as well as the maximum observed current data point for that period of the data, and the mean nontidal current, also for the period of the data. In the particular plots shown in Figure 6.10a one sees that the ebb phase lasts much longer than the flood phase, which is due to the mean nontidal current.

Figure 6.10b shows these same results on a polar plot. Here one can get a better idea of the direction in which the current flows, and how that direction changes over a tidal cycle. This particular example shows that the current does not necessarily rotate as a simple ellipse. Here the tip of the current vector actually traces out a figure eight, which is due to the geography (shoreline, channels, and bathymetry) of the location of the current station. The mean nontidal current has shifted the center of the figure away from zero.

6.6.4 Special Considerations and Choices To Be Made For the Rotary Analysis

6.6.4a Editing Out Data During the Analysis

Current data can be quite noisy, but the averaging process of the analysis can take care of most real and reasonable noise. Extreme outliers that do not look real will usually be taken care of in the quality control part of the data processing procedure prior to being analyzed with the rotary method. However, within the rotary analysis itself there is the option to edit out data determined to be bad by some criteria. One of two methods is typically used.

The first method edits out speeds and directions separately. (This method is justified for some current meters that measure speed and direction separately.) Speeds are thrown out where the speed is outside some range (typically two standard deviations from the calculated average speed for the interval). Directions are thrown out in a three-step process, first all directions more than 90° from the average direction for the interval, then after recalculating the average direction, the process is repeated for 60° and 45°. If more than 80% of the directions in an interval are thrown out, that interval is flagged (for narrow current ellipses this often happens near times of slack water since the direction of flow changes rapidly around that time).

The second editing method removes velocity outliers vectorially in a two-step process. All current velocity values that are beyond a certain distance vectorially from the average current vector for an interval are removed. That distance value is initially the absolute value of the average current speed, and then after recalculating the average current vector the distance is half the absolute value of the average current speed. This method tends to be used for low signal-to-noise currents. Near times of slack water it generally throws out less than 80% of the values.

6.6.4b Selecting the Start and Stop Times For the Analysis

It is important to use a whole number of tidal cycles in the analysis, especially for short analyzes, where the fragment of a tidal cycle could bias the results. One should determine the largest number of whole tidal cycles that can fit within the time period of the data, and analyze that many cycles,

selecting what appears to be the best quality data (leaving data off at the end or at the beginning, or some off from both the beginning and end.)

6.6.4c *Selecting which aspect of the tidal current (maximum flood, maximum ebb, or slack/minimum) to use to divide up the data record into tidal cycles*

The most likely value to be adversely affected by an erroneous rotary analysis (for example, when one uses a reference station that is not similar enough in tidal characteristics) are the speeds of the maximum floods and ebbs. The time shifts in the data for each superimposed tidal cycle do not significantly hurt the calculation of the minimums, or even the times of the maximums, but they can make the maximums smaller than they should be. The true average maximum flood or ebb will come out of the analysis only if all the individual maximums line up in time perfectly with each other. (This is a problem that does not occur in the reversing reduction, since the actual maximum flood and ebb values are chosen to be averaged.) Thus, it is usually preferable to use reference times (to break up the data time series into tidal cycles) that will put all the maximum floods in the same half-hour interval. This often means that the maximum flood times and/or the maximum ebb times are best to use as the reference point for the analysis.

If one chooses to use the times of maximum flood and there is some variation in the length of the tidal cycle, then while the maximum floods (or each tidal cycle) are likely to line up with each other fairly well, the maximum ebbs will be less likely to line up with each other, and the result will be a smaller mean maximum ebb speed than should be. Thus, it may actually be better to use both the maximum flood (MF) times and the maximum ebb (ME) times, and have two reference times per tidal cycle, to try to minimize the time shifting around the two maximums. In this case one might have for example, MF-3, MF-2½, MF-2, MF-1½, MF-1, MF-½, MF, MF+½, MF+1, MF+1½, MF+2, MF+2½, and MF+3, and likewise for maximum ebb. If there ends up being 26 intervals, then there will likely be some overlap between MF+3 and ME-3, which will have to be worked out.

6.6.4d *Selecting the Size of the Time Intervals Used in the Analysis.*

The most typical selection of time interval for a rotary analysis is to use 25 half-hour intervals to cover the tidal cycle. The 25th interval will usually vary in length, often being less than a half-hour. If two reference points are used per tidal cycle (such as maximum flood and maximum ebb) then the intervals near the change over from flood to ebb may vary in size. The length of the time intervals, however, does not have to be a half hour and can be varied as desired, depending on the sampling interval of the current data time series. However, it should be remembered that the wider the interval the more the average maximum flood and ebb will be reduced by the analysis (especially if the rise to the maximum is steep) because slightly smaller values near each actual maximum in the data will be included in the interval average.

It is very difficult to accurately represent a mixed tidal current with the rotary reduction analysis, because with a mixed tidal current the length of the duration of the flood phase and the duration of the ebb phase will vary from tidal cycle to tidal cycle, sometimes significantly. To try to make this method work for the diurnal situation, one must not use a constant time interval, because for this situation this will cause some half-hour segments to be in the flood phase during part of the data and in the ebb phases during other parts of the data. As an alternative scheme, one can instead divide the duration of flood phase into the same number of interval (and likewise the duration of the ebb

phase), no matter what the length in time of the flood (or ebb). Then, each interval will vary in width, but will always represent the same portion of the flood (or ebb) phase. To break the data up into flood phases and ebb phases, one can use the slack (minimum) times at the reference station. However, if the subordinate and reference stations are too far apart, using the reference station slack times may not break up the subordinate station appropriately. In this case, one might try to break up the subordinate station time series using its own slack(minimum) times. Whether this will help better represent the varying diurnal inequality of the mixed tidal current will have to be looked at closely. It cannot work when a mixed tidal current goes diurnal for part of the month.

6.6.4e Interpreting the mean nontidal current from the analysis

The rotary analysis provides a mean nontidal current value for the time period of the particular data time series analyzed. The mean current value for another data time series from that location might be quite different. It depends on what caused the mean flow. In a river or estuary the mean flow could be due to river flow. River flow varies considerably over the year, from high values during spring runoff to low values during the summer. The mean flow might also be due to the wind, in which case, it will vary significantly with time.

There are, however, situations where the geography of the waterway (for example a point jutting out into the waterway, or a bending channel) causes tidally-induced eddies to occur (sometimes only during one phase of the current). This results from a nonlinear lateral inertial effect (see Section 2.3.6). When averaged over a tidal cycle, the result is a mean current. Such mean currents are fairly permanent, and being tidally induced should be included in the final total current of the rotary analysis. An example of such tidally induced mean currents is shown in Figure 2.35.

6.7 Selecting a Reference Station

It is important to select a reference station with similar tidal characteristics. While for tide stations it is usually enough to select a geographically close station, this is not always the case for tidal currents. The frequency characteristics of tidal currents can change dramatically over a short horizontal distance, as a result of bathymetry and the shape of the shoreline. Channel bends and points jutting out into channels can (via nonlinear inertial mechanism, see Section 2.3.6) transfer diurnal energy into the semidiurnal band and transfer semidiurnal energy into the quarter diurnal band, e.g., in the latter case, from M_2 to M_4 (see Figure 2.35), which will make the time differences and speed ratios between two stations vary considerably throughout the month.

One should also not use a tide station as a reference station for a tidal current analysis without careful consideration. In many areas the type of tidal current can be quite different than the type of tide. For example, in the eastern end of the Strait of Juan de Fuca, where it meets Haro Strait the tide is mixed mainly diurnal and the tidal currents are mixed mainly semidiurnal.

When the tidal characteristics are different, one will see changing differences between, for example, successive times of maximum flood, which will make the superimposed tidal cycles in a rotary reduction analysis have a variety of lengths. In that case, the mean maximum flood may still come out of the analysis with reasonable accuracy, but the mean maximum ebb velocity will probably come out smaller than it should (because all the individual maxi ebbs were shifted in time relative to each other). As was discussed, the use of a reference station with tidal characteristic not similar to those at the subordinate station will show up clearly in a reversing reduction analysis, but it will not be apparent in a rotary reduction analysis.

To try to select the best reference station, carry out the following steps: (1) identify the nearest reference stations that might be used; if analyzing water level data, choose a reference tide station; if analyzing current data, choose a reference tidal current station; don't refer a current station to a tide reference station, or vice versa; (2) compare the harmonic constants at the station to be analyzed (if available) with the harmonic constants at the candidate reference stations; (3) select the reference station with the most similar harmonic constant relationships, that is, with ratios of $(K_1 + O_1)/M_2$, M_4/M_2 , S_2/M_2 , etc. that are most similar, as well as phase lag (epoch) differences, e.g., $\frac{1}{2}(M_2^o - K_1^o - O_1^o)$, that are most similar. If there is a reasonably strong diurnal signal, then the $(K_1 + O_1)/M_2$ ratio should be given precedence, since that ratio will change more quickly with geographic distance between the two stations. However, M_4/M_2 ratios for tidal currents can vary significantly from location to location, and this overtide effect can shift the time of maximum flood and/or maximum ebb significantly; and (4) if no harmonic constants are available for the station to be analyzed, initially choose the reference station that is closest geographically (however, if one is analyzing a current station, the closest reference station geographically may not be the one with the most similar harmonic constants; if possible, do not choose a reference station that is in a different channel, or around a bend or on the other side of a point of land).

6.8 Putting a Subordinate Station In a Tide or Tidal Current Table and On a Tidal Current Chart

Today the two primary uses for a nonharmonic comparison analysis are for the inclusion of a subordinate station in Table 2 of a Tide or Tidal Current Table (or sometimes in Table 5 of a Tidal Current Table) and for the construction of Tidal Current Charts. Based on what has been learned in this chapter, the use of nonharmonic analyses for these purposes is briefly summarized.

Putting a subordinate station in Table 2 of a Tide Table has been fairly routine for decades. For many water level stations there are many years of data, numerous harmonic analysis results, and numerous results of monthly mean analyses. Only the limited pages allowable in a Tide Table prevents most tide stations from becoming (harmonically predicted) reference stations in Table 1. The standard procedure for putting the mean time and height differences of one of these stations into Table 2, is merely to use the differences between corresponding monthly mean analyses from the subordinate station and from the reference station. However, for short tide stations, the tide-by-tide analysis (usually called "Comparison of Simultaneous Observations") has been used to find the mean time and height differences. This last analysis has typically also shown the time differences for each tidal cycle (although until recently the height differences for each cycle were not shown) and so one could see how much they varied from cycle to cycle.

As quality control, to make sure that the subordinate tide station is referred to a reference tide station with similar enough tidal characteristics, and to calculate the expected error in predictions made with the mean time and height differences, one should run a tide-by-tide analysis on the subordinate station. One should make sure to tabulate all the height differences (and not just the time differences) for each tidal cycle.

Putting a subordinate station in Table 2 of a Tidal Current Table has in the past been done by either using the reversing reduction analysis or the rotary reduction analysis (see previous sections for the circumstances under which each was used). In reality both methods should be used, because each has a unique benefit that one should take advantage of. The rotary analysis will provide entire mean tidal current curves (a speed curve, a direction curve, and a polar plot) for a mean tidal cycle. Thus, one will not only have mean values for maximum flood, maximum ebb, slack (minimum)

before flood, and slack (minimum) before ebb, but one will be able to see the complete rotation of the tidal current over the whole tidal cycle, plus any nonlinear distortions due to shallow-water or lateral inertial effects. It will also provide the time differences and speed ratios that will go into Table 2. For current stations off the coast, where the current ellipse widens out to a circle, and thus where there are no clear flood or ebb directions, one can put all the hourly (or half-hourly) results from the rotary reduction analysis into Table 5 of the Tidal Current Tables.

What the rotary reduction analysis does not tell us is how much variation there will be in the time differences and speed ratios throughout the month (and how similar the tidal characteristics of the tidal current are at the two stations, subordinate and reference). This information must come out of the reversing reduction analysis, which is used for quality control purposes. This analysis tells us what kind of errors one can expect in the tidal current predictions made with the above mean values put into Table 2. This is especially important for currents, for as was seen, there are many nonlinear hydrodynamic mechanisms (but especially the lateral inertial effect) that can cause a great deal of variability in the harmonic makeup of currents stations, even ones that are geographically close to each other (see Section 2.3.6).

If the variation in the time differences and speed ratios (which equate to the errors one would see in the predictions using the mean time differences and mean speed ratios) is larger than acceptable (for a particular application, such a maritime safety), then one may need to establish a new harmonically produced reference station for this (and other nearby) subordinate current stations. If that is not possible, one might try to use the results of the reversing reduction analysis to calculate additional types of mean time difference and mean speed ratios, for example, for times of maximum lunar declination. Such values might be added to the Endnotes for Table 2. If there are many subordinate stations in need of those additional time differences and speed ratios, one could even change the format of the Table 2 page (for those stations) to more efficiently handle it, for example, adding columns to handle the extra time differences and speed ratios for the maximum declination situation.

It should be added that sometimes the mean values for maximum floods and ebbs and slacks (minimums) that come out of the two types of analysis (rotary and reversing) are not exactly the same. Most likely the mean maximum flood and ebb speeds obtained from the rotary reduction analysis will be a little smaller than those obtained from the reversing reduction. That is because the maximum values in the rotary reduction are obtained by averaging over half-hour (or worse, hour) intervals, so some speeds lower than the actual maximum get included in the calculation. The difference between the rotary value and the reversing value is usually not great, but when one has both, one should probably use the values from the reversing reduction.

For constructing a set of Tidal Current Charts for a waterway, the rotary reduction analysis is the best nonharmonic comparison method to use (such charts can also be produced with numerical hydrodynamic models, or with tidal current predictions from harmonic constants). Only the rotary reduction analysis can give the current speed and direction for each hour (or half-hour) of the tidal cycle. This is discussed in more detail in Section 9.4.

6.9 Minimizing the Errors Due to the Variations Throughout the Month Of Nonharmonically Determined Time and Height Differences

When producing a Tide or Tidal Current Table the intention is to have enough reference stations so that no subordinate station is forced to be associated with a reference station whose tidal characteristics are dissimilar enough that significant variations in time differences and other

differences or ratios will occur. However, this may not always be possible. In mixed tidal regimes the reference stations need to be closer because the diurnal-to-semidiurnal ratios change more quickly with distance than do the ratios between two semidiurnal constituents. The phase differences between the K_1 's and O_1 's, respectively, at two stations, have a significant effect on the average (essentially M_2) time differences. In addition, shallow-water generated distortions in the tide or tidal current (the effect of M_4 in particular) may shift the times of (e.g.) high water or maximum flood around during the month, also leading to variations in time differences between two stations.

Tidal currents have an additional problem. The lateral advective (inertial) terms in the conservation of momentum equation (see Sections 2.3.6 and 7.3.2), which generate tidally induced residual currents off points and around channel bends, also shift energy into the next harmonic, changing the K_1/M_2 ratio or the M_2/M_4 ratio in the tidal current. The area around the San Juan Islands, including the Strait of Juan de Fuca, Haro Strait, and many other connecting waterways, provides an example (see Figure 2.35). A combination of the large diurnal inequalities and the inertial effects due to the complex geometry lead to tidal current characteristics that can change dramatically over a short distance. While the K_1/M_2 ratio for the tide changes gradually and smoothly in this area, the K_1/M_2 ratio for the tidal current varies considerably (see Parker, 1977).

Even though there are six reference stations in the NOS Tidal Current Tables for the Strait of Juan de Fuca – Haro Strait – San Juan Islands area, there are times during the month when the tidal current at some subordinate stations will become diurnal a day earlier or later than at the reference station, making it almost impossible to make a prediction using a Table 2 correction. Even at times of the month when both reference station and subordinate station have not become diurnal, there is significant variation in time differences and speed ratios. For such situations one really needs several sets of time differences and speed ratios for each tidal parameter in Table 2 — for example, one set for maximum southern declination, one set for equatorial lunar declination, and one set for maximum northern lunar declination.

There may also be subordinate stations in the Tide or Tidal Current Tables which are associated with an inappropriate reference station merely because their relationship was not examined closely enough. It is not enough that two stations are both semidiurnal or that their harmonic constituents look similar. It is also not enough that two stations are geographically close, especially in the case of current stations, where two stations right around a channel bend or on opposite sides of a point, can have different tidal characteristics.

At each subordinate station variation in time differences and height differences throughout the month should be calculated and compared against an accepted standard.

6.10 Summary Overview: Steps In Analyzing Water Level or Current Data With a Nonharmonic Comparison Method

In this section the steps to take in nonharmonically analyzing a water level or current data times series will be summarized. Sections where more information can be found are in [] at the end of each step. These steps, in bullet form are:

6. Nonharmonic Analysis of Water Level and Current Data

- (1) identify the nearest reference stations that might be used; if analyzing water level data, choose a reference tide station; if analyzing current data, choose a reference tidal current station; don't refer a current station to a tide reference station, or vice versa. [Section 6.7]
- (2) compare the harmonic constants at the station to be analyzed (if available) with the harmonic constants at the candidate reference stations; [Section 6.7]
- (3) select the reference station with the most similar harmonic constant relationships, that is, with ratios of $(K_1 + O_1)/M_2$, M_4/M_2 , S_2/M_2 , etc. that are most similar, as well as phase lag (epoch) differences, e.g., $\frac{1}{2}(M_2^{\circ} - K_1^{\circ} - O_1^{\circ})$, that are most similar. If there is a reasonably strong diurnal signal, then similarity in the $(K_1 + O_1)/M_2$ ratio should be given precedence, since that ratio will change more quickly with geographic distance between the two stations. However, M_4/M_2 ratios for tidal currents can vary significantly from location to location, and this overtide effect can shift the time of maximum flood and/or maximum ebb significantly.
- (4) if no harmonic constants are available for the station to be analyzed, initially choose the reference station that is closest geographically; (however, if one is analyzing a current station, the closest reference station geographically may not be the one with the most similar harmonic constants; if possible, do not choose a reference station that is in a different channel, or around a bend or on the other side of a point of land) [Section 6.7]
- (5a) *for water level data*, if one intends to use a mean monthly analysis, one should still also run at least a month-long tide-by-tide analysis (comparison of simultaneous observations) in order to assess the size of the variation throughout the month in the time differences between high waters (and also between low waters) at the two stations, as well as the height differences; [Section 6.3 and 6.4]
- (5b) *for current data*, if one intends to use a rotary reduction analysis, one should still also run a reversing reduction analysis in order to assess the size of the variation throughout the month in the time differences between maximum floods (and also between maximum ebbs, and between slacks) at the two stations, as well as the speed ratios. [Section 6.5]
- (6) if the variation in these differences throughout the month, as determined by a tide-by-tide analysis of water level data or a reversing reduction analysis of current data, is large (according to a criterion based on the intended users of the resulting tide or tidal current predictions) then there are three options with regard to including the subordinate station(s) in the Tide or Tidal Current Tables: [Section 6.8 and 6.9]
 - (a) use another reference station that might have a more similar harmonic makeup;
 - (b) establish a new reference station from a suitable nearby long-term station; or
 - (c) use the tide-by-tide analysis (for tides) or the reversing reduction analysis (for currents) to calculate mean time and height differences or speed ratios for special astronomical conditions (such as maximum lunar declination), and put these in the Endnotes section for Table 2; or if there are many stations with this problem, reformat a Table 2 page with extra columns to handle these additional values;
- (7a) *to get a full picture of the tidal current*, one should use both a reversing reduction analysis and a rotary reduction analysis on the current data series; the rotary analysis will capture the rotation in the tidal current flow, as well as any distortions in the shape of the tidal current curve due to shallow-water effects or lateral inertial effects, and the reversing analysis will capture the variation in time differences and speed ratios throughout the month; both are important; Table 2 Endnotes may have to be used to indicate such occurrences as double max floods or ebbs, longer than normal periods of slack water (or minimum flow), flattened maximums, and/or variations in the time differences and speed ratios over a month etc.; if

- the current ellipse is very wide, the station might have to be put in Table 5; if the current data is being analyzed for a Tidal Current Chart, one must always use a rotary reduction analysis, since values are required for each hour of the tidal current cycle.
- (7b) *to get the full picture of the tide*, one should usually carry out (at least initially) a month-long tide-by-tide analysis (along with the numerous mean monthly analyses that will routinely be carried out) to show the variation in time differences and speed ratios throughout the month; if the water level data is in shallow water, one should also carry out (at least initially) a one-month mean tide curve analysis (analogous to the rotary analysis in currents) from which information about the average distortion of the tide can be ascertained (including possible double high or low waters); the results of these analyses can be included in a Table 2 Endnote for the station. [Section 6.9]

7 Interpretation of Tidal Analysis Results Based On Hydrodynamics

The accurate prediction of the tide or tidal current, though a major objective of tidal analysis, is not the only objective. Another important goal is to obtain a better understanding of the hydrodynamics of a waterway. This may in turn allow one to improve the analysis or better implement a numerical hydrodynamic model, which then ultimately could produce better predictions. Although tidal analysis results are used to understand the tidal dynamics of a particular waterway, the opposite can also be true – a basic understanding of tidal hydrodynamics in a variety of waterways can help one better interpret and quality control the tidal analysis results from a newly surveyed waterway. For example, the calculated harmonic constants should change spatially over this waterway in a way that makes sense with respect to hydrodynamics.

In this chapter, therefore, the tidal hydrodynamics of a waterway will again be looked at, but this time in more detail. There may be some redundancy with Section 2.3 and with some parts of other sections in this book, but those sections were meant to provide just enough hydrodynamic background to allow one to make the best choices when statistically analyzing the tides and tidal currents. Now the hydrodynamics will be looked at more thoroughly (and mathematically) in order to help in the interpretation of the results of the statistical analysis.

In this chapter some simple analytical models will be used to illustrate typical variations in tide and tidal current characteristics for a variety of conditions and situations. Analytical models, though representing simple special cases in basin shape and depths (which is the reason the equations of motion can be solved analytically rather than numerically) have the advantage of being able to illustrate many cases simply by changing parameters in one or two formulas. To accomplish the same thing with a numerical hydrodynamic model, one must rerun the model many times. However, use of a numerical model is unavoidable when dealing with nonlinear effects (such as in shallow waterways) or dealing with complicated geometries, neither of which can be solved analytically.

7.1 *Products for Showing Tidal Analysis Results*

Prior to looking at what analytical models can tell one about the tidal hydrodynamics of a waterway, a few typical ways of graphically displaying tide and tidal current analysis results will be looked at.

7.1.1 Cotidal, Corange, and Coamplitude Charts

A corange tidal chart is nothing more than a group of contour lines representing different tide ranges throughout a waterway. Each corange line is a line of constant tide range. These corange lines can be for the total tide, or they can be for single tidal constituent, such as M_2 , in which case

sometimes the tidal constituent amplitudes (half the constituent ranges) are contoured instead of the ranges. An example of a corange chart for the M_2 tidal constituent was shown in Figure 2.5 for the Strait of Juan de Fuca - Straight of Georgia based on the harmonic analysis of 95 tide stations along that waterway (Parker, 1977). Another example of a corange chart, for Chesapeake Bay, was shown in Figure 2.24.

A cotidal chart is nothing more than a group of contour lines representing different hours (or phase lags) of high water throughout a waterway. Each cotidal line is a line of constant phase lag or of constant high water time, relative to the same time meridian (usually the local time meridian, but sometimes the Greenwich time meridian). These cotidal lines can be for the total tide, or they can be for single tidal constituent. An example of a cotidal chart for the M_2 tide was shown in Figure 2.6.

One more example of cotidal and coamplitude lines is given in Figure 7.1 for Delaware River and Bay, in this case for M_2 again. In this figure the coamplitude (half the tide range) and cophase lines are put on the same chart, with the actual values at each tide station (the black dots) also given. Because the upper part of the waterway is so narrow, there are contour lines only in the lower bay. The phase lags relative to the local time meridian can be converted to hours after moon transit over that time meridian by dividing by 360° and multiplying by 12.42 hours. In this figure one sees that it takes 193° or 6.7 hours for high water to move from the bay entrance to the head of tide near Trenton, NJ. (These M_2 results will be referred to in later sections of this chapter.)

When one has harmonic analysis results from a sufficient number of water level stations along a waterway and one wishes to produce cotidal and corange (or coamplitude) charts for the total tide and/or for various tidal constituents, one begins by putting the ranges and high water times, or the constituent amplitude and epoch (i.e., phase lags), on the chart at the exact locations of the water level stations. Then one must decide how best to draw the contours to represent the entire tide regime based on these results at these particular locations. The more water level stations one has, of course, the easier this job is. But even when there are many stations, those stations will be mainly along both shorelines, as well as on whatever islands may be available, and so the middle of the waterway is usually not well covered. For a narrow waterway where Coriolis does not have much of an effect, drawing (the short) contour lines will be straight forward, and one is basically left with interpolating between neighboring stations to determine where to put the lines. However, for wider bays one must consider the fact that the contour lines will likely cross the waterway at an angle due to effect of Coriolis (see Sections 2.3.1 and 7.5). With enough stations (and especially with some stations in the middle of the waterway, e.g., on islands or structures) one may still be able to obtain the correct angles. If there are not enough tide gauges on both sides and/or the waterway is long enough to have a quasinode (a location of minimum tide range where the tide range is larger both up the waterway and down the waterway from that location), then one may need the help of a hydrodynamic tide model to help decide how to angle the lines.

A second problem occurs in deeper waterways, where the ranges and time of high water (or the constituent amplitudes and epochs) may change too slowly over geographic distance. For this situation the construction of the chart may put demand a level of accuracy from the harmonic analysis results that may not be attainable if one has to rely on many stations that are less than six months long. In other words, the results from these short tide stations will (because of their shortness) have various errors (unless all the stations happened to be installed over the same time period, which is usually unlikely) that will make it difficult to determine accurate contour lines. In Section 4.2.2 a reference station approach was used to improve the results from short harmonic analyses, so that coamplitude and cophase charts could be produced. This method was, in fact, used to construct the charts in Figures 2.5 and 2.6 (and other charts found in Parker, 1977).

7. Interpretation of Tidal Analysis Results Based On Hydrodynamics

The creation of cotidal and corange charts is a form of quality control of the harmonic constants for the stations in a waterway, because these constants must make sense with respect to each other over space. If the harmonic constants from a particular station do not seem to make sense relative

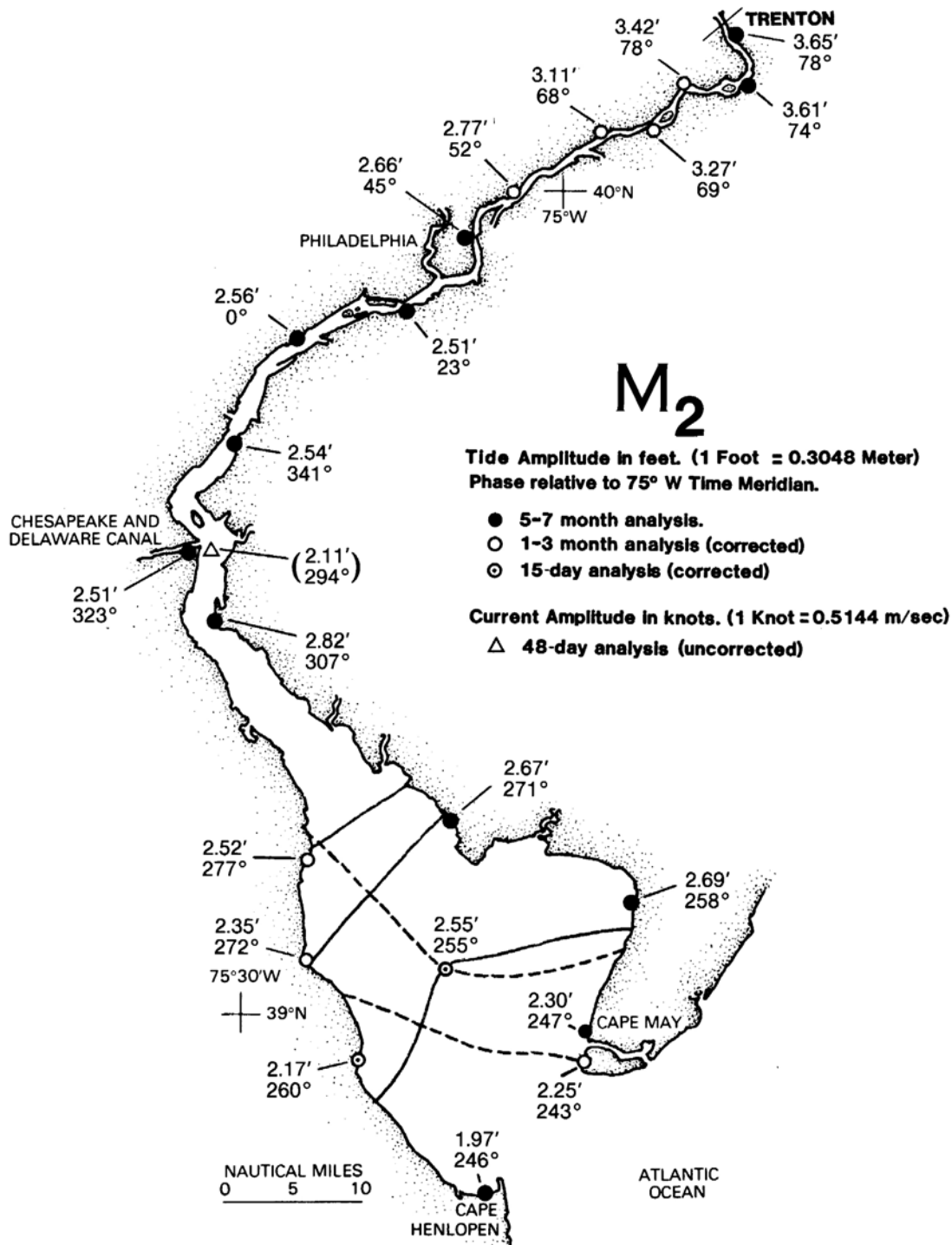


Figure 7.1. Coamplitude and cophase chart for the M_2 tide constituent for the Delaware River and Bay, showing the geographic variation in M_2 amplitude and epoch (phase lag). Coamplitude lines are dashed; cophase lines are solid. (From Parker, 1984.)

to the harmonic constants at surrounding stations, there either may be a problem with the data from that station, or the results are actually good and one must figure out the hydrodynamic cause of the observed variation over space relative to the other stations. These results will help verify hydrodynamic models (analytical or numerical), and likewise the models will then help us understand the tidal analysis results.

Later in this chapter it will be seen how a number of simple analytical models, as well as more complex numerical models, explain how the tide and tidal current are likely to vary over space and time for a variety of different conditions, such as different basin depths, widths, length, and shapes.

Corange and cotidal charts also have other practical uses. Some form of them (whether hardcopy or in some electronic form) are normally used for carrying out hydrographic surveys, where the depth soundings made during the survey must be adjusted so that they are referenced to chart datum, which in the United States is mean lower low water (MLLW). This will be discussed more in Section 8.7.2, because tide models now play an important role for this application.

7.1.2 Cospeed and Cophase Charts

Cospeed and cophase charts for tidal currents in a waterway are much more difficult to produce, and often end up not looking like their tide equivalents. This is because so many factors can affect the speed amplitude and phase lags of the tidal current constituents that there is often so much spatial variability among the results from the current stations that it is impossible to produce meaningful contour lines. This is especially true for waterways with bends, sudden-width changes, and variable bathymetry, since the tidal current speeds and phase lags are very sensitive to such changes. Current sensors are often at different depths, and current speeds and lags are very depth dependent. Tidal current speeds will be much faster in a narrow entrance (because of continuity) compared with the speeds outside the entrance (see for example, the very long tidal current ellipses in Figure 7.3 in the next section).

Current station data time series are also frequently short, on the order of only 15 to 30 days, and correction using a reference station is often difficult or impossible, because there are few long-enough current stations, and those that are long enough may not have similar enough tidal characteristics. Thus, one will often see just the values at the specific current stations put on the charts, with no contour lines. For example, Figure 7.2 shows the cophase chart for the M_2 tidal current in the Strait of Juan de Fuca – Strait of Georgia. Only in the western end of the Strait of Juan de Fuca were cophase line attempted. In the rest of the waterway the phase lags (epochs) from the harmonic analyses were so variable in space that no such lines could be attempted. This variation is primarily due to the effect of the lateral inertial nonlinear terms described in Sections 2.3.6 and 5.1.

7.1.3 Tidal Current Ellipses

Tidal current ellipses were described in Section 5.2 with a sample result for several tidal current constituents from a single current station showed in Figure 5.4. Placing many such ellipses on a chart of the waterway at the locations of the current meters can provide insights into the dynamics of the tidal currents in that waterway. Such an example is provided in Figure 7.3, which shows numerous M_2 ellipses (from Parker, 1977) for the eastern end of the Strait of Juan de Fuca, Haro and

7. Interpretation of Tidal Analysis Results Based On Hydrodynamics

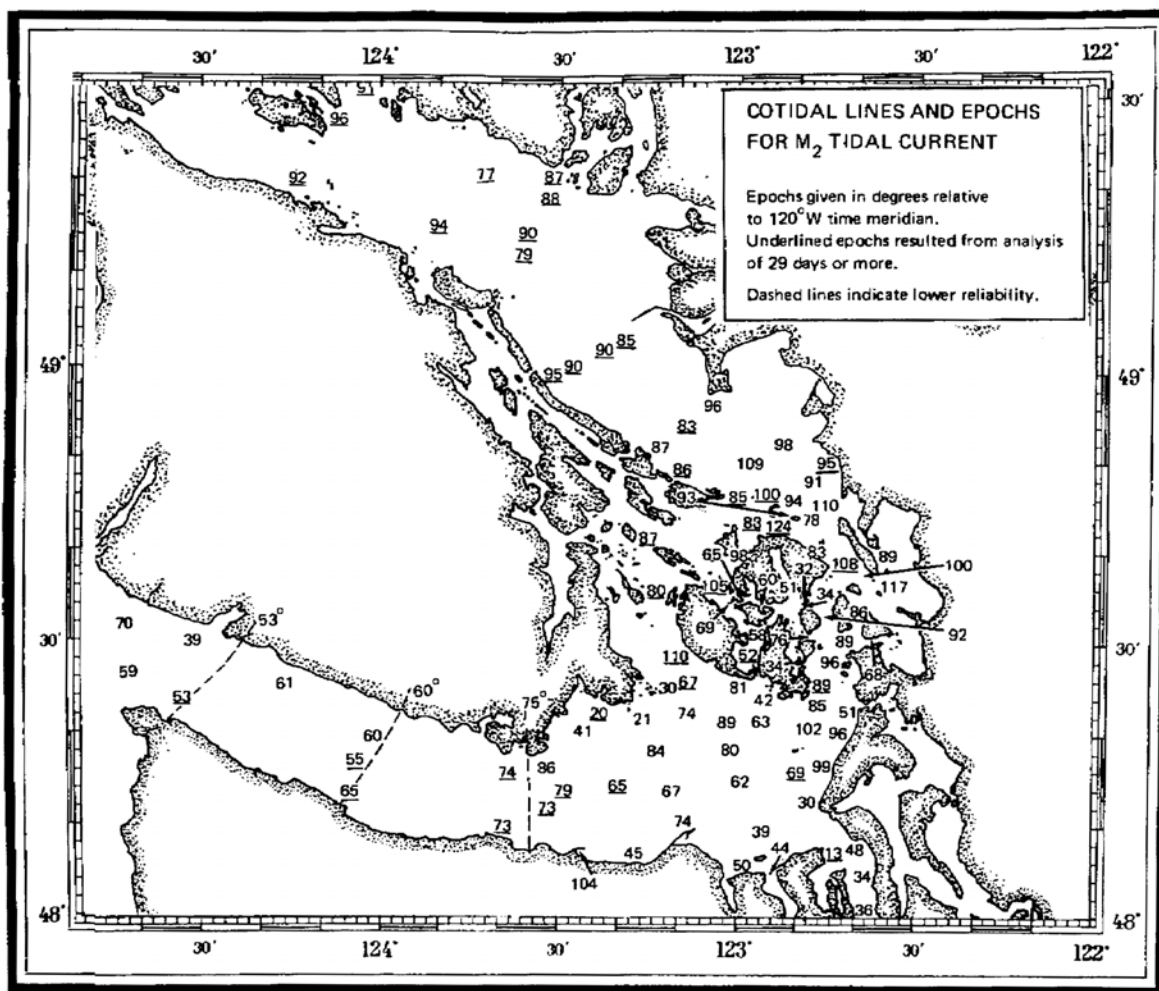


Figure 7.2. Chart with epochs (phase lags) for maximum flood for the M_2 tidal currents in the Strait of Juan de Fuca – Strait of Georgia, given in degrees of phase lag relative to the local time meridian (120°W).

Rosario Straits, and the southern end of the Strait of Georgia. All the ellipses are drawn to the same scale, so longer ellipses indicate higher M_2 maximum flood and ebb speeds. For each ellipse, connecting the center dot to the dot for a particular hour indicates the speed and direction of the tidal constituent for that hour of the constituent cycle. Zero hour indicates the lunar transit over the local time meridian (in this case 120°W). For ellipses that are wide enough for the rotation of the tidal current to be clear, one can see whether that rotation is clockwise or counterclockwise by looking at the hour numbers. The hour number at the end of the major axis of the ellipse that comes after the zero hour is the hour of maximum flood current (relative to 120°W).

Most the current data analyzed to produce this chart were measured at 70 feet below MLLW (because the current meters were mounted from bottom-mounted tautline buoys). Looking at the many ellipses shown in this figure, one can see a great deal of variability in their length, width, time of maximum flood, and direction of rotation. There are very long narrow ellipses in narrow and channels and in small entrances. The M_2 flood-ebb orientation tends to follow the geography or the bathymetry. Wider ellipses tend to be in wider parts of the waterway, but not always. The wide



Figure 7.3. Numerous M₂ tidal current constituent ellipses for the eastern end of the Strait of Juan de Fuca, the southern end of the Strait of Georgia, and around and between the San Juan Islands. See key on chart, and the text. For the flow for a particular hour of the M₂ cycle, draw a vector from the center of the ellipse to the dot with the number of the hour of the cycle. Note the different directions of rotation of the flow and the different degrees of narrowness of the ellipses.

ellipse just south of Victoria, BC is probably affected by the lateral inertial effects of the channel bending north into Haro Strait (see Section 2.3.6 and 5.1). The timing of each M_2 maximum flood can vary quite a bit from station to station, due to differing water depths, as well as due to the lateral inertial effects of channel bends, points sticking out into the waterway, and other geographic effects. The majority of the ellipses show a clockwise rotation, but there are also some that are counterclockwise (lateral inertial effects again probably playing a role in this, but bottom friction may also play a role). Some of this variation may be the result of the short data time series (from different time periods) harmonically analyzed to produce the ellipses (most of the current stations analyzed only had 15 to 29 days of data). The possible causes of the variability in tidal currents will be described in the following sections of this chapter (see also Section 2.3.6).

7.1.4 Various Types of Graphs

For wider waterways, corange and cotidal charts created from harmonic analysis results may be most useful for visualization of the tide regime over the waterway and for comparison to numerical models results, but for a narrower waterway a simple plot of (e.g.) the tide ranges along the length of the waterway may be just as useful. For example, Figure 7.4 shows the variation in tide amplitude (half the tide range) for the five largest semidiurnal constituents in Delaware River and Bay – M_2 , N_2 , S_2 , $2MN_2$, and $2MS_2$. The M_2 values are the same as those on the coamplitude chart in Figure 7.1 (and the values for the other four constituents can be found on corange charts in Parker, 1984). Clearly M_2 is the dominant constituent, being much larger than the other four semidiurnal constituents. One also sees that in the lower bay (which is wider) the tidal amplitude is higher on the right side of the waterway (looking up the estuary) due to the Coriolis effect.

More useful is Figure 7.5, which shows the amplification of these same five constituents (i.e., for each constituents each amplitude value is divided by the amplitude value at the entrance). Here M_2 has an amplification of 1.7 at Trenton, but N_2 and S_2 have smaller amplifications (approximately 1.3 and 1.4, respectively) and $2MN_2$, and $2MS_2$ have much greater amplifications (5 and 6, respectively). Other plots from Parker (1984) show K_1 with even less amplification than N_2 and S_2 , and M_4 and M_6 with even larger amplifications than $2MN_2$, and $2MS_2$. The reasons for these differences in amplification will be explained in Section 7.6.2. The shallow-water constituents $2MN_2$, and $2MS_2$ have the same frequencies as the astronomical constituents L_2 and μ_2 , and the original harmonic analyses may have had L_2 and μ_2 listed as the constituents being solved for, but these amplification plots would have clearly indicated that $2MN_2$ and $2MS_2$ were the actual constituents being calculated by the analysis.

There are, of course, many other graphs of various statistical analysis outputs that can be useful, including frequency domain plots of the harmonic constants, various spectra, EOF analysis results, and graphs from various nonharmonic analyses (such as the rotary and reversing reductions).

7.2 Spatial Variation in Tidal and Tidal Current Parameters In a Waterway Due to Hydrodynamic Processes

Throughout physical oceanography (and geophysics in general) data analysis and dynamical modeling go hand in hand and complement each other. A model is a mathematical representation of the particular laws of physics that are believed to govern the specific dynamics with which we are concerned. The data (and the data analysis results) are used in that model to see how well that

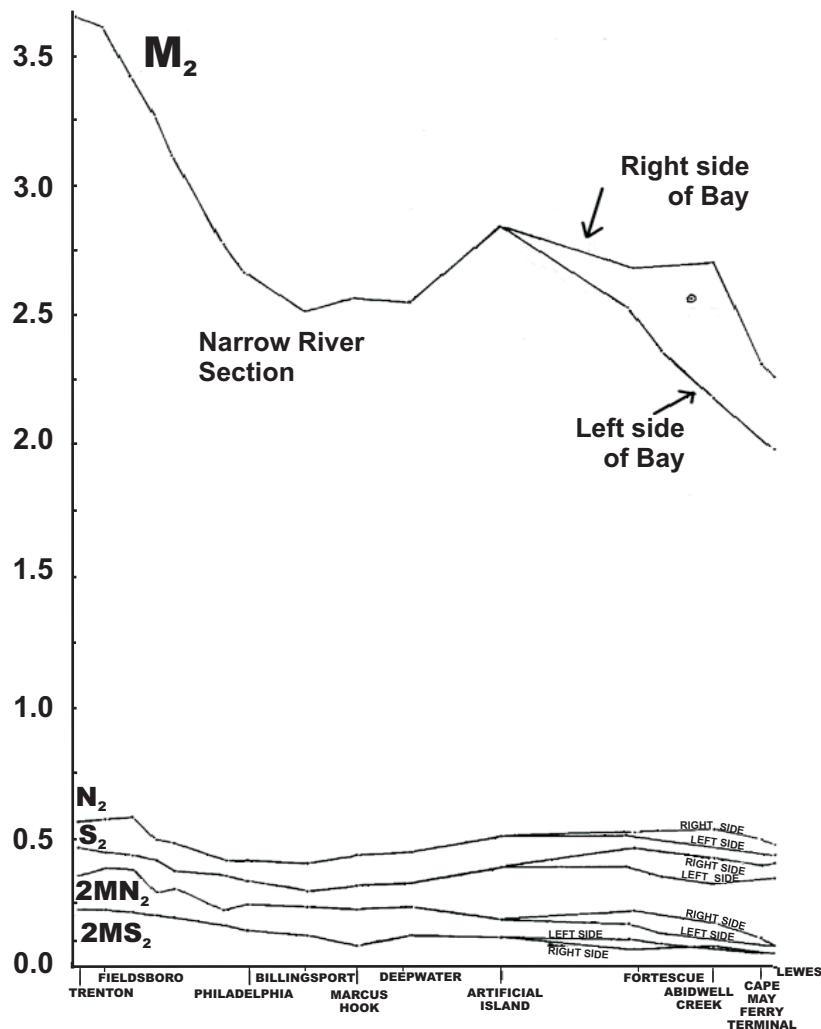


Figure 7.4. Variation in the amplitude (half range) of the five largest semidiurnal constituents in the Delaware River and Bay, from the ocean entrance on the right to the head of tide on the left. (From Parker, 1984.)

model can describe that particular dynamic phenomenon and how well it can make predictions. Once a model has been validated using the data, it can in turn be used to better understand the data. It can provide values at locations where there are no data. And it can provide better insights with regard to how the data should vary over space and time. Models can provide synoptic pictures of tide regimes that can help us understand our data analysis results. It can, in fact, provide some quality assurance with regard to the results of our harmonic or nonharmonic tidal analyses, for example, giving one an idea whether harmonic constants at a particular station look reasonable relative to harmonic constants found at other nearby stations. Hydrodynamics can help one answer questions like, how do we expect the M_2 amplitude or epoch to change along a particular waterway, or how do we expect the M_4/M_2 ratio or the K_1/O_1 ratio to change with distance?

Hydrodynamic models can provide insights about the how the tide regime varies in different types of waterways. In this chapter many of these models will have been greatly simplified by using an idealized geometry or by ignoring a particular aspect of the physics (such as the nonlinear terms), but the features they demonstrate usually are a good first approximation and for some (no too shallow) waterways, they can even fairly accurately represent the tide. The advantage of these

7. Interpretation of Tidal Analysis Results Based On Hydrodynamics

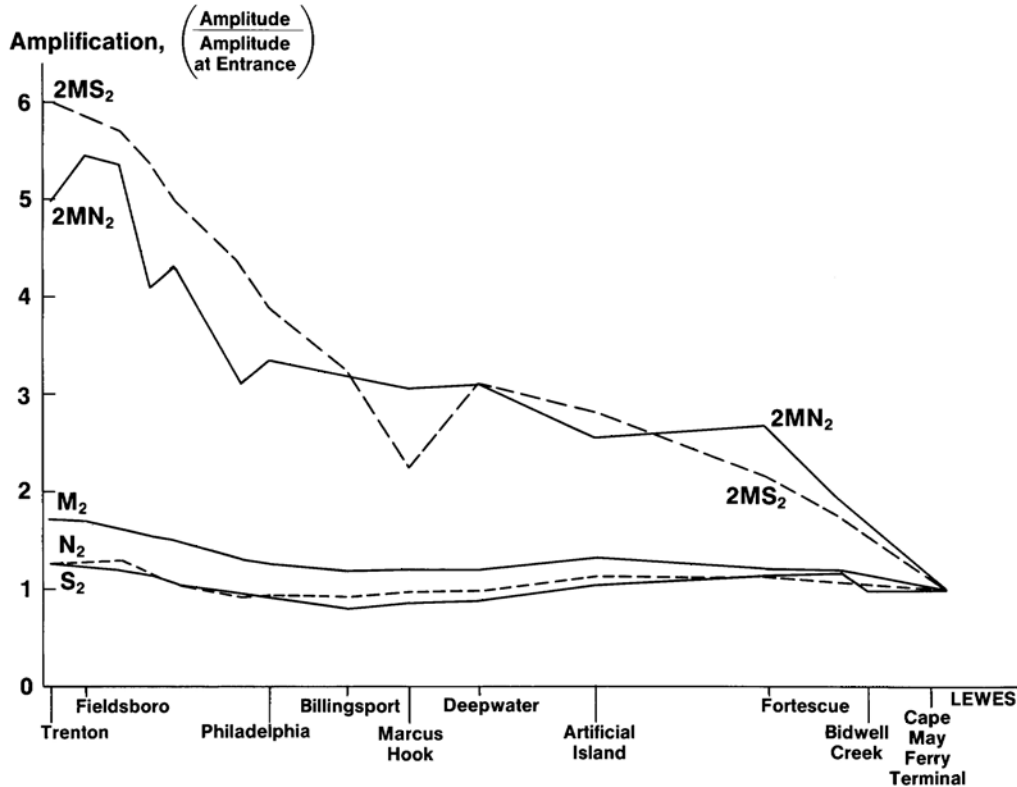


Figure 7.5. The amplification of the five largest semidiurnal constituents in the Delaware River and Bay. M_2 , N_2 , and S_2 are astronomical constituents, while $2MN_2$ and $2MS_2$ are compound constituents generated by nonlinear mechanisms in the shallow water (see text). (From Parker, 1991a.)

simple models is that they can be solved analytically, with the resulting solution being one or more formulas, which can then be used to directly provide information about the tide or tidal current over a whole waterway for a whole host of situations. Incorporating the more complete physics requires fully nonlinear numerical solutions, often with high-resolution grids. The analytical models allow us to easily see how the tide or tidal current changes for different water depths, frictional dissipation, etc. by simply changing a few parameters in the formulas. The numerical models, while much more accurate, require rerunning the model many times to be able to summarize the different cases.

One way to interpret the results of a tidal harmonic analysis is to see whether those results make sense within a synoptic description of the tidal hydrodynamics of the waterway from which the analyzed data came. Even if one is analyzing data from a particular waterway for the first time, and expects to describe the tidal hydrodynamic system in that waterway for the first time (assuming one has enough stations to do so), there will be certain expectations (based on the physics of the waterway) of how the various tidal harmonic constituents should vary in horizontal (geographic) space, and in vertical space (i.e., with depth) when looking at tidal currents. However, the use of such information, primarily from tidal hydrodynamic models, can only be carried so far from a quality control point of view, since the data analysis results are usually meant to validate a model, rather than the other way around. Models can be of all varieties and levels of resolution and accuracy, and thus may not provide the detail or accuracy to finely quality control the analysis results, especially if one is interested in tidal current analysis results (knowing how quickly such results can change with distance; see Section 2.3.6). But as an approximate indicator of quality

control, this tidal hydrodynamic understanding from models can point out large errors in analysis results. Simply from the standpoint of better understanding what a waterway can do to the tide wave that enters it from the ocean, it is important to understand what such models can tell us. The following sections of this chapter are a more detailed extension of what was described in Section 2.3, but with reference to the equations of motion (on which the various models are based, to different degrees of approximation), which will be discussed next.

7.3 The Equations of Motion As the Basis for Tidal Hydrodynamic Models

Tidal models are mathematical representations of the physics of the waterway that affect the tide and tidal current (which are two manifestations of the same phenomenon, one vertical one horizontal). They make use of conservation equations that are usually referred to as the *equations of motion*. These equations are derived based on the assumptions that mass (or volume) and momentum must be conserved, as well as energy in some cases, with additional equations of state if one includes salinity and water temperature effects. The various tidal models that will be looked at in this chapter will each involve some kind of simplification of these equations of motion (such as ignoring certain nonlinear terms), and their analytical solution will usually be made possible by using some kind of idealized geometry for the waterway (e.g., a rectangular basin). Numerical solutions, however, will also be used in Section 7.6 when looking at nonlinear effects.

Derivations of the basic original equations of motion (before being simplified for particular cases) will not be given here, but some key information will be provided about where the equations came from, as well as references where one can go to see the derivations. These are partial differential equations. If the reader lacks experience with advanced calculus it will hopefully not be too much of a liability because the physical meaning of these equations will be described. The final outcome, at least for the analytical solutions, will be fairly straightforward formulas.

7.3.1 The Equation of Continuity

The *conservation of mass* is described by the following equation:

$$\frac{\partial \rho}{\partial t} + \frac{\partial(\rho u)}{\partial x} + \frac{\partial(\rho v)}{\partial y} + \frac{\partial(\rho w)}{\partial z} = 0 \quad . \quad (7.1)$$

where t is time, x , y , and z are the three orthogonal dimensions in space, ρ is the water density (mass per unit volume; a scalar quantity) and u , v , and w are the three orthogonal components of the current speed (a vector quantity). [For those not familiar with partial differential equations, one can simply think of the $\partial \rho / \partial t$ as a change in density over a small time interval. Similarly $\partial(\rho u) / \partial x$ can be thought of as a change in mass over a small distance in the x direction.]

The visualization typically used in the derivation of this equation is to picture a cubic box (as a control volume) with water flowing through it, such as in Figure 7.6. The second term in equation (7.1) is the difference between the mass flowing into the box (in the x -direction) through one face of the box and the mass flowing out of the box through the opposite face (and likewise for the y and z directions). The first term in equation (7.1), the change in density with time, will go up if more mass enters the cube than leaves the cube, and vice versa.

Here, for simplicity, one assumes that the density remains constant everywhere and for all time.

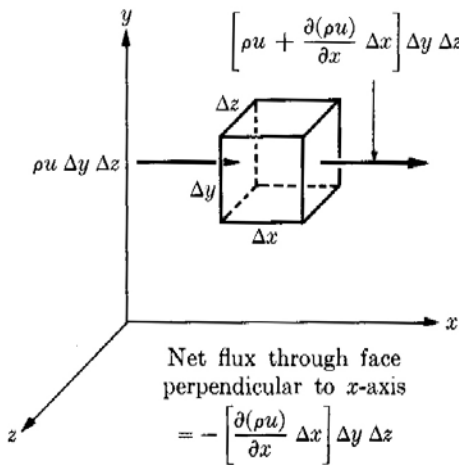


Figure 7.6. A cubic control volume used in deriving the conservation of mass equation. (From Daily and Harleman, 1966.).

Then equation (7.1) reduces to the basic *continuity equation* (which now really represents a conservation of volume):

$$\frac{\partial \mathbf{u}}{\partial x} + \frac{\partial \mathbf{v}}{\partial y} + \frac{\partial \mathbf{w}}{\partial z} = 0 \quad . \quad (7.2)$$

(There is actually a less drastic assumption that will also lead to equation (7.2), i.e., the assumption that water is incompressible. This is approximately true for water, but is not true for air and so cannot be used when the fluid dynamic equations are applied to the atmosphere.)

7.3.2 The Momentum Equations

The *conservation of momentum equation* comes from Newton's second law, $\mathbf{F} = \mathbf{ma}$, i.e., force (F) equals mass (m) times acceleration (a). *Momentum* is mass times velocity, so \mathbf{ma} is actually the rate of change of momentum. To obtain a momentum equation useful in a tidal model, Newton's second law is put into a different form, where the rate of change of momentum is balanced with the various forces that may be acting on the water (such as gravity and friction).

To visualize the derivation of this equation one can again use a cube as a control volume, and look at how various changing forces on a cube (similar to the one in Figure 7.6) will affect the rate of change of momentum of the water moving through the cube. There are pressure forces pressing in on the cube due to the effect of gravity (i.e., the pressure due to the weight of the water above it) as well as shear stress forces rubbing on the faces of the cube (due to such things as the effect of bottom friction, or the wind stress from the water surface, both transmitted through the water, from water particle to water particle). One usually deals again with density (ρ) instead of mass, and one makes another simplifying assumption in order to more easily handle ρ in the equations. The so-called *Boussinesq Approximation* says that one can ignore small changes in density except as it affects the weight/pressure of the water. This lets one divide all the terms in the momentum equation by ρ , so that the acceleration is being balanced by changing forces divided by mass.

At this point, in order to jump quickly to a momentum equation usable for our purposes (and skipping many steps, which can be found in the references), use will be made of several geometric assumptions dealing with the length scales of the waterway and the length scale of the tide wave in

the waterway. If one does a scaling analysis of the equations of motion, and some of these length scales are disparate from each other, then one will see that certain terms will be much smaller than others and so can be left out of the equations, greatly simplifying them, and making them easier to solve.

For example, since the tide wave is a very long wave, one can make the assumption that its wave length (λ) is much greater than the water depth (D). When this is the case ($\lambda \gg D$) the vertical acceleration (of moving water particles) will be negligibly small and the third of the three momentum equations will be greatly simplified (see below). As a result of this assumption, the change in pressure in the vertical direction will be due solely to the effect of gravity on the water (i.e., the deeper one goes the greater the pressure will be due to the weight of the water above). This is usually referred as either the *long-wave approximation* or the *shallow-water approximation* or the *hydrostatic approximation*. Other length-scale based simplifications will be seen in later sections.

Another length-scale assumption doesn't eliminate any of the terms, but does have another benefit. One assumes that the length of our waterway is much smaller than the radius of the Earth, and this allows the use of Cartesian coordinates instead of (the much more cumbersome) spherical coordinates.

And finally (to skip one more step in the derivation of the equations below) a shift is made from a fixed reference frame (relative to a distant star in outer space) to a reference frame that rotates with the rotating Earth. The result of this transformation of the equations to a rotating reference frame adds terms to the equations that represent an *apparent* force, i.e., the *Coriolis force*. The Coriolis force appears to push moving objects to the right in the Northern Hemisphere and to the left in the Southern Hemisphere (relative to a fixed reference frame, however, those objects would still move straight and the Earth would turn under it; see Parker, 1998). The slower the motion of the object and the longer distance it goes, the more it pushed to the right (or left). The Coriolis force increases from zero at the equator to a maximum near the north or south pole. However, for simplicity, it is assumed that the waterway is small enough that one can ignore the variation in the Coriolis force with latitude. This is the so-called *f-plane approximation* (where $f = 2\Omega \sin \varphi$ and φ is the latitude and 2Ω is the planet vorticity of the Earth, i.e., its rotation), and f is assumed to be constant. (For hydrodynamic models covering a large area of the ocean, one instead makes the so-called *beta-plane approximation*, which keeps the latitudinal variation of the Coriolis force, but says that over short distances one can assume it to be linear.)

Thus, the momentum equations become (in three dimensions):

$$\begin{aligned} \frac{\partial u}{\partial t} + u \frac{\partial u}{\partial x} + v \frac{\partial u}{\partial y} + w \frac{\partial u}{\partial z} - fv &= -\frac{1}{\rho} \frac{\partial p}{\partial x} - (\text{frictional forces})_x \\ \frac{\partial v}{\partial t} + u \frac{\partial v}{\partial x} + v \frac{\partial v}{\partial y} + w \frac{\partial v}{\partial z} + fu &= -\frac{1}{\rho} \frac{\partial p}{\partial y} - (\text{frictional forces})_y \\ 0 &= -\frac{1}{\rho} \frac{\partial p}{\partial z} - g \end{aligned} \quad (7.3)$$

where p = pressure and g = the acceleration due to gravity, and the x and y components of the frictional forces have been left vague for the moment.

So far in these equations, while the currents have been clearly indicated (u, v, w), there has yet been no mention of the elevation of the water level surface. This will come next, with the help of the third equation (which is in a greatly simplified form since vertical acceleration was neglected

7. Interpretation of Tidal Analysis Results Based On Hydrodynamics

as a result of the long-wave approximation). This third equation is called the *hydrostatic equation*, and if one integrates it over depth (i.e., with respect to z) and uses the boundary condition that the pressure at the water surface is equal to the atmospheric pressure, p_a one obtains

$$p = \rho g (\eta - z) + p_a \quad (7.4)$$

where η is the *water level elevation*. From this equation one can see that when $z = \eta$, namely, when one is at the water surface, the pressure equals atmospheric pressure, but as one goes deeper the pressure increases linearly (in this equation, $z=0$ at mean sea level and z is positive above mean sea level and negative below it). By neglecting the horizontal variation in p_a and differentiating equation (7.4) with respect to x and y , the pressure terms in equation (7.3) can be replaced with terms that have the water level elevation, η , namely :

$$\frac{1}{\rho} \frac{\partial p}{\partial x} = g \frac{\partial \eta}{\partial x} \quad \text{and} \quad \frac{1}{\rho} \frac{\partial p}{\partial y} = g \frac{\partial \eta}{\partial y} .$$

The frictional forces are usually treated by handling the turbulence (that friction causes) with the so-called *Reynolds equations*. The typical approach is to break up each velocity component into a so-called a mean portion and a rapidly fluctuating portion (the latter due to the turbulence caused by frictional effects, such as the current flowing along a rough sea bottom). The so-called mean portion is a mean only in the sense of short-term averaging and is really the current that is measured and modeled. One ends up (again skipping the steps in the derivation) with Reynolds stress terms, often indicated as τ_x and τ_y . At this point in our discussion the first two momentum equations now are:

$$\begin{aligned} \frac{\partial u}{\partial t} + u \frac{\partial u}{\partial x} + v \frac{\partial u}{\partial y} + w \frac{\partial u}{\partial z} - fv &= -g \frac{\partial \eta}{\partial x} + \frac{1}{\rho} \frac{\partial \tau_x}{\partial z} \\ \frac{\partial v}{\partial t} + u \frac{\partial v}{\partial x} + v \frac{\partial v}{\partial y} + w \frac{\partial v}{\partial z} + fu &= -g \frac{\partial \eta}{\partial y} + \frac{1}{\rho} \frac{\partial \tau_y}{\partial z} \end{aligned} \quad (7.5)$$

There has been much research on the best ways to represent the energy loss due to the friction terms on the extreme right ends of these two equations (which again must be skipped over here). The type of approach usually depends on whether one stays with the full three-dimensional equations (in which case some type of a so-called *turbulence closure scheme* would be used) or go down to two dimensions (e.g., by integrating the equations over the depth) or go down to one dimension (by integrating over the depth and the width). As will be seen below, the integration over depth (with boundary conditions at the bottom and water surface) ends up giving us some type of parameter for the bottom friction and another for the surface friction (which would be due to the wind blowing on the surface). The most frequently used representation for bottom friction is a quadratic law such as $\tau_b = c_f \rho u |u|$, where c_f is a friction coefficient that is determined empirically. (The absolute sign $| |$ is necessary to keep the frictional stress in the same direction as the current flow, but still with a quadratic character, i.e., still like u^2 .)

So at this point one has a continuity equation (7.2) and two momentum equations (7.5), the later having the water level elevation (η) as a variable (as a result of using the hydrostatic equation), along with the currents, whose three components are u , v , w . (The water level elevation η will also

come into the continuity equation once it is integrated over depth.) In each component equation of (7.5) there is a balance between the change in current speed with time and space (i.e., the acceleration) and three forces: (1) the Coriolis force (actually an apparent force due to being in a rotating reference frame); (2) the pressure forces of the weight of the water (now represented by elevation times the acceleration due to gravity, because of the hydrostatic equation); and (3) the frictional forces that dissipate energy. The spatial change in the current speed (terms two, three, and four), called the *inertial terms*, are nonlinear since the velocity values multiply each other. These nonlinear terms will have to be neglected in order to find simple analytical solutions, but in Section 7.6 numerical solutions will be used to deal with them because of their importance in producing overtides, compound tides, and nonlinear interactions with nontidal phenomena like storm surge and river flow. The representations for the friction terms will also end up being nonlinear, but in the analytical models friction will be linearized, not neglected, since it is too important. Nonlinear terms will still come into play in the continuity equation when it is integrated over depth. Scaling arguments will be used in order to determine when such simplifications are allowable. For example, one will be able to neglect the inertial terms when the depth of the waterway is much greater than the amplitude of the tide wave and the waterways is straight.

In the above discussion many mathematical steps have been skipped over to get from the most general and most comprehensive equations of motion down to much simpler equations. Many assumptions have been made (and there is more simplification still to come). For the derivation of these equations, and a much more thorough discussion of them, there are many texts in fluid dynamics, geophysical fluid dynamics, and physical oceanography to which one can go. Only a few are mentioned here, and even in these there are differences in their mathematical complexity. On the less complex side is the physical oceanography text by Knauss (1978). The more engineering oriented fluid dynamics text by Daily and Harleman (1966) provides a clear derivation of the equations of motion, as do the fluid mechanics texts by Yih (1969) and Batchelor (1967). A more comprehensive (and more complex) discussion can be found in the geophysical fluid dynamics text by Pedlosky (1987). There are, of course, many others from which to choose.

7.3.3 Simplifying the Equations of Motion For Idealized Cases

In order to obtain some useful easy-to-use analytical tide models one must further simplify the continuity equation (7.2) and the momentum equations (7.5), again by using scaling arguments that take advantage of disparate length scales.

First, the very simplest case will be looked at, that is, the case of a long narrow straight waterway, where one expects there to be no appreciable cross-channel motion. Here another length-scale assumption is made, namely, that the length of the waterway (L) is much greater than the width (B), i.e., $L \gg B$, which is called the *narrow basin approximation*. Adding this assumption to the previous assumptions that have been made about length scales, they can be summarized by the following inequalities:

$$\text{tidal wavelength} > \text{length of waterway} \gg \text{width of waterway} \gg \text{depth of waterway}$$

7. Interpretation of Tidal Analysis Results Based On Hydrodynamics

As a result of the narrow basin assumption the second (v) momentum equation in (7.5) reduces to:

$$f u = - g \frac{\partial \eta}{\partial y}$$

For this case, due to Coriolis, the water level elevation on one side of the waterway will be higher than the elevation on the other side of the waterway, and this will depend on the current speed u .

The length scale associated with the effect of Coriolis is the *Rossby radius of deformation*. The constant-density version, usually called R_o , is defined as

$$R_o = \frac{(gD)^{1/2}}{f} = \frac{c}{f} = \frac{\sigma}{f} L$$

where c is the propagation speed of the crest (high water) of the tide wave, which for frictionless situations is $(gD)^{1/2}$, and σ is the tidal frequency. In order to be able to neglect the effect of Coriolis, the width of the waterway must be narrow enough such that $B/R_o \ll 1$, or equivalently $B/L \ll \sigma/f$. This assumption will be made now (but in Section 7.5 the case where the waterway is wide enough for Coriolis to be important will be treated). [However, one still needs to retain the nonlinear inertial terms, in which case the condition for being able to neglect Coriolis, but keep the nonlinear terms is $B/R_o \ll N/D$ or equivalently $B/L \ll (\sigma/f)(N/D)$, where N is the scale of the amplitude of the tide wave. For more information on a complete scaling analysis, see Parker (1984).]

To make the continuity equation and the remaining momentum equation truly one-dimensional, one must integrate over the cross-sectional area of the waterway. The cross-sectional area (A) is assumed to be rectangular with $A=b(h+\eta)$, where the width b and the depth h are constants, and η is the tidal amplitude, which must be still included since the nonlinear terms have not been neglected (i.e., one has not yet said that $N/D \ll 1$).

For the continuity equation, many steps will be again skipped over (which make use of Leibnitz's Rule several times; see Parker, 1984), and again the surface boundary condition is used to bring in the water level elevation, η . Finally, one ends up with

$$\frac{\partial \eta}{\partial t} + \frac{1}{b} \frac{1}{\partial x} (b(h+\eta) u) = 0 \quad (7.6)$$

Similarly integrating the first momentum equation in (7.5) over the cross-sectional area one ends up with

$$\frac{\partial u}{\partial t} + u \frac{\partial u}{\partial x} = -g \frac{\partial \eta}{\partial x} - \frac{1}{h+\eta} c_f u |u| \quad (7.7)$$

where the $c_f u |u|$ is the classic representation of the bottom friction, and surface friction has been neglected by assuming there will be no wind.

Equations (7.6) and (7.7) will be looked at more closely in Section 7.6, where the effect of the various nonlinear terms will be looked at, including the generation of overtides and compound tides, and the nonlinear interaction of the tide with nontidal phenomena such as storm surge and river flow.

But for now one assumes that the depth of the waterway is much greater than the amplitude of the tide ($N \ll D$), so that all the nonlinear terms can be neglected except friction. There are two nonlinear aspects to friction term in equation (7.7), the $(h+\eta)$ in the denominator, in which the η will be neglected, and the quadratic part, i.e., the $u |u|$ (which is like u^2 except the use of the absolute value allows the energy loss to be in the direction of flow). It is important to keep some term for

the energy dissipation, so the quadratic friction is linearized and the energy loss is made proportional to simply u (with N as a frictional coefficient, which will be determined empirically). The linearized continuity and momentum equations, for which one will be able to find analytical solutions (for simple geometries) then become

$$\begin{aligned}\frac{\partial \eta}{\partial t} + \frac{1}{b} \frac{1}{\partial x} (bhu) &= 0 \\ \frac{\partial u}{\partial t} &= -g \frac{\partial \eta}{\partial x} - N u\end{aligned}\tag{7.8}$$

7.4 Tidal Variations Along a Very Narrow Waterway

7.4.1 Tidal Variations In a Narrow Rectangular Waterway

In this section the simplest possible analytical tidal model is looked at, namely, a model describing the tide and tidal current in a long very narrow shallow waterway, and assuming that the tidal amplitude is much smaller than the depth. In terms of length scales one is assuming that

$$\text{tidal wavelength} > \text{length of waterway} \gg \text{width of waterway} \gg \text{depth of waterway} \gg \text{tidal amplitude}$$

With the assumption of a small tidal amplitude relative to the water depth one can then neglect all the nonlinear terms except friction. Friction is linearized, that is, it is assumed that energy loss is directly proportional to the current speed (rather than to $u|u|$). One also assumes that the waterway is rectangular with a constant width b and depth h , in which case equations (7.8), become:

$$\begin{aligned}\frac{\partial \eta}{\partial t} &= -h \frac{\partial u}{\partial x} \\ \frac{\partial u}{\partial t} &= -g \frac{\partial \eta}{\partial x} - N u\end{aligned}\tag{7.8a}$$

where N is some type of a frictional coefficient, which will be determined empirically.

A simple solution of these two equations (see Redfield, 1950; Ippen and Harleman, 1966; Parker, 1984) is an *exponentially damped progressive wave* (see Figure 2.21) whose water level elevation is described by the formula

$$\eta_i = a_0 \cos(\sigma t - kx) e^{-\mu x}\tag{7.9}$$

where σ is the frequency of the progressive wave, k is the wave number (the inverse of the wavelength λ , i.e., $k=1/\lambda$), μ is a frictional damping coefficient, and a_0 is the tidal amplitude at the $x=0$ ($x=0$ is at the closed end of the waterway). The frictional term $e^{-\mu x}$ wears down the wave as it moves up the waterway. If one labels the frictionless values for wave number, wavelength, and

7. Interpretation of Tidal Analysis Results Based On Hydrodynamics

wave speed (also called celerity) as k_o , λ_o , and c_o , one effect of friction can be seen from the formula

$$\frac{k_o}{k} = \frac{\lambda}{\lambda_o} = \frac{c}{c_o} = \frac{1}{[1 + (\mu/k_o)^2]^{1/2}}$$

From this formula once sees that friction shortens the tidal wavelength and slows up the tide wave. As friction increases (i.e., as μ increases), the tidal wavelength decreases, as does the propagation speed of the tide wave. Since friction increases as the water depth decreases, one will expect to see shorter tidal wavelengths in shallower waterways. (μ is related to N coefficient originally used in the momentum equation (7.8) by the formula $N = 2\mu k c_o / k_o$)

For this same exponentially damped progressive wave, the current velocity can be obtained by putting (7.9) in the continuity equation, the result being the formula

$$u_i = \frac{a_o \sigma}{h} \frac{1}{(\mu^2 + k^2)^{1/2}} \cos(\sigma t - kx + \alpha) e^{-\mu x} \quad (7.10)$$

where $\alpha = \tan^{-1}(\mu/k)$ is the phase difference between the time of high water and the time of maximum flood current. For no friction ($\mu=0$) high water and maximum flood occur at the same time. As friction increases (as the depth decreases) the time difference between high water and maximum flood current increases. However, this only applies for a damped progressive wave, which primarily exist in essentially open-ended waterways like rivers where there is no reflection of the tide wave and the progressive wave moves up the waterway until friction wears it down to nothing.

To look at the case where the waterway has a closed end (see Figure 7.7 for schematic and coordinate system), one simply adds a reflected damped progressive wave to the incident progressive damped wave, with the boundary condition that the incident wave must equal the reflected wave at the closed end, where the reflection takes place. Thus,

$$\eta = \eta_i + \eta_r = a_o \cos(\sigma t - kx) e^{-\mu x} + a_o \cos(\sigma t + kx) e^{\mu x} \quad (7.11)$$

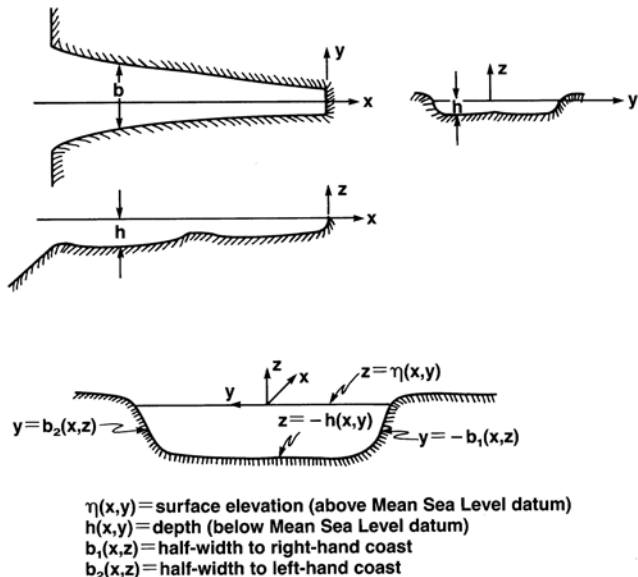


Figure 7.7. Schematic of waterway with a Cartesian coordinate system.

where $\eta_i = \eta_r$ at $x=0$. To find the time and height of high water, one takes the first derivative of (7.11) and sets it equal to zero, solves for the time of high water, and puts it back into (7.11).

$$\frac{\partial \eta}{\partial t} = - a_o \sigma \sin(\sigma t - kx) e^{-\mu x} - a_o \sigma \sin(\sigma t + kx) e^{\mu x} = 0$$

The $a_o \sigma$ drops out, and expanding the sine and cosine terms and rearranging, one has

$$0 = \sin \sigma t \cos kx (e^{\mu x} + e^{-\mu x}) + \cos \sigma t \sin kx (e^{\mu x} - e^{-\mu x}).$$

Dividing through by $\cos \sigma t \cos kx$ one has

$$\frac{\sin \sigma t}{\cos \sigma t} = \frac{\sin kx}{\cos kx} \frac{(e^{\mu x} - e^{-\mu x})}{(e^{\mu x} + e^{-\mu x})}$$

which is

$$\tan \sigma t = - \operatorname{tanh} kx \operatorname{tanh} \mu x$$

where $\operatorname{tanh} \mu x$ is the hyperbolic tangent. The time of high water is given by the formula:

$$\sigma t_H = \tan^{-1} (-\operatorname{tanh} kx \operatorname{tanh} \mu x) \quad (7.12)$$

where t_H is the time of high water, and σt_H is the phase of high water (both are relative to the time or phase of high water at the reflection point at the closed end of the waterway). Putting (7.12) into (7.11) one obtains the following formula for the high water level elevation

$$\eta_H = 2a_o [\cos \sigma t \cos kx \cosh \mu x - \sin \sigma t \sin kx \sinh \mu x] \quad (7.13)$$

where \cosh and \sinh are hyperbolic sine and cosine, and $2a_o$ is the high water elevation at the closed end. (7.12) and (7.13) are the equations for a *frictionally damped standing wave* (see Figure 2.22).

σt_H is plotted versus kx in Figure 7.8 for various values of the damping coefficient μ . In this figure, kx represents distance from the closed end (x is distance in portions of a tidal wavelength). In Figure 7.8, kx equals 0° at the left end of the horizontal axis (representing the closed end of the waterway) and becomes more negative as one moves to the right toward the mouth of the waterway (which can be placed anywhere along the horizontal axis). From this figure one can see that for the case of very little friction (e.g., $\mu=0.5$), such as in a deeper waterway, one has almost a pure standing wave, where high water occurs at approximately the same time everywhere on one side of $kx=90^\circ$, and occurs a half cycle (180°) later on the other side of $kx=90^\circ$. Here $kx=90^\circ$ is one quarter of a tidal wavelength from the closed end. When it is high water to the left of $kx=90^\circ$ it is low water to the right of it (and vice versa); see Figure 2.22. For much higher frictional damping (e.g., $\mu=8.0$, such as in a very shallow waterway) one has almost a pure damped progressive wave, where the time of high water get progressively later as one moves up the waterway. (For this last case, it looks basically like the incident damped progressive wave, because the reflected wave is worn down so much that it has no effect except very close to the point of reflection.) For both these cases, and all the cases in between, the phase of high water is always the same at $kx= - 90^\circ$ (but this location changes with changing μ because the wavelength changes with μ , and thus k changes with μ).

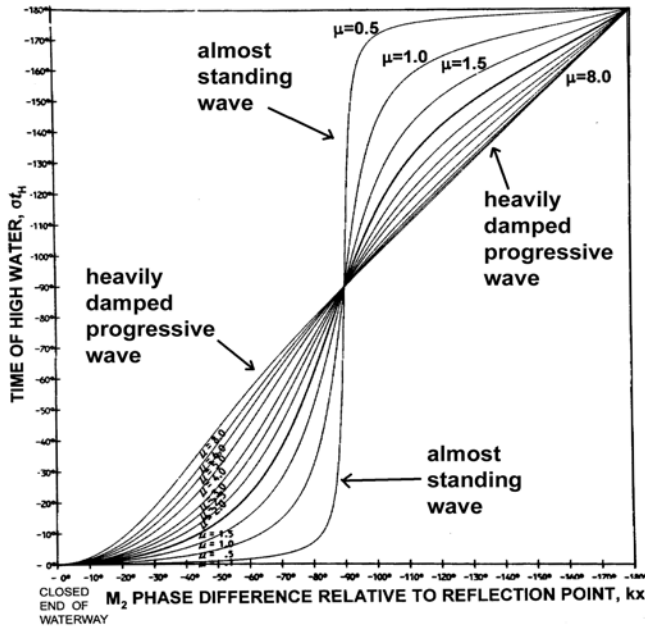


Figure 7.8. The phase (time) of high water, σt_H , versus distance from the closed end (extreme left) of the waterway in terms of wavenumber phase, kx , for different values of the frictional damping coefficient μ . See text. x is distance in portions of a tidal wavelength. $kx = -90^\circ$ is one quarter of a tidal wavelength from the closed end. (Very similar to Figure 1 in Redfield, 1950.)

One can use some trigonometric angle relationships to simplify (7.13) and obtain the formula for the amplitude of the tide (i.e., half the tide range) at high water (η_H) relative to the high water amplitude at the closed end [$\eta_o = \eta_H(0) = 2a_o$], i.e.,

$$\frac{\eta_H}{\eta_o} = [\frac{1}{2} (\cos 2kx + \cosh 2\mu x)]^{\frac{1}{2}} \quad (7.14)$$

a result obtained by Fjeldstad (1929), Redfield (1950), and Ippen and Harleman (1966). This amplitude ratio (which is the same as the ratio of the tide ranges) is plotted in Figure 7.9 for various values of the damping coefficient μ , again plotted relative to the closed end of the waterway at the left end of the figure. Again, for very little frictional damping (i.e., $\mu=0.5$, such as in a deeper waterway) one sees an almost standing wave with an almost zero tide range at $kx = -90^\circ$, that location being a *quasinode* (or a *node*, for the frictionless situation). For a (frictionless) standing wave and frictional cases where μ does not get too large, the largest tide range occurs at the closed end of the waterway. For very large μ (e.g., $\mu=8.0$, such as for a very shallow waterway) one sees that the smallest tide ranges are at the closed end of the waterway and one again has almost a pure damped progressive wave that decreases in tide range as it moves up the waterway. (For this last case, it again looks basically like the incident damped progressive wave, because the reflected wave is worn down so much that it has no effect except very close to the point of reflection.)

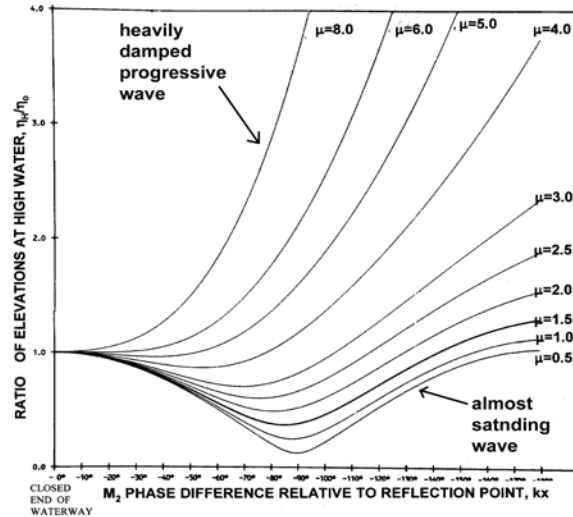


Figure 7.9. The amplitude ratio (=tide range ratio) plotted versus distance from the closed end (extreme left) of the waterway in terms of wavenumber phase, kx , for several values of the frictional coefficient, μ . (See text and Figure 7.8.) (Very similar to Figure 2 in Redfield, 1950.)

From Figure 7.9 one can also see how the length of waterway affects the amplification of the tide. If one has a waterway whose length is, for example, one quarter of a tidal wavelength long, then in Figure 7.9 one would mark the entrance at $kx = -90^\circ$ on the horizontal axis. One would then pick the μ curve for a particular frictional situation (lower μ for deeper waterways; higher μ for shallower). The amplification for the tide would be the closed end value (1.0) divided by the value at $kx = -90^\circ$ for that μ curve. Thus one sees very large amplification for small μ . For $\mu=0$ (no friction) there is infinite amplification at $kx = -90^\circ$, which is called *resonance*. That never happens in the real world (because of friction) but very large amplifications do occur in bays with lengths that are near a quarter tidal wavelength (e.g., the Bay of Fundy). For waterways that are not as long, the amplification is not as great (for the small μ case).

Figure 7.9 is a convenient way to put many cases on the same plot, because every case can be plotted relative to the closed end, but such things as amplification may be easier to understand if values are plotted relative to the entrance. Figure 7.10 shows such a set of plots, for one frictional damping value ($\mu=1.5$, typical for many bays) and for six different waterway lengths (here the entrance to the waterway is now on the left). This gives a better idea of how the length of the waterway can affect the amplification of the tide. The greatest amplification occurs at a length of $kx=90^\circ$ (1/4 of a tidal wavelength), as one would expect from the discussion in the last paragraph. Smaller amplifications result when the length of the waterway is 60° (1/6 of a tidal wavelength) or 30° (1/12 of a tidal wavelength). For a length of 180° (1/2 a tidal wavelength) there is no amplification, the tide range actually decreasing halfway up the waterway, then increasing again but not getting back to the value at the entrance. For a length of 120° (1/3 a tidal wavelength) the tide range at first decreases but then increases and eventually is larger than the value at the entrance.

7. Interpretation of Tidal Analysis Results Based On Hydrodynamics

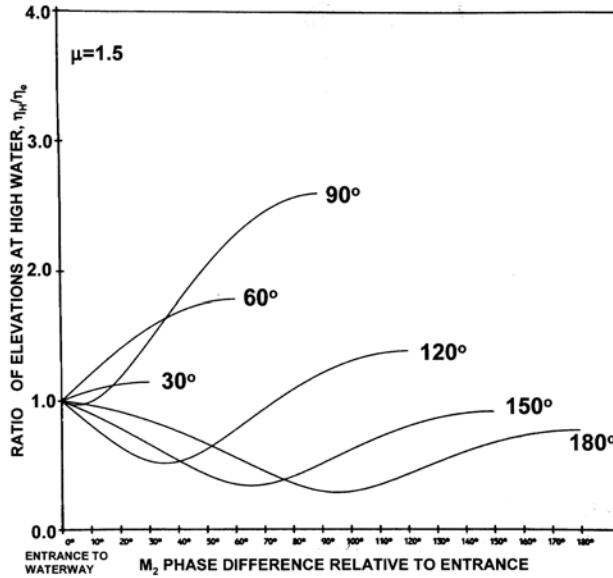


Figure 7.10. The tide range ratio (relative to the value at the entrance to the waterway on the left) for one frictional damping coefficient ($\mu=1.5$) for six different length waterways. A 90° waterway length is $\frac{1}{4}$ of a tidal wavelength. A 60° length is $\frac{1}{3}$ of a tidal wavelength, etc. (Very similar to Figure 15 in Redfield, 1950.)

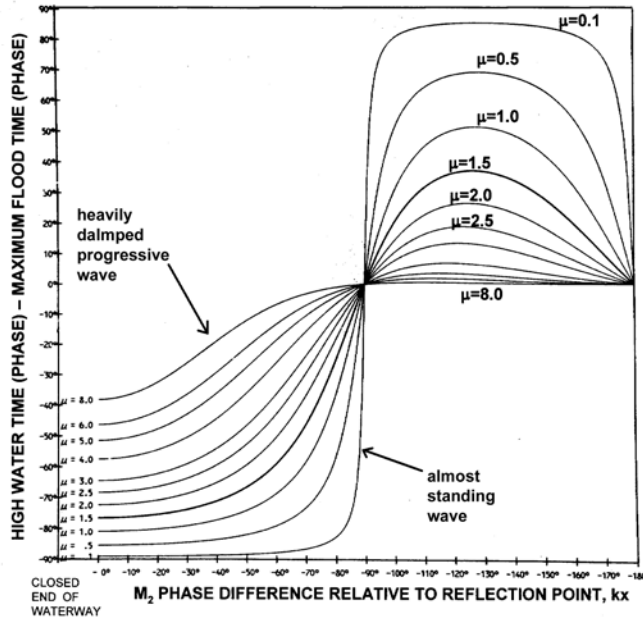


Figure 7.11. The phase (time) difference between high water and maximum flood versus distance form the closed end of the waterway for different values of the frictional coefficient, μ . (Very similar to Figure 5 in Redfield, 1950.)

To look at the tidal currents in our waterway with a closed end, one simply adds the formulas for the tidal current of the incident and reflected damped progressive waves, i.e.,

$$u = u_i + u_r = \frac{a_0 \sigma}{h} \frac{1}{(\mu^2 + k^2)} [\cos(\sigma t - kx + \alpha) e^{-\mu x} + \cos(\sigma t + kx + \alpha) e^{\mu x}] \quad (7.15)$$

(where again $\alpha = \tan^{-1}(\mu/k)$ is the phase difference between high water and maximum flood in the incident damped progress wave). The phase of maximum flood is obtained by setting the derivative of this equation equal to zero, ending up with

$$\sigma t_M = \tan^{-1}(-\tan kx \coth \mu x) \quad . \quad (7.16)$$

Figure 7.11 shows plots of the difference between times of high water and maximum flood ($\sigma t_H - \sigma t_M$). Between the closed end and 1/4 of a tidal wavelength downstream (i.e., $kx = -90^\circ$, the location of the quasinode) the maximum flood current occurs before high water, but further downstream from $kx = -90^\circ$ it occurs after high water. For the almost standing wave case ($\mu = 0.5$) maximum flood occurs approximately 1/4 of tidal period before high water (-90°) when the tide is at mean tide level (which means that slack water occurs at high water and at low water). Beyond this location it occurs 1/4 of tidal period after high water ($+90^\circ$) when the tide again is at mean tide level heading for low water. For a high frictional case ($\mu = 8.0$, almost a pure damped progressive wave) the times of maximum flood and high water get closer and closer together, especially as the waterway becomes longer. Here again, it looks basically like the incident damped progressive wave, because the reflected wave is worn down so much that it has no effect except very close to the point

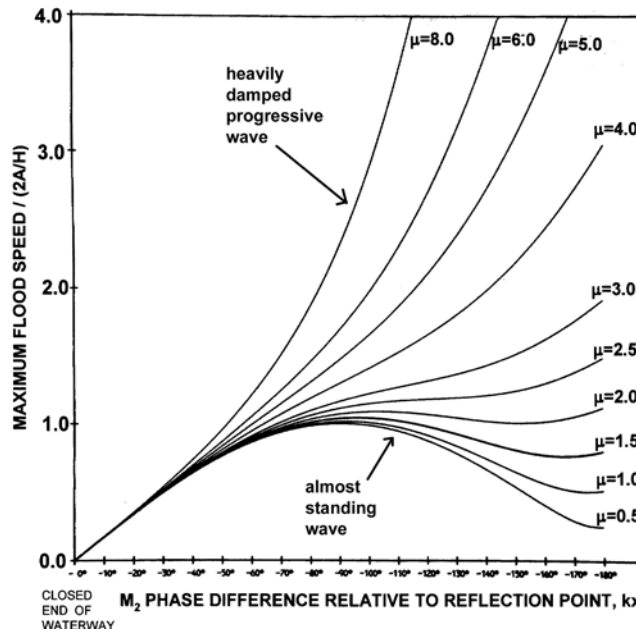


Figure 7.12. Maximum flood speed versus distance from the closed end of the waterway for various values of the frictional damping coefficient, μ . (See text.)

7. Interpretation of Tidal Analysis Results Based On Hydrodynamics

To obtain the current speed value for the maximum flood, (7.16) is substituted into a simplified form of (7.15), again for various values of μ , from which is obtained

$$u_M = \frac{2a_0}{h} \sigma \frac{1}{(\mu^2 + k^2)^{1/2}} [\frac{1}{2} (\cosh 2\mu x - \cos 2kx)]^{1/2} \quad (7.17)$$

The maximum flood speed is plotted in Figure 7.12 for various frictional damping values, μ . (In this figure, the speed value is divided by $2a_0/h$.) For all values of μ the current speed equals zero at the closed end ($x=0$), as it must. For small to moderate frictional damping, the highest values of maximum flood speed occur at $1/4$ of a tidal wavelength downstream (i.e., $kx = -90^\circ$), the location where the tide range value is the smallest. Again for the highest frictional values (e.g., $\mu=8.0$, an almost a pure damped progressive wave) the maximum flood speeds decrease all the way up the waterway (as do the tide range values).

One can also use these simple analytical formulas to look at the relationship between the semidiurnal and diurnal tide waves with changing frictional dissipation and different length waterways. For example, the K_1/M_2 tide range ratio, relative to the K_1/M_2 tide range ratio at the closed end of the waterway, can be expressed as

$$\frac{\eta_{K1}}{\eta_{M2}} = \frac{[\frac{1}{2} (\cos 2kx/1.927 + \cosh 2\mu x/1.927)]^{1/2}}{[\frac{1}{2} (\cos 2kx + \cosh 2\mu x)]^{1/2}} \quad (7.18)$$

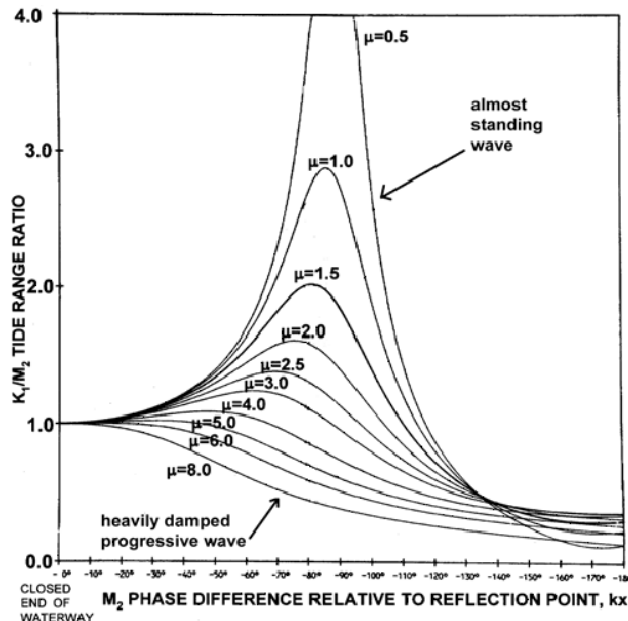


Figure 7.13. The K_1/M_2 ratio (relative to the K_1/M_2 ratio at the closed end of the waterway) plotted versus distance from the closed end, for several values of the frictional damping coefficient, μ . $kx = -90^\circ$ is $1/4$ of a tidal wavelength from the closed end. (Very similar to Figure 16 in Redfield, 1950.)

This is plotted in Figure 7.13, where the horizontal axis is in terms of the M_2 phase number change (kx). This figure must be viewed remembering that the 1.0 value at the closed end can be misleading if one forgets that all these plotted ratios are relative to the K_1/M_2 ratio at the closed end. That being said, one can see from this figure that for low μ values, the K_1/M_2 ratio tends to be largest near 1/4 of an M_2 tidal wavelength from the closed end of the waterway (i.e., $kx = -90^\circ$). This is the location of the M_2 quasinode, but the K_1 quasinode is near $kx = -180^\circ$; the M_2 tide wave has reached its minimum but the K_1 tide wave has not.

The wavelengths of the M_2 and K_1 constituent waves depend on the depth of the waterway. Thus the changing tide regime moving along a waterway depends on: (1) the depth of the waterway; (2) the length of the waterway; and (3) the K_1/M_2 ratio at the entrance to the waterway. Figure 7.14 shows six K_1/M_2 ratio curves plotted relative to the K_1/M_2 ratio at the entrance, for one frictional damping value ($\mu=1.5$, typical for many bays) and six different waterway lengths (in the figure the entrance to the waterway is on the left). In this figure one can see that if the length of the waterway is less than 80° of phase number length, then the K_1/M_2 ratio will decrease from the entrance up the waterway. For longer waterways one sees that the K_1/M_2 ratio increases as one moves up the waterways from the entrance. (This figure must be viewed remembering that all plotted ratios are relative to the K_1/M_2 at the entrance, and the K_1/M_2 value shown at the entrance is 1.0. Whatever the actual K_1/M_2 ratio is at the entrance should therefore multiply the values on this figure. If the tide is, for example, very semidiurnal at the entrance (e.g., the entrance value of K_1/M_2 is 0.25), then even after the amplification shown on the plot the tide might still be semidiurnal.)

[A caution here on the interpretation of model results when dealing with more than one tidal frequency. Although here we have acted as though there are two separate long waves, one for M_2 and one for K_1 , the tide-producing forces actually act on the water in a waterway to produce only one long wave, but that one wave changes shape with time because it has many frequency components. Breaking that one wave into waves representing its frequency components is a useful

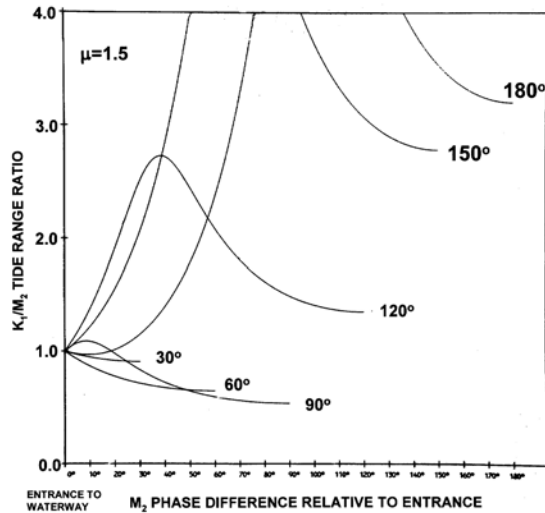


Figure 7.14. K_1/M_2 tide range ratio (relative to the ratio at the entrance, on the left) versus distance from the entrance, for six different length waterways, for a value of $\mu=1.5$ for the frictional damping. (See text.)

7. Interpretation of Tidal Analysis Results Based On Hydrodynamics

way to represent it statistically (as was seen in using harmonic analysis and prediction) and it also seems to work fine when using linear hydrodynamic models, where those component waves do not interact and can simply be added to recreate that one long wave that changes shape with time. However, when the nonlinear terms have been included, there will be energy transfer to new frequencies (and to some already existing frequencies), so that the waves representing those components will be changing amplitude and phase, not only because of the effects of the basin (just looked at) but because of the energy they will be receiving from (or giving up to) other component waves through the nonlinear interactions. Numerical models, on the other hand, act in the time domain, time stepping forward with all hydrodynamic effects acting at the same time on the water. This is much closer to reality, but then one usually still ends up looking at the results in the frequency domain to better understand what has happened.]

Although the relationships obtained in this section were for very narrow situations, one also finds that they match the values found at the center of wider waterways where the Coriolis effect has been included. The case including Coriolis effects is treated in Section 7.5.1, but first the effect of changing widths on the tide will be investigated.

7.4.2 Tidal Variations In a Narrowing Waterway

If there is a change in width as one moves up a waterway, that will also affect the tide and tidal current. Generally if the waterway becomes narrower the tide range increases. If the decrease in width can be approximately described with an exponential function (as some natural waterways can, especially rivers) then one can find a simple analytical solution to the equations of motion that will provide insights into how changing width can affect the tide regime in such a waterway.

Starting with the version of the continuity and momentum equations in equation (7.8)

$$\begin{aligned} \frac{\partial \eta}{\partial t} + \frac{1}{b} \frac{1}{\partial x} (bhu) &= 0 \\ \frac{\partial u}{\partial t} &= -g \frac{\partial \eta}{\partial x} - N u \end{aligned} \quad (7.8)$$

Neglecting nonlinear terms, linearizing friction, assuming constant depth h and an exponential width decrease described by $b=b_0 e^{-x/\ell}$, where ℓ is the length scale associated with the decreasing width (see Figure 7.7), one obtains

$$\begin{aligned} \frac{\partial \eta}{\partial t} + h \frac{1}{2\ell} \frac{\partial u}{\partial x} &= 0 \\ \frac{\partial u}{\partial t} &= -g \frac{\partial \eta}{\partial x} - N u \end{aligned} \quad (7.19)$$

Solutions to these two equations will be of the form (see Parker, 1984)

$$\eta(x) \propto e^{-x/2\ell} e^{\pm i\kappa x} e^{\pm \mu x}$$

where $\kappa = k \left[\frac{1}{2} \left(1 + \frac{N^2 \sigma^2}{k^4} \right)^{1/2} + \frac{1}{2} \right]^{1/2}$ and $\mu = k \left[\frac{1}{2} \left(1 + \frac{N^2 \sigma^2}{k^4} \right)^{1/2} - \frac{1}{2} \right]^{1/2}$ and

where $k = \sigma [1 - \frac{1}{(2\sigma\ell)^2}]^{\frac{1}{2}}$ is the wave number for the frictionless case [assuming $\sigma > 1/(2\ell)$, in

which case the frictionless solution is oscillatory; otherwise the frictionless solution is monotonic]. If $\sigma > 1/(2\ell)$, then κ is the wave number and μ is the damping factor. As the rate of width-decrease increases (i.e., as ℓ decreases) the wave number decreases and the wavelength increases as does the wave propagation speed. Thus, a decreasing width has the opposite effect of increasing friction (since the latter decreases the wavelength and the wave propagation speed). Thus, as a tide wave propagates up a shallow narrowing river, friction will be wearing it down and the decreasing width will be building it up.

From the solution of equations (7.19) one obtains two messy looking formulas, but at least an analytical solution is possible, and using them one can see a limitless number of cases by simply changing parameters in these formulas. The formula for the phase of high water (relative to the phase of high water at the closed end of the waterway) is:

$$\sigma t_H = \tan^{-1} \left(- \frac{e^{\mu x} \operatorname{seca}_2 - e^{-\mu x} \operatorname{seca}_1}{e^{\mu x} \operatorname{seca}_2 + e^{-\mu x} \operatorname{seca}_1} \tan(\kappa x + \varphi) \right) - \tan^{-1} \left(- \frac{\operatorname{seca}_2 - \operatorname{seca}_1}{\operatorname{seca}_2 + \operatorname{seca}_1} \tan \varphi \right) \quad (7.20)$$

and the formula for the high water elevation relative to the high water elevation at the closed end of the waterway (which equals the tide range relative to the tide range at the closed end) is:

$$\frac{\eta(x)}{\eta(0)} = \frac{1}{2} \frac{\kappa^2}{(\kappa^2 + \mu^2)^{\frac{1}{2}}} e^{x/2\ell} [e^{2\mu x} \sec^2 \alpha_2 + e^{-2\mu x} \sec^2 \alpha_1 + 2 \operatorname{seca}_1 \operatorname{seca}_2 \cos 2(\kappa x + \varphi)]^{\frac{1}{2}} \quad (7.21)$$

where (to make it a little less messy) the following parameters were defined

$$\varphi = \frac{1}{2} (\alpha_1 - \alpha_2), \quad \alpha_1 = \tan^{-1} \left(\frac{1/(2\ell) + \mu}{\kappa} \right), \quad \text{and} \quad \alpha_2 = \tan^{-1} \left(\frac{-1/(2\ell) + \mu}{\kappa} \right).$$

The width change in the upper 70 percent of the Delaware estuary can be described fairly well with an exponential formula using a value of $\ell=0.136$. Using that value, formula (7.20) is plotted in Figure 7.15a for eight different values of the frictional coefficient N. The asterisks (*) on the plot represent the center-waterway M₂ high water phase lag (relative to the value at the closed end) for nine locations along the estuary, from actual harmonically analyzed water level data. They fall nicely along the N=8 curve, showing that this simple analytical model can represent the M₂ phase change reasonably well. (For a constant-width model, there would have been no N curves along which these data values would have fallen.)

Similarly, in Figure 7.15b formula (7.21) is plotted for eight different values of the frictional coefficient N again for a width decrease represented by $\ell=0.136$. The asterisks (*) on the plot this time represent the center-waterway M₂ tidal amplitudes (relative to the value at the closed end) for the nine locations along the estuary. Again they fall nicely along the N=8 curve (and again for a constant-width model there would have been no N curves along which these data values would have fallen.). The same proved to be true for the K₁ amplitudes and phases, only they fell nicely along the N=10 curve (see Parker, 1984). (As will be seen in Section 7.6, the larger value of N for K₁ is due to the nonlinear effect of the larger M₂ constituent increasing the frictional momentum loss from the smaller K₁ constituent.)

7. Interpretation of Tidal Analysis Results Based On Hydrodynamics

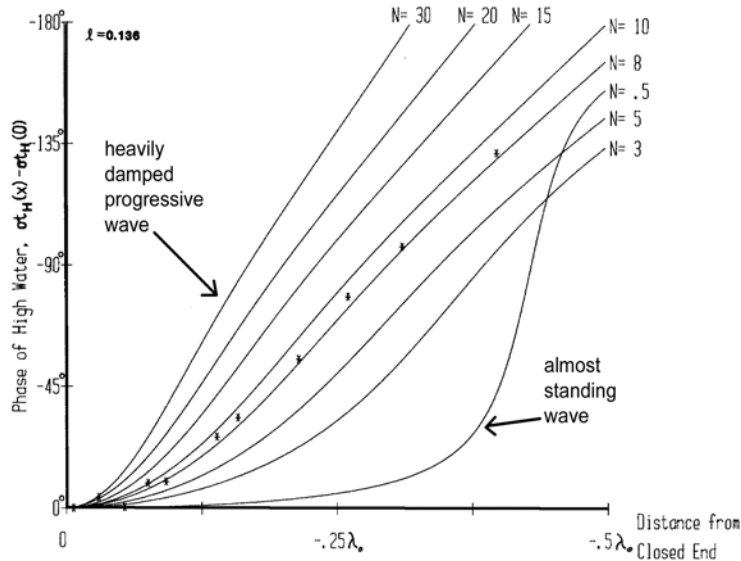


Figure 7.15a. The phase (time) of M_2 high water (relative to the value at the closed end, on the left) for eight different values of the frictional coefficient N in a bay with an exponential width decrease ($\ell=0.136$) matching Delaware River. The *'s are M_2 phase lags from harmonically analyzed water level data in the Delaware River (see text). (From Parker, 1984.)

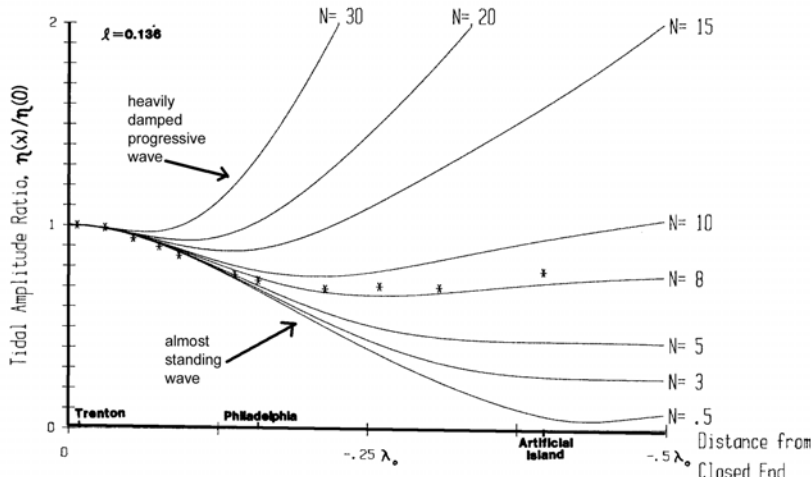


Figure 15b. The M_2 tide range (relative to the value at the closed end of the waterway, on the left) versus distance from the closed end (in portions of a tidal wavelength) for eight different values of the frictional coefficient N in a bay with an exponential width decrease ($\ell=0.136$) matching that in the Delaware River. The *'s indicate the M_2 tide range (relative to the value at the closed end) from harmonically analyzed water level data from stations along the Delaware River. (From Parker, 1984.)

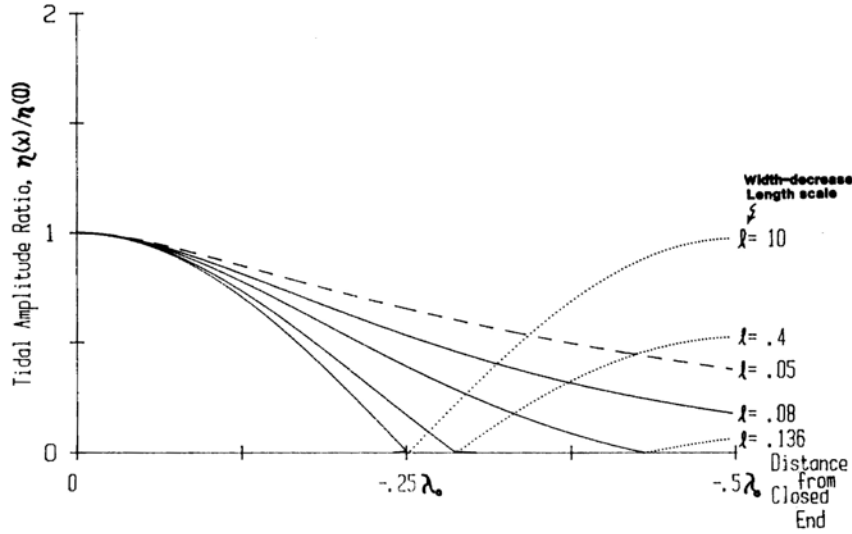


Figure 7.16. Tide range (relative to the range at the closed end, on the left) for five different exponential width decreases, for the frictionless case ($N=0$). $\ell=0.136$ represents the width decrease of the Delaware River. Dashed line are for monotonic solutions. Solid-dotted curves are for oscillatory solutions, which represent standing waves (since this is a frictionless case). (See text.)

Figure 7.16 shows how different rates of width-decreases (i.e., different values of ℓ) can affect the M_2 tidal amplitude along the waterway. To isolate the width effect one looks at the case for no friction ($N=0$). The frictionless case is interesting in that it actually has two types of solutions, one oscillatory [if $\sigma > 1/(2\ell)$] and one monotonic [if $\sigma \leq 1/(2\ell)$]. For the M_2 tidal frequency the solution goes monotonic for $\ell \leq 0.08$ (represented by dashed lines in the figure). Each oscillatory solution is represented by a solid line up to a node (zero tide range) and then by a dotted line (where the phase is now a half cycle out of phase with the solid curve portion). For $\ell=10$ the width is essentially constant, and the node occurs at 1/4 of a constant-width frictionless M_2 tidal wavelength from the closed end. As the rate of width-decrease increases (i.e., ℓ decreases) one sees that the wavelength increases and the node moves further away from the closed end. (This again is the opposite effect of friction, which shortens the tide wave length.) By the time ℓ decreases to 0.08, the wavelength has become infinite and the water level oscillation is in phase everywhere in the waterway (the monotonic solution).

For the $\ell=0.136$ value in the Delaware estuary, the frequency at which the frictionless solution goes monotonic (the so-called *cutoff frequency*) happens to fall between the frequency of the K_1 and O_1 , with O_1 falling below it. In Section 2.3.4 we saw that in the Delaware estuary the calculated lunar nodal factor curve for O_1 very closely matched the astronomically determined curve, while the K_1 somewhat matched, and the curves for the semidiurnal and higher order constituents did not match at all. It was mentioned that the exponential width decrease probably inhibited the tidal hydrodynamics for the diurnal constituents and the nonlinear interactions that would have modified the astronomically-based lunar nodal factor curves.

In this section an exponential width change has been used to illustrate the effects of width changes on the tide, but also see Prandle and Rahman (1980) and Prandle (1991) for the effects on the tide when the width varies according to a power law. The classic paper on the effects of width

(and depth) changes is by Green (1837) in which he showed that the wave amplitude is inversely proportional to the square root of the width of the basin (and inversely proportional to the fourth root of the depth of the basin), but that relationship ignores friction and assumes slowly changing width and/or depth. Jay (1991) looked at cases with more rapid changes in width and/or depth.

For very sudden changes in width and/or depth, the tide wave is partially reflected and partially transmitted. A sudden reduction in width (looking up a bay) leads to a partial reflection-transmission that amplifies the tide wave, leading to larger tide ranges at the head of the bay. A sudden widening of the bay (again, looking up the bay) has the opposite effect, reducing the tide range at the head of the bay. One can analytically model the tide for this type of situation by using transmission and reflection wave coefficients similar to those used by Eagleson and Dean (1966, pp 71-7).

Some large tide ranges are actually due to several successive sudden reductions in width moving up a waterway with partial reflection-transmissions at each location, which amplify the tide wave. This contributes to the 38.4 mean tide range (43.5 mean spring range; with ranges sometimes reaching 50 feet) at the head of Minas Basin at the northeastern end of the Bay of Fundy. There is an amplification from the partial reflection-transmission at the transition from the continental shelf to the Gulf of Maine-Bay of Fundy, and then again at the transition from the Bay of Fundy into Minas Basin, before being further amplified by the total reflection at the head of Minas Basin. In each case the length of that portion of the waterway is conducive to amplification (as explained in Section 7.4.1), each portion of the waterway falling somewhere among the first three curves of Figure 7.10, with the Bay of Fundy portion covering almost 90° of wave number phase (k_x), namely, almost $\frac{1}{4}$ of an M_2 tidal wavelength. One can, in fact, see these three regions in Figure 9 from Redfield (1950) (reproduced along with Redfield's Figure 10 in Figure 7.17 below), which shows the ratio of the tide range for stations along the Bay of Fundy, Gulf of Maine, and part of the continental shelf (relative to the tide range at the head of the Bay of Fundy) versus the time (phase) of high water at those stations (relative to the time of high water at the head of the Bay). Stations 16 through 21 are along the Atlantic coast of Nova Scotia and represent some of the amplification on the continental shelf. Stations 24 and 23 are in Minas Basin and 22 is at the end of Cumberland Basin, a little to the west of Minas Basin. The stations along the northwest coast of the Bay of Fundy are shown lying approximately along a curve representing a frictional coefficient of $\mu=1.0$, while those along the southeast coast lie somewhere between $\mu=1.5$ and $\mu=2.0$. However, this supposed difference in frictional dissipation is not real, being a result of Redfield not including the Coriolis force in his analytical model but still using coastal tide stations, when center-bay values would have been more appropriate. He also did not include the slow decrease in width going up the Bay of Fundy, which if included would have probably resulted in a higher μ value.

7.5 Tidal Variations In Wider Waterways – the Effect of Coriolis

If the waterway is not narrow enough that so that the following equalities are true, $B/R_o \ll 1$, or equivalently $B/L \ll \sigma/f$ (see Section 7.3.3), where R_o is the constant-density version of the *Rossby radius of deformation*, i.e.

$$R_o = \frac{(gD)^{\frac{1}{2}}}{f} = \frac{c}{f} = \frac{\sigma}{f} L$$

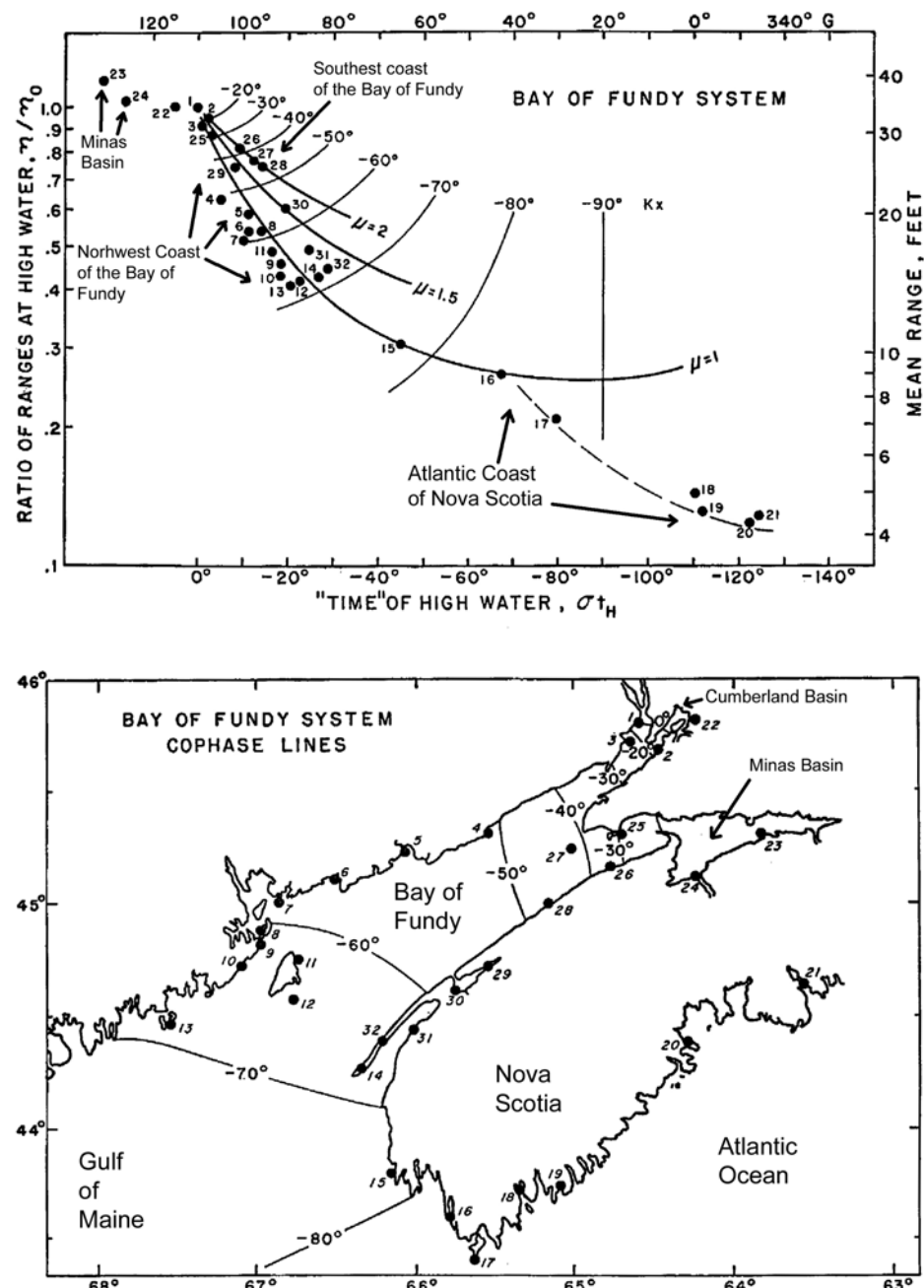


Figure 7.17. (Top panel) The tide range for stations along the Bay of Fundy, Gulf of Maine, and part of the Atlantic Coast along Nova Scotia (relative to the tide range at the head of the Minas Basin at the northeastern end of the Bay of Fundy) plotted versus the time (phase) of high water at those same stations (relative to high water time at the head of Minas Basin). See text. (Bottom panel) Map showing water level station locations. (From Redfield, 1950, with some labels added.)

7. Interpretation of Tidal Analysis Results Based On Hydrodynamics

then one must include the effect of the Coriolis force ($f = 2\Omega \sin\varphi$; see Section 7.3.2). The equations of motions for this case (neglecting the nonlinear terms and linearizing the friction term) are:

$$\begin{aligned}\frac{\partial \eta}{\partial t} &= - h \frac{\partial u}{\partial x} \\ \frac{\partial u}{\partial t} &= - g \frac{\partial \eta}{\partial x} - N u \\ fu &= - g \frac{\partial \eta}{\partial y}\end{aligned}\tag{7.22}$$

which is the same as (7.8a) except for the cross-bay momentum equation (the 3rd equation above). The first solution for this case was probably Fjeldstad (1929); the solution for the frictionless case was given by Taylor (1920) (see also Hendershott and Speranza, 1971). The solution is still an exponentially damped progressive wave but now there is a term representing the cross-bay variation in water level due to the Coriolis force. The water level elevation for a damped progressive wave under the influence of Coriolis is described by the formula

$$\eta_i = a_o \cos(\sigma t - kx - \mu\zeta y) e^{-\mu x} e^{-k\zeta y}\tag{7.23}$$

where σ is the frequency of the progressive wave, k is the wave number (the inverse of the wavelength λ , i.e., $k=1/\lambda$), μ is a frictional damping coefficient, c_o is the frictionless wave speed $(gD)^{1/2}$, a_o is the tidal amplitude at the $x=0, y=0$ (located at the center of the closed end of the waterway), and ζ is defined by

$$\zeta = \frac{f\sigma}{c_o^2(k^2 + \mu^2)} = \frac{f}{\sigma} \frac{k^2 - \mu^2}{k^2 + \mu^2}.$$

The wave described by formula (7.23) is called a frictionally damped *Kelvin wave* (the frictionless case was first looked at by Lord Kelvin). From the last formula it can be seen that as the frictional damping (μ) increases the Coriolis effect on the water level elevation decreases, so even if a waterway is wide the effect of Coriolis may be small if the waterway is very shallow. As in Section 7.4.1, to find the elevation in a closed waterway, one adds incident and reflected damped progressive Kelvin waves, i.e.,

$$\eta = \eta_i + \eta_r = a_o \cos(\sigma t - kx - \mu\zeta y) e^{-\mu x} e^{-k\zeta y} + a_o \cos(\sigma t + kx + \mu\zeta y) e^{-\mu x} e^{+k\zeta y}$$

and simplifies to obtain

$$\eta = 2a_o [\cos\sigma t \cos(kx + \mu\zeta y) \cosh(\mu x + \zeta y) - \sin\sigma t \sin(kx + \mu\zeta y) \sinh(\mu x + \zeta y)]\tag{7.24}$$

By setting the derivative of this equation to zero one obtains the phase of high water

$$\sigma t_H = \tan^{-1} [-\tan(kx + \mu\zeta y) \tanh(\mu x + \zeta y)]\tag{7.25}$$

which when substituted into (7.24) gives the high water elevation (relative to the high water elevation at the center of the closed end) as

$$\frac{\eta_H}{\eta_0} = [\frac{1}{2} \{ \cos 2(kx + \mu\zeta y) + \cosh 2(\mu x + k\zeta y) \}]^{1/2} \quad (7.26)$$

This amplitude ratio is the same as the tide range relative to the tide range at the center of the closed end. For this case, however, the reflection isn't perfect. η_i does not equal η_r at the closed end except at $y=0$, nor is the tidal current equal to zero at the closed end (again) except at $y=0$. To make this reflection of Kelvin waves perfect, one must add additional waves [of the type known as *Poincaré waves*, as Taylor (1920) first did with the frictionless case]. However, the effect of these added waves is small for a narrow waterway and also disappears as one moves away from the closed end.

The only difference between equation (7.26) above and equation (7.14) in Section 7.4.1 for the non Coriolis case, is that kx is replaced by $(kx + \mu\zeta y)$ and μx is replaced by $(\mu x + k\zeta y)$. The same is true for the equation for the tidal current. One will also notice that at $y=0$, i.e., down the center of the waterway, these equations reduce to those found in Section 7.4.1. Thus, those equations in Section 7.4.1 can still be used to represent the tide and tidal current down the center of a waterway, even if that waterway is wide enough for Coriolis to have an effect.

Figure 7.18 shows the cotidal and corange lines in the closed waterway for different values of the frictional damping coefficient μ . In each case the width is 1/10th of a frictionless tidal wavelength and the length is $\frac{1}{2}$ a frictionless tidal wavelength. For the frictionless case ($\mu=0$, i.e., a very deep waterway) there is a *node*, i.e., a point of zero tide range, $1/4$ of a tidal wavelength from the closed end, in the center of the waterway. As friction increases (μ increases) this node moves to the right (when looking down the waterway), until for the $\mu=1.0$ case it moves onto land and becomes a *virtual node* (for this particular width).

The cotidal and corange lines in many waterways approximately match those seen in one of the examples in Figure 7.18. In Figures 2.5 and 2.6, even though the Strait of Juan de Fuca -Strait of Georgia waterway bends around, one can see the similarity in the M_2 cotidal and corange lines with those for the case $\mu=1.0$ in Figure 7.18, including a virtual node at the southeastern tip of Vancouver Island. Likewise, in Figure 2.24 one can see a virtual node on the western shore of Chesapeake Bay near South Point. In corange charts for the open ocean (which are so deep that $\mu=0$ is not a bad approximation) one does see nodes, which are usually called *amphidromic points* (see Section 7.8). [Tahiti happens to be located near an M_2 amphidromic point in the Pacific Ocean, allowing S_2 to be of comparable size, and therefore leading to the very unusual situation of high water there occurring at approximately the same time every day (see Marmer, 1926).]

In a wide waterway, there are other mechanisms besides Coriolis that can affect the tide or tidal current, including the effects of changing bathymetry and the nonlinear effects of the lateral inertial terms (see Section 7.6.7).

7.6 Nonlinear Shallow-water Effects on Tides

7.6.1 The Nonlinear Terms In the Equations of Motion

Returning now to the nonlinear one-dimensional continuity and momentum equations from Section 7.3.3, equations (7.6) and (7.7) are

$$\frac{\partial \eta}{\partial t} + \frac{1}{b} \frac{\partial}{\partial x} (b(h+\eta) u) = 0 \quad (7.27)$$

7. Interpretation of Tidal Analysis Results Based On Hydrodynamics

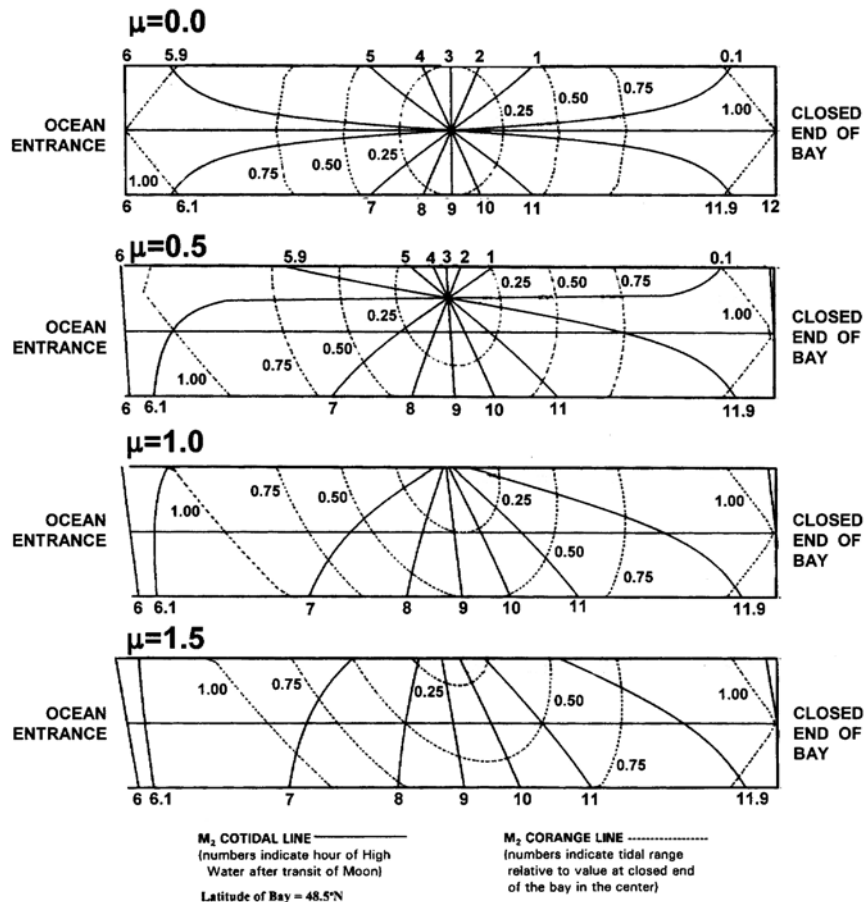


Figure 7.18. Cotidal and corange lines in a semi-enclosed rectangular waterway (the closed end on the right) caused by the Coriolis force, for four different values of the frictional damping coefficient (including the frictionless case (top panel)).

and

$$\frac{\partial u}{\partial t} + u \frac{\partial u}{\partial x} = -g \frac{\partial \eta}{\partial x} - \frac{1}{h+\eta} c_f u |u| \quad (7.28)$$

where η is the tidal elevation, u is the cross-sectionally averaged tidal current velocity, b is the width of the basin, h is the width-averaged depth of the basin, and c_f is the friction coefficient (which is usually determined empirically for a particular waterway, but is often on the order of 0.0025).

There are three nonlinear terms in these two equations:

- (1) $u \frac{\partial u}{\partial x}$, the inertial (advective) term in the momentum equation;
 - (2) $\frac{\partial(b\eta u)}{\partial x}$, in the continuity equation (where one lets $b=\text{constant}$, for simplicity); and
 - (3) $\frac{1}{h+\eta} c_f u |u|$, the friction term in the momentum equation

The first two terms were the terms considered in the classical works on shallow-water tides. The third term, the friction term, actually has two nonlinear aspects, the quadratic part $u|u|$ and the effect of η in the denominator. The η effect in the denominator of the friction term is the effect of elevation on the frictional momentum loss per unit volume of fluid. The energy dissipation due to bottom friction has less of an effect if spread over a deeper depth than over a shallower depth. When the tidal elevation is comparable in size to the water depth there is good deal less energy loss per unit volume of fluid under the crest (high water) than under the trough (low water) of the tide wave. These two frictional effects can be separated into two separate terms. First (3) is put into the form

$$\frac{1}{h} \frac{1}{(1+\eta/h)} c_f u|u| = \frac{1}{h} (1+\eta/h)^{-1} c_f u|u|$$

and then a binomial expansion of $(1+\eta/h)^{-1}$ is carried out, namely,

$$(1+\eta/h)^{-1} = 1 - \eta/h + (\eta/h)^2 - (\eta/h)^3 + \dots$$

Then, assuming $\eta \ll h$ and neglecting terms with $(\eta/h)^2$ and higher order, the friction term can be written as

$$\frac{1}{h} c_f u|u| - \frac{1}{h^2} c_f \eta u|u|$$

The $\eta u|u|$ is the elevation effect just discussed, and it will be seen below that its effects are similar to the effects of terms (1) and (2) above, all three having asymmetric effects, while the effect of $u|u|$ is a symmetric effect. These nonlinear terms transfer energy from one tidal frequency to another, and also cause the interaction between the tide and nontidal phenomena such as storm surge and river flow.

Because of these nonlinear terms the equations of motion, (7.27) and (7.28), cannot be solved analytically, and so there cannot be any formulas comparable to those in Sections 7.4 for telling how (for example) high waters or maximum floods will be affected by different conditions. These equations can be solved using numerical methods, but in order to obtain some idea of the effect of these terms one must run a numerical model many times – a very time consuming process. However, there is one alternative method, which will provide at least an approximate idea of the effects of each of these nonlinear terms, and that is to carry out a Fourier decomposition of equations (7.27) and (7.28).

7.6.2 The Generation of Compound Tides and Overtides

A Fourier decomposition of the equations of motion will first be used to determine which nonlinear mechanisms generate which compound tides and overtides. First the total tidal current is represented as the sum of two astronomical tidal constituents, i.e.:

$$u(x,t) = u_1(x) \cos(\sigma t - \phi_1(x)) + u_1'(x) \cos(\sigma' t - \phi_1'(x))$$

where σ, σ' are the frequencies of the two tidal current constituents, and u_1, u_1' , and ϕ_1, ϕ_1' are the tidal current constituent amplitudes and phase lags. To simplify this for use in later calculations let $\sigma_r = \sigma - \sigma'$, i.e., the difference in frequency between the two constituents. Then rewrite $u(x,t)$ as

7. Interpretation of Tidal Analysis Results Based On Hydrodynamics

$$u = u_1 \cos(n\sigma_r t - \phi_1) + u_1' \cos([n+\beta]\sigma_r t - \phi_1') \quad (7.29)$$

where $\beta = \pm 1$ and n is an integer. Also let $n\theta = (n\sigma_r t - \phi_1)$, again to make later calculations a little simpler to keep track of. Then rewrite $u(x,t)$ as

$$u = u_1 \cos n\theta + u_1' \cos([n+\beta]\theta - [\phi_1' - \frac{n+\beta}{n} \phi_1]) \quad (7.30)$$

Similarly for the total tidal elevation:

$$\eta(x,t) = \eta_1(x) \cos(\sigma t - \psi_1(x)) + \eta_1'(x) \cos(\sigma' t - \psi_1'(x))$$

again using $\sigma_r = \sigma - \sigma'$ and $n\theta = (n\sigma_r t - \phi_1)$ and $\beta = \pm 1$, one has:

$$\eta = \eta_1 \cos(n\theta - [\psi_1 - \phi_1]) + \eta_1' \cos([n+\beta]\theta - [\psi_1' - \frac{n+\beta}{n} \phi_1]) \quad (7.31)$$

One also makes the assumption that $u_1' \ll u_1$ and $\eta_1' \ll \eta_1$, which is true for semidiurnal tide regime, since in such an area M_2 is much larger than the other tidal constituents. So for convenience the larger constituent will be called M_2 .

The inertial term then becomes:

$$\begin{aligned} u \frac{\partial u}{\partial x} &= \frac{1}{2} \frac{\partial}{\partial x} (u^2) = \frac{1}{2} \frac{\partial}{\partial x} ([u_1 \cos n\theta + u_1' \cos([n+\beta]\theta - [\phi_1' - \frac{n+\beta}{n} \phi_1])]^2) \\ &= \frac{1}{2} \frac{\partial}{\partial x} (\frac{1}{2} u_1^2 + u_1 u_1' \cos(\beta\theta - [\phi_1' - \frac{n+\beta}{n} \phi_1]) + \frac{1}{2} u_1^2 \cos 2n\theta \\ &\quad + u_1 u_1' \cos([2n+\beta]\theta - [\phi_1' - \frac{n+\beta}{n} \phi_1'])) \end{aligned} \quad (7.32)$$

The first term inside the () on the right-hand side of (7.32), involving u_1^2 , is a mean flow generated by the inertial term's effect on M_2 , namely, the so-called *tidally induced residual current*. The third term is the second harmonic of M_2 , namely, the overtide M_4 . (The higher amplification of M_4 mentioned in Section 7.2 results from this generation of M_4 along the length of the waterway.) The second and fourth terms are new compound tides generated by the interaction between M_2 and the second constituent. If this second constituent is N_2 then the second term is a low-frequency shallow-water tidal constituent, MN , which happens to have the same frequency as the astronomical constituent Mn . The fourth term is a higher-frequency shallow-water tidal constituent, MN_4 . (The inertial term can also produce M_6 , but this results from an interaction between M_2 and M_4 , and thus is a smaller second-order effect. As will be seen below, M_6 is primarily generated by the quadratic friction term from M_2 alone.)

The nonlinear term from the continuity equation becomes:

$$\begin{aligned} \frac{\partial}{\partial x} (\eta u) &= \frac{\partial}{\partial x} (\{\eta_1 \cos(n\theta - [\psi_1 - \phi_1]) + \eta_1' \cos([n+\beta]\theta - [\psi_1' + \frac{n+\beta}{n} \phi_1])\} \\ &\quad \{\[u_1 \cos n\theta + u_1' \cos([n+\beta]\theta - [\phi_1' - \frac{n+\beta}{n} \phi_1])\}\}) \\ &= \frac{1}{2} \frac{\partial}{\partial x} (\eta_1 u_1 \cos[\psi_1 - \phi_1] + \eta_1 u_1' \cos(\beta\theta + [\psi_1 - \phi_1] + \beta\phi_1) \\ &\quad + \eta_1' u_1 \cos(\beta\theta - [\psi_1' - \frac{n+\beta}{n} \phi_1]) + \eta_1 u_1 \cos(2n\theta - [\psi_1 - \phi_1])) \end{aligned}$$

$$\begin{aligned}
 & + \eta_1 u_1' \cos([2n+\beta]\theta - [\psi_1 - \phi_1' - \frac{2n+\beta}{n} \phi_1]) \\
 & + \eta_1' u_1 \cos([2n+\beta]\theta - [\psi_1' - \phi_1' - \frac{n+\beta}{n} \phi_1]))
 \end{aligned} \tag{7.33}$$

The same new tidal constituents are generated as by the inertial term, but the phase lag relationships are different, and the amplitudes are also different. In situations where one expects slow currents this nonlinear continuity term will be larger than the inertial term. One will notice that this term also produces a shift in mean sea level (the first term to the right of the second equal sign). Thus, if the tide range of a waterway changes for some reason, then one will also see a change in the mean sea level of the waterway (especially near the closed end) due to this nonlinear effect.

The two above derivations were quite straight forward, but for the two friction terms, $u|u|$ and $\eta u|u|$, a complete Fourier decomposition of each term must be done. $u|u|$ can be represented as a Fourier series, i.e.,

$$u|u| = \frac{a_o}{2} + \sum_n^{\infty} [a_m \cos m\theta + b_m \sin m\theta] \tag{7.34}$$

To find a_m one multiplies equation (7.34) by $\cos m\theta$ and integrates over all possible frequencies, and to find b_m one does the same but instead multiplies the equation by $\sin m\theta$, i.e.:

$$\begin{aligned}
 a_m &= \frac{1}{\pi} \int_0^{2\pi} (u_1 \cos(n\sigma_r t - \phi_1) + u_1' \cos([n+\beta]\sigma_r t - \phi_1')) \\
 &\quad |(u_1 \cos(n\sigma_r t - \phi_1) + u_1' \cos([n+\beta]\sigma_r t - \phi_1'))| \cos m\theta d\theta \\
 b_m &= \frac{1}{\pi} \int_0^{2\pi} (u_1 \cos(n\sigma_r t - \phi_1) + u_1' \cos([n+\beta]\sigma_r t - \phi_1')) \\
 &\quad |(u_1 \cos(n\sigma_r t - \phi_1) + u_1' \cos([n+\beta]\sigma_r t - \phi_1'))| \sin m\theta d\theta ,
 \end{aligned}$$

The tedious steps in carrying out this Fourier expansion can be found in Parker, 1984 (see also Dronkers, 1964; LeProvost, 1976; and Fang, 1987). Here only the resulting values for a_m and b_m will be given. First one notes that $a_o = 0$, so no mean flow is generated by the effect of $u|u|$ for this case. For the larger tidal constituent (M_2), with frequency $n\theta$, one obtains

$a_n = \frac{8}{3\pi} u_1^2$, which represents the first-order momentum loss due to friction. One also gets

$a_{3n} = \frac{8}{15\pi} u_1^2$, with frequency $3n\theta$, which represents the generation of a third harmonic of M_2 ,

namely, the second overtide, M_6 . (The higher amplification of M_6 mentioned in Section 7.2 results from its nonlinear generation along the length of the waterway.)

If the second smaller astronomical constituent has a frequency of $(n-1)\theta$ then one has

$$a_{(n-1)} = \frac{8}{3\pi} u_1 u_1' \cos [\phi_1' - \frac{n-1}{n} \phi_1'] \quad \text{and} \quad b_{(n-1)} = \frac{8}{3\pi} u_1 u_1' \sin [\phi_1' - \frac{n-1}{n} \phi_1']$$

which represents its first-order momentum loss from the smaller tidal constituent due to friction, but this loss is greater because of the presence of the larger tidal constituent, i.e., the $u_1 u_1'$ is larger than $(u_1')^2$. (In Figure 7.5 this is why the amplifications of S_2 and N_2 are smaller than amplification of M_2 .)

7. Interpretation of Tidal Analysis Results Based On Hydrodynamics

The interaction of the two astronomical tidal constituents also produces a new *compound tidal constituent*, with frequency $(n+1)\theta$, whose formulas for $a_{(n+1)}$ and $b_{(n+1)}$ look the same as those just shown for $a_{(n-1)}$ and $b_{(n-1)}$ except with the $n-1$ replaced with $n+1$. One can see that if the smaller astronomical tidal constituent is semidiurnal then the compound tidal constituent will also be semidiurnal. If the smaller astronomical constituent is N_2 then the generated compound tidal constituent will be $2MN_2$. If the smaller astronomical constituent is S_2 then the generated compound constituent will be $2MS_2$. ($2MN_2$ and $2MS_2$ have the same frequencies as the two astronomical constituents L_2 and μ_2 . The large amplifications of $2MN_2$ and $2MS_2$ seen in Figure 7.5 are because they are nonlinearly generated along the length of the waterway. Such amplifications are much larger than would be the amplifications of L_2 and μ_2 , which would be comparable to the amplifications of N_2 and S_2 seen in that figure.) There are also high frequency compound tidal constituents generated that are close in frequency to M_6 (for example, $2MN_6$ and $2NM_6$).

For the $\eta u|u|$ friction term one must also do a complete Fourier decomposition, where $\eta u|u|$ is represented as a Fourier series, i.e.,

$$\eta u|u| = \frac{c_o}{2} + \sum_n^{\infty} [c_m \cos m\theta + d_m \sin m\theta] \quad (7.35)$$

and the coefficients c_m and d_m are found in a similar manner (see Parker, 1984) with even more terms involved. Again only the results are summarized. This time there is a mean effect, since for c_o we get a nonzero value of

$$\frac{c_o}{2} = \frac{4}{3\pi} \eta_1 u_1^2 \cos(\psi_1 - \phi_1)$$

where $(\psi_1 - \phi_1)$ is the phase difference between high water and maximum flood. One also obtains values for c_{2n} and d_{2n} , which also generate the second harmonic, M_4 , but with a different amplitude and phase lag contribution (than those from the inertial or nonlinear continuity terms), i.e.,

$$c_{2n} = \frac{8}{15\pi} \eta_1 u_1^2 \cos(\psi_1 - \phi_1) \quad \text{and} \quad d_{2n} = \frac{8}{15\pi} \eta_1 u_1^2 \sin(\psi_1 - \phi_1)$$

In addition the same compound tidal constituents (both low frequency and higher frequency) are generated as by the inertial term and the nonlinear continuity term, but again with different amplitude and phase lag contributions. (For c_1 and d_1 , and the other compound coefficients, see Parker, 1984.)

Table 2.4 (presented in Chapter 2) summarizes the nonlinear interactions between M_2 and four other astronomical tidal constituents (N_2 , S_2 , K_1 , O_1), as well as with itself, and shows what compound and overtide tidal constituents are generated by these interactions, and which nonlinear terms can be responsible. There is a distinct difference between the symmetric nonlinear effect of quadratic friction, $u|u|$, and the asymmetric nonlinear effect of the nonlinear continuity term, $\partial(\eta u)/\partial x$, the inertial term $u\partial u/\partial x$, and the elevation effect on friction, $\eta u|u|$. The semidiurnal compound tides (such as $2MN_2$ and $2MS_2$) are only generated by $u|u|$. The asymmetric nonlinear terms generate low-frequency compound tides, such as MN and MS , which have the same frequencies as the astronomical constituents Mm and MSf (and which are often dominated anyway by meteorological noise). They also generate overtones (e.g., M_4 , S_4 , etc.) and quarter-diurnal compound tides (e.g., MN_4 and MS_4). Terdiurnal constituents can be generated by all the nonlinear terms (i.e., by both symmetric and asymmetric mechanisms), through the interaction of M_2 with either K_1 or O_1 . For example, MK_3 is generated by one or more asymmetric nonlinear mechanisms,

while $2MO_3$ is generated by the symmetric quadratic friction mechanism; both have the same frequency (but different node factors). In some research papers one will see either MK_3 or $2MO_3$ listed, when in fact, both are really present; and likewise for MO_3 and $2MK_3$.

The symmetric quadratic frictional interaction between M_2 with either K_1 or O_1 also produces fifth and seventh diurnal constituents. There are also many more compound tidal constituents (not shown in the Table) that can be generated through the nonlinear interaction of two or more tidal constituents. Only in waterways with very shallow depths and a large tide range will these other constituents be important enough to use in a tide prediction, but there are cases where over a hundred tidal constituents (more than half of them shallow-water constituents) are used. For example, Zetler and Cummings (1967) used 114 constituents for the tide at Anchorage, Alaska, as did Rossiter and Lennon (1967) for the tide in the Thames estuary in the United Kingdom. However, only 74 constituents of each 114 were the same for both groups. Thus each group, included 40 different constituents in their analysis that the other group did not use, which points to the confusion that can occur in deciding which shallow-water constituents are most important to include. Understanding the nonlinear mechanisms that generated them, and which one are first, second, or third order helps in that decision making.

M_8 is often larger than many of the shallow-water constituents shown in Table 2.4. This table only goes up to seventh diurnal tidal constituents, because it includes only constituents generated by a first-order interaction between two astronomical constituents. M_8 is generated by the interaction of M_6 with M_2 via the asymmetric nonlinear terms and is thus a second-order interaction. It often reaches a significant size only because M_2 is usually so much larger than the other tidal constituents.

As mentioned earlier, M_6 can also be generated by the interaction of M_4 with M_2 via the asymmetric nonlinear terms, but this second-order contribution is significantly smaller than the effect of quadratic friction directly on M_2 . Although the quadratic friction mechanism was first pointed out by Proudman in 1923, for many decades M_6 was treated as though it was produced by the classic shallow-water nonlinear terms through the interaction of M_2 and M_4 . (One can see this in Schureman's (1958) choice of a node factor for M_6 , which he erroneously specifies as being the cube of the node factor for M_2 instead of the square of the node factor).

Table 3.2 lists some of the shallow-water constituents typically included in a harmonic analysis. It also shows the shallow-water compound constituent equivalents for many of the astronomical constituents. Tables A.1 and A.2 include many more shallow-water constituents. In all three of these tables the asymmetric or symmetric nonlinear mechanisms are also indicated for each shallow-water constituent.

The same nonlinear mechanisms that generate overtide and compound tide constituents also cause the interaction between the tide and various nontidal phenomena such as river flow and storm surge. The next two sections will look at such interactions and the roles played by the specific nonlinear terms.

7.6.3 The Nonlinear Interaction of the Tide With River Flow

In Table 2.4 there a fourth way listed to generate the asymmetric nonlinear effects produced by the other three nonlinear mechanisms (the continuity term $\partial(\eta u)/\partial x$, the inertial term $u\partial u/\partial x$, and the elevation effect on friction $\eta u|u|$). It turns out that quadratic friction $u|u|$ can produce asymmetric effects if there is a mean flow present, such as river flow. This can be shown by doing a Fourier decomposition similar to the one done in the previous section, but including a mean flow, i.e., let

7. Interpretation of Tidal Analysis Results Based On Hydrodynamics

$u(x,t) = u_o(x) + u_1(x) \cos(\sigma t - \phi_1(x))$ and again for $u|u|$ one has

$$u|u| = \frac{a_o(x)}{2} + \sum_n^{\infty} [a_n(x) \cos n\theta_1 + b_n(x) \sin n\theta_1] \quad (7.36)$$

To find a_n one multiplies equation (7.36) by $\cos n\theta_1$ and integrates over all possible frequencies, and to find b_n one does the same but instead multiplies the equation by $\sin n\theta_1$, i.e.:

$$a_n = \frac{1}{\pi} \int_0^{2\pi} (u_o + u_1 \cos\theta_1) |(u_o + u_1 \cos\theta_1)| \cos n\theta_1 d\theta_1$$

$$b_n = \frac{1}{\pi} \int_0^{2\pi} (u_o + u_1 \cos\theta_1) |(u_o + u_1 \cos\theta_1)| \sin n\theta_1 d\theta_1$$

The steps in the complete Fourier decomposition can be found in Parker (1984) (and see also Dronkers, 1964, and Fang, 1987). Here only some of the results are presented.

Since a mean current flow has been included one expects to get a value for a_o , but it also includes an effect from the tidal current, namely,

$$\begin{aligned} a_o &= (8/\pi) u_1 u_o && \text{when } u_o \ll u_1 \quad \text{or} \\ a_o &= 2(u_o^2 + \frac{1}{2} u_1^2) && \text{when } u_o \gtrsim u_1 \end{aligned}$$

namely, in the second case, when the river flow is fast enough so that the direction of flow is always downstream (although current speed oscillates, becoming faster and then slower due to the effect of the tidal current).

For the main tidal constituent one obtains the same result as in Section 7.6.2 when $u_o \ll u_1$, i.e., $a_1 = (8/3\pi)u_1^2$ (a result first gotten by Proudman, 1923). But when $u_o \sim u_1$ we obtain

$$a_1 = \frac{4}{\pi} u_1^2 \left[\frac{u_o}{u_1} \sin^{-1} \frac{u_o}{u_1} + \frac{1}{3} \left(\frac{u_o^2}{u_1^2} + 2 \right) \left(1 - \frac{u_o^2}{u_1^2} \right)^{\frac{1}{2}} \right]$$

(a result obtained by Bowden, 1953) and one sees that the river flow will increase the frictional momentum loss from the main tidal constituent, thus reducing the tide range. This is a little more obvious when $u_o = u_1$, for which one gets $a_1 = 2u_o u_1$.

The result for a_2 shows that second harmonics (e.g., M_4) can be generated by $u|u|$ when there is a mean flow present. For the case where $u_o \ll u_1$ one obtains $a_2 = (8/3\pi) u_o u_1$. For the case when $u_o \sim u_1$ one obtains

$$a_2 = \frac{1}{\pi} u_1^2 \left[\sin^{-1} \frac{u_o}{u_1} + \frac{1}{3} \frac{u_o}{u_1} \left(5 - 2 \frac{u_o^2}{u_1^2} \right) \left(1 - \frac{u_o^2}{u_1^2} \right)^{\frac{1}{2}} \right]$$

When $u_o = u_1$ this reduces to $a_2 = \frac{1}{2} u_1^2$, and maximum generation of M_4 .

As was seen in the last section, $u|u|$ directly generates third harmonics such as M_6 . From the result here for a_3 one sees that adding a mean flow reduces this third harmonic generation. For $u_o \ll u_1$ one again gets $a_3 = (8/15\pi) u_1^2$ (a result also obtained by Proudman, 1923), but for $u_o \sim u_1$ one obtains

$$a_3 = \frac{8}{15\pi} u_1^2 \left[\left(1 - 2 \frac{u_o^2}{u_1^2} + \frac{u_o^4}{u_1^4} \right) \left(1 - \frac{u_o^2}{u_1^2} \right)^{\frac{1}{2}} \right]$$

and once the flow reaches $u_o = u_1$, then $a_3 = 0$ and all M_6 generation by $u|u|$ disappears (because with the river speed now the same as the tidal current amplitude there is no more flood and ebb and

$u|u|$ has become u^2). [However, one also sees an increase in M_6 generation by $\eta u|u|$ with a small increase in river flow; see Parker, 1984.]

Figure 7.19 graphically illustrates the results for a_1 , a_2 , and a_3 , resulting from the interaction between the tide and river flow as a result of the quadratic friction term $u|u|$. It shows how these three coefficients change as u_o/u_1 increases from zero to 2 (that is, from no river flow to river flow with a current speed twice that of the tidal current). The friction coefficient a_1 increases with increasing u_o/u_1 indicating increased momentum loss from the main tidal constituent due to the increased river flow. River flow decreases the tide range through this frictional effect. Coefficient a_2 represents momentum input into the second harmonic (e.g., M_4), which increases as the river flow increases (but only up to the point where $u_o = u_1$). Coefficient a_3 represents momentum input into the third harmonic (e.g., M_6), which decreases as the river flow increases, reaching zero when $u_o = u_1$.

7.6.4 The Nonlinear Interaction of the Tide With Low-Frequency Storm Surge

The same nonlinear mechanisms that generate compound and overtide constituents and that cause the interaction between the tide and river flow, also cause the interaction between the tide and low-frequency (i.e., subtidal) storm surge. Of the four nonlinear terms that have been looked at (the nonlinear continuity term $\partial(\eta u)/\partial x$, the inertial term $u\partial u/\partial x$, the quadratic friction term $u|u|$, and the elevation effect on friction $\eta u|u|$), $u\partial u/\partial x$ and $u|u|$ do not usually play a major role here because a low-frequency storm surge changes the water level elevation slowly and the accompanying

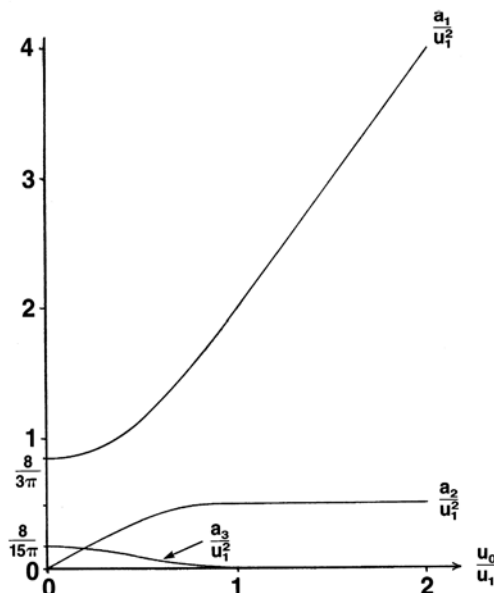


Figure 7.19. The effect of mean river flow (u_o) on the first three tidal harmonics from a Fourier decomposition of the quadratic friction term, $u|u|$. u_1 is the M_2 tidal current amplitude. a_1 and a_2 represent momentum input to the M_4 and M_6 . a_1 represent frictional momentum loss from M_2 . (See text.)

currents are therefore usually very small. Thus, at least for subtidal storm surge, nonlinear continuity term $\partial(\eta u)/\partial x$ and the elevation effect on friction $\eta u|u|$ are the two nonlinear terms one will need to consider. (For storm surge with frequencies higher than the tidal frequency $u\partial u/\partial x$ and $u|u|$ are much more important. For a discussion of the interaction of the tide with storm surge that have frequencies higher than the tidal frequency see Prandle and Wolf (1978). This interaction depends more on the quadratic friction mechanism because the higher frequencies of the surge mean stronger currents.)

At the crest of a storm surge the total depth will greater than if the storm surge were not there. This will increase the tidal wavelength and may also slightly affect the proximity of the hydrodynamic system to a (damped) resonant condition. The opposite occurs at the trough of the storm surge. The larger depth under the crest of the storm surge may also lead to slower tidal current velocities and therefore less (first-order) frictional attenuation, and likewise more frictional attenuation under the trough of the storm surge. The tidal amplitude is thus larger at the surge crest than it would be if no surge were present, and smaller at the surge trough than it would be if the surge were not present. These are the effects of the nonlinear continuity term, $\partial(\eta u)/\partial x$, with first-order friction playing a role. The $\eta u|u|$ term also causes the same effects. The greater depth at the crest of the storm surge leads to less frictional momentum loss per unit volume of fluid and thus less attenuation of the wave and larger tidal amplitudes. At the trough of the surge the smaller depth leads to greater frictional momentum loss per unit volume of fluid, and thus greater attenuation and smaller tidal amplitudes. An example of such effects by a low-frequency subtidal storm surge was seen in Figure 2.31, in which one can see smaller tide ranges along the entire Delaware River and Bay coinciding with the trough of a subtidal storm surge, and larger tide ranges coinciding with the crest of the storm surge.

If low-frequency (subtidal) storm surge were truly periodic (they are really transient oscillatory phenomena caused by the wind, and to some degree by atmospheric pressure), one could use a Fourier decomposition similar to that in Section 7.6.2 to show that, in water level spectra from coastal areas and bays, such "periodic" subtidal storm surges would produce side bands around each astronomical constituent spectral line via these nonlinear mechanisms. The lower the frequency of such a "periodic" storm surge the closer the side bands would be to each spectral tidal line. However, since storm surges are indeed transient with their energy spread over many frequencies, the result is a smearing of each spectral line, called a "*tidal cusp*" by Munk, *et al.* (1965) (the name coming from the shape of the spectrum as it rises up to each tidal spectral line on both sides. (See Section 3.10.2 for more discussion of tidal cusps.)

7.6.5 A Physical Explanation of the Nonlinear Mechanisms

The effect of the nonlinear terms in the equations of motion on a tidal constituent is to cause a modulation or distortion of that constituent, which can be represented by the combination of that constituent with one or more new constituents. The Fourier decomposition in the previous sections reveals what these new tidal constituents are, but does not provide physical insight into the cause of such modulations or distortions. Here some physical insight will be provided, which will be seen to involve predominantly wave propagation velocity of the tide wave and frictional attenuation.

The generation of second harmonics (e.g. M_4) in shallow water by the so called "shallow-water" terms (the inertial term in the momentum equation and the nonlinear term in the continuity equation) has been studied at least since Airy (1845). The wave propagation velocity for long waves without friction [$c_o = (gh)^{1/2}$] is approximately constant over a tidal cycle only if the tidal amplitude, η , is

much smaller than the depth, h , i.e., if $\eta/h \ll 1$. For a progressive long wave in shallow water, where η/h is not negligibly small and where η will therefore significantly affect the total depth, the wave crest will travel faster than the trough. Thus the faster moving crest (high water) will move closer to the trough ahead of it, which at the same time is falling more behind the next crest. Thus, high water arrives sooner than it would in deeper water, and one sees a faster rise to high water and a slower fall to low water. This can be seen in the water level curves in Figure 2.25 as one moves further up the Gironde River (in France). The resulting wave profile will be distorted from a perfect sinusoid. Subtracting the original sinusoid from this distorted profile, one finds energy in the second harmonic. This is the asymmetric effect of the nonlinear continuity term, $\partial(\eta u)/\partial x$.

The tidal current amplitude is approximately $u = (\eta/h)c_o$, ignoring friction. When η/h is not very small, u cannot be neglected with respect to c_o , so the wave propagation velocity at the crest is actually $c_o + u$ and at the trough is $c_o - u$. The result again is a similarly distorted wave profile. This is the effect of the inertial term in the momentum equation, $u \partial u / \partial x$. The importance of the inertial term in distorting the tidal elevation is reduced by friction, by a width-decrease, and by reflection (making the tide wave closer to a standing wave). As will be seen in Section 7.6.7, however, the lateral inertial terms in the two-dimensional momentum equation have can have a very important effect on the tidal current.

The first-order effects of friction are to decrease the wave propagation velocity and to attenuate the wave amplitude. This linear effect will not distort the wave profile; both high and low waters will be delayed and decreased in amplitude. However, the two nonlinear aspects of the frictional momentum loss, $u|u|$ and $\eta u|u|$, will lead to distortion. The effect of $\eta u|u|$ is that the frictional loss of momentum per unit volume of fluid is smaller for greater depths and greater for smaller depths, so the crest will travel faster than the trough. This asymmetric effect can thus generate M_4 and other even harmonics just like the classic shallow-water terms, and in fact is usually more important than the inertial term.

Second harmonics (first over tides) are generated by the above three mechanisms because the maximum wave propagation velocity and minimum attenuation occur at the crest, and the opposite occurs at the trough. The tide is distorted in an asymmetric manner (see Figure 7.20).

Quadratic friction, $u|u|$, on the other hand, has a symmetric effect, causing maximum attenuation (and minimum wave propagation velocity) at both maximum flood and maximum ebb (which coincides approximately with the crest and trough if the wave is progressive), and minimum attenuation (and maximum wave propagation velocity) at slack waters. The result of this symmetric effect is a third harmonic (e.g. M_6) and other smaller odd harmonics (see Figure 7.21).

When two astronomical tidal constituents are present quadratic friction modulates their combined effects, producing new compound tidal constituents. For example, when M_2 and N_2 are in phase, so that their respective high waters occur at the same time, the total depth under the crest of the combined wave will be greater than when they are out of phase 13.8 days later. Similarly, the total depth under the trough when M_2 and N_2 are in phase will be smaller than when they are out of phase. Thus, M_4 generation due to greater depth at the crest than at the trough will be modulated by the 27.6-day variation of the combined M_2+N_2 effects, leading to a 27.6-day modulation of M_4 and a new constituent, NM_4 .

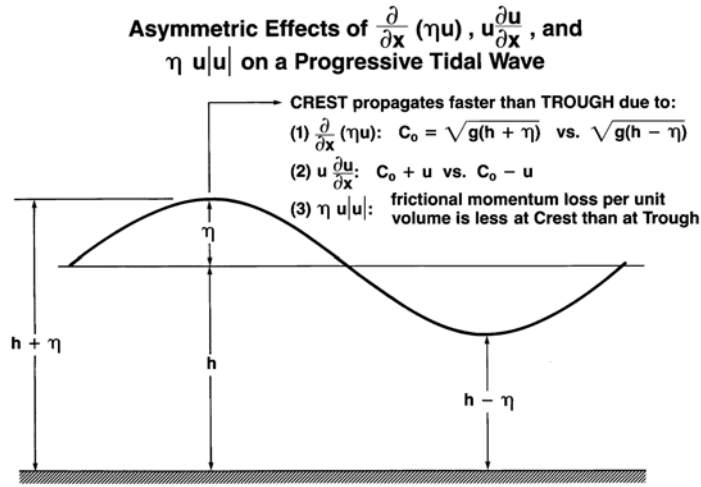


Figure 7.20. Diagram illustrating the asymmetric effects of the nonlinear continuity term, the inertial(advection) term, and the term representing the elevation effect on frictional momentum loss per unit volume of fluid. (See text.)

Maximum flood and ebb currents will be greatest when M_2 and N_2 tidal currents are in phase. Because of the quadratic nature of frictional momentum loss, the loss when M_2 and N_2 are in phase will be greater than the sum of the individual losses if M_2 and N_2 existed independently. The combined wave will travel slower and be damped more. The opposite will be true 13.8 days later when M_2 and N_2 are out of phase and the combined maximum currents are less. The increased frictional momentum loss at in-phase times, will be greater than the decreased loss at out-of-phase times, and each constituent will lose more momentum than if it existed alone. Since M_2 is larger than N_2 , M_2 will reduce N_2 by a higher percentage than N_2 will reduce M_2 (see Figure 7.5).

There will also be a 27.6 day modulation of the frictional momentum loss from M_2 and N_2 , and thus a 27.6-day modulation of their frictional damping and wave propagation speed. The result is represented by two new compound tidal constituents, $2MN_2$ and $2NM_2$ (which have the same

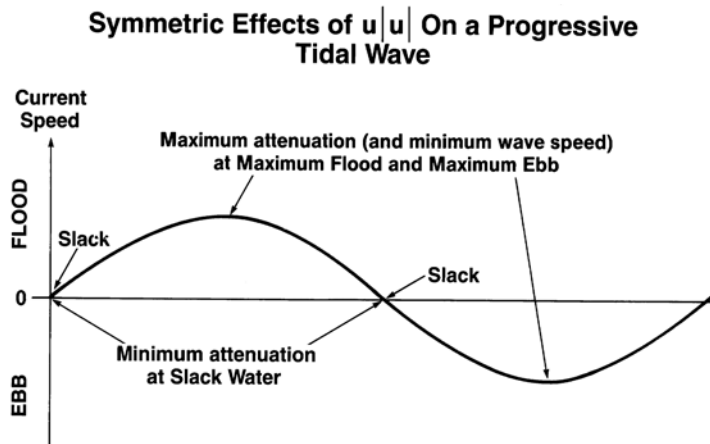


Figure 7.21. Diagram illustrating the symmetric nonlinear effect of quadratic friction.

frequencies as the astronomical constituents, L_2 and $2N_2$). Third harmonics (e.g. M_6) will also be modulated to produce new sixth diurnals (such as $2MN_6$ and $4MN_6$).

In all of the above examples a progressive wave was used for simplicity. For tidal waves in real estuaries, which, due to first-order "linear" frictional effects are always somewhere between a damped progressive wave and a damped standing wave, the effects are similar but the phase relationships and relative amplitudes will vary.

The effects on the tide of a mean flow (e.g. river flow) can also be explained in terms of changes in wave propagation velocity and frictional attenuation. Quadratic friction generally has a greater effect than the other nonlinear terms, especially at high river current speeds. A mean river flow makes ebb current speeds larger and flood current speeds smaller. Due to the quadratic nature of the frictional momentum loss, the increased loss during the ebb phase is greater than the decreased loss during the flood phase. The result is a greater energy loss than if the mean flow were not present, and thus the river flow dampens the tidal wave reducing the tide range.

Quadratic friction effects, being greater during ebb than during flood and thus being asymmetric, also lead to the generation of M_4 . Low waters are delayed and high waters come earlier. Frictional generation of M_6 will continue as long as the river current speed is less than the tidal current speed and there are still slack waters (see upper half of Figure 7.22). When the river flow is greater than the tidal current the flow becomes unidirectional (there are no more slack waters) and the minimum attenuation then occurs at what would have been maximum flood (if the river flow hadn't overwhelmed the tidal current); see lower half of Figure 7.22. Figure 7.19 shows the effect of a

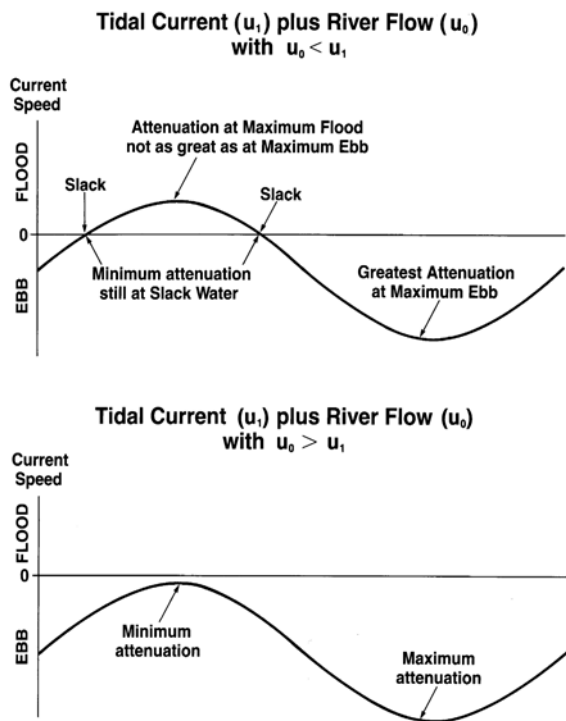


Figure 7.22. Diagram illustrating the nonlinear interaction of the tide with river discharge via quadratic friction, for two cases: (1) the river flow is less than the maximum tidal current; and (2) the river flow is greater than the maximum tidal current. (See text.)

7. Interpretation of Tidal Analysis Results Based On Hydrodynamics

mean flow on the first three harmonics from a Fourier decomposition of $u|u|$. The increase in the friction coefficient a_1 with increasing u_o/u_1 increases momentum loss from the main tidal constituent. Coefficients a_2 and a_3 represent momentum input into the second harmonic (e.g., M_4) and third harmonic (e.g., M_6), the former increasing with increasing u_o/u_1 and the latter decreasing.

The quadratic frictional effect described above, may be slightly modified by the other nonlinear terms, but these smaller effects will probably depend on the specific situation and may be competing with each other. For example, when increased river discharge raises the mean sea level due to frictional momentum loss from the mean flow, the resulting increase in water depth will (via the nonlinear continuity term) increases the wave propagation speed and the tide wavelength to some degree. Yet, increased (linear) friction tends to decrease the wave propagation speed and wavelength. A changing wavelength due to one or both of these effects can move the location of a quasinode (i.e. the point of minimum tide range) and actually increasing the tide range at that location. This appears to happen in Figure 7.24 (in Section 7.6.6c) south of Philadelphia.

The effect on the tide of storm surge can also be explained in terms of changes in wave propagation velocity and frictional damping. The relative importance of the four nonlinear terms depends on the frequency of the surge. The lower the frequency of the surge the smaller the current velocities accompanying the water level changes, and the less important are $u \partial u / \partial x$ and $u|u|$. A low-frequency storm surge affects the tide primarily through the slowly changing depth on which the tide propagates. At the crest of the storm surge the total depth will greater and the tidal wave propagation velocity will be greater. This will increase the tidal wavelength and may slightly affect the proximity of the hydrodynamic system to a (damped) resonant condition. The opposite occurs at the trough of the storm surge. The larger depth under the crest of the storm surge also leads to slower tidal current velocities and therefore less (first-order) frictional attenuation, and likewise more frictional attenuation under the trough of the storm surge. The tidal amplitude is thus larger at the surge crest than it would be if no surge were present. Likewise, the tidal amplitude at the surge trough is smaller than it would be if the surge were not present. These are the effects of the nonlinear continuity term, $\partial(\eta u) / \partial x$, with first-order friction playing a key role. The $\eta u|u|$ term also causes the same effects. The greater depth at the crest of the storm surge leads to less frictional momentum loss per unit volume of fluid and thus less attenuation of the wave and larger tidal amplitudes. At the trough of the surge the smaller depth leads to greater frictional momentum loss per unit volume of fluid, and thus greater attenuation and smaller tidal amplitudes.

7.6.6 A Real-World Example of Nonlinear Shallow-water Effects Using a Numerical Model

The nonlinear effects demonstrated by the Fourier analysis and explained above can be demonstrated using a numerical hydrodynamic model. That model must be calibrated and verified with harmonic analysis results obtained from actual data. The model must be run long enough to produce a times series (at its hundreds of grid points) that can be harmonically analyzed. Since for simplicity we have been working with a nonlinear one-dimensional model, we will use here a numerical hydrodynamic model for a long narrow shallow estuary, one that approximately meets the criteria used in the above sections for simplifying (at least geometrically) the equations of motion. The Delaware River and Bay estuary is a convenient choice; not only is it long and narrow and shallow, but it also has an exponential width decrease as one moves up the estuary. Using a numerical model for this waterway, one can turn the nonlinear terms on and off for different runs of the model, and not only confirm the effects of each nonlinear term, but also estimate the relative importance of several nonlinear mechanisms that might have the same effect.

7.6.6a The Numerical Model

There are, of course, a whole host of hydrodynamic numerical models, using a wide variety of numerical schemes, and with also a wide variety of assumptions made about the equations of motion. Here we use one of the simplest models that still includes the nonlinear terms that we have been discussing. The model used in this section is a finite-difference numerical model of the nonlinear one-dimensional equations of motion (7.6) and (7.7) applied to the Delaware River and Bay, which matches the geometric assumptions of these equations fairly well. For those familiar with basic numerical modeling a few of the details of this simple model will be described (no attempt is made to define the terms mentioned, see modeling texts such as Haidvogel and Beckman, 1999, and Kantha and Clayson, 2000); see also Section 8.2).

This numerical model uses a staggered grid spatial scheme (elevation is determined at odd grid points and velocity is determined at even grid points). Centered second-order spatial differences are used for all spatial derivatives. The explicit time integration scheme uses centered second-order time differences (the "leapfrog" scheme), except for the friction term, for which a backward first-order time difference scheme is used. The friction term (in this very shallow waterway) has such a stabilizing effect that the model will reach the correct solution from a motionless flat initial condition in just a couple of tidal cycles; the larger the friction term the faster the correct solution is reached. Because the friction term has such a strong damping effect, nonlinear instabilities, if they occurred, never cause the model to blow up, but instead show themselves as very short wavelength, high-frequency spurious oscillations. Such oscillations result only from the nonlinear terms involving spatial gradients, i.e. the inertial term and the nonlinear continuity term, leaking in from the boundaries because of the uncentered second-order spatial differences required there. Once these two terms are turned off (only) at the boundaries, all spurious oscillations cease (see Parker, 1984). Other details about this simple numerical model are give in Section 8.2.

The model was calibrated for the Delaware River and Bay using the M_2 harmonic constants at 15 locations along the estuary. The model was forced at the ocean entrance with the appropriate M_2 tide at Lewes, Delaware and Cape May, New Jersey. The boundary at the upriver end of the model was a closed end with respect to the tide, which could not get past the rapids north of Trenton (see Figure 7.1), but still allowed river discharge to enter the model. The model was run for 8 days and the last 4 days were harmonically analyzed for M_2 and over tides.

Although M_2 greatly dominates all other constituents, the cumulative effect of the other constituents is to reduce M_2 via nonlinear frictional interaction. If those constituents are left out of a calibration run (as was done above), then their effect on M_2 will be compensated for by a larger friction coefficient, when one tries to match the model to the harmonic analysis results from the data. Thus, calibrating the model only with M_2 will lead to an empirically determined friction coefficient that is too large, and when one then adds all the other tidal constituents into the model, there will be too much frictional dissipation. The ideal calibration would have the model forced by all important constituents (for every run), but then each run would have to generate a month of calculated tidal heights if one used, M_2 , S_2 , N_2 , K_1 , and O_1 , or a half year of heights if one used these five plus P_1 , in order to separate all the constituents with harmonic analysis. [Actually one might be able to analyze a shorter time series because there will be no noise, and a least squares harmonic analysis would be used; see Section 3.3.] Because of this additional (erroneous) frictional effect, the model (calibrated only with M_2) will also generate M_6 amplitudes that are too large, as well as compound tides (such as $2MN_6$ and $2MS_6$) that are too large (although the shape of the model-produced constituent plots along the estuary will look similar in shape to the plots from the harmonic

analysis of data. Figure 7.23 shows plots of M_2 , M_4/M_2 , and M_6/M_2 produced by the one-dimensional nonlinear model of the Delaware waterway described above (solid lines) compared with harmonic analysis results (the * and + symbols) from Delaware water level data. One can see that the model-predicted M_6/M_2 graph is larger than the M_6/M_2 values from the harmonic analyses of the data (although both curves have very similar shapes). [A better way to calibrate a hydrodynamic numerical tide model is to start with an M_2 , but then add the additional important constituents and re-calibrate (even though one will have to generate and harmonically analyze longer model-produced time series); see Section 8.6.]

7.6.6b Overtides Generated By the Numerical Model Compared With Analysis Results

Repeated model runs with different nonlinear terms turned on and off, confirmed that quadratic friction, $u|u|$, was the dominant M_6 generating term. When the rest of the nonlinear terms were also turned on, producing M_4 , the third-order interaction between M_2 and M_4 (also via these terms) produced an M_6 out of phase with the frictionally generated M_6 , such that the total model-produced M_6 decreased a little.

The M_4 values produced by the model were close to the actual Delaware data analysis results (see Figure 7.23 and also Parker, 1984). Running the model with different nonlinear terms turned on, showed that the nonlinear continuity term, $\partial(\eta u)/\partial x$, accounted for 73% of the M_4 . The term representing the elevation effect on frictional momentum loss (per unit volume of fluid), $\eta u|u|$, accounted for 20% of the M_4 . The inertial term, $u\partial u/\partial x$, accounted for only 7%.

These same three terms also caused a small shift in mean sea level, although in this case the inertial term had a very small effect. The largest change in mean sea level occurred near

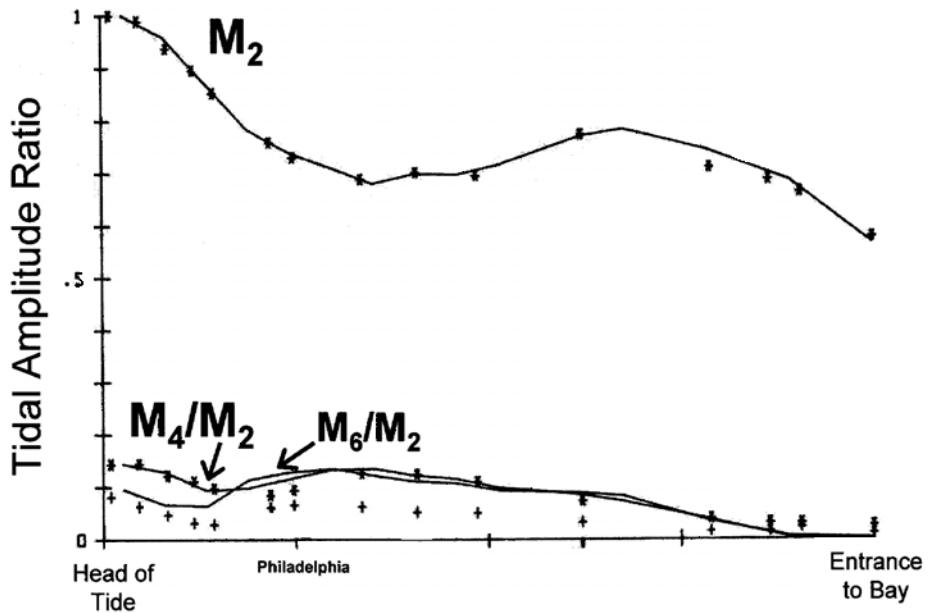


Figure 7.23. Plots of tidal M_2 amplitude and M_4/M_2 and M_6/M_2 amplitude ratios produced by a calibrated one-dimensional nonlinear numerical model of the Delaware River and Bay (solid lines) compared with harmonic analysis results for stations along the waterway (*s and +s). (See text) (From Parker, 1984.)

Philadelphia, an increase of approximately 0.16 ft (5cm) (i.e., 7.7% of the M_2 amplitude at the entrance to the bay). The term representing the elevation effect on frictional momentum loss was most important, accounting for 69% of the change in mean sea level; the nonlinear continuity term accounted for the rest. The term representing the elevation effect on frictional momentum loss had its greatest effect at Trenton (6% of the M_2 amplitude), while the nonlinear continuity term had its greatest effect near the Chesapeake and Delaware Canal (3.4% of the M_2 amplitude).

The model, forced with M_2 and N_2 , was run for 28 days and the resulting data were harmonically analyzed. The results confirmed that $u|u|$ generated the compound tide $2MN_2$. The results also confirmed that $u|u|$ reduced the amplification of N_2 due to the presence of M_2 .

7.6.6c Numerical Model Results Illustrating Nonlinear Tidal Interaction With River Flow

The numerical model was also run with seven different (constant) river discharges (with only M_2 forcing at the entrance). Figure 7.24 shows the M_2 amplitude curve for the runs with $u|u|$ as the only nonlinear term turned on; all values are plotted relative to the entrance amplitude value. The river effect is localized in the narrower upper river north of Philadelphia, where the river current speeds are greater than in the wider portions of the river and bay (due to continuity). In the upper river one sees a significant decrease in the M_2 amplitude. [Downstream of Philadelphia the M_2 amplitude actually increases slightly for higher river flows. This is the location of a quasinode under no flow conditions, but for higher flows there is a shortening of the M_2 wavelength and a marked reduction in the amplitude of the reflected wave by the time it reaches this location, which leads to a small increase in amplitude there.] Model runs with all nonlinear terms turned on, gave only slightly different M_2 amplitudes (approximately 1-2% larger) than the $u|u|$ -only run.

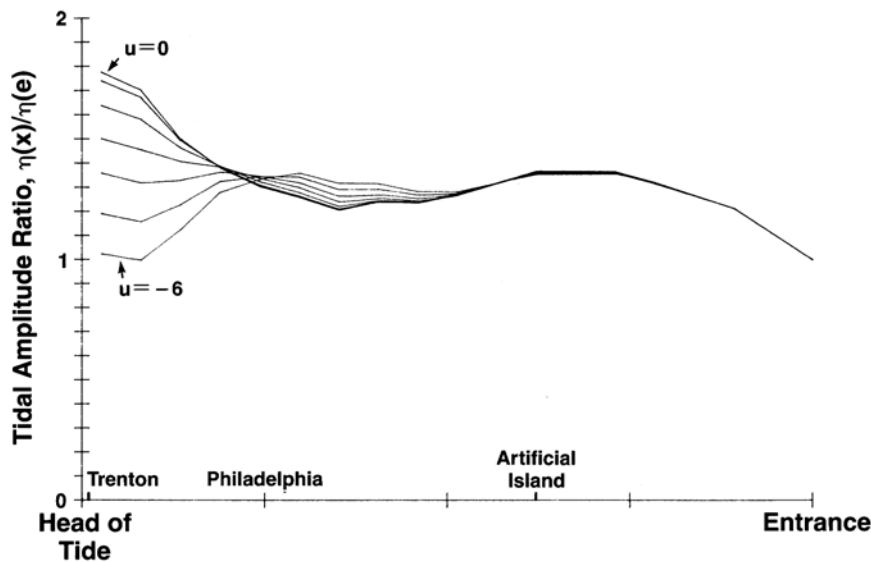


Figure 7.24. M_2 amplitudes produced by a one-dimensional nonlinear numerical model along the Delaware River and Bay for seven different amounts of river discharge, with quadratic friction as the only nonlinear term turned on in the model. $U=-1$ corresponds to a discharge of approximately $10,000 \text{ ft}^3/\text{sec}$ ($283\text{m}^3/\text{sec}$). All values are relative to the M_2 at the entrance.

Increased river discharge delays M_2 high and low waters. For example, near Trenton the $u|u|$ -only run with discharge equivalent to approximately 50,000 ft³/sec (1416 m³/sec) produced a 17.2° later phase lag. With all the other nonlinear terms turned on this lag decreased to 9.4° because the increased depth (due to the increased river flow) increased the wave propagation speed of the M_2 wave (via the nonlinear continuity term). Figure 7.25 shows the M_4/M_2 amplitude ratio resulting from the river flow effect (only the $u|u|$ terms was turned on; all other nonlinear terms were turned off). As river discharge increased so did the M_4/M_2 ratio. Eventually, however, at the highest discharges, the M_4/M_2 ratio begins to decrease, because the greater (first-order) frictional damping of M_4 than M_2 finally overcomes the M_4 generating effect, which has leveled off. The increased M_4/M_2 ratio was also reflected in an increased delay in the time of low water relative to the high water.

Model runs with only $u|u|$ also showed the expected decrease in M_6/M_2 amplitude ratio with increased river flow (see Figure 7.26.). The mean sea level increased with increased river flow as expected (see Parker, 1984).

7.6.6d Numerical Model Results Illustrating Nonlinear Tidal Interaction With Storm Surge

Storm surges are transient and approximately periodic for short time periods. However, to simulate the effects of a low-frequency storm surge the model was forced with an M_2 tide plus a low-frequency oscillation with the same amplitude but with 1/10th the frequency (roughly a 5-day period of oscillation). Runs were made with tide and surge separately and combined, with each nonlinear term turned on individually and then with all the nonlinear terms turn on together. The

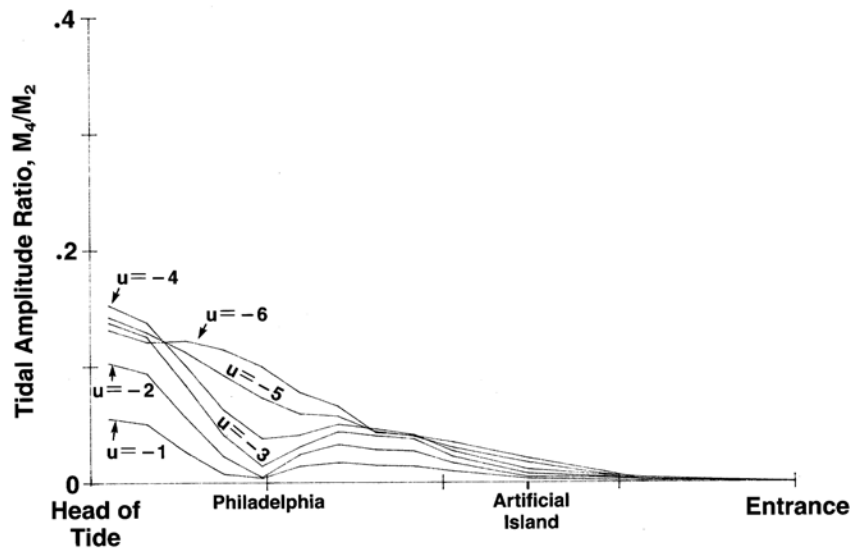


Figure 7.25. Numerical model-produced M_4/M_2 tide range ratios along the Delaware River and Bay for seven different river discharge amounts, with quadratic friction as the only nonlinear term turned on in the model. (From Parker, 1984.)

7. Interpretation of Tidal Analysis Results Based On Hydrodynamics

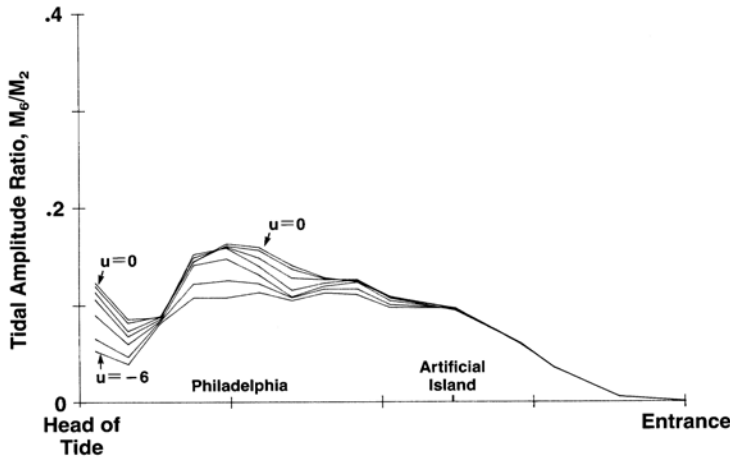


Figure 7.26. Numerical-model produced M_6/M_2 tide range ratios along the Delaware River and Bay for seven different river discharge amounts, with quadratic friction as the only nonlinear term turned on in the model. (See text.) (From Parker, 1984.)

results are summarized in Table 7.1. With all nonlinear terms turned on there was a reduction in tide range at the trough of the low-frequency storm surge, which increased as one moved up the estuary (the results in Table 7.1 are near Trenton). There was also an increase in tide range at the crest of the surge. The model with quadratic friction as the only nonlinear term showed none of these effects, nor did it with the inertial term added to quadratic friction. The decrease in the tide range under the trough of the storm surge was due solely to the effects of the nonlinear continuity term and the term representing the elevation effect on frictional momentum less, with both terms being of

Nonlinear Terms turned on:	At Crest of LF Surge		At Trough of LF Surge	
	Tidal Amplitude*	Increase over $ u $ only	Tidal Amplitude*	Decrease from $ u $ only
$ u $ only	1.661	—	1.682	—
$ u + u \frac{\partial u}{\partial x}$	1.660	0.0%	1.683	0.0%
$ u + \eta u u $	1.778	7.0%	1.569	6.7%
$ u + \frac{\partial}{\partial x} (\eta u)$	1.788	7.6%	1.530	8.6%
all nonlinear terms	1.917	15.4%	1.439	14.4%

*relative to entrance amplitude

Table 7.1. Effect of a low-frequency storm surge on the tide near the head of tide in the Delaware River, using a nonlinear numerical model. The amplitude of the surge equaled the tide amplitude at the entrance to Delaware Bay, but had a frequency of 1/10th of the M_2 tide frequency. (See text.) (From Parker, 1991a.)

approximately equal importance. The same two terms were also responsible for the increase in tide range under the crest of the storm surge.

The model was also run with a down-estuary wind blowing over only the lower bay for one tide cycle and then turned off. With quadratic friction as the only nonlinear term turned on, there was simply a shift down in water level that propagated up the estuary, but with no effect on the tidal range. Turning on the inertial term did not change this. But turning on the nonlinear continuity term and/or the term representing the elevation effect on frictional momentum loss produced a tide range reduction (in addition to the shift down in water level) that became more significant as one moved up the estuary. The nonlinear continuity term had the greater effect of the two terms, but both were significant.

7.6.7 The Effect of the Nonlinear Lateral Inertial Terms

In the one-dimensional approach in the previous sections the third and fourth terms in each of the momentum equations in (7.3) were neglected; the (7.3) equations are repeated below.

$$\begin{aligned} \frac{\partial u}{\partial t} + u \frac{\partial u}{\partial x} + v \frac{\partial u}{\partial y} + w \frac{\partial w}{\partial z} - fv &= -\frac{1}{\rho} \frac{\partial p}{\partial x} - (\text{frictional forces})_x \\ \frac{\partial v}{\partial t} + u \frac{\partial v}{\partial x} + v \frac{\partial v}{\partial y} + w \frac{\partial v}{\partial z} + fu &= -\frac{1}{\rho} \frac{\partial p}{\partial y} - (\text{frictional forces})_y \end{aligned} \quad (7.3)$$

Here one will still neglect the fourth term in each, still assuming that the vertical acceleration is small. Now, however, one needs to consider the effects of the lateral inertial terms, which as was seen in Section 2.3.6e can have a very important effect on tidal currents when there are irregular geometries such as bends in the waterway or points of land sticking out into the waterway. A good example was shown in Figure 2.36, which showed the change in the $(K_1+O_1)/M_2$ ratio, the M_4/M_2 ratio, and the mean (residual) current across the entrance to Haro Strait due to the effects of the lateral inertial terms.

As with the nonlinear shallow-water terms, there is no simple analytical solution that allows one to see the effects of the nonlinear lateral inertial terms (and one can best see these effects with a high-resolution two- or three-dimensional numerical hydrodynamic model). However, as was done in Section 7.6.2, one do a Fourier decomposition of these terms to get an understanding of what they will do to tidal harmonic constituents. For example, for the third term in the second momentum equation in (7.3) one can do the following Fourier decomposition. As usual the tidal current will be broken into two orthogonal components, u and v , such as in the major axis and minor axis directions. Representing the total cross-waterway component of the tidal current, v , as the sum of two astronomical tidal constituents, one has:

$$v(x,y,t) = v_1(x,y) \cos(\sigma t - \phi_1(x,y)) + v_1'(x,y) \cos(\sigma' t - \phi_1'(x,y))$$

where σ, σ' are the frequencies of the two tidal current constituents, and v_1, v_1' , and ϕ_1, ϕ_1' are the tidal current constituent amplitudes and phase lags for the cross-waterway component. To simplify this for use in later calculations let $\sigma_r = \sigma - \sigma'$, i.e., the difference in frequency between the two constituents. Then rewrite $v(x,y,t)$ as

7. Interpretation of Tidal Analysis Results Based On Hydrodynamics

$$v = v_1 \cos(n\sigma_r t - \phi_1) + uv'_1 \cos([n+\beta]\sigma_r t - \phi'_1)$$

where $\beta = \pm 1$ and n is an integer. Also let $n\theta = (n\sigma_r t - \phi_1)$, again to make later calculations a little simpler to keep track of. Then rewrite $v(x,y,t)$ as

$$v = v_1 \cos n\theta + v'_1 \cos([n+\beta]\theta - [\phi'_1 - \frac{n+\beta}{n} \phi_1])$$

One also makes the assumption that $v'_1 \ll v_1$, which is true for semidiurnal tide regime, since in such an area M_2 is much larger than the other tidal constituents (it may be less true in some areas when the second tidal constituent is K_1 , but here we are only trying to demonstrate effects in the frequency domain and we don't necessarily expect very accurate answers). So for convenience we will call the larger constituents M_2 .

This lateral inertial term then becomes:

$$\begin{aligned} v \frac{\partial v}{\partial y} &= \frac{1}{2} \frac{\partial(v^2)}{\partial y} = \frac{1}{2} \frac{\partial}{\partial x} ([v_1 \cos n\theta + v'_1 \cos([n+\beta]\theta - [\phi'_1 - \frac{n+\beta}{n} \phi_1])]^2) \\ &= \frac{1}{2} \frac{\partial}{\partial y} (\frac{1}{2} v_1^2 + v_1 v'_1 \cos(\beta\theta - [\phi'_1 - \frac{n+\beta}{n} \phi_1]) + \frac{1}{2} v'_1^2 \cos 2n\theta \\ &\quad + v_1 v'_1 \cos([2n+\beta]\theta - [\phi'_1 - \frac{n+\beta}{n} \phi_1])) \end{aligned}$$

The first term inside the $()$ on the right-hand side of the second $=$ sign is a mean flow generated by the inertial term's effect on M_2 . This helps generate the *tidally induced residual currents* seen in Figure 2.3.6 (along with the other lateral inertial terms). This is also called *tidal rectification*. The third term is the second harmonic of M_2 , namely, the overtide M_4 . This term helps produce the increased M_4/M_2 ratio seen on the west side of Haro Strait in Figure 2.3.6. It also helps produce the decreased $(K_1+O_1)/M_2$ ratio in that figure [but to show that with this Fourier decomposition, one would have to let v_1 represent K_1 and let v'_1 represent O_1 ; the result would produce the compound tidal current KO_2 , which has the same frequency as M_2]. The second and fourth terms are new compound tidal currents generated by the interaction between M_2 and the second constituent. If this second constituent is N_2 then the second term is a low-frequency shallow-water tidal constituent, MN, which happens to have the same frequency as the astronomical constituent Mn. The fourth term is a higher-frequency shallow-water tidal constituent, MN_4 . The nonlinear lateral inertial terms have the same asymmetric effect as the asymmetric nonlinear mechanisms $(\partial(\eta u)/\partial x, u \partial u / \partial x, \text{ and } \eta u |u|)$ discussed in Section 7.6.2 and summarized in Table 2.4.

7.7 Variation of Tidal Currents With Depth

Tidal currents vary with depth, due to frictional momentum loss at the sea bottom. The current speed increases from zero right at the bottom to a maximum often near (but not always at) the water surface. The shape of the current profile can vary, depending on the roughness of the bottom and other factors. There is usually some distance from the bottom over which there is a fairly rapid increase in current speed (which is usually called the *bottom boundary layer*), and then a more gradual increase upward after that. The turbulence caused by the rough bottom makes the thickness of the bottom boundary layer larger than it would be with slow flow over a smooth bottom (in which case there is no turbulence and one has what is called a laminar boundary layer), but this is found only in a laboratory, and not in the ocean or bays, where the flow is always turbulent. In Figure 2.33

we saw the vertical variation in tidal current speed and direction in a cross section in Chesapeake Bay, which showed that at particular times the tidal current can be flowing in opposite directions near the bottom versus near the water surface. Bottom friction causes the current to slow up and change direction sooner near the bottom, and then this change slowly works its way up the water column.

There is also vertical variation in the current due to density effects when there are vertical gradients in salinity and/or water temperature. This latter *baroclinic* effect includes the effects of (usually intermittent) internal tide waves. When there is sufficient stratification an internal tide wave will propagate along an interface between an upper fresher layer and a lower saltier layer (the interface does not actually have to be sharp, but can be blurred by mixing). This interface moves up and down (in much the same way as the interface between air and water moves up and down at the water's surface), at the same time causing an oscillating current back and forth horizontally. These oscillations have a tidal period and so the baroclinic tidal currents are superimposed on the barotropic tidal currents (i.e., those associated with the regular tide, that we have been looking at in this book). The tidal currents will therefore vary most around the interface. [A horizontal density (salinity) gradient up an estuary can also generate a so-called *estuarine* or *gravitation circulation*, where there is outflow near the water surface and inflow near the bottom, this nontidal effect being superimposed on the tidal current.]

To accurately account for these effects on the tidal currents one must go back to the full three dimensional equations of motion [i.e., equations (7.1) and (7.3)]. To include the baroclinic effects one can no longer keep density constant, and one must add a conservation of salt equation and/or conservation of heat equation (equations of state). Needless to say, this makes solutions more complex, and obviously solvable only with numerical methods. The frictional momentum loss (and its effect on the currents along the water column) must be represented with some kind of a turbulence closure scheme (e.g., Mellor and Yamada, 1982). This is beyond the scope of this book. For a treatment of possible shapes of the vertical current profile see Dronkers (1964, pp145-152), but these are generally simpler than one will usually see in a real waterway.

In a real waterway there are a variety of hydrodynamic effects that can alter the vertical current profile, such as bathymetry, which will have more of an effect on deeper currents than on currents closed to the surface. Because of this (and the changing stratification) there can be great variety in measured current profiles. This can be seen in Figure 7.27, which shows current profiles measured with bottom-mounted upward-looking acoustic Doppler current profilers (ADCPs) at eight different locations in Chesapeake Bay, all taken at the same time (but the bay is so large, each of these locations is at a different stage of the tide).

As was seen in Sections 5.2 and 7.1.3, tidal constituent ellipses can vary significantly, and that includes with depth. Frequently one will see tidal current ellipses become narrower with depth and then change from clockwise rotation to counterclockwise rotation (or vice versa). For example in Figure 7.28 one sees the M_2 ellipse at the upper two depths (near the surface) rotating clockwise but then the ellipse at a depth much closer to the bottom rotates counterclockwise. At the same station the N_2 ellipse starts out with a fairly wide ellipse at the depth closest to the surface, then becomes very narrow a little deeper, both these having clockwise rotation, and then near the bottom getting even narrower, but rotating counterclockwise. The K_1 at the same station (not shown in the figure) had fairly narrow ellipses at all three depths, but it started out with counterclockwise rotation at the top two depths and changed to clockwise rotation at the bottom depth.

When the wind blows on the water surface it produces a wind-driven current that decreases with depth as the frictional stress is transmitted from layer to layer. This, of course, is a nontidal current

7. Interpretation of Tidal Analysis Results Based On Hydrodynamics

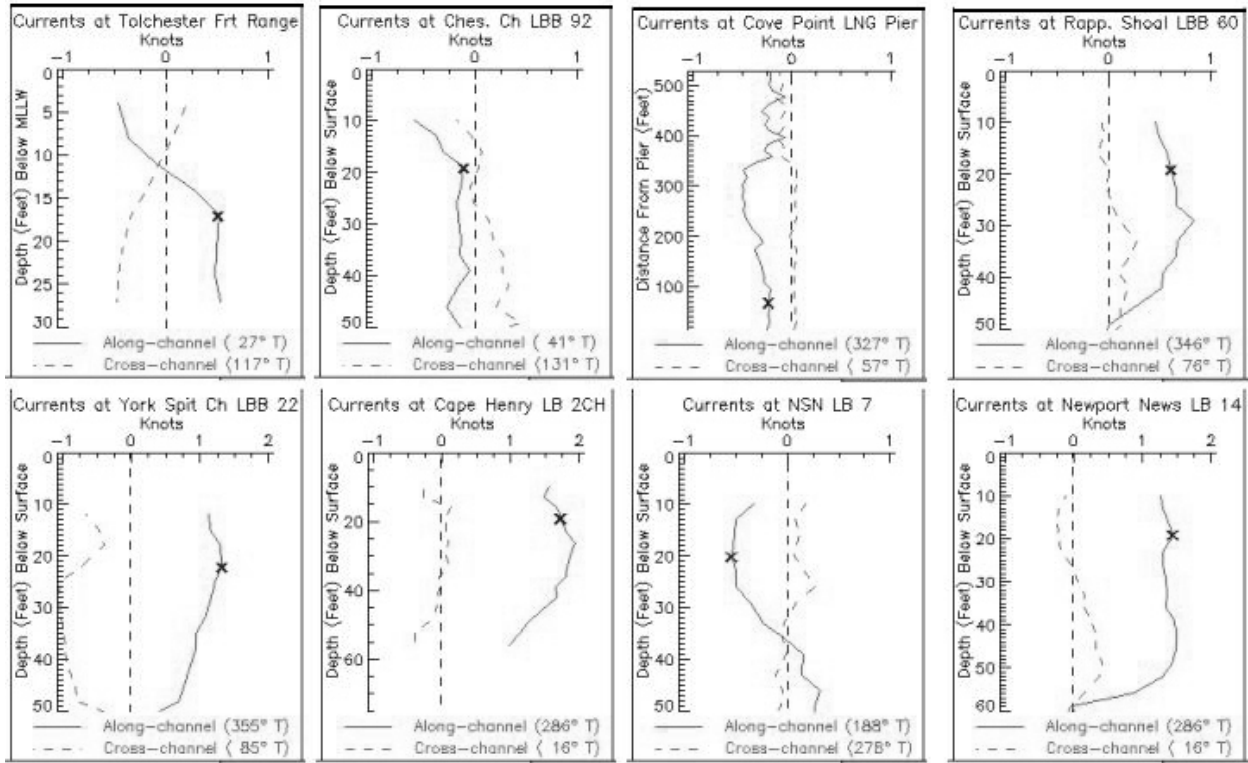


Figure 7.27. Current profiles from bottom-mounted upward-looking ADCPs at eight locations in Chesapeake Bay, all measured on October 26, 2006 at noon. The solid line is the along-channel component, and the dashed line is the cross-channel component. Negative speeds are in the ebb direction.

but as was seen, there can be interactions with the tidal current, and this could possibly affect the tidal current, also giving it a depth dependency, in addition to the depth dependency it has from bottom friction and from density effects. In waterways wide enough for Coriolis to have an effect, one sees that not only does the wind-driven current decrease with depth, but it slowly changes direction, each lower layer of water moving slower and further to the right of the wind (in the Northern Hemisphere), describing the classic *Ekman spiral*. A similar effect can happen with the bottom frictional effect on tidal currents, and this may be responsible for the change in rotation of tidal current ellipses with depth (but there may also be topographic effects involved also).

For more discussion of and approaches to handling the vertical structure of tidal currents see also Prandle (1982).

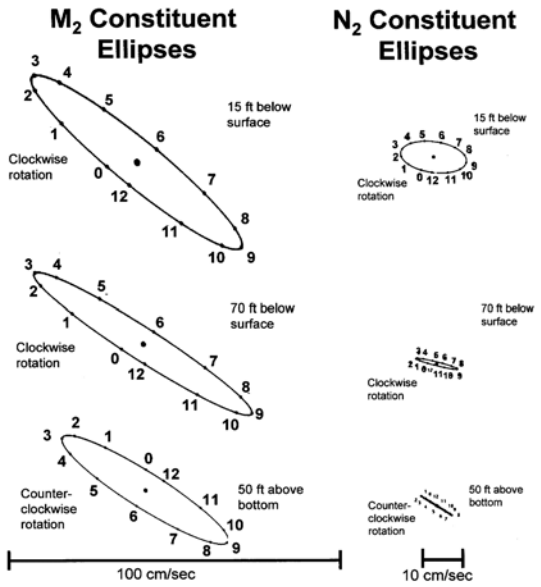


Figure 7.28. M₂ and N₂ constituent ellipse for three different depths for a current station in the Strait of Georgia. (Reworked from Parker, 1977.)

7.8 Tidal Dynamics of the Oceans of the World

Even though the oceans are where the tide is first generated, they are the most difficult waterways to model hydrodynamically. The tide in other bodies of water (the bays and estuaries connected to the oceans), being too small for the tide-producing forces to generate a tide, result from the tidal forcing at their entrances by the ocean tide (modified by the continental shelves). This makes the hydrodynamic modeling of a bay or estuary much easier, for the tidal forcing at the entrance can be done with accurate harmonic constants obtained from water levels stations (which often are on both sides of the entrance). (Even when one wishes to move the open boundary conditions offshore from the entrance there are usually ways to figure out what those offshore boundary conditions should be. See Section 8.5.) No such convenient open boundary conditions exist when modeling the tide in the Atlantic Ocean or in the Pacific Ocean. In fact, some modelers have felt that it is simpler to model all the ocean basins of the world as one, which avoids the problem of open boundaries that are not well known. For even if one had good harmonics constant for some line of latitude or longitude that one would like to make an open boundary, technically the ocean is not being “forced” at that boundary. The tide in a particular ocean is a combination of the tide created directly by the tide-producing forces in that ocean, and the tides that propagate into that ocean from other ocean basins (where they were generated). This is another reason why modeling all the oceans together as one large connected ocean makes sense (Kuo, 1991).

Another problem has been the data against which to compare one's ocean model. For decades, oceanographers have been trying to construct accurate cotidal and corange charts for the oceans, against which models can be compared. However, water level gauges along the coastlines of the world have data that have been affected by the continental shelves, and so in order to use harmonic constants from these stations to develop a model, that model must have the continental shelves

7. Interpretation of Tidal Analysis Results Based On Hydrodynamics

represented in the model. That increases the resolution requirements of the model. Water level gauges on islands provide the best data to harmonically analyze, usually not having large enough shallow water areas around them to dramatically change the ocean tide signal. Only in the last couple of decades has satellite altimetry provided a way to accurately measure the tide in the middle of the ocean. For although there is a very large sampling period for the data from satellite altimeters, this does not keep one from harmonically analyzing the data (one does, however, have to worry about periodicities in the satellite orbits that may interfere with particular tidal constituents); see Cartwright, 1991; Egbert, *et al.*, 1994.

The first attempts to understand the tides in the open ocean were based on whatever cotidal and corange charts could be produced from the available water level data (with all its coastal limitations, as mentioned above). (See Chapter 9 in Cartwright, 1999.) In that pre-computer era, analytical solutions were attempted by adding together combinations of Kelvin waves, Poincare waves, and other specialized solutions of some version of the long wave equation on a rotating Earth (which often obtained the name of the first person to solve them). It was not until the advent of high-resolution global tide models and satellite altimetry (to provide global tidal data) that oceanographers were able to gain some real understanding of the tidal dynamics of the oceans, and were able to produce reasonably accurate cotidal and corange charts for the oceans (see Figure 7.29 for one example). For more information on the modeling of oceans see Doodson, 1958; Cartwright, 1977; Schwiderski, 1978, 1980, 1991; Platzman, 1991; Le Provost and Vincent, 1991; Kuo, 1991; Andersen, *et al.*, 1995; and Shum, *et al.*, 1997.

The continental shelves are sometimes modeled separately from the rest of the much deeper ocean, the open ocean providing the boundary conditions along the continental slope. A continental shelf, especially if it is reasonably shallow, can be a significant co-oscillating tidal system in itself. Looking at the tidal system over a continental shelf in the simplest possible way, a long tide wave from the ocean will undergo a partial reflection-transmission at the depth discontinuity along the continental slope, increasing the tide range over the shelf. Another full reflection of the tide wave at the coast will further increase the tide range, that increase depending on the width of the shelf compared with the tidal wavelength over the shelf (that wavelength being dependent on the water depth over the shelf). A shallower continental shelf has a shorter tidal wavelength and its width is thus more likely to be closer to $\frac{1}{4}$ of a tidal wavelength, leading to a larger tide range. The largest tide range along an open coast is along the coast of Argentina because of the very wide continental shelf, reaching to the Falkland Islands. The above discussion, of course, is an over simplification. Tide waves can propagate along the continental shelf as Kelvin waves or other types of long waves, with the tidal frequency's relationship to the Coriolis parameter (which depends on latitude) having an important effect. Strong tidal amplification can occur across wide continental shelves in mid and low latitudes. For more information on tides over the continental shelf see the review on the subject by Clarke (1991).

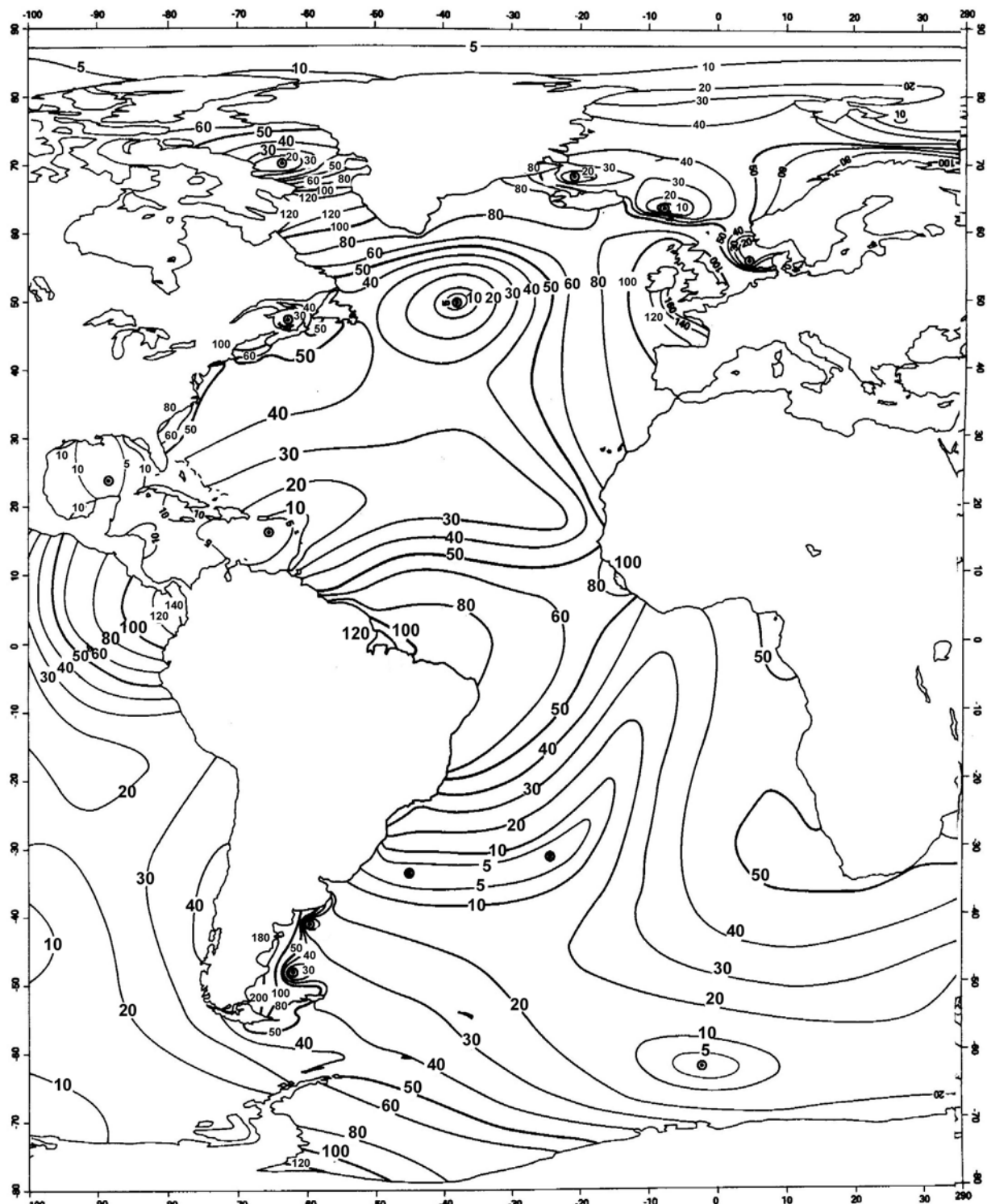


Figure 7.29. An example of an ocean M_2 amplitude chart, this one for the Atlantic Ocean produced by Schwiderksi (1979). Amplitudes are in cm. Circles with a dot in the center denote amphidromic points (i.e., points where the amplitude is zero).

7. Interpretation of Tidal Analysis Results Based On Hydrodynamics

8. The Use of Numerical Hydrodynamic Models For Predicting Tides and Tidal Currents

8.1 Introduction

The alternative to making a tide or tidal current prediction at a particular location using a statistical technique (such as harmonic analysis) is to make a tide or tidal prediction using a numerical hydrodynamic model of the waterway in which that particular location is found. As has been seen, the harmonic analysis technique relies solely on the knowledge of the frequencies where the astronomically and shallow-water produced tidal energy is found. The numerical hydrodynamic model, on the other hand, makes the prediction using the physics of the water movement as described by a discretized version of the equations of motion (such as those seen in Section 7.3). Such a model still relies on astronomical forcing, but for a bay or river this forcing is needed only at the entrance (usually in the form of harmonically produced tide predictions) and the model then uses physics to determine how the tide wave propagates up the waterway and what the tide and tidal current will be at the location(s) of interest. [For a global ocean tide model, instead of tide predictions at an entrance, the model uses the actual tide producing forces throughout the ocean(s), with the forced equations of motion determining how the tide wave propagates throughout the ocean and up the bays and rivers.]

As one steps forward in time when making a harmonically-based tide prediction, one is, for each time step, merely adding up the contributions of the cosine values for each tidal frequency for which one has harmonic constants. This is done independently of the previous time step. However, as one steps forward in time when making a prediction using a numerical hydrodynamic model, the calculation at each time step makes use of values at one or more previous time steps both at the location (grid point) where the prediction is being made and at one or more nearby locations (grid points). The formulas for calculating the tidal height or tidal current at a particular time step (using the values at previous time steps) come from the rearranged discretized equations of motion. The next section will show a simple example so that those not familiar with numerical modeling theory can gain some insight into how this type of prediction process works.

8.2 The Workings of a Very Simple Numerical Hydrodynamic Model

It is beyond the scope of this book to go into great detail about how numerical hydrodynamic models are created and how they work. There are thousands of papers on the subject, and a few good textbooks such as Haidvogel and Beckman, 1999, and Kantha and Clayson, 2000. Here a little background is merely provided for those without any experience with numerical models.

Numerical hydrodynamic models are computer programs that calculate numerical solutions of the equations of motion [such as equations (7.1) and (7.3)] for a specific waterway, whose shoreline and bathymetry determine the solid boundaries of the model, and whose forcing at its entrances (such as the tide at the ocean entrance and discharge from rivers that flow into the waterway)

provides the momentum and energy to drive the motion inside the waterway. The model may also include additional equations for salinity and temperature/heat, if one wants to include baroclinic (density) effects on the tide and tidal current.

Chapter 7 provided examples of a few *analytical hydrodynamic models*, that is, very simple mathematical equations that can be solved using algebra and trigonometry to produce formulas with which one can calculate the tide or tidal current at any point in time at any place within the idealized geometry of the waterway. However, such analytical models do not accurately represent any real-world waterways. In order to solve the equations of motion one had to leave out all but the slightest variation in the geography of the waterway, and one had to leave out all the nonlinear terms in the equations. When those nonlinear terms and the complex geometry are left in, the only alternative is to solve the equations *numerically*.

When one uses the complete three-dimensional equations of motion (including the extra equations to include density effects) to describe the tidal hydrodynamic over the full three-dimensional geometry of a waterway, the resulting numerical model is large and complex, as one might expect. However, to get across the basic idea of how a numerical solution works, a very simple geometry will be used, along with a very simple numerical solution technique, the *finite-difference* technique. (There are a whole host of numerical modeling techniques, most more sophisticated than the finite-difference technique, but for our purposes this simple technique gets across the basic idea of numerical models.)

This basic finite-difference numerical modeling technique will be applied to a simple one-dimension nonlinear set of equations of motion, equations (7.27) and (7.28), which is repeated here

$$\frac{\partial \eta}{\partial t} + \frac{1}{b} \frac{\partial}{\partial x} (b(h+\eta) u) = 0 \quad (7.27)$$

$$\frac{\partial u}{\partial t} + u \frac{\partial u}{\partial x} = -g \frac{\partial \eta}{\partial x} - \frac{1}{h+\eta} c_f u |u| \quad (7.28)$$

where η is the tidal elevation, u is the cross-sectionally averaged tidal current velocity, b is the width of the basin, h is the width-averaged depth of the basin, and c_f is the friction coefficient (which is usually determined empirically for a particular waterway, but is often on the order of 0.0025).

Let Δx be the distance between points on a grid representing the waterway (which for a one-dimensional model is nothing more than a single string of boxes running up the waterway). Let Δt be the time interval between time steps, as the predictions are created by *time stepping* through the solution. Each time step makes use of the values calculated in the previous time step. The partial derivatives in equations (7.27) and (7.28) are replaced with small differences in speed (Δu) and elevation ($\Delta \eta$) divided by small differences in space (Δx) and time (Δt), creating *finite-difference analogs* of these equations. For example, $\partial \eta / \partial t$ becomes $\Delta \eta / \Delta t$, but for numerical reasons involving stability (discussed in the above mentioned numerical modeling texts) it is better to use what is called a centered difference, i.e. $[u(x,t+\Delta t) - u(x,t-\Delta t)]$ and divide it by $2\Delta t$. [In other words, one takes the u value at time interval $(t+\Delta t)$ and subtracts from it the u value at time interval $(t-\Delta t)$, and then divides by $2\Delta t$.] Likewise, $u \partial u / \partial x$, first becomes $\frac{1}{2} \partial(u^2) / \partial x$, this spatial derivative being replaced by $\frac{1}{2} \Delta(u^2) / \Delta x$, but a centered spatial difference is used, i.e., $\frac{1}{2} [u^2(x+\Delta x,t) - u^2(x-\Delta x,t)]$ and it is divided it by $2\Delta x$. [In other words, one takes the u^2 value at the grid point after x , i.e., $(x+\Delta x)$, and subtracts from it the u^2 value at the grid point before x , i.e., $(x-\Delta x)$, and then divides by $2\Delta x$.]

8. The Use of Numerical Hydrodynamic Models For Predicting Tides and Tidal Currents

The finite-difference analogs of these one-dimensional nonlinear equations of motion then become

$$\frac{\eta(x,t+\Delta t) - \eta(x,t-\Delta t)}{2\Delta t} + \frac{1}{b(x)} \frac{1}{2\Delta x} \{ b(x+\Delta x) [h(x+\Delta x) + \eta(x+\Delta x,t)] u(x+\Delta x,t) - b(x-\Delta x) [h(x-\Delta x) + \eta(x-\Delta x,t)] u(x-\Delta x,t) \} = 0 \quad (8.1)$$

$$\frac{u(x,t+\Delta t) - u(x,t-\Delta t)}{2\Delta t} + \frac{1}{2} \frac{u^2(x+\Delta x,t) - u^2(x-\Delta x,t)}{2\Delta x} = -g \frac{\eta(x+\Delta x,t) - \eta(x-\Delta x,t)}{2\Delta x} - \frac{1}{h(x)+\eta(x-\Delta x,t)} c_f u(x,t-\Delta t) |u(x,t-\Delta t)| \quad (8.2)$$

This particular model often uses a so-called staggered spatial scheme, where the elevation, $\eta(x,t+\Delta t)$, is determined at odd grid points using equation (8.1) and the velocity, $u(x,t+\Delta t)$, is determined at even grid points using equation (8.2). One essentially calculates a value for $\eta(x,t+\Delta t)$ from the rest of the terms in equation (8.1), which all involve values at two previous time steps, t and $(t-\Delta t)$ [at three grid points, $x-\Delta x$, x , and $x+\Delta x$]. Likewise, one calculates a value at $u(x,t+\Delta t)$ from the rest of the terms in equation (8.2), which also involves values at t and $t-\Delta t$ [again at three grid points, $x-\Delta x$, x , and $x+\Delta x$]. And one continues to step forward in time, producing as many predicted elevations and velocities as one needs.

The model is forced at the entrance with predicted tide elevations (from accurate harmonic constants) at grid point 1, and with river flow (or a no flow condition) at the highest numbered even grid point in the model. Centered second-order spatial differences are used for all spatial derivatives. The inertial term, which is the second term in equation (8.2), requires velocities at odd grid points, which are obtained by averaging the velocities at each surrounding pair of even grid points. The nonlinear continuity term in equation (8.2) requires elevation values at even grid points, which are obtained by averaging the elevations at each pair of surrounding odd grid points. [At the two open boundaries one is forced to use uncentered second-order spatial differences, which can lead to instabilities, so these two nonlinear terms are turned off at these two points.]

The explicit time integration scheme, using the rearranged equations (8.1) and (8.2), uses centered second-order time difference (the so-called *leapfrog* scheme), except for the friction term (for which such a scheme would cause the numerical solution to be unstable), so for this term a backward, first-order time difference scheme is used. In fact, the friction term has a very stabilizing effect, which allows this model to reach a correct solution after (time stepping forward) from a completely flat initial condition (*a zero startup*) in just a couple of tidal cycles. The larger the friction term (i.e., the shallower the waterway being modeled) the faster the correct solution is reached. There is a commonly used stability criterion (the *Courant-Friedrichs-Lowy criterion*) that specifies how small the time step should be for a particular grid spacing, so that the model will stay stable. The higher the resolution of a model (i.e., the smaller Δx is) the smaller the time step Δt must be and the longer it will take the model to run.

There are two types of two-dimensional models. The most typical solves the depth-integrated two-dimensional equations of motion [of which equations (7.22) are a very simplified form]. For a narrow waterway, a model might instead use the width-integrated two-dimensional equations of motion, in order to better look at how current speed changes with depth. With a two-dimensional depth-integrated model (and again using a basic finite-difference technique), one can have hundreds

or many thousands of square grid cells filling up the entire the entire waterway (see Figure 8.1, which shows only a part of a grid). Using square grid cells does not make it easy to accurately match the complicated shoreline at the model's boundaries. One approach is to increase the resolution, i.e., have smaller cells, for specific parts of a waterway (a so-called high-resolution nested grid), for example, needing more cells in a narrow channel where it is important to predict accurately the tidal current. But there are other forms of finite-difference models where the grid cells do not have to be squares, and can be shapes that help the model better match the shorelines, for example, using a *boundary fitted* coordinate system or an *unstructured* coordinate system. With models that use a *finite-element* solution technique the grid cells are (usually) triangles, which makes it very easy to match the shorelines, and very easy to change the resolutions of a particular part of the model.

For three-dimensional models there can be many layers of grid cells, and there are many approaches with regard to the vertical spacing of the grid points (see Mellor, *et al*, 2002). The frequently used *sigma coordinate* grid allows higher resolution near the bottom (to better resolve the bathymetry and the bottom boundary layer) and near the surface (to better handle wind effects), but can cause problems when there are large scale changes in depth, and so other systems for vertical spacing have also been developed. For models covering a waterway with high horizontal resolution and many layers, there can be hundreds of thousands of grid cells, but with today's computer power, that is usually not a serious problem.

Today there many types of numerical hydrodynamic models that are used to model the tide, or to model water level and currents with the tide being a predominant driver of this motion (along with changing wind, atmospheric pressure, river flow, and water density). These models use a whole host of numerical solution techniques, grid coordinate systems, and/or specialized forms of the equations of motion (only a few of which include: Blumberg and Mellor, 1987; Le Provost and Vincent, 1991; Lynch and Werner, 1991; Cheng, *et al*, 1991; Hess, 1989;). Some of these models have been standardized, with the same basic model being used by many oceanographers. Yet even with this increased standardization, the approaches to calibrating and verifying a model can still vary.

8.3 Advantages of Using a Numerical Hydrodynamic Model

When making tide or tidal current predictions using harmonic constants extracted from water level data or current data, there can be a number of limitations or problems. Now we will look at how we can overcome those limitations by making tidal predictions using numerical hydrodynamic computer models. [In the following discussion, the term "model" is used to mean a well calibrated and accurately verified three-dimensional high-resolution numerical hydrodynamic model, that accurately captures the relevant physics for the type of application for which the model is being used. Sections 8.5 and 8.6 will present a discussion about how to assure that a model meets these criteria.]

The first limitation using the results of a harmonic (or nonharmonic) tidal analysis is that one can make tide or tidal current predictions *only* at the locations for which one has data. Often one wants predictions at locations where one doesn't have data. With tide predictions that is usually not too serious a problem, because generally the tide regime changes slowly enough that either a nearby station can be used, or one can do reasonably well linearly interpolating between two nearby tide stations. However, this is not the case for tidal currents, which (as has been discussed many times

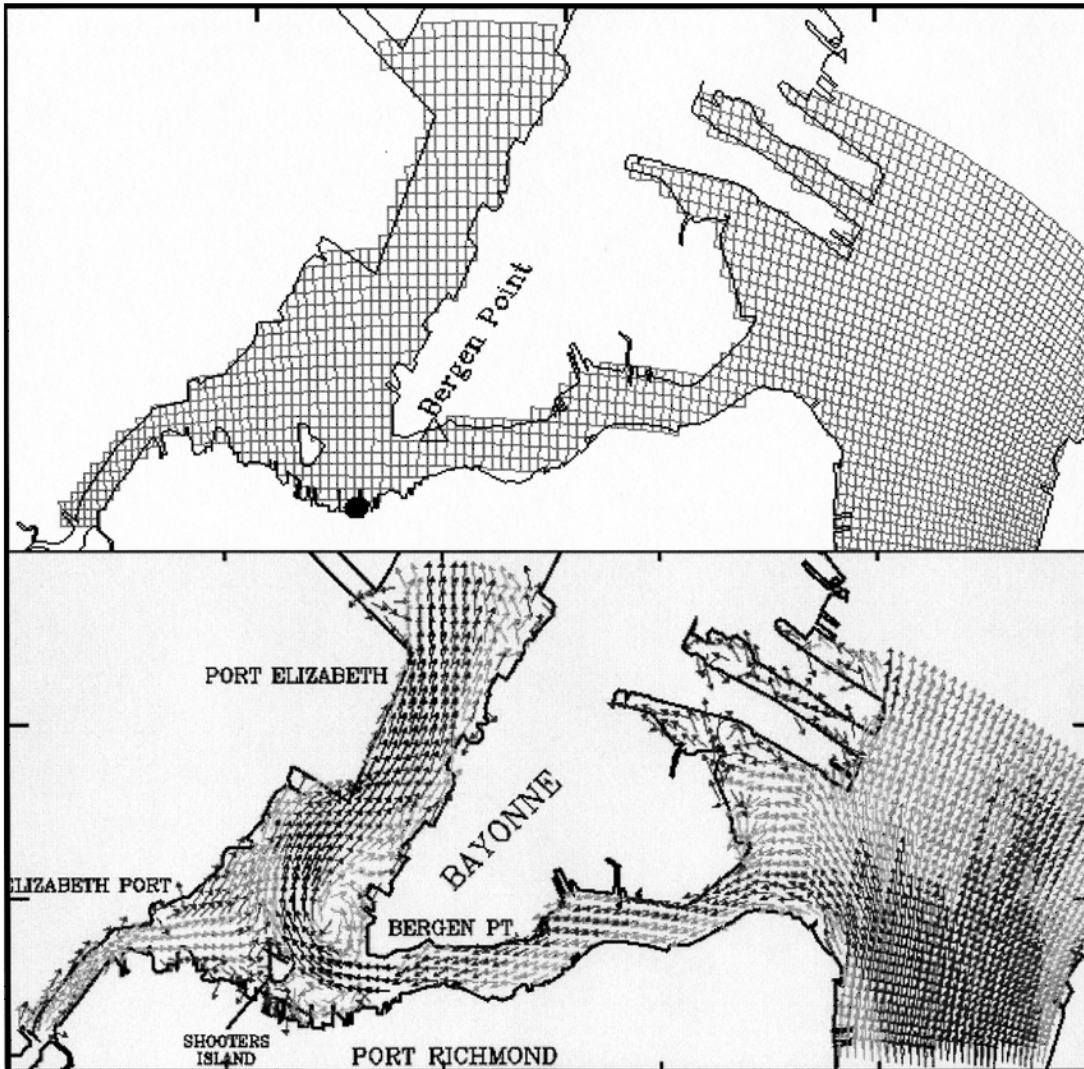


Figure 8.1. (Upper panel) A fine grid section of the NOS New York New Jersey Operational Forecast Model. (Lower panel) The predicted currents in the same section of the model illustrating the complex horizontal structure of the tidal currents (including current shears and eddies). (From Wei, 2003.)

in this book) can vary dramatically with distance, both horizontally and vertically. The lower panel in Figure 8.1 shows a section of the Port of New York and New Jersey where one can see a complex structure in the tidal currents, including current shears and eddies. This figure was produced by a numerical model of the port (a portion of the model grid is shown in the upper panel); see Wei, 2003. To try describe this complex a current pattern based on harmonically analyzing data, one would need hundreds of bottom-mounted ADCPs, or many towed ADCPs (e.g., see Figure 2.35), or still better, a high-resolution microwave radar system (which, however, provides only surface currents), and even then, to harmonically analyze all these data would be extremely labor intensive and inefficient compared to using a numerical hydrodynamic model.

Numerical hydrodynamic models can provide tide and tidal current predictions at many thousands of locations. The finer the resolution of the model grid the more places one can provide

predictions. Normally one will not want predictions at all the possible locations but it makes it easier to select them for specific locations of interest.

Models are especially important for tidal current predictions. It has been seen that tidal currents near the sea bottom can be very different in speed and direction and timing than tidal currents near the water surface. They can also be quite different in a channel and in the shallows just a few feet away. It is very difficult to obtain enough data to adequately describe all the spatial variability of the tidal currents. With a bottom-mounted upward-looking ADCP one can get only a single vertical velocity profile over time. With a side-mounted ADCP one can get only a single horizontal velocity profile at over time (or possibly sweep it around to get coverage of one water depth for one small area). With HF radar current measurement systems one can get spatial variation in the surface layer over a larger area, but not with enough resolution for a small bay or harbor unless one uses very high frequencies like microwaves. Only a validated high-resolution numerical model can really provide accurate tidal current predictions over an entire waterway.

Because of their great spatially variability, if one wants tidal current predictions for a particular location in the waterway, one will want to look at predictions at all the grid points around that location, and in all the (depth) layers of the model at that location, to see how much the current speed and direction changes from grid cell to grid cell (see Figure 8.1 again for an example of horizontal variation) and at various depth intervals. One can then decide how best to present the information to a user, like a pilot or ship's captain. One can graphically present synoptic views of nowcast and forecast model outputs (and even animate them) and/or select time series from key grid points to harmonically analyze for inclusion in the Tidal Current Tables (instead of basing it on a current sensor record that perhaps was not installed at a good location to best represent the tidal currents for that area).

The second limitation using the results of harmonic (or nonharmonic) tidal analysis, is the problem with making accurate tidal current predictions in waterways like that shown in Figures 7.2, 7.3, and 2.34 that was discussed in Section 3.6.3 (see also Section 9.2.6). Because of the complex geography affecting the mixed tidal currents in this waterway, there are such rapid changes in the harmonic make up of the tidal currents over short distances, that the six reference stations for that area now in the Tidal Current Tables are not nearly enough. The $(K_1+O_1)/M_2$ ratios and the M_4/M_2 ratios change from location to location, and permanent tidally induced "mean" currents are also generated (that should be included in the tidal current predictions). The only way to reasonably handle such a complex situation is with a high-resolution numerical hydrodynamic model. The predictions from the model may have to be provided only electronically, since convenient graphical representations in hardcopy form of all the possible dynamic situations remains difficult. A numerical model was developed in Canada to make predictions for the above complicated dynamic area (Crean, *et al*, 1988), but when they tried to turn the results in to a Tidal Current Chart it took more than a hundred charts to fairly accurately represent the results in a way that a mariner could (try to use to) make a prediction (Huggett, 1998). See also Section 9.4.3b.

With regard to our third limitation, using the results of harmonic (or nonharmonic) analysis it has been seen in Sections 2.3.3, 4.1.4, 5.3.4, 7.6.3, and 7.6.4 that in shallow waterways the tide nonlinearly interacts with nontidal phenomena such as river flow and storm surges. These nontidal phenomena can modify the harmonic constants during strong events, so that they cannot be used to make tide or tidal current predictions for other time periods (and they are generally not even usable for the time period of the nontidal event, because such events are too short for a reliable harmonic analysis to be done). However, a numerical hydrodynamic model can easily handle the nonlinear interactions between the tide and the various nontidal

8. The Use of Numerical Hydrodynamic Models For Predicting Tides and Tidal Currents

phenomena at the same time (including their interactions), and predict the total water level and the total currents. If the model includes the appropriate equations for salinity and water temperature, it can also include all the transient baroclinic effects on the tide and tidal current (such as internal tide waves). It can even include the gravitational (estuarine) circulation due to salinity gradients up the waterway, another nontidal effect.

As mentioned in the first paragraph, when we say “model”, we are talking about validated three-dimensional numerical hydrodynamic models with good resolution. With today’s computer power, there is no reason to settle for less. Sometimes more important than having access to predictions at many locations is the fact that high-resolution three-dimensional numerical models usually do a much better job of representing the physics of the waterway, than do one- or two-dimensional models, especially when it comes to the tidal currents, and so they provide more accurate predictions.

8.4 Disadvantages of Using a Numerical Hydrodynamic Model

With all the advantages discussed in the last section, one must remember that a lot of work and skill goes into developing a numerical hydrodynamic model that can provide accurate tide and tidal current predictions when forced only with the tide, or accurate water level and current predictions when forced at the entrance with actual water levels, plus inputs of wind, atmospheric pressure, and river discharge.

There are many ways that an inadequate model can be developed. The harmonic constants for the entrance may not be accurate enough, because there was not a long enough data time series to harmonically analyze. There may not be enough data at enough locations in the waterway to adequately calibrate it and verify it. It may not have high enough spatial resolution to do a good job on the tidal currents. Sometimes the available bathymetry is too old and the depths have changed (which can be a serious problem for shallow waterways). Or the calibration and verification procedure itself may not have been done in a way that resulted in a model that could reproduce all the important tidal frequencies accurately. When models are not producing as accurate results as desired, sometimes certain coefficients are played with and sometimes bathymetry is changed, and wrong choices can be made. One may make changes that allow the model to reproduce a particular data set, but those changes might not work well for a different set of data (covering a different dynamic situation).

One error that was often made in the past occurred when depths were taken off nautical charts for assigning depths to all the grid cells of the model. Sometimes the modeler forgot that the depths on a nautical chart are referenced to mean lower low water (MLLW) and not to mean sea level (MSL), which the model is usually referenced to. For example, a six-foot depth is six feet below MLLW; it would be larger if it were referenced to MSL. Such an error essentially reduces the depths over the entire model by half the tide range, making the waterway shallower by that amount. This might not matter much if the waterway is very deep, but for a shallow waterway such an error can make a significant difference (and when the model did not produce the desired results, the modeler then often played with various coefficients to make the model match the data).

Of course, to correct these depths from MLLW to MSL, one must know the tide range at every point in the waterway, which in fact, is what is to be calculated by the numerical model and so is not known (at least accurately) when the model is first set up. One can initially do this depth correction with some approximate spatial description of the changing tide range, and then re-correct the depths

with the new spatial description of the tide range that comes out of the first model run, and then rerun the model (perhaps re-correcting one more time, if necessary).

Of course, the charted depths themselves were originally calculated by adjusting the depth soundings for the tide at the time they were measured, and only recently have models been used in that correction process (see Hess *et al*, 1999). So there is some unknown error built into those charted depths (see Section 8.7.2). The most promising approach for accurately measuring bathymetry with respect to a known datum is to make the depth measurements with respect to a known ellipsoid datum using GPS, and then to transform them to a tidal datum (e.g. MLLW) using a tool like VDatum (see Parker, 2002, and Parker, *et al*, 2003). A tool like VDatum requires some type of a numerical tide model to produce the horizontal variation in the tidal datums, either by dynamically interpolating the harmonic constants from all the available water level stations (Hess *et al*, 1999) or by a more typical calculation based on the tidal forcing at the entrance (but with data assimilation to make sure that the model matches the tide exactly at the available water level stations).

A three-dimensional numerical hydrodynamic model that is well calibrated and verified using a good deal of high quality water level and current data, can usually do a better overall job of tide prediction and especially tidal current prediction. However, at a particular station where there are many years of water level data that can be analyzed, a prediction based on a quality set of harmonic constants obtained from those data is usually more accurate than a model-produced tide prediction.

It takes a lot of effort to develop a well calibrated and verified numerical hydrodynamic model. It takes much less effort to harmonically analyze a water level time series. So if one has a long enough time series of quality water level data, and one needs tide predictions at only a few locations, the harmonic analysis approach is probably best. However, If one needs tidal current predictions, the choice is not as clear. In some cases, one may have a long data time series from a current sensor that was deployed in a good location (i.e., in an area with little horizontal variation in the tidal current) and covers enough depths. The harmonic constants from this current station will be very useful and will provide tidal current predictions that are as good or even better than those produced by a numerical hydrodynamic model. But for many other situations, one has to believe that the model (again if well calibrated and verified) will do the better job.

8.5 Proper Tidal Forcing of a Numerical Hydrodynamic Model

After the above discussions of the advantages and disadvantages of using a numerical hydrodynamic model to produce tide and tidal current predictions, one must remember that such models still must be forced at their open boundaries to the ocean with very accurate tide predictions. And even if the model is eventually going to be forced by actual real-time water level data at the ocean open boundary (e.g., as part of a real-time data-based nowcast-forecast system to provide water levels and currents), it is important to first show that the model can produce accurate tide and tidal current predictions throughout the waterway when forced at the entrance with accurate tide predictions.

To provide proper tidal forcing at the ocean entrance(s) to the waterway, one should have at least one water level station with at least one year's worth of data for each ocean entrance. If the entrance is reasonably wide, it is important to have at least two water level stations, one on each side of each entrance. For each of these stations one should follow essentially the same procedures for producing a reference station in a Tide Table (see Section 4.4).

8. The Use of Numerical Hydrodynamic Models For Predicting Tides and Tidal Currents

The water level data time series for such a station must be at least a year long in order to be able to use as many tidal constituents as possible in the harmonic analysis. The most recent data should be used (especially in small waterways) in case there have been bathymetric changes which may have affected the tide regime. Typically the standard 37 tidal harmonic constituents listed in Table 3.2 have been used in CO-OPS (and its predecessor organizations) unless the station is located in a shallow waterway with a large tide range, in which case additional tidal constituents are used (see Table A.2). At Anchorage, Alaska, 114 tidal constituents were used to produce accurate tide predictions, the 77 additional shallow-water constituents being needed because of the 30-ft tide range and the very shallow-water conditions at the upper end of Cook Inlet. (The tidal bore that occurs at Turnagain Arm near Anchorage will be a challenge for most numerical hydrodynamic models.) However, at entrances to shallow waterways, the extra constituents are usually not needed, because the shallow-water over tides and compound tides are usually not large at the entrance (it requires some distance along the shallow waterway for them to grow large).

As with analyzing data for a reference station in the Tide Tables, one must try to include as many tidal constituents as possible. This may include a number of very small constituents, that are sometimes rejected because of their small size (0.03 feet being a typical arbitrarily chosen cutoff), the reasoning being that they are unreliable because they are small enough to be down in the nontidal noise continuum. However, to avoid throwing out possibly real tidal constituents, one should do a number of one-year analyses on different time periods to see if the amplitude and epoch (phase lag) for these constituents are similar from year to year. Such consistency is a better acceptance criterion than an arbitrary lower cutoff value.

One might be tempted to put the open boundary condition, with the tidal forcing, further up the waterway (perhaps) to make the model smaller, but this is never a good idea. The ideal place for an open boundary condition is at a location that will not be affected by the dynamics of the waterway itself. One is, in fact, assuming this to be the case when one forces a waterway at the entrance; nothing is allowed to change the tide predictions (or water level values) used at the entrance. Only for the ideal case of a waterway attached to a semi-infinite ocean (i.e., with infinite width and depth) is this absolutely true. For waterways with deep entrances directly to the ocean, it may be very approximately true. But for a waterway whose entrance is shallow in places and connects to a shallow continental shelf, there are likely to be some local hydrodynamic effects, and putting the forced boundary there might not produce as good results as one would like.

For this reason, some modelers move the open boundary offshore of the entrance onto the continental shelf. That usually solves the problem of local hydrodynamic effects at the open boundary, but it presents another problem, which can be much worse. Offshore there are unlikely to be any long water level data time series for the points along this new open boundary on the continental shelf, from which accurate harmonic constants can be derived for tide predictions. (It is even less likely that real-time water levels will be available there to drive a nowcast-forecast model.)

The accuracy of the predictions inside the waterway from the numerical hydrodynamic model is critically dependent on the forcing at the entrance, and by going offshore one adds a great deal of uncertainty to that forcing. There are several possible approaches to developing a good offshore tidal forcing boundary condition for the numerical hydrodynamic model of a bay or estuary.

First, one can actually put several water level measuring devices out on the continental shelf at the locations appropriate for the extended model grid. Bottom pressure sensors have been used for this purpose, but they have had a variety of problems (including water density effects, and the lack of a datum), which can take some effort to overcome (Filloux, 1991). (Recently additional bottom

pressure sensors have been deployed as part of the DART system to detect tsunamis. The water level data from these bottom pressure sensors have been harmonically analyzed, so that tide predictions can be subtracted from real-time water level data and the real-time residual data will better show tsunami signals.) A more promising technique for measuring offshore water level data is the use of GPS receivers on buoys. Such systems make water level measurements relative to a known ellipsoid datum, and they are not affected by the changing density of the seawater as pressure sensors are.

Second, one can try to use satellite altimetry data. Even though the sampling interval is very large (on the order of a day or more at cross-over points), one can still extract tidal constituents from these data using a least squares harmonic analysis technique or a modified response method (see Cartwright, 1991; Egbert, *et al*, 1994; Woodworth and Thomas, 1990; and Cherniawsky *et al*, 2001). Results have typically been better in the deep ocean compared with over the continental shelves and near the coasts, because of the shorter tidal wavelengths over the shelf, which require better spatial resolution in the data, and there are also less altimetric data over the shelves (see LeProvost, 2001).

Third, one can try to use the output from a shelf model. An often-used approach is to use such a model with altimetry data analyzed for the tides. It is also likely be forced with an ocean or global tide model (e.g., Schwiderski, 1980 and 1991; Bennett, 1992). Another approach is to start with a such a shelf or coastal model and then use some type of data assimilation technique (using the tides predicted from accurate harmonic constants at stations along the coast) to improve the model (see Zhang, Wei and Parker, 2003; Chen and Mellor, 1999; Myers and Baptista, 2001.)

For many waterway entrances (to a shelf area) none of the offshore modeling approaches may turn out to be as good as simply using tide predictions right at the entrance based on harmonic constants from long data time series (and perhaps not using the tidal current predictions in the immediate vicinity of the entrance. However, the shelf modeling approach is likely a better choice if one is predicting total water levels, including wind and pressure driven changes over the shelf. Wind and pressure data fields and forecast wind and pressure fields are used in the model, and then can be adjusted using a data assimilation technique to better match the nontidal coastal water levels (see Zhang, Parker, and Wei, 2002).

However it is accomplished, once the best possible tidal forcing is provided at the ocean open boundary to the model of the bay or estuary, then one must go through a careful process to calibrate and validate the model, which will be discussed in the next section.

8.6 Tidal Validation a Numerical Hydrodynamic Model

With most numerical hydrodynamic models there are particular constants/coefficients that can be adjusted to try to make the predictions of the model better match the available data. (For fully nonlinear three-dimensional models, this theoretically should not be necessary, but that may still depend on the type of turbulence closure scheme used.) If the predictions of the model do not match the available data, there must be a reason, and the first thing often tried is to play with whatever coefficients are in the model. (This is assuming that one has done the best possible job of matching the shoreline and bathymetry of the waterway, using adequate resolution.) The second thing often tried is to adjust the depths in particular grid cells (which might be wrong if the bathymetry used is old). One may also decide to increase the resolution of the model, especially if the shorelines of the waterway are complex, but this takes a lot of effort and so may not be done until other approaches are tried. Adjusting coefficients and depths sometimes seems more like art than science, because it is sometimes not obvious which way to change the coefficients or the depths (since the

8. The Use of Numerical Hydrodynamic Models For Predicting Tides and Tidal Currents

hydrodynamics of a shallow waterway with a complex geometry is usually complicated). For deep-water waterways there is usually much less of a problem.

The shallow-water areas will always be the biggest problem in calibrating and verifying a numerical model. The worst situation is when there are many small little bays, inlets, and streams connected to the main waterway, most of which do not have water level data, or even worse, perhaps not even accurate bathymetry. Even when the rest of the model is producing accurate tides (and even good tidal currents) one cannot know how well the model is doing in these shallow bays, inlets, and streams where there is no corroborating data. One cannot assume the model does well there because it does well elsewhere, because these shallow-water areas are usually at the edge of the model (as opposed to being areas between stations with data). Also, if the model is not doing as well in main areas of the waterway, one cannot be sure that the cause may not be these shallow areas (which can often absorb energy and store water in significant amounts).

Except for tides, all the energy in a water level record or current record are stochastic, i.e., random or quasi-periodic (e.g., periodic for a short while, but then gone). The tides are deterministic and truly periodic (because of the astronomical forcing behind them), and one can figure out from harmonically analyzed data records exactly what the response of a particular waterway is to the periodic tidal forcing at its entrance. There are a number of different tidal frequencies one can look at with respect to how well the model is doing, combined with a knowledge of the frequency effects of each term in the equations of motion on which the model is based (from Fourier decompositions such as done in Section 7.6). Thus, in carrying out the detective work necessary to make a model match the available data, the periodic tide provides many useful hints. One can learn a lot from looking at cotidal and corange maps of the waterway for all the important tidal constituents. Corange ratio maps of M_4/M_2 for the tide, for example, will give one an idea of where nonlinear shallow-water effects are important.

It is difficult to calibrate and verify a hydrodynamic model for stochastic nontidal effects, because there are too many different situations to cover (with a whole host of wind, pressure, density, and river effects). One ends up dealing in probabilities. But luckily one has the tides, with known energy at known frequencies, with which to test a model. If a model can handle the tides and tidal currents, it will most likely be able to handle wind effects, river discharges, and storm surge (as long as one has good boundary conditions for those effects and accurate nontidal forcing data).

In calibrating and verifying a numerical hydrodynamic model for tides and tidal currents, one should first get the tides right (because they are affected primarily by the entire waterway), and then deal with the tidal currents (which are also greatly influenced by local conditions). The local conditions may be adjustable to make the tidal currents at a particular location better, but that should not be done until one knows that the overall hydrodynamic system is being represented well by the model.

In calibrating the model to do a good job with the tides, modelers often started by first running the model with only M_2 , typically largest tidal constituent. This was done to save analysis time. Some percentage of the hundreds of predicted time series output at hundreds of grid points must be harmonically analyzed to see if the predicted M_2 amplitudes and epochs (phase lags) match those from the harmonically analyzed water level data at the various stations around the waterway. By predicting with only M_2 one only needs to analyze only a couple of days of predicted time series. If one adds the next four important tidal constituents (S_2 , N_2 , K_1 , and O_1), one needs to predict and analyze month-long time series. Including the 37 most important constituents requires year-long times series for analysis in order to resolve some of the smaller constituents. This was usually done

in stages, first using M_2 only, but then adding the other constituents. However, with today's computer power, forcing with all available tidal constituents and analyzing longer predicted times series is not a problem.

It is important to remember that one should never calibrate a numerical model only using M_2 (and then not going on to more refined calibrations by adding the other constituents). As has been seen in Sections 2.3.2 and 7.6, there are important nonlinear interactions between tidal constituents (even in areas as deep as the continental shelf) which cause additional energy loss from each constituent. In other words, because of the presence of M_2 , the constituents N_2 and S_2 , will be smaller than they would be if M_2 was not present. This is because of the (nonlinear) quadratic aspect of frictional energy loss. The M_2 effect on N_2 or S_2 is much greater than the effect of N_2 or S_2 on M_2 (since M_2 is so much larger than N_2 and S_2), which explains the smaller amplifications of N_2 and S_2 in Figure 7.5 compared with the amplification of M_2 . However, the cumulative effects of all the constituents on M_2 is significant. Thus, if one calibrates a model only using M_2 , then the additional energy loss due to the nonlinear effect on M_2 of the other tidal constituents will not be present in the model (but it will be in the data), and so to make the model match the data, it will be calibrated to frictionally reduce M_2 more than it should be. Then, when the other constituents are included in the model, too much energy will be lost. [For the very simple case of the one-dimensional nonlinear model used in Section 7.6.6 one can see the result of this in Figure 7.24, where the friction coefficient was made too large (trying to compensate for the added energy loss due to all the other constituents), and as a result the model over predicts M_6 (which is generated by the same quadratic frictional effect that reduces these other constituents)].

The relative size of certain constituent ratios, such as M_4/M_2 or $(K_1+O_1)/M_2$, in the data versus in the predictions from the model, should also provide clues as to where the model might possibly be adjusted. There are many aspects of the tidal hydrodynamics of a waterway with unique frequency dependencies, that once learned can also help with the detective work.

Section 8.4 described the consequence of using the depths from a nautical chart (which are referenced to the MLLW datum) without adjusting them to a MSL datum, and therefore essentially changing all the depths in the model by half the tide range, i.e., making the waterway shallower by that amount. Making the entire waterway shallower shortens the tidal wavelength and slows the wave propagation velocity. Depending on the length of the waterway (relative to 1/4 of a tidal wavelength), this shortening of the tidal wavelength could move the situation closer to resonance or farther from resonance. Learning whether this increases the tide range or decreases is a useful piece of information, and one might in fact artificially decide to decrease the overall average depth of the waterway for one model run, and then artificially increase it for another, just to see how the tide ranges (as well as the amplitudes and epochs of the different tidal constituents) are affected. This is just one way to do a *sensitivity analysis* on the model, in order to have some idea of what kinds of adjustments might be made to fix a model that is not performing well enough. Closing off small inlets or adjoining bays for one model run is another type of artificial adjustment whose effects can be enlightening. Such small inlets and adjoining bays can soak up energy, and may have a cumulative effect similar to adjusting the effect of bottom friction over the entire waterway.

As mentioned above, making adjustments to improve tidal current predictions is usually much more of a local accommodation. The speed and direction and timing of the tidal current at a specific location (and at a specific depth below the water surface) is greatly affected by the water depth at that location, the distance from that point in the water column to the sea bottom, the orientation of the bathymetry at that exact location, and the nearby water depths. As has been discussed the tidal currents are very sensitive to frictional, continuity, and inertial/advection effects. And examples

have been give illustrating how complex the structure of the current field can be. For example, the currents in a channel can be much faster than in the shallows right next to it, and yet varying considerably from top to bottom in the channel, sometimes flowing in opposite directions due to frictional effects. It is even more complicated at channel bends or near points of land, due to inertial effects that create eddies (resulting in zero frequency "residual currents" and shifts of tidal energy into higher harmonics).

One should not attempt to make local adjustments that might improve tidal currents in a specific area until after all necessary adjustments have been made to get the tide right, because this also affects the tidal current. For the local effects, grid resolution will be a critical factor in how accurately the tidal currents can be predicted, and one common "fix" for poor tidal current predictions is to increase the spatial resolution in the areas where the predicted tidal currents are not matching the data well. This can become almost more art than science, since the situations can be so varied that it is difficult to develop too many rules of thumb for making adjustments to improve predicted tidal currents.

As has been already mentioned, trying validate the numerical model for its prediction of currents is difficult because of the lack of suitable current data fields that can show the current flow structure with suitable resolution, and over long enough time periods. There are limitations to the information one can obtain even from ADCPs (bottom-mounted , side-mounted, or towed) or from HF radar systems. Although limited to the surface layer, and often without high enough resolution for some waterways, an HF Radar system is the closest thing one has to being able to see if a three-dimensional numerical hydrodynamic model is outputting current fields that are close to the real-world (or at least the "real world" as measured by an HF radar). Figure 8.2 shows one typical example of a comparison between an HF radar synoptic view of a surface current field at a specific day and time and the output of a three-dimensional finite-element hydrodynamic model of Chesapeake Bay for the same day and time (Gross, 2002). There are similarities in the two circulation fields, and there are many differences. In the model output one sees the signature of the navigation channels in the current field, which does not appear in the output from the HF radar. This may be a resolution issue, the radar not having a high enough resolution to resolve the current over the navigational channel.

When trying to validate a model with data, especially data from a relatively new remote measurement technique, there will always be some uncertainty. In the example in Figure 8.2, is the model right or is the radar right? In this case, one believes the model because one knows about the navigation channels and the fact that currents are fast in and over those deeper depths, but one may not always be able to so easily make a judgement.

8.7 The Operational Use of Numerical Hydrodynamic Models

There are a number of applications where it is usually better to obtain tide and tidal current predictions (or water level and current predictions that include the tide and tidal current) from a numerical hydrodynamic model. A few of these will be briefly discussed below.

8.7.1 Creation of Tidal Current Charts, Forecast Atlases and Digital Tidal Prediction Products

A numerical hydrodynamic tide model can be used to produce Tidal Current Charts, Tidal Circulation and Water Level Forecast Atlases, and Digital Tidal Prediction Products (see Sections

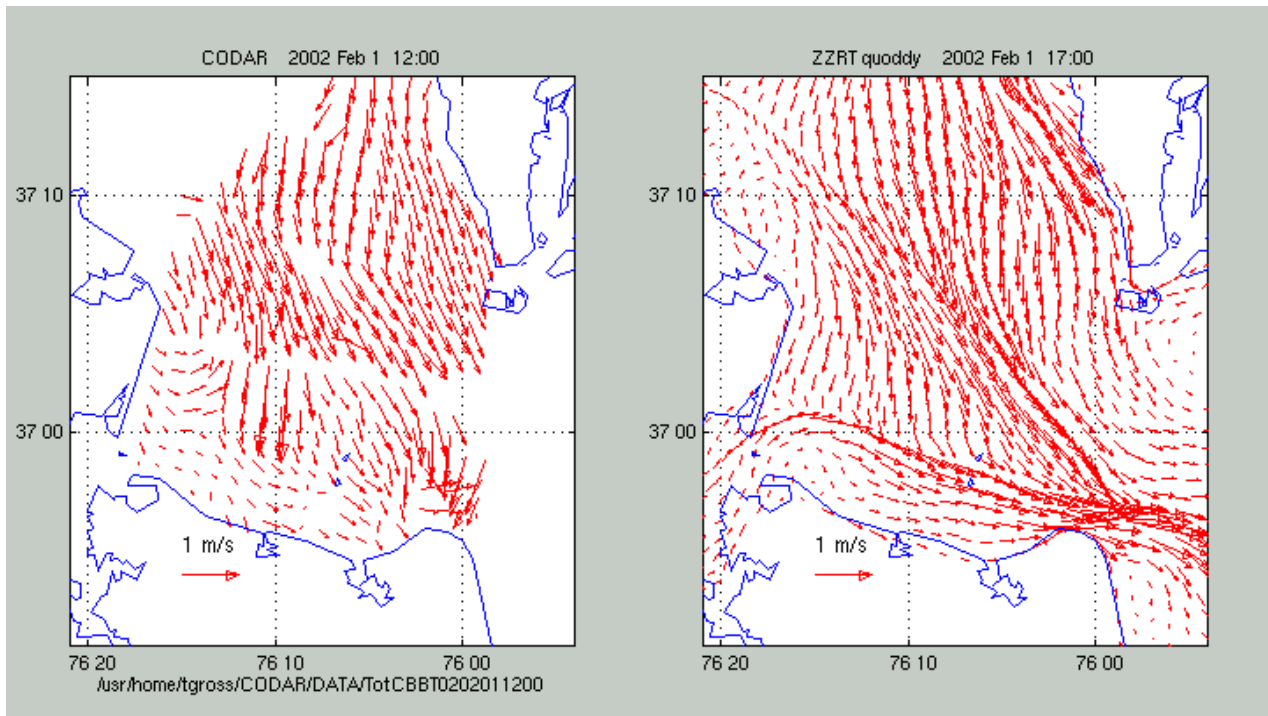


Figure 8.2. Comparison between a surface current field measured by an HF radar system (left panel) in lower Chesapeake Bay and the output of a three-dimensional finite element hydrodynamic model for the same time period. (from Gross, 2002)

8.3, 8.4 and 8.6). Such a model (Patchen, 1986) was used to produce the *Delaware River and Bay Tidal Circulation and Water Level Forecast Atlas* (NOAA, 1987); see Figures 9.10 and 9.11, and Parker, 1988.

With the hundreds of locations for which a model can predict tidal currents, one can produce a Tidal Current Chart with many more current vectors covering more of the waterway, and covering multiple depths. The large number of vectors allows one to choose the current vectors that are most representative of the circulation at each location. When producing a Forecast Atlas, the hundreds of locations for which the model can predict tidal heights allows one to produce very detailed height contours for the entire waterway. The numerical hydrodynamic tide model can also produce such charts for any astronomical situation. Thus for waterways with mixed tides or mixed tidal currents (the most difficult situation to accurately represent in Tidal Current Charts or in Tide or Tidal Current Tables), one can create different charts for (e.g.) equatorial lunar declination and for maximum lunar declination, or (e.g.) for spring, mean, and neap situations.

As will be discussed in Section 9.7, a digital tidal prediction product can provide more accurate tide and tidal current predictions than a Tide Table or a Tidal Current Table or a Tidal Current Chart. This is because predictions based on harmonic constants can be used for every station, and thus the problems with Table 2 nonharmonic-based predictions discussed in Sections 3.6.3 and 6.8 (and to be discussed further in Sections 9.2.5, 9.3.6, and 9.4.2) can be avoided. The one problem, however, is obtaining harmonic constants for all the necessary locations, especially for the tidal currents. Because of the greater spatial variability in currents, current data are required for more locations than are needed for water level data, but it is more difficult and expensive to acquire current data. And so here again, a numerical hydrodynamic model is the best way to obtain the required time

8. The Use of Numerical Hydrodynamic Models For Predicting Tides and Tidal Currents

series for harmonic analysis. A model also gives one the flexibility to provide tide or tidal current predictions at locations where one does not even have data.

8.7.2 Tide-Based Corrections In Hydrographic Surveys

When hydrographic (bathymetric) surveys are carried out and millions of depth soundings are acquired using a multibeam sonar system, each of those soundings is a measure of the total water depth at the exact time the measurement was made. That total water depth measurement includes the water level elevation (of which a major portion is usually the tide) at that exact time. At another time, during a different phase of the tide, a total water depth measurement at that same location will be different. The difference between the two water depth measurements at the same location is due to the different water level heights at the two different times (and again, most of which is usually due to the different tidal heights). To be able to provide depths on charts that are good for any time, all depth sounding must be corrected for the water level elevation at the time the depth sounding measurement was made. Both the eventual charted depth and the water level must be referenced to a vertical datum. In the U.S., that vertical datum (the *chart datum*) is the mean lower low water (MLLW).

The key question then is: what is the water level elevation (relative to MLLW) at the exact location where the depth sounding measurement is being made? If one subtracts the water level elevation referenced to MLLW, from the total depth, then one will have a water depth referenced to MLLW, i.e., the charted depth. (See Parker and Huff, 1998.) There are, however, no water level measuring devices at all the locations where soundings are being made. For the earliest hydrographic surveys a single water level station might be installed in the area of the survey, and then it was assumed that the water level at that station applied to the entire area being surveyed. Since the tide regime changes with horizontal distance (and the shallower it is, the more quickly the tide regime changes), most hydrographic surveys have used more than one water level gauge, and a method of interpolating between the gauges was used to provide water level heights for the entire survey area.

This was called *tidal zoning*, because the variation in the water level over the survey area was assumed to be the same as the variation in the tide (there being no equally reliable way to consider wind or other effects on the water level; and the tide was usually the dominant part of the water level change). But there could still be problems. Zoning techniques often involved representing the spatial variation of the water level in terms of connected polygon “zones” based on the variation in tide range and times of high and low water. The drawbacks of such methods included: (1) treating the variation of the water level as though it were exclusively tidal (when the wind-induced component could vary spatially and temporally in a much different way than the tide); (2) the sudden jumps in value when crossing the boundary between two polygon zones; and (3) the constant time differences assumed between the tide at two geographic points over all astronomical tidal situations over a month (the same problem looked at for Table 2 stations in the Tide Tables).

The use of numerical tide models can improve this situation, using two different techniques (Parker and Huff, 1998). In the first technique, a model is used to provide the spatial variation of all major tide constituents over the survey area, which can then be used to accurately predict the tide at any point in space at any time. To these tide predictions one can then add the nontidal part of the water level signal (due to the wind, atmospheric pressure, density changes, and/or river flow), as interpolated between the nontidal elevations determined at the installed water level gauges (by subtracting the tide predictions at those gauges from the water levels). Such *continuous water level*

zoning can also be provided using less computer intensive (but still numerical) interpolation techniques, such as a Laplacian technique (Hess, *et al*, 1999).

The second technique is an even more attractive approach for accurately measuring depths with respect to a common (chart) datum. This technique uses differential GPS on a moving ship, and techniques for rapid ambiguity resolution, often referred to as on-the-fly (OTF) GPS (Parker and Huff, 1998). Since the transducer of a multibeam sonar system is at a known position below a GPS receiver on the ship, then the depth measurements are known relative to the an ellipsoid datum. If the spatial variation of the MLLW tidal datum with respect to the ellipsoid has been determined in advance, then the measured depths can be directly referenced to the chart datum as they are measured (and no corrections based on water level zoning are necessary). The spatial variation in the chart datum (with respect to the ellipsoid) can be determined with a numerical hydrodynamic model (Schmalz, 1996) or with a numerical interpolation technique such as the Laplacian technique mentioned above (Hess *et al*, 1999). (Using OTF-GPS also eliminates the need to correct the depth soundings for effects on the survey vessel's dynamic draft.)

A depth sounding measurement made relative to an ellipsoid datum can be transformed to a value relative to MLLW using NOS's *Vertical Datum Transformation Tool* (VDatum), in which is included the spatial variation of all the various tidal, ellipsoid, and orthometric datums for the waterway being surveyed (see Parker *et al*, 2003, and Parker, 2002). The geographic distribution of the tidal datums in VDatum is calculated using a numerical tide model.

VDatum can also be used to calculate MHW shoreline from a digital elevation model (DEM) by transforming the DEM from the ellipsoid datum (used when the Lidar was taken from a GPS-positioned aircraft) to the MHW tidal datum, the MHW shoreline being the zero elevations points in the MHW reference frame (see Parker, 2003). This is a more accurate and efficient way to measure shoreline than traditional photogrammetric methods.

8.7.3 Real-time Based Nowcast/Forecast Model Prediction Systems

Although the tide and tidal current are usually the largest cause of changes in water level and currents, the nontidal contributions (due to wind, atmospheric pressure, water density changes, and river flow) can still be very important, depending on the needs of the mariner. (Of course, there are times, such as during a storm or a river flow event, when the nontidal part can dominate the tidal part.) For example, the pilot bringing into port a deep-draft commercial ship wants to know exactly the underkeel clearance that his ship will have, so that it does not run aground, and to know this he must know the total water level, not just the tide prediction. Or, a HAZMAT team wants to know which direction an oil spill will move, and to predict this they need (in addition to good wind information) accurate information on the currents, not just a tidal current prediction.

In respond to such needs, systems such as CO-OPS' the Physical Oceanographic Real-Time System (PORTS) were developed to provide real-time water level and current information to the maritime community (Appell, *et al*, 1994; Parker, 1995; Parker, 1986). Such systems could provide real-time data and information, but they originally could not provide short-term forecasts of water level and currents, which were important for short-term on-the-water decisions (e.g., the ship's pilot and the HAZMAT team benefit greatly from short-term forecasts of water level and currents). More recently PORTS was expanded to include a real-time based nowcast/forecast model prediction system (Parker, 1998a; Parker, 2002; Aikman *et al*, 1996), which consists of an accurately calibrated and validated numerical hydrodynamic model, as well as a surrounding system for managing the real-time input of data and output of predictions, including graphics, quality control assessments,

8. The Use of Numerical Hydrodynamic Models For Predicting Tides and Tidal Currents

etc. For nowcasts, such models are driven by real-time water levels as well as real-time surface wind fields (Patchen, 1986, describes one of the earliest experimental real-time models). For forecasts, sometimes the tidal and nontidal component are provided separately, with the forecast nontidal water level signal provided by a coastal nowcast/forecast model (Aikman, et al, 1996; Zhang, Parker, and Wei, 2002), which is driven by the predictions from a numerical weather forecast model. For such coastal models other real-time data are often necessary, including satellite sea surface temperature and salinity and water temperature profiles from ships (Szabados, *et al*, 1987).

Nowcast/forecast models are first calibrated and validated for accurately predicting the tide and tidal current. If the real-time instrumentation fails one can still provide tide and tidal current predictions over the entire waterway. Over the last decade a number of accurately calibrated and validated hydrodynamic models for operation in the real-time based nowcast/forecast mode have been developed and validated (see: Bosley and Hess, 1997; Wei, 2003; Schmalz, 1996; Kelley, *et al*, 20002; Gross, *et al*, 2000; Patchen and Blaha, 2002). Such real-time based nowcast/forecast model systems either support or become a component of other forecast models, such as storm surge models, oil spill trajectory models, and water quality models.

9. Products For Presenting Tide and Tidal Current Predictions

9.1 Introduction

Since the first time that mankind began to regularly predict the tide or the tidal current (or the arrival of a tidal bore in a few rivers) there have been products devised to provide these predictions to the general public in some type of convenient form. Most maritime nations have been producing such products for at least a century, and in some cases for many centuries. Because of the nature of the tide and tidal current these products have been very similar from nation to nation, and they generally fall into one of only few categories. This chapter will briefly look at some of these tide and tidal current prediction products. The products of the Center for Operational Oceanographic Products and Services (CO-OPS) in the National Ocean Service (NOS) in NOAA are used as typical examples, but they are very similar to the analogous products from other nations and from some private companies. The advantages and disadvantages of each type of product, discussed in this chapter, generally apply no matter which country produces that product. There has been, of course, an occasional special variation of a particular product designed to overcome one of the typical shortcomings of that type of product, which will be mentioned where relevant. This chapter only very briefly touches on some of the history of such products. For a much more thorough and fascinating coverage of the history of tide and tidal current products one should read Cartwright, 1999, which also includes many historical references. Sections 9.2 through 9.6 cover what might be termed the classic hardcopy/printed tidal prediction products (even if delivered on the Internet), while Section 9.7 discusses the improvements possible in tidal predictions delivered digitally.

9.2 Tide Tables

The Tide Table is the oldest method of providing tide predictions to mariners, and even today it is still the primary way in which most users acquire tide predictions, whether obtained as hard copy books, on CDs, or on the World Wide Web of the Internet. Prior to being published in their own volumes, tide predictions were provided in other publications. The first published tide predictions in the U.S. appeared in 1830 as part of *The American Almanac and Repository of Useful Knowledge for the Year 1830*, published by Gray and Bowen in Boston. Tide notes on nautical charts began in 1844. Tables for obtaining tide predictions appeared in 1853 in the Appendix to the Annual Report of the Coast & Geodetic Survey. In 1864 a thousand copies of tide tables for that year were provided during the Civil War to the Union naval forces. In all these early tables the tide predictions were produced using a nonharmonic interval method.

In 1867 the U.S. Tide Tables were published in their own separate volumes. There were two volumes with daily predictions for 19 reference stations and time and height differences for 124 subordinate stations. Those first tide tables provided only high water predictions (since most large vessels usually left a port on the high tide). Low water predictions were included beginning in 1887.

Two years earlier, in 1885, the U.S. Tide Tables began to be produced harmonically using the first U.S. tide predicting machine, Ferrel's maxima and minima tide predictor. In 1912 the Harris-Fischer tide predicting machine was introduced and used to produce the Tide Tables. That machine could predict actual hourly tidal heights (and not just the high and low waters).

By the 1920s the Tide Tables looked fairly similar in format to those used today. But even before Ferrel developed his harmonic analysis and prediction method in the late 1800s (later improved by Harris and then Schuremen), Tide Tables tended to be made up of two type of tables. The first, referred to as Table 1, contains daily tide predictions for the most important ports and harbors. These locations are referred to as *reference stations* in the U.S. (and as *primary ports* in the U.K. and some other countries]). The second type of table, referred to as Table 2, contains time and height differences for thousands of other locations, which are referred to as *subordinate stations* in the U.S. (and as *secondary ports* in the U.K. and some other countries). The predictions at a subordinate station are produced by applying the time and height differences to the daily predictions at the reference station with the most similar tidal characteristics (usually the closest reference station geographically). The daily predictions in Table 1 are produced with the harmonic tide prediction equation (see Section 3.4.2 and Chapter 4), using the constituents calculated from a harmonic analysis of at least a year's worth of water level data. The time and height differences in Table 2 are produced using one of several nonharmonic methods (see Section 3.6 and Chapter 6), which compare the high and low waters of a water level data time series at the subordinate station to the predicted high and low waters for the same time period at the station.

At the time of the writing of this book there are four volumes of Tide Tables produced by CO-OPS that cover the entire globe. In the 2007 *Tide Tables, East Coast of North and South America* there are 76 reference stations and 2589 subordinate stations. The 2007 *Tide Tables, West Coast of North and South America* have 60 reference stations and 1318 subordinate stations. In the 2007 *Tide Tables, Central and Western Pacific Ocean and Indian Ocean* there are 95 reference stations and 1998 subordinate stations. The 2007 *Tide Tables, Europe and West Coast of Africa* have 38 reference stations and 982 subordinate stations. The predictions for locations in other countries included in these volumes are generally received through bilateral exchange with each nation.

Table 1 and Table 2, as well as other tables that have been added to the Tide Tables, will be described in the following sections.

9.2.1 Table 1 – Daily Predictions for References Stations

Figure 9.1 shows one page of the four pages of a typical Table 1 reference station, in this case showing the daily predictions of high and low waters for Boston, covering January, February, and March 2006. On each day of each month the predicted times and heights of high waters and low waters are provided in chronological order, high water alternating with low water. The times of high and low waters are given in hours and minutes (relative to the local time meridian, in this case 75° west). The heights of high and low waters are given in both feet and centimeters (relative to MLLW). To get a height at some point between a high water and a low water the user of the Tide Table is referred to Table 3 (see Section 9.2.4), which provides a cosine-based interpolation scheme. This scheme works reasonably well for deep-water tide stations, but less well for shallow-water stations where the tide curve is distorted away from a cosine shape by nonlinear hydrodynamic mechanisms (see Sections 2.3.2 and 7.6.2).

9. Products For Presenting Tide and Tidal Current Predictions

Boston, Massachusetts, 2006

Times and Heights of High and Low Waters

January				February				March			
	Time	Height			Time	Height			Time	Height	
	h m	ft cm			h m	ft cm			h m	ft cm	
1	0530	-0.1	-3	16	0018	8.8	268	1	0053	10.8	329
Su	1142	11.6	354	M	0608	1.0	30	W	0657	-1.2	-37
	1811	-1.5	-46		1221	10.0	305		1310	11.6	354
					1842	0.1	3		1928	-1.7	-52
2	0025	9.9	302	17	0055	8.8	268	2	0143	10.9	332
M	0621	-0.3	-9	Tu	0648	1.0	30	Th	0750	-1.1	-34
	1233	11.6	354		1300	9.8	299		1403	11.1	338
	1900	-1.6	-49		1919	0.3	9		2017	-1.2	-37
3	0115	10.1	308	18	0132	8.9	271	3	0233	10.8	329
Tu	0713	-0.4	-12	W	0729	1.0	30	Sa	0845	-0.8	-24
	1326	11.5	351		1340	9.6	293		1458	10.4	317
	1950	-1.4	-43		1957	0.5	15		2108	-0.6	-18
4	0207	10.2	311	19	0210	8.9	271	4	0326	10.6	323
W	0808	-0.3	-9	Th	0811	1.1	34	Sa	0942	-0.4	-12
	1421	11.0	335		1421	9.2	280		1556	9.6	293
	2042	-1.1	-34		2035	0.7	21		2201	0.1	3
5	0300	10.2	311	20	0249	8.9	271	5	0421	10.3	314
Th	0905	-0.2	-6	F	0856	1.3	40	Su	1042	0.1	3
	1518	10.5	320		1504	8.8	268		1657	8.9	271
	2135	-0.6	-18		2116	1.0	30	O	2258	0.8	24
6	0356	10.2	311	21	0331	8.9	271	6	0520	9.9	302
F	1005	0.0	0	Sa	0943	1.4	43	M	1147	0.5	15
	1618	9.9	302		1551	8.5	259		1803	8.4	256
O	2230	-0.1	-3		2200	1.3	40		2358	1.3	40
7	0451	10.2	311	22	0416	8.9	271	7	0622	9.6	293
Sa	1107	0.2	6	Th	1034	1.4	43	Tu	1253	0.7	21
	1721	9.3	283		1643	8.1	247		1911	8.1	247
	2327	0.4	12	O	2249	1.5	46				
8	0550	10.1	308	23	0504	9.0	274	8	0101	1.6	49
Su	1211	0.3	9	M	1129	1.3	40	W	0725	9.5	290
	1826	8.9	271		1738	7.9	241		1559	0.7	21
					2342	1.7	52		2015	8.1	247
9	0026	0.8	24	24	0557	9.2	280	9	0201	1.6	49
M	0849	10.1	308	Tu	1227	1.1	34	Th	0825	9.5	280
	1315	0.3	9		1837	7.9	241		1457	0.6	18
	1930	8.6	262						2112	8.2	250
10	0124	1.0	30	25	0038	1.6	49	10	0256	1.5	46
Tu	0747	10.1	308	W	0653	9.5	290	Sa	0918	9.6	293
	1416	0.2	6		1326	0.7	21		1546	0.5	15
	2032	8.5	259		1937	8.1	247		2200	8.4	256
11	0221	1.1	34	26	0135	1.4	43	11	0344	1.3	40
W	0842	10.1	308	Th	0750	10.0	305	Sa	1004	9.8	299
	1512	0.1	3		1424	0.2	6		1628	0.3	9
	2127	8.6	262		2036	8.4	256		2241	8.6	262
12	0313	1.2	37	27	0232	0.9	27	12	0427	1.0	30
Th	0933	10.1	308	F	0846	10.5	320	Su	1045	9.9	302
	1602	0.0	0		1519	-0.5	-15		1705	0.2	6
	2216	8.6	262		2131	8.9	271	O	2317	8.8	268
13	0401	1.1	34	28	0327	0.4	12	13	0508	0.8	24
F	1019	10.2	311	Sa	0941	11.1	338	M	1123	10.0	305
	1646	0.0	0		1611	-1.1	-34		1739	0.2	6
	2300	8.7	265		2224	9.5	290		2352	9.0	274
14	0445	1.0	30	29	0420	-0.2	-6	14	0546	0.7	21
Sa	1102	10.2	311	Su	1034	11.6	364	Tu	1200	9.9	302
	1726	0.0	0		1702	-1.5	-46		1813	0.2	6
O	2340	8.7	265		2315	10.0	305				
15	0527	1.0	30	30	0513	-0.7	-21	15	0025	9.2	280
Su	1142	10.1	308	M	1751	-1.8	-55	W	0624	0.6	18
	1805	0.0	0						1236	9.8	299
									1848	0.3	9
31	0004	10.5	320								
	0605	-1.0	-30								
	1218	11.9	363								
	1839	-1.9	-58								

Time meridian 75° W. 0000 is midnight. 1200 is noon. Times are not adjusted for Daylight Saving Time.
Heights are referred to mean lower low water which is the chart datum of soundings.

Figure 9.1. A page from the Table 1 daily predictions for Boston, MA, from the *Tide Tables, East Coast of North and South America*.

The phases of the moon are also indicated on the days that they occur with symbols for new moon, first quarter, moon, and third quarter. The rest of the important astronomical data for the entire year is provided on the inside of the back cover of the Tide Table, including: moon in apogee, moon in perigee, moon farthest north of Equator, moon on equator, moon farthest south of equator, March equinox, June solstice, September equinox, and December solstice. (See Section 2.2.1 for definitions.) Boston is one of 76 reference stations in the *Tide Tables, East Coast of North and South America*. These reference stations are listed in the front of the Tide Tables, along with the year(s) of the data from which the harmonic constants were calculated that were used to make the daily predictions. For example, the Boston daily predictions in the 2006 Tide Tables (Figure 9.1) were produced using harmonic constants from the harmonic analysis of five years of water level data, from 1994 through 1998.

9.2.2 Table 2 – Time and Height Differences for Subordinate Stations

Figure 9.2 shows one typical page of the 42 pages of Table 2 in the *Tide Tables, East Coast of North and South America*. This page provides tidal information for 59 subordinate stations, one station per line, 43 stations of which are referred to the Boston reference station (which also has a line in the table) and 16 stations which are referred to the Portland reference station (listed on the previous page). For each station the information includes: its latitude and longitude, the time and height differences for the high waters and the low waters, the mean and spring ranges, and the mean tide level. All height differences, ranges, and levels are given in feet. Sometimes height ratios are provided instead of height differences (in rare cases both differences and ratios are used). The tide at the 60 stations shown on the page in this figure are predominantly semidiurnal, so the spring range is given. At stations where there is a significant diurnal inequality, the diurnal range is given instead of the spring range.

The subordinate stations are split up into groups of stations referred to the same reference station, which is listed above each group. There are two groups on this page, one group referred to Portland and one to Boston. To make a prediction on a particular day at a subordinate station, the time and height differences (or ratios) are applied to the daily prediction for that day at the reference station listed above that group of subordinate stations. For stations with special situations that cannot be totally handled by this format, there are Endnotes with additional information. In some special cases an entire page will be devoted to the so-called “peculiarities in the behavior of the tide” at a station, an example of which is shown in Figure 9.3. In this case the nonlinear effect of shallow water has distorted and flattened out the low water half of the tide cycle, but that distortion changes with different astronomical conditions, so the user is warned not to use Table 3 to interpolate between low and high waters. Such “peculiarities” are actually fairly common, although few are highlighted in the Tide Tables as in Figure 9.3. They are even more common in tidal currents.

The time and height differences in Table 2 were produced using one of several nonharmonic comparison methods, which compare the high and low waters of a water level data time series at the subordinate station to the predicted high and low waters for the same time period at the most appropriate reference station (see Sections 6.3 and 6.4).

Tidal Analysis and Prediction

TABLE 2 – TIDAL DIFFERENCES AND OTHER CONSTANTS

No.	PLACE	POSITION		DIFFERENCES				RANGES		Mean Tide Level
		Latitude	Longitude	Time	Height	High Water	Low Water	High Water	Low Water	
	MAINE and NEW HAMPSHIRE—cont. Time meridian, 75° W	North	West	h m	h m	ft	ft	ft	ft	ft
		on Portland, p.36								
803	Piscataqua River Atlantic Heights	43° 05.4'	70° 46.0'	+0 37	+0 28	*0.82	*0.82	7.5	8.6	4.0
805	Dover Point	43° 07'	70° 50'	+1 33	+1 27	*0.70	*0.70	6.4	7.4	3.4
807	Dover, Cocheco River	43° 11.9'	70° 52.1'	+1 45	+1 39	*0.77	*0.76	7.04	8.03	3.78
809	Salmon Falls River	43° 11.4'	70° 49.5'	+1 35	+1 52	*0.75	*0.75	6.8	7.8	3.6
811	Squamscott River RR. Bridge	43° 03.2'	70° 54.8'	+2 19	+2 41	*0.75	*0.75	6.8	7.8	3.6
813	Gosport Harbor, Isles of Shoals	42° 58.7'	70° 36.9'	+0 02	-0 02	*0.93	*0.93	8.5	9.8	4.5
815	Hampton Harbor	42° 54'	70° 49'	+0 14	+0 32	*0.91	*0.91	8.3	9.5	4.5
	MASSACHUSETTS, outer coast									
		on Boston, p.40								
817	Merrimack River Plum Island, Merrimack River Entrance	42° 49.0'	70° 49.2'	+0 06	+0 29	*0.88	*0.88	8.00	9.12	4.30
819	Newburyport	42° 48.7'	70° 51.9'	+0 31	+1 11	*0.86	*0.86	7.8	9.0	4.2
821	Salisbury Point	42° 50.3'	70° 54.5'	+0 55	+1 18	*0.83	*0.56	7.64	8.71	4.01
823	Merrimacport	42° 49.5'	70° 59.3'	+1 26	+2 08	*0.76	*0.50	7.05	8.04	3.70
825	Riverside	42° 45.8'	71° 04.6'	+1 56	+3 30	*0.62	*0.35	5.72	6.52	2.80
827	Plum Island Sound (south end)	42° 42.6'	70° 47.3'	+0 12	+0 37	*0.94	*0.94	8.6	9.9	4.6
829	Essex	42° 37.9'	70° 46.6'	+0 22	+0 31	*1.00	*0.94	9.18	10.47	4.90
831	Annisquam, Lobster Cove	42° 39.3'	70° 40.6'	+0 11	+0 03	*0.97	*0.97	8.81	10.04	4.74
833	Rockport	42° 39.5'	70° 36.9'	+0 06	+0 06	*0.95	*0.97	8.70	9.92	4.71
	Boston Harbor									
841	Boston Light	42° 19.7'	70° 53.5'	-0 01	-0 02	*0.95	*0.97	9.05	10.03	4.85
843	Deer Island (south end)	42° 20.7'	70° 57.5'	+0 01	+0 00	*0.97	*0.97	9.3	10.8	4.9
845	BOSTON	42° 21.3'	71° 03.1'					9.49	11.07	5.09
847	Charlestown, Charles River entrance	42° 22.5'	71° 03.0'	+0 00	+0 01	*1.00	*1.00	9.5	11.0	5.0
849	Amelia Earhart Dam, Mystic River	42° 23.7'	71° 04.6'	+0 01	+0 02	*1.01	*0.97	9.56	10.89	5.11
851	Chelsea St. Bridge, Chelsea River	42° 23.2'	71° 01.4'	+0 01	+0 06	*1.01	*1.01	9.6	11.1	5.1
853	Nepponset, Nepponset River	42° 17.1'	71° 02.4'	-0 02	+0 03	*1.00	*1.00	9.5	11.0	5.0
855	Moon Head	42° 18.5'	70° 59.3'	+0 01	+0 04	*0.99	*0.99	9.4	10.9	5.0
	Hingham Bay									
857	Nut Island, Quincy Bay	42° 16.8'	70° 57.3'	+0 01	+0 01	*0.99	*1.00	9.42	10.74	5.05
859	Weymouth Fore River Bridge	42° 14.7'	70° 58.1'	+0 09	+0 06	*1.00	*1.00	9.5	11.0	5.0
861	Crow Point, Hingham Harbor entrance	42° 15.7'	70° 53.6'	+0 02	+0 05	*0.99	*0.99	9.4	10.9	5.0
863	Hingham	42° 14.8'	70° 53.1'	+0 09	+0 08	*1.00	*1.00	9.5	11.0	5.0
865	Nantasket Beach, Weir River	42° 16.2'	70° 51.6'	+0 06	+0 07	*0.99	*0.99	9.4	10.9	5.0
867	Hull	42° 18.2'	70° 55.2'	+0 05	+0 07	*0.97	*0.97	9.3	10.8	5.0
	Cohasset Harbor to Davis Bank									
869	Cohasset Harbor (White Head)	42° 14.9'	70° 47.0'	+0 04	-0 02	*0.92	*0.92	8.8	10.2	4.7
871	Scituate, Scituate Harbor	42° 12.1'	70° 43.6'	+0 03	-0 01	*0.95	*1.03	8.94	10.19	4.83
873	Damons Point, North River	42° 09.6'	70° 44.0'	+0 20	+0 36	*0.89	*0.89	8.5	9.9	4.5
875	Brant Rock, Green Harbor River	42° 05.0'	70° 38.8'	+0 05	+0 03	*0.96	*1.03	9.08	10.35	4.89
	Cape Cod Bay									
877	Duxbury, Duxbury Harbor	42° 02.3'	70° 40.2'	+0 06	+0 33	*1.04	*1.03	9.89	11.27	5.30
879	Plymouth	41° 57.6'	70° 39.7'	+0 04	+0 18	*1.03	*1.00	9.76	11.13	5.22
881	Cape Cod Canal, east entrance	41° 46.3'	70° 30.4'	-0 01	-0 03	*0.91	*0.68	8.74	9.96	4.59
883	Cape Cod Canal, Sagamore	41° 46.5'	70° 32.1'	-0 15	-0 06	*0.83	*0.88	7.90	9.01	4.25
885	Cape Cod Canal, Bourne Dale	41° 46.2'	70° 33.7'	-0 29	-0 21	*0.66	*0.79	6.18	7.05	3.37
887	Cape Cod Canal, Bourne Bridge	41° 44.7'	70° 35.6'	-1 13	-0 24	*0.46	*0.79	4.29	4.89	2.42
889	Barnstable Harbor, Beach Point	41° 43.3'	70° 17.1'	+0 11	+0 30	*1.00	*1.00	9.5	11.0	5.0
891	Sesuit Harbor, East Dennis	41° 45.1'	70° 09.3'	+0 02	-0 01	*1.02	*0.82	9.73	11.09	5.14
893	Wellfleet	41° 55.8'	70° 02.5'	+0 14	+0 30	*1.05	*1.05	10.0	11.6	5.4
895	Provincetown	42° 03'	70° 11'	+0 16	+0 18	*0.95	*0.95	9.1	10.6	4.8
	Cape Cod									
897	Chatham, Stage Harbor	41° 40.0'	69° 58.0'	+0 46	+0 19	*0.43	*0.43	3.95	4.50	2.23
899	Chatham Harbor, Aunt Lydia's Cove	41° 41.6'	69° 57.0'	+1 08	+1 57	*0.48	*0.35	4.63	5.27	2.43
901	Pleasant Bay	41° 44.2'	69° 58.9'	+2 28	+3 27	*0.34	*0.34	3.2	3.7	1.7
903	Georges Shoal	41° 41.3'	69° 45.6'	-0 47	-0 43	*0.44	*0.44	4.2	4.8	2.2
	Nantucket Sound, north side									
905	Stage Harbor	41° 39.9'	69° 58.2'	+0 57	+0 48	*0.41	*0.41	3.9	4.7	2.0
907	Saquisset Harbor	41° 40.1'	70° 03.4'	+0 46	+0 16	*0.41	*0.41	3.72	4.24	2.14
909	Wychmere Harbor	41° 39.9'	70° 03.9'	+0 52	+0 25	*0.39	*0.39	3.7	4.3	1.9
911	Dennisport	41° 39.5'	70° 06.9'	+1 03	+0 38	*0.36	*0.36	3.4	4.1	1.8
913	South Yarmouth, Bass River	41° 39.9'	70° 11.0'	+1 48	+1 46	*0.29	*0.29	2.8	3.4	1.5
915	Hyannis Port	41° 37.8'	70° 18.0'	+1 03	+0 31	*0.32	*0.32	3.1	3.7	1.6
917	Cotuit Highlands	41° 36.5'	70° 26.2'	+1 17	+0 47	*0.26	*0.26	2.5	3.0	1.3
919	Poponesset Island, Poponesset Bay	41° 35.2'	70° 27.8'	+2 03	+1 52	*0.24	*0.24	2.3	2.8	1.2
921	Falmouth Heights	41° 32.7'	70° 35.9'	-0 16	-0 09	*0.14	*0.14	1.3	1.6	0.6

Endnotes can be found at the end of table 2.

Figure 9.2. A page from Table 2 of the *Tide Tables, East Coast of North and South America* showing 60 subordinate tide stations.

CAUTION**Cape Cod Canal, Railroad Bridge, No. 1117**

Predictions of the times of low water must be used with caution because of the peculiarities in the behavior of the tide. Since the tide may be practically at a stand for as much as two hours before or after the predicted times of low water, the levels at other than high and low water times cannot be obtained in the usual way as in Table 3 (Height of Tide at Any Time). The peculiar behavior of the tide near low water, which is prevalent at this place, is illustrated by the first three curves; however there are brief periods each month when the behavior is as depicted by the fourth curve.

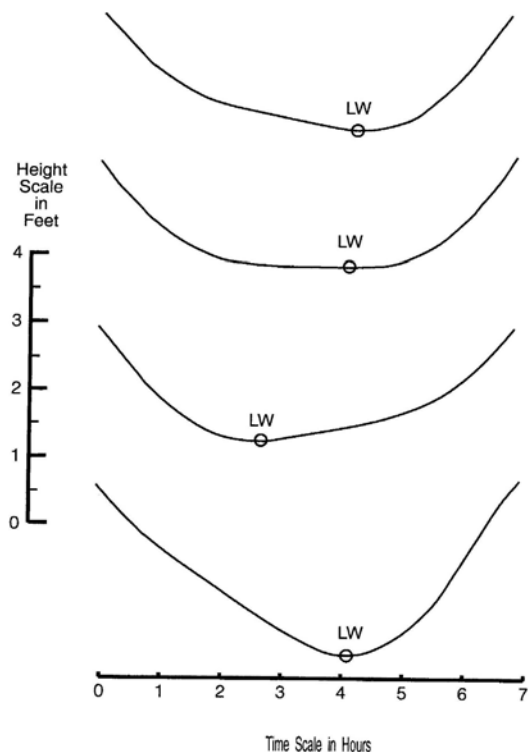


Figure 9.3. A caution in the Tide Tables about variations in low water times due to shallow-water effects.

9.2.3 Table 8 – Tide Prediction Accuracy

Table 8 provides some statistical figures on the “*tide prediction accuracy*” of the reference stations in a Tide Table. Figure 9.4 shows Table 8 from the *Tide Tables, East Coast of North and South America*, which includes 32 stations. The statistical values provided for the times and heights of the high and low waters at each station include the:

- (1) *90% distribution level*, which means that 90% of the absolute values of the difference are less than or equal to the value shown in the column;
- (2) *standard deviation of differences*, which is the square root of the average of all the squares of the differences; and
- (3) *average difference*, which is the average of the all the differences (with their signs taken into consideration).

These values are determined by comparing predicted and observed high waters (and low waters) for one year of data (the specific year is listed in the third column of the table), the observed values being subtracted from the predicted values.

Technically, since one is comparing predicted and observed values, one is not really looking at the accuracy of the astronomical tide prediction, but at how well this tide prediction can represent

9. Products For Presenting Tide and Tidal Current Predictions

Table 8. - TIDE PREDICTION ACCURACY

Station ID	Station Name	Year	90% Distribution Level Time Differences				Standard Deviation of Differences Times				Average Differences Times			
			High Water (Hours)	Low Water (Hours)	High Water (Feet)	Low Water (Feet)	High Water (Hours)	Low Water (Hours)	High Water (Feet)	Low Water (Feet)	High Water (Hours)	Low Water (Hours)	High Water (Feet)	Low Water (Feet)
841-0140	Eastport, ME	1998	0.2	0.2	0.7	0.6	0.09	0.11	0.41	0.40	-0.07	-0.10	-0.08	-0.10
841-8150	Portland, ME	1998	0.3	0.2	0.6	0.6	0.14	0.13	0.40	0.39	-0.10	-0.07	-0.11	0.06
844-3970	Boston, MA	1998	0.3	0.3	0.8	0.7	0.14	0.14	0.49	0.48	-0.10	-0.10	-0.10	-0.09
844-7930	Woods Hole, MA	2003	0.5	>1.0	0.7	0.7	0.48	0.77	0.43	0.40	-0.03	0.01	-0.02	-0.01
844-9130	Nantucket, Ma	2003	0.3	0.3	0.6	0.6	0.23	0.21	0.40	0.39	-0.03	0.03	-0.03	0.03
845-2660	Newport, RI	1997	0.3	0.6	0.7	0.7	0.19	0.14	0.41	0.40	-0.06	-0.04	-0.07	-0.05
846-1490	New London, CT	1998	0.4	0.3	0.7	0.7	0.25	0.22	0.47	0.47	-0.11	-0.08	-0.10	-0.09
846-7150	Bridgeport, CT	1998	0.3	0.3	0.8	0.8	0.13	0.13	0.55	0.56	-0.12	-0.15	-0.11	-0.16
841-6945	Kings Point, NY	1999	0.9	>1.0	0.8	0.8	0.59	0.54	0.55	0.56	-0.12	-0.15	-0.11	-0.16
851-8750	The Battery, NY	2003	0.6	0.5	0.9	0.9	0.37	0.31	0.59	0.60	-0.07	-0.06	0.03	-0.02
853-1680	Sandy Hook, NJ	2002	0.4	0.4	0.8	0.9	0.25	0.25	0.51	0.54	-0.13	-0.12	0.19	0.21
853-4720	Atlantic City, NJ	2000	0.3	0.4	0.9	0.9	0.24	0.24	0.57	0.57	-0.02	-0.01	0.02	-0.02
854-5530	Philadelphia, PA	1989	0.5	0.6	1.0	1.0	0.30	0.36	0.72	0.65	0.14	0.11	-0.12	0.28
855-1910	Reedy Point, DE	2002	0.5	0.7	0.9	0.9	0.23	0.31	0.55	0.56	-0.18	-0.35	0.09	-0.02
855-7380	Breakwater Harbor, DE	1998	0.3	0.3	0.9	0.9	0.18	0.18	0.62	0.68	-0.06	-0.03	-0.03	-0.01
857-4680	Baltimore, MD	1998	0.8	1.0	1.0	1.38	1.43	0.64	0.62	-0.21	-0.09	-0.21	-0.11	
859-4900	Washington, DC	1998	0.5	0.8	1.0	1.0	0.33	0.48	0.73	0.83	-0.05	-0.19	-0.03	-0.23
863-8863	Chesapeake Bay Bri Tunnel	2002	0.3	0.4	0.8	0.8	0.25	0.27	0.50	0.52	-0.06	-0.08	-0.07	-0.08
863-8610	Hampton Roads, VA	1995	0.4	0.4	0.8	0.9	0.27	0.25	0.51	0.56	0.07	0.05	0.03	-0.01
865-8120	Wilmington, NC	2003	0.5	0.5	0.6	0.8	0.34	0.29	0.38	0.46	-0.01	-0.08	0.11	0.16
8661070	Myrtle Beach, SC	2003	0.4	0.4	0.8	0.8	0.28	0.29	0.48	0.50	0.00	0.01	0.00	0.00
866-5530	Charleston, SC	2000	0.4	0.4	0.6	0.7	0.19	0.20	0.42	0.47	0.14	-0.10	0.05	-0.02
867-0870	Savannah R. Ent., GA	1995	0.3	0.3	0.7	0.9	0.21	0.19	0.47	0.58	-0.01	-0.07	0.05	0.03
872-0030	Fernandina Beach, FL	1995	0.2	0.3	0.9	0.9	0.15	0.19	0.48	0.56	-0.02	0.06	0.33	0.30
872-0218	Mayport, FL	2003	0.2	0.3	0.6	0.8	0.14	0.21	0.41	0.51	-0.04	0.01	-0.02	0.01
872-3178	Miami, Government Cut, FL	1985	0.3	0.3	0.4	0.4	0.18	0.17	0.25	0.24	-0.07	0.01	-0.02	-0.01
872-4580	Key West, FL	2000	0.5	0.4	0.3	0.3	0.29	0.25	0.19	0.20	-0.18	-0.06	-0.15	-0.10
872-6520	St. Petersburg, FL	2003	0.7	0.7	0.6	0.5	0.56	0.44	0.38	0.34	0.07	0.00	0.01	0.2
872-9840	Pensacola, FL	1995	>1.0	>1.0	0.6	0.9	2.61	2.72	0.48	0.41	0.04	0.10	-0.04	0.07
873-7048	Mobile, AL	1984	>1.0	>1.0	0.8	0.7	2.56	2.49	0.48	0.45	0.05	-0.09	-0.05	0.04
876-1724	Grand Isle, LA	2003	>1.0	>1.0	0.5	0.5	1.21	1.22	0.30	0.30	-0.24	-0.33	0.00	0.00
877-1450	Galveston, TX	1995	>1.0	>1.0	0.7	0.8	1.29	1.25	0.50	0.54	-0.15	-0.12	-0.03	0.00

Figure 9.4. An example of a Table 8 showing statistical figures related to the tide prediction accuracy of the reference stations from the 2006 *Tide Tables, East Coast of North and South America*. The values in this table, however, are actually greatly influenced by nontidal changes in water level (see text).

the actual water level (on average over a year). The water level observations include nontidal influences, such as the effects of winds and atmospheric pressure and river flow on water level. For the average difference values, most of these nontidal contributions are averaged out over a year, but there can still be asymmetries in seasonal effects on the nontidal water level that will not average out and will show up in the time and height differences. Thus, for example, in Figure 9.4 one sees larger average differences for high and low waters at Philadelphia, which is on the upper Delaware River and thus is influenced by river flow. During high runoff periods the river flow raises the mean sea level, reduces the tide range, and distorts the tide curve asymmetrically, all of which affect the average differences in Table 8 (see Sections 2.3.3 and 7.6.6).

Being based on only one year of data, the average differences in Table 8 may primarily represent the nontidal contributions, and, in fact, the astronomical tide itself could be totally captured by the harmonically produced tide predictions, and thus could really be 99.99% accurate. (One can say, at least, that the average difference due to errors in predicting the astronomical tide will be no worse than the value in Table 8.) If the comparison between predicted and observed high waters is done over many years the mean difference values may be smaller and closer to representing any missing tidal energy in the tide prediction (and thus a truer indication of the accuracy of the astronomical tide prediction). But seasonal effects might still have an influence. Section 3.7.1 and

specifically Figure 3.11 showed how much the seasonal sea level range can vary from year to year. It is possible that the year chosen for the statistics in Table 8 could have been a typical year or it could have been an unusual year.

The standard deviations listed in Table 8, however, will include nontidal effects no matter how many years of data are used, because the positive and negative differences are squared and do not cancel each other out. One sees larger standard deviations for high water differences at Philadelphia (as expected based on the discussion in the last paragraph). The four stations shown in Table 8 from the northern Gulf of Mexico (Pensacola, Mobile, Grand Isle, and Galveston) all have even larger standard deviations for the time differences between predicted and observed times of high water and low water (and there is an explanatory note for this Table 8 mentioning the influence of weather conditions). At these locations the tide range is small and is often dominated by water level variations caused by wind and pressure effects (even a front passing over the waterway can significantly affect the water level). Likewise the 90% distribution level values also reflect the nontidal influences, no matter how long the length of the observed and predicted time series analyzed, because absolute values of the differences are used (and thus the nontidal variations do not average out).

Even though the statistical values in Table 8 are not strictly speaking a measure of how well the astronomical tide has been predicted, the statistical information in Table 8 has been useful for mariners who use tide prediction as the best estimate of actual high and low waters that they will experience with their ships. Even then, however, there will always be some confusion because the average differences shown in Table 8 (being averaged over a year) are less than the differences between the predicted tide and the observed water level seen on any given day (and much less than the differences seen when there is a large storm surge or strong river flow).

9.2.4 Other Tables and Information in the Tide Tables

There are other small tables in the Tide Tables that provide additional information such as how to determine: the height of the tide between a high water and a low water, the local mean time of sunrise and sunset, the reduction of local mean time to standard time, the conversion from feet to centimeters, and the lowest and highest astronomical tide and other tidal datums.

Table 3 provides a method for getting a tidal height at some point between a high water and a low water using a cosine-based interpolation scheme. This scheme works reasonably well for deep-water tide stations, but less well for shallow-water stations where the tide curve is distorted away from a cosine shape. A graphic method is also provided for the same purpose, also assuming cosine interpolation.

Table 4 is nine pages of tables that give the local mean time of the rising sun and the setting of the sun's *upper limb* (i.e., the sun's upper outer edge) for every fifth day of the year for every 5 degrees of latitude.

Table 5 allows a value from Table 4 to be converted to standard time.

Table 6 gives the time of the rising and setting of the moon's upper limb for every day of the year, but for only 8 locations (Boston, New York, Washington, D.C., Charleston, Savannah, Galveston, and the Panama Canal) in the *Tide Tables, East Coast of North and South America*.

Table 7 provides a way to convert feet to centimeters.

Table 9 shows five tidal datum values for all the reference stations, including: the lowest astronomical tide (LAT); mean lower low water (MLLW); mean low water (MWL); mean high water (MHW); mean higher high water (MHHW); and the highest astronomical tide (HAT). LAT

and HAT are the highest and lowest predicted tide values at a given location over a 19-year period (i.e., over the 18.6-year lunar nodal cycle). LAT and HAT are calculated by generating tide predictions for the most recent National Tidal Datum Epoch (presently 1983-2001) using the latest set of tidal harmonic constants.

9.2.5 Limitations of Tide Tables

Tide Tables are “hardcopy” products that have been printed for more than a century, and only in recent years have been extended to electronic media such as CDs and the World Wide Web on the Internet. As printed documents there were certain limitations put on what could be included in a tide table, because of page limitations and because of the lack of ease with which certain information could be conveyed to a user. With electronic media those limitations go away, but the traditional format for tide tables continues to survive, if only because of its familiarity, but also because extensive new data may be required to produce digital tide prediction products based on the harmonic analysis of all stations (see Section 9.7). [One alternative to this is the use of numerical hydrodynamic models forced with accurate tide predictions at the entrance based on long-term tide stations (see Chapter 8). However, that requires more data than for just the entrance. The extensive validation of the model, that is required to make sure it produces accurate predictions everywhere in the modeled waterway, requires a reasonable amount of data for those validation sites.]

The first limitation of a tide table is that (harmonically produced) daily predictions can only be provided for a relatively few stations out of the thousands in the table. This is a page limitation, since the daily predictions for a reference station take four pages in Table 1, while the time and height differences for a subordinate station take only one line in Table 2, with roughly 60 stations per page. Most stations must therefore be included as subordinate stations in Table 2. As was seen in Section 3.6.3, in the introduction to Chapter 6, and in Section 6.9, serious prediction errors can occur if the harmonic makeup of the subordinate stations in Table 2 is not similar enough to the harmonic makeup of the reference station in Table 1. In this situation the mean time and height differences in Table 2 (that come out of a nonharmonic comparison analysis) are really good only for certain times of the month. This problem is most likely to occur in a waterway with a mixed tide and a strong diurnal signal, because the tidal characteristics will change relatively quickly with geographic distance, and the subordinate station will often be too far from the reference station. In this case, tide predictions using Table 2 time and height differences will be least accurate around the times of maximum lunar declination, and most accurate near times of equatorial declination (see Sections 3.6.3 and 6.5.1 for examples). But this problem also arises when shallow water distorts the tide curve, shifting around the times of high water or low water so that the time differences between the subordinate station and the reference stations can vary considerably (see Figures 3.7, 3.8, and 3.9 for one example). If this problem occurs, one solution is to add an additional reference station to the Tide Table, one that is closer to the subordinate stations and has more similar tidal characteristics. (But sometimes more additional reference stations may be needed than one would like, considering the four additional pages required for each new reference station).

The second limitation of a tide table is that only high and low waters predictions are given. For predictions of tidal heights between a low water and a high water the user is sent to Table 3 and forced to use a cosine-based interpolation scheme. However, the tide curve only looks like a cosine curve for deep-water stations (for example, stations on oceanic islands and continental coasts), and such an interpolation scheme may not work well for stations inside bays and estuaries and rivers where nonlinear shallow-water effects distort the tide curve away from a pure cosine. Figure 9.3

shows one example of this, but there are others, and in a Tide Table it can only be treated with an Endnote or a diagram such as in Figure 9.3.

Both these problems can be solved in electronic/digital tide predictions products where for every station an entire tide curve is predicted harmonically (at any time interval desired). This eliminates the need for time and height differences, and it eliminate the need for interpolation between high and low waters.

9.2.6 The Construction of Tide Tables

Here a short overview is given on the constructions of tide tables (that repeats some of what was said in Sections 4.4 and 6.8.). There are two primary activities: (1) producing accurate daily predictions (of high and low waters) for references stations in Table 1 using harmonic analysis and prediction, and (2) calculating time and height differences for subordinate stations in Table 2 using nonharmonic analysis. Predictions at a subordinate station are made by applying its time and height differences to the daily predictions at the reference station that was used in the nonharmonic analysis.

To produce the daily predictions for a reference station for Table 1 one must have very accurate tidal harmonic constants, since such predictions will be made for many years in future, and many subordinate stations in Table 2 will be referenced to that station. Thus, the water level data time series for a reference station must be long (at least a year) in order to be able to use as many tidal constituents as possible in the least squares harmonic analysis. If many years of water level data are available for the station, the most recent will be the best (since bathymetry and shorelines can change in waterways), but rather than have to revise harmonic constants every year, it makes more sense to do quality analyses on the predictions (versus observations) each year, to see how well the present set of harmonic constants is doing. (When one revises the harmonic constants at a reference station one must then carry out new nonharmonic comparison analyses for all the subordinate stations referred to that reference station.)

Typically the standard 37 constituents (listed in Table 3.2) are used, but for a station far inside a very shallow waterway with large tide range, one may need to use additional shallow-water tidal constituents (the 114 constituents needed for Anchorage, Alaska being an example). However, when creating a new reference station, or updating an old reference station, one should not feel it necessary to stick with the standard 37 constituents even for stations with situations less extreme than Anchorage. One should use the methods mentioned in Section 4.3 for assessing the quality of the predicted tide series to decide whether more constituents are needed, in which case a time series longer than a year can be analyzed, if required. By calculating as many tidal constituents as can be obtained from the available time series, one will probably eliminate the need to use a build-up factor (see Section 4.3.5). But to assure the use of the maximum number of tidal constituents possible, one must look carefully at the smallest constituents that come out of the harmonic analysis. In the past such small constituents have often been rejected because they fell below an (arbitrarily selected) standard cutoff criterion for acceptance (e.g., 0.03 feet). However, one should run several one-year harmonic analyses and look at the variation in the amplitude and epoch (phase lag) for these constituents from year to year. If there is not much variation (especially in the epochs), then such consistency indicates that these constituents though small are real (and not simply a representation of quasiperiodic nontidal noise at that frequency). They should be kept and used in the tide predictions. The inclusion of several small constituents that fall below a standard rejection criterion (e.g., 0.03 foot historically in NOS) but appear to be consistent from year to year and thus are real,

may allow one to resist the temptation to use a build-up factor. If one wishes to go still further in improving tide predictions, one can also assess the true variation in constituent amplitudes over a 19-year period versus the astronomically determined variation represented in the node factor, f , obtained from Table 15 in Schureman (1958). (See Section 2.3.4) One might even decide to use dozens of additional satellite constituents in the harmonic analysis and prediction, and do away with the use of node factors (but this requires a 19-year harmonic analysis, and usually does not improve the predictions enough to be worth the effort).

To put a subordinate station in Table 2 of a Tide Table one must use some type of nonharmonic analysis method. For many decades the standard procedure for putting the mean time and height differences into Table 2 has been merely to use the differences between corresponding monthly mean analyses from the subordinate station and from the reference station. Only for a water level station with a short data time series was the tide-by-tide analysis (usually called “Comparison of Simultaneous Observations”) used. This tide-by-tide analysis also shows the time and height difference for each tidal cycle, and so one can see how much these differences vary from cycle to cycle throughout the month. This makes the tide-by-tide analysis valuable as a quality analysis tool. When one finds significant periodic variations in the time and/or height differences from cycle to cycle this indicates that the selected reference station does not have similar enough tidal characteristic to the subordinate station. These periodic variations equate to errors in tide predictions made with these mean time and height differences (in Table 2) when applied to the daily tide predictions at that reference station (in Table 1). In such cases, selection of a better reference station is recommended, which may mean creating a new reference station in that Tide Table to handle that subordinate station and probably other subordinate stations around it.

9.3 Tidal Current Tables

Tidal Current Tables are not as old as the Tide Tables, but they still have a long history. In the U.S. the first published tidal current predictions were in 1890 for New York Harbor and vicinity. The Tidal Current Tables were first published separately from the Tide Tables in 1923, as two volumes, one for the Atlantic coast of the U.S. and one for the Pacific coast, as they are today. In the 2007 *Tidal Current Tables, Atlantic Coast of North America* there are 31 reference stations and 1787 subordinate stations. The 2007 *Tidal Current Tables, Pacific Coast of North American and Asia* have 32 reference stations and 1126 subordinate stations. Both include some foreign stations (18 in the Atlantic tables, and 162 in the Pacific tables).

As with the Tide Tables there are two primary kinds of tables within the Tidal Current Tables. Table 1 contains daily tidal current predictions for a restricted number of *reference stations*, which includes the times and speeds of maximum floods and ebbs and the times of slack water. Table 2 contains time differences and current speed ratios for thousands of *subordinate stations*. The predictions at a subordinate station are produced by applying these time and speed ratios to the daily tidal current predictions at the reference station with the most similar tidal characteristics (usually the closest reference station geographically). The daily predictions in Table 1 are produced with the harmonic tidal current prediction equations (see Section 3.4.3 and Chapter 5), using the constituents calculated from a harmonic analysis of (preferably but not always) a year’s worth of current data. The time differences and speed ratios in Table 2 are produced using one of two nonharmonic methods (the rotary reduction and the reversing reduction), which compare the maximum floods and ebbs and slack waters (or minimum currents) in a current data time series at the subordinate station

with those predicted for the same time period at the most appropriate reference station (see Sections 3.6, 6.5, and 6.6).

In addition to Tables 1 and 2, there is another table (Table 5) to handle rotary tidal currents that are so circular that one cannot decide on a flood or ebb direction. Such current stations usually are in open water off the coast. Stations close to shore and in bays and estuaries are also rotary, but their shape is usually elliptical so that maximum flood and maximum ebb directions are clear.

The following sections will look at Table 1, Table 2, and Table 5, as well as other tables that have been added to the Tidal Current Tables for other purposes.

9.3.1 Table 1 – Daily Predictions for References Stations

Figure 9.5 shows one page of the four pages of a typical Table 1 tidal current reference station, in this case showing the daily predictions of slack waters and of maximum floods and ebbs for Chesapeake Bay Entrance, covering January, February, and March 2006. On each day of each month the predicted times of slacks (first column) and maximums (second column) are provided in chronological order, maximum floods waters (F) alternating with maximum ebbs (E). The third column contains the maximum speeds (in knots). The times are given in hours and minutes relative to the local time meridian (in this case 75° west). To get a current speed at some point between a slack and a maximum flood or ebb, the user is referred to Table 3 (see Section 9.3.4), which provides a cosine-based interpolation scheme. This scheme may work reasonably well for a current station in a deep narrow channel, but often much less well for other stations, since the tidal current curve is often fairly rotary and is often distorted away from a simple cosine shape by nonlinear shallow-water effects and lateral inertial effects.

The phases of the moon are also indicated in Table 1 on the days that they occur with symbols for new moon, first quarter, full moon, and third quarter. The rest of the important astronomical data for the entire year is provided on the inside of the back cover of the Tidal Current Table, including: moon in apogee, moon in perigee, moon farthest north of Equator, moon on equator, moon farthest south of equator, March equinox, June solstice, September equinox, and December solstice (see Section 2.2.1 for definitions). Chesapeake Bay Entrance is one of 31 reference stations in the *Tidal Current Tables, Atlantic Coast of North America*. These reference stations are listed in the front of the Tide Tables with the length of the data time series from which the harmonic constants were calculated that were used to make the daily predictions. Chesapeake Bay Entrance was based on a least squares harmonic analysis using 330 days of current data from 1982. Because of the shortage of long-term current stations, many other tidal current reference station daily predictions are based on harmonic constants from shorter time series.

9.3.2 Table 2 – Differences and Ratios for Subordinate Stations

Figure 9.6 shows one typical page of the 47 pages of Table 2 in the *Tidal Current Tables, Atlantic Coast of North America*. This page provides tidal current information for 30 subordinate stations that are referenced to Chesapeake Bay Entrance, one station per line. (The page also includes 13 stations that are referred to the reference station at Delaware Bay Entrance, including two offshore current stations that were rotary enough that the reader is referred to Table 5.) For each station the information includes: the depth of the current station, its latitude and longitude, the time differences for minimum (slack) before flood, maximum flood, minimum (slack) before ebb, and maximum ebb, the speed ratios for maximum flood and maximum ebb, and the average speeds and

9. Products For Presenting Tide and Tidal Current Predictions

Chesapeake Bay Entrance, Virginia, 2006

F—Flood, Dir. 300° True E—Ebb, Dir. 129° True

January					February					March				
	Slack	Maximum		Slack	Maximum		Slack	Maximum		Slack	Maximum		Slack	Maximum
1 Su	0245 1.6E 0546 0837 1.4F 1209 1528 1.6E 1841 2103 0.9F 2356	h m h m knots 0245 1.6E 0634 0917 0.9F 1238 1603 1.2E 1930 2146 0.6F	16 M	0028 0352 1.1E 0715 0954 0.8F 1307 1633 1.1E 2008 2226 0.6F	h m h m knots 0318 1.2E 0917 0.9F 1311 1638 1.7E 1949 2225 1.2F	1 W	0049 0415 1.7E 0723 0958 1.3F 1355 1730 1.6E 2038 2319 1.2F	16 Th	0056 0408 1.1E 0732 1000 0.7F 1252 1622 1.2E 1954 2229 0.8F	1 W	0038 0400 1.8E 0711 0939 1.2F 1241 1609 1.7E 1916 2200 1.4F	16 Th	0000 0313 1.2E 0632 0900 0.7F 1145 1518 1.3E 1838 2123 0.9F	
2 M	0334 1.6E 0640 0926 1.4F 1256 1615 1.6E 1930 2153 1.0F		17 Tu	0028 0352 1.1E 0715 0954 0.8F 1337 1706 1.1E 2024 2247 1.0F	h m h m knots 0318 1.2E 0917 0.9F 1148 0.8F 1440 1826 1.4E	2 Th	0148 0514 1.6E 0822 1051 1.1F 1400 1826 1.4E	17 F	0135 0448 1.0E 0814 1035 0.6F 1315 1658 1.1E 2026 2305 1.2F	2 Th	0038 0400 1.8E 0711 0939 1.2F 1241 1609 1.7E 1916 2200 1.4F	17 F	0037 0347 1.2E 0712 0932 0.7F 1212 1548 1.3E 1908 2153 0.9F	
3 Tu	0056 0429 1.6E 0738 1016 1.2F 1341 1708 1.5E 2021 2247 1.0F		18 W	0111 0431 1.0E 0757 1031 0.7F 1333 1706 1.1E 2042 2309 0.6F	h m h m knots 0318 1.2E 0917 0.9F 1148 0.8F 2131	3 F	0247 0620 1.4E 0928 1148 0.8F 1440 1826 1.4E	18 Sa	0214 0536 0.9E 0900 1114 0.5F 1337 1740 1.0E 2100 2343 0.7F	3 F	0130 0456 1.6E 0810 1029 1.0F 1325 1657 1.5E 2004 2249 1.3F	18 Sa	0112 0425 1.1E 0755 1006 0.6F 1238 1623 1.2E 1941 2225 0.9F	
4 W	0157 0532 1.4E 0837 1111 1.1F 1426 1804 1.5E 2112 2346 1.0F		19 Th	0156 0517 0.9E 0840 1111 0.6F 1357 1744 1.0E 2119 2353 0.6F	h m h m knots 0318 1.2E 0917 0.9F 1148 0.8F 1531 1922 1.2E	4 Sa	0014 1.1F 0351 0725 1.3E	19 Su	0256 0629 0.8E 0954 1157 0.3F 1400 1827 1.0E 2141	4 Sa	0223 0558 1.5E 0910 1125 0.8F 1410 1753 1.3E 2056 2342 1.1F	19 Su	0148 0510 1.0E 0840 1043 0.4F 1304 1706 1.1E 2019 2303 0.8F	
5 Th	0303 0639 1.3E 0941 1210 0.9F 1514 1859 1.4E 2208		20 F	0243 0609 0.8E 0929 1154 0.5F 1420 1825 1.0E 2158	h m h m knots 0318 1.2E 0917 0.9F 1148 0.8F 1637 2023 1.0E	5 Su	0111 0.9F 0503 0834 1.2E	20 M	0026 0.7F 0349 0722 0.8E 1100 1246 0.8F 1430 1918 0.9E	5 Su	0320 0702 1.3E 0919 1224 0.6F 1459 1852 1.1E 2155	20 M	0226 0603 0.9E 0931 1127 0.3F 1330 1757 1.0E 2104 2349 0.8F	
6 F	0045 0.9F 0418 0745 1.2E 1056 1310 0.7F 1609 1954 1.3E 2306		21 Sa	0035 0.6F 0339 0701 0.8E 1029 1238 0.4F 1444 1907 0.9E 2239	h m h m knots 0318 1.2E 0917 0.9F 1148 0.8F 1749 2136 0.9E	6 M	0215 0.8F 0614 0950 1.1E	21 Tu	0114 0.7F 0457 0821 0.8E 1210 1341 * 1519 2014 0.9E	6 M	0038 0.9F 0427 0808 1.2E 1134 1325 0.4F 1602 1953 1.0E	21 Tu	0314 0659 0.9E 1033 1218 0.3F 1405 1853 0.9E 2200	
7 Sa	0145 0.9F 0533 0857 1.2E 1213 1418 0.5F 1712 2055 1.2E		22 Su	0117 0.6F 0444 0755 0.7E 1138 1326 0.3F 1517 1953 0.9E	h m h m knots 0318 1.2E 0917 0.9F 1148 0.8F 1857 2246 1.0E	7 Tu	0041 0347 0.7F 0721 1058 1.1E	22 W	0216 0.7F 0606 0934 0.8E 1315 1456 * 1650 2124 1.0E	7 Tu	0140 0.7F 0541 0923 1.0E 1251 1443 0.3F 1719 2108 0.9E	22 W	0043 0.7F 0421 0758 0.8E 1142 1315 * 1457 1953 0.9E	
8 Su	0005 0254 0.9F 0641 1011 1.2E 1330 1543 0.4F 1816 2202 1.1E		23 M	0206 0.6F 0546 0858 0.7E 1247 1427 * 1616 2049 0.9E	h m h m knots 0318 1.2E 0917 0.9F 1148 0.8F 1522 1732 0.4F	8 W	0150 0503 0.7F 0825 1155 1.2E	23 Th	0040 0333 0.7F 0710 1041 1.0E 1410 1612 0.3F 1822 2233 1.1E	8 W	0020 0313 0.6F 0653 1036 1.0E 1405 1626 0.3F 1831 2225 0.9E	23 Th	0144 0.7F 0536 0907 0.9E 1246 1427 * 1633 2104 1.0E	
9 M	0104 0410 0.9F 0743 1114 1.3E 1439 1651 0.5F 1917 2302 1.1E		24 Tu	0017 0308 0.7F 0644 1008 0.8E 1349 1541 * 1735 2153 1.0E	h m h m knots 0318 1.2E 0917 0.9F 1148 0.8F 1604 1813 0.5F	9 Th	0250 0551 0.8F 0919 1246 1.2E	24 F	0143 0437 0.9F 0810 1134 1.1F 1455 1705 0.6F 1939 2333 1.3E	9 Th	0135 0459 0.6F 0759 1134 1.0E 1501 1719 0.4F 1935 2324 0.9E	24 F	0018 0301 0.7F 0642 1015 1.0E 1340 1551 0.4F 1819 2219 1.1E	
10 Tu	0202 0504 0.9F 0840 1209 1.3E 1533 1739 0.5F 2015 2355 1.1E		25 W	0110 0410 0.8F 0740 1106 1.0E 1439 1638 0.4F 1845 2254 1.1E	h m h m knots 0318 1.2E 0917 0.9F 1148 0.8F 1640 1853 0.5F	10 F	0033 1.1E 0340 0631 0.8F 1002 1332 1.2E	25 Sa	0242 0528 1.1F 0902 1224 1.4E 1537 1754 0.8F 2049	10 F	0239 0544 0.6F 0852 1222 1.1E 1541 1758 0.5F 2031	25 Sa	0125 0415 0.9F 0739 1110 1.2E 1428 1650 0.7F 1939 2322 1.3E	
11 W	0258 0548 0.9F 0931 1301 1.3E 1618 1822 0.5F 2105		26 Th	0206 0500 1.0F 0836 1157 1.1E 1521 1724 0.5F 1952 2349 1.3E	h m h m knots 0318 1.2E 0917 0.9F 1148 0.8F 1713 1933 0.6F	11 Sa	0117 1.1E 0421 0710 1.2E 1038 1409 1.2E	26 Su	0031 1.5E 0337 0617 1.2F 0949 1313 1.6E	11 Sa	0013 1.0E 0328 0616 0.7F 0932 1304 1.1E	26 Su	0228 0509 1.0F 0830 1158 1.4E 1509 1738 0.9F	
12 Th	0045 1.1E 0346 0631 0.9F 1016 1348 1.3E 1658 1905 0.6F 2148		27 F	0259 0547 1.2F 0927 1248 1.3E 1601 1811 0.7F 2056	h m h m knots 0318 1.2E 0917 0.9F 1148 0.8F 1508 1811 0.7F	12 O	0156 1.2E 0459 0747 0.9F 1108 1440 1.2E 1747 2011 0.7F	27 M	0127 1.7E 0429 0709 1.3F 1032 1359 1.7E 2151	12 O	0056 1.1E 0407 0647 0.7F 1002 1338 1.2E 1642 1911 0.7F	27 M	0020 1.5E 0325 0558 1.1F 0917 1246 1.6E 1550 1825 1.2F	
13 F	0131 1.2E 0430 0716 0.9F 1056 1429 1.3E 1736 1948 0.6F 2227		28 Sa	0045 1.5E 0350 0636 1.3F 1015 1337 1.5E 1643 1902 0.9F 2156	h m h m knots 0318 1.2E 0917 0.9F 1148 0.8F 1819 2047 0.7F	13 M	0229 1.2E 0537 0821 0.9F 1136 1505 1.2E	28 Tu	0220 1.8E 0520 0801 1.4F 1116 1442 1.8E 1743 2026 1.4F	13 M	0135 1.1E 0441 0719 0.8F 1028 1405 1.2E 1710 1948 0.8F	28 Tu	0116 1.7E 0418 0648 1.2F 1000 1332 1.7E 1631 1914 1.4F	
14 Sa	0211 1.2E 0511 0800 0.9F 1133 1504 1.3E 1813 2029 0.6F 2305		29 Su	0140 1.6E 0440 0728 1.4F 1100 1423 1.6E 1727 1954 1.0F 2253	h m h m knots 0318 1.2E 0917 0.9F 1148 0.8F 1851 2122 0.8F	14 Tu	0301 1.2E 0613 0855 0.9F 1201 1528 1.2E	29 W	0210 1.2E 0518 0753 0.8F 1053 1429 1.3E	29 W	0209 1.8E 0510 0740 1.2F 1043 1416 1.8E			
15 Su	0246 1.2E 0552 0840 0.9F 1207 1535 1.2E 1851 2107 0.6F 2345		30 M	0232 1.8E 0532 0820 1.4F 1145 1507 1.7E 1812 2046 1.2F 2351	h m h m knots 0318 1.2E 0917 0.9F 1148 0.8F 1822 2155 0.8F	15 W	0015 1.2E 0652 0927 0.8F 1227 1553 1.2E	30 Th	0242 1.2E 0553 0827 0.8F 1119 1452 1.3E	30 Th	0258 1.8E 0604 0831 1.1F 1127 1459 1.8E 1758 2049 1.6F			
31 Tu	0322 1.8E 0628 0909 1.4F 1229 1551 1.8E 1900 2135 1.2F					31 F	0021 0346 1.8E 0700 0919 1.0F 1211 1542 1.7E 1845 2134 1.5F	31 F	0021 0346 1.8E 0700 0919 1.0F 1211 1542 1.7E 1845 2134 1.5F					

Time meridian 75° W. 0000 is midnight. 1200 is noon. Times are not adjusted for Daylight Saving Time.

* Current weak and variable.

Figure 9.5. One page from Table 1 predictions for a tidal current reference station at Chesapeake Bay Entrance from the *Tidal Current Tables, Atlantic Coast of North America*.

Tidal Analysis and Prediction

TABLE 2 – CURRENT DIFFERENCES AND OTHER CONSTANTS

No.	PLACE	Meter Depth	POSITION		TIME DIFFERENCES				SPEED RATIOS		AVERAGE SPEEDS AND DIRECTIONS								
			Latitude	Longitude	Min. before Flood		Min. before Ebb		Flood	Ebb	Minimum before Flood		Maximum Flood		Minimum before Ebb		Maximum Ebb		
					ft	North	West	h m	h m	h m	h m	knots	Dir.	knots	Dir.	knots	Dir.	knots	Dir.
DELAWARE BAY and RIVER CONT. Time meridian, 75° W																			
4471	PHILADELPHIA, PENNS LANDING, Petty Point (west end), Main Channel	15d	39° 56.76'	75° 08.33'	+5 34	75° 08.49'	+4 18	+5 00	1.3	1.3	—	—	1.5	017°	—	—	2.0	201°	
4471	Petty Point	24d	39° 56.73'	75° 08.13'	+6 03	75° 08.45'	+4 15	+5 27	1.0	1.5	—	—	1.3	026°	—	—	1.8	248°	
4481	Five Mile Point Bridge, northern end of	35d	39° 59.18'	75° 03.75'	+5 29	75° 04.52'	+4 33	+4 20	1.1	1.0	—	—	1.4	041°	—	—	1.7	229°	
4491	Torresdale, west of channel	40d	40° 02.4'	74° 59.4'	+6 55	75° 03.55'	+4 51	+6 07	0.6	1.2	—	—	0.9	038°	—	—	1.3	14°	
4496	Rancocas Creek, off Delanco	40d	40° 02.6'	74° 57.6'	+6 37	+6 24	+5 43	+6 29	0.7	0.7	—	—	1.0	090°	—	—	0.9	227°	
4501	College Point, 0.4 n.mi. east of	21d	40° 04.65'	74° 53.20'	+6 34	+4 54	+5 01	+4 50	0.8	0.9	—	—	1.2	064°	—	—	1.2	252°	
4506	Bristol, south of	8	40° 05.3'	74° 51.6'	+6 56	+5 30	+4 49	+6 31	0.9	1.2	—	—	1.3	024°	—	—	1.6	200°	
4516	Burlington Island, channel east of	40d	40° 05.7'	74° 49.2'	+7 33	+5 48	+4 08	+6 07	0.7	1.1	—	—	0.9	018°	—	—	1.6	204°	
4521	Newark Island north of, Main Channel	15d	40° 08.03'	74° 45.38'	+6 27	+4 29	+4 28	+3 51	0.5	0.4	—	—	0.7	084°	—	—	0.5	250°	
	Whitehill <27>		40° 08.2'	74° 44.2'	—	—	—	+7 28	—	1.1	—	—	—	—	—	—	1.4	233°	
DEL., MD. and VA. COAST																			
4526	Indian River Inlet (bridge)	38° 37'	75° 04'	—	—	+0 04	—	+0 31	1.3	1.6	—	—	1.8	265°	—	—	2.1	085°	
4531	Fenwick Shoal Lighted Whistle Buoy 2	38° 25'	74° 46'	—	—	See table 5.	—	—	—	—	—	—	—	—	—	—	—	—	
4536	Winter-Quarter Shoal Buoy 6WQS <28>	37° 55'	74° 56'	—	—	See table 5.	—	—	—	—	—	—	—	—	—	—	—	—	
on Delaware Bay Entrance, p.52																			
4541	Smith Island Shoal, southeast of	7	37° 05.3'	75° 43.5'	-1 36	-1 17	-1 35	-1 34	0.4	0.3	—	—	0.3	298°	—	—	0.4	068°	
4546	Cape Henry Light, 2.2 miles southeast of		36° 53.9'	75° 58.7'	-1 16	-0 23	-0 10	-1 10	1.2	0.7	—	—	1.0	346°	—	—	0.9	165°	
on Chesapeake Bay Entrance, p.68																			
4551	Cape Henry Light, 3.4nm NNE of	7d	36° 58.79'	75° 58.85'	-0 03	+0 00	+0 09	-0 01	1.3	1.3	0.2	206°	1.0	287°	0.2	016°	1.6	116°	
	do	15d	36° 58.79'	75° 58.85'	-0 14	-0 04	-0 11	-0 05	1.2	1.0	0.1	199°	1.1	290°	0.1	193°	1.2	172°	
	do	30d	36° 58.79'	75° 58.85'	-0 09	+0 01	-0 03	-0 08	0.5	0.5	0.0	009°	0.6	277°	—	195°	0.6	024°	
4556	Cape Henry Light, 2.95nm NNE of	15d	36° 57.74'	75° 59.14'	+0 17	+0 33	+0 18	+0 07	1.3	1.0	—	—	1.0	291°	0.1	029°	1.2	116°	
	do	30d	36° 57.74'	75° 59.14'	-0 36	+0 00	+0 07	-0 25	1.5	0.8	—	—	1.2	294°	0.1	208°	1.0	233°	
	do	45d	36° 57.74'	75° 59.14'	-1 05	-0 08	-0 10	-0 41	1.7	0.7	—	—	1.4	294°	0.1	205°	0.9	125°	
4561	Cape Henry Light, 1.4nm NE of	6d	36° 57.74'	75° 59.14'	-1 22	-0 18	+0 04	-0 56	1.4	0.6	—	—	1.2	294°	0.1	204°	0.7	124°	
	do	30d	36° 57.73'	75° 59.38'	+0 43	+0 44	+0 47	+0 21	1.1	1.2	0.1	205°	0.2	290°	—	1.5	117°	—	
	do	45d	36° 57.73'	75° 59.38'	-0 19	-0 25	-0 10	-0 01	1.5	1.0	0.1	205°	1.2	290°	—	1.2	119°	—	
4566	Cape Henry Light, 0.8 n.mi. NNE of	15d	36° 56.73'	75° 59.38'	-0 18	+0 09	-0 30	-0 01	1.5	0.9	0.1	203°	1.2	293°	0.1	199°	1.1	114°	
	do	60d	36° 56.73'	75° 59.38'	-0 32	+0 07	-0 30	-0 11	1.3	0.8	—	—	1.0	282°	0.1	191°	1.0	107°	
4567	Cape Henry Light, 2.0 n.mi. north of	15d	36° 56.33'	75° 59.98'	+0 26	+0 03	-0 04	+0 10	1.3	1.3	—	—	1.0	298°	—	—	1.7	113°	
	do	30d	36° 56.33'	75° 59.98'	-1 42	-1 41	-1 36	-1 52	1.4	1.0	0.2	003°	1.1	275°	0.2	189°	1.2	106°	
4571	Cape Henry Light, 2.0 n.mi. north of	15d	36° 57.53'	76° 00.63'	+0 12	+0 25	+0 00	+0 20	1.5	0.9	0.1	210°	1.2	289°	—	1.1	110°	—	
	do	30d	36° 57.53'	76° 00.63'	-0 23	+0 10	-0 55	-0 17	1.5	0.5	0.1	201°	1.2	277°	0.1	190°	1.7	107°	
4576	Lynnhaven Inlet bridge	5d	36° 57.53'	76° 00.63'	-1 03	-0 07	+0 34	-1 05	1.1	0.4	0.1	002°	0.9	263°	0.2	177°	0.5	111°	
CHESAPEAKE BAY ENTRANCE																			
4581	Cape Henry Light, 4.6 miles north of	14d	36° 58.80'	75° 59.89'	-0 27	+0 09	+0 19	+0 23	1.6	1.0	—	—	1.3	294°	—	—	1.3	104°	
4586	Cape Henry Light, 5.9 n.mi. north of	14d	37° 01.40'	75° 59.55'	-0 59	-0 09	-0 26	-0 36	0.8	0.5	0.1	228°	0.6	307°	—	0.7	140°	—	
4591	Cape Henry Light, 8.3 mi. NW of	12	37° 02.20'	76° 06.60'	+0 16	+0 43	+0 45	+0 26	1.2	0.9	—	—	1.0	329°	—	—	1.1	133°	
4596	Lynnhaven Inlet bridge	36d	36° 55.1'	76° 04.9'	-0 20	+0 18	+0 15	-0 10	1.0	0.7	—	—	0.8	280°	—	—	0.9	070°	
4601	Chesapeake Bay Bridge Tunnel	36d	36° 54.4'	76° 05.6'	-1 18	-1 10	-1 43	-2 30	0.7	1.1	0.6	180°	—	—	—	—	1.4	000°	
4606	Chesapeake Beach, 1.5 miles north of	6d	36° 56.69'	76° 07.33'	+0 29	+0 48	+0 06	+0 00	1.0	0.7	—	—	0.8	305°	—	—	0.9	100°	
4611	0.75nm west, Thimble Shoal Channel	16d	36° 58.64'	76° 07.45'	-0 03	+0 18	+0 13	+0 08	1.5	0.8	0.3	205°	1.2	288°	0.2	013°	1.1	113°	
	do	16d	36° 58.64'	76° 07.45'	-0 30	+0 19	+0 45	+0 02	1.4	0.6	0.1	200°	1.1	289°	0.1	017°	0.8	111°	
	do	29d	36° 58.64'	76° 07.45'	-0 22	+0 13	+0 05	+0 11	0.6	0.1	0.08	0.9	244°	—	—	0.3	017°	—	—
	do	39d	36° 58.64'	76° 07.45'	-0 43	+0 19	+0 22	+0 01	0.8	0.4	—	—	0.6	281°	—	—	0.5	096°	—
4616	Tail of the Horseshoe		36° 59.57'	76° 06.20'	+0 05	+0 30	+0 16	+0 28	1.1	0.8	—	—	0.9	300°	—	—	1.0	110°	—

Endnotes can be found at the end of table 2.

Figure 9.6. A page from Table 2 from the *Tidal Current Tables, Atlantic Coast of North America* showing subordinate tidal current stations.

directions for the minimum before flood, maximum flood, minimum before ebb, and maximum ebb. All speeds are given in knots (1 knot = 51.4 cm/sec). The subordinate stations are split up into groups of stations referred to the same reference station, which is listed above each group (two groups are shown on this page). To make a prediction on a particular day at a subordinate station, the time differences and speed ratios are applied to the daily predictions for that day at the reference station listed above that group of subordinate stations. For stations with special situations that cannot be totally handled by this format, there are Endnotes with additional information, and for stations that are rotary enough there is no clear flood or ebb direction the reader is referred to Table 5.

The time differences and speed ratios in Table 2 were produced using the rotary reduction analysis and/or the reversing reduction analysis, which are two nonharmonic methods that compare the slacks/minima and maximum floods and ebbs in a current data time series at the subordinate station with the predicted slacks/minima and maximum floods and ebbs for the same time period at the most appropriate reference station (see Sections 6.5 and 6.6). The column headings say “Minimum before Flood” instead of “Slack before Flood” and “Minimum before Ebb” instead of “Slack before Ebb” because the more recent current data were analyzed with a computerized rotary reduction analysis. Most current stations are rotary to some degree, although the ones listed in Figure 9.6 trace out fairly narrow ellipses so that the minimum current flow perpendicular to the main flood-ebb axis is only on the order of a tenth of a knot or two. The dashes in those columns are for older stations that were analyzed using a manual reversing reduction analysis.

9.3.3 Table 5 – Rotary Tidal Currents

Figure 9.7 shows a typical page of Table 5 in the *Tidal Current Tables, Atlantic Coast of North America*, which shows tidal current stations that are very rotary, i.e., the tips of the rotating vector trace out a very wide ellipse or even a circle. For such current stations there are either no clear flood and ebb directions, or if such directions can be determined, the minimum flows (perpendicular to the flood-ebb axis) are not much smaller than the maximum flows. Since most current stations are rotary to some degree, almost all the stations could be put into Table 5 if one wanted (and that would serve a useful purpose for seeing how each station rotates, and also how it is distorted by shallow-water effects). However, usually only offshore stations have been put in Table 5, as well as some inshore stations with very wide ellipses. For these stations Table 5 gives a current speed and direction for each hour of a mean tidal current cycle. These hours are relative to a particular time at a particular reference station. For example, the hourly time increments in Figure 9.7 for Frying Pan Shoals are after the time of maximum flood at the reference station, Charleston Harbor. (That reference station had been used in a rotary reduction analysis of the current data at Frying Pan Shoals, to come up with the twelve speed and direction pairs found in this table for this station.) The direction of each hourly value is given in degrees true clockwise from north.

9.3.4 Other Tables and Information

There are other small tables in the Tidal Current Tables that provide additional information such as: a table for determining the speed of current at any time (between maximum and slacks); a table

TABLE 5.—ROTARY TIDAL CURRENTS

Station Name	Depth	Hourly time increments												
		0	1	2	3	4	5	6	7	8	9	10	11	
After Maximum Flood at THE RACE														
Little Gull Island, 3.7 miles ESE		0.8 271	0.5 284	0.2 320	0.2 068	0.7 077	1.1 095	1.6 118	1.2 128	0.6 150	0.2 171	0.4 221	0.7 228	knots degrees
Great Round Shoal Channel		1.0 047	1.3 060	1.3 070	0.8 091	0.5 153	0.7 211	0.9 234	1.3 247	1.1 252	0.9 260	0.3 305	0.4 035	knots degrees
After Maximum Flood at THE NARROWS, NEW YORK														
Sandy Hook Approach Lighted Horn Bouy 2A, 0.2 miles W		0.4 313	0.3 325	0.2 356	0.2 055	0.3 094	0.4 118	0.6 136	0.5 147	0.2 177	0.2 256	0.3 290	0.4 298	knots degrees
After Maximum Flood at DELAWARE BAY ENTRANCE														
Fenwick Shoal Lighted Whistle Bouy 2		0.2 342	0.2 349	0.1 357	0.1 043	0.1 110	0.2 135	0.3 150	0.2 165	0.2 185	0.1 226	0.1 282	0.2 318	knots degrees
After Maximum Flood at CHESAPEAKE BAY ENTRANCE														
Point Lookout, 1.5nm east of	16	0.31 197	0.26 217	0.24 242	0.24 266	0.22 290	0.22 311	0.18 330	0.10 358	0.09 073	0.13 113	0.20 152	0.29 179	knots degrees
After Maximum Flood at CHARLESTON HARBOR														
Frying Pan Shoals, off Cape Fear		0.3 335	0.2 010	0.2 050	0.3 090	0.3 110	0.3 128	0.3 150	0.2 188	0.2 235	0.3 268	0.3 290	0.3 305	knots degrees
Cape Romain, 5 miles SE		0.2 006	0.2 038	0.3 055	0.3 067	0.3 093	0.3 114	0.2 167	0.2 212	0.3 242	0.4 244	0.3 262	0.3 292	knots degrees
Cape Romain, 6.9 miles SW		0.3 317	0.2 350	0.2 019	0.3 071	0.3 115	0.3 111	0.2 132	0.2 160	0.2 216	0.2 251	0.3 266	0.3 303	knots degrees
Capers Inlet, 1.9 miles east of		0.1 012	0.1 058	0.2 052	0.2 053	0.1 067	0.1 098	0.1 129	0.1 214	0.2 222	0.2 254	0.1 246	0.1 247	knots degrees
Capers Inlet, 3.6 miles SE of		0.2 302	0.1 357	0.1 034	0.2 017	0.2 089	0.2 094	0.2 112	0.2 116	0.1 189	0.2 249	0.2 268	0.2 282	knots degrees

Figure 9.7. Rotary tidal currents presented in Table 5 of the *Tidal Current Tables, Atlantic Coast of North America*.

for determining the durations of slack; and descriptive information about coastal tidal currents and wind-driven currents and how to combine them.

Table 3 provides a method for calculating the tidal current speed at some point between a slack water and a maximum flow based on cosine interpolation of the speeds of a reversing tidal current. There are actually two tables, one for most of the stations listed in Table 2, and the second for a few particular stations. This cosine-based interpolation scheme may not work very well for many current stations, because in shallow water the tidal current speed curve is distorted away from a cosine shape and the current direction also rotates around the compass, which is not considered in Table 3.

Table 4 gives information about the duration of slack water at any station in Table 2. Although “slack water” is defined as one point along a tidal current speed curve where the speed is exactly zero, there will be some period of time before and after this zero-speed point that the speeds are so low that it will appear to be slack water to the mariner. Table 4 helps calculate how long a period of time that the currents at a particular station will stay below some current speed value (the choices being, 0.1, 0.2, 0.3, 0.4 or 0.5 knot), based on the maximum current at that particular station. As with Table 3, there are two tables for this, one for most of the stations listed in Table 2, and the second for a few particular stations. Table 4 is also based on cosine interpolation of the speeds of a reversing tidal current and therefore will not necessarily give accurate results for stations with rotary currents or shallow-water distortions.

9.3.5 Current Diagrams

The *Tidal Current Tables, Atlantic Coast of North America* also include five examples of another type of presentation for tidal currents, the *current diagram*. A current diagram is a graphic that shows the velocities of the flood and ebb currents (and the time of slacks and maximum floods and ebbs) over a “considerable stretch of the channel of a tidal waterway.” At definite intervals along the channel the current velocities are shown with reference to the times of slack waters (when the current changes direction from flood to ebb or vice versa) at a particular reference current station. An example, for Chesapeake Bay, from the entrance (Cape Henry) to Baltimore, a distance of about 150 nautical miles, is shown in Figure 9.8. Along the top and bottom horizontal axes one sees hourly time intervals referred to slack flood begins (i.e., slack before flood, SBF) or to slack ebb begins (i.e., slack before ebb, SBE) at the reference tidal current station, in this case Chesapeake Bay Entrance (CBE). The first six intervals are 3 hours before SBF at CBE, 2 hours before SBF, 1 hour before SBF, SBF, 1 hour after SBF, and 2 hours after SBF. The next six intervals are 2 hours before SBE at CBE, 1 hour before SBE, SBE, 1 hour after SBE, 2 hours after SBE, and 3 hours after SBE. And then the first set of intervals repeats. This added set of time intervals is needed in the diagram, because the distance from the entrance to Baltimore is so long that it takes more than a tidal cycle for a particular slack water to progress up the Bay from the entrance to Baltimore. The same tidal cycle starts progressively later going up the Bay. The changing current speed for each station is shown on a horizontal line to the right of the station. Flood and ebb phases are shown with appropriate shading and labeling. The speed lines to the right of the diagram were for the captain of a ship moving at a particular speed (from 5 to 15 knots, which correspond to the slanted speed lines, one set for the ship sailing northward and one set for southward) to use to figure out (with parallel rulers) what the current speeds will be along the ship’s route.

9. Products For Presenting Tide and Tidal Current Predictions

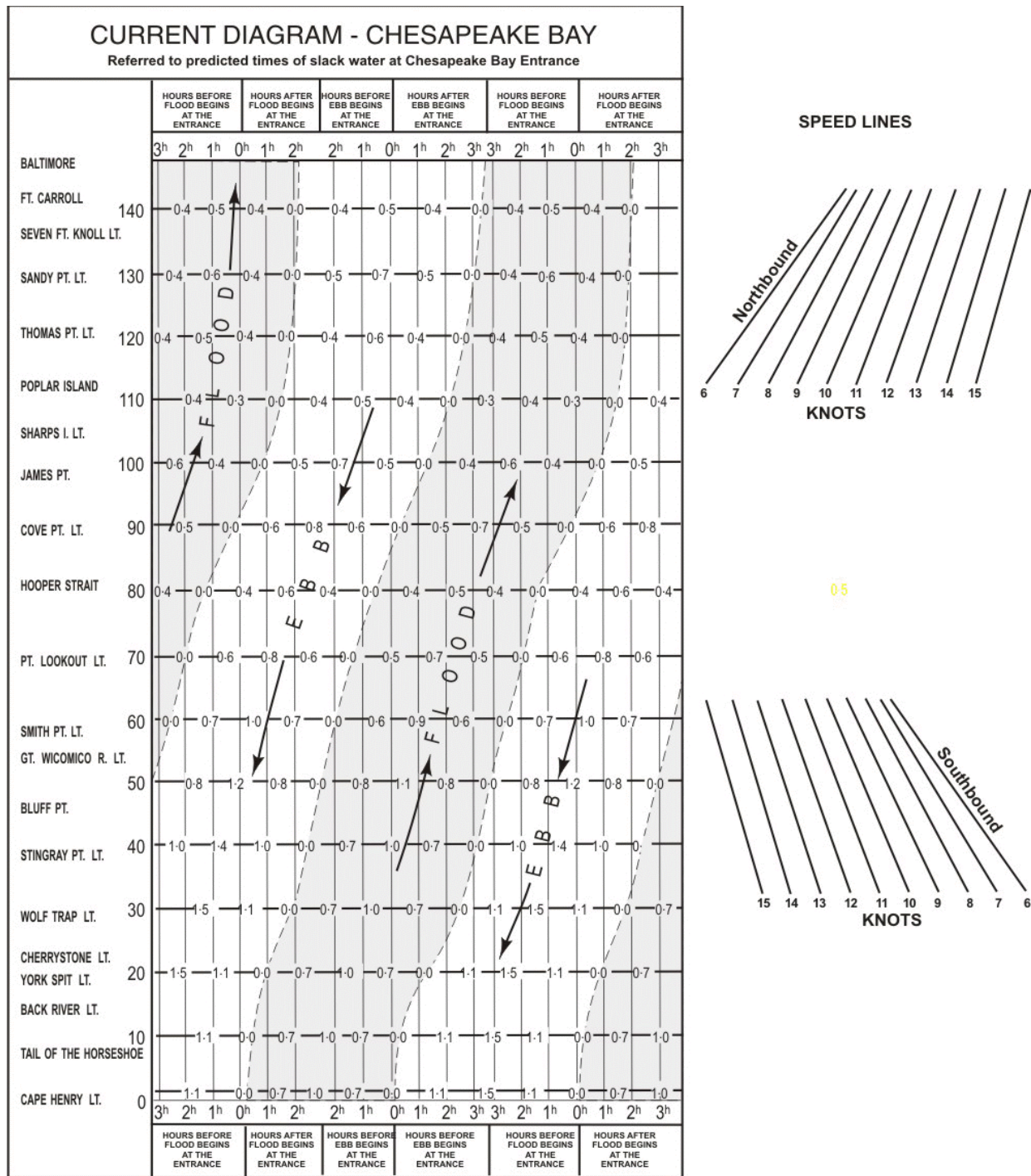


Figure 9.8. A tidal current diagram for Chesapeake Bay included in the *Tidal Current Tables, Atlantic Coast of North America*.

9.3.6 Limitations of Tidal Current Tables

Tidal Current Tables, like Tide Tables (see Section 9.2.5), are “hardcopy” products that have been printed for many decades, and only in recent years have been extended to electronic media such as CDs and the World Wide Web on the Internet. As printed documents these tables have had certain limitations on what could be included in them, because of page limitations and also because of the lack of ease with which certain information could be conveyed to a user. With electronic media those limitations go away, but the traditional format for tidal current tables continues to survive, both because of its familiarity but also because of the extensive new data that will be required to produce digital tidal current prediction products based on the harmonic analysis of all stations (see Section 9.7).

One alternative to this, mentioned in Section 9.2.5, is the use of numerical hydrodynamic models forced with accurate tide predictions at the entrance based on long-term tide stations. Such a method for predicting tidal currents has many advantages (see Section 8.3) since they provide tidal current predictions at hundreds or even thousands of locations, and they can show how the tidal currents vary spatially (often in a dramatic fashion) over short distances. For example, they can show the very different speed and directions near the bottom compared with near the mid and surface levels, as well as the dramatic differences between tidal currents in a channel and in the nearby shallows. However, a model requires new data, and for more than just the entrance, because of the extensive validation of the model that is required to make sure it produces accurate predictions everywhere in the modeled waterway. Thus, a reasonable amount of new data is necessary for numerous validation sites. This is especially true for current data since the currents can change so dramatically from place to place, which puts a great pressure on suitable validation.

The same two primary limitations apply to a tidal current table as to a tide table, only they are usually more serious for a tidal current table (See Section 9.2.5.). The first limitation is that in a tidal current table (harmonically produced) daily predictions can only be provided for a relatively few of the thousands of tide stations in the table. This is a page limitation, since the daily predictions of a reference takes four pages in Table 1, while the time differences and speed ratios for a subordinate station takes only one line in Table 2, with roughly 50 stations per page. Most stations must therefore be included as subordinate stations in Table 2. As was seen in Section 3.6.3, in the introduction to Chapter 6, and in Section 6.9, serious prediction errors can occur if the harmonic makeup of the subordinate stations is not similar enough to the harmonic makeup of the reference station. In this situation the mean time differences and speed ratios in Table 2 (that come out of a nonharmonic comparison analysis) are really good only for certain times of the month.

This can be a very serious problem for tidal currents especially in a waterway with a mixed tidal current and a strong diurnal signal, because the tidal characteristics will change relatively quickly with geographic distance, and the subordinate station will often be too far from the reference station. With tidal currents this can happen much more frequently than with the tide, because for currents in channel bends and around points sticking out into a waterway, nonlinear lateral inertial effects transfer energy from diurnal frequencies to semidiurnal frequencies (see Section 2.3.6e and Figure 2.36). In this case tidal current predictions made using Table 2 time differences and speed ratios will be least accurate around the times of maximum lunar declination, and most accurate near times of equatorial declination. If this occurs, one solution is to add an additional reference station to the Tidal Current Table, one that is closer to the subordinate stations and has more similar tidal characteristics. But for an area like the Strait of Juan de Fuca, the San Juan Islands, and the Strait of Georgia (see Figures 2.36, 7.2 and 7.3) there is so much variation in diurnal-to-semidiurnal ratios

in the area, that dozens of new tidal current reference stations would have to be created to handle the situation.

The second limitation of a tidal current table is that only predictions for slacks/minimums and maximum floods and ebbs are given. For predictions of the tidal current speed and direction between the slacks/minimums and the maximum floods or maximum ebbs the user is sent to Table 3 and forced to use a cosine-based interpolation scheme (only a very few stations are included in Table 5, for very rotary tidal currents). However, the tidal current curve looks like a cosine for only a few special cases such as a reversing current in a deep narrow channel or waterway. And even if Table 3 worked fine for speeds, it does not give the direction of flow, which for most current stations is different for each hour. Most current stations are rotary to some degree and are distorted by nonlinear shallow water and lateral inertial effects, for which a cosine curve will not work at all. For example, of the tidal current examples shown in Figure 2.4 a cosine curve interpolations scheme might only work for the left-hand bottom example (and then only if the speed curve is not too distorted by shallow water, which is difficult to tell from that plot).

Both these problems can be solved using electronic/digital tide predictions products where all the stations are predicted harmonically, which eliminates the need for time differences and speed ratios, and which allows prediction of an entire tidal current curve for every station (showing all rotations of direction as well as the distortions by shallow water and lateral inertial effects) so that no interpolation is needed.

9.3.7 The Construction of Tidal Current Tables

Here a short overview on the constructions of Tidal Current Tables is presented that repeats some of what was said in Sections 5.6 and Sections 6.8. There are two primary activities: (1) producing accurate daily predictions (of slacks/minimums and maximum floods and ebbs) for references stations in Table 1 using harmonic analysis and prediction; and (2) calculating time differences and speed ratios for subordinate stations in Table 2 using nonharmonic comparison analysis. Predictions at a subordinate station are made by applying its time differences and speed ratios to the daily predictions at the reference station that was used in the nonharmonic analysis.

To produce reference stations for Table 1 of the Tidal Current Tables, one should use as long a current data time series as possible, preferably at a dynamically simple location (such as in the center of the entrance to the waterway or in the straight section of a channel; away from channel bends, junctures of channel, points sticking out into the waterway, etc.). It is preferable, if possible, that this location should be important for navigational purposes, as many mariners will rely mainly on the reference station and may not go through the adjustment process using Table 2 time differences and speed ratios. One should carry out a harmonic analysis using as many tidal constituents as the length of the time series will allow (see Section 5.3.1), perhaps being able to push this limit in some situations if one needs to include an important tidal constituent (see Section 3.3). Because of the importance of this reference station, and because predictions for this station will be produced for many years, one should do a careful quality analysis (see Section 5.5).

Using this reference station one should then analyze the numerous subordinate current stations nonharmonically. One should use both the rotary reduction analysis and the reversing reduction analysis on every subordinate station, since they both provide different but necessary information. Since the tidal current at most locations (other than very narrow channels) is rotary to some degree (the tip of the current vector approximately tracing out ellipses of various widths), a rotary reduction must be run to show this rotation in direction over a tidal current cycle. The rotary reduction

analysis also shows how the current speeds are distorted by shallow-water effects (so that the speed curve is often far from looking like a pure cosine curve). The reversing reduction must also be run, primarily for quality assurance purposes, in order to see how much the time differences and speed ratios between the subordinate station and the reference station for each tidal cycle change throughout the month. For example, if there is too much periodic variation from a tidal cycle near equatorial lunar declination to a tidal cycle near maximum lunar declination, then the tidal characteristics of the reference station are not similar enough to those at the subordinate station. In this case a different reference station should be used if possible, or even a new reference station developed. If neither of these is an option, then one should determine (from the reversing reduction analysis) how much the time differences and speed ratios will vary (and under what astronomical conditions) and put that information in an Endnote for Table 2. If there are many stations with this problem, one can even modify the format of one page of Table 2 for those stations, and add columns for differences and ratios that apply to, for example, maximum lunar declination.

9.4 Tidal Current Charts

9.4.1 Description of Tidal Current Charts

Typically a set of *Tidal Current Charts* consists of a chart of the waterway repeated twelve times (sometimes thirteen), one for each hour of the tidal cycle, each chart having numerous current vectors showing the speed and direction of the tidal current flow for that hour of the tidal cycle at various locations in the waterway. (In other countries similar charts can be called Tidal Stream Atlases or Tide Stream Charts.) These charts allow one to produce tidal current predictions at numerous locations in a waterway (using a reference station from the Tidal Current Tables), but one of the main advantages of these charts is their visualization of the tidal current flow over the entire waterway at hourly intervals throughout a tidal cycle. Figure 9.9 shows an example of (a portion of) one tidal current chart from the 12 that make up the *Upper Chesapeake Bay Tidal Current Charts* (2nd Edition, 1973). Some of the more recent Tidal Current Charts show current vectors for more than one depth.

The first time that tidal currents (tidal streams) were presented on a chart may have been in 1702 when Edmond Halley (of comet fame) published a chart based on five months of observations that he made in the English Channel the year before using the Admiralty ship *Paramour*. What he actually recorded for many locations in the Channel (and put on the chart) were the times when his anchored ship swung around when the tidal current changed from flood direction to ebb direction (“the end of the stream that sets to the eastward”), as well as the direction of this flood current (predominantly parallel to the coasts, and thus eastward); these would be essentially slack times if the currents were not rotary. At numerous locations on his tidal stream chart, the hours for these *turning times* were given for the first day of the new moon or full moon (and they were generally one or two hours earlier than high water times, which were measured on the coasts). It would not be for another 130 years before others would also produce some type of tidal stream chart. (See Proudman, 1942)

In the U.S. in the Coast Survey, tidal current charts first appeared in a series of Special Publications (S.P.) in the 1920s and 1930s, as part of some very thorough and detailed studies of the tides and tidal currents in particular bays and harbors (which usually also included water temperature and density data, as well). For example, fairly crude looking tidal current charts appeared in *Tide and Currents in San Francisco Bay* by Disney and Overshiner (1925, S.P.115) in their Figures 19

9. Products for Presenting Tide and Tidal Current Predictions

through 30. Three years later more precise looking tidal current charts appeared in an S.P. by Paul Schureman entitled *Tide and Currents in Boston Harbor* (Schureman, 1928, S.P. 142). In later S.P.s the tidal current charts became larger and more detailed and required fold-out pages, such as in *Tide and Currents in Long Island and Block Island Sounds* by LeLacheur and Sammons (1932, S.P. 174). In more recent decades Tidal Current Charts were published as separate documents, one set each for various bays and harbors around the United States.

Each individual tidal current chart (of the 12 or 13 provided for a particular waterway) is referenced to one or two key points in the tidal current cycle [e.g. slack before flood (SFB) and/or slack before ebb (SBE), or maximum flood (MF), etc.] or sometimes in the tide cycle [e.g. high water (HW) and/or low water(LW)]. For some tidal current charts, each chart was for one or more hours after or before the key point used. For example, the *Upper Chesapeake Bay Tidal Current Charts* had 12 charts depicting the currents at: two hours before *maximum flood* at Baltimore Harbor Approach (F-2), F-1, F, F+1, F+2, F+3, two hours before *maximum ebb* (E-2), E-1, E, E+1, E+2, and E+3. The *Narragansett Bay Tidal Current Charts* (1st edition, 1971) had 13 charts depicting the currents at: the time of *high water* (HW) at Newport, one hour after high water (HW+1), HW+2,, HW+12. Several tidal current charts used *slack, flood begins* (SFB) and *slack, ebb begins* (SEB), but instead of each chart being one or more hours before or after SFB or SEB, the flood phase (i.e., from the time of SFB to the time of SEB) was divided into six equal periods, as was the ebb phase. The *Boston Harbor Tidal Current Charts* had 13 charts depicting the currents at: SFB, SFB+1, SFB+2, SFB+3, SFB+4, SFB+5, SEB, SEB+1, SEB+2, SEB+3, SEB+4, SEB+5, and SEB+6, but here the 1, 2, 3, etc, refer to equal intervals after SFB or SEB, not hours.

Making tidal current predictions using a Tidal Current Chart still requires use of a tidal current reference station (or sometimes a tide reference station) for the waterway depicted on the chart. Although the tidal current chart applies to any year, each year a new set of daily predictions for the reference station is needed. Such reference station daily predictions, of course, appear in Table 1 of the annual Tidal Current Table (or Tide Table), but were sometimes provided separately.

To make a prediction of the tidal current at a particular time on a particular day, the user would go to the daily predictions at the reference station, from which the user first would determine which of the 12 or 13 tidal current charts is needed to make the prediction. For Chesapeake Bay, which had hourly charts before and after maximum flood at Baltimore Harbor Approach, one would look at the reference station predictions for the day of interest and see how many hours before or after the nearest maximum flood or maximum ebb the time of interest fell and then select the corresponding chart.

The tidal speeds depicted on the charts are usually for mean springs (i.e., near times of full moon or new moon). Since the tidal current varies throughout the month (being faster near times of springs, perigee, and maximum lunar declination, and slower near times of neaps, apogee, and equatorial declination) a method was used to adjust the spring values shown on the charts for other astronomical conditions. A factor for correcting the speeds on the selected chart was chosen from a table on the inside front cover of the Tidal Current Charts, where one looked up the predicted speed of the nearest maximum flood or maximum ebb at the reference station and then selected the corresponding correction factor (from the column to the right) and applied it to the speeds on the selected chart.

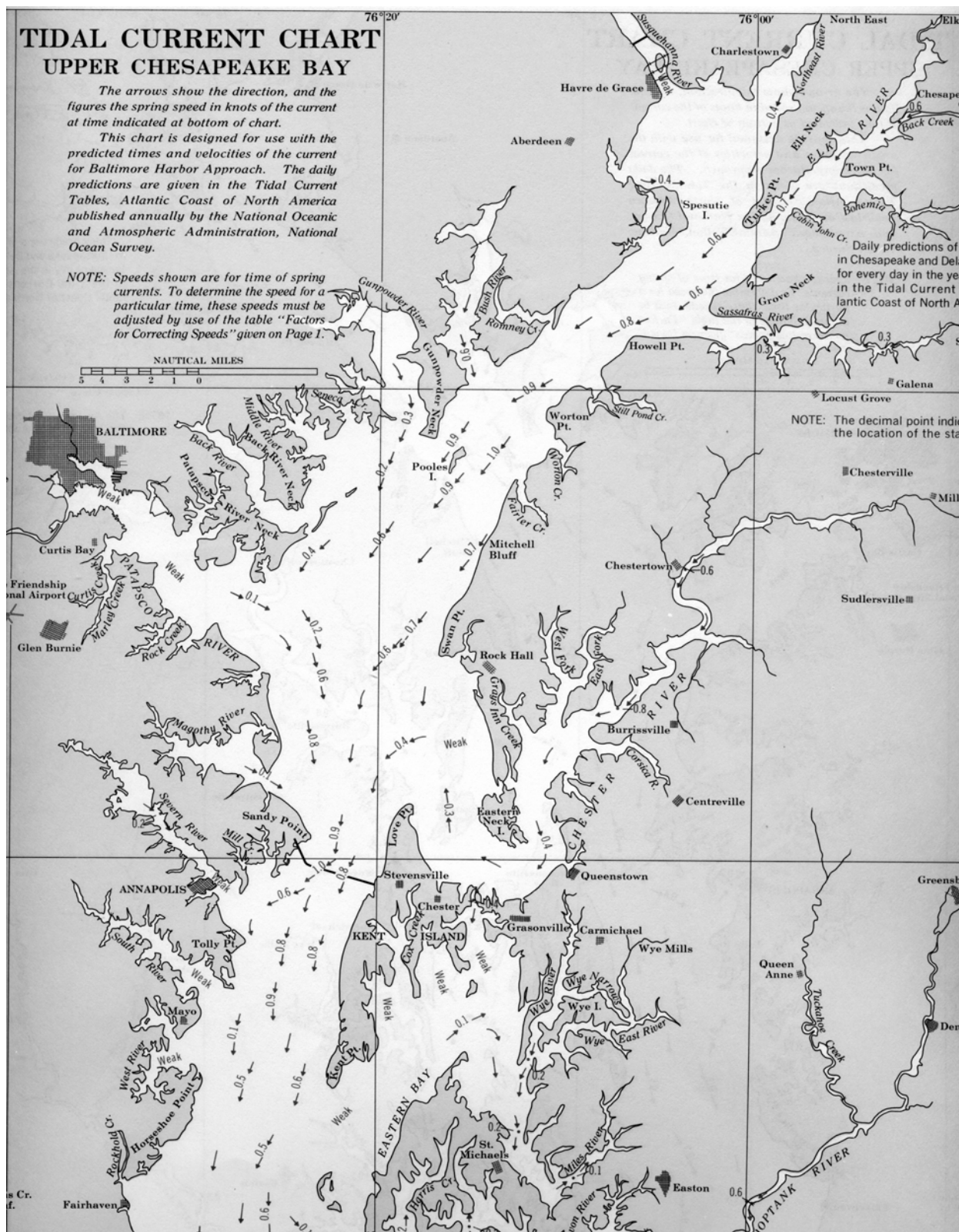


Figure 9.9. A portion of one of the 12 hourly tidal current charts for the Upper Chesapeake Bay.

9. Products for Presenting Tide and Tidal Current Predictions

For the tidal current charts that used equal intervals for the ebb and flood phases (rather than simply used hours after or before) the procedure was similar to that above, with one difference. To select the correct chart to use one had to first figure whether the time of interest fell in the flood phase or the ebb phase. Using the two slack water times that straddled the time of interest to determine the duration of the flood or ebb phase, and then dividing the duration by six to determine the start and stop times for each of the six charts for that phase, one selected the chart that the time of interest fell in. To make this simpler, for some Tidal Current Charts a special set of 12 *Tidal Current Diagrams* was published annually, one diagram for each month of the year. On each diagram the days of the month ran down the left side, and the hours of the day ran across the top side. By lining up the day of interest and time of interest one could directly obtain the correct tidal current chart to use, those being indicated by contour lines generally running in parallel from upper left to low right. (These diagrams should not be confused with the diagrams in Section 9.3.5 or Section 9.6.)

9.4.2 The Advantages and Limitations of Tidal Current Charts

Since Tidal Current Charts show the tidal current for each hour of a mean tidal current cycle it has the advantage of being able to accurately show the changing current direction (as well as the changing current speed) as the current rotates around compass over one tidal cycle. For currents in narrow channels the ellipses traced out by the tips of the hourly current vectors will be narrow (and so almost a reversing currents) but for wider waterways and for areas where various channels meet, the tips of the hourly current vectors can trace out wide ellipses as well as some other shapes (even figure eights), which can be correctly depicted on the Tidal Current Charts. Also, tidal current curves are frequently distorted due to shallow-water and lateral inertial effects (the M_4/M_2 ratio is often larger in the tidal current than in the tide), and the changing speeds (which will look quite different than a cosine curve) can also be represented accurately on Tidal Current Charts. Thus, Tidal Current Charts should be able to provide better tidal current predictions than a Tidal Current Table, since with the latter, cosine-base interpolations are used to provide the tidal current flows between the slacks and maximum floods or ebbs that are provided in the Tables. (Unfortunately, because the reversing reduction analysis was most frequently used during the pre-computer era, because it took much less manual effort, there appear to have been a few examples of Tidal Current Charts where the currents, even in wide waterways or areas with complicated geometry, are depicted as strictly reversing and where cosine interpolation was probably used to produce many charts representing the times between slacks and maximum floods and ebbs. A rotary reduction analysis should always be used for analyzing all current stations put on a Tidal Current Chart.)

Tidal Current Charts also have some limitations. For example, they cannot easily be made to represent mixed tidal currents, that is, tidal currents with a significant diurnal inequality. For such situations not only does this inequality vary throughout the month (from a minimum near times of equatorial declination to a maximum near times of maximum lunar declination), but the length of the flood phase and the length of the ebb phase will also vary throughout the month (often being quite different for the morning tide versus the afternoon tide). One can try to use the above mentioned equal-interval method, with each flood or ebb phase divided up into six equal intervals (instead of simply using hours before or after the slacks), so that all the shorter phases could still be averaged with the longer phases. However, even if that method produced consistent reasonable values, it could not be used when the tidal current goes diurnal during part of the month (as can happen in mixed tidal currents that have a strong diurnal signal).

The distortions to the mean tidal current curve caused by nonlinear shallow-water effects or lateral inertial effects are represented on a tidal current chart, but not easily visualized because the actual mean tidal current curves are not provided (but probably should be added at the back of the charts). These distortions, however, also vary throughout the month, and this variation would be very difficult to represent with some kind of a correction technique.

9.4.3 The Construction of the Tidal Current Charts

9.4.3a Using the Rotary Reduction Analysis – the Traditional Method

To construct a set of tidal current charts for a particular waterway one must analyze all available current data of accepted quality from that waterway. Unless the waterway is very deep the current data should be fairly recent. Currents are greatly affected by changes in bathymetry, changes in shoreline or other geographic features, changes in average river discharge (perhaps due to a dam), etc. Thus, current data from a time period before major dredging or shoaling occurred should not be used.

One will use the rotary reduction to analyze these current data (reading Section 6.6 may be necessary to fully appreciate some comments below). One must also have a long enough current station time series to be able to harmonically analyze it and to produce a reliable reference tidal current station, predictions from which will be used in the rotary analysis. Often that has already been done for the Tidal Current Tables, in which case predictions from that reference station will be used in the analysis. One should also do a few reversing reduction analyses for quality control purposes, to make sure that the tidal characteristics of each subordinate station are similar enough to those of the reference stations (i.e., that the time differences and speed ratios do not vary too much throughout the month). If for that particular waterway a second reference station is required for some of the subordinate stations, then essentially two sets of tidal current charts will have to be produced, one set referred to each reference station (but they could perhaps be put on opposite facing pages in the finished product).

One must next decide which (one or two) key points on a tidal current curve one would like to use in the rotary analysis (the rotary analysis can handle both one or two key points). As was seen in Section 9.4.1, in the past different Tidal Current Charts used different key points on a tidal current curve, for example, the times of maximum flood, the times of maximum floods and ebbs, the slacks before flood and slacks before ebb, and even the high waters and/or low waters at a nearby tide gauge (which probably should only be used if there are absolutely no usable tidal current reference stations; see Section 6.9). The rotary reduction analysis has a tendency to reduce the values of maximum flood and maximum ebb if the individual maximums (from each tidal cycle) shift around in time. To minimize this effect it might be better to choose maximum flood (MF) and maximum ebb (ME) times at the reference station, as the way of breaking the subordinate time series into tidal-cycle-sections of the data time series that will be superimposed and averaged (in this case, the flood phase section around maximum flood and the ebb phase section around maximum ebb).

When using the rotary reduction analysis one usually divides these sections of data into half-hour intervals, but one will probably decide to use the analysis results for only the hour intervals when creating the actual tidal current charts. These charts might, for example, be for: MF-3, MF-2, MF-1, MF, MF+1, MF+2, MF+3, ME-3, ME-2, ME-1, ME, ME+1, ME+2, and ME+3, where perhaps only one of MF+3 or ME-3 might be used (or similarly only one of ME+3 or MF-3). The rotary analysis puts out mean results, and if one wants to have spring results depicted on the Tidal Current Charts,

9. Products for Presenting Tide and Tidal Current Predictions

one will have to adjust the analysis results accordingly (perhaps using the spring-to-mean relationship at the reference station), or one could selectively run the rotary analysis only for periods of time surrounding full moon and new moon.

9.4.3b Using Numerical Hydrodynamic Models

High-resolution numerical hydrodynamic models now can do a good job at representing tidal currents, as long as the resolution is high enough for the particular geographic and bathymetric situation in the waterways where the currents are being represented. Such models, after being fully calibrated and verified, can be forced with tide predictions at the waterway's entrance in order to carry out a tidal-only simulation. This simulation should be for at least a month, but could be run for an entire year, from which specific time periods to be analyzed could be extracted (e.g., perhaps all the time periods bracketing full and new moon). These simulations could then be analyzed using a rotary reduction in the same way as described in the previous section. One would have hundreds (even thousands) of locations to choose from, and those that seem most representative in depicting the tidal currents throughout the waterway would be chosen. However, a much less labor intensive (and probably more accurate) approach is to instead select a tidal-cycle-length time period within the year that is shown to be closest to what would be (e.g.) a mean spring situation, and then simply directly use the model output for that time period to create the Tidal Current Charts.

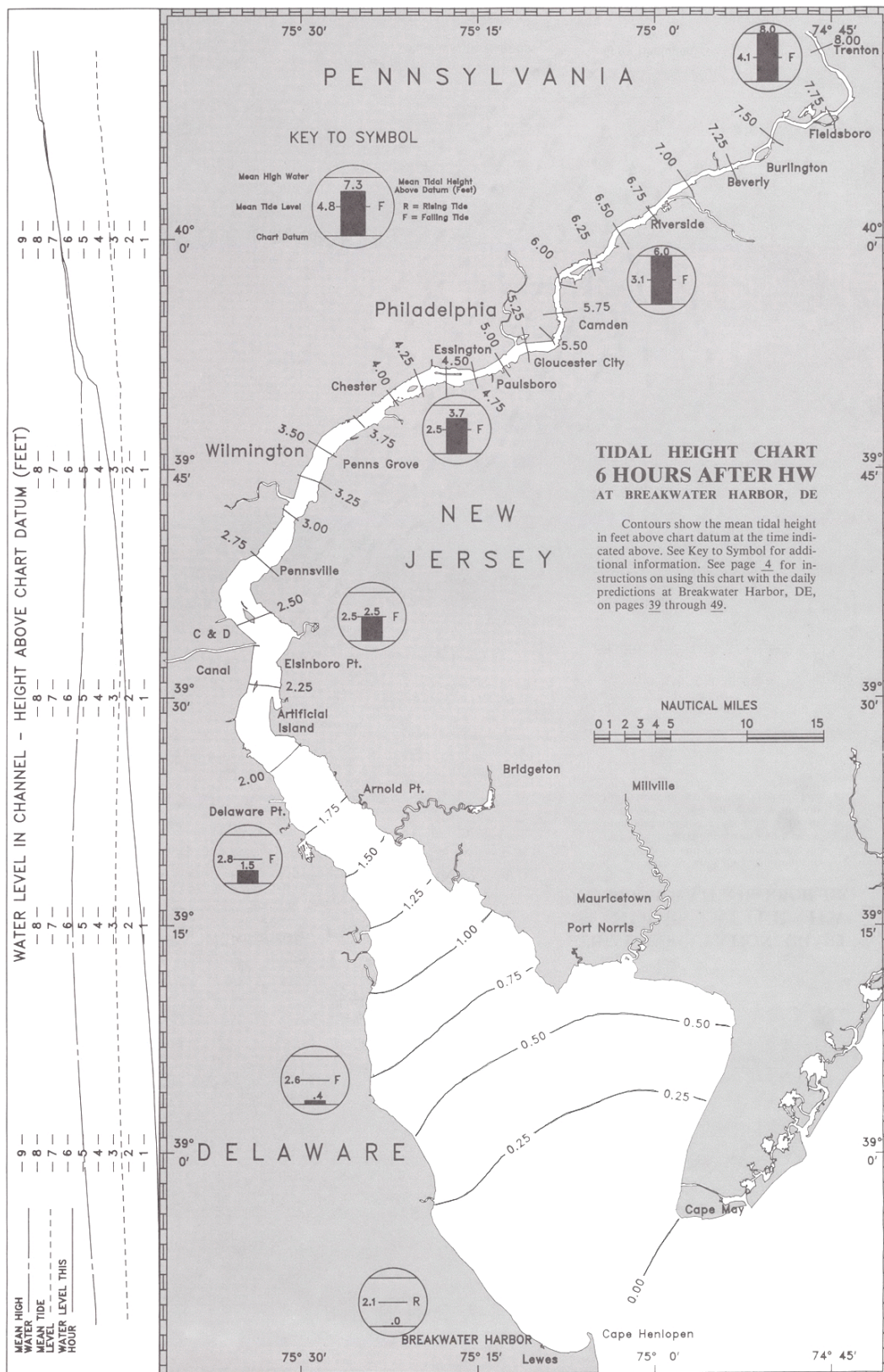
A calibrated and verified numerical hydrodynamic model was used by a predecessor organization of CO-OPS in the National Ocean Service in 1987 to produce the *Delaware River and Bay Tidal Circulation and Water Level Forecast Atlas*, which is described in Section 9.5.

To take this modeling approach a step further, one can use it to try to solve one of the primary limitations of the traditionally produced Tidal Current Charts, i.e., dealing with a mixed tidal current situation with a strong diurnal signal. One can select a tidal-cycle-length time period that represents a mean equatorial declination situation and another that represents a mean maximum declination situation (or one might need to have two maximum declination situations, one for northern declination and one for souther declination, if they have different effects). Something like this was, in fact, attempted for the very dynamically complex area of the Strait of Juan de Fuca-Strait of Georgia, which had a strong diurnal signal and much variance of diurnal-to-semidiurnal ratios and M_4/M_2 ratios due to lateral inertial effects (Crean, *et al.*, 1988; Huggett, 1988). But, because of that complexity, more than a hundred individual tidal current charts had to be produced to try to cover all possible dynamic situations.

9.5 *Tidal Circulation and Water Level Forecast Atlases*

The *Tidal Circulation and Water Level Forecast Atlas* was a new type of product for providing tide and tidal current predictions first published by the National Ocean Service in 1987 for the Delaware River and Bay (NOAA, 1987). Its basic design was similar to that of the Tidal Current Charts, but in addition to providing a tidal current chart for each hour of the tidal cycle, it also provided a tidal height chart for each hour of the cycle. (See Parker, 1988) (see Figures 9.10 and 9.11)

Tidal Analysis and Prediction



9. Products for Presenting Tide and Tidal Current Predictions

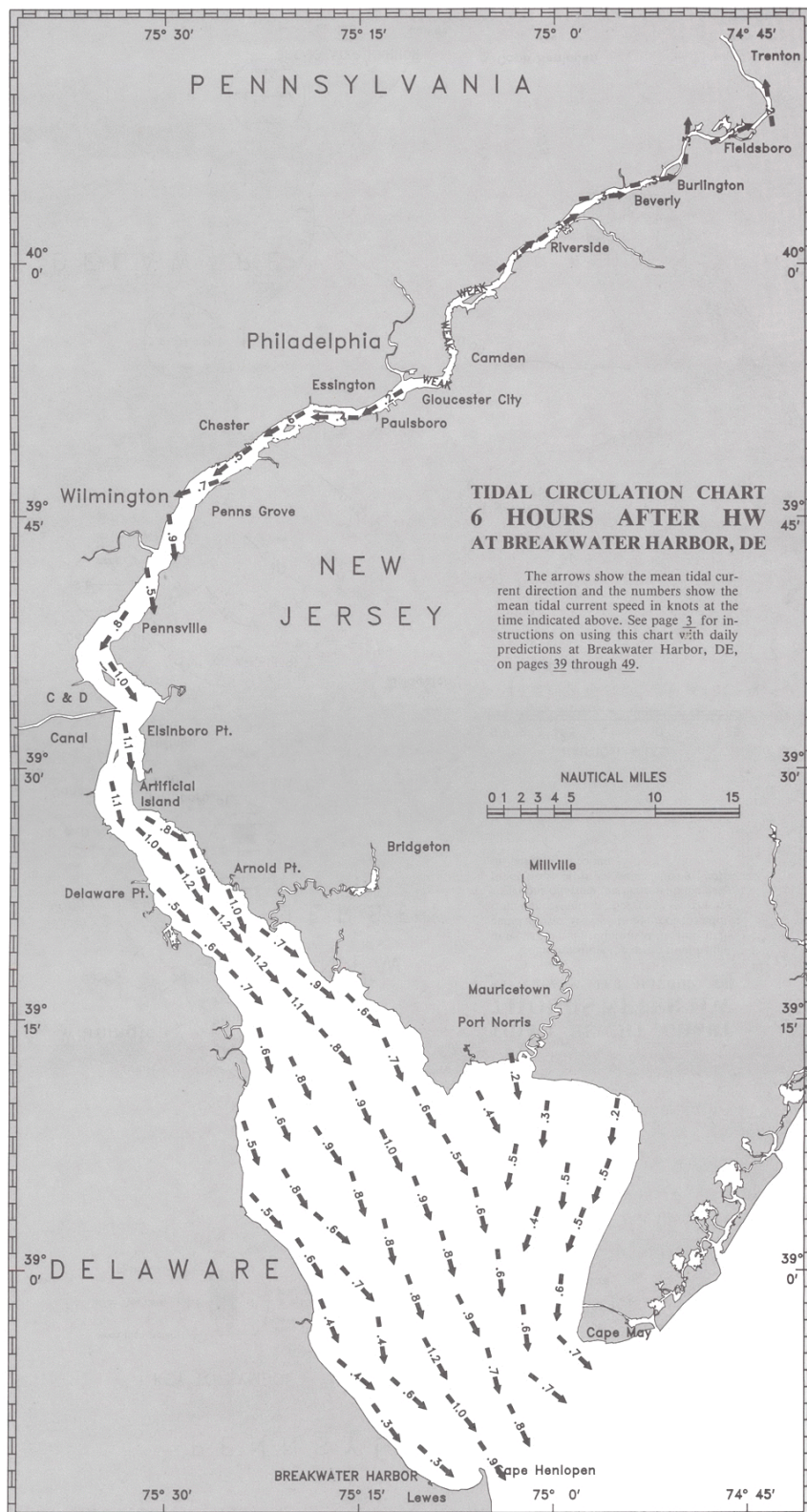


Figure 9.11. One of the hourly tidal circulation charts from the *Delaware River and Bay Tidal Circulation and Water Level Atlas*.

The same methods that allowed fairly easy prediction of the tidal current could now be used to predict tidal heights, with the same added benefit, namely, that one could more easily visualize the change in tidal heights over the entire waterway. This was done in three ways, using: (1) tidal height contours; (2) tide curves for the center of the entire length of the waterway, for mean high water, for mean tide level, and for the actual water level heights for that hour of the tidal cycle; and (3) symbols for a few key locations along the waterway that by means of a histogram showed the height for that hour of the tidal cycle relative to mean high water, mean tide level, and chart datum (i.e., mean lower low water).

A calibrated and verified numerical hydrodynamic model was used to produce the atlas (Patchen, 1986). With the hundreds of locations for which the model could predict tidal currents, one could produce tidal circulation charts with many more current vectors covering more of the waterway. With the hundreds of locations for which the model could predict tidal heights, one could produce detailed height contours for the entire waterway.

In addition to the tidal height charts and tidal circulation charts, the atlas also provided corange and cotidal charts for the tide, and coamplitude and cophase charts for the tidal currents, as well as a chart showing the bathymetry in the bay. The atlas also provided five years of daily predictions for the reference station, in this case Breakwater Harbor, Delaware, so that predictions could be made without having a separate Tide Table or Tidal Current Table.

9.6 *The Tide and Light Diagram – a bit of history*

A special type of product for providing tide predictions was devised in the Coast and Geodetic Survey during World War II. Tide predictions had always been important for navigating large ships out of shallow harbors at times of high water, but with the outbreak of World War II, tide predictions became extremely important for a truly life-or-death purpose – amphibious landings. Capturing enemy-held islands in the Pacific often meant knowing whether there was enough water covering treacherous coral reefs so that U.S. Marines could safely cross them and reach the beaches. In Europe the Allies often wanted to land near high tide to reduce the length of beach their soldiers would have to run across under fire (but actually a little before high tide so that a landing craft would have time to leave and not be left high and dry when the tide receded).

But often the stages of tide were not the only consideration. The day and time for landing would be selected based on the combination of a certain stage of the tide occurring at a particular time of the day (e.g., just after sunrise) after a night with a full moon or a new moon, or some other combination. The Coast and Geodetic Survey produced *Tide and Light Diagrams* for most islands in the Pacific and for North Africa (Zetler, 1991; Hicks, 1967).

An example of a Tide and Light Diagram (from Zetler, 1991) is shown in Figure 9.12 (this one was for October 1945 and so was never used). It depicted graphically for one month the daily times of high and low water, moonrise, moonset, sunrise, sunset, and various degrees of twilight. These top-secret diagrams, which were primarily conceived by Walter Zerbe, Chief of the Predictions Section at that time, and worked on also by Bernard Zetler, Chief of the Tides Section. The Tide and Light Diagram became the principal product produced by these Sections during the war, which grew to 25 people and eventually came under the Joint Army Navy Intelligence Service. Almost one thousand Tide and Light Diagrams were produced during the war for the Pacific and for North Africa. For security reasons many Diagrams were produced that the U.S. had no intention of using, while others were requested on very short notice.

Tidal Analysis and Prediction

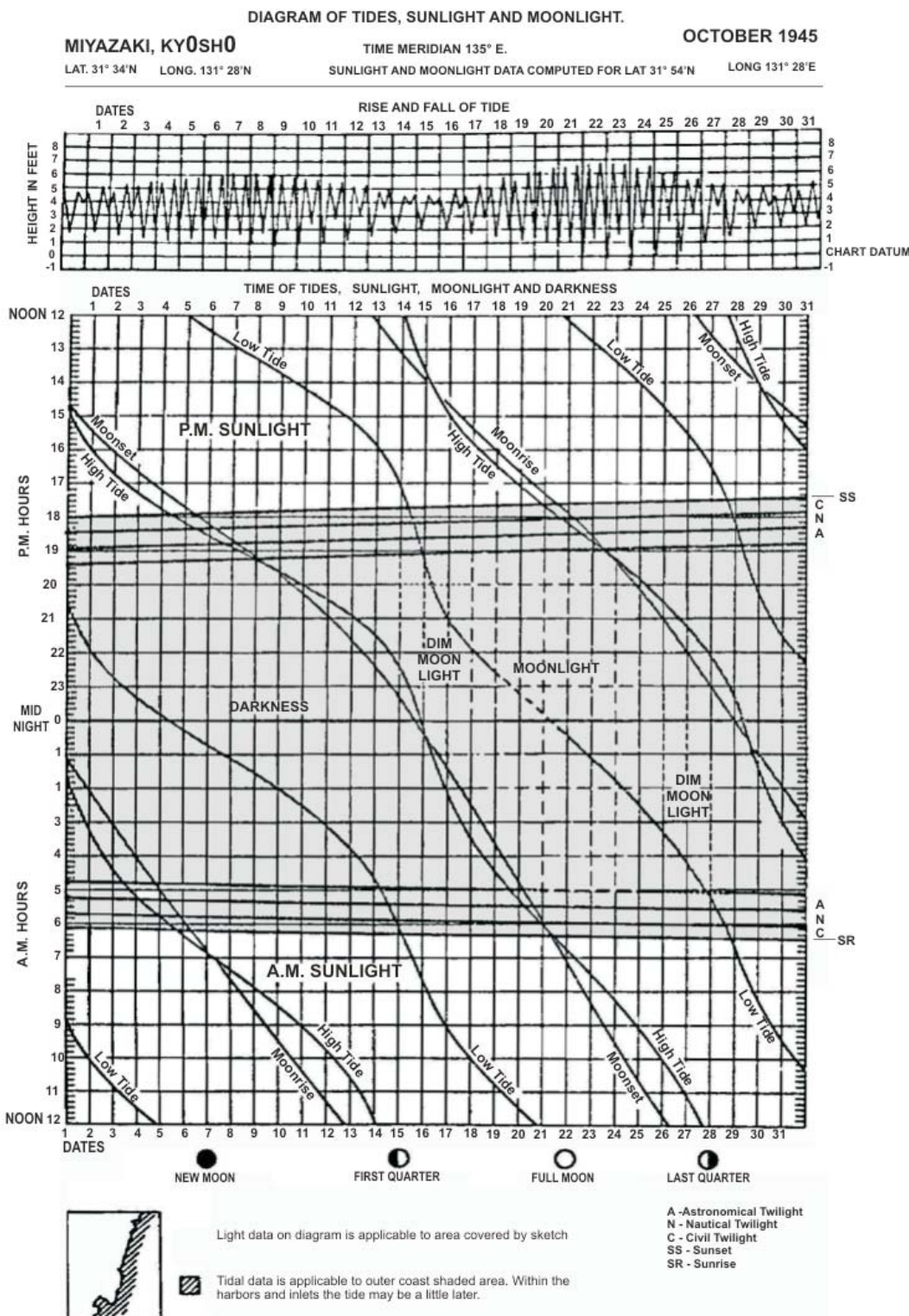


Figure 9.12. A Tide and Light Diagram produced during World War II to show the times of high and low water, along with the times of moonrise, moonset, sunrise, sunset, and various degrees of twilight. (From Zetler, 1991.)

9. Products for Presenting Tide and Tidal Current Predictions

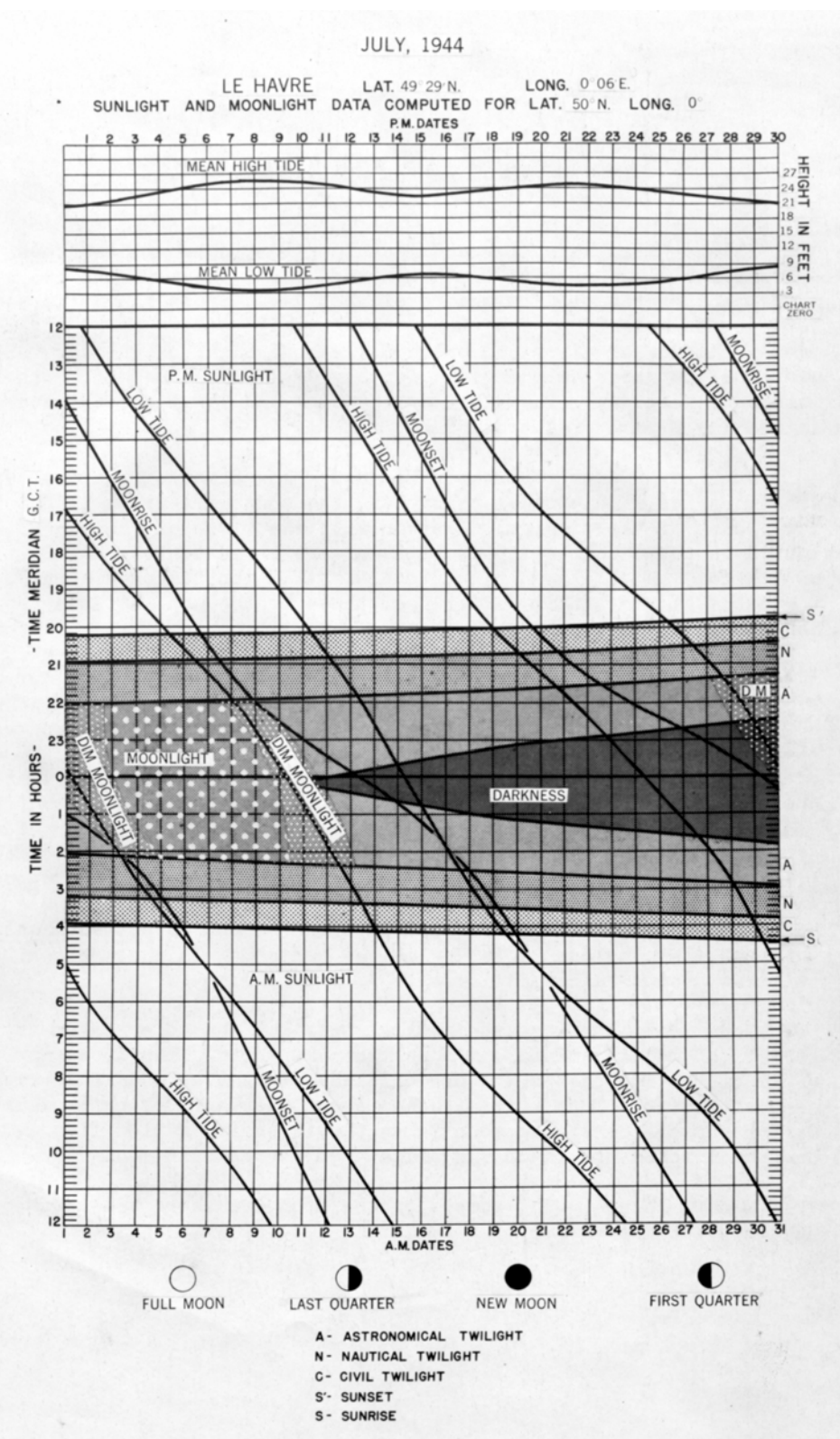


Figure 9.13a. A Tidal Illumination Diagram for LeHarve, France, for July 1944, produced from tide predictions calculated by the British for Allied forces.

9. Products for Presenting Tide and Tidal Current Predictions

In the upper portion of the Tide and Light Diagram (see Figure 9.12) there is a low-resolution tide curve for the particular month of the diagram, primarily to show the general tidal characteristics, such as days when there were spring tides or neap tides, or when the tide might become more diurnal or more semidiurnal. The majority of the diagram is devoted to a two-dimensional graphic on which exact daily times are provided for high water, low water, moonrise, moonset, sunrise, sunset, and various degrees of twilight (both morning and evening). Various degrees of darkness, which depended on the phase of the moon, were outlined by dotted overlays. Using all this information found on one sheet, military planners could select the best time during the month when both the tide and light conditions were optimum for a landing operation.

Similar diagrams, called *Tidal Illumination Diagrams*, were produced by the British for the Allies to use in Europe, including for the beaches of Normandy for the D-Day landings. Figure 9.13a shows a Tidal Illumination Diagram for LeHarve, France, a little east of Normandy, for July 1944. The explanation of the diagram, found on the back, is shown in Figure 9.13b. The actual tide predictions used in these diagrams were produced by Arthur Doodson at the Liverpool Observatory and Tidal Institute and provided to the Commander William Ian Farquharson, the Superintendent of Tides at the Hydrographic Department of the Admiralty in Bath.

Explanation of Diagram

Tides.--Mean high tide and mean low tide, shown in the upper part of the diagram, give the heights of the average of the two high waters and of the two low waters of each day. Since the difference between the heights of the two successive high waters is relatively small, the height given can be used for both highs of the day. Likewise the low water height given for any day can be used for both low waters of that day. The times of the high and low tides are shown in the lower part of the diagram.

Sunrise, Sunset, Moonrise, Moonset.--The times of sunrise, sunset, moonrise, and moonset throughout the month are given in the lower part of the diagram, together with the times of the tide. It should be noted that all p.m. times are referred to P.M. DATES (top of diagram) and all a.m. times to A.M. DATES (bottom of diagram). The dates at the bottom differ from those at the top, because the date changes in passing through midnight.

Solar Twilight.--Distinction is made between 3 types of twilight. Civil twilight starts at sunset and ends when the sun is 6° below the horizon. Objects can be readily distinguished and a newspaper can be read. At the end of civil twilight, the brightness of the sky is about 20 times as great as when the full moon is at the zenith. Civil twilight is followed by nautical twilight which ends when the sun is 12° below the horizon. All the brighter stars are visible, general outlines can be distinguished, but the horizon will usually be indistinct. The end of nautical twilight may appear to be the beginning of solar darkness, but some light from the sun may still be refracted or reflected until the end of astronomical twilight when the sun is 18° below the horizon. In the morning the twilights occur in reverse order.

Moonlight.--During astronomical twilight and solar darkness, periods of moonlight and dim moonlight are shown. The intensity of light, during the period of moonlight, varies between the brightness of the full moon at zenith and about one-third of this value. During the period of dim moonlight, the intensity varies from about one-third to one-tenth of the brightness during full moon.

Moon's Phases.--The phases of the moon are shown below the day on which they occur.

Figure 9.13b. The “Explanation of Diagram” found on the back of the Tidal Illumination Diagram in Figure 9.13a.

9.7 Digital Tidal Prediction Products

In Sections 9.2.5 and 9.3.6 we looked at the two primary limitations of the standard hardcopy/paper tidal prediction products, the Tide Tables and Tidal Current Tables.

The first limitation is that nonharmonic comparison methods have to be used for thousands of subordinate stations in Table 2, because it would take far too many pages to include them as harmonically predicted reference stations. (A reference station takes four pages in Table 1, while a subordinate station takes one line of 60 lines on one page in Table 2.) As was seen in Sections 3.6.3 and 6.9, the use of nonharmonic comparison analyses can cause prediction errors if the reference station does not have tidal characteristics similar enough to the secondary station (which is most likely to happen in waterways with mixed tides or tidal currents and a strong diurnal signal). These errors oscillate throughout the month, usually being worse near times of maximum lunar declination. If this occurs, one solution is to add an additional reference station to the Tide or Tidal Current Table, one that is closer to the subordinate stations and has more similar tidal characteristics. But for some areas with complex hydrodynamics there is so much variation in diurnal-to-semidiurnal ratios in the area, that dozens of new tidal current reference stations would have to be created to handle the situation.

The second limitation is that only high and low waters predictions are presented in Tide Tables and only predictions of slacks and maximum floods and ebbs are presented in the Tidal Current Tables. For predictions at other times (between these key points) the user is forced to use a cosine-based interpolation scheme. Such an interpolation scheme only works well for deep-water stations. It does not work well for stations in bays and estuaries and rivers where nonlinear shallow-water effects distort the tide or tidal current curve away from a pure cosine shape. It is especially bad for tidal currents since most are rotary to some degree and the Tidal Current Tables do not show this rotation in Table 1 or Table 2.

Both these problems can be solved by producing *digital tidal predictions products* where all the stations are predicted harmonically, which eliminates the need for Table 2-like time and height differences and speed ratios. It also allows prediction of the entire tide or tidal current curve for every station, showing all rotations of direction for tidal currents, as well as the distortions in the tide and tidal current by nonlinear shallow water and lateral inertial effects (so that no cosine-based interpolation is needed). Such digital products, whether provided to the user on CDs for use on their home computer or provided via a special Website on the World Wide Web, provide more accurate harmonically-based predictions for all locations and times, using a variety of graphical outputs. If one still wants hardcopy, one can print out a detailed tide or tidal current curve for the particular place and time of interest, or even special tidal current charts for a specific day. Predictions from such harmonically-based products are much easier to use than Tide or Tidal Current tables or even Tidal Current Charts; they would require no calculations or corrections by the mariner. Such products can also provide additional useful features such as providing predicted values directly on charts on the screen, as animated results (such as current vectors changing over time), and even Lagrangian drift calculations (in areas with enough density of current stations).

To produce a digital tidal prediction product, one needs harmonic constants for all water level and current stations. For most tide stations in the Tide Tables this is not be a problem, because most usually have long enough time series for adequate harmonic analyses (and most already have calculated harmonic constants). However, most current stations in the Tidal Current Tables have short data time series, so producing a digital tidal prediction product can mean the expense of installing new current sensors for periods of at least a month (although for many of these stations,

9. Products for Presenting Tide and Tidal Current Predictions

one might be able to infer some of the harmonic constants). One alternative to this is to produce long time series of predicted tidal currents using an accurately calibrated and verified high-resolution three-dimensional numerical hydrodynamic model forced with accurate tide predictions at the entrance (see Chapter 8). Then selected current time series for all locations of interest (to be included in the digital tidal prediction product) could be harmonically analyzed.

CO-OPS is, in fact, moving towards electronically delivering harmonically based tidal predictions for many more locations than just the standard reference stations in the Tide and Tidal Current Tables. Other nations and private companies are also developing new ways to conveniently present digital tide and tidal current predictions.

Appendix

Table A.1. 149 tidal constituents in order of increasing frequency.

Table A.2. 149 tidal constituents in order of increasing synodic period.

See explanation in the detailed key following the second Table.

Table A.1 Tidal Constituents In Order of Increasing Frequency

Tidal Harmonic Constituent	Origin of Constituent	Cartwright (Doodson) Number	Shallow-water equivalent	Nonlinear mechanism, sym or asym	Angular Speed (o/hour)	Freq. (cpd)	Period (hours)	Synodic Period	wrt Const. (name)	Cartwright Potential
Sa	solar (*met)	0 0 1 0 0 0			0.0410686	0.0027	8765.8211	365.2	Ssa	0.01156
Ssa	solar (*met)	0 0 2 0 0 0			0.0821373	0.0055	4382.9052	365.2	Sa	0.07281
Msm		0 1 -2 1 0 0			0.4715521	0.0314	763.4364	206.0	Mn	0.01579
Mm	lunar (*met)	0 1 0 -1 0 0	MN	asym	0.5443747	0.0363	661.3092	31.8	MSF	0.08254
MSf	lunar	0 2 -2 0 0 0	MS	asym	1.0158958	0.0677	354.3671	182.6	Mf	0.01369
Mf	lunar	0 2 0 0 0 0	KO	asym	1.0980331	0.0732	327.8590	182.6	MSf	0.15647
α_1		1 -4 2 1 0 0			12.3827652	0.8255	29.0727	1.3	Mf	0.00278
2Q ₁	lunar	1 -3 0 2 0 0			12.8542862	0.8570	28.0062	13.8	O ₁	0.00955
σ_1	lunar	1 -3 2 0 0 0			12.9271398	0.8618	27.8484	14.8	Q ₁	0.01152
Q ₁	lunar	1 -2 0 1 0 0	NK ₁	asym	13.3986609	0.8932	26.8684	27.6	O ₁	0.07217
p ₁	lunar	1 -2 2 -1 0 0			13.4715145	0.8981	26.7231	205.9	Q ₁	0.01371
O ₁	lunar	1 -1 0 0 0 0	MK ₁	asym	13.9430356	0.9295	25.8193	13.7	K ₁	0.37694
τ_1	lunar	1 -1 2 0 0 0	MP ₁	asym	14.0251729	0.9350	25.6681	23.9	Q ₁	-0.00493
β_1		1 0 -2 1 0 0			14.4145548	0.9610	24.9748	193.6	M ₁	-0.00278
M ₁	luni-solar	1 0 0 1 0 0	NO ₁	asym	14.4920521	0.9661	24.8412	27.3	K ₁	0.02964
χ_1	lunar	1 0 2 -1 0 0			14.5695476	0.9713	24.7091	193.6	M ₁	-0.00567
π_1	solar	1 1 -3 0 0 1	TK ₁	asym	14.9178647	0.9945	24.1321	365.3	P ₁	0.01023
P ₁	lunar	1 1 -2 0 0 0	SK ₁	asym	14.9589314	0.9973	24.0659	182.6	K ₁	0.17543
S ₁	solar (*met)	1 1 -1 0 0 0			15.0000000	1.0000	24.0000	365.2	K ₁	0.00416
K ₁	luni-solar	1 1 0 0 0 0	MO ₁	asym	15.0410686	1.0027	23.9345	1.1	M ₂	0.53011
Ψ_1	solar	1 1 1 0 -1 0	RP ₁	asym	15.0821353	1.0055	23.8693	365.2	Φ_1	-0.00422
φ_1	solar	1 1 2 0 0 0	2KP ₁	sym	15.1232058	1.0082	23.8045	182.6	K ₁	-0.00756
θ_1	lunar	1 2 -2 1 0 0			15.5125897	1.0342	23.2070	205.9	J ₁	-0.00567
J ₁	lunar	1 2 0 -1 0 0	MQ ₁	asym	15.5854433	1.0390	23.0985	27.6	K ₁	-0.02964
2PO ₁	shallow water		2PO ₁	sym	15.9748272	1.0650	22.5355	38.5	J ₁	
SO ₁	lunar	-1 3 -2 0 0 0	SO ₁	asym	16.0569644	1.0705	22.4202	182.6	2PO ₁	-0.00492
OO ₁	lunar	1 3 0 0 0 0	2KO ₁	sym	16.1391017	1.0759	22.3061	13.7	K ₁	-0.01624

v_1		1 4 0 -1 0 0		16,6834764	1.1122	21.5782	27.6	00,	-0.00078
2MNS ₂	shallow water		2MNS ₂		26,4079379	1.7605	13,6323	31.8	2NS ₂
2NS ₂	shallow water		2NS ₂	sym	26,8794590	1.7920	13,3931	14.8	2N ₂
3M2S ₂	shallow water		3M2S ₂		26,9523126	1.7968	13,3569	205.9	2NS ₂
2NK2S ₂	shallow water		2NK2S ₂		26,9615963	1.7974	13,3523	1615.7	3M2S ₂
OQ ₂	shallow water		OQ ₂	asym	27,3416965	1.8228	13,1667	182.6	ε_2
ε_2		2 -3 2 1 0 0	MNS ₂		27,4238337	1.8283	13,1273	31.8	2N ₂
MNK2S ₂	shallow water		MNK2S ₂		27,5059710	1.8337	13,0881	182.6	ε_2
2MS2K ₂	shallow water		2MS2K ₂		27,8039338	1.8536	12,9478	182.6	O ₂
O ₂	shallow water		O ₂	asym	27,8860712	1.8591	12,9097	1615.8	2N ₂
2N ₂	lunar	2 -2 0 2 0 0	2NM ₂	sym	27,8953548	1.8597	12,9054	205.9	μ_2
μ_2	lunar	2 -2 2 0 0 0	2MS ₂	sym	27,9682084	1.8645	12,8718	31.8	N2
N ₂	lunar	2 -1 0 1 0 0			28,4397295	1.8960	12,6583	27.6	M2
ν_2	lunar	2 -1 2 -1 0 0			28,5125831	1.9008	12,6260	205.9	N2
MKL2S ₂	shallow water		MKL2S ₂		28,5947204	1.9063	12,5897	182.6	ν_2
2KN2S ₂	shallow water		2KN2S ₂		28,6040041	1.9069	12,5857	164.1	v2
OP ₂	shallow water		OP ₂	asym	28,9019669	1.9268	12,4559	38.5	ν_2
Γ_2		2 0 -2 2 0 0			28,9112508	1.9274	12,4519	205.9	M ₂
α_2		2 0 -1 0 1 0	SO ₂	asym	28,9430356	1.9295	12,4382	365.2	M ₂
M ₂	lunar	2 0 0 0 0 0	KO ₂	asym	28,9841042	1.9323	12,4206	---	***
MKS ₂	shallow water		MKS ₂		29,0662415	1.9377	12,3855	182.6	M ₂
δ_2	lunar	2 0 2 0 0 0	M2(KS) ₂		29,1483788	1.9432	12,3506	91.3	M ₂
2SN(MK) ₂	shallow water		2SN(MK) ₂		29,3734880	1.9582	12,2559	182.6	λ_2
λ_2	lunar	2 1 -2 1 0 0			29,4556253	1.9637	12,2218	205.9	-0.00273
L ₂	lunar	2 1 0 -1 0 0	2MN ₂	sym	29,5284789	1.9686	12,1916	31.8	S ₂
2SK ₂	shallow water		2SK ₂	sym	29,9178627	1.9945	12,0329	38.5	L ₂
T ₂	solar	2 2 -3 0 0 1			29,9589333	1.9973	12,0164	365.3	S ₂
S ₂	solar	2 2 -2 0 0 0	KP ₂	asym	30,0000000	2.0000	12,0000	14.8	M ₂
R ₂	solar	2 2 -1 0 0 -1	SK ₂	asym	30,0410667	2.0027	11,9836	365.3	S ₂
K ₂	luni-solar	2 2 0 0 0 0			30,0821373	2.0055	11,9672	182.6	S ₂
MSN ₂	shallow water		MSN ₂		30,5443747	2.0363	11,7861	32.5	K ₂
ζ_2		2 3 -2 1 0 0			30,5536572	2.0369	11,7826	205.9	η_2
η_2	lunar	2 3 0 -1 0 0	KL ₂	asym	30,6265119	2.0418	11,7545	27.6	K ₂
									0.00643

$2\text{MK}_s/3\text{MO}_s$	shallow water		$2\text{MK}_s/3\text{MO}_s$	sym	73.0092770	4.8673	4.9309	1.1	M_6
MSK_s	shallow water		MSK_s		74.0251728	4.9350	4.8632	14.8	2MK_s
3KM_s	shallow water		3KM_s		74.1073100	4.9405	4.8578	182.6	MSK_s
N_6	shallow water		N_6	sym	85.3191885	5.6879	4.2194	205.9	3MNS_6
3MNS_6	shallow water		3MNS_6		85.3920421	5.6928	4.2158	1615.7	3NKS_6
3NKS_6	shallow water		3NKS_6		85.4013258	5.6934	4.2154	32.5	2NM_6
2NM_6	shallow water		2NM_6	sym	85.8635632	5.7242	4.1927	205.9	4MS_6
4MS_6	shallow water		4MS_6	sym	85.9364168	5.7291	4.1891	14.8	M_6
2NMKS_6	shallow water		2NMKS_6		85.9457005	5.7297	4.1887	1615.7	4MS_6
2MN_6	shallow water		2MN_6	sym	86.4079380	5.7605	4.1663	27.6	M_6
2Mv_6	shallow water		2Mv_6	sym	86.4807916	5.7654	4.1628	205.9	2MN_6
2MNKS_6	shallow water		2MNKS_6		86.4900752	5.7660	4.1623	32.5	M_6
M_6	shallow water		M_6	sym	86.9523127	5.7968	4.1402	0.5	M_4
MSN_6	shallow water		MSN_6		87.4238337	5.8283	4.1179	205.9	4MN_6
4MN_6	shallow water		4MN_6		87.4966873	5.8331	4.1144	27.6	M_6
MKN_6	shallow water		MKN_6		87.5059710	5.8337	4.1140	1615.7	4MN_6
2MS_6	shallow water		2MS_6	sym	87.9682084	5.8645	4.0924	14.8	M_6
2MK_6	shallow water		2MK_6		88.0503457	5.8700	4.0886	182.6	2MS_6
3MSN_6	shallow water		3MSN_6		88.5125831	5.9008	4.0672	32.5	2MK_6
NSK_6	shallow water		NSK_6		88.5218668	5.9015	4.0668	32.5	2SM_6
2SM_6	shallow water		2SM_6	sym	88.9841042	5.9323	4.0457	7.4	M_6
MSK_6	shallow water		MSK_6		89.0662415	5.9377	4.0419	7.1	M_6
S_6	shallow water		S_6	sym	90.0000000	6.0000	4.0000	4.9	M_6
4MP_7	shallow water		4MP_7	sym	100.9774854	6.7318	3.5652	182.6	4MK_7
$4\text{MK}_7/3\text{MO}_7$	shallow water		$4\text{MK}_7/3\text{MO}_7$	sym	100.8953500	6.7264	3.5681	1.1	M_6
$4\text{MO}_7/3\text{MK}_7$	shallow water		$4\text{MO}_7/3\text{MK}_7$	sym	101.9933600	6.7996	3.5296	13.7	4MK_7
4MJ_7	shallow water		4MJ_7	sym	100.3509735	6.6901	3.5874	9.1	4MO_7
2MNK_7	shallow water		2MNK_7		100.9046318	6.7270	3.5677	27.1	4MJ_7
4Mt_7	shallow water		4Mt_7	sym	101.9112440	6.7941	3.5325	14.9	2MNK_7
$4\text{M}\sigma_7$	shallow water		$4\text{M}\sigma_7$	sym	103.0092771	6.8673	3.4948	13.7	4MTAU_7
$2(\text{MN})_8$	shallow water		$2(\text{MN})_8$		114.8476674	7.6565	3.1346	27.6	3MN_8
3MN_8	shallow water		3MN_8		115.3920422	7.6928	3.1198	27.6	M_8

3MNKS ₈	shallow water		3MNKS ₈		115.4741794	7.6983	3.1176	182.6	3MN ₈
M ₈	shallow water	M ₈	both	115.9364169	7.7291	3.1052	0.5	M ₆	
2MSN ₈	shallow water	2MSN ₈		116.4079380	7.7605	3.0926	182.6	2MNK ₈	
2MNK ₈	shallow water	2MNK ₈		116.4900752	7.7660	3.0904	32.5	3MS ₈	
3MS ₈	shallow water	3MS ₈		116.9523127	7.7968	3.0782	14.8	M ₈	
3MK ₈	shallow water	3MK ₈		117.0344500	7.8023	3.0760	182.6	3MS ₈	
MSNK ₈	shallow water	MSNK ₈		117.5059710	7.8337	3.0637	31.8	3MK ₈	
2(MS) ₈	shallow water	2(MS) ₈		117.9682084	7.8645	3.0517	14.8	3MS ₈	
2MSK ₈	shallow water	2MSK ₈		118.0503457	7.8700	3.0495	182.6	2(MS) ₈	
2M2NK ₉	shallow water	2M2NK ₉		129.8887360	8.6592	2.7716	13.8	4MK ₉	
3MNK ₉	shallow water	3MNK ₉		130.4331108	8.6955	2.7600	27.6	4MK ₉	
4MK ₉	shallow water	4MK ₉		130.9774855	8.7318	2.7486	1.0	M ₈	
3MSK ₉	shallow water	3MSK ₉		131.9933813	8.7996	2.7274	14.8	4MK ₉	
4MN ₁₀	shallow water	4MN ₁₀		144.3761464	9.6251	2.4935	27.6	M ₁₀	
M ₁₀	shallow water	M ₁₀		144.9205211	9.6614	2.4841	0.5	M ₈	
3MNS ₁₀	shallow water	3MNS ₁₀		145.3920422	9.6928	2.4761	27.6	4MS ₁₀	
4MS ₁₀	shallow water	4MS ₁₀		145.9364169	9.7291	2.4668	14.8	M ₁₀	
2MNNSK ₁₀	shallow water	2MNNSK ₁₀		146.4900752	9.7660	2.4575	27.1	4MS ₁₀	
3M2S ₁₀	shallow water	3M2S ₁₀		146.9523127	9.7968	2.4498	32.5	2MNSK ₁	
4MSK ₁₁	shallow water	4MSK ₁₁		160.9774855	10.7318	2.2363	0	M ₁₀	
4MNS ₁₂	shallow water	4MNS ₁₂		174.3761464	11.6251	2.0645	27.6	5MS ₁₂	
5MS ₁₂	shallow water	5MS ₁₂		174.9205211	11.6614	2.0581	0.5	M ₁₀	
3MNKS ₁₂	shallow water	3MNKS ₁₂		175.4741794	11.6983	2.0516	32.5	4M2S ₁₂	
4M2S ₁₂	shallow water	4M2S ₁₂		175.9364169	11.7291	2.0462	14.8	5MS ₁₂	

Table A.2 Tidal Constituents In Order of Increasing Synodic Period

Tidal Harmonic Constituent	Origin of Constituent	Cartwright (Doodson) Number	Shallow-water equivalent	Nonlinear mechanism, sym or asym	Angular Speed (o/hour)	Freq. (cpd)	Period (hours)	Synodic Period (name)	wrt Const. (name)	Cartwright Potential	
M_2	lunar	2	0	0	0	KO ₂	asym	28.9841042	1.9323	12.4206 ***	
M_4	shallow water			M ₄	asym	57.9682084	3.8645	6.2103	0.5	M ₂	
M_6	shallow water			M ₆	sym	86.9523127	5.7968	4.1402	0.5	M ₄	
M_8	shallow water			M ₈	both	115.9364169	7.7291	3.1052	0.5	M ₆	
M_{10}	shallow water			M ₁₀		144.9205211	9.6614	2.4841	0.5	M ₈	
$5MS_{12}$	shallow water			5MS ₁₂		174.9205211	11.6614	2.0581	0.5	M ₁₀	
$4MSK_{11}$	shallow water			4MSK ₁₁		160.9774855	10.7318	2.2363	0.9	M ₁₀	
K_1	lumi-solar	1	1	0	0	MO ₁	asym	15.0410686	1.0027	23.9345	
$4MK_9$	shallow water			4MK ₉		130.9774855	8.7318	2.7486	1.0	M ₈	
$2MK_s/3MO_5$	shallow water			2MK _s /3MO ₅	sym	73.0092770	4.8673	4.9309	1.1	M ₆	
$4MK_7/3MO_7$	shallow water			4MK ₇ /3MO ₇	sym	100.8953500	6.7264	3.5681	1.1	M ₆	
α_+		1	-4	2	1	0	0	12.3827652	0.8255	29.0727	
S_6	shallow water			S ₆	sym	90.0000000	6.0000	4.0000	4.9	M ₆	
MSK_6	shallow water			MSK ₆		89.0662415	5.9377	4.0419	7.1	M ₆	
$2SM_6$	shallow water			2SM ₆	sym	88.9841042	5.9323	4.0457	7.4	M ₆	
$4M\zeta_2$	shallow water			4M\zeta ₂	sym	100.3509735	6.6901	3.5874	9.1	4MO ₂	
O_1	lunar	1	-1	0	0	MK ₁	asym	13.9430356	0.9295	25.8193	
OO_1	lunar	1	3	0	0	2KO ₁	sym	16.1391017	1.0759	22.3061	
$2Q_1$	lunar	1	-3	0	2	0	0	12.8542862	0.8570	28.0062	
$2MK_3(MO_3)$	shallow water			2MK ₃ (MO ₃)	sym (asym)	42.9271398	2.8618	8.3863	13.7	K ₁	
$MK_3(2MO_3)$	shallow water			MK ₃ (2MO ₃)	asym (sym)	44.0251729	2.9350	8.1771	13.7	2MK ₃	
$2MO_s/3MO_5$	shallow water			2MO _s /3MO ₅	sym	71.9112440	4.7941	5.0062	13.7	2MK _s	
$4MO_7/3MK_7$	shallow water			4MO ₇ /3MK ₇	sym	101.9933600	6.7996	3.5296	13.7	4MK ₇	
$4M\sigma_7$	shallow water			4M\sigma ₇	sym	103.0092771	6.8673	3.4948	13.7	4MTAU ₇	
$2M2NK_o$	shallow water			2M2NK _o		129.8887360	8.6592	2.7716	13.8	4MK _o	
S_2	solar	2	2	-2	0	0	KP ₂	asym	30.0000000	2.0000	12.0000
$2SM_2$	shallow water			2SM ₂	sym	31.0158958	2.0677	11.6070	14.8	S ₂	

3MSK ₉	shallow water			3MSK ₉		131.9933813	8.7996	2.7274	14.8	4MK ₉
3MS ₈	shallow water			3MS ₈		116.9523127	7.7968	3.0782	14.8	M ₈
2NS ₂	shallow water			2NS ₂	sym	26.8794590	1.7920	13.3931	14.8	2N ₂
4MS ₆	shallow water			4MS ₆	sym	85.9364168	5.7291	4.1891	14.8	M ₆
S ₄	shallow water			S ₄	asym	60.0000000	4.0000	6.0000	14.8	MS ₄
MSK ₅	shallow water			MSK ₅		74.0251728	4.9350	4.8632	14.8	2MK ₅
MS ₄	shallow water			MS ₄	asym	58.9841042	3.9323	6.1033	14.8	M ₄
σ_1	lunar	1	-3	2	0	0	12.9271398	0.8618	27.8484	14.8
4MS ₁₀	shallow water			4MS ₁₀		145.9364169	9.7291	2.4668	14.8	M ₁₀
2MS ₆	shallow water			2MS ₆	sym	87.9682084	5.8645	4.0924	14.8	M ₆
2(MS) ₈	shallow water			2(MS) ₈		117.9682084	7.8645	3.0517	14.8	3MS ₈
4M τ_7	shallow water			4M τ_7	sym	101.9112440	6.7941	3.5325	14.9	2MNK ₇
4M2S ₁₂	shallow water			4M2S ₁₂		175.9364169	11.7291	2.0462	14.8	5MS ₁₂
SP ₃	shallow water			SP ₃	sym	44.9589314	2.9973	8.0073	16.1	MK ₃
τ_1	lunar	1	-1	2	0	0	MP ₁			O ₁
M ₁	luni-solar	1	0	0	1	0	NO ₁			-0.00493
M ₃	lunar	3	0	0	0	0				
2MNSK ₁₀	shallow water			2MNSK ₁₀		146.4900752	9.7660	2.4575	27.1	4MS ₁₀
2MNK ₇	shallow water			2MNK ₇		100.9046318	6.7270	3.5677	27.1	4MN ₇
MO ₄ /3MK ₄	shallow water			MO ₄ /3MK ₄		56.8701754	3.7913	6.3302	27.1	MN ₄
N ₂	lunar	2	-1	0	1	0				
J ₁	lunar	1	2	0	-1	0	MQ ₁			
Q ₁	lunar	1	-2	0	1	0	NK ₁			
MNK ₅	shallow water			MNK ₅		72.4649023	4.8310	4.9679	27.6	2MK ₅
MNO ₅	shallow water			MNO ₅		71.3668693	4.7578	5.0444	27.6	2MO ₅
3MNS ₁₀	shallow water			3MNS ₁₀		145.3920422	9.6928	2.4761	27.6	4MS ₁₀
2MN ₆	shallow water			2MN ₆	sym	86.4079380	5.7605	4.1663	27.6	M ₆
MN ₄	shallow water			MN ₄	asym	57.4238337	3.8283	6.2692	27.6	M ₄
4MN ₆	shallow water			4MN ₆		87.4966873	5.8331	4.1144	27.6	M ₆
4MN ₁₀	shallow water			4MN ₁₀		144.3761464	9.6251	2.4935	27.6	M ₁₀
NO ₄	shallow water			NO ₄		56.3258007	3.7551	6.3914	27.6	MO ₄
2(MN) ₈	shallow water			2(MN) ₈		114.8476674	7.6565	3.1346	27.6	3MN ₈
η_2	lunar	2	3	0	-1	0	KJ ₂			0.00643

4MNS ₁₂	shallow water				4MNS ₁₂			174.3761464	11.6251	2.0645	27.6	5MS ₁₂			
v ₁		1	4	0	-1	0	0		16.6834764	1.1122	21.5782	27.6	OO ₁	-0.00078	
3MN ₈	shallow water			3MN ₈				115.3920422	7.6928	3.1198	27.6	M ₈			
3MNK ₉	shallow water			3MNK ₉				130.4331108	8.6955	2.7600	27.6	4MK ₉			
NO ₂	shallow water			NO ₂		sym		42.3827651	2.8255	8.4940	27.6	2MK ₃			
L ₂	lunar	2	1	0	-1	0	0	2MN ₂	sym	29.5284789	1.9686	12.1916	31.8	S ₂	-0.02567
l ₂	lunar	2	-2	2	0	0	0	2MS ₂	sym	27.9682084	1.8645	12.8718	31.8	N2	0.02776
Mm	lunar (*met)	0	1	0	-1	0	0	MN	asym	0.5443747	0.0363	661.3092	31.8	MSF	0.08254
2MNS ₂	shallow water			2MNS ₂				26.4079379	1.7605	13.6323	31.8	2NS ₂			
3MS ₄	shallow water			3MS ₄				56.9523127	3.7968	6.3211	31.8	MN ₄			
MSNK ₈	shallow water			MSNK ₈				117.5059710	7.8337	3.0637	31.8	3MK ₈			
ε ₂		2	-3	2	1	0	0	MNS ₂		27.4238337	1.8283	13.1273	31.8	2N ₂	0.00671
SN ₄	shallow water			SN ₄		asym		58.4397295	3.8960	6.1602	31.8	M ₄			
MSN ₂	shallow water			MSN ₂				30.5443747	2.0363	11.7861	32.5	K ₂			
3MNKS ₁₂	shallow water			3MNKS ₁₂				175.4741794	11.6983	2.0516	32.5	4M2S ₁₂			
2MNKS ₆	shallow water			2MNKS ₆				86.4900752	5.7660	4.1623	32.5	M ₆			
3M2S ₁₀	shallow water			3M2S ₁₀				146.9523127	9.7968	2.4498	32.5	2MNSK ₁₀			
3NKS ₆	shallow water			3NKS ₆				85.4013258	5.6934	4.2154	32.5	2NM ₆			
3MSN ₆	shallow water			3MSN ₆				88.5125831	5.9008	4.0672	32.5	2MK ₆			
SL ₄	shallow water			SL ₄		asym		59.5284789	3.9686	6.0475	32.5	MK ₄			
2NP ₃	shallow water			2NP ₃		sym		41.9205276	2.7947	8.5877	32.5	NO ₃			
NSK ₆	shallow water			NSK ₆				88.5218668	5.9015	4.0668	32.5	2SM ₆			
2MNK ₈	shallow water			2MNK ₈				116.4900752	7.7660	3.0904	32.5	3MS ₈			
KN ₄	shallow water			KN ₄				58.5218668	3.9015	6.1515	32.5	MS ₄			
OP ₂	shallow water			OP ₂		asym		28.9019669	1.9268	12.4559	38.5	v ₂			
2SK ₂	shallow water			2SK ₂		sym		29.9178627	1.9945	12.0329	38.5	L ₂			
2PO ₁	shallow water			2PO ₁		sym		15.9748272	1.0650	22.5355	38.5	J ₁			
2KM(SN) ₂	shallow water			2KM(SN) ₂				30.7086493	2.0472	11.7231	48.8	2SM ₂			
δ ₂	lunar	2	0	2	0	0	0	M2(KS) ₂		29.1483788	1.9432	12.3506	91.3	M ₂	0.00104
2KN2S ₃	shallow water			2KN2S ₃				28.6040041	1.9069	12.5857	164.1	v2			
P ₁	lunar	1	1	-2	0	0	0	SK ₁	asym	14.9589314	0.9973	24.0659	182.6	K ₁	0.17543
K ₂	luni-solar	2	2	0	0	0	0			30.0821373	2.0055	11.9672	182.6	S ₂	0.11498
MSf	lunar	0	2	-2	0	0	0	MS	asym	1.0158958	0.0677	354.3671	182.6	Mf	0.01369

Mf	lunar	0	2	0	0	0	KO	asym	1.0980331	0.0732	327.8590	182.6	MSf	0.15647
$3MP_5$	shallow water						$3MP_5$	sym	71.9933813	4.7996	5.0005	182.6	$2MO_5$	
MKS_2	shallow water						MKS_2		29.0662415	1.9377	12.3855	182.6	M_2	
$2MP_5$	shallow water						$2MP_5$	sym	72.9271398	4.8618	4.9364	182.6	$2MK_5$	
ϕ_1	solar	1	1	2	0	0	$2KP_1$	sym	15.1232058	1.0082	23.8045	182.6	K_1	-0.00756
SO_1	lunar	-1	3	-2	0	0	SO_1	asym	16.0569644	1.0705	22.4202	182.6	$2PO_1$	-0.00492
$3KM_5$	shallow water						$3KM_5$		74.1073100	4.9405	4.8578	182.6	MSK_5	
$3MNS_8$	shallow water						$3MNS_8$		115.4741794	7.6983	3.1176	182.6	$3MN_8$	
$2SN(MK)_2$	shallow water						$2SN(MK)_2$		29.3734880	1.9582	12.2559	182.6	λ_2	
SO_4	shallow water						SO_4		57.8860712	3.8591	6.2191	182.6	M_4	
$3MK_8$	shallow water						$3MK_8$		117.0344500	7.8023	3.0760	182.6	$3MS_8$	
$4MP_7$	shallow water						$4MP_7$	sym	100.9774854	6.7318	3.5652	182.6	$4MK_7$	
$MKL2S_2$	shallow water						$MKL2S_2$		28.5947204	1.9063	12.5897	182.6	V_2	
SK_3	shallow water						SK_3	sym	45.0410686	3.0027	7.9927	182.6	SP_3	
MK_4	shallow water						MK_4		59.0662415	3.9377	6.0949	182.6	MS_4	
OQ_2	shallow water						OQ_2	asym	27.3416965	1.8228	13.1667	182.6	ε_2	
SO_3	shallow water						SO_3	sym	43.9430356	2.9295	8.1924	182.6	MK_3	
SKM_2	shallow water						SKM_2		31.0980331	2.0732	11.5763	182.6	$2SM_2$	
$2MSK_8$	shallow water						$2MSK_8$		118.0503457	7.8700	3.0495	182.6	$2(MS)_8$	
MSf	lunar	0	2	-2	0	0	MS	asym	1.0158958	0.0677	354.3671	182.6	MF	0.01369
$2MK_6$	shallow water						$2MK_6$		88.0503457	5.8700	4.0886	182.6	$2MS_6$	
$2MSN_8$	shallow water						$2MSN_8$		116.4079380	7.7605	3.0926	182.6	$2MNK_8$	
$2MS2K_2$	shallow water						$2MS2K_2$		27.8039338	1.8536	12.9478	182.6	O_2	
$MNK2S_2$	shallow water						$MNK2S_2$		27.5059710	1.8337	13.0881	182.6	ε_2	
β_1		1	0	-2	1	0			14.4145548	0.9610	24.9748	193.6	M_1	-0.00278
γ_1	lunar	1	0	2	-1	0			14.5695476	0.9713	24.7091	193.6	M_1	-0.00567
$2N_2$	lunar	2	-2	0	2	0	$2NM_2$	sym	27.8953548	1.8597	12.9054	205.9	μ_2	0.02301
ρ_1	lunar	1	-2	2	-1	0			13.4715145	0.8981	26.7231	205.9	Q1	0.01371
v_2	lunar	2	-1	2	-1	0			28.5125831	1.9008	12.6260	205.9	N2	0.03302
λ_2	lunar	2	1	-2	1	0			29.4556253	1.9637	12.2218	205.9	L_2	-0.00670
MSN_6	shallow water						MSN_6		87.4238337	5.8283	4.1179	205.9	$4MN_6$	
$3M2S_2$	shallow water						$3M2S_2$		26.9523126	1.7968	13.3569	205.9	$2NS_2$	
$2Mv_6$	shallow water						$2Mv_6$	sym	86.4807916	5.7654	4.1628	205.9	$2MN_6$	

θ_1	lunar	1	2	-2	1	0	0		15.5125897	1.0342	23.2070	205.9	J_1	-0.00567	
N_6	shallow water				N_6		sym	85.3191885	5.6879	4.2194	205.9	$3MN_6$			
Γ_2		2	0	-2	2	0	0		28.9112508	1.9274	12.4519	205.9	M_2	-0.00273	
$3MN_4$	shallow water				$3MN_4$			58.5125831	3.9008	6.1525	205.9	SN_4			
Mv_2	shallow water				$2MLS_4$			57.4966873	3.8331	6.2612	205.9	MN_4			
N_4	shallow water				N_4		asym	56.8794590	3.7920	6.3292	205.9	$3MS_4$			
ζ_2		2	3	-2	1	0	0		30.5536572	2.0369	11.7826	205.9	η_2	0.00123	
$2NM_6$	shallow water				$2NM_6$		sym	85.8635632	5.7242	4.1927	205.9	$4MS_6$			
M_{sm}		0	1	-2	1	0	0		0.4715521	0.0314	763.4364	206.0	Mn	0.01579	
Sa	solar (*met)	0	0	1	0	0	0		0.0410686	0.0027	8765.8211	365.2	Ssa	0.01156	
Ssa	solar (*met)	0	0	2	0	0	0		0.0821373	0.0055	4382.9052	365.2	Sa	0.07281	
R_2	solar	2	2	-1	0	0	-1	SK_2		30.0410667	2.0027	11.9836	365.3	S_2	-0.00355
T_2	solar	2	2	-3	0	0	1		29.9589333	1.9973	12.0164	365.3	S_2	0.02476	
S_1	solar (*met)	1	1	-1	0	0	0		15.0000000	1.0000	24.00000	365.2	K_1	0.00416	
α_2		2	0	-1	0	0	1	SO_2		28.9430356	1.9295	12.4382	365.2	M_2	-0.00313
Ψ_1	solar	1	1	1	0	0	-1	RP_1		15.0821353	1.0055	23.8693	365.2	ϕ_1	-0.00422
π_1	solar	1	1	-3	0	0	1	TK_1		14.9178647	0.9945	24.1321	365.3	P_1	0.01023
MNK_4	shallow water				MNK_4			57.5059710	3.8337	6.2602	1615.7	MV_2			
$3MN_6$	shallow water				$3MN_6$			85.3920421	5.6928	4.2158	1615.7	$3NK_6$			
$2NK2S_2$	shallow water				$2NK2S_2$			26.9615963	1.7974	13.3523	1615.7	$3M2S_2$			
$2NMKS_6$	shallow water				$2NMKS_6$			85.9457005	5.7297	4.1887	1615.7	$4MS_6$			
MKN_6	shallow water				MKN_6			87.5059710	5.8337	4.1140	1615.7	$4MN_6$			
O_2	shallow water				O_2		asym	27.8860712	1.8591	12.9097	1615.8	$2N_2$			
NK_5	shallow water				NK_5		sym	43.4807981	2.8987	8.2795	3231.5	M_5			

Tables A.1 and A.2. 149 tidal harmonic constituents listed first in order of increasing frequency (Table A.1) and then in order of increasing synodic period (Table A.2).

103 of these constituents are shallow-water constituents up through the 12th diurnals. There are a few cases where the astronomical constituent is listed, but the shallow-water constituent at the same frequency can often be larger (e.g., $2MN_2$ is larger than L_2 in shallow bays and estuaries). No satellite constituents (representing the 18.6-year nodal cycle) are included in these tables (see table 4.1, and Zetler *et al.*, 1985).

In the **2nd column** (“origin of constituent”), the term “shallow water” indicates that the constituent was produced by nonlinear mechanisms in shallow water. A (“*met”) indicates that the calculated harmonic constants for this constituent usually include mostly quasi-periodic meteorological effect energy. The **4th column** (“shallow-water equivalent”) gives the shallow-water constituent with the same frequency as the astronomical constituent listed in the 1st column (or if the constituent is only a shallow-water constituent, it simply repeats the name). The **5th column** (“NL mechanism, sym or asym”) indicates whether the shallow-water constituent is produced by the symmetric nonlinear mechanism ($\mathbf{u}|\mathbf{u}|$) or by the asymmetric nonlinear mechanisms ($\partial(\mathbf{u}\mathbf{u})/\partial\mathbf{x}$, $\mathbf{u}\partial\mathbf{u}/\partial\mathbf{x}$, and $\mathbf{q}\mathbf{u}|\mathbf{u}|$) as indicated in Table 2.4 and discussed in Section 7.6. Constituents listed as asymmetric can also be produced by the lateral initial terms as discussed in Section 7.6.7. (A “sym or asym” assessment is not given for higher order interactions, especially involving more than two constituents.)

The **3rd column** (“Cartwright number”) gives the six digits that indicate which combination of astronomical frequencies (from Table 2.1) produces that astronomical tidal constituent (examples are shown in Table 2.2). The classic *Doodson numbers* are the same as the Cartwright numbers but with a 5 added to each digit (except the first), which Doodson did to keep these digits from being negative. These six digits are the multiplying coefficients in front of the six frequencies ω_L , and ω_i through ω_5 from Table 2.1 (the classic Doodson labeling for these six astronomical frequencies was τ, S, h, p, N, P_1). The angular speeds (frequencies) for the six astronomical motions listed in Table 3.2.1 are (in °/hour): $\omega_L = 14.49205236$, $\omega_1 = 0.54901656$, $\omega_2 = 0.0410688$, $\omega_3 = 0.00011408$, $\omega_4 = 0.0045422$, $\omega_5 = 0.00220644$ (Table 2.1 gives the equivalent astronomical periods). As an example, the Cartwright number for N_2 is 2-1-0-1-0-0; to obtain the angular speed for N_2 one multiplies ω_L by 2, subtracts ω_1 from it, and then adds ω_3 . Cartwright numbers are not given for shallow-water constituents (even though a combination of Cartwright numbers could be constructed that would produce the correct frequency of that constituent) because shallow-water constituents are not produced directly by a combination of those six astronomical frequencies; they are produced hydrodynamically by energy transferred from other constituents through the nonlinear mechanisms discussed in Sections 2.3.2 and 7.6.2.

The **6th column** gives the “angular speed” of the constituent in degrees per hour. Dividing the angular speed by 360° (=one cycle) and multiplying by 24 (hours) gives the frequency of the constituent in cycles per day (cpd) shown in the **7th column**. Dividing 360° by the angular speed gives the period of the constituent in hours shown in the **8th column**.

The **9th column** gives the synodic period for the constituent with respect to (wrt) the constituent which is closest in frequency among the constituents with a larger amplitude (shown in the **10th column**). Table 3.1 shows several synodic periods for each constituent, each paired with another constituent, but among the possibilities only the longest synodic period for a larger constituent is shown in the 9th column. The synodic period given in the 9th column depends on which larger nearby constituent (listed in the 10th column) it is decided

is most important; for the shallow-water constituents it may not always be clear which nearby constituent should be in the 10th column (unless one has a very high resolution spectra to look at).

The 11th column shows a coefficient of the relative strength of the tide potential (the tide producing force) for each astronomical constituent as determined by Cartwright and Edden (1973), in order to give one a first guess at the expected relative sizes of the tidal constituents (at least the astronomical ones). However, hydrodynamics can change these relative strengths. (In Table 3.2, the 12th column gives, as just one example, the constituent amplitudes for a water level station at Trenton, NJ, on the Delaware River. In this case, N_2 is larger than S_2 , unlike with the tide producing forces. Also, for that station one is really calculating $2MN_2$ and not L_2 , and likewise $2MS_2$ not μ_2 .) This Cartwright potential is not given for the shallow-water constituents, since they are not produced directly from the astronomical tide producing forces.

The relative size of a shallow-water term will be different for every hydrodynamic situation, but as an approximate estimate can be initially based on: (1) the sizes of the astronomical constituents from which it was produced; (2) the particular nonlinear mechanism that produced it; and (3) and the “order” of the nonlinear interaction (i.e., was it a first-order interaction or second-order, or even a third-order). Generally one can guess that a shallow-water constituent will be larger (compared with other shallow-water constituents) if its name includes fewer letters, and one or more of those letters represents one of the larger astronomical constituents. The examples of compound tides and overides shown in Table 2.4 were all first-order terms involving only two constituents at a time (one of them M_2), and thus are likely to be the most important of the shallow-water constituents. Compound tides and overides similarly generated with K_1 or O_1 are also likely to be important.

In the past, shallow-water frequencies were “found” by simply adding and/or subtracting the frequencies for two, three, and even four astronomical frequencies. A large number of combinations were possible, and the choices did not always represent a particular nonlinear generating mechanism. To choose which shallow-water constituents should be included in Tables A.1 and A.2, first various references were looked at including Godin (1988), Foreman (2004), Zettler et al (1967), and others (most references agreed on most of the astronomical frequencies, but there was not agreement on which shallow-water constituents to use); then the nonlinear generating mechanisms were considered (such as in Table 2.4). However, Tables A.1 and A.2 should still not be considered definitive, and a more precise and thorough Fourier decomposition (similar to that in Section 7.6) needs to be done. However, even with that done, the relative sizes of the shallow-water constituents, and thus the order in which they should be included in a harmonic analysis, will vary depending on the sizes of the astronomical constituents in the particular waterway from where the data came.

References

- Aikman, F. III, G.L. Mellor, T. Ezer, D. Sheinin, P. Chen, L. Breaker, K. Bosley, and D.B. Rao, 1996. Towards an operational nowcast/forecast system for the U.S. East Coast. In: *Modern Approaches to Data Assimilation in Ocean Modeling*, P. Malanotte-Rizzoli (ed.), Elsevier Oceanography Series, 61, pp. 347-376.
- Andersen, O.B., P.L. Woodworth, and R.A. Flather, 1995. Intercomparison of recent ocean tide models. *Journal of Geophysical Research*, **100**(C12):25261-25282.
- Amin, M., 1976. The fine resolution of tidal harmonics. *Geophysical J. Royal Astronomical Soc.*, **44**:293-310.
- Amin, M., 1977. Some recent investigations into the harmonic shallow water corrections method of tidal predictions. *International Hydrographic Review*, **56**(1): 87-108.
- Amin, M., 1991. Superfine resolution of tidal harmonic constants. In: *Tidal Hydrodynamics*, (ed.) B.B. Parker, John Wiley & Sons, New York, pp 771-724.
- Appell, G.F., T.N. Mero, and T.D. Bethem, and G.W. French, 1994. The development of a real-time port information system, *IEEE Journal of Oceanic Engineering*, **19**(2):149-157.
- Batchelor, G.K., 1977. *An Introduction to Fluid Mechanics*, Cambridge University Press, Cambridge, UK., 615 pages.
- Bennett, A.F., 1992. *Inverse Methods in Physical Oceanography*. Cambridge University Press, Cambridge, UK..
- Blackman, R.B. and J.W. Tukey, 1959. *The Measurement of Power Spectra: from the point of view of communications engineering*, Dover Publications, New York.
- Blumberg, A.F. and G.L. Mellor, 1987. A Description of a Three-Dimensional Coastal Ocean Circulation Model. In: *Three-Dimensional Coastal Ocean Models*, (Ed.) N. Heaps, pp 1-16, American Geophys. Union.
- Bosley, K T and K.W. Hess, 1997. Development of an Experimental Nowcast/Forecast System for Chesapeake Bay Water Levels. *Estuarine and Coastal Modeling*, pp. 413-426.
- Bowden, K.F., 1953. Note on wind drift in a channel in the presence of tidal currents, *Proc. Royal Soc. London*, A219:425-446.
- Burg, J.P., 1972. The relationship between maximum entropy spectra and maximum likelihood spectra. *Geophysics*, **37**:375-6.
- Cartwright, D.E., 1968. A unified analysis of tides and surges round north and east Britain. *Philosophical Transactions Royal Society London*, A263:1-55.
- Cartwright, D.E., 1977. Oceanic tides. *Reports On Progress In Physics*, **40**:665-708.
- Cartwright, D.E., 1991. Detection of tides from artificial satellites (review). In: *Tidal Hydrodynamics*, (ed) B.B. Parker, John Wiley & Sons, New York, pp 547-567.

- Cartwright, D.E., 1999. *Tides – A Scientific History*, Cambridge University Press, Cambridge, UK, 292 pages.
- Cartwright, D.E. and M. Amin, 1986. The variances of tidal harmonics. *Deutsche Hyrogr. Zeit.*, **6**:235-253.
- Cartwright, D.E. and R.J. Tayler, 1971. New computations of the tide-generating potential. *Geophys. J. Royal Astronomical Society*, **23**:45-74.
- Cartwright, D.E. and Anne C. Edden, 1973. Corrected tables of tidal harmonics. *Geophys. J. Royal Astronomical Society*, **33**:253-264.
- Chen, P, and G. Mellor, 1999. Determination of tidal boundary forcing using tide station data. In: *Coastal Ocean Prediction*, Christopher N.K. Mooers (Ed.), Coastal and Estuarine Studies, 56, AGU Publications, Washington, D.C., pp 329-351..
- Cheney, R., L. Miller, R. Agreen, N. Doyle, and J. Lillibridge, 1994. TOPEX/POSEIDON: the 2-cm solution. *Journal of Geophysical Research*, **99**(C12):24555-24563.
- Cheng, Ralph T., Jon R. Burau, and Jeff W. Gartner, 1991. Interfacing data analysis and numerical modeling for tidal hydrodynamic phenomena. In: *Tidal Hydrodynamics*, (ed.) B.B. Parker, John Wiley & Sons, New York, pp 201-220.
- Cherniawsky, J.Y., M.G.G. Foreman, W.R.Crawford, and R.F. Henry, 2001. Ocean tides from TOPEX/POSEIDON sea level data. *Journal of Atmospheric and Oceanic Technology*, **18**(4):649-664.
- Clarke, A.J., 1991. The dynamics of barotropic tides over the continental shelf and slope (Review). In: *Tidal Hydrodynamics*, (ed.) B.B. Parker, John Wiley & Sons, New York, pp 79-108.
- Cooley, J.W. and J.W. Tukey, 1965. An algorithm for machine calculation of complex Fourier series. *Mathematical Computations*, **19**:297-301.
- CO-OPS, 2000. *Tides and Currents Glossary*. Center for Operational Oceanographic Products and Services, National Ocean Service, NOAA, U.S. Dept. of Commerce.
- CO-OPS, 2003. *Computational Techniques For Tidal Datums Handbook*, NOAA Special Publication NOS CO-OPS2, Center for Operational Oceanographic Products and Services, National Ocean Service, NOAA, U.S. Dept. of Commerce, 90 pages.
- Crean, P. B., T. S. Murty, and J. A. Stronach, 1988: Mathematical modeling of tides and estuarine circulation: The coastal seas of southern British Columbia and Washington State. *Lecture Notes on Coastal and Estuarine Studies*, M. Bowman et al.,Eds., Springer-Verlag, 471 pp.
- Daily, James W. and Donald R.F. Harleman, 1966. *Fluid Dynamics*. Addison-Wesley Publishing Company, Reading, MA, 454 pages.
- Darwin, George H., 1883. The harmonic analysis of tidal observations. *British Assoc. Report for 1883*, pp 49-118.
- Darwin, G. H., 1883. On the harmonic analysis of tidal observations of high and low water. *Proc. Royal Society*, **48**:278-340.
- Dean, R.G., 1966. Tides and Harmonic Analysis. In: *Estuary and Coastline Hydrodynamics*, (Ed.) Arthur T. Ippen, McGraw-Hill Book Company, New York, pp. 197-230..

References

- Defant, Albert, 1961. *Physical Oceanography*, Vol.II, Pergamon Press, The Macmillan Co, New York, pp 254-516.
- Dennis, R.E. and E.E Long, 1971. *A User's Guide to a Computer Program for Harmonic Analysis of Data at Tidal Frequencies*, NOAA Technical Reort NOS, National Ocean Survey, NOAA, Dept. of Commerce, 31 pages.
- Disney, L.P. and W.H. Overshiner, 1925. *Tides and Currents in San Francisco Bay*. Special Pub. 115, U.S. Coast and Geodetic Survey, Dept. of Commerce, Washington, DC, 125 pages.
- Dietrich, G., 1967. *General Oceanography*, Wiley, New York, 588 pages.
- Doodson, A.T., 1921. The harmonic development of the tide-generating potential. *Proc. Royal Society A*, **100**:305-329.
- Doodson, A.T., 1928a. The analysis of tidal observations. *Philosophical Transactions of the Royal Society of London*, **227**:223-279.
- Doodson, A.T., 1928b. The analysis and prediction of tidal currents from observations of time of slack water. *Proceedings of the Royal Society of London. Series A*, **121**(787):72-88.
- Doodson, A.T., 1951. The analysis of high and low waters. *International Hydrographic Review*, **28**(1):13-77.
- Doodson, A.T., 1957. The analysis and prediction of tides in shallow water. *International Hydrographic Review*, **34**:85-111.
- Doodson, A.T. and H.D.Warburg, 1941. *Admiralty Manual of Tides*. Hydrographic Department, Admiralty, London, 270 pages.
- Dronkers, J.J., 1964. *Tidal Computations In Rivers and Coastal Waters*. North-Holland Publishing Co., Amsterdam, 518 pages.
- Eagleson, P.S. and R.G. Dean, 1966. Small amplitude wave theory. In: *Estuarine and Coastline Hydrodynamics*, (Ed) Arthur T. Ippen, McGraw-Hill Book Company, New York, pp 1-92.
- Egbert, G.D., A.F. Bennett, and M.G.G. Foreman, 1994. TOPX/POSEIDON tides estimated using a global inverse model, *Journal of Geophysical Research*, **99**(C12):24821-52.
- Emery, William J. and Richard E. Thomson, 2001. *Data Analysis Methods in Physical Oceanography*. Elsevier, New York, 638 pages.
- Fang, G., 1987. Nonlinear effect of tidal friction. *Acta Oceanologica Sinica*, vol **6**, suppl.1, pp 105-122.
- Fjeldstad, J.E., 1929. Contributions to the dynamics of free progressive tidal waves. In: *The Norwegian North Polar Expedition with the Maud, 1919-1925, Scientific Results*, vol. IV, no. 3, Geofysisk Institute, Bergen.
- Ferrel, William E., 1874. *Tidal Researches*. United States Coast Survey Report, 1874. Appendix, Washington, DC., 270 pages.
- Filloux, J.H., D.S. Luther, and A.D.Chave,1991. Update on seafloor pressure and electric field observations from the north-central and noreastern Pacific: Tides, Infratidal fluctuations, and barotropic flow. In: *Tidal Hydrodynamics*, (ed.) B.B. Parker, John Wiley & Sons, New York, pp 617-640.
- Fisher, Carl, 1986. *Tidal Circulation In Chesapeake Bay*. Ph.D. Dissertation, Old Dominion University, 255 pages.

- Foreman, M.G.G., 2004a. *Manual for Tidal Heights Analysis and Prediction*. Pacific Marine Science Report 77-10, Inst. of Ocean Sciences, Patricia Bay, Victoria, B.C., 101 pages. (Online revised version of 1977 original)
- Foreman, M.G.G., 2004b. *Manual for Tidal Currents Analysis and Prediction*. Pacific Marine Science Report 78-6, Inst. of Ocean Sciences, Patricia Bay, Victoria, B.C., 70 pages. (Online revised version of 1978 original)
- Foreman, M.G.G. and R.F. Henry, 1989. The harmonic analysis of tidal model time series. *Advances In Water Resources*, **12**(3):109-120.
- Foreman, M.G.G. and R.F. Henry, 2004. *Tidal Analysis Based On High and Low Water Observations*. Pacific Marine Science Report 79-15, Inst. of Ocean Sciences, Patricia Bay, Victoria, B.C., 36 pages. (Online revised version of 1979 original)
- Foreman, M.G.G., and E.T. Neufeld, 1991. Harmonic analysis of long time series. *International Hydrographic Review*, **68**(1):85-108.
- Forrester, Warren D., 1983. *Canadian Tide Manual*, Dept. of Fisheries and Oceans, Ottawa, CA, 137 pages.
- George, K.J. and B. Simon, 1984. The species concordance method of tide prediction in estuaries. *International Hydrographic Review*, **65**(1):121-145.
- Gill, S.K., T.N. Mero, and B.B. Parker, 1992. NOAA operational experience with acoustic sea level measurement. In: *Sea Level Measurement and Quality Control*. Joint IAPSO/IOC Workshop, October 12-13, 1992, Intergovernmental Commission, Paris, France.
- Gill, S.K. and J.R. Schultz (eds), 2001. *Tidal Datums and Their Applications*. NOAA Special Publication NOS CO-OPS1, Center for Operational Oceanographic Products and Services, National Ocean Service, NOAA, U.S. Dept. of Commerce, 111 pages.
- Glenn, S.M., T.D. Dickey, B. Parker, and W. Boicourt, 2000. Long-term real-time coastal ocean observation networks, *Oceanography*, **13**(1):24-34.
- Glenn, S.M., W. Boicourt, B. Parker, and T.D. Dickey, 2000. Operational observation networks for ports, a large estuary and an open shelf, *Oceanography*, **13**(1):12-23.
- Godin, G., 1972. *The Analysis of Tides*. University of Toronto Press, Toronto, Canada, 264 pages.
- Godin, G., 1986. The use of nodal corrections in the calculation of harmonic constants. *International Hydrographic Review*, **63**(2):143-162.
- Godin, Gabriel, 1988. *Tides*. CICESE, Ensenada, Mexico, 290 pages.
- Godin, G., 1991. The analysis of tides and currents. In: *Tidal Hydrodynamics*, (ed.) B.B. Parker, John Wiley & Sons, New York, pp 675-709.
- Gonella, J., 1972. A rotary-component method for analysing meteorological and oceanographic vector time series, *Deep Sea Research*, **19**:833–846.
- Green, G., 1837. On the motion of waves in a variable canal of small depth and width. *Transactions, Cambridge Philosophical Society*, **6**:457-462.
- Gross, T.F., K.T. Bosley, K.W. Hess, 2000. *The Chesapeake Bay Operational Forecast System (CBOFS): Technical Documentation*, National Ocean Service, NOAA, U.S. Dept. of Commerce.
- Gross, T.F., 2002. (Personal communication)

References

- Groves, G., 1955. Numerical filters for discrimination against tidal periodicities. *Trans. American Geophysical Union*, **36**(6):1073-84.
- Groves, G.W. and E.J. Hannan, 1968. Time series regression of sea level on weather, *Reviews of Geophysics*, **6**:129-174.
- Haidvogel, D. B., and A. Beckman, 1999. *Numerical Ocean Circulation Modeling*, Imperial College Press, River Edge, N. J., 318 pp.,
- Harris, D.L., 1962. The equivalence between certain statistical prediction methods and linearized dynamical methods, *Monthly Weather Review*, vol. 90, No. 8, Aug. 1962.,
- Harris, D.L., N.A. Pore, and R. Cummings, 1963. The Application of High Speed Computers to Practical Tidal Problems. Abstracts of Papers, vol 6, IAPO, XIII General Assembly, IUGG, Berkeley, VI-16.
- Harris, Rollin A., 1887-1907. *Manual of Tides*. Parts 1, 2, 3, 4, and 5, originally Appendices to the U.S. Coast and Geodetic Annual Reports.
- Hendershott, M.C., Speranza, A., 1971. Co-oscillating tides in long narrow bays; the Taylor problem revisited. *Deep Sea Research*, **8**:959-980.
- Hess KW. 1989. *MECCA Program Documentation*. NOAA Technical Report NESDIS 46, NOAA, U.S. Department of Commerce, 156 pp.
- Hess, K., R. Schmalz, C. Zervas, W. Collier, 1999. *Tidal Constituent And Residual Interpolation (TCARI): A New Method for the Tidal Correction of Bathymetric Data*, NOAA Technical Report NOS CS 4, National Oceanic and Atmospheric Administration.
- Hess, Kurt, 2003. Water level simulation in bays by spatial interpolation of tidal constituents, residual water levels, and datums. *Continental Shelf Research*, **23**:395-414.
- Hicks, Steacy D. 1967. The prediction centenary of the United States Coast and Geodetic Survey, *International Hydrographic Review*, **44**:123-131.
- Hicks, Steacy D. 2006. *Understanding Tides*, Center for Operational Oceanographic Products and Services, National Ocean Service, NOAA, U.S. Dept. of Commerce, 66 pages.
- Huggett, W.S., 1988. Juan de Fuca Strait and Strait of Georgia Current Atlas. The *Hydrographical Journal*, **47**:5-16.
- IOC, 2006. *Manual On Sea Level Measurement and Interpretation*, Vol. IV, an update to 2006, Intergovernmental Oceanographic Commission, JCOMM Technical Report No. 31, WMO/TD No. 1339, UNESCO, 88 pages.
- Ippen, A.T. and D.R.F Harleman, 1966. Tidal dynamics in estuaries. In: *Estuary and Coastline Hydrodynamics*, (Ed.) Arthur T. Ippen, McGraw-Hill Book Company, New York, pp. 493-545.
- Jay, David A., 1991. Green's law revisited: tidal long wave propagation in channels with strong topography. *Journal of Geophysical Research*, **96**:20,585-20,598.
- Jay, David A. and Edward P. Flinchem, 1999. A comparison of methods of analysis of tidal records containing multi-scale non-tidal background energy. *Continental Shelf Research*, **19**:1695-1731.
- Jay, David A. and Tobias Kukulka, 2003. Revising the paradigm of tidal analysis – the uses of non-stationary data. *Ocean Dynamics*, **53**:110-125.

- Kantha, Lakshmi H. and Carol Anne Clayson, 2000. *Numerical Models of Oceans and Oceanic Processes*. International Geophysics Series, Vol 66, Academic Press, 940 pages.
- Kelley, John G.W., D.W.Behringer, J.H. Thiebaux, and B. Balasubramaniyan 2002. Assimilation of SST data into a real-time coastal ocean forecast system for the U.S. East Coast. *Weather and Forecasting*, **17**(4):670-690.
- Knauss, John A., 1978. *Introduction To Physical Oceanography*. Prentice-Hall, Englewood Cliffs, NJ, 338 pages.
- Kuo, John T., 1991. Synoptic predictions of tide and currents everywhere in the world. In: *Tidal Hydrodynamics*, (ed.) B.B. Parker, John Wiley & Sons, New York, pp 61-76.
- Laplace, P.S., 1775. *Mem. Acad. R. Sci.*, **88**:75-182, **89**:177-267.
- LeLacheur, E.A. and J.C. Sammons, 1932. *Tide and Currents in Long Island and Block Island Sounds*, Special Publications 174, U.S. Coast and Geodetic Survey, Dept. of Commerce, Washington, DC, 187 pages.
- Le Provost, Christian, 1976. Theoretical analysis of the structure of the tidal wave spectrum in shallow water areas, *Mémoires Société Royale des Sciences de Liège*, 6^e série, tome C, pp 97-111.
- Le Provost, Christian, 1992. On the use of sea-level gauge data for satellite altimetry validation, a review. *Oceanologica Acta*, **15**:431-440.
- LeProvost, Christian, 2001. Tide over ridges, shelves and near coasts. In: *Report of the High-Resolution Ocean Topography Science Working Group Meeting*, (Ed) D.B. Chelton, convened at U. of Maryland, College Park, MD.
- Le Provost, Christian and Patrick Vincent, 1991. Finite-element method for modeling ocean tides. In: *Tidal Hydrodynamics*, (ed.) B.B. Parker, John Wiley & Sons, New York, pp 41-60.
- Loder, J.W. and C. Garrett, 1978. The 18.6-year cycle of sea surface temperature in shallow seas due to variations in tidal mixing. *Journal of Geophysical Research*, **83**(C4):1967-1970.
- Lynch, Daniel R. and Francisco E. Werner, 1991. Three-dimensional velocities from a finite-element model of English Channel/Southern Bight tides. In: *Tidal Hydrodynamics*, (ed.) B.B. Parker, John Wiley & Sons, New York, pp 183-200.
- Marmer, Harry A., 1926. *The Tide*. D. Appleton and Company, New York, 282 pages.
- Marmer, Harry A., 1951. *Tidal Datum Planes*, U.S. Coast and Geodetic Survey, Dept. of Commerce, Washington, DC, 142 pages.
- Mellor, G.L., and T. Yamada, 1982. Development of a turbulence closure model for geophysical fluid problems, *Review Geophys. Space Physics*, **20**:851-875.
- Mellor, George, Sirpa Hakkinen, Tal Ezer, and Richard Patchen, 2002. A generalization of a sigma coordinate ocean model and an intercomparison of model vertical grids. In: *Ocean Forecasting: Conceptual Basics and Applications*, N. Pinardi and J. Woods (Eds.), Springer, Berlin, pp 55-72.
- Myers, E.P. and A.M. Baptista, 2001. Inversion for tides in the Eastern North Pacific Ocean. *Advances in Water Resources*, **24**(5):505-519.

References

- Mooers, C.N.K., 1973. A technique for the cross spectrum analysis of pairs of complex-valued time series, with emphasis on properties of polarized components and rotational invariants. *Deep-Sea Research*, **20**:1129-1141.
- Munk, W.H. , B. Zetler, and G.W.Groves, 1965. Tidal cusps. *Geophysical Journal*, **10**:211-219.
- Munk, W.H. and D.E. Cartwright, (1966). Tidal spectroscopy and prediction. *Phil. Trans. R. Soc. A*, **259**:533-581.
- Munk, Walter and Klaus Hasselmann, 1964. Super-resolution of tides. *Studies on Oceanography*, University of Tokyo Press, Tokyo, Japan, pp 339-344.
- National Ocean Service, 1987. *Delaware River and Bay Tidal Circulation and Water Level Forecast Atlas*. National Ocean Service, NOAA, U.S. Dept. of Commerce, 49 pages.
- Noble, M.A. and G.R. Gelfenbaum, 1992. Seasonal fluctuations in sea level on the South Carolina Shelf and their relationship to the Gulf Stream. *Journal of Geophysical Research*, **97**(C6):9521-9529.
- O'Brien, J.J. and R.D. Pillsbury, 1974. Rotary wind spectra in a sea breeze regime. *Jour. Of Applied Meteorology*, **13**(7):820-825.
- Parker, Bruce B. 1977. *Tidal Hydrodynamics In the Strait of Juan de Fuca-Strait of Georgia*, NOAA Technical Report, NOS 69, 56 pages.
- Parker, Bruce B., 1984. *Frictional Effect on the Tidal Dynamics of a Shallow Estuary*. Ph.D. Dissertation, The Johns Hopkins University, Baltimore, Maryland, 292 pages.
- Parker, Bruce B., 1986. Applications of real-time oceanographic data systems, *The Marine Technology Society Journal*, **20**(3):18-27.
- Parker, Bruce B., 1988. An atlas for forecasting circulation and water levels. *Sea Technology*, **29**(8): 21-25.
- Parker, Bruce B., 1991a. The relative importance of the various nonlinear mechanisms in a wide rage of tidal interactions. In: *Tidal Hydrodynamics*, pages 237-268, John Wiley & Sons, New York..
- Parker, Bruce B., 1991b. On the use of nonharmonic tidal analyses and their effect on the quality of subordinate station predictions. In: *Tidal Hydrodynamics*, pages 771-788, John Wiley & Sons, New York.
- Parker, Bruce B., 1994. Sea level variability along the East Coast of the United States. In: *Studies In Eastern Energy and the Environment*, AAPG Eastern Section Special Volume, (Eds.) A.P. Schultz and E.K. Rader, Virginia Div. of Mineral Resources Publication 132, pp 66-72.
- Parker, Bruce B., 1995. PORTS makes navigation safer. *Proceedings of the Marine Safety Council*, **52**(5):30-2, Sept-Oct, 1995.
- Parker, Bruce B., 1996. Monitoring and modeling of coastal waters in support of environmental preservation. *Journal of Marine Science and Technology*, **1**(2):75-84.
- Parker, Bruce B., 1997. Coastal Currents, *Mariners Weather Log*, **40**(3):24-28.
- Parker, Bruce B., 1998a. Development of Model-Based Regional Nowcasting/ Forecasting Systems. In: Spaulding, M.L. and A.F. Blumberg (Eds.), *Estuarine and Coastal Modeling*, American Society of Civil Engineers, New York, refereed proceedings of the 5th International Conference, Alexandria, VA, pp 355-373.

- Parker, Bruce B., 1998b. The Coriolis Effect: Motion On a Rotating Planet, *Mariners Weather Log*, **42**(2):17-33.
- Parker, Bruce B., 1998c. Why Are the Tides So Predictable? *Mariners Weather Log*, **42**(3):21-27.
- Parker, Bruce B., 1999. Tides In Shallow Water *Mariners Weather Log*, **43**(3):16-23.
- Parker, Bruce, B., 2002. The integration of bathymetry, topography, and shoreline and the vertical datum transformations behind it. *International Hydrographic Review*, vol.3, no.3(New Series), pp 35-47, Nov 2002.
- Parker, Bruce B., 2002. Integrated real-time/forecast information for safe, efficient, and environmentally-friendly ports, *Singapore Maritime and Port Journal*, pp 1-10.
- Parker, Bruce B., 2003. The difficulties in measuring a consistently defined shoreline -- the problem of vertical referencing. *Journal of Coastal Research*, Special Issue 38:44-56.
- Parker, Bruce B., 2004. Tides. In: *Encyclopedia of Coastal Science*, (ed.) M. Schwartz, Kluwer Academic Publishers, Encyclopedia of Earth Sciences Series, pp 987-996..
- Parker, Bruce B. and Bryan R. Pearce. 1975. *The Response of Massachusetts Bay To Wind Stress*, Massachusetts Institute of Technology Technical Report No. 198, Dept. of Civil Engineering, 109 pages.
- Parker, Bruce B. and Lloyd C. Huff, 1998. Modern under-keel clearance management. *International Hydrographic Review*, LXXV(2):143-165.
- Parker, Bruce B., Alan Davies, and Jiuxing Xing, 1999. Tidal Height and Current Prediction. Chapter 12 in: *Coastal Ocean Prediction*, Christopher N.K. Mooers (Ed.), Coastal and Estuarine Studies, 56, pages 277-327, AGU Publications, Washington, D.C..
- Parker, B., K. Hess, D. Milbert, and S. Gill, 2003. A National Vertical Datum Transformation Tool. *Sea Technology*, 44(9):1-15.
- Patchen, R. C., 1986. A real-time operational model/measurement system for Delaware River and Bay. In *Applications of Real-Time Oceanographic Circulation Modeling*, (ed) Bruce B. Parker, pp. 47-58.
- Patchen, Richard C., Elmo E. Long, and Bruce B. Parker. 1976. *Analysis of Current Meter Observations In New York Bight Apex, August 1973-June 1974*, NOAA Technical Report ERL 368-MESA 5, 24 pages.
- Patchen, R. and J. Blaha, 2002. Implementation of an infrastructure to support operation and evaluation of Gulf of Mexico models. In: *Oceans'02 MTS/IEEE*, vo. 2, pp 803-809.
- Pawlowicz, Rich, Bob Beardsley, and Steven Lenz, 2002. Classical tidal harmonic analysis including error estimates in MATLAB using T_TIDE, *Computers & Geosciences*, **28**:929-937.
- Pedlosky, Joseph, 1987. *Geophysical Fluid Dynamics*. Spring-Verlag, New York, 624 pages.
- Platzman, George, 1971. Ocean tides and related waves. *Lectures in Applied Math*, vol. 14, pp 239-291.
- Platzman, George, 1991. Tidal evidence for ocean normal modes. In: *Tidal Hydrodynamics*, (ed.) B.B. Parker, John Wiley & Sons, New York, pp 13-26.

References

- Porter, David L. and H.H. Shih, 1996. Investigations of temperature effects on NOAA's Next Generation Water Level Measurement system. *Jour. of Atmospheric and Oceanic Technology*, **13**:714-725.
- Prandle, David, 1982. The vertical structure of tidal currents and other oscillatory flows. *Geophysical and Astrophysical Fluid Dynamics*, **22**:29-49.
- Prandle, David, 1991. Tides in estuaries and embayments (Review). In: *Tidal Hydrodynamics*, (ed.) B.B. Parker, John Wiley & Sons, New York, pp 125-152.
- Prandle, D. and J. Wolf, 1978. The interaction of surge and tide in the North Sea and River Thames. *Geophysical Journal of the Royal Astronomical Society*, **55**:203-216.
- Prandle, D. and M. Rahman, 1980. Tidal response in estuaries. *Journal of Physical Oceanography*, **10**(10):1552-73.
- Press, W.H., B.P. Flannery, S.A. Teukolsky, and W.T. Vetterling, 1992. *Numerical Recipes: The Art of Scientific Computing*. (2nd. Edition) Cambridge University Press, 992 pages.
- Preisendorfer, R.W., 1988. *Principal Component Analysis in Meteorology and Oceanography*, Developments in Atmospheric Sciences, 17, Elsevier, Amsterdam.
- Proudman, J., 1923. Tides: Appendix. *Reports on the State of Science*, etc., Section A - Liverpool, pp 1-6, British Association.
- Proudman, J., 1942. Halley's tidal chart. *The Geophysical Journal*, **100**(4):174-6.
- Pugh, D.T., 1987. *Tides, Surges, and Mean Sea Level*. John Wiley & Sons, New York, 472 pages.
- Pugh, D.T., 2004. *Changing Sea Levels. Effects of Tides, Weather, and Climate*, Cambridge University Press, Cambridge, UK, 265 pages.
- Ray, Richard D. and Gary T. Mitchum, 1997. Surface manifestation of internal tides in the deep ocean: observations from altimetry and island gauges. *Progress In Oceanography*, **40**:135-162.
- Redfield, A., 1950. The analysis of tidal phenomena in narrow embayments, *Papers In Physical Oceanography and Meteorology*, **11**(4), Massachusetts Inst. of Tech. and Woods Hole.
- Rossiter, J.R. and G.W. Lennon, 1967. An intensive analysis of shallow water tides. *Geophysical J. Royal astronomical Soc.*, **16**:275-293.
- Schureman, P., 1958. *Manual of Harmonic Analysis and Prediction of Tides*. Special Publication 98, Coast and Geodetic Survey, U.S. Dept. of Commerce, Washington, D.C., 317 pages.(Revised 1940 Edition with corrections; first published in 1924)
- Schwiderskii, E.W., 1978. *Global Ocean Tides, Part I: A Detailed Hydrodynamic Interpolation Model*, NSWC/DX TR-3866, U.S. Naval Surface Warfare Center.
- Schwiderskii, E.W., 1979. *Global Ocean Tides, Part II: The Semidiurnal Principle Lunar Tide (M_2)*, Atlast of Tidal Charts and Maps, NSWC TR-79-414, U.S. Naval Surface Warfare Center.
- Schwiderski, E.W., 1980. On charting global ocean tides, *Rev. of Geophysics and Space Physics*, **18**(1):243-268.
- Schwiderski, Ernst W., 1991. High-precision modeling of mean sea level, ocean tides, and dynamic ocean variations with GEOSAT altimeter signals. In: *Tidal Hydrodynamics*, (ed.) B.B. Parker, John Wiley & Sons, New York, pages 593-616.

- Schmalz, Richard, 1996. *DGPS-Supported Hydrosurvey, Water Level Measurement, and Modeling of Galveston Bay: Development and Application of the Numerical Circulation Model*. NOAA Technical Report NOS OES 012, Silver Spring, Maryland, 136 pages.
- Schmalz, Richard, 2000. *Three-dimensional Hydrodynamic Model Development For a Galveston Bay Nowcast/Forecast System*, NOAA Technical Report NOS CS9, Silver Spring, MD, 167 pages.
- Shih, H.H. and L. Baer, 1991. Some errors in tide measurement caused by dynamic environment. In: *Tidal Hydrodynamics*, (ed.) B.B. Parker, John Wiley & Sons, New York, pp 641-671.
- Shum, C.K., P.L. Woodworth, O.B. Anersen, G.D. Egbert, O. Francis, C. King, S.M. Klosko, C. LeProvost, X. Li, J-M Molines, M.E. Parke, R.D. Ray, M.G. Schlax, D. Stammer, C.C. Tierney, P. Vincent, and C.I. Wunsch, 1997. Accuracy assessment of recent ocean tide models. *Journal of Geophysical Research*, **102**(C11)::25173-25194.
- Simon, B., 1991. The species concordance method of tide prediction. In: *Tidal Hydrodynamics*, (ed.) B.B. Parker, John Wiley & Sons, pp 725-735.
- Smith, A.J., B.A.C. Ambrosius, K.F. Wakker, P.L. Woodworth, and J.M. Vassie, 1997. Comparison between the harmonic and response methods of tidal analysis using TOPEX/POSEIDON altimetry. *Journal of Geodesy*, **71**:695-703.
- Speer, Paul, David G. Aubrey, and Carl T. Friedrichs, 1991. Nonlinear hydrodynamics of shallow tidal inlet/bay systems. In: *Tidal Hydrodynamics*, (ed.) B.B. Parker, John Wiley & Sons, New York, pp 321-340.
- Szabados, Michael, Chuck Roman, and Bobby Taylor, 1987. Transmission of real time oceanographic and meteorological data from ships. *Oceans*, vol. 19, pp 863-869.
- Taylor, G. I., 1920. Tidal oscillations in gulfs and rectangular basins. *Proceedings London Mathematical Society*, **20**:148-181.
- Thomson, Sir William (Lord Kelvin), 1869. Report of the Committee for the purpose of promoting the extension, improvement and harmonic analysis of Tidal Observations. In: Report of the 38th Meeting of the BAAS, 1868, pp 489-510, John Murray, London.
- Thomson, Sir William (Lord Kelvin), 1881. The tide gauge, tidal harmonic analyzer and tide predicter. *Proceedings Institute of Civil Engineering*, London, **65**:4-74.
- Tsimplis, M.N. and P.L. Woodworth, 1994. The global distribution of the seasonal sea level cycle calculation from coeastal tide gauge data. *Journal of Geophysical Research*, **99**(C8):16031-16039.
- U.S. Coast and Geodetic Survey, 1950. *Manual of Current Observations*, Special Publication No. 215, Washington, D.C., 87 pages.
- U.S. Coast and Geodetic Survey, 1952. *Manual of Harmonic Constant Reductions*, Special Publication 260, U.S. , U.S. Dept. of Commerce, 74 pages.
- U.S. Coast and Geodetic Survey, 1965. *Manual of Tide Observations*, Publication 30-1, Washington, D.C., 72 pages.
- Wei, Eugene, 2003. The new Port of New York and New Jersey Operational Forecast System (NYOFS), *Bulletin of the American Meteorological Society*, Sept 2003, pp 1004-6.

References

- Woodworth, P.L. and J.P. Thomas, 1990. Determination of the major semidiurnal tides of the northwester European continental shelf from Geosat altimetry. *Journal of Geophysical Research*, **95**(C3):3061-3068.
- Wunsch, C., 1972. Bermuda sea level in relation to tides, weather, and baroclinic fluctuations. *Reviews in Geophysics, Space Physics*, **10**:1-49.
- Yih, Chia-Shun, 1969. *Fluid Mechanics*. McGraw-Hill Book Company, New York, 622 pages.
- Zervas, Chris, 1999. *Tidal Current Analysis Procedures and Associated Computer Programs*. NOAA Technical Report NOS CO-OPS 0021. National Ocean Service, NOAA, U.S. Dept. of Commerce, 101 pages.
- Zetler, Bernard D, 1953. A method of inferring the amplitudes of the tidal constituents M_2 and (K_1+O_1) . *International Hydrographic Review*, vol. 30.
- Zetler, Bernard D, 1959. Tidal characteristics from harmonic constants. *J. of the Hydraulics Div, Proc American Soc. Civil Engineers*, vol 85, HY12, pp 77-87.
- Zetler, Bernard D, 1982. *Computer Applications to Tides in the National Ocean Survey*. National Ocean Survey, NOAA, Dept. of Commerce, 85 pages.
- Zetler, Bernard.D, 1987. The evolution of modern tide analysis and prediction – some personal memories. *International Hydrographic Review*, **64**(1):124-139.
- Zetler, Bernard.D, 1991. Military Tide Predictions in World War II.. In: *Tidal Hydrodynamics*, (ed.) B.B. Parker, John Wiley & Sons, New York, pp 791-797.
- Zetler, B.D., M.D. Schuldert, R.W. Whipple, and S.D. Hicks, 1965. Harmonic analysis of tides from data randomly spaced in time. *Journal of Geophysical Research*, **70**(12):2805-2811.
- Zetler, Bernard D. and Robert E. Cummings, 1967. A harmonic method for prediction shallow-water tides. *Journal. of Marine Research*, **25**(1):103-114.
- Zetler, B.D., D.E. Cartwright, and W.H. Munk, 1969. Tidal constants derived from response admittances. *Symp. on Earth Tides*, Strasbourg, 175-178.
- Zetler, B.D., D.E. Cartwright, and S. Berkman, 1979. Some comparisons of response and harmonic tide predictions. *International Hydrographic Review*, **56**(2):105-115.
- Zetler, B.D. and W.H. Munk, 1975. The optimum wiggliness of tidal admittances. *J. of Marine Research*, **33**(Suppl.):1-13.
- Zetler, B.D., E.E. Long, and L.F. Ku, 1985. Tide predictions using satellite constituents. *International Hydrographic Review*, **62**(2):135-142.
- Zhang, Aijun, Bruce B. Parker, and Eugene Wei, 2002. Assimilation of water level data into a coastal hydrodynamic model by an adjoint optimal technique. *Continental Shelf Research*, **22**:1909-1934.
- Zhang, Aijun, Eugene Wei, and Bruce B. Parker, 2003. Optimal estimation of tidal open boundary conditions using predicted tides and adjoint data assimilation technique. *Continental Shelf Research*, **23**:1055-1070.
- Zhang, Aijun, K.W. Hess, E.Wei, and E.Myers, 2006. *Implementation of Model Skill Assessment Software for Water Level and Current In Tidal Regions*, NOAA Technical Report NOS CS 24., 59 pages.
- Zuosheng, Yang, K.O. Emery, and Xui Yui, 1989. Historical development and use of thousand-year-old tide-prediction tables. *Limnology and Oceanography*, **34**(5):953-957.

List of Figures

Figure 1.1.	Harris tide predicting machine	4
Figure 1.2.	Gear and pulley system of an early analog tide predicting machine.	9
Figure 2.1.	Simple tide curve with definitions.	16
Figure 2.2.	Four tide curves showing how the tide range (high water minus low water) varies throughout the month.	17
Figure 2.3.	Simple tidal current curve with definitions for a reversing tidal current.	18
Figure 2.4.	Examples of three rotary tidal currents and one reversing tidal current.	18
Figure 2.5.	Corange chart showing the geographic variation of the tidal range of the largest tidal constituent, M_2 , for the Strait of Juan de Fuca-Strait of Georgia,	20
Figure 2.6.	Cotidal chart showing the geographic variation in the time of high water for the largest tidal constituent, M_2 , for the Strait of Juan de Fuca-Strait of Georgia.	21
Figure 2.7.	The relationship between tidal datums and U.S. marine boundaries.	23
Figure 2.8.	The Earth-Moon system (viewed from very high above the North Pole) revolving around a common point (inside the Earth) with two tidal bulges.	25
Figure 2.9.	The tide generating forces on the Earth resulting from the difference between gravitational attraction and centrifugal force.	25
Figure 2.10.	A very long tide wave of relatively small amplitude produced in the ocean by the tide-generating forces caused by the moon and the sun.	26
Figure 2.11.	Asymmetric tidal bulges when the moon is at maximum declination north or south of the equator, resulting in a diurnal component in the tidal forces	28
Figure 2.12.	The orbits of the moon around the Earth and of the Earth around the sun, as viewed from a distant star.	30
Figure 2.13.	The moon's orbit moon and the sun's orbit (the ecliptic) with respect to the Earth's equatorial plane.	30
Figure 2.14.	The combined effect of the moon and the sun at Full Moon and New Moon (causing larger tidal ranges, <i>spring tides</i>), and at First Quarter and Last Quarter (causing smaller tidal ranges, <i>neap tides</i>).	33
Figure 2.15.	A demonstration of aliasing.	36
Figure 2.16.	Water level spectrum from near Anchorage, Alaska, at the end of a shallow waterway with a large tide range.	36
Figure 2.17.	Tidal Spectra, with diurnal species and semidiurnal species further split into tidal spectral lines.	38

Figure 2.18.	A 100-year record of monthly and annual mean tide ranges at Seattle, WA, illustrating the 18.6-year lunar nodal cycle.	42
Figure 2.19.	Tide curves for particular combinations of $(K_1+O_1)/M_2$ amplitude ratios and phase differences defined as $\frac{1}{2}(M_2^\circ - K_1^\circ - O_1^\circ)$.	44
Figure 2.20.	Chart illustrating the geographic variation in the $(K_1+O_1)/(M_2+S_2)$ tidal constituent amplitude ratio, as well as the <i>type of tide</i> classification for each location, in the Strait of Juan de Fuca - Strait of Georgia.	45
Figure 2.21.	The tide propagating up a river as a <i>progressive wave</i> .	50
Figure 2.22.	The tide in a bay as a <i>standing wave</i>	51
Figure 2.23.	The effect of Coriolis force on M_2 tidal range (corange lines) and the times of high water (cotidal lines) for an idealized rectangular bay.	53
Figure 2.24.	M_2 coamplitude chart for Chesapeake Bay.	54
Figure 2.25.	Typical tide curves for an area with no shallow-water effects (top panel) and for three areas with different degrees of distortion caused by the shallow water.	56
Figure 2.26.	Water level curves from the Gironde River in France showing the effects of nonlinear shallow-water distortion.	57
Figure 2.27.	Tide curves for particular combinations of M_4/M_2 amplitude ratios and phase differences between M_4 and M_2 (defined as $2M_2^\circ - M_4^\circ$).	60
Figure 2.28.	Tide curves for particular combinations of M_6/M_2 amplitude ratios and phase differences between M_6 and M_2 (defined as $3M_2^\circ - M_6^\circ$).	61
Figure 2.29.	Water level data from the tide gauge at Trenton, NJ, during a high river discharge period.	63
Figure 2.30.	Comparison of 15-day harmonic analyses of water level data from Delaware River and Bay during a high runoff period and during a low runoff period, both periods with similar astronomical conditions.	64
Figure 2.31.	The tidal portion of a water level record from Trenton, NJ, on the Delaware River, during a high river discharge period, plotted with the tide predictions for the same period as if there were no river discharge.	65
Figure 2.32.	The tidal portion of water level recorded plotted with tidal predictions for three locations along the Delaware River and Bay and a station on the Atlantic Coast showing the effect on the tide of subtidal storm surge.	66
Figure 2.33.	Calculated node factors for six tidal constituents from 19 one-year (uncorrected) least squares harmonic analyses of Philadelphia water level data plotted with node factors determined from astronomical/equilibrium-tide considerations.	68
Figure 2.34.	Current flow through a cross section near the Chesapeake Bay Bridge.	71
Figure 2.35.	The spatial variation in tidal currents near the surface to the west of Bergen Point in the Port of New York and New Jersey, acquired from a towed ADCP.	72
Figure 2.36.	Variation in $(K_1+O_2)/M_2$ and M_4/M_2 tidal current amplitude ratios, and tidally-induced residual current, across the entrance to Haro Strait, due to the effect of the lateral inertial terms in the equations of motion	74
Figure 2.37.	Speed and direction plots of the unusual occurrence of dominant quarter-diurnal tidal currents at an NOS current station in Ramshorn Creek, SC.	75

Figure 3.1.	A very simple demonstration of extracting tidal constituents from a water level time series.	83
Figure 3.2.	A graphical representation of the amplitude and epoch of a single tidal constituent and its time relationship to moon's transit.	91
Figure 3.3.	Example of a tide curve produced with the harmonic tide prediction equation, along with seven of the individual tidal constituent curves.	93
Figure 3.4.	A current vector with speed and direction, broken up into north and east components and into major and minor components.	96
Figure 3.5.	The harmonic characteristics for two water level stations and two current stations in San Francisco Bay, where the tide regime is mixed.	114
Figure 3.6a.	Plot of the differences between predicted low water times at Port Chicago and predicted low water times at Golden Gate, for the first 120 tidal cycles of 1980.	115
Figure 3.6b.	Plot of the differences between the heights of predicted low waters at Port Chicago and the heights of predicted low waters at Golden Gate.	115
Figure 3.7.	Plot of time differences between harmonically predicted maximum ebbs at two current stations in Delaware River and Bay.	116
Figure 3.8.	Predicted tidal current at Philadelphia on the Delaware River illustrating the dramatically varying time interval between successive maximum floods and between successive maximum ebbs due to shallow-water effects.	118
Figure 3.9.	Plot of time differences between harmonically predicted (but leaving out the overtide and compound tidal constituents) maximum ebbs at two current stations in Delaware River and Bay.	118
Figure 3.10.	The mean annual sea level cycle at 14 NOS stations along the East Coast and Gulf Coast of the U.S. for the period 1948-1984.	121
Figure 3.11.	The variation from year to year of the seasonal sea level range from 1935 to 1992 at four NOS stations along the U.S. East Coast.	122
Figure 3.12a.	Filtering a data time series. In this simple example each group of 13 data points is averaged to produce one data point in the filtered data series.	124
Figure 3.12b.	A water level time series filtered to remove the tidal oscillations and leave a predominantly nontidal time series.	125
Figure 3.13.	Water level data from Trenton, NJ, filtered with a tidal filter compared with river discharge data at Trenton filtered with the same filter.	126
Figure 3.14.	The difference between two tidally filtered water level records at opposite ends of Massachusetts Bay compared with the wind stress component along the axis of the Bay, which was similarly filtered.	127
Figure 3.15.	The simple box filter (running mean) and its effect in the frequency domain.	128
Figure 3.16.	An idealized low-frequency nontidal continuum decreasing from its highest value near zero frequency, but then rising up around a tidal spectral line in the shape of a so-called tidal cusp.	136
Figure 4.1.	The residual water level at Trenton, NJ, on the Delaware River, showing the temporary appearance of tidal energy in the residual during a period of increasing river discharge.	147

Figure 4.2.	Schureman's formulas for inferring tidal constituents from constituents already calculated.	153
Figure 5.1.	A current station deployed at a bend in the waterway, so that the flood direction and the ebb direction are not 180° apart; because of this geometry a harmonic analysis will show a mean current toward the east and a significant second harmonic, M_4 .	172
Figure 5.2.	A fairly narrow tidal constituent ellipse (i.e., eccentricity approaching 1.0).	175
Figure 5.3.	The geometry and trigonometry for converting between north-east components and major-minor components.	176
Figure 5.4.	Tidal current constituent ellipses for M_2 , S_2 , N_2 , K_1 , and O_1 , for a current station in the Strait of Georgia, based on a 29-day harmonic analysis of a data time series.	178
Figure 6.1.	A copy of Form 2211, on which tabulations were done in the pre-computer era when carrying out a monthly mean analysis.	198
Figure 6.2.	Form 657, which was used in the pre-computer era for calculating and recording comparison of monthly means.	200
Figure 6.3.	Form 248, which was used in the pre-computer era to carry out a comparison of simultaneous observations (a tide-by-tide analysis).	201
Figure 6.4.	A short tide-by-tide analysis produced with a recent computer program.	203
Figure 6.5.	An early version of Form 451, which was used in the pre-computer era to carry out a reversing reduction analysis of current data.	206
Figure 6.6.	Results of a computerized reversing reduction analysis for Kent Island, MD, relative to a reference station at Chesapeake Bay Entrance.	208
Figure 6.7.	Plotted time differences between slack before flood at Kent Island, MD, and a reference station at Chesapeake Bay Entrance.	208
Figure 6.8.	Plotted results from a reversing reduction analysis showing the time differences between maximum ebbs at Carquinez Strait and Alcatraz-North Point, both in San Francisco Bay.	209
Figure 6.9.	Plotted results of a reversing reduction showing the ratio of maximum ebb speeds at Carquinez Strait and Alcatraz-North Point, both in San Francisco Bay.	209
Figure 6.10a.	Speed and direction plots of the total current (tidal current plus mean nontidal current) resulting from a rotary reduction analysis of current data from a station in Boston Harbor.	214
Figure 6.10b.	Polar plot showing the rotation of the total current (tidal current plus mean nontidal current) resulting from a rotary reduction analysis of current data from a station in Boston Harbor.	214
Figure 7.1.	Coamplitude and cophase chart for the M_2 tide constituent for the Delaware River and Bay waterway, showing the geographic variation in M_2 amplitude and epoch.	225

Figure 7.2.	Chart with epochs (phase lags) for maximum flood for the M_2 tidal currents in the Strait of Juan de Fuca – Strait of Georgia waterway, given in degrees relative to the local time meridian (120°W).	227
Figure 7.3.	Numerous M_2 ellipses for the waterways around the San Juan Islands.	228
Figure 7.4.	Variation in the amplitude (half-tide range) of the five largest semidiurnal constituents in the Delaware River and Bay.	230
Figure 7.5.	The amplification of the five largest semidiurnal constituents in Delaware River and Bay, namely, M_2 , N_2 , S_2 , $2MN_2$, and $2MS_2$.	231
Figure 7.6.	A cubic control volume used in deriving the conservation of mass equation.	233
Figure 7.7.	Schematic of waterway with Cartesian coordinate system.	239
Figure 7.8.	The phase (time) of high water for various values of the friction coefficient plotted along the length of the waterway from the closed end versus the change in wave number phase	241
Figure 7.9.	The tide range ratio for various values of the friction coefficient plotted along the length of the waterway from the closed end versus the change in wave number phase.	242
Figure 7.10.	Plots of the tide range ratio (relative to the value at the entrance) for six different length waterways (and the same frictional damping coefficient).	243
Figure 7.11.	Plots of the phase (time) difference between high water and maximum flood for various frictional damping coefficients.	243
Figure 7.12.	Maximum flood speed for various frictional damping values plotted relative to the closed end of the waterway.	244
Figure 7.13.	Plots of the K_1/M_2 tide range ratio (relative to the ratio at the closed end) for various values of the frictional damping coefficient.	245
Figure 7.14.	K_1/M_2 ratios for six different waterways lengths, for frictional damping coefficient $\mu=1.5$ (typical for many waterways), plotted relative to the K_1/M_2 value at the entrance.	246
Figure 7.15a.	The phase (time) of M_2 high water (relative the value at the closed end) for eight different values of the frictional coefficient N in an estuary with an exponential width decrease matching that in the Delaware River and Bay.	249
Figure 7.15b.	The M_2 tide range (relative the value at the closed end) for eight different values of the frictional coefficient N in an estuary with an exponential width decrease matching that in the Delaware River and Bay.	249
Figure 7.16.	Tide range (relative to that at the closed end) for five different values of exponential width decrease, for the frictionless case ($N=0$).	250
Figure 7.17.	Tide range for stations in the Bay of Fundy plotted verus the time (phase) of high water, and a map of the locations of the tide stations.	252
Figure 7.18.	Cotidal and corange lines in a semi-enclosed waterway for four different values of the frictional damping coefficient (including the frictionless case).	255
Figure 7.19.	The effect of a mean river flow on the first three tidal harmonics, from a Fourier decomposition of the quadratic friction term, $u u $.	262
Figure 7.20.	Diagram illustrating the asymmetric effects of the nonlinear continuity term, the inertial term, and the term representing the elevation effect on frictional momentum loss per unit volume of fluid.	265
Figure 7.21.	Diagram illustrating the symmetric nonlinear effects of quadratic friction.	265

Figure 7.22.	Diagrams illustrating the nonlinear interaction of the tide with river flow via the quadratic friction term, for two cases: the river flow is less than the maximum tidal current, and the river flow is greater than the maximum tidal current.	266
Figure 7.23.	Plots of the tidal amplitudes M_2 , M_4/M_2 , and M_6/M_2 produced by a one dimensional nonlinear model of Delaware River and Bay compared with harmonic analysis results from Delaware River and Bay water level data.	269
Figure 7.24.	M_2 amplitudes produced by a nonlinear numerical model along the Delaware River and Bay for seven amounts of river discharge, with only the quadratic friction term turned on.	270
Figure 7.25.	Numerical model-produced M_4/M_2 amplitude ratios along the Delaware River and Bay for seven different river discharge amounts, with quadratic friction as the only nonlinear term turned on in the model.	271
Figure 7.26.	Numerical model-produced M_6/M_2 amplitude ratios along the Delaware River and Bay for seven different river discharge amounts, with quadratic friction as the only nonlinear term turned on in the model.	272
Figure 7.27.	Current profiles from bottom-mounted upward-looking ADCPs at eight locations in Chesapeake Bay, all measured on October 26, 2006 at noon.	276
Figure 7.28.	M_2 and N_2 constituent ellipses for three different depths for a current station in the Strait of Georgia.	277
Figure 7.29.	An example of an ocean M_2 co-amplitude chart for the Atlantic Ocean.	279
Figure 8.1.	A fine grid section of the NOS New York -New Jersey Operational Forecast Model System, and the predicted currents in the same section of the model, illustrating the complex horizontal structure of the tidal currents including current shear and eddies.	285
Figure 8.2.	Comparison between a surface current field measured by an HF radar system in lower Chesapeake Bay and the output of a three-dimensional finite element hydrodynamic model for the same time period.	294
Figure 9.1.	A Table 1 page of daily tide predictions for Boston, MA.	301
Figure 9.2.	A Table 2 page showing subordinate tide stations.	303
Figure 9.3.	A caution in the Tide Tables about the variation in low water time due to shallow-water effects.	304
Figure 9.4.	An example of Table 8 from the 2006 Tide Tables for the <i>East Coast of North and South America</i> , showing statistical figures related to the tide prediction accuracy of the reference stations.	305
Figure 9.5.	Table 1 daily predictions for a the tidal current reference station at Chesapeake Bay Entrance from the <i>Tidal Current Tables for the Atlantic Coast of North America</i> .	311
Figure 9.6.	A Table 2 page of subordinate tidal current stations from the <i>Tidal Current Tables for the Atlantic Coast of North American</i> .	312
Figure 9.7.	Rotary tidal currents presented in Table 5 of the <i>Tidal Current Tables for the Atlantic Coast of North America</i> .	313

List of Figures

Figure 9.8.	A tidal current diagram for Chesapeake Bay included in the <i>Tidal Current Tables for the Atlantic Coast of North America</i> .	315
Figure 9.9.	A portion of one of the 12 hourly tidal current charts for the Upper Chesapeake Bay.	320
Figure 9.10.	One of the hourly tidal height charts from the <i>Delaware River and Bay Tidal Circulation and Water Level Atlas</i> .	324
Figure 9.11.	One of the hourly tidal circulations charts from the <i>Delaware River and Bay Tidal Circulation and Water Level Atlas</i> .	325
Figure 9.12.	A tide and light diagram produced during World War II to show the times of high and low tides, plus the times of moonrise, moonset, sunrise, sunset, and various degrees of twilight for a month.	327
Figure 9.13a.	A Tidal Illumination Diagram for LeHarve, France, for July 1944, produced from tide predictions calculated by the British for the Allied forces.	328
Figure 9.13b.	The “Explanation of Diagram” found on the back of the Tidal Illumination Diagram in Figure 9.13a.	329

List of Tables

Table 2.1.	Fundamental astronomical periods of the motions of the earth, moon, and sun.	29
Table 2.2.	Tidal constituents and their origin from key astronomical frequencies.	40
Table 2.3.	Table showing the effect of the phase difference $P = \frac{1}{2}(M_2^\circ - K_1^\circ - O_1^\circ)$ on the sequence of tide and the acceleration or retardation of the high or low water.	46
Table 2.4.	Compound and overtide constituents generated by four nonlinear terms in the one-dimensional equations of motion.	59
Table 3.1.	Schureman's Table 39 showing the synodic periods for a number of pairs of semidiurnal tidal constituents and diurnal tidal constituents.	85
Table 3.2.	The 37 tidal harmonic constituents that typically had been included in a harmonic analysis at CO-OPS and its predecessor organizations (unless it was an extreme shallow-water situation).	88-9
Table 4.1.	55 tidal constituents from a 19-year harmonic analysis of Seattle water level data, including 30 satellite constituents.	151
Table 4.2.	Corrections factors for ten different reference stations in the Strait of Juan de Fuca-Strait of Georgia for the 29-day period beginning March 1, 1974, for use in correcting the harmonic constants from other stations with only 29 days of data.	156
Table 7.1.	A low-frequency storm effect on tide amplitude near the head of tide in the Delaware River produced with a nonlinear numerical model.	272
Table A.1.	149 tidal harmonic constituents listed in order of increasing frequency.	334-8
Table A.2.	149 tidal harmonic constituents listed in order of increasing synodic period.	339-5

Acknowledgments

Mike Szabados provided the support for this project, and totally believed in the need for this book; without his support this book would not have been written. Brenda Via managed the publication and printing process for the book and also improved many of the graphics. Steve Gill coordinated the internal review process for the book and provided many valuable comments himself. Chris Zervas, Pat Burke, and Chris Paternostro of CO-OPS provided significant comments and useful suggestions. Others inside CO-OPS who reviewed the book were Kate Bosley, Karen Earwaker, Kathleen Fisher, and Laura Rear. Members of the Coast Survey Development Laboratory who also provided useful comments were Kurt Hess, John Kelley, Richard Patchen, Dick Schmalz, Eugene Wei, and Aijun Zhang. Outside of NOAA, very beneficial comments and suggestions were provided by four true experts in the field, Mike Foreman (Institute of Ocean Sciences, Canada), Philip Woodworth (Proudman Oceanographic Laboratory, UK), David Jay (Portland State University), and Alan Blumberg (Stevens Institute of Technology). Over the years, working in tides in the Coast and Geodetic Survey (C&GS) and its later organizational forms in the National Ocean Service in NOAA, the author has had the privilege of working with many dedicated tidalists, who have contributed much to tidal science and operations, many of whose names one will see in the References section of this book. In addition to those mentioned above, this included early in his career, scientists who were carrying on the advancement of tidal science within the C&GS such as Bernard Zetler, Robert Cummings, D. Lee Harris, Elmo Long, Robert Dennis, and Steacy Hicks.

About the Author

Dr. Bruce Parker spent most of his career in NOAA and much of his time working on tide related problems as a specialty even while tackling jobs with a much broader scope. Positions he held at NOAA included: Chief Scientist of the National Ocean Service; Director of the Coast Survey Development Laboratory; Director of the World Data Center for Oceanography; Principal Investigator for the NOAA Global Sea Level Program; and head of the U.S. national tides and currents program (in a earlier organizational form before it became CO-OPS). Among his awards are the NOAA Bronze Medal, the Department of Commerce Silver and Gold Medals, and the Commodore Cooper Medal from the International Hydrographic Organization. Dr. Parker is presently a Visiting Professor at the Center for Maritime Systems at the Stevens Institute of Technology. Dr. Parker has written many papers on tidal subjects, some of which are included in the References section of this book, as well as many tidal analysis programs, some still being used in some form in CO-OPS. He also had the privilege of organizing the program for the International Conference On Tidal Hydrodynamics in 1988 and editing the book that resulted. Dr. Parker received his Ph.D. in physical oceanography from The Johns Hopkins University, and prior to that an M.S. in physical oceanography from the Massachusetts Institute of Technology, and a B.S./B.A. in biology and physics from Brown University.

Index

A

accelerated tide 46
age
 the tide (age of phase inequality) 47
 of diurnal inequality 47
 of parallax inequality 47
 of the moon 110
aliasing 35-36, 103
amphidromic point 254, 279
 (see “node, point of zero range”)
analysis
 (see “tidal analysis, types of”)
angular speed 15, 39-40, 47, 84, 89, 91-94,
 152, 157, 333-45
 (see also “tidal frequencies”)
apogee, lunar 30, 32-35, 38, 49, 58, 113,
 302
 apogean tides 32-34
 apogean neap tides 34
aphelion (solar apogee) 31, 37, 39, 119
astronomical frequencies 11, 29, 35-40,
 91, 108, 333-45
astronomical periods (inverse of
 astronomical frequencies) 29-30

B

baroclinic effects 71, 105, 171, 185, 275
benchmark 22
bore, tidal (see “tidal bore”)
bottom boundary layer 274, 284
Boussinesq Approximation 233
build-up factor 142, 163-65, 308

C

Cartwright tide potential of 39, 89, 149,
 333-45
Cartwright number 39, 88-89, 150, 333-45
 (see also “Doodson number”)
centrifugal force 24-26
compound tide 1, 11, 31, 37, 49, 58-60,
 104, 108, 141, 167, 171, 179,
 193-94, 231, 236-67, 256-62,
 264-65, 268, 270, 274, 289, 303
generation of 58-60, 256-62, 285, 289
 with same frequency as an astronomical
 constituent 141, 333
conservation of mass, volume, and
 momentum
 (see “equations of motion”)
consistency
 in calculated amplitudes and epoch 87,
 142, 160, 164-66, 179, 193, 289
 in calculating maxima 129-32
 in calculated Sa and Ssa from year to
 year 120
constituent ellipse
 (see “ellipse”)
constituents (see “tidal constituents”)
continental shelf, tides on 278
continuous wavelet transform 65, 105-6
 126, 147, 158, 171, 185
continuum (nontidal) 35, 37, 82, 132,
 134-36, 142, 165, 289
 (see also “spectra”)
corange (or coamplitude) chart 20, 54,
 137, 224-25, 223-26, 255, 279

- Coriolis force 27, 53, 234
 effects in wider waterways 27, 53,
 251-55
 effect on inertial currents 78, 136
 effect on land breeze-sea breeze 78,
 136
 f-plane approximation 234
 Ekman spiral 276
 Rossby radius of deformation 237
 cospeed chart 226
 cotidal (or co-phase) chart 20-21, 52-53,
 223-26
 current data, analysis of
 (see “harmonic analysis”)
 (see “nonharmonic comparison
 analysis”)
 (see “tidal analysis, types of”)
 current diagrams, 314-15
 current meters
 errors from 180-84
 types of 180-84
 current pole and log line 181
 cusp (see “tidal cusp”)
 cycle-by-cycle analysis 111, 112-19, 202-4
 (see “tide-by-tide analysis”)
 (see “reversing reduction analysis”)
- D**
- datum (vertical)
 chart 22, 92, 295
 ellipsoid (3-D) 22-24,
 marine boundaries based on 23,
 orthometric 22-24,
 tidal 6, 22-24, (also see separate entry
 under “tidal datum”)
 vertical datum transformation tool
 (VDatum) 24,
- day
 lunar 15, 29
 sidereal 29
 solar 15, 29
- declination
 lunar declination
 equatorial 28-31, 34,
 northern or southern 28-31, 34
 (see also “tropic tide”)
- solar declination 29-31, 34
 definitions 15-24, 42-48
 deterministic (data) 81, 133
 detiding 7, 123-29
 differences (time, height, speed)
 from nonharmonic analyses 111-12,
 195-222
 in Table 2 112, 195, 218-19, 302-3,
 308-9, 310, 312, 317-18
 variation throughout month 112-19,
 195-97, 219-220
 digital tidal prediction products 330-31
 diurnal inequality 19, 34,
 diurnal tide 17, 35, 43-46
 Doodson tidal potential 39
 Doodson number 30, 89, 333-45
 (see also “Cartwright number”)
- E**
- ebb current 16, 50
 eccentricity 174
 ecliptic 29-31, 34,
 obliquity of 31
 (see also “orbits”)
 elimination 154
 (see “inference and elimination”)
 Ekman spiral 276
 (see “Coriolis force”)
 ellipse
 rotary tidal current 18
 (see “tidal current constituent ellipse”)
 empirical orthogonal function analysis
 137-38
 epoch 8, 28, 31, 39, 43, 47, 91-95, 97, 107-8
 (see “harmonic constants”)
 Epoch, National Tidal Datum 22-23, 46
 equilibrium argument 39, 41-42, 69, 91-95,
 99, 141, 148-49, 152, 158
 equilibrium theory 26, 28, 42, 67-68,
 91-92, 152, 154-55, 162
 equations of motion 232-38
 continuity equation 232-33
 finite-difference analog 281-84
 momentum equations 233-35
 nonlinear terms in 254-56
 physical explanation of 263-67

simplifying for idealized cases 223-28
 equatorial declination 28, 34,
 (see “lunar declination”)
 equinox
 autumnal 29, 34,
 vernal 29, 34,
 errors, instrument
 in current data time series data 180-84
 in water level data time series data
 142-46
 establishment of the port 47

F

fair tide 7,
 filtering 123
 band pass 128
 band-stop 128
 high pass 128
 low pass 125-28
 weights 124, 128
 (see “tidal filtering”)
 finite-difference technique 283-84
 (see “numerical hydrodynamic models”)
 finite-element technique 284
 (see “numerical hydrodynamic models”)
 flood current 16, 50
 folding (see “aliasing”)
 folding frequency (see “Nyquist frequency”)
 Fourier decomposition of the equations of motion 256-62, 273-74
 Fourier harmonic analysis 97-99
 frequency
 astronomical 29, 39
 Nyquist 35
 tidal (see tidal frequency)
 friction (bottom) 52, 57
 energy loss due to 57
 damping of tide wave 52, 238
 generation of compound tides and
 overtides 59-60, 256-60
 linearized 238
 nonlinear effects, types of 255-60
 frictionally damped progressive wave 52,
 238
 frictionally damped standing wave 52, 240

G

geoid 23
 gravitation (estuarine) circulation 275

H

harmonic analysis 8, 39, 42, 91-101,
 complex algebra form 97, 179
 constituents solved for 139-41
 (see also “synodic period”)
 Fourier-based method 97-99
 historical development 8, 10
 harmonic tide prediction equation 90-95
 harmonic tidal current prediction
 equation 95-97
 inference and elimination 152-59
 least-squares method 99-101
 of a long series of high and low waters
 106-9
 of current data 169-94
 constituent ellipses from harmonic
 constants 96, 132, 169, 172-80,
 226-29, 275-79
 mean current from 186
 orthogonal axes 179-80
 summary overview 192-94
 special problems with 169-72
 of water level data 139-68
 summary overview 166-68
 reference station, use of 154-55
 Sa and Ssa, analysis for determining
 122-23
 satellite constituents, using 150-51
 short time series, analyzing 150-59, 187
 small constituents, keeping or rejecting
 142
 harmonic constants 1, 8, 42-48, 90
 harmonic constituents (see “tidal
 constituents”)
 harmonic-shallow-water corrections method
 103
 high and low waters 15
 calculating (consistently defined)
 129-31
 diurnal inequality 19

- harmonic analysis of a long time series
of 106-9
types of 17-18, 46-47
- hydraulic tidal currents 76
- hydrodynamic models 223-79, 281-97
analytical hydrodynamic models 223,
238-54
- long narrow rectangular waterway
238-47
- exponentially narrowing waterway
247-50
- numerical hydrodynamic models
267-73, 281-84
use in tidal prediction 281-97
advantages 284-87
disadvantages 287-88
operational uses of 293-97
sensitivity analysis 292
tidal forcing, proper 288-90
validation of 290-93
- real-time based nowcast/forecast model
prediction systems 296-97
- wider waterways (Coriolis effects)
251-55
(see "equations of motion")
(see "tidal prediction, numerical model")
- hydrodynamics 10-11, 15, 48-79, 223-79
importance of 10-11
- hydrographic surveys 295-96
tidal modeling for 295-96
tide-based corrections in 295-96
VDatum used in 296
- hydrostatic approximation 234
- hydrostatic equation 235
- I**
- inference and elimination 150, 152-58,
187
- inertial currents 78-79, 186,
inertial effects
(see "lateral inertial effects")
(see "shallow-water tides")
- inertial terms in equations of motion 236
- internal tides 135, 146, 171, 185, 275
- interpretation of tidal analysis results
223-79
- interval, lunital (see "lunital interval")
- J**
- K**
- Kelvin wave 253-55, 278
- L**
- lateral inertial effects (on tidal current)
73-75, 273-74
- long-period tides 40-41
lunar fortnightly constituent (Mf)
37-38, 40
- lunar monthly constituent (Mm)
37-38, 40
- lunar synodic fortnightly constituent
(MSf) 37-38
(see "Sa and Ssa")
- long wave approximation 234
(see "hydrostatic approximation")
(see "equations of motion")
- low waters (see "high and low waters")
- lunar declination (see "declination")
- lunar nodal regression 31, 40,
ascending lunar node 31, 40
(see "node factor")
- lunital interval 47, 205,
(see also "cotidal chart")
- M**
- marine boundaries 22-23
- maximum floods and ebbs 16
calculating consistently defined 131-32
- mean current
from a harmonic analysis 172, 186-88
from a nonharmonic analysis 212-14
tidally induced 69, 73-74
(see also "tidally induced residual
current")
- mean cycle analysis 111
(see "rotary reduction analysis")
- mean sea level 15, 19
tidally induced change in 69
- mixed tide 18, 43-46, 135,
- models (see "hydrodynamic models")

modulation of tidal force 32-34, 37
 (see also “splitting of tidal species”)
 momentum 233
 (see “equations of motion”)
 month
 synodic 30
 tropical 29
 monthly mean analysis 111, 197-202
 moon
 (see “lunar”)
 (see “orbits”)

N

narrow basin approximation 236
 (see “equations of motion”)
 narrowing waterway, effect on tide 247-51
 natural period of oscillation 27
 nodal regression (see “lunar nodal regression”)
 neap tide 16, 32-33
 node (point of zero tide range) 50-53, 55, 77-78, 241, 250, 254, 267
 amphidromic point 268
 quasinode 52-53, 77-78, 224, 241, 244, 246, 254, 257, 259, 267, 270
 virtual 52, 254
 node factor (lunar) 37, 39-42, 60-61, 67-69, 91-94, 99, 141, 148-50, 152-59, 165, 167, 171-73, 187, 193
 hydrodynamic effects on 67-69
 nonharmonic comparison tidal analysis 8, 87, 109-19, 195-222
 hydrodynamic considerations 196-97
 need for 196
 problems with 112-18, 219-20
 variation of values throughout a month 112-18, 219-20
 minimizing errors due to 219-20
 reference station, selecting a 217-18
 subordinate station, putting in a Tide or Tidal Current Table 218-19
 types of 111-12, 197-217
 monthly mean analysis 197-201
 tide-by-tide analysis 202-5
 reversing reduction analysis 205-9
 rotary reduction analysis 210-17

nonlinear interaction of tides with nontidal phenomena 63-67
 with river flow 63-66, 260-62
 with storm surge 66-67, 262-63
 nonlinear mechanisms 55, 59, 263-67, 333-45
 (see “nonlinear tides”)
 nonlinear tides
 asymmetric effect 55-62, 69, 73-75, 88-89, 259-60, 264-65, 274, 333-46
 lateral inertial effects (see “lateral inertial effects on tides”)
 physical explanation of nonlinear mechanisms 263-67
 shallow-water (see “shallow-water tides”)
 symmetric effect (of quadratic friction) 56-62, 259-60
 zero-frequency effects 70
 (see “compound tides” and “overtides”)
 nontidal phenomena (river flow and storm surge)
 nonlinear interaction with tide and tidal current 63-67, 146, 260-63, 266-67, 270-73
 nontidal water level change
 causes of 19
 numerical hydrodynamic models (see “hydrodynamic models”)
 Nyquist frequency 35

O

orbits

Earth orbit around sun (ecliptic) 27-34
 Moon orbit around Earth 27-34
 overtide 1, 11, 36, 55-61, 78, 116, 171-72, 179, 256-60, 251-52, 264, 269, 274
 generation of 256-60

P

parallax 32
 perigee, lunar 30-35, 37, 40-41, 47, 58
 perigean spring tides 34
 (see also “apogee, lunar”)
 perihelion (solar perigee) 31, 37-38, 119

- period 15
 - natural period of oscillation 27
 - phase age 47
 - phase lag (see “epoch”)
 - Poincaré waves 254, 278
 - predicted series
 - assessing quality of 159-63, 188-90, 304-6
 - changes in bathymetry and shoreline, looking for 164, 190
 - comparison of high and low waters (predicted versus data) 161-62, 304-6
 - comparison of maximum floods and ebbs (predicted versus data) 188-89
 - residual series, spectral analysis
 - spectral analysis of 162, 189
 - transient tidal oscillations, looking for 169-70, 198-99
 - build-up factors, use and misuse of 163-64
 - reference station, for 165, 191
 - prediction (see “tidal prediction”)
 - principal component analysis 137-38
 - products, tidal prediction (see “tidal prediction products”)
 - progressive tide wave
 - frictionally damped 49, 51, 238-41, 244-45, 253, 264, 266
 - frictionless 49-52, 250
- Q**
- quality assessment
 - of harmonic analysis of current data 190-94
 - of harmonic analysis of water level data 158-63
 - of nonharmonic analysis 219-20
 - of tidal current predictions 190-94
 - of tide predictions 158-63
 - quasinode (see “node, point of zero range”)
- R**
- range (see “tide range”)
- Rayleigh criterion 36, 84-87, 101, 158
 - (see “synodic period”)
 - reduction factor 42
 - (see “node factor”)
 - reference station 2, 87, 90, 103-4, 108, 110-11, 113, 116-17, 149, 154-57, 161, 164, 189, 191, 195-96, 204
 - producing a reference station
 - for Table 1 of a Tide Table 165, 308
 - for Table 1 of a Tidal Current Table 191, 317
 - selecting for a nonharmonic comparison analysis 217-18
 - use of in improving a short harmonic analysis 154-56
 - reflected tide wave 51
 - (see “standing wave”)
 - resonance 27, 50-51
 - residual current
 - (see “tidally induced residual current”)
 - residual time series 100-1, 121, 123, 125-26, 147-49, 159-68, 185-86, 188-90, 192, 194
 - spectral analysis of 161, 191, transient tidal oscillations, looking for 162, 192
 - response method 5, 9, 90, 102-3, 104, 105, 133, 137, 290
 - admittance 102-3
 - credo of smoothness 103
 - radiational input 103
 - resonance 27, 49, 50, 55, 67, 72, 242
 - retarded tide 50
 - Reynolds equations 235
 - (see “equations of motion”)
 - reversing reduction analysis 111-12, 116, 205-10, 212, 216, 219, 221
 - reversing tidal current
 - defined 16, 18,
 - river flow (river discharge)
 - effect on tide (see “nonlinear interaction of tide with nontidal phenomena”)
 - effect on nontidal water level 267
 - Rossby radius of deformation 237, 251
 - rotary reduction analysis 111-12, 204-5, 207, 210-19, 221

- rotary tidal current
defined 17, 18, 214,
- S**
- Sa and Ssa 38, 88, 103, 119-23, 143, 145, 148, 162
considerations in whether to use 120-22
meteorological origins of 119-23
methods for calculating 122-23
- satellite constituents 37, 39, 41, 92-93, 141, 148-50, 151, 158, 165
(see “node factor”)
- satellites 39
- sea level 15, 19, 22
(also see “mean sea level”)
- sea level change
absolute 22
relative 22
steric sea level change 119-20, 122, 159
tidally induced 69
- secondary port (see “subordinate station”)
- semidiurnal tide 18-19, 43-46,
sequence of tide 45-46
- shallow-water approximation 234
(see “hydrostatic approximation”)
(see “equations of motion”)
- shallow-water constituents 11, 38, 39, 57-78, 60-2, 75, 141, 156-67, 165, 166, 179, 191, 193-94, 229, 257, 260, 274
(see “compound tides” and “overtides”)
(see also “nonlinear tides”)
- simultaneous observations, comparison of
(see “tide-by-tide analysis”)
- shoreline
legal U.S. shoreline 22-23
mean high water shoreline defined 22
- slack water 16, 48-50, 57, 76, 107, 112, 129, 132, 188, 194, 205, 208, 211, 214-15, 244, 264, 266
- solar declination (see “solstice”)
- solstice
summer 29, 34,
winter 29, 34,
(see “declination”)
- species concordance method 104
- spectra 36-37
(see “tidal spectra”)
- spectral analysis 132-37
autocorrelation method 133
autospectrum 133
cross-spectrum 133
cross-spectral analysis 135-37
direct method using the FFT 134
maximum entropy method 134
maximum likelihood method 134
of water level data 133-34
of current data 135-36
Parseval’s theorem 133
rotary spectral analysis 135-36
(see also “tidal cusps”)
- spectroscopy 37
- splitting of tidal species 37
(see also “modulation of tidal force”)
- spring tide 16, 32-34, 46-48,
- standard port (see “reference station”)
- standing tide wave
frictionally damped 50, 51, 57, 240-41, 244, 264, 266
frictionless 50, 250
- stand of tide 61
- stationary data 81
- stochastic (data) 81, 133
- storm surge 6, 19, 66-67, 262-63
- storm tide 6,
- subordinate station 2, 87, 90, 110-11, 113, 117, 154-55, 165, 191, 195-96, 200, 202-4, 206, 210, 213, 216-221, 299-300, 216-21, 299-300, 302-3, 307-310, 312, 316-18, 322, 330
- putting
in Table 2 of a Tide Table 218-19, 302, 308
in Table 2 of a Tidal Current Table 218-89, 310, 317
in Table 5 of a Tidal Current Table 218-89, 313, 317
on a Tidal Current Chart 218-89, 322
- sun
(see “solar”)
(see “orbits”)
- superfine resolution method 105

synodic period 84-89, 99, 101, 139-41,
 160, 166-68, 192-94, 333-45
 (see also "Rayleigh criterion")

T

tidal analysis, types of 81-138
 simple demonstration of extracting tidal constituents from a data time series 83-85
 (see "continuous wavelet transform analysis")
 (see "harmonic analysis, Fourier")
 (see "harmonic analysis, least squares")
 (see "harmonic-shallow-water corrections method")
 (see "nonharmonic analysis")
 (see "response method")
 (see "species concordance method")
 (see "spectral analysis")
 (see "superfine-resolution method")
 (see "tidal filtering")
 tidal bore 7, 55, 57, 299
 tidal circulation and water level forecast atlases 323-26
 tidal bulges (in equilibrium theory) 24-25
 tidal constituents
 amplification of 201, 243
 constituents solved for 139-41, 166, 179, 192
 (see "synodic period")
 origin of 31-39, 88-89, 333-45
 naming convention 39
 calculation of from data (see "harmonic analysis")
 shallow-water (see "shallow-water constituents")
 spectral lines for 38
 table of 37 constituents 88-89
 table of 149 constituents 334-45
 tidal current
 constituent ellipses 96, 136, 169, 172-79, 180, 191, 193
 defined 15
 ebb current 16, 50
 errors, types of instrument errors 180-84

flood current 16
 hydraulic tidal currents 76
 limitations on predictions 78-81
 locations with high speeds 20-21
 mean current
 tidally induced 69, 73-74, 195
 whether to include 195-96
 nonlinear lateral inertial effects on 73-75, 273-74
 nontidal influences, potential effects of 184-86
 orthogonal axes, selection of 179-80
 reversing 16, 18, 205
 rotary 18, 210
 shallow-water effects on 75-76
 slack water 16, 48-50, 57, 76, 107, 112, 129, 132, 188, 194, 205, 208, 211, 214-15, 244, 264, 266
 special aspects of 69-80
 special problems when analyzing 169-72
 types of 19
 variation over depth 71-72, 274-77
 variation over horizontal distance 72-75
 tidal current charts 318-23
 advantages and limitations of 321-22
 construction of 322-23
 tidal current tables 309-18
 construction of 317-18
 current diagrams 314-15
 limitations of 316-17
 Table 1 (harmonically produced reference stations) 310
 Table 2 (nonharmonically produced subordinate stations) 310-12
 Table 5 (for rotary tidal currents) 313
 tidal cusp 65, 134-36, 263
 tidal datum 7, 22
 types of 22-24,
 lowest astronomical tide 23
 mean high water 22-23
 mean lower low water 22-23
 relationship to marine boundaries 22-23
 relationship to shoreline 22-23
 (see also "datums (vertical)")

- tidal filtering 123-29
 Doodson filter 128
 tidal frequencies 15, 94
 derivation of 35-40
 (see also "angular speed")
 tidal harmonic constituent (see "tide constituent")
 tidal illumination diagram, 328-29
 tidal period 15-16
 tidal prediction
 complex tidal prediction equation 97, 179
 harmonic tide prediction equation 90-95
 harmonic tidal current prediction equation 95-96
 numerical model, using a 281-97
 advantages 284-87
 disadvantages 287-88
 sensitivity analysis 292
 tidal forcing, proper 288-90
 validation of 290-93
 operational uses of 293-97
 uses of 6-7
 (see "predicted series, assessing quality of")
 tidal prediction products 299-331
 (see "tide tables")
 (see "tidal current tables")
 (see "tidal current charts")
 (see "tidal circulation and water level forecast atlases")
 (see "tide and light diagram")
 (see "digital tidal prediction products")
 tidal range (see "tide range")
 tidal rectification (see "tidally induced residual current")
 tidal spectra 35-39, 82
 tidal spectral lines 38, 41, 82, 136
 tidal stream (see "tidal current")
 tidal stream atlas (see "tidal current chart")
 tidal wavelength 50, 55, 239-46, 249-51, 254, 263, 267, 278
 tidal wave number 238, 248, 251, 253
 tidal zoning 295
 continuous water level zoning 295
 (see "hydrographic surveys")
 tidally induced mean sea level change 69, 258
 tidally induced residual current 69, 73-74, 257, 273-74
 tide
 astronomical versus hydrodynamic aspects 15, 19-20
 astronomical considerations 27-48
 hydrodynamic considerations 48-80
 defined 15
 generation of 24-27
 sequence of 46
 type of 17-19, 43
 versus water level 6
 tide and light diagram 326-27
 tide-by-tide analysis 112, 115, 202-5
 tide gauge (tide gage)
 (see "water level gauge")
 tide-generating potential 39, 88-89, 149, 333-45
 tide predicting machine 3-4, 8-9
 tide-producing forces 25, 39
 tide range 15, 48
 hydrodynamics effects on 49-45, 241-43, 248-50, 251-54
 large ranges, locations with 21, 52
 types of 48
 (see also "corange chart")
 tide staff (see "water level gauge")
 tide tables 299-309
 construction of 308-9
 limitations of 307-8
 Table 1 (harmonically produced reference stations) 300-2
 Table 2 (nonharmonically produced subordinate stations) 302-4
 tropic tide 43
 turbulence closure scheme 235, 275, 290
 (see "equations of motion")
 type of tide 17-19, 43-45
 (see also "semidiurnal", "mixed", and "diurnal")

U

uses of tidal analysis and prediction 6-7

V

vertical datum

(see “datum, vertical”)

VDatum (vertical datum transformation tool) 24, 296

virtual node (see “node, point of zero range”)

vulgar establishment 47

W

wavelength

(see tidal “wavelength”)

water level

nontidal effects on 19, 267

versus tide 6

water level data, analysis of

(see “harmonic analysis”)

(see “nonharmonic comparison analysis”)

(see “tidal analysis, types of”)

water level gauge 22, 143-46

errors from 143-46

types of 143-46

wave number (see “tidal wave number”)

X

Y

year

tropical 31

Z

zero-frequency effects from nonlinear tidal interaction 69, 73-74, 257-78, 273-74